

Some pages of this thesis may have been removed for copyright restrictions.

If you have discovered material in AURA which is unlawful e.g. breaches copyright, (either yours or that of a third party) or any other law, including but not limited to those relating to patent, trademark, confidentiality, data protection, obscenity, defamation, libel, then please read our [Takedown Policy](#) and [contact the service](#) immediately

**OXIDATION AND STABILISATION CHEMISTRY OF METALLOCENE-
BASED POLYOLEFINS DURING MELT PROCESSING**

XI PENG

Doctor of Philosophy

ASTON UNIVERSITY

March 2004

This copy of the thesis has been supplied on condition that anyone who consults it is understood to recognise that its copyright rests with its author and that no quotation from the thesis and no information derived from it may be published without proper acknowledgement.

ASTON UNIVERSITY
**OXIDATION AND STABILISATION CHEMISTRY OF METALLOCENE-BASED
POLYOLEFINS DURING MELT PROCESSING**

XI PENG

Doctor of Philosophy
March 2004

SUMMARY

Metallocene catalyzed linear low density polyethylene (m-LLDPE) is a new generation of olefin copolymer. Based on the more recently developed metallocene-type catalysts, m-LLDPE can be synthesized with exactly controlled short chain branches and stereo-regular microstructure. The unique properties of these polymers have led to their applications in many areas. As a result, it is important to have a good understanding of the oxidation mechanism of m-LLDPE during melt processing in order to develop more effective stabilisation systems and continue to increase the performance of the material.

The primary objectives of this work were, firstly, to investigate the oxidative degradation mechanisms of m-LLDPE polymers having different comonomer (1-octene) content during melt processing. Secondly, to examine the effectiveness of some commercial antioxidants on the stabilisation of m-LLDPE melt. A Ziegler-polymerized LLDPE (z-LLDPE) based on the same comonomer was chosen and processed under the same conditions for comparison with the metallocene polymers.

The LLDPE polymers were processed using an internal mixer (torque rheometer, TR) and a co-rotating twin-screw extruder (TSE). The effects of processing variables (time, temperature) on the rheological (MI, MWD, rheometry) and molecular (unsaturation type and content, carbonyl compounds, chain branching) characteristics of the processed polymers were examined. It was found that the catalyst type (metallocene or Ziegler) and comonomer content of the polymers have great impact on their oxidative degradation behavior (crosslinking or chain scission) during melt processing. The metallocene polymers mainly underwent chain scission at lower temperature (< 220°C) but crosslinking became predominant at higher temperature for both TR and TSE processed polymers. Generally, the more comonomers the m-LLDPE contains, a larger extent of chain scission can be expected. In contrast, crosslinking reactions were shown to be always dominant in the case of the Ziegler LLDPE. Furthermore, it is clear that the molecular weight distribution (MWD) of all LLDPE became broader after processing and tended generally to be broader at elevated temperatures and more extrusion passes. So, it can be concluded that crosslinking and chain scission are temperature dependent and occur simultaneously as competing reactions during melt processing. Vinyl is considered to be the most important unsaturated group leading to polymer crosslinking as its concentration in all the LLDPE decreased after processing. Carbonyl compounds were produced during LLDPE melt processing and ketones were shown to be the most important carbonyl-containing products in all processed polymers. The carbonyl concentration generally increased with temperature and extrusion passes, and the higher carbonyl content formed in processed z-LLDPE and m-LLDPE polymers having higher comonomer content indicates their higher susceptibility of oxidative degradation.

Hindered phenol and lactone antioxidants were shown to be effective in the stabilization of m-LLDPE melt when they were singly used in TSE extrusion. The combination of hindered phenol and phosphite has synergistic effect on m-LLDPE stabilization and the phenol-phosphite-lactone mixture imparted the polymers with good stability during extrusion, especially for m-LLDPE with higher comonomer content.

Keywords: Metallocene Polyolefins, LLDPE, Polyethylene, Polyolefin, Oxidation, Melt Stabilisation

ACKNOWLEDGEMENTS

I would like to sincerely acknowledge with gratitude all that my supervisor, Dr. Sahar Al-Malaika, has done for me during this work, especially her kind and constructive suggestions, detailed and crucial comments, which greatly widened my views and perspective.

I am also indebted to Dr. Husam Sheena and Dr. Mike Perry for their technical support and valuable discussion. I am very grateful to other members of Polymer Processing and Performance Research Unit, Umar Daraz, Eddiyanto, Mark Lay, Mark Jones, Elizabeth Lakin, especially Chinese fellow, Dr. Wei Kong, as well as the project (UG) students, Stella Mui, Helen Weston, for their great help, useful discussion, advice and opinions.

I also thank Aston University for the financial support for my research and Dow Chemical Company for providing experimental materials.

Finally, I would like to dedicate this thesis to the memory of my beloved father, who was an excellent researcher in polymer science and passed away ten years ago. I learnt much from him in my life, not only knowledge in polymer science, but also the kind personality. My thanks are also given to my dear wife, Mrs Jing Wang, my mother, my mother in law and my lovely son, little Mingke, for their love, care and support through all these years.

CONTENT

| | Page |
|---|------|
| SUMMARY | 1 |
| ACKNOWLEDGEMENTS | 2 |
| CONTENT | 3 |
| LIST OF TABLES | 9 |
| LIST OF FIGURES | 13 |
| LIST OF SCHEMES | 27 |
| LIST OF ABBREVIATIONS | 29 |
| CHAPTER 1. INTRODUCTION | 31 |
| 1.1. Metallocene Catalysed Polyolefins and Linear Low Density Polyethylene (m-LLDPE) | 31 |
| 1.1.1. Synthesis of Polyolefins Using Metallocene-based Catalysts | 31 |
| 1.1.2. Structural Differences Between Metallocene and Ziegler-based LLDPE Polymers | 37 |
| 1.1.3. Properties of Metallocene and Ziegler-based LLDPE | 40 |
| 1.1.4. Characterisation Techniques for Molecular Structure of m-LLDPE | 42 |
| 1.1.5. Commercial Development of m-LLDPE | 45 |
| 1.1.6. Applications and New Markets of m-LLDPE | 47 |

| | |
|---|--------|
| 1.2. Polymer Oxidative Degradation | 49 |
| 1.2.1. General Oxidation Mechanisms of Hydrocarbon Polymers | 49 |
| 1.2.2. Thermal Oxidation of Polyethylene During Melt Processing | 58 |
| 1.3. Antioxidant and Stabilisation of Polyolefins | 67 |
| 1.3.1. Stabilisation Mechanisms of the Major Antioxidant Classes | 67 |
| 1.3.2. Stabilisation Systems Generally Used in Hydrocarbon Polymers | 70 |
| 1.3.3. Stabilisation of Polyethylene During Melt Processing | 76 |
| 1.4. Aims and Objectives of Present Work | 78 |
| CHAPTER 2. EXPERIMENTAL TECHNIQUES AND METHODOLOGIES | 80 |
| 2.1. Materials | 80 |
| 2.2. Polymer Processing and Sample Preparation | 81 |
| 2.2.1. Processing Using an Internal Mixer (Torque Rheometer) | 81 |
| 2.2.2. Processing Using Twin-Screw Extruder (TSE) | 82 |
| (a) Twin-screw Extrusion of “Virgin” LLDPE (with no added antioxidants) | 84 |
| (b) Twin-screw Extrusion of LLDPE in the Presence of Antioxidants (AO) | 84 |
| 2.2.3. Preparation of Polymer Films and Plaques by Compression Moulding | 86 |
| 2.2.3.1. Preparation of Polymer Films for FTIR Analysis | 86 |
| 2.2.3.2. Preparation of Polymer Plaques for Colour Analysis | 87 |
| 2.3. Polymer Characterisation | 87 |
| 2.3.1. Rheological Measurements | 88 |

| | |
|--|---------|
| 2.3.1.1. Melt Index (MI) and High Load Melt Index (HMI) | 88 |
| 2.3.1.2. Rheological Properties Measured Using a Capillary Rheometer | 90 |
| 2.3.2. Characterisation of the Molecular Structure of LLDPE | 93 |
| 2.3.2.1. Fourier Transform Infrared Spectroscopy (FTIR) | 93 |
| (a) Determination of Unsaturated Group Concentrations | 93 |
| (b) Determination of Concentrations of Carbonyl Containing Compounds | 94 |
| 2.3.2.2. ¹³ C-NMR Spectroscopy for Quantification of the Level of Branching ... | 95 |
| 2.3.3. Determination of Antioxidant Concentration in LLDPE | 97 |
| 2.3.3.1. Calibration of Standard Antioxidant Solutions | 98 |
| 2.3.3.2. Determination of Antioxidant Concentration in Polymers | 99 |
| 2.3.4. Spectrophotometry for Colour Measurements of Polymer Plaques | 100 |
| CHAPTER 3. THERMAL OXIDATION OF LLDPE DURING PROCESSING USING AN INTERNAL MIXER (TORQUE RHEOMETER, TR) | 130 |
| 3.1. Objectives and Methodology | 130 |
| 3.2. Results | 132 |
| 3.2.1. Effects of TR Processing on Characteristics of the Polymer Melt | 132 |
| 3.2.1.1. Effects of Processing on the Changes in Torque | 132 |
| 3.2.1.2. Effects of Processing on Melt Flow Properties | 133 |
| 3.2.2. Effects of TR Processing on Structural Characteristics of LLDPE | 133 |
| 3.2.2.1. Effects of Processing on the Type and Extent of Unsaturation | 133 |
| 3.2.2.2. Effects of Processing on the Concentration of Carbonyl Compounds ... | 134 |
| 3.3. Discussion | 135 |

| | |
|---|-----|
| CHAPTER 4. THERMAL OXIDATION OF LLDPE DURING PROCESSING USING A TWIN-SCREW EXTRUDER (TSE) | 153 |
| 4.1. Objectives and Methodology | 153 |
| 4.2. Results | 155 |
| 4.2.1. Extrusion Parameters of Processed LLDPE Polymers | 155 |
| 4.2.2. Rheological Characteristics of Extruded LLDPE Polymers | 156 |
| 4.2.2.1. Effects of TSE Processing on Melt Flow Behaviour Measured from Melt Flow Index | 156 |
| 4.2.2.2. Effects of Melt Processing on Rheological Properties Measured Using a Twin-Bore Capillary Rheometer | 158 |
| 4.2.3. Structural Characteristics of Extruded LLDPE Polymers | 162 |
| 4.2.3.1. Effects of Extrusion on the Extent and Nature of Unsaturation Determined by FTIR | 163 |
| 4.2.3.2. Effects of Extrusion on the Type and Level of Carbonyl Containing Compounds Determined by FTIR | 164 |
| 4.2.3.3. Effects of Extrusion on the Extent of Branching Determined by ^{13}C -NMR | 167 |
| 4.2.4. Effects of Extrusion on Discoloration (Yellowing) of the TSE Processed Polymers | 167 |
| 4.3. Discussion | 168 |
| 4.3.1. Melt Stabilities of LLDPE Polymers during TSE Extrusion | 169 |
| 4.3.2. Changes in Micro-structure of m-LLDPE with Lower SCB Content | 173 |
| 4.3.3. Changes in Micro-structure of m-LLDPE with Higher SCB Content | 182 |
| 4.3.4. Changes in Micro-structure of z-LLDPE | 188 |

| | |
|---|-----|
| 4.3.5. Relationship between the Concentration of Carbonyl Compounds and Unsaturated Groups in TSE Extruded LLDPE Polymers | 193 |
| 4.4. Overview of the Oxidative Degradation of LLDPE Polymers in Melt Processing .. | 193 |
| 4.4.1. Comparison of the Oxidative Degradation of LLDPE Polymers Processed by TR and TSE | 193 |
| 4.4.2. Comparison of the Oxidative Degradation of Different LLDPE Polymers Processed by TSE | 197 |
| CHAPTER 5. EFFECTS OF DIFFERENT CLASSES OF ANTIOXIDANTS ON THE STABILISATION OF EXTRUDED LLDPE | |
| 5.1. Objectives and Methodology | 241 |
| 5.2. Results | 245 |
| 5.2.1. Extrusion Characteristics of Stabilised LLDPE | 245 |
| 5.2.1.1. Extrusion Characteristics of LLDPE Containing Single Antioxidants ... | 245 |
| 5.2.1.2. Extrusion Characteristics of LLDPE Containing Antioxidant Mixtures.. | 246 |
| 5.2.2. Effects of Single Antioxidants on the Extent of LLDPE Stabilisation | 247 |
| 5.2.2.1. Effects on the Melt Stability | 247 |
| 5.2.2.2. Effects on the degree of Unsaturation | 248 |
| 5.2.2.3. Effects on the Level of Carbonyl Containing Compounds | 250 |
| 5.2.2.4. Effects on the Extent of Branching | 251 |
| 5.2.2.5. Effects on the Discoloration of Extruded Polymers | 252 |
| 5.2.3. Synergistic and Antagonistic Effects of Antioxidant Mixtures on Stabilisation of Extruded LLDPE | 252 |
| 5.2.3.1. Effects on the Melt Stability | 252 |
| 5.2.3.2. Effects on the Degree of Unsaturation | 254 |

| | |
|--|-----|
| 5.2.3.3. Effects on the Level of Carbonyl Containing Compounds | 255 |
| 5.2.3.4. Effects on the Discoloration | 256 |
| 5.3. Discussion..... | 257 |
| 5.3.1. Stabilisation Mechanisms of LLDPE Polymers in the Presence of Different Antioxidants Used Singly | 257 |
| 5.3.1.1. Effects of Antioxidants on the Melt Stability of LLDPE Polymers | 257 |
| 5.3.1.2. Effects of Antioxidants on Structural Changes in LLDPE Polymers | 262 |
| 5.3.1.3. Effects of Antioxidants on the Discoloration of LLDPE Polymers | 268 |
| 5.3.2. Melt Stabilisation Mechanisms of Antioxidant Mixtures in LLDPE | 270 |
| CHAPTER 6. CONCLUSIONS AND SUGGESTIONS FOR FURTHER WORK | 339 |
| 6.1. Conclusions | 339 |
| 6.2. Suggestions for Further Work | 345 |
| REFERENCES | 347 |
| APPENDIX | 358 |

LIST OF TABLES

| | Page |
|---|------|
| Table 1.1. Summary of Different Analytical Tools Used for Structural Characterisation of LLDPE | 45 |
| Table 2.1. Characteristics of LLDPE Used in This Study (as specified by the manufacturer, Dow Chemical Company) | 102 |
| Table 2.2. Characteristics of Unprocessed LLDPE (as received) (measured in Aston's PPP Labs) | 102 |
| Table 2.3. Details of Antioxidants Used in this Work | 103 |
| Table 2.4. Details of Chemicals Used in this Work | 105 |
| Table 2.5. Different Temperature Profiles Used for the Twin-Screw Extrusions of LLDPE (Profiles of T_2 ~ T_5 were used respectively for all five extrusion passes for each polymer) | 105 |
| Table 2.6. A Typical Example Showing the Characteristics of TSE Extrusion for LLDPE Polymers | 106 |
| Table 2.7. Twin-Screw Extrusion of LLDPE with Antioxidants (100rpm) | 107 |
| Table 2.8. Deviation in MI and HMI Measurements Determined from Replicate Measurements of Representative Polymer Samples | 108 |
| Table 2.9. Deviation of MI and HMI Measurements Determined from Repeat Processing of Representative Polymer Samples under the Same Conditions | 109 |
| Table 2.10. IR-Extinction Coefficients of Double Bonds and Some Carbonyl Containing Compounds | 110 |
| Table 2.11. Deviation of the Double Bond Concentrations Determined from the Measurements of Different Samples Taken out from the Same Processed Polymer | 111 |
| Table 2.12. Deviation of the Double Bond Concentrations Determined from the Samples of Repeat Processing of Representative Polymer Samples Under the Same Conditions | 112 |

| | | |
|-------------|---|-----|
| Table 2.13. | Deviation of the Carbonyl Concentration Determined from Different Samples of the Same Processed Polymer and from Repeat Processing of a Representative Polymers under the Same Conditions | 113 |
| Table 2.14. | Deviation of the Branching Amount Determination Derived from Repeat Integration of the Same Sample and from Different Samples of the Same Representative Polymers | 114 |
| Table 2.15. | Deviation of the Yellow Index Determined from Different Samples and Replicate Processing for the Representative Polymers | 115 |
| Table 3.1. | MI, HMI and MFR of TR Processed LLDPE Polymers | 145 |
| Table 3.2. | Relative Concentrations (from IR absorption area indices) of Unsaturated and Carbonyl Groups Contained in Virgin and TR Processed LLDPE Polymers | 145 |
| Table 4.1. | TSE Parameters Used for Processing LLDPE (screw speed fixed at 100rpm) | 200 |
| Table 4.2. | Branching Amount of TSE Processed Unstabilised LLDPE (P1) Measured by ^{13}C -NMR | 201 |
| Table 4.3. | Branching Amount of TSE Processed Unstabilised LLDPE (265°C) Measured by ^{13}C -NMR | 201 |
| Table 4.4. | Yellow Index (YI) of TSE Processed LLDPE (unstabilised) | 201 |
| Table 5.1. | TSE Extrusion of LLDPE Samples Containing Single Antioxidants | 242 |
| Table 5.2. | TSE Extrusion of LLDPE Containing Antioxidant Mixture (265°C, 100rpm, 4.8kg/hr) | 243 |
| Table 5.3. | Comparison of the Target and Actual AO Concentrations in m-LLDPE Measured in P ₀ Processed PL-1840 (Determined from IR Spectroscopy and Calibration Curves, see Section 2.3.3 in Chapter 2 and v in the table) | 243 |
| Table 5.4. | TSE Extrusion Characteristics of P ₀ for LLDPE Compounded with Single and Combined Antioxidants | 280 |
| Table 5.5. | TSE Extrusion Characteristics of P ₁ ~P ₅ for Stabilised LLDPE Containing Single Antioxidants | 281 |
| Table 5.6. | TSE Extrusion Characteristics of P ₁ ~P ₅ for Stabilised LLDPE Containing AO Mixtures | 282 |

| | | |
|-------------|---|-----|
| Table 5.7. | SCB Content (weight %) in TSE Processed LLDPE (265°C, 100rpm) Containing Different Single Antioxidants (Measured by ¹³ C-NMR) | 283 |
| Table 5.8. | Yellow Index (YI) and Its Changes (YI-YI ₀) of TSE Extruded LLDPE Containing Single Antioxidant Measured by Spectrophotometry | 283 |
| Table 5.9. | Yellow Index (YI) and Its Changes (YI-YI ₀) of TSE Extruded LLDPE Containing Antioxidant Mixtures (Measured by Spectrophotometry) | 284 |
| Table A3.1 | Branching Amount (from ¹³ C-NMR) and Relative Concentrations of Double Bonds (from IR absorption area index) Contained in Virgin LLDPE (measured in Aston) | 372 |
| Table A4.1. | MI, HMI and MFR of TSE Processed LLDPE Polymers | 374 |
| Table A4.2. | Double Bond Concentration (from IR extinction coefficient) of TSE Processed FM-1570 | 375 |
| Table A4.3. | Double Bond Concentration (from IR extinction coefficient) of TSE Processed PL-1840 | 375 |
| Table A4.4. | Double Bond Concentration (from IR extinction coefficient) of TSE Processed PL-1880 | 376 |
| Table A4.5. | Double Bond Concentration (from IR extinction coefficient) of TSE Processed VP-8770 | 376 |
| Table A4.6. | Double Bond Concentration (from IR extinction coefficient) of TSE Processed Dowlex2045E | 377 |
| Table A4.7. | Content of Carbonyl Groups (from IR extinction coefficient) Contained in TSE Processed LLDPE | 377 |
| Table A5.1. | MI and Its Change of TSE Processed LLDPE Containing Single Stabiliser (265°C, 100rpm, 4.8kg/hr) | 378 |
| Table A5.2. | MFR and Its Change of TSE Processed LLDPE Containing Single Stabiliser (265°C, 100rpm, 4.8kg/hr) | 379 |
| Table A5.3. | Concentrations of Double Bonds and Carbonyl Compounds in Extruded LLDPE Containing Irg1076 (Calculation Based on IR Extinction Coefficients) | 380 |

| | | |
|--------------|--|-----|
| Table A5.4. | Concentrations of Double Bonds and Carbonyl Compounds in Extruded LLDPE Containing HP136 (Calculation Based on IR Extinction Coefficients) | 380 |
| Table A5.5. | Concentrations of Double Bonds and Carbonyl Compounds in Extruded LLDPE Containing Ultrinox626 (Calculation Based on IR Extinction Coefficients) | 381 |
| Table A5.6. | Concentrations of Double Bonds and Carbonyl Compounds in Extruded LLDPE Containing IrganoxE201 (Calculation Based on IR Extinction Coefficients) | 381 |
| Table A5.7. | MI and Its Change of TSE Processed LLDPE Containing Antioxidant Mixtures (265°C, 100rpm, 4.8kg/hr) | 382 |
| Table A5.8. | MFR and Its Change of TSE Processed LLDPE Containing Antioxidant Mixture (265°C, 100rpm, 4.8kg/hr) | 383 |
| Table A5.9. | Trans-vinylene Concentration in TSE Extruded LLDPE Containing Antioxidant Mixture (Measured by FTIR) | 384 |
| Table A5.10. | Vinyl Concentration in TSE Extruded LLDPE Containing Antioxidant Mixture (Measured by FTIR) | 384 |
| Table A5.11. | Vinylidene Concentration in TSE Extruded LLDPE Containing Antioxidant Mixture (Measured by FTIR) | 385 |
| Table A5.12. | Carbonyl Concentration in TSE Extruded LLDPE Containing Antioxidant Mixture (Measured by FTIR) | 385 |

LIST OF FIGURES

| | Page |
|---|------|
| Figure 1.1. The Evolution of Metallocene Olefin Polymerisation Catalysts | 32 |
| Figure 1.2. Typical Unit Structure of MAO Cocatalysts among Different Oligomers | 33 |
| Figure 1.3. Cossee-Arlman Mechanism of Metallocene-Based Olefin Polymerisation | 34 |
| Figure 1.4. Solution Polymerisation Process of Metallocene-Catalysed Linear Low Density Polyethylene | 37 |
| Figure 1.5. Molecular Structure of Ethylene/1-Octene LLDPE | 38 |
| Figure 1.6. SCB and MWD; Schematic Representation of Molecular Structure of Metallocene and Ziegler-Natta Catalysed LLDPE | 39 |
| Figure 1.7. Schematic Illustration of Relation between Oxidation Rate and Hydroperoxide Accumulation during Polymer Oxidation | 55 |
| Figure 1.8. Representation of Unsaturated Impurities in Polyethylene | 61 |
| Figure 1.9. Schematic Representation of Changes in Melt Flow Index of Processed PE under Different Temperatures Reflecting Cross-linking (decrease in MI) and Chain Scission (increase in MI) | 66 |
| Figure 2.1. FTIR Spectrum of Virgin Dowlex2045-E (z-LLDPE) | 116 |
| Figure 2.2. FTIR Spectrum of Virgin VP-8770 (m-LLDPE) | 116 |
| Figure 2.3. The Screw Configurations of the Co-rotating Screw in the BETOL 30mm Twin-Screw Extruder | 117 |
| Figure 2.4. Twin-Screw Extruder Line and Arrangements Shown for P ₀ Compounding and Multi-pass Extrusion | 118 |
| Figure 2.5. Schematic Diagram of the Davenport Melt Flow Indexer | 119 |
| Figure 2.6. Schematic Diagram of the Rosand RH2000 Twin-Bore Capillary Rheometer | 120 |
| Figure 2.7. Outline of the Material Degradation Test of Virgin LLDPE Polymers Using the Rosand Twin-Bore Capillary Rheometer | 121 |

| | | |
|--------------|---|-----|
| Figure 2.8. | FTIR Spectrum of Virgin Dowlex2045-E (z-LLDPE) at the Region of Unsaturation | 122 |
| Figure 2.9. | FTIR Spectrum of Virgin VP-8770 (m-LLDPE) at the Region of Unsaturation | 122 |
| Figure 2.10. | FTIR Spectrum of Virgin Dowlex2045-E (z-LLDPE) at Carbonyl Region | 123 |
| Figure 2.11. | FTIR Spectrum of Virgin VP-8770 (m-LLDPE) at Carbonyl Region | 123 |
| Figure 2.12. | Schematic Diagram of Sample Preparation for ^{13}C -NMR Analysis | 124 |
| Figure 2.13. | ^{13}C -NMR Spectrum of Virgin EG8150 (m-LLDPE) | 125 |
| Figure 3.1. | Torque Changes of LLDPE Polymers during TR Processing | 146 |
| Figure 3.2. | Percentage MI Change of TR Processed LLDPE Polymers | 147 |
| Figure 3.3. | Percentage HMI Change of TR Processed LLDPE Polymers | 147 |
| Figure 3.4. | Percentage MFR Change of TR Processed LLDPE Polymers | 148 |
| Figure 3.5. | t-Vinylene Relative Concentration Change of TR Processed LLDPE Polymers | 148 |
| Figure 3.6. | Vinyl Relative Concentration Change of TR Processed LLDPE Polymers | 149 |
| Figure 3.7. | Vinylidene Relative Concentration Change of TR Processed LLDPE Polymers | 149 |
| Figure 3.8. | Percentage Changes of Relative Carbonyl Concentrations in TR Processed LLDPE Polymers | 150 |
| Figure 3.9. | FTIR Spectra in the Carbonyl Region of TR Processed FM-1570 (60rpm, 10min) | 150 |
| Figure 3.10. | FTIR Spectra in the Carbonyl Region of TR Processed PL-1840 (60rpm, 10min) | 151 |
| Figure 3.11. | FTIR Spectra in the Carbonyl Region of TR Processed VP-8770 (60rpm, 10min) | 151 |

| | | |
|--------------|--|-----|
| Figure 3.12. | FTIR Spectra in the Carbonyl Region of TR Processed EG8150 (60rpm, 10min) | 152 |
| Figure 3.13. | FTIR Spectra in the Carbonyl Region of TR Processed Dowlex2045-E (60rpm, 10min) | 152 |
| Figure 4.1. | Change of Temperature Difference (between melt and die) with Die Temperature for LLDPE during Extrusion of Pass1 | 202 |
| Figure 4.2. | Change of Die Pressure with Die Temperature for LLDPE during Extrusion of Pass1 | 202 |
| Figure 4.3. | a: Change of Feeding Rate with Die Temperature for LLDPE during Extrusion of Pass1; b: Changes of Feeding Rate and Die Pressure with the Density of Virgin m-LLDPE Polymers (210°C, Pass1) | 202 |
| Figure 4.4. | Changes in Melt Flow Index (MI) for Different LLDPE Polymers during Multiple Extrusions at Different Temperatures | 203 |
| Figure 4.5. | Changes in Melt Flow Index (MI) of Different LLDPE Polymers during Multiple Extrusions Each Compared at the Different Processing Temperatures | 204 |
| Figure 4.6. | Changes in Melt Flow Rate (MFR) for Different LLDPE Polymers during Multiple Extrusions at Different Temperatures | 205 |
| Figure 4.7. | Changes in Melt Flow Rate (MFR) of Different LLDPE Polymers during Multiple Extrusions Each Compared at the Different Processing Temperatures | 206 |
| Figure 4.8. | Changes in Melt Flow Index (MI) with Temperature for Different LLDPE Polymers after TSE Extrusion of Different Passes | 207 |
| Figure 4.9. | Changes in High Load Melt Flow Index (HMI) with Temperature for Different LLDPE Polymers after TSE Extrusion of Different Passes | 208 |
| Figure 4.10. | Changes in Melt Flow Rate (MFR) with Temperature for Different LLDPE Polymers after TSE Extrusion of Different Passes | 209 |
| Figure 4.11. | Rheological Behaviours of Different Virgin LLDPE Polymers Measured by a Rosand Capillary Rheometer at Different Temperatures | 210 |
| Figure 4.12. | Comparison of Rheological Behaviours of Different Virgin LLDPE Polymers Tested by a Rosand Capillary Rheometer at 210°C and 265°C | 211 |

| | | |
|--------------|--|-----|
| Figure 4.13. | Rheological Behaviours of Different Virgin LLDPE Polymers Measured by a Rosand Capillary Rheometer, Each Polymer Compared at the Different Temperatures | 212 |
| Figure 4.14. | Comparison of Rheological Behaviours of Different Virgin LLDPE Polymers Tested by a Rosand Capillary Rheometer at Different Temperatures | 213 |
| Figure 4.15. | Shear Viscosity Changes with Shear Rate for Different Extruded LLDPE Polymers (under the conditions of 265°C, 100rpm) Measured by a Capillary Rheometer at 265°C | 214 |
| Figure 4.16. | Shear Viscosity Changes with Shear Rate for Individual Extruded LLDPE Polymers (under the conditions of 265°C, 100rpm) Tested by a Rosand Capillary Rheometer at 265°C. The Rheological Properties of the Corresponding Virgin Polymers (as received not extruded) Tested in the Rheometer at 265°C (same testing conditions) Are also Shown | 215 |
| Figure 4.17. | Shear Stress Changes with Shear Rate for Different Extruded LLDPE Polymers (under the conditions of 265°C, 100rpm) Measured by a Capillary Rheometer at 265°C | 216 |
| Figure 4.18. | Shear Stress Changes with Shear Rate for Individual Extruded LLDPE Polymers (under the conditions of 265°C, 100rpm) Tested by a Rosand Capillary Rheometer at 265°C. The Rheological Properties of the Corresponding Virgin Polymers (as received not extruded) Tested in the Rheometer at 265°C (same testing conditions) Are also Shown | 217 |
| Figure 4.19. | Changes of Shear Stress (compared with virgin polymers) at Fixed Shear Rate Values for Different Extruded LLDPE Polymers (under the conditions of 265°C, 100rpm) Measured by a Rosand Capillary Rheometer at 265°C | 218 |
| Figure 4.20. | Extensional Viscosity versus Extensional Stress for Individual Virgin LLDPE Polymers Tested by a Rosand Capillary Rheometer at Different Temperatures | 219 |
| Figure 4.21. | Extensional Viscosity versus Extensional Stress for Different Virgin LLDPE Polymers Measured by a Rosand Capillary Rheometer at Different Temperatures | 220 |
| Figure 4.22. | Extensional Viscosity versus Extensional Stress for Extruded LLDPE Polymers (265°C, Pass3) Measured by a Rosand Capillary Rheometer at 265°C | 220 |

| | | |
|--------------|--|-----|
| Figure 4.23. | Shear Stress versus Time for Material Degradation Test of Different Virgin LLDPE Polymers Carried out in a Capillary Rheometer at 265°C | 220 |
| Figure 4.24. | Concentrations of Double Bonds in Different Virgin LLDPE Polymers Measured by FTIR Based on Corresponding IR Extinction Coefficients | 221 |
| Figure 4.25. | trans-Vinylene Concentration with Temperature Curves for Extruded LLDPE Polymers after Different Extrusion Passes | 222 |
| Figure 4.26. | Percentage Changes of trans-Vinylene Concentration (compared to corresponding virgin polymers) with Temperature for Extruded LLDPE Polymers after Different Extrusion Passes | 222 |
| Figure 4.27. | Vinyl Concentration with Temperature Curves for Extruded LLDPE Polymers after Different Extrusion Passes | 223 |
| Figure 4.28. | Percentage Changes of Vinyl Concentration with Temperature for Extruded LLDPE Polymers after Different Extrusion Passes | 223 |
| Figure 4.29. | Vinylidene Concentration with Temperature Curves for Extruded LLDPE Polymers after Different Extrusion Passes | 224 |
| Figure 4.30. | Percentage Changes of Vinylidene Concentration with Temperature for Extruded LLDPE Polymers after Different Extrusion Passes | 224 |
| Figure 4.31. | Total Double Bond Concentration with Temperature Curves for Extruded LLDPE Polymers after Different Extrusion Passes | 225 |
| Figure 4.32. | Percentage Changes of Total Double Bond Concentration (with respect to virgin polymers) with Temperature for Extruded LLDPE Polymers after Different Extrusion Passes | 225 |
| Figure 4.33. | Carbonyl Group Concentration with Temperature Curves for Extruded LLDPE Polymers after Different Extrusion Passes | 226 |
| Figure 4.34. | Percentage Changes of Carbonyl Group Concentration with Temperature for Extruded LLDPE Polymers after Different Extrusion Passes | 226 |
| Figure 4.35. | FTIR Spectra at Carbonyl Region for FM-1570 Extruded at Different Temperatures for Different Passes | 227 |
| Figure 4.36. | FTIR Spectra at Carbonyl Region for FM-1570 after Different Extrusion Passes at Different Temperatures | 228 |

| | | |
|--------------|---|-----|
| Figure 4.37. | FTIR Spectra at Carbonyl Region for VP-8770 Extruded at Different Temperatures for Different Passes | 229 |
| Figure 4.38. | FTIR Spectra at Carbonyl Region for VP-8770 after Different Extrusion Passes at Different Temperatures | 230 |
| Figure 4.39. | FTIR Spectra at Carbonyl Region for Dowlex2045-E Extruded at Different Temperatures for Different Passes | 231 |
| Figure 4.40. | FTIR Spectra at Carbonyl Region for Dowlex2045-E after Different Extrusion Passes at Different Temperatures | 232 |
| Figure 4.41. | Percentage Change of SCB Amount (with respect to virgin polymer) with Extrusion Temperature for Different LLDPE Polymers after One Pass Extrusion (P1), from ^{13}C -NMR Measurement | 233 |
| Figure 4.42. | Percentage Change of SCB Amount with Extrusion Passes for Different LLDPE Polymers Extruded at 265°C, from ^{13}C -NMR Measurement | 233 |
| Figure 4.43. | Variation of Yellow Index (YI) with Temperature for Extruded LLDPE Polymers after Different Extrusion Passes | 234 |
| Figure 4.44. | Yellow Index Changes (YI-YI ₀ , with respect to virgin polymer) for Extruded LLDPE Polymers after Different Extrusion Passes | 234 |
| Figure 4.45. | Relationship between the Concentrations of Carbonyl and Different Double Bonds (based on FTIR) for LLDPE Polymers Extruded under Different Conditions | 235 |
| Figure 4.46. | Absolute Amount of Vinyl Group Consumed in Different LLDPE Polymers during TSE Extrusions | 236 |
| Figure 4.47. | Comparison of the Percentage Changes of Double Bonds and Carbonyl Concentrations in FM-1570 Polymer after TSE Extrusions at Different Temperatures | 237 |
| Figure 4.48. | Comparison of the Percentage Changes of Double Bonds and Carbonyl Concentrations in PL-1840 Polymer after TSE Extrusions at Different Temperatures | 238 |
| Figure 4.49. | Comparison of the Percentage Changes of Double Bonds and Carbonyl Concentrations in VP-8770 Polymer after TSE Extrusions at Different Temperatures | 239 |

| | | |
|--------------|---|-----|
| Figure 4.50. | Comparison of the Percentage Changes of Double Bonds and Carbonyl Concentrations in Dowlex2045-E Polymer after TSE Extrusions at Different Temperatures | 240 |
| Figure 5.1. | Power Consumption of TSE Extrusion for LLDPE Stabilised with Single Antioxidants (210°C, 100rpm, 4.0kg/hr for P ₀ , 265°C, 100rpm, 4.8kg/hr for P ₁ ~P ₅) | 285 |
| Figure 5.2. | Die Pressure of TSE Extrusion for LLDPE Stabilised with Single Antioxidants (210°C, 100rpm, 4.0kg/hr for P ₀ , 265°C, 100rpm, 4.8kg/hr for P ₁ ~P ₅) | 286 |
| Figure 5.3. | Power Consumption of TSE Extrusion for PL-1840 Stabilised with Antioxidant Mixtures (210°C, 100rpm, 4.0kg/hr for P ₀ , 265°C, 100rpm, 4.8kg/hr for P ₁ ~P ₅) | 287 |
| Figure 5.4. | Power Consumption of TSE Extrusion for LLDPE Stabilised with Commercial Antioxidants (210°C, 100rpm, 4.0kg/hr for P ₀ , 265°C, 100rpm, 4.8kg/hr for P ₁ ~P ₅) | 288 |
| Figure 5.5. | Die Pressure of TSE Extrusion for LLDPE Stabilised with Commercial Antioxidants (210°C, 100rpm, 4.0kg/hr for P ₀ , 265°C, 100rpm, 4.8kg/hr for P ₁ ~P ₅) | 288 |
| Figure 5.6. | Die Pressure of TSE Extrusion for PL-1840 Stabilised by Antioxidant Mixtures (210°C, 100rpm, 4.0kg/hr for P ₀ , 265°C, 100rpm, 4.8kg/hr for P ₁ ~P ₅) | 289 |
| Figure 5.7. | Percentage MI Change with Passes for Different TSE Processed LLDPE Polymers Containing Single Antioxidants (265°C, 100rpm) | 290 |
| Figure 5.8. | Percentage MI Change with Passes for Each of the Extruded LLDPE Polymers Containing Different Single Antioxidants (265°C, 100rpm) | 291 |
| Figure 5.9. | Percentage MFR Change with Passes for Different TSE Processed LLDPE Polymers Containing Single Antioxidants (265°C, 100rpm) | 292 |
| Figure 5.10. | Percentage MFR Change with Passes for Each of the Extruded LLDPE Polymers Containing Different Single Antioxidants (265°C, 100rpm) | 293 |
| Figure 5.11. | Percentage Concentration Change of Unsaturated Groups and Carbonyl Compounds in Unstabilised LLDPE Polymers Extruded at 265°C | 294 |

| | |
|---|-----|
| Figure 5.12. Concentration of Trans-vinylene as a Function of Extrusion Passes for TSE Processed LLDPE Polymers Containing Single Antioxidants (265°C, 100rpm) | 295 |
| Figure 5.13(a). Percentage Concentration Change of Trans-vinylene with Extrusion Passes for Individual LLDPE Polymers Containing Different Single Antioxidants Extruded under the Condition of 265°C, 100rpm | 296 |
| Figure 5.13(b). Percentage Concentration Change of Trans-vinylene with Extrusion Passes for Different LLDPE Polymers Containing Single Antioxidants Extruded under the Condition of 265°C, 100rpm | 297 |
| Figure 5.14. Concentration of Vinyl as a Function of Extrusion Passes for TSE Processed LLDPE Polymers Containing Single Antioxidants (265°C, 100rpm) | 298 |
| Figure 5.15(a). Percentage Concentration Change of Vinyl with Extrusion Passes for Individual LLDPE Polymers Containing Different Single Antioxidants Extruded under the Condition of 265°C, 100rpm | 299 |
| Figure 5.15(b). Percentage Concentration Change of Vinyl with Extrusion Passes for Different LLDPE Polymers Containing Single Antioxidants Extruded under the Condition of 265°C, 100rpm | 300 |
| Figure 5.16. Concentration of Vinylidene as a Function of Extrusion Passes for TSE Processed LLDPE Polymers Containing Single Antioxidants (265°C, 100rpm) | 301 |
| Figure 5.17(a). Percentage Concentration Change of Vinylidene with Extrusion Passes for Individual LLDPE Polymers Containing Different Single Antioxidants Extruded under the Condition of 265°C, 100rpm | 302 |
| Figure 5.17(b). Percentage Concentration Change of Vinylidene with Extrusion Passes for Different LLDPE Polymers Containing Single Antioxidants Extruded under the Condition of 265°C, 100rpm | 303 |
| Figure 5.18. Concentration of Carbonyl Compounds (determined by FTIR in carbonyl region of 1680~1780 cm ⁻¹) as a Function of Extrusion Passes for Different TSE Processed LLDPE Polymers Containing Single Antioxidants (265°C, 100rpm) | 304 |
| Figure 5.19(a). Percentage Concentration Change of Carbonyl Groups with Extrusion Passes for Individual LLDPE Polymers Containing Different Single Antioxidants Extruded under the Condition of 265°C, 100rpm | 305 |

| | |
|---|-----|
| Figure 5.19(b). Percentage Concentration Change of Carbonyl Groups with Extrusion Passes for Different LLDPE Polymers Containing Single Antioxidants Extruded under the Condition of 265°C, 100rpm | 306 |
| Figure 5.20. FTIR Spectra in Carbonyl Region for TSE Processed (265°C, 100rpm) LLDPE Polymers Containing Irganox1076 (1772 cm ⁻¹ γ-Lactone, 1739 cm ⁻¹ Ester, 1718 cm ⁻¹ Ketone, 1699~1701 cm ⁻¹ Carboxylic acid, 1684~1685 cm ⁻¹ Unsaturated ketone) | 307 |
| Figure 5.21. FTIR Spectra in Carbonyl Region for TSE Processed (265°C, 100rpm) LLDPE Polymers Containing IrganoxE201 (1772 cm ⁻¹ γ-Lactone, 1739~1741 cm ⁻¹ Ester, 1730 cm ⁻¹ Aldehyde, 1718 cm ⁻¹ Ketone, 1701 cm ⁻¹ Carboxylic acid, 1684 cm ⁻¹ Unsaturated ketone) | 308 |
| Figure 5.22. FTIR Spectra in Carbonyl Region for TSE Processed (265°C, 100rpm) LLDPE Polymers Containing IrganoxHP136 (1772 cm ⁻¹ γ-Lactone, 1739~1741 cm ⁻¹ Ester, 1730 cm ⁻¹ Aldehyde, 1718 cm ⁻¹ Ketone, 1701 cm ⁻¹ Carboxylic acid, 1684~1685 cm ⁻¹ Unsaturated ketone) | 309 |
| Figure 5.23. FTIR Spectra in Carbonyl Region for TSE Processed (265°C, 100rpm) LLDPE Polymers Containing Ultrinox626 (1768~1772 cm ⁻¹ γ-Lactone, 1739~1741 cm ⁻¹ Ester, 1730 cm ⁻¹ Aldehyde, 1714~1718 cm ⁻¹ Ketone, 1697~1701 cm ⁻¹ Carboxylic acid, 1684~1685 cm ⁻¹ Unsaturated ketone) | 310 |
| Figure 5.24. Yellow Index Change (YI-YI ₀) for TSE Processed LLDPE Polymers Containing Single Antioxidants (265°C, 100rpm) | 311 |
| Figure 5.25. Percentage MI Change with Extrusion Passes for TSE Processed PL-1840 Containing Different Antioxidant Mixtures (265°C, 100rpm, see Table 5.2 for AO composition) | 312 |
| Figure 5.26. Percentage MI Change with Extrusion Passes for TSE Processed PL-1840 Containing Irg1076 and Different Phosphite Antioxidants (265°C, 100rpm, see Table 5.2 for AO composition) | 313 |
| Figure 5.27. Percentage MI Change with Extrusion Passes for TSE Processed PL-1840 Containing Irg1076, HP136 and Different Phosphite Antioxidants (265°C, 100rpm, see Table 5.2 for AO composition) | 313 |
| Figure 5.28. Percentage MFR Change with Extrusion Passes for TSE Processed PL-1840 Containing Different Antioxidant Mixtures (265°C, 100rpm) | 314 |

| | | |
|-----------------|--|-----|
| Figure 5.29. | Percentage MI Change with Extrusion Passes for TSE Processed LLDPE Containing Commercial Antioxidant Mixtures (265°C, 100rpm, IrgXP490 – Irg1076: IrgP-EPQ: HP136 = 3:2:1, IrgHP2921 – Irg1076: Irg168: HP136= 2:4:1) | 315 |
| Figure 5.30. | Percentage MFR Change with Extrusion Passes for TSE Processed LLDPE Containing Commercial Antioxidant Mixtures (265°C, 100rpm, IrgXP490 – Irg1076: IrgP-EPQ: HP136 = 3:2:1, IrgHP2921 – Irg1076: Irg168: HP136= 2:4:1) | 315 |
| Figure 5.31. | Percentage MI Change with Extrusion Passes for Extruded LLDPE Containing Different Commercial Antioxidant Mixtures (265°C, 100rpm) | 316 |
| Figure 5.32. | Changes in Trans-vinylene Concentration with Extrusion Passes for TSE Processed PL-1840 Containing Different Antioxidant Mixtures (265°C, 100rpm) | 317 |
| Figure 5.33. | Percentage Concentration Change of Trans-vinylene with Extrusion Passes for TSE Processed PL-1840 Containing Different Antioxidant Mixtures (265°C, 100rpm) | 318 |
| Figure 5.34. | Changes in Vinyl Concentration with Extrusion Passes for TSE Processed PL-1840 Containing Different Antioxidant Mixtures (265°C, 100rpm) | 319 |
| Figure 5.35. | Percentage Concentration Change of Vinyl Group with Extrusion Passes for TSE Processed PL-1840 Containing Different Antioxidant Mixtures (265°C, 100rpm) | 320 |
| Figure 5.36. | Changes in Vinylidene Concentration with Extrusion Passes for TSE Processed PL-1840 Containing Different Antioxidant Mixtures (265°C, 100rpm) | 321 |
| Figure 5.37. | Percentage Concentration Change of Vinylidene Group with Extrusion Passes for TSE Processed PL-1840 Containing Different Antioxidant Mixtures (265°C, 100rpm) | 322 |
| Figure 5.38(a). | Changes of Unsaturated Group Concentrations with Extrusion Passes for TSE Processed PL-1840 Containing Different Antioxidant Mixtures (265°C, 100rpm) | 323 |
| Figure 5.38(b). | Percentage Concentration Change of Unsaturated Groups with Extrusion Passes for TSE Processed PL-1840 Containing Different Antioxidant Mixtures (265°C, 100rpm) | 324 |

| | | |
|--------------|---|-----|
| Figure 5.39. | Double Bond Concentration Change with Extrusion Passes for TSE Processed LLDPE Polymers Containing Commercial Antioxidant Mixtures (265°C, 100rpm) | 326 |
| Figure 5.40. | Percentage Change of Double Bond Concentrations with Extrusion Passes for TSE Processed LLDPE Polymers Containing Commercial Antioxidant Mixtures (265°C, 100rpm) | 327 |
| Figure 5.41. | The Changes of Unsaturated Concentrations with Extrusion Passes for TSE Processed LLDPE Polymers Containing Different Commercial Antioxidant Mixtures (265°C, 100rpm) | 328 |
| Figure 5.42. | Changes in Carbonyl Concentration with Extrusion Passes for TSE Processed PL-1840 Containing Different Antioxidant Mixtures (265°C, 100rpm) | 329 |
| Figure 5.43. | Percentage Concentration Change of Carbonyl Group with Extrusion Passes for TSE Processed PL-1840 Containing Different Antioxidant Mixtures (265°C, 100rpm) | 330 |
| Figure 5.44. | Changes of Carbonyl Concentrations with Extrusion Passes for TSE Processed PL-1840 Containing Irg1076 and Different Phosphite Antioxidants (265°C, 100rpm, see Table 5.2 for AO composition) | 331 |
| Figure 5.45. | Changes of Carbonyl Concentrations with Extrusion Passes for TSE Processed PL-1840 Containing Irg1076, HP136 and Different Phosphite Antioxidants (265°C, 100rpm, see Table 5.2 for AO composition) | 331 |
| Figure 5.46. | Carbonyl Concentration Change with Extrusion Passes for TSE Processed LLDPE Polymers Containing Commercial Antioxidant Mixtures (265°C, 100rpm, IrgXP490 – Irg1076: IrgP-EPQ: HP136 = 3:2:1, IrgHP2921 – Irg1076: Irg168: HP136= 2:4:1) | 332 |
| Figure 5.47. | Percentage Concentration Change of Carbonyl Group with Extrusion Passes for TSE Processed LLDPE Polymers Containing Commercial Antioxidant Mixtures (265°C, 100rpm,) | 332 |
| Figure 5.48. | The Changes of Carbonyl Concentrations with Extrusion Passes for TSE Processed LLDPE Polymers Containing Different Commercial Antioxidant Mixtures (265°C, 100rpm) | 332 |
| Figure 5.49. | Yellow Index Change (YI-YI ₀) with Extrusion Passes for TSE Processed PL-1840 Containing Different Antioxidant Mixtures (265°C, 100rpm) | 333 |

| | | |
|--------------|--|-----|
| Figure 5.50. | Yellow Index Change (YI-YI ₀) with Extrusion Passes for TSE Processed PL-1840 Containing Irg1076 and Different Phosphite Antioxidants (265°C, 100rpm) | 334 |
| Figure 5.51. | Yellow Index Change (YI-YI ₀) with Extrusion Passes for TSE Processed PL-1840 Containing Irg1076, HP136 and Different Phosphite Antioxidants (265°C, 100rpm) | 334 |
| Figure 5.52. | Yellow Index Change (YI-YI ₀) with Extrusion Passes for Different Extruded LLDPE Polymers Containing Commercial Antioxidant Mixtures (265°C, 100rpm, IrgXP490 – Irg1076: IrgP-EPQ: HP136 = 3:2:1, IrgHP2921 – Irg1076: Irg168: HP136= 2:4:1) | 335 |
| Figure 5.53. | Yellow Index Change (YI-YI ₀) with Extrusion Passes for TSE Processed LLDPE Polymers Containing Different Commercial Antioxidant Mixtures (265°C, 100rpm, IrgXP490 – Irg1076: IrgP-EPQ: HP136 = 3:2:1, IrgHP2921 – Irg1076: Irg168: HP136 = 2:4:1) | 335 |
| Figure 5.54. | FTIR Spectra in Carbonyl Region for TSE Processed (265°C, 100rpm) PL-1840 Containing Irganox1076 and Other Antioxidants (1772cm ⁻¹ γ-Lactone, 1739~1740 cm ⁻¹ Ester, 1730 cm ⁻¹ Aldehyde, 1718 cm ⁻¹ Ketone, 1701 cm ⁻¹ Carboxylic acid, 1685 cm ⁻¹ Unsaturated ketone) | 336 |
| Figure 5.55. | FTIR Spectra in Carbonyl Region for TSE Processed (265°C, 100rpm) PL-1840 Containing IrganoxE201 and Other Antioxidants (1772 cm ⁻¹ γ-Lactone, 1739~1740 cm ⁻¹ Ester, 1730 cm ⁻¹ Aldehyde, 1718 cm ⁻¹ Ketone, 1701 cm ⁻¹ Carboxylic acid, 1685 cm ⁻¹ Unsaturated ketone) | 337 |
| Figure 5.56. | FTIR Spectra in Carbonyl Region for TSE Processed (265°C, 100rpm) LLDPE Polymers Containing IrganoxXP490 (1772 cm ⁻¹ γ-Lactone, 1739~1741 cm ⁻¹ Ester, 1730 cm ⁻¹ Aldehyde, 1718 cm ⁻¹ Ketone, 1701 cm ⁻¹ Carboxylic acid, 1685 cm ⁻¹ Unsaturated ketone) | 338 |
| Figure A2.1. | FTIR Spectrum of Irganox 1076 and the Expansion at 2000~900 cm ⁻¹ (KBR windows) | 359 |
| Figure A2.2. | UV Spectrum of Irganox 1076 in Hexane | 359 |
| Figure A2.3. | FTIR Spectrum of Irganox HP136 and the Expansion at 2000~900 cm ⁻¹ (KBR windows) | 360 |
| Figure A2.4. | UV Spectrum of Irganox HP136 in Hexane | 360 |

| | |
|--|-----|
| Figure A2.5. FTIR Spectrum of Irganox E201 and the Expansion at 2000~900 cm ⁻¹ (KBr windows) | 361 |
| Figure A2.6. UV Spectrum of Irganox E201 in Hexane | 361 |
| Figure A2.7. FTIR Spectrum of Weston 399 and the Expansion at 2000~900 cm ⁻¹ (KBr windows) | 362 |
| Figure A2.8. UV Spectrum of Weston 399 in Hexane | 362 |
| Figure A2.9. FTIR Spectrum of Ultrinox 626 and the Expansion at 2000~900 cm ⁻¹ (KBr windows) | 363 |
| Figure A2.10. UV Spectrum of Ultrinox 626 in Hexane | 363 |
| Figure A2.11. FTIR Spectrum of Irgafos 168 and the Expansion at 2000~900 cm ⁻¹ (mixture with Nujol) | 364 |
| Figure A2.12. UV Spectrum of Irgafos 168 in Hexane | 364 |
| Figure A2.13. FTIR Spectrum of Irgafos P-EPQ and the Expansion at 2000~900 cm ⁻¹ (KBr windows) | 365 |
| Figure A2.14. UV Spectrum of Irgafos P-EPQ in Hexane | 365 |
| Figure A2.15. FTIR Spectra of Irganox1076 Standard Solutions (DCM) (the Numbers are ppm concentration of each solution) | 366 |
| Figure A2.16. FTIR Spectrum of TSE Processed PL-1840, P ₀ (Irg1076: Irg168 = 500:1250 ppm) | 366 |
| Figure A2.17. FTIR Spectra of Irgafos168 Standard Solutions (DCM) (the Numbers are ppm concentration of each solution) | 367 |
| Figure A2.18. FTIR Spectrum of TSE Processed PL-1840, P ₀ (Irg1076: Irg168: HP168 = 500:1250:250 ppm) | 367 |
| Figure A2.19. FTIR Spectra of Irgafos P-EPQ Standard Solutions (DCM) (the Numbers are ppm concentration of each solution) | 368 |
| Figure A2.20. FTIR Spectrum of TSE Processed PL-1840, P ₀ (Irg1076: IrgP-EPQ = 500: 1000 ppm) | 368 |
| Figure A2.21. FTIR Spectra of Irganox HP136 Standard Solutions (DCM) (the Numbers are ppm concentration of each solution) | 369 |

| | |
|---|-----|
| Figure A2.22. FTIR Spectrum of TSE Processed PL-1840, P ₀ (Irg1076: IrgP-EPQ: HP136 = 500:1000:250 ppm) | 369 |
| Figure A2.23. Calibration Curve of Irganox 1076 | 370 |
| Figure A2.24. Calibration Curve of Irganox HP136 | 370 |
| Figure A2.25. Calibration Curve of Irgafos 168 | 371 |
| Figure A2.26. Calibration Curve of Irgafos P-EPQ | 371 |
| Figure A3.1. FTIR Spectrums of TR Processed PL-1840 (60rpm, 10min) at the Region of Unsaturated Groups | 372 |
| Figure A3.2. FTIR Spectrums of TR Processed EG8150 (60rpm, 10min) at the Region of Unsaturated Groups | 373 |
| Figure A3.3. FTIR Spectrums of TR Processed Dowlex2045-E (60rpm, 10min) at the Region of Unsaturated Groups | 373 |
| Figure A5.1. Concentration Changes of Double Bonds with Passes for Extruded FM-1570 Containing Different Single Antioxidants (265°C, 100rpm, Pass0 of unstabilised polymer represents the virgin sample) | 386 |
| Figure A5.2. Concentration Changes of Double Bonds with Passes for Extruded PL-1840 Containing Different Single Antioxidants (265°C, 100rpm, Pass0 of unstabilised polymer represents the virgin sample) | 387 |
| Figure A5.3. Concentration Changes of Double Bonds with Passes for Extruded VP-8770 Containing Different Single Antioxidants (265°C, 100rpm, Pass0 of unstabilised polymer represents the virgin sample) | 388 |
| Figure A5.4. Concentration Changes of Double Bonds with Passes for Extruded Dowlex2045E Containing Different Single Antioxidants (265°C, 100rpm, Pass0 of unstabilised polymer represents the virgin sample, Dowlex2045E containing Irg1076 was old batch and the others were new batch polymers) | 389 |
| Figure A5.5. Carbonyl Concentration (determined by FTIR in carbonyl region of 1680~1780 cm ⁻¹) Change with Extrusion Passes for Extruded LLDPE Polymers Containing Different Single Antioxidants (265°C, 100rpm, virgin LLDPE with 0 pass represent unprocessed polymers) | 390 |

LIST OF SCHEMES

| | Page |
|---|------|
| Scheme 1.1. Elementary Steps of Radical Reactions Included in Polymer Oxidation | 50 |
| Scheme 1.2. Transition State of Hydrogen Abstraction in Hydrocarbon Oxidation | 52 |
| Scheme 1.3. Major Decomposition of Hydroperoxide in Polymer Oxidation | 56 |
| Scheme 1.4. Supplementary General Steps for Polyethylene Thermal Oxidation | 59 |
| Scheme 1.5. Reactions Leading to Molecular Enlargement and Chain Scission of Polyethylene | 60 |
| Scheme 1.6. Oxidative Reactions of Polyethylene Main Chains | 61 |
| Scheme 1.7. Reactions Involving Vinyl and trans-Vinylene in PE Oxidation | 62 |
| Scheme 1.8. Basic Radical Reactions Involved in PE Thermo-oxidation | 64 |
| Scheme 1.9. Mechanisms of Antioxidant Action in Polymer Oxidation | 67 |
| Scheme 1.10. Kinetic Chain-breaking Processes | 68 |
| Scheme 1.11. Stabilisation Reactions of Hindered Phenol and Aromatic Amine | 71 |
| Scheme 1.12. Stabilisation Reaction of Quinone (CB-A) | 72 |
| Scheme 1.13. Complementary Mechanisms Involving Hydroquinones and its Oxidation Products | 73 |
| Scheme 1.14. Regeneration of Galvinoxyl Used in Polypropylene Stabilisation | 74 |
| Scheme 1.15. Stabilisation Reaction by Tris-nonyl Phenylphosphite | 74 |
| Scheme 1.16. Reaction of Dialkyl-thiodipropionates with Hydroperoxide | 75 |
| Scheme 2.1. Flow Chart of the Procedure Used to Process Polymers in Torque Rheometer | 126 |
| Scheme 2.2. Basic Operation of Twin-Screw Extruder for LLDPE Processing | 127 |

| | | |
|-------------|--|-----|
| Scheme 2.3. | The Amount of Polymers Used during a Typical 5-Multi-pass Extrusions of LLDPE at 100rpm Speed Using BETOL Twin-Screw Extruder | 128 |
| Scheme 2.4. | Flow Diagram of the General Procedure of Rheological Test Using the Rosand Twin-Bore Capillary Rheometer | 129 |
| Scheme 3.1. | Methodology Used in the Investigation of Oxidative Degradation of LLDPE Polymers During TR Processing | 131 |
| Scheme 4.1. | Methodology Used in Investigation of Unstabilised LLDPE Oxidation during Melt Extrusion | 154 |
| Scheme 5.1. | Overall Methodology Used in the Stabilisation of LLDPE Using Single and Combined Antioxidants | 244 |
| Scheme 5.2. | Co-operative Interaction between Hindered Phenol (Irganox1076) and Phosphite Ester (Irgafos168) in PL-1840 melt During TSE Extrusion | 271 |
| Scheme 5.3. | Co-operative Interaction between Lactone (IrganoxHP136) and Phosphite Ester (Irgafos168) in PL-1840 melt During TSE Extrusion | 273 |

LIST OF ABBREVIATIONS

| | |
|---------|---|
| AO | Antioxidant |
| CB-A | Chain-breaking Acceptor |
| CB-D | Chain-breaking Donor |
| DCB | 1,4-Dichlorobenzene |
| DCM | Dichloromethane |
| DETA | Dielectric Thermal Analysis |
| DMTA | Dynamic Mechanical Thermal Analysis |
| DSC | Differential Scanning Calorimetry |
| ESCA | Electron Spectroscopy for Chemical Analysis |
| FTIR | Fourier Transform Infrared Spectroscopy |
| GC | Gas Chromatography |
| GPC | Gel Permeation Chromatography |
| HDPE | High Density Polyethylene |
| HMI | High Load Melt Flow Index |
| HPLC | High Performance Liquid Chromatography |
| IR | Infrared Spectroscopy |
| LCB | Long Chain Branch |
| LDPE | Low Density Polyethylene |
| LLDPE | Linear Low Density Polyethylene |
| MAO | Methylaluminoxane |
| MD | Metal Deactivator |
| MFR | Melt Flow Rate (MI/HMI) |
| MI | Melt Flow Index |
| m-LLDPE | Metallocene-Based Linear Low Density Polyethylene |
| MS | Mass Spectroscopy |
| MW | Molecular Weight |
| MWD | Molecular Weight Distribution |
| NMR | Nuclear Magnetic Resonance |
| NOE | Nuclear Overhauser Enhancement |

| | |
|---------|---|
| PD | Hydroperoxide Decomposition |
| PD-C | Catalytic Peroxide Decomposer |
| PD-S | Stoichiometric Peroxide Decomposer |
| PE | Polyethylene |
| PP | Polypropylene |
| PPP | Polymer Processing and Performance Unit |
| PS | Polystyrene |
| PVC | Polyvinylchloride |
| SCB | Short Chain Branch |
| SCBD | Short Chain Branch Distribution |
| TA | Thermal Analysis |
| TCB | 1,2,4-Trichlorobenzene |
| TGA | Thermogravimetric Analysis |
| TMP | Trimethylolpropane ethoxylate |
| TR | Torque Rheometer |
| TREF | Temperature Rising Elution Fractionation |
| TSE | Twin-screw Extruder |
| UV | Ultraviolet Spectroscopy |
| UVA | UV Light Absorber |
| YI | Yellow Index |
| z-LLDPE | Ziegler-Natta Catalysed Linear Low Density Polyethylene |

CHAPTER 1. INTRODUCTION

1.1. METALLOCENE CATALYSED POLYOLEFINS AND LINEAR LOW DENSITY POLYETHYLENE (m-LLDPE)

1.1.1. Synthesis of Polyolefins Using Metallocene-based Catalysts

Polyolefins particularly polyethylene (PE) and polypropylene (PP) are synthetic thermoplastic polymers widely used in modern society. Polyethylene has the simplest structure among all commercial polyolefins and been classified by different densities and extent of branching [1]. Low-density polyethylene (LDPE), which is often produced by free radical vinyl polymerisation, is a branched polymer and contains both long chain (LCB) and short chain (SCB) branches. High-density polyethylene (HDPE, sometimes referred to as linear polyethylene), on the other hand, which is normally polymerised via Ziegler-Natta catalyst, is free of long branches and has fewer short branches [1, 2].

In more recent years, linear low-density polyethylene (LLDPE), a series of polyolefin polymers based on copolymers of ethylene and certain α -olefins, were synthesized and commercialised for use in a diverse range of applications. LLDPE is synthesised by copolymerising ethylene monomer with an alkyl-branched olefin comonomer such as propylene, 1-butene, 1-hexene, 1-octene. As a result, it is a copolymer with short hydrocarbon branches attached on the polymer backbone. The polymerisation process leading to synthesis of LLDPE has traditionally been achieved using Ziegler-Natta catalysts and more recently using metallocene catalysts [3, 4]. The new generation metallocene-based polyolefins will almost certainly make a significant impact on the plastics industry due to their unique and excellent properties.

Indeed, metallocene based catalyst technology is expected to revolutionize the polyolefin industry with particular impact in polyethylene and polypropylene

Metallocenes as olefin polymerisation catalysts also have a long history. As early as 1957 Natta reported the polymerization of ethylene with the titanocene catalyst Cp_2TiCl_2 and the co-catalyst triethylaluminum, a co-catalyst traditionally used in Ziegler-Natta olefin polymerisation systems. The activity of the metallocene with the Ziegler-Natta co-catalyst was very low and therefore it was only used for scientific purpose, e.g. in mechanistic studies and showed little commercial promise [6]. However, the situation changed dramatically in the mid 1970's due to an accidental discovery by W. Kaminsky (University of Hamburg) and his colleagues. While an NMR measurement was conducted in a mixture of homogenous $\text{Cp}_2\text{ZrCl}_2/\text{Al}(\text{CH}_3)_3$ and ethylene, a trace of water was accidentally introduced into the NMR tube leading to an extremely active ethylene polymerisation system; the above system was known at that time to be inactive for olefin polymerisation [4]. Subsequent studies revealed that the high activity was due to the formation of the co-catalyst methylaluminoxane (MAO), see Figure 1.2 [4], as a result of hydrolysis of the trimethyl aluminum, $\text{Al}(\text{CH}_3)_3$. It is because of the discovery of this new co-catalyst that metallocenes are now also commonly called "Kaminsky" catalysts.

Generally, metallocene catalysts consist of metallocene complexes of group 4 metals such as zirconium, hafnium or titanium and cocatalysts such as MAO or borates. Bis(cyclopentadienyl)zirconium dichloride (Cp_2ZrCl_2) in combination with MAO is the most widely used metallocene catalyst system for olefin polymerisation. The role of MAO cocatalyst is believed [4] to i) alkylate the metallocene, forming the active complex, ii) act as scavenger for impurities, iii) stabilise the cationic center via an ion-pair interaction, and iv) possibly prevent bimetallic deactivation processes from occurring.

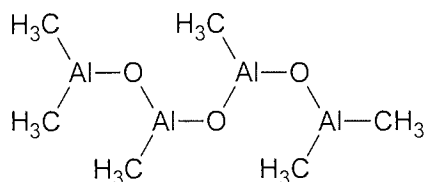


Figure 1.2. Typical Unit Structure of MAO Cocatalysts among Different Oligomers

Olefin polymerisation catalysed by metallocenes is believed to occur via the Cossee-Arlman mechanism as derived from traditional Ziegler-Natta catalysis, see Figure 1.3 [4]. A significant amount of experimental and theoretical evidence suggests that a cationic alkyl-metallocene complex is the active species in the polymerisation. The metal atom in the metallocene complex forms a **single site** active centre and enables the olefin monomer to insert into the polymer chain effectively and linearly.

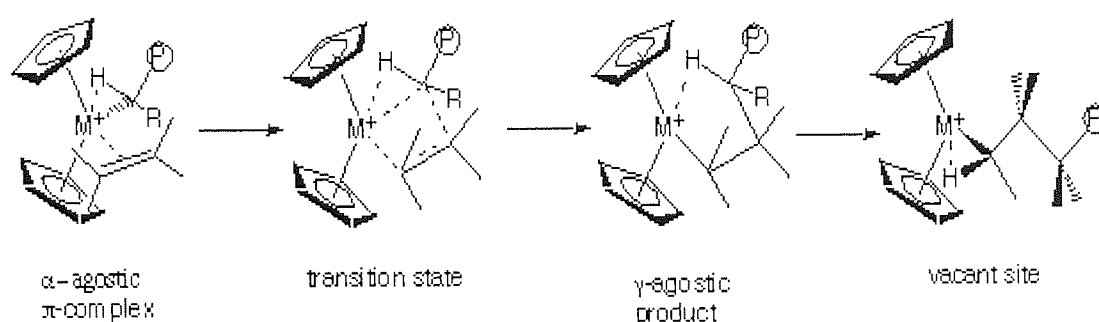


Figure 1.3. Cossee-Arlman Mechanism of Metallocene-Based Olefin Polymerisation [4]

Since Kaminsky's discovery of the high activity $\text{Cp}_2\text{ZrCl}_2/\text{MAO}$ ethylene polymerisation system, metallocene catalysts have slowly evolved as producers started to commercialise the technology [4]. The innovations have primarily been directed at solving the deficiencies associated with the early metallocene systems. The most serious shortcoming being that, in order to achieve the high activities, extremely high molar Al to transition metal ratios (Al:M) of between 1000-15000:1 were required. Such ratios are commercially unacceptable in terms of the cost and the amount of residues left in the polymer (Commercial Ziegler-Natta systems typically require Al to M ratios of between 50~200:1). A significant effort has been put into reducing the amount of MAO required and this has led to the development of many systems with non-aluminum cocatalysts, such as $[\text{B}(\text{C}_6\text{F}_5)_4]^-$ and $[\text{H}_3\text{CB}(\text{C}_6\text{F}_5)_3]^+$.

Other developments include the mono-Cp constrained geometry catalysts which have been primarily developed by Dow and Exxon [7]. These are typically titanium based and have one Cp ligand replaced by a **heteroatom** that is "**constrained**" by a **bridging group** (Nitrogen is the preferred heteroatom and silicon the most preferred bridging centre as shown in Figure 1.1). The properties of bridged and non-bridged metallocene catalysts differ markedly in α -olefin polymerisations. The non-bridged catalysts are traditionally used in the polymerisation of ethylene, whereas the bridged ones are used in propylene and longer α -olefin polymerisation. Both catalyst types have also been investigated in ethylene/ α -olefin copolymerisation [8]. Significant effort has also gone into heterogenizing the catalyst system by supporting the metallocene and cocatalyst onto an inorganic support such as silica. However, despite all the innovations Zr still remains the most common metal centre, followed by Ti and Hf. Work has also been done with Sc, Cr, and lanthanides [9, 10].

The first patent for a metallocene catalyst was filed in 1980 but it has been the last decade that have seen a dramatic increase in the volume of research into metallocenes and the maturing of metallocene technology. The high degree of control exerted by metallocene catalysts (also known as **single-site catalysts**) during the olefin polymerisation results in property advantages over the traditional Ziegler-Natta catalysts (**multi-site catalysts**). There are four main features that distinguish metallocene catalysts from the conventional Ziegler-Natta catalysts used in the polyolefin industry [11 - 14], in that the former can:

1. Polymerise almost any vinyl monomer irrespective of its molecular weight or steric hindrance.
2. Produce uniform polymers and co-polymers of narrow molecular weight distributions (MWD).
3. Control the level of vinyl unsaturation in the polymer produced.
4. Polymerise α -olefins with very high stereoregularity to give isotactic or syndiotactic polymers.

Furthermore, if metallocenes, especially zirconocenes, are combined with MAO, the resulting catalyst can polymerise olefins 10~100 times faster than those used in even the most active Ziegler-Natta systems [4, 15]. The structure of metallocene catalysts can also be varied to produce polymer with specially required properties. Thus, for the first time it is possible to tailor carefully the properties of large-volume commodity polymers. Overall, the advent of metallocene catalysts has opened the doors to a challenging new area of polymer reaction engineering, where catalyst types and reaction conditions can be carefully selected in order to produce polyolefins with controlled microstructure for advanced applications [16].

Metallocenes have been highly successful in the production of linear low-density polyethylene via the copolymerisation of ethylene with other α -olefins. Most commercially available metallocene-based LLDPEs are copolymers of ethylene-butene, ethylene-hexene and ethylene-octene [17, 18]. The metallocene catalyst can be used in a number of polymerisation processes including slurry, solution, and gas phase operations. The catalyst is usually first mixed with co-catalyst and very low levels of the catalyst mixture are then continuously metered into a reactor along with a predetermined ratio of ethylene and the comonomer of choice. The molecular weight of the polymer continues to build up with the polymerisation of ethylene and comonomer at the catalyst site until stopped by catalyst deactivation or chain termination with hydrogen introduction to the reactor (see Figure 1.4). The reactions are effected by the variation of the Al/Zr ratio, temperature and catalyst concentration [4]. These variations result in changes in structural characteristics of the copolymer such as the molecular weight (MW), molecular weight distribution (MWD) and the ethylene content. Many different metallocene aluminoxane catalysts have been thoroughly studied so far and their applications in olefin copolymerisation have been reported extensively [19, 20].

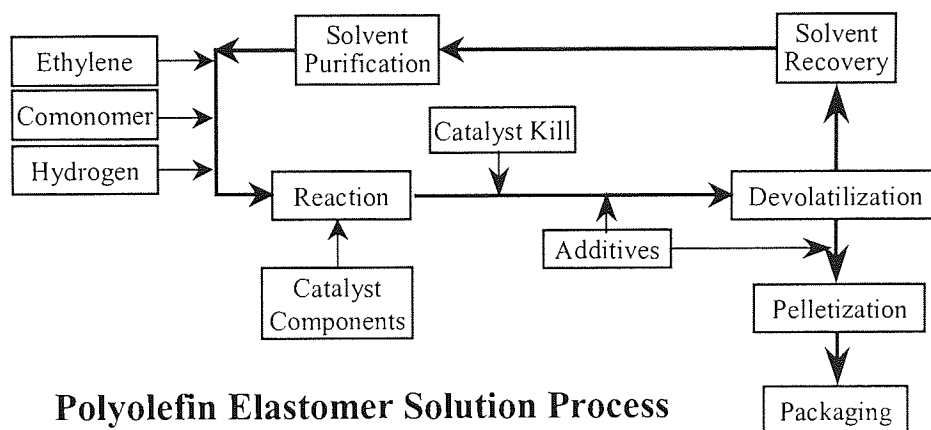


Figure 1.4. Solution Polymerisation Process of Metallocene-Catalysed Linear Low Density Polyethylene [20]

1.1.2. Structural Differences Between Metallocene and Ziegler-based LLDPE Polymers

A remarkable difference between metallocene and Ziegler-Natta catalysis technologies is based on the fact that Ziegler-Natta catalysts give rise to non-uniformity within the polymeric matrix whereas the metallocene catalysts furnish high uniformity to the polymer since it permits polymerisation at only a single site [21].

Polymerisation of olefin monomers with single-site metallocene catalysts allows the production of polyolefins with a highly defined structure and superior properties. This means that the monomers can be built up stereoregularly, with building blocks in the chain having a defined constantly repetitive configuration. In contrast, conventional Ziegler-Natta catalysts have multiple reaction sites that would make the control of polymer structure much more difficult resulting in non-uniformly structural polymers [4].

In addition to the high stereo-regularity of the molecular structure, the metallocene catalysed linear low-density polyethylene also possesses other unique structural

characteristics compared to the Ziegler type polymers. The primary parameters affecting the processing and ultimate properties of LLDPE are branching (amount and distribution), crystallinity, molecular weight (MW) and molecular weight distribution (MWD) (see Figure 1.5) [22].

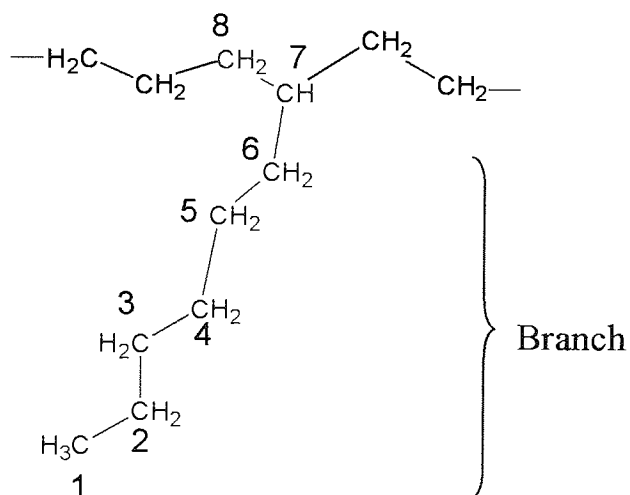


Figure 1.5. Molecular Structure of Ethylene/1-Octene LLDPE

The controlled addition of an α -olefin comonomer to ethylene during polymerisation produces a linear polymer with short chain branches (SCB). The α -olefin added during polymerisation determines the length and concentration of the SCB. It has been shown that in the case of metallocene catalysts, an α -olefin comonomer can be polymerised with ethylene at a concentration for up to 40%, whereas, for most of the Ziegler type LLDPE, the proportion of the comonomer is generally less than 10% [23]. Moreover, the homogenous nature of the metallocene catalyst provides an even distribution of SCB in LLDPE compared to non-uniform distribution of the SCB exhibited by Ziegler-Natta catalysed LLDPE (see Figure 1.6).

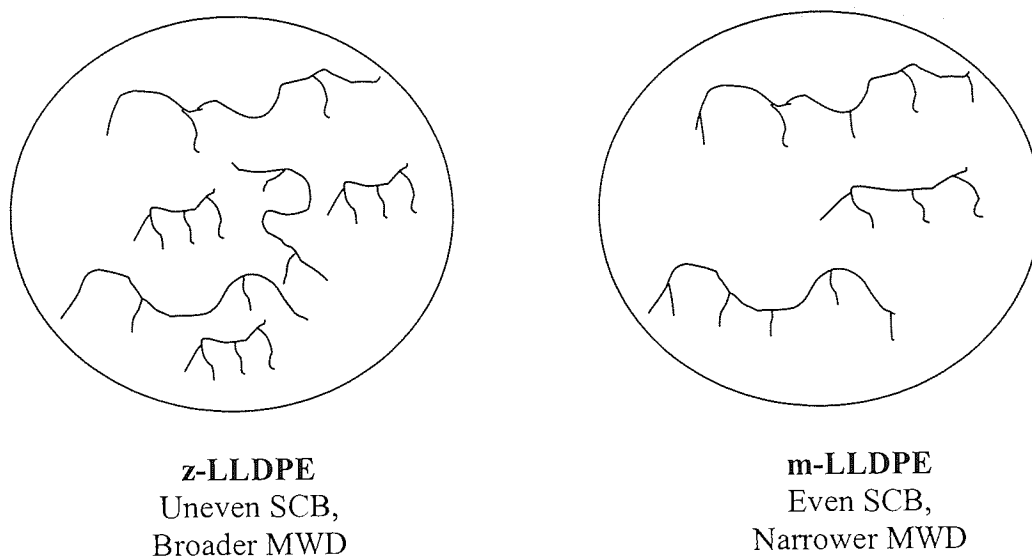


Figure 1.6. SCB and MWD; Schematic Representation of Molecular Structure of Metallocene and Ziegler-Natta Catalysed LLDPE

The crystallisation of polymers is of enormous technological importance. Most of polyolefins, e.g. LLDPE, will crystallise to some extent when the polymer is cooled below its melting point from the melt state, or concentrated in polymer solution. There are many factors that can affect crystal morphology and crystallinity for a particular polyolefin, for instance, the amount and size of the chain branches, MW and MWD as well as the conditions of the polymer crystallisation [24].

The crystal morphology of LLDPE develops from lamellae formed from the ordering of folded chains. The rate of folding is interrupted significantly by the presence of SCB, especially with high molecular weight α -olefin co-monomer (e.g. 1-hexene, 1-octene). The SCB cannot be incorporated into the main chain crystal and, is therefore, excluded from crystallising with the rest of the chain [23, 24]. For this reason, a major part of the regular chain close to the short branches cannot be incorporated into the crystal structure. This results in significant lowering of the overall crystallinity and the crystal size of the polymer. In m-LLDPE (with a narrow MWD and SCB distribution), crystallisation including nucleation and growth proceeds at a similar rate throughout the polymer (as the chains are of similar size with SCB evenly distributed along the polymer backbone). On the other hand, in the

heterogeneous z-LLDPE polymer, which has a broader MWD and co-monomer (SCB) distribution, crystallisation progresses at distinctively different rates. A larger portion of SCB are found in the lower molecular weight fraction of the Ziegler-Natta catalysed polymer, thus nucleation and crystal growth take place at a much slower rate and the crystal size is much smaller than in the higher molecular weight fraction (lower co-monomer content) of the polymer. This leads to differences in the lamella thickness and explains the broader melting points associated with z-LLDPE [25].

Polymerisation reactions lead to polymer heterogeneity in molecular weight, i.e. the polymer is a mixture of molecules of various molecular weights. The MW, therefore, is expressed as an average value of all molecular weight fractions in the polymer. The heterogeneity in MW of a polymer is termed as molecular weight distribution (MWD) or polydispersity. The MWD is defined as a ratio of weight average molecular weight to the number average molecular weight. The MW and MWD are very significant parameters in determining the end use of PE polymers. In general, copolymerisation initiated by ordinary Ziegler-Natta catalysts gives rise to z-LLDPE with a wider co-monomer distribution and broader MWD, whereas the homogeneous metallocene catalysts lead to m-LLDPE with a narrower MWD and even shorter chain branch (SCB) distribution [4, 22, 23].

1.1.3. Properties of Metallocene and Ziegler-based LLDPE

Due to the short branching from the incorporated α -olefin co-monomer (e.g. 1-butene, 1-hexene, 1-octene), the LLDPE generally shows lower melting point, lower density and lower crystallinity compared to the traditional HDPE. The molecular structure of such polymers has a significant influence on the physical and hence the ultimate performance properties of the material. Fortunately, the greatest possibility of structure control offered by metallocene catalysts during polymerisation provides opportunities to tailor polymers for specific applications [4].

Metallocene catalysed LLDPE exhibits far superior physical properties such as tensile strength, optical clarity, impact strength, crack resistance, and has also lower melting properties, compared to the conventional Ziegler-based LLDPE [14, 16]. The most important application of the LLDPE copolymers is film manufacture. The deliberate addition of an α -olefin comonomer in ethylene polymerisation makes films formed from these materials more flexible and have better processing characteristics [26, 27]. The narrow MWD and a uniform stereo-regularity exhibited by metallocene catalysed LLDPE films are distinguished in general by their high tensile strength, stiffness, gloss and barrier properties along with good optical clarity. Both tensile strength and stiffness are important properties in the conversion of films to final products. Improved stiffness offers the opportunity for down gauging, an industry demand, to reduce the cost and volume of packaging material. Improved barrier properties mean better flavour preservation and therefore longer shelf life of the final packaging goods [28, 29].

The primary characteristic of narrow MWD and SCB distribution offers m-LLDPE many other advantages such as sharper melting point, better hot tack and heat seal properties, compared to the Ziegler analogues [16]. Additionally, LLDPE with higher comonomer content is an excellent impact modifier for plastics. As LLDPE is compatible with most olefinic materials, they offer unique performance capabilities for compounded products [30, 31]. Overall, the high performance of metallocene-based LLDPE is not derived from one characteristic but from a superior group of properties.

One slight drawback, on the other hand, is the high melt viscosity of metallocene-catalysed LLDPE, which results in poor melt flow ability that above a critical (very low) shear stress gives rise to the appearance of instable flow in extrusion processes. This is the major reason for normal processing difficulties that m-LLDPE polymers experience during melt extrusion [32, 33]. The poor melt flow behaviour exhibited by m-LLDPE is related to the high degree of entanglement and uniform shear stresses incurred by the majority of m-LLDPE polymer chains (with evenly

distributed SCB along the main backbone) during extrusion. Thus, the narrow MWD and uniform SCB distribution of m-LLDPE typically result in poor melt processability, low melt strength, high-extruded backpressure and high-energy power consumption during extrusion. Whilst, the good melt flow behaviour exhibited by z-LLDPE during high temperature extrusion has been attributed to low degree of entanglement between the higher and lower molecular weight chains. The higher molecular weight chains (containing a small fraction of SCB) suffer a disproportionately high degree of shear stress, and form a 'protective' network around the lower molecular weight polymer chains. The lower molecular weight chains lubricate the flow of the higher molecular weight chains, thus enhancing the flow of polymer material during high temperature processing [34, 35].

Since a typical processing operation of polyethylene may be carried out by extrusion at a temperature range from 175°C to 300°C (depending on the type of polymer and application), the various polymer structural parameters must be considered carefully before melt processing in order to determine proper processing conditions and have a good control of the product quality. These include the type of the co-monomer used in the polymerisation, the content and distribution of chain branching, the molecular weight (MW) and molecular weight distribution (MWD). They can greatly affect the processability and product properties of the metallocene-based polyolefin [36].

1.1.4. Characterisation Techniques for Molecular Structure of m-LLDPE

Since the introduction of short chain branches (SCB) significantly affects the morphology and properties of m-LLDPE, which are largely dependent upon the nature and quantity of the co-monomer present in the chain, a combination of different analytical techniques would be required in order to examine the molecular characteristics of these polymers [37, 38, 39, 40]. Characterisation of the molecular structure has revealed that the chain microstructure depends mainly on the average weight percent of short chain branching (SCB) and its distribution (SCBD),

molecular weight, molecular weight distribution, and the amount of SCB in a given molecular weight portion [40].

^{13}C -NMR spectroscopy has been one of the primary analytical tools used for the determination of the type and amount of branching in these polymers [41]. The most important advantage of NMR method is that it is an absolute method which does not require standards and specificity, since the location of the resonance identifies the exact type of the branch. Branches shorter than six carbons in length can be unambiguously assigned from their ^{13}C -NMR spectrum. But branches longer than five carbons cannot be differentiated from long chain branches [42]. In order to obtain a precise spectrum for quantitative analysis of branching in m-LLDPE, the appropriate parameters and analytical conditions described in an internationally accepted reference, ASTM, are normally applied [43].

Infrared spectroscopy is another powerful method for the determination of the level of branching in LLDPE, it utilise the absorbance of the methyl group at 1380 cm^{-1} [44]. The main weakness of this method is that the absorbance must be corrected due to interference of the methylene groups and other bands [45]. However, comparing with ^{13}C -NMR, the IR method has some distinct advantages in precision and analysis time. Furthermore, IR spectroscopy can also be used to determine the concentrations of unsaturated bonds, carbonyl groups and hydroperoxide in the LLDPE [46]. Since the ^{13}C -NMR spectroscopy has the advantages of accuracy and specificity, and it is an absolute method for quantitative determination of branching in LLDPE if the appropriate parameters are employed, it can be utilised to define standard materials which can then be used to standardise the IR method [44, 45]. The continued interest in IR quantitative analysis has led to improvement in the methodology used [47, 48].

Molecular weight parameters and molecular weight distribution (MWD) for m-LLDPE can be measured using gel permeation chromatography (GPC) which provides data on MWD of different polymers [48]. A temperature rising elution fractionation (TREF) technique has been employed to provide data that reveals SCBD of polyolefin. In TREF, methylene contents of various fractions are measured and weight distribution as a function of temperature is taken as a measure of SCBD. Fractions with decreasing SCB contents elute at increasing temperatures. TREF is an effective method for measuring SCBD, but it is time consuming and requires special equipment [49]. Differential scanning calorimetry (DSC) is a popular, fast and useful method for investigating the crystallization process and crystalline morphology in polymers. The existence of SCB in LLDPE inhibits regular ordered packing of polymer chains. Crystallinity is reduced and polymer morphology is changed [50]. DSC may easily examine these changes. Therefore, DSC technique may be used to determine the co-monomer or SCB distributions in LLDPE especially for solution crystallized mixtures [40, 51].

Unsaturation is also a very important structural parameter in LLDPE, as it is a key factor which affects the mechanisms when the polymer undergoes oxidative degradation [52]. The contents of unsaturated groups (mainly including vinylidene, vinyl and trans-vinylene) can be exactly and quantitatively measured by ^1H -NMR analysis [53]. Unsaturation can also be quantified more easily by IR spectroscopy, on the basis of average molar extinction coefficients of model compounds such as hexenes, heptenes, octenes, and so on [54]. Table 1.1 summarizes the main techniques used for structural characterisation of LLDPE.

Table 1.1. Summary of Different Analytical Tools Used for Structural Characterisation of LLDPE

| Technique | Quantitatively Determined Characteristics | Comments | Reference |
|--|---|---|---------------------------|
| ¹³ C-NMR | 1. Type of branching 2. Amount of branching 3. Short chain branching distribution (SCBD) | Absolute method Accurate and specific Branches<6 carbons, can be assigned; Branches>5, can't be differentiated from LCB | [41] [42] [43]-ASTM |
| ¹ H-NMR | Content of different unsaturation | Time consuming | [53] |
| FTIR | 1. Amount of branching via absorbance at 1380 cm ⁻¹ 2. Content of unsaturated and carbonyl groups | Precise and fast Correction needed due to interference | [44] [45] [54]-ASTM |
| NMR-IR | 1. Amount of branching 2. Double bond quantity | Standardization of the two techniques | [44] [45] |
| GPC | MW and MWD | | [48] |
| TREF (Temperature Rising Elution Fractionation) | SCBD, Measuring methylene content and weight distribution as a function of temperature | Effective and accurate Time consuming Special equipment needed | [49] |
| DSC | 1. Crystallisation and morphology 2. SCBD | Fast and effective | [50] [40], [51] |

1.1.5. Commercial Development of m-LLDPE

There has been significant developmental activity in the past decade related to the applications of LLDPE and to the implementation of metallocene catalysts in the industrial production of LLDPE. The market for metallocene LLDPE has been growing very fast due to greatly improved properties, e.g. strength and puncture-, tear- and impact-resistance, compared to those of ordinary (e.g. z-based) resins. The two worldwide leading suppliers of metallocene LLDPE are Exxon Mobil Company and Dow Chemical Company [55, 56, 57].

Exxon Mobil Chemical Company introduced metallocene-LLDPE polymers on the market in 1991, which are based on ethylene-hexene copolymer synthesized by **gas phase polymerisation** using metallocene catalysts [58]. In 1995, the company commercialised **Exceed™**, a metallocene catalysed linear low-density polyethylene resin with more outstanding properties [59]. They took advantage of the company's patented **Exxpol®** technology to produce the resin used for blown and cast film manufacture with five "grades" being available to meet various application needs. The films made from the resin are reported to withstand 50% more puncture force and offer 40% greater tensile strength than conventional z-LLDPE [59]. Clarity, gloss, lower extractable, improved sealing and good organoleptics for food packaging are additional merits claimed by Exxon Chemical Company. Metallocene catalysed ethylene copolymers, which were positioned between traditional LLDPE plastics and elastomers also became first commercially available from Exxon (**Exact™**). They were generally referred to as Plastomers, as they possessed many of the characteristics of both plastics and elastomers. These novel materials offer improved strength and toughness, enhanced optical and sealing properties, increased elasticity and cling performance. They are widely used in stretched film, wire and cable coating, packaging, flooring and medical applications [59].

LLDPE with longer branches (copolymer of ethylene and 1-octene) were initially manufactured by Dow Chemical Company through **solution polymerisation** in 1993 using the metallocene catalyst technology referred to as “**constrained geometry**” single site catalyst (**In-site® Technology**). Fourteen grades of plastics (**AFFINITY®**) and seven grades of elastomers (**ENGAGE®**) have been developed since 1994 [59]. It is reported that these flexible metallocene polyolefin can replace currently used plasticised PVC in many applications without requiring the addition of environmentally damaging phthalate plasticisers. These metallocene catalysed LLDPE may also be used as substitute of poly(ethylene-co-propylene) rubber (EPDM) and poly(vinyl acetate) (PVAc). In 1996, Dow Chemical Company

successfully commercialised new metallocene-based LLDPE so-called “semi-crystalline PE with tie chain” and “narrow compositional distribution PE” using “In-site®” technology [59]. These novel polyolefin resins not only maintain the excellent properties of metallocene type LLDPE, but also have a greatly improved processability [23, 60].

In recent years, the big companies in this field have collaborated and succeeded in developing and commercialising new metallocene catalysts and provided significant advanced metallocene-based LLDPE resins. Both Dow and Exxon-Mobil entered into joint efforts with the leading gas technology firms (BP and Carbide, respectively) to develop and commercialise metallocene catalysts for use in gas reactors. Some of the world's most widely licensed metallocene LLDPE polymerisation technologies such as “Unipol®”, “Innovene®”, were developed by Dow/BP and Exxon/Carbide joint development programs [59].

1.1.6. Applications and New Markets of m-LLDPE

Applications of the m-LLDPE copolymers include packaging, shrink films with low steam permeation, elastic films, which incorporate a high comonomer concentration, cable coatings, in the medical field due to the low content of extractable materials, foams, elastic fibres, adhesives. Therefore, this new generation of metallocene-based olefin copolymers has a great industrial potential and has opened up brand-new markets and opportunities [4].

Metallocene catalysed ethylene copolymers may be used in a variety of end applications. Many of them are consumer oriented, such as highly flexible and tenacious films, one of the top-tier end use markets [27, 28]. Metallocene-based LLDPE films can be produced, bi-axially oriented or non-oriented. Bi-axially oriented films, with their high clarity, moisture-barrier (low water vapour

transmission rate) and high stiffness, are widely used in tape and food packaging. Non-oriented films are used in the packaging of textile products, stationary products and food packaging [61]. Other segments of the bi-axially oriented film market where metallocene catalysed LLDPE shows potential are shrink and heat-sealing film. In the shrink film market, improved shrinkage performance, low heat sealing temperature and good hot tack properties accompanied by balanced bi-axially oriented physical properties are desired. Whilst, in the heat sealing film market, easy seal-ability and high hot tack strength are desired [62]. Overall, film applications seek to maximise the exceptional mechanical, optical and heat-sealing attributes of m-LLDPE. Film manufacturers have incorporated this unique set of properties into a variety of film making applications.

Some of the key attributes of metallocene catalysed LLDPE plastomers, which make them of interest as alternatives to plasticised polyvinylchloride (PVC) are clarity (especially in thick sections), softness, low modulus, flexibility, superior low temperature toughness, and a low level of extractable (no extractable plasticisers). This culmination of properties have made LLDPE plastomers ideal for medical applications e.g. intravenous tubes, caps (made *via* injection moulding), fittings and connectors to large articles such as face-masks [62, 63]. For many of these applications, clarity is essential. Plastomers with densities below about 0.95g/cm^3 are usually clear enough even in thick sections to meet the requirements for the product [62].

It is estimated that about 13 million metric tons of LLDPE were consumed worldwide in 2001. About 80% of commercial LLDPE goes into films for packaging, bags and other applications. Other important uses for the polymer are, in descending order of consumption, injection molded parts, rotationally molded parts, and wire and cable. Among them, metallocene LLDPE consumption exceeded one million metric tons in 2001, an increase of more than 10% from the year before [64].

1.2. POLYMER OXIDATIVE DEGRADATION

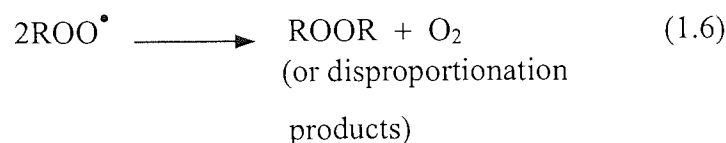
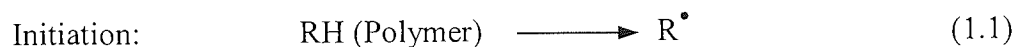
1.2.1. General Oxidation Mechanisms of Hydrocarbon Polymers

Like all other organic compounds, oxidative degradation of hydrocarbon polymers can be initiated by atmospheric oxygen. The degradation reactions are ubiquitous so that they can occur at any stage of macromolecule's lifetime [65, 66, 67]. During processing, heat, oxygen and mechanical stress are the main factors that contribute to polymer degradation; and during the useful life of the materials oxygen and sunlight are the most important degradative agents. In some specialised applications, degradation may be induced by high energy radiation, ozone, atmospheric pollutants, biological action, hydrolysis and many other influences [68, 69, 70]. The mechanisms of these reactions must be understood if the properties of polymer products are to continue to be improved.

Degrading polymer molecules undergo a series of reactions whose effects can be side-group reactions or crosslinking which lead to structural modification [71]. In most cases, however, bond scissions will take place on the polymer main chains, yielding radical species that may initiate chain processes where depolymerization, intra- and intermolecular radical transfers, and termination reactions are in competition, leading to the formation of monomeric molecules, oligomers, chain fragments, and new compounds, while average molecular weights and molecular weight distributions change continuously [72, 73]. To understand the way polymer molecules degrade the effects of such reactions must be carefully analysed.

Evidence from former investigation has indicated that the mechanism of oxidative degradation of hydrocarbon polymer is free radical chain reaction. Depending on the type of polymer and even the catalyst used to produce it, the polymer may undergo many different radical reactions. Polymer oxidation is a complex chain reaction, which includes several simple (elementary) steps, i.e. initiation, propagation, and termination. The main (simplified) reaction steps involved in the

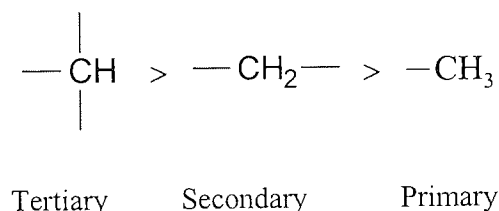
oxidation of hydrocarbon polymers are illustrated in Scheme 1.1 (RH represents a polymer chain) [74]:



Scheme 1.1. Elementary Steps of Radical Reactions Included in Polymer Oxidation

In the initiation step a hydrogen atom is removed from a polymer molecule leaving a macroalkyl radical (R^\bullet). Commercial polymers usually contain either traces of hydroperoxides or other sensitising groups which activate hydrogen on adjacent carbon atoms.

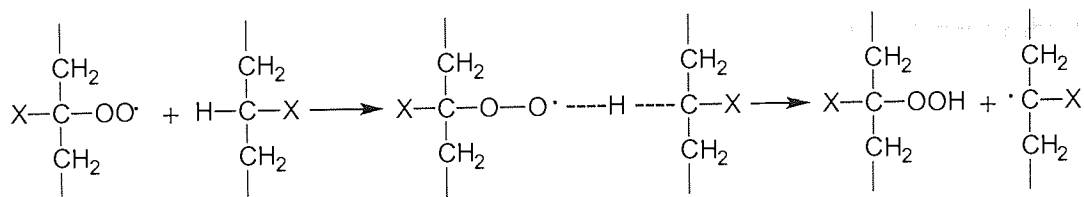
Once initiation has started and few radicals are formed in the polymer, propagation would then follow in a series of reactions. The first of these is a rapid reaction of R^\bullet with oxygen to form a peroxy radical (ROO^\bullet). This is then followed by abstraction of a H from the same or another polymer molecule by the ROO^\bullet radical (rate determining step) [75]. There is also a wide variation in the ease of removal of hydrogen from different hydrocarbon polymer structures [66], with the relative ease of removal following the order shown below:



The reaction will stop in time by the process of “autotermination”. The structure of the autoxidising hydrocarbon and the oxygen concentration determine which of the termination steps (Reactions 1.4 to 1.6) leads to the removal of radicals from an oxidising substrate. Since alkylperoxyl radicals are the dominant radical species present during polymer oxidation, termination occurs primarily through Reaction 1.6. If, however, oxygen access is limited by diffusion, for example during melt processing of polymers, Reactions 1.4 and 1.5 may play a more important role [74].

The continuing search for new polymeric materials with enhanced stability has created much interest in the relationships between stability (or degradability) and polymer structure and a great deal is now known about the structural features necessary for optimum stability.

Polymers vary widely in their vulnerability to deterioration when exposed to the same environment. These variations in stability are caused primarily by differences in chemical structure [65, 66]. For example, it is quite clear that aromatic and ladder structures built into the main chain of polymers are especially desirable in their resistance to oxidative degradation. In the hydrogen abstraction reaction of polymer oxidation, a transition state exists and the carbon atom to which the labile hydrogen is attached may assume a partial electron delocalisation, a partial ionic charge or a combination of both depending on the nature of X group (see Scheme 1.2) [65]:



Scheme 1.2. Transition State of Hydrogen Abstraction in Hydrocarbon Oxidation

In hydrocarbon polymers, the rate of oxidation is primarily affected by the electron delocalisation of the attached group. In polymers containing hetero-atoms (e.g. PVC), polarity normally predominates in the hydrogen abstraction reaction.

Minor structural impurity in both natural and synthetic polymers is another very important factor that determines their oxidative stability. Impurities that promote degradation can be foreign materials, such as residues from polymerisation catalysts, or they can be an integral part of polymer molecules, such as unsaturated groups and branching points [76]. For example, low-density polyethylene (LDPE) contains considerably more chain branching than high-density polyethylene (HDPE). Furthermore, both polymers contain unsaturation which markedly increase the oxidative ability of adjacent methylenic groups. Polypropylene is much more susceptible to oxidation compared to high-density polyethylene, with oxidation stability of low-density polyethylene lying between the two [72].

Polymer degradation depends on the chemical effects, physical structure, and polymer morphology [77]. The effects of physical structure are related to the arrangement of molecules in ordered (crystalline) and disordered (amorphous) regions of the polymer matrix. Many polymers are semi-crystalline and thus have both ordered and disordered regions.

Amorphous polymers oxidise homogeneously and uniformly throughout the bulk of the polymeric matrix. In general, polymers above their glass transition temperature oxidise more rapidly than those in the glassy state due to the faster rate of diffusion

of oxygen in the former. Therefore, the factors influencing reactant permeability have an important effect on polymer degradation. Permeability of reactants (e.g. oxygen) into a polymer matrix is dependent on the density of the material which varies with the degree of crystallinity and the compactness of amorphous and crystalline regions. In many polymers, the degree of crystallinity can be increased by annealing in an inert atmosphere. The density increases with annealing and permeation of reactant into the polymer is reduced [65].

Semi-crystalline polymers are essentially two-phase systems consisting of spherical clusters of crystals embedded in the amorphous continuum. Oxygen can diffuse readily through the amorphous regions of polyolefin but cannot penetrate the crystalline regions, consequently most of the oxidation damage occurs at the spherulite boundaries, thus weakening the “adhesive” which holds the crystalline regions together. A consequence of this is that the same amount of oxidation creates much more damage in a highly crystalline polymer than it does in a less crystalline polymer of similar chemical structure [77].

The surface-to-volume ratio of a polymer sample is also important in determining the rate of oxidation. In samples which are too thick to permit diffusion of oxygen throughout the polymer mass, the reaction rate is limited by the concentration gradient of oxygen in the sample. The concentration of oxygen and the reaction rate are highest at the surface. When reactants cannot diffuse completely into the polymer matrix, the processes of oxidation are just limited to surface layers with little change in bulk properties [65, 77].

Many commercial polymers are relatively stable to oxidation as they are manufactured. However, in their conversion to fabricated end products they are subjected to high temperature and high shearing forces in the polymer melt (generally at temperature above 150°C and sometimes as high as 300°C). Since it is impossible to exclude molecular oxygen completely from such procedures, important chemical modification inevitably occurs at this stage in the history of the

polymer and this has a profound effect on its subsequent service performance [77]. The conversion of a thermoplastic polymer to a finished article normally involves heating it to the liquid state followed by extrusion through a die or into a mould. The polymer is mixed continuously by means of a screw which conveys it to the extrusion port. During this processing operation, considerable shear is applied to the viscous polymer melt which causes some of the polymer chains to undergo homolytic scission at the carbon-carbon bonds with the formation of macro-alkyl radicals. Additionally, macro-alkyl radicals can also be generated under the action of oxygen molecules at high temperature. Although both of these are infrequent processes, the alkyl radicals so produced are highly active chemical species which, like lower molecular weight radicals, initiate the radical chain reaction, see Scheme 1.1 Reactions 1.2 and 1.3, and generate oxygen-containing groups [65, 78].

Autoxidation proceeds by a typical free radical chain reaction mechanism and although most polymers undergo autoxidation, there is a considerable variation in their resistance to this type of deterioration. The reaction is usually autocatalytic, following a rate curve similar to that shown in Figure 1.7. Radicals that initiate autoxidation in polymers are formed by thermal energy, ultraviolet radiation, bombardment by high-energy particles, mechanical stress, metal catalysis, and the addition of initiators. When polymer bonds are ruptured under any of these conditions and oxygen is present in the environment, autoxidation can occur [66, 79, 80, 81].

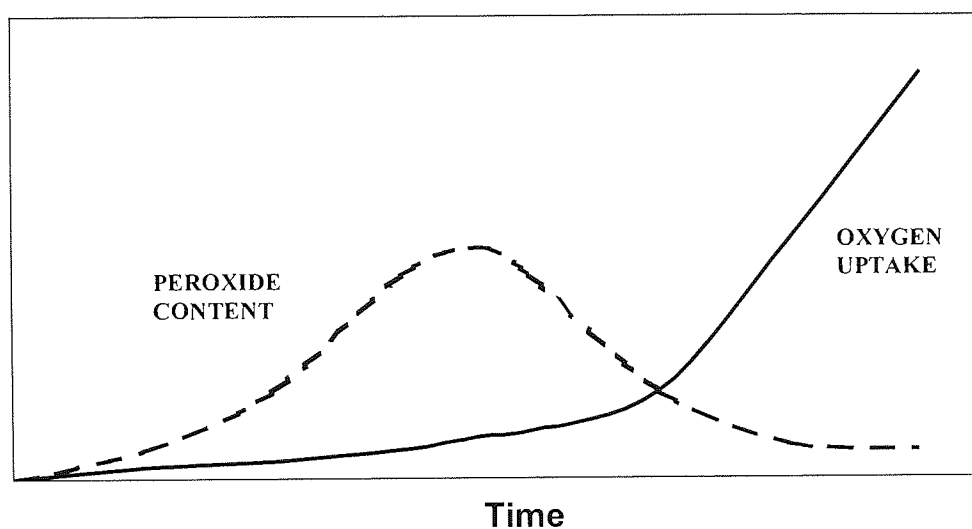


Figure 1.7. Schematic Illustration of Relation Between Oxidation Rate and Hydroperoxide Accumulation During Polymer Oxidation

Ruptures of polymer chains can also occur when polymeric materials are frequently or continually subjected to mechanical stresses during normal application. Mechanical destruction generates the mechano-radical that initiates chemical reactions in which the mechano-radicals easily react with an oxygen molecule to form peroxy radicals. In addition, the application of stress renders some unsaturated polymers vulnerable to attack by ozone. These chemical reactions originate from the physical action, are characteristics of a polymer, and result in changes of the physical nature of the polymer [79].

Since hydroperoxides were first assigned the correct structure, they were soon recognised as the most important molecular intermediate in polymer oxidation [82]. The reactions of hydroperoxide are much more complicated compared to that of alkyl peroxide radical. Alkyl hydroperoxides at low concentrations in inert solvent are quite stable and undergo monomolecular homolytic cleavage at elevated temperatures. In concentrated solutions or at high temperature bimolecular decomposition processes can occur (see Scheme 1.3) [79].



Scheme 1.3. Major Decomposition of Hydroperoxide in Polymer Oxidation

The course of hydroperoxide decomposition is not only determined by temperature and concentration, it is also influenced by the structure of the hydroperoxide. Therefore, the key to the understanding of polymer oxidation lies in the thorough study of the reactions and structures of the polymer hydroperoxides [74]. Hydroperoxide decomposition begins to occur at a rapid rate and the oxidation becomes autocatalytic, see Figure 1.7. After the decomposition of hydroperoxides, an additional series of elementary reactions will occur. As a result, the hydroperoxides cause additional changes in the oxidised polymer [75], normally:

- (1) Formation of oxidised structures in the chain
- (2) Fragmentation and crosslinking of the polymer chain
- (3) Formation of low molecular weight products

The majority of the oxidation products result from hydroperoxide decomposition processes. In addition, a considerable proportion is formed in the transformation of peroxy radicals and a smaller fraction from radical termination processes. Most of the free radicals formed from hydroperoxide decomposition undergo cage-recombination. About 80% of the end products resulting from PE-hydroperoxides and 90% of those from PP-hydroperoxides are formed in cage processes, whereas, a smaller proportion, which is likely to be responsible for the broad spectrum of products, is generally formed by reactions of radicals escaping the cage and of active intermediate products formed from them [74].

The information obtained from fundamental studies of polymer oxidation can be used to explain the technologically important processes which take place during polymer processing and application. Examination of the nature of the products and kinetics of oxidation is, therefore, quite important. Different types of testing methods have been used in measurements of oxidative effects in organic substrates which lead to better understanding of the nature, kinetics and thermodynamics of the oxidation process and products formed from it. Furthermore, the role of the structure of the polymer repeat unit on the oxidation process and the changes in molar mass of polymers as function of extent of degradation can also be investigated [65, 83].

The nature of chemical compounds obtained from polymer oxidative degradation, are normally characterised using spectroscopic measurements e.g. IR, UV, electron spectroscopy for chemical analysis (ESCA), nuclear magnetic resonance (NMR), and mass spectroscopy (MS), whereas chromatographic methods are generally employed for the separation of the mixtures produced during degradation. In such a context, it is desirable to combine separation techniques with specific detectors for on-line product identification. Polymer degradation is, in fact, the process of choice for applications like gas chromatography (GC)-fourier transform infrared (FTIR), GC-MS, thermogravimetric (TG)-FTIR, and high-performance liquid chromatography (HPLC)-MS [84, 85, 86, 87, 88].

Infrared spectroscopy (IR) is a powerful technique to elucidate the mechanisms taking place during the thermal oxidative degradation of polymers. IR analyses are based on measuring absorbance, which is proportional to the thickness of the sample being analysed and the concentration of the absorbing groups. FTIR analysis is most often used to determine the oxygen content and unsaturated groups in the reacted substrates. This technique has undergone a number of refinements and is suitable for both qualitative and quantitative analyses [89].

The techniques of thermal analysis (TA) are very important to the whole field of polymers in that they provide essential information relating both to their

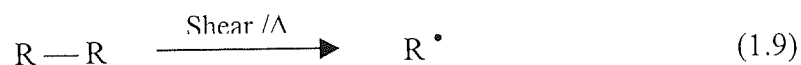
characterisation and their degradation. TA techniques are a group of techniques in which the property of a sample is monitored against time or temperature while the temperature of the sample, in a specified atmosphere, is programmed. This program may involve heating or cooling at a fixed rate of temperature change, or holding the temperature constant, or any sequence of these. Single techniques, such as thermogravimetric analysis (TGA), differential scanning calorimetry (DSC), dynamic mechanical thermal analysis (DMTA), and dielectric thermal analysis (DETA) provide important information on the thermal behaviour of materials. To obtain a more complete profile of polymer degradation, the use of a simultaneous thermal analyser (notably a TGA-DSC instrument), coupled to a mass spectrometer or to a FTIR, can provide a very powerful system for such studies [90, 91].

1.2.2. Thermal Oxidation of Polyethylene during Melt Processing

Oxidative degradation of polyolefin can be initiated by oxygen, shear, heat, catalyst residues or any combination of these factors during melt processing. The rate of degradation increases greatly due to high temperatures and high shear rates [65]. Overall, thermo-oxidative degradation results in undesirable reactions such as crosslinking, chain scission and the formation of detrimental oxygen containing functional groups (carbonyls, peroxides and unsaturation), which would ultimately lead to deterioration of the original properties of the polymers and reduction in their useful lifetime [81]. The oxidation extent depends on the type of the polymer examined, and the catalyst used to produce it. Polyethylene is one of the largest volume polyolefin yet structurally one of the simplest. The grades of polyethylene are differentiated based on the MW, MWD, density, co-monomer, SCB and SCB distribution. These variations in polyethylene composition produce wide variations in performance, including variations in susceptibility to oxidative degradation [92, 93]. Thus, understanding the oxidation mechanism of polyethylene is very important in order to develop appropriate stabilisation packages.

The thermal oxidation of polyethylene is also an autocatalytic process. In addition to the general steps shown in Scheme 1.1, other primary reactions involved in polyethylene thermal oxidation are shown in Scheme 1.4 (where RH represents the polyethylene chain) [78].

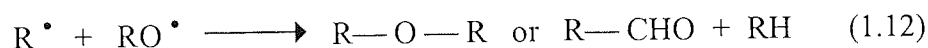
INITIATION:



PROPAGATION:



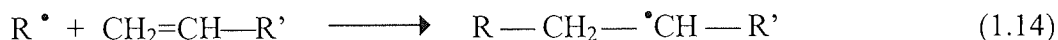
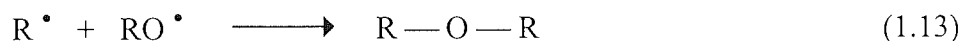
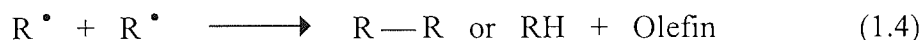
TERMINATION:



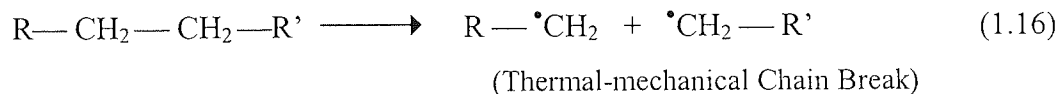
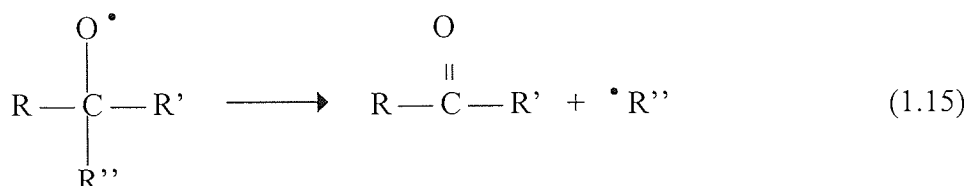
Scheme 1.4. Supplementary General Steps for Polyethylene Thermal Oxidation

Generally, chain branching and crosslinking, leading to molecular enlargement, may occur simultaneously with chain scission as competitive reactions during polyethylene processing (see Scheme 1.5). As a result, a change in molecular weight is accompanied by changes in melt viscosity, which may affect efficient processing of polyethylene [78].

MOLECULAR ENLARGEMENT:

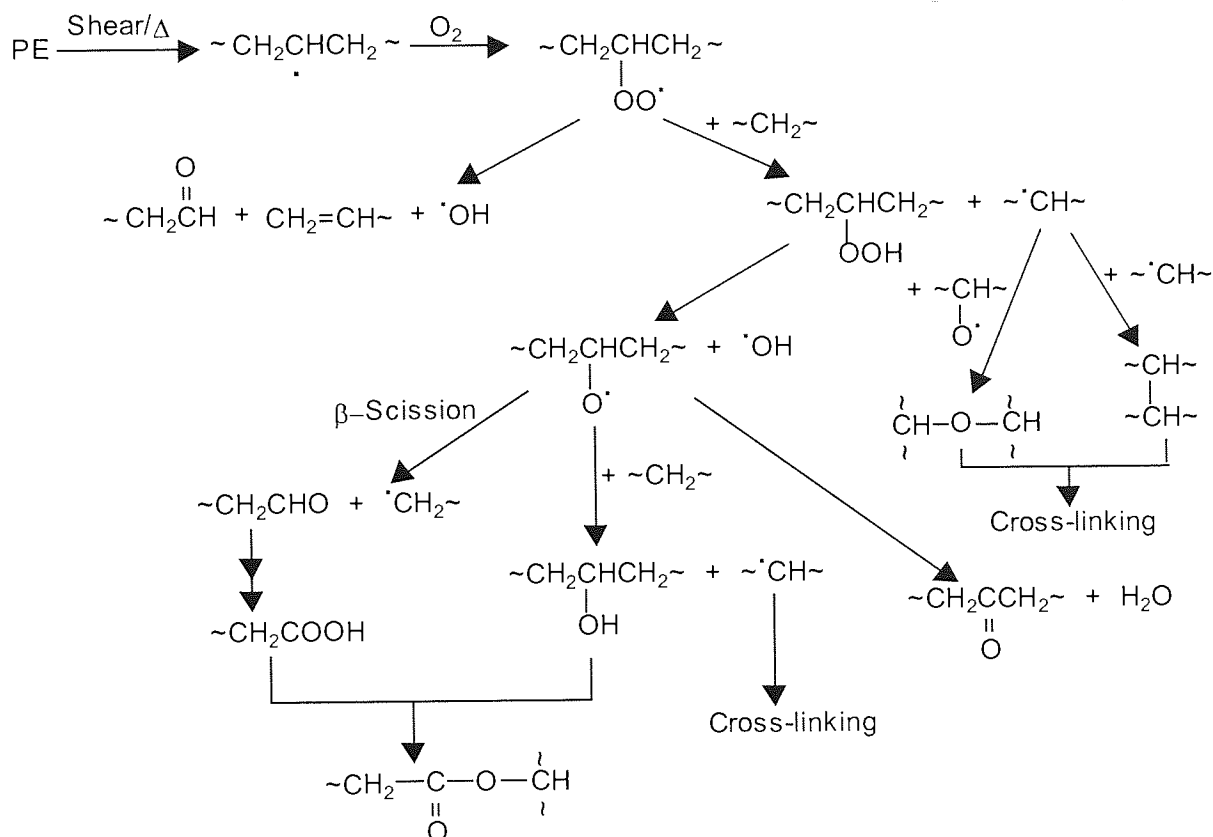


CHAIN SCISSION:



Scheme 1.5. Reactions Leading to Molecular Enlargement and Chain Scission of Polyethylene

At low and medium oxygen pressures, reactions of R^{\bullet} and RO_2^{\bullet} radicals dominate the termination step, whereas at high oxygen pressure, reactions of RO_2^{\bullet} radicals become predominant. The detailed mechanisms of oxidation and consequently the nature of the products formed will ultimately depend on the structural features of the polyethylene and the processing conditions applied [94, 95, 96]. However, different grades of polyethylene undergo thermo-oxidative degradation in the melt in a quite similar way [97], the basic oxidation reactions are outlined in Scheme 1.6 [98].



Scheme 1.6. Oxidative Reactions of Polyethylene Main Chains

In the case of the HDPE, chain branching and crosslinking, leading to an increase of the molecular weight of the polymer, is generally favoured compared to thermo-oxidative and thermo-mechanical induced chain scission. The study of thermo-oxidation during extrusion has revealed that vinyl group reactions (see Figure 1.8) are primarily responsible for the observed molecular weight increase [78].

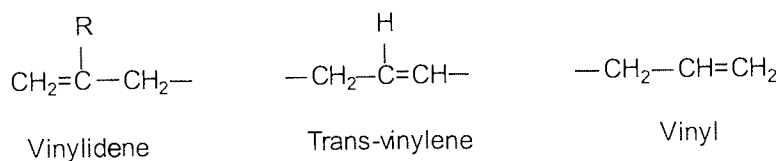
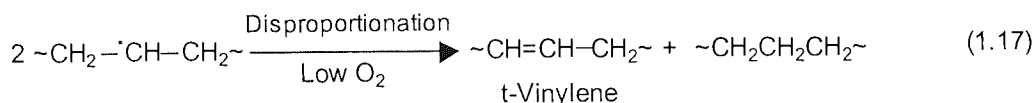
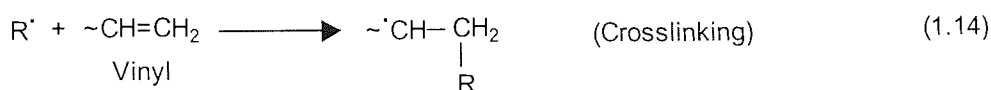


Figure 1.8. Representation of Unsaturated Impurities in Polyethylene

It has been shown that the MW increases correlate well with the content of vinyl groups originally present in the polymer. Chain branching and crosslinking reactions can be assigned to the addition of alkyl radicals to vinyl groups (Scheme 1.7, Reaction 1.14) [99]. However, addition reactions of substituted trans-vinylene and vinylidene groups (see Figure 1.8) with alkyl radicals were found not to occur, at least not to the same extent, as vinyl group [52, 99]. The steric environment allows an alkyl radical addition most likely on an un-substituted double bond. Any further substitution of the $-C=C-$ bond prevents such a reaction [99]. The formation of trans-vinylene groups can be explained by disproportionation reactions of secondary radicals at low oxygen concentration (Scheme 1.7, Reaction 1.17). The dominating role of alkyl radicals in degradation reactions of HDPE is evident, where molecular weight changes (chain scission or crosslinking) are determined by the ratio of R^\bullet and RO_2^\bullet concentration [74].



Scheme 1.7. Reactions Involving Vinyl and trans-Vinylene in PE Oxidation

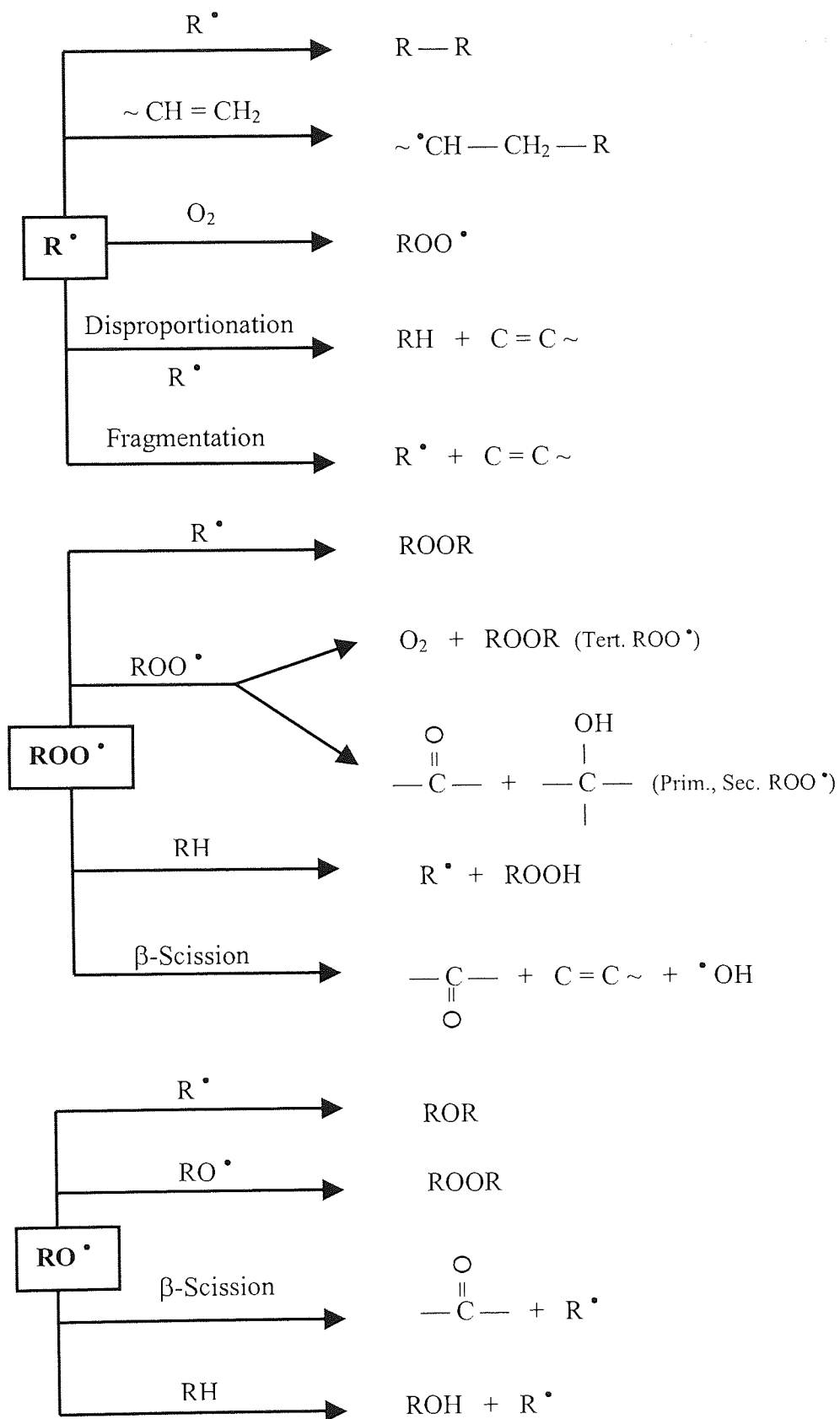
LDPE has been shown to have more tendencies to cross-link and form LCB at high temperatures compared with HDPE and this was attributed to differences in their molecular microstructures. However, although molecular enlargement dominates, a considerable molecular diminishment (chemical scission) also occurs. As a result the molecular weight distribution becomes broader [97]. In some cases of LDPE, chain scission may be favoured depending on the processing conditions.

In contrast, polypropylene (PP) primarily undergoes chain scission in thermo-oxidation, leading to a decrease in the average molecular weight of the polymer.

This is mainly caused by β -scission of the tertiary alkoxyl radicals, the breakdown of peroxy radicals and shear. Disproportionation reactions of alkyl radicals are terminating steps. Comparing the products of PE and isotactic PP, the most striking difference is in the kinetics of formation of carboxyl group and in that of fragmentation [100, 101]. Accordingly, the formation of primary radicals takes place preferentially at the branching points, e.g. on tertiary carbon atoms or at other structural defects. The primary initiation of oxidation occurs mainly at allylic C-H bonds, while in propagation the tertiary C-H bonds play an important role [74].

The primary mechanisms for chain scission of polyethylene, which occurs by β -cleavage of oxygen centred radicals (ROO^\bullet , RO^\bullet) and alkyl radicals, include oxidative and thermal scissions. Oxidative scission is the dominant reaction at moderate temperatures under conditions of high oxygen pressures. Thermal scission involves β -cleavage of secondary alkyl radicals thereby giving rise to vinyl groups ($\text{CH}_2=\text{CH-R}$) whilst tertiary alkyl radicals giving rise to vinylidene groups ($\text{CH}_2=\text{CR}'\text{-R}''$). Thermal scission does not require high oxygen pressures, hence becoming increasingly important as processing temperatures increases. Many studies of polyethylene degradation have shown that the tendency for crosslinking dominates at lower processing temperatures ($< 250^\circ\text{C}$) and chain scission starts to become more important at higher processing temperatures ($> 250^\circ\text{C}$) in oxygen deficient conditions. In oxygen excess conditions, chain scission is the dominant reaction [52, 74].

Summarily, the basic reactions of the most important radical intermediates involved in polyethylene thermal oxidation are shown in Scheme 1.8 [99].



Scheme 1.8. Basic Radical Reactions Involved in PE Thermo-oxidation

On the one hand, oxidation of polyolefins of different structures leads to active species of different structures, which would consequently determine the behaviour of the oxidation and composition of the end products [102, 103]. On the other hand, the oxidative degradation process is similar to some extent for different polyolefins. Oxygen is absorbed chemically according to an autocatalytic curve. The kinetic curves for the formation of different end products (carbonyl compounds with different structures, water, volatile organic products, chain fragments) have the same shape. The concentrations of intermediate products (propagating radicals, hydroperoxide groups) as well as the mass of the polymer go through a maximum. The molecular weight distribution steadily becomes broader, owing to the enlargement and fragmentation of the polymer chains [74].

The thermal-oxidative degradation of polyethylene copolymers (i.e. LLDPE) depends on the type, content and distribution of the co-monomers [104]. It also depends on the type and amount of unsaturation present and the type and amount of catalyst residues. Under some circumstances, thermal-oxidative crosslinking occurs in LLDPE during melt processing predominantly via reaction of unsaturated groups, especially vinyl groups (Scheme 1.7, Reaction 1.14). The mechanism of molecular weight increase is not via simple crosslinking. Under shearing conditions, a clear increase of long-chain branching was observed [105]. Molecular weight increase and bond scission are temperature dependent and occur simultaneously as competitive reactions [52]. In addition, the co-monomer content was shown to have a major impact on the degradation mechanism. The higher the co-monomer content, the more pronounced is the β -scission [105].

A model was developed by some researchers to show how olefin-based reaction affects the balance of crosslinking versus chain scission during LLDPE melt processing [52]. Such a model will allow estimation of the temperature above which a given LLDPE will show predominant scission during melt processing. Estimation of the dominance of crosslinking versus chain scission in a given polyethylene must take into account the vinyl and vinylidene concentrations, temperature, relative

oxidation rate, and possibly the concentration of trans-vinylene. If the oxidation rate is assumed to be similar for different polyethylenes processed under the same conditions, then it is quite plausible that the major factor that causes different PEs to degrade differently during processing depends on the unsaturation type and content. It has been proposed that for most classes of polyethylene, vinyl concentration is the most important variables, followed by the vinylidene concentration [52].

The melt flow behavior (*via* measurement of melt flow index, MI) has been widely and successfully used to give a quick indication of the type of chemical change that may occur during polyethylene processing. The MI, which is the mass (in grams) of molten polymer extruded through a standard die in a given time (normally 10 minutes), is inversely related to its molecular weight. An increase in MI is associated with chain scission whereas a decrease in MI reflects crosslinking and an increase in molecular weight (see Figure 1.9) [106].

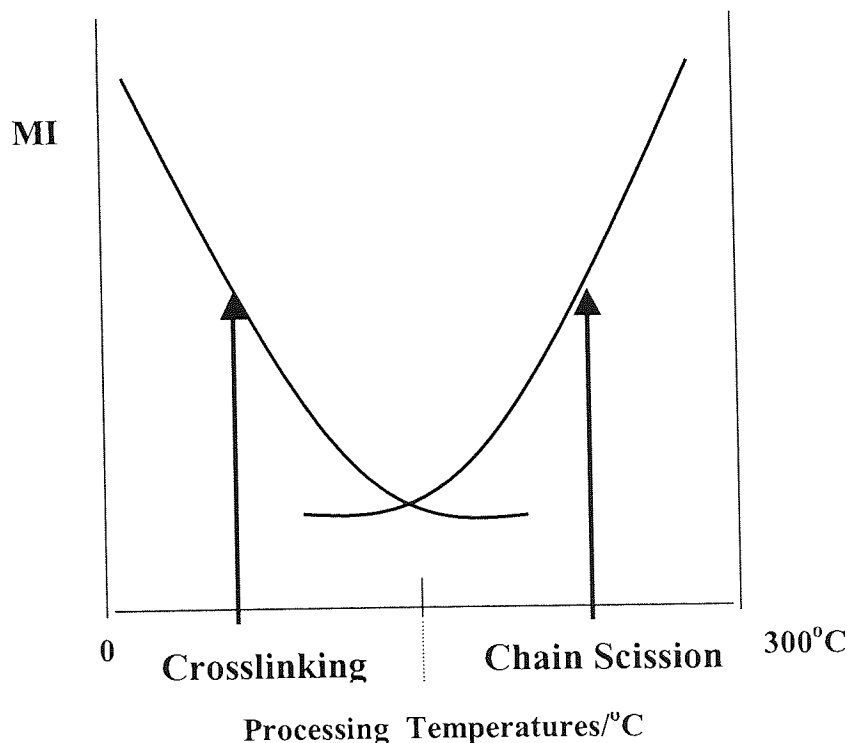


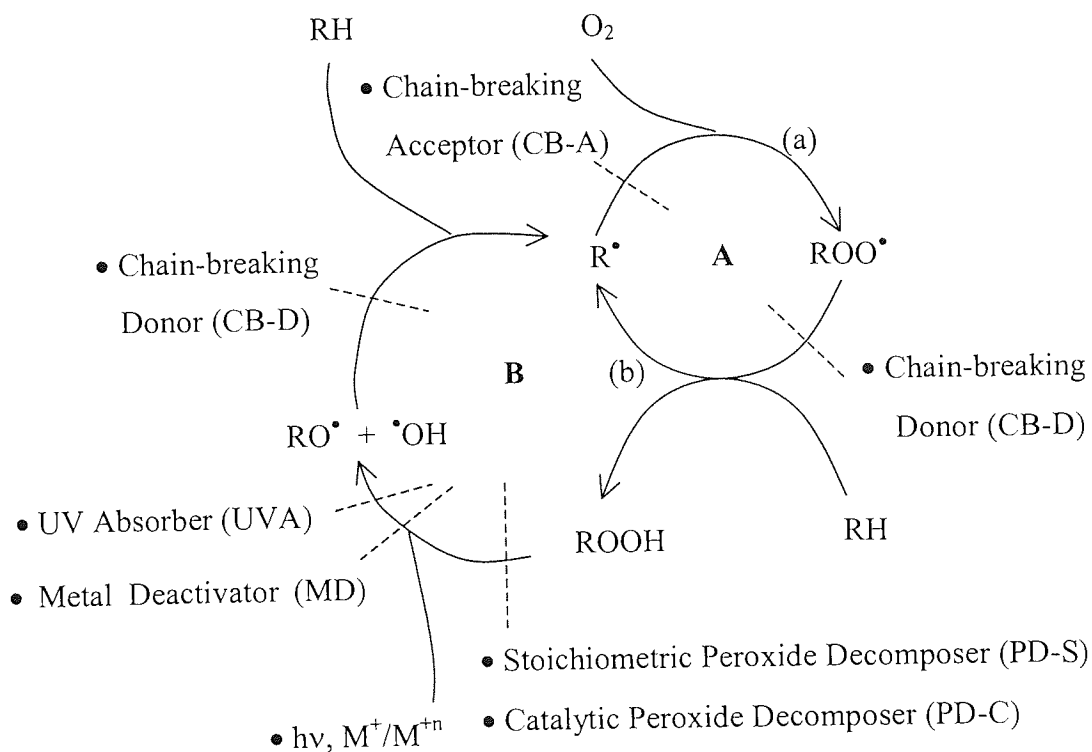
Figure 1.9. Schematic Representation of Changes in Melt Flow Index of Processed PE under Different Temperatures Reflecting Crosslinking (decrease in MI) and Chain Scission (increase in MI)

Although there has been extensive study of oxidation of Ziegler-based LLDPE in recent years [47, 80, 93, 105], very little has been published on the oxidative degradation mechanisms of the newer m-LLDPE polymers.

1.3. ANTIOXIDANT AND STABILISATION OF POLYOLEFINS

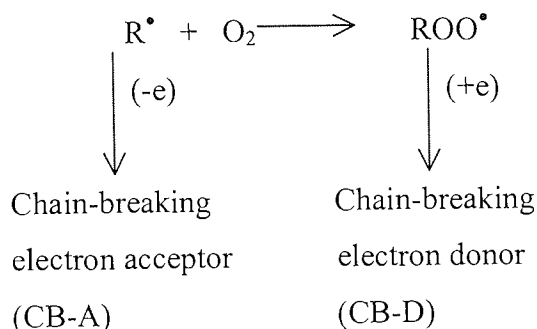
1.3.1. Stabilisation Mechanisms of the Major Antioxidant Classes

Antioxidants are generally recognised as being inhibitors of either radical chain reactions involving alkyl and alkylperoxyl radicals as the chain propagating species or production of hydroperoxides as the indigenous initiators of autoxidation. Oxidation inhibition processes have been classified into two main types: kinetic chain-breaking processes and initiation prevention mechanisms. The effects of antioxidants on polymer stabilisation are summarised in Scheme 1.9 [107-109].



Scheme 1.9. Mechanisms of Antioxidant Action in Polymer Oxidation

The first type embraces the traditional rubber antioxidants, the aromatic amines and hindered phenols, the second includes the hydroperoxide decomposers, the transition metal deactivators and u.v. stabilisers. The sum of the various methods of retardation of polymer oxidation and the decrease of the undesired consequences of the oxidation process is referred to as “polymer stabilization” [107].



Scheme 1.10. Kinetic Chain-breaking Processes

The free radical chain reactions of polymer oxidation might be interrupted by two ways summarised in Scheme 1.10. The first involves removal of the alkyl radical by an oxidation process to give a carbonium ion or a derived product (CB-A mechanism) and the second involves the reduction of the alkylperoxyl radical to give a hydroperoxide (CB-D mechanism). Antioxidants acting by these two mechanisms are electron acceptors (oxidising agents) and electron donors (reducing agents), respectively [109].

If both alkyl and alkylperoxyl radicals are present in an autoxidising system in comparable concentration at the same time, then CB-A and CB-D mechanisms may operate simultaneously. Moreover, if the oxidised and reduced forms of an antioxidant form a reversible redox couple, then more than one kinetic chain may be broken per antioxidant molecule. Under these favourable conditions catalytic inhibition may occur and is in competition with the propagation processes of polymer oxidation. Generally, the abstraction of H from polymer backbone by the ROO^\bullet radical is the rate controlling reaction. As a result, the CB-A process in

catalytic chain-breaking mechanism will only operate effectively if the oxygen concentration is low during oxidation. If it is not, then oxygen can successfully compete with the oxidised form of the antioxidant for the alkyl radical, in this case only the CB-D mechanism can terminate chain-propagating radicals efficiently [110, 111].

Antioxidants whose primary function is to interfere with the generation of free radicals are assorted into preventive antioxidants. The most important preventive mechanism, both theoretically and practically, is hydroperoxide decomposition (PD) in a process that does not involve the formation of free radicals. These kinds of antioxidants fall into two classes; stoichiometric peroxide decomposers (PD-S), such as phosphite esters that are reagents for the reduction of hydroperoxides to alcohols, and catalytic peroxide decomposers (PD-C). A variety of sulfur compounds which are of considerable importance as commercial antioxidants fall into the latter class and their mechanisms have been extensively studied in recent years [112].

Although complete destruction of hydroperoxides from the manufacture of the polymer articles through their service life is the ideal to be aimed at, other agents that can slow down their decomposition may act as retarders of peroxide initiated oxidation. Many transition metal ions are effective catalysts for the homolytic decomposition of hydroperoxides. They are therefore effective pro-oxidants and their activity depends on the availability of oxidised and reduced states of comparable stability. Complex agents that have the ability to co-ordinate the vacant orbitals of transition metal ions to their maximum co-ordination number and thus inhibit the co-ordination of hydroperoxides to the metal ions are therefore effective metal deactivators (MD) and hence inhibitors for metal catalysed auto-oxidation [112].

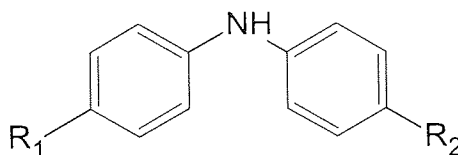
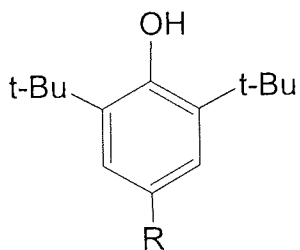
Similarly, in the case of UV-initiated oxidation, UV light absorbers (UVA), screens and filters, effectively inhibit the photo-excitation of light absorbing species present in the polymers. Another way in which preventive antioxidants may be in principal

act, is by quenching of photo-excited states of chromophores present in polymers (e.g. carbonyl compounds). In practice, many commercial stabilisers have been found to operate by a combination of these mechanisms [113, 114].

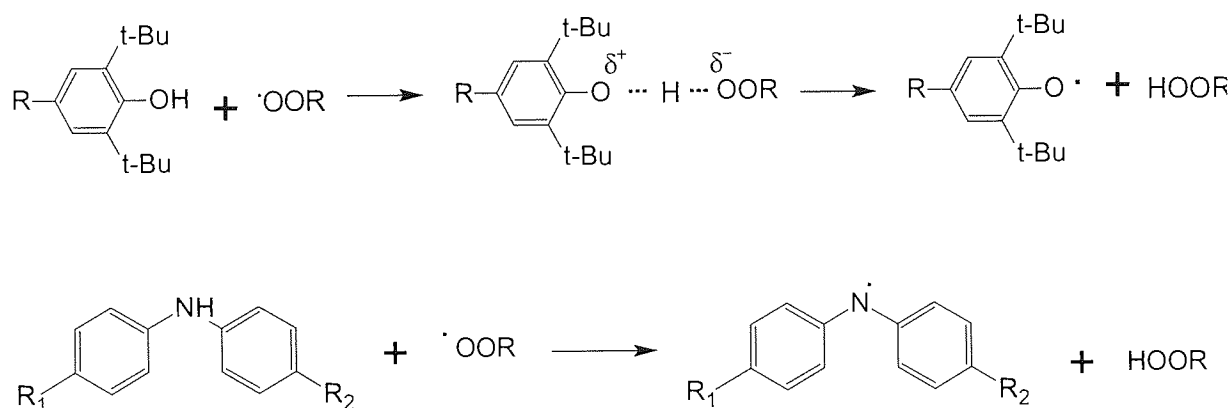
Most stabilisers for polymers contain a combination of antioxidants acting by different and normally complementary mechanisms. It has been shown that antioxidants that destroy hydroperoxides, thereby reducing the concentration of initiating radicals, will as a consequence, slow down the depletion of chain-breaking antioxidants [107, 112]. By the same token, an effective chain-breaking antioxidant reduces the amount of hydroperoxides formed in an autoxidising system and hence “protects” the peroxide decomposer antioxidants used in the system. This co-operative interaction, which is commonly called synergism, leads to an overall antioxidant effect that is greater than the sum of the individual effects and very often to an effectiveness much greater than can be achieved by either antioxidant alone even at much higher concentrations. The phenomenon is therefore of considerable practical and theoretical significance. Occasionally the reverse phenomenon is observed; that is, two antioxidants interact to decrease the sum of their individual effects. This is described as antagonism [112, 115, 116, 117].

1.3.2. Stabilisation Systems Generally Used in Hydrocarbon Polymers

The earliest antioxidants to be investigated fall into the chain-breaking donor (CB-D) mechanism. The two best known classes of commercial antioxidants for hydrocarbon polymers in this class are the hindered phenols and the aromatic amines. Both classes are able to donate a hydrogen to an alkylperoxy radical [112].



The effect of substituent groups in the aromatic rings is to reduce the energy of the transition state which involves electron transfer to the peroxy radicals and electron delocalisation in the aromatic ring (see Scheme 1.11).

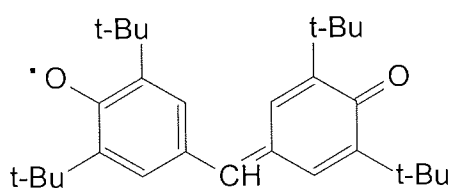


Scheme 1.11. Stabilisation Reactions of Hindered Phenol and Aromatic Amine

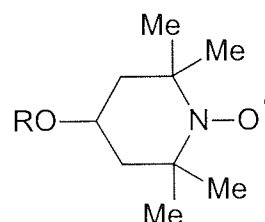
The activities of phenolic antioxidants are strongly dependent on their structures. In general, groups in the 2, 4 and 6 positions that extend the delocalisation of the unpaired electron increase activity. Electron-releasing groups decrease the energy of the transition state and consequently increase antioxidant activity, whereas electron-attracting groups decrease activity. The presence of at least one tertiary alkyl group in the ortho position is necessary for high antioxidant activity. Many of the most effective antioxidants are substituted in both ortho positions by tertiary alkyl groups [112, 118].

Arylamine antioxidants with higher molecular weight such as octylated diphenylamine are commercial antioxidants for rubbers used at high temperatures. A disadvantage of the arylamines is that they cause considerable discolouration of the polymers to which they are added. This is due to the formation of extensively conjugated quinonoid oxidation products [107, 112].

Macro-alkyl radicals, unlike alkylperoxyl radicals, are not powerful oxidising agents, but they are themselves readily oxidised by electron acceptors. A variety of oxidising agents are capable of removing alkyl radicals from an autoxidising system and provided they are able to do this in competition with alkylperoxyl radicals, they have antioxidant activity. In general, the molecular requirements for a CB-A antioxidant are the same as for polymerisation inhibitors. This class includes quinones and nitro compounds, but by far the most important are the “stable” free radicals, of which galvinoxyl and nitroxyls are the most effective [110, 112].

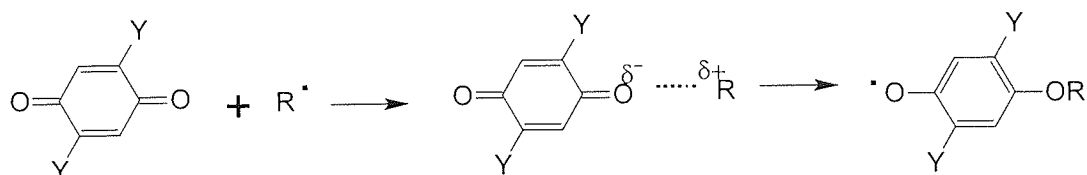


Galvinoxyl



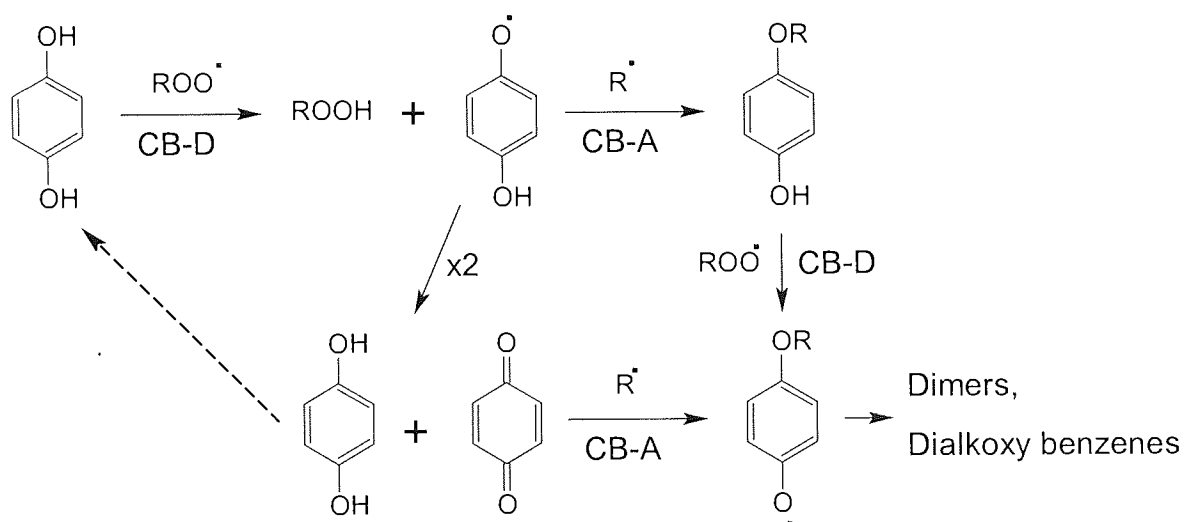
Nitroxyls

The transition state for the reaction of quinone with an alkyl radical involves charge separation (see Scheme 1.12). Electron withdrawing and delocalising groups (Y) both increase the alkyl radical affinity, and hence antioxidant activity of quinones. Quinones and nitro compounds have little practical effectiveness in the presence of excess oxygen since they are not able to compete with oxygen in the alkyl-oxidising reactions [107, 112].



Scheme 1.12. Stabilisation Reaction of Quinone (CB-A)

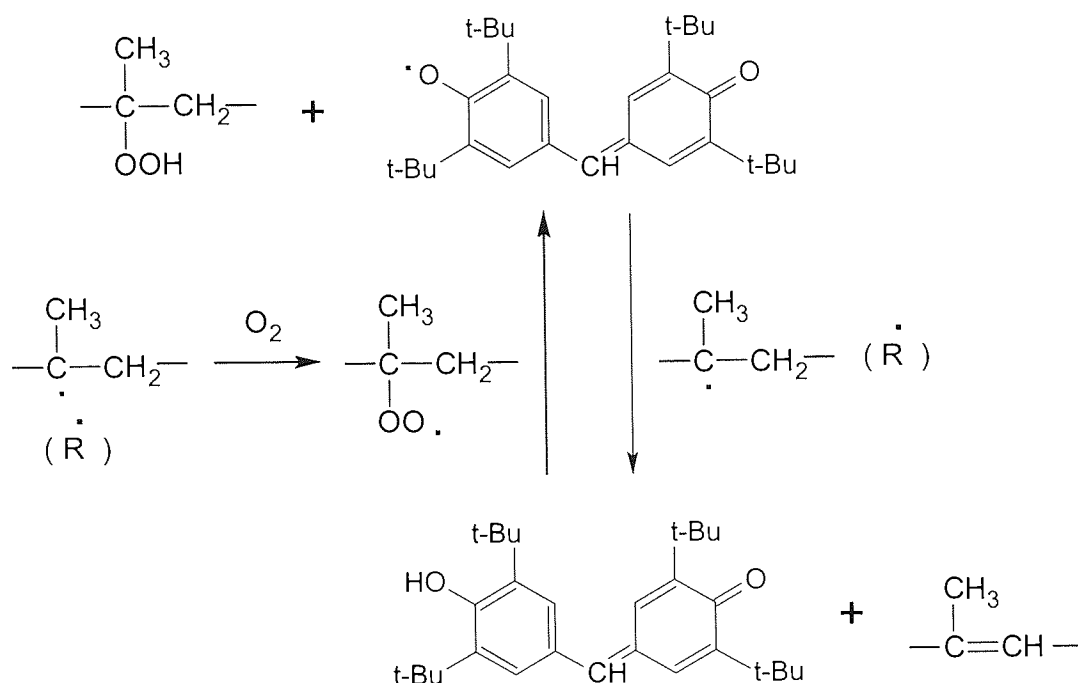
CB-D antioxidants function most effectively when the alkylperoxyl radical is the chain propagating species present in highest concentration in the system; that is, in the presence of excess oxygen. The CB-A mechanism, on the other hand, operates best in oxygen deficiency or at high initiation rates. Antioxidants which exhibit both kinds of activity clearly have an advantage over those operating by a single mechanism since in most oxidation processes both alkyl and alkylperoxyl radicals are present to some extent. Several types of antioxidant are known to involve both mechanisms. The best known is hydroquinone itself that is converted to benzoquinones by the CB-D mechanism (see Scheme 1.13). However, benzoquinones is itself a very effective alkyl radical trap and many radicals may be removed from the system before antioxidant inactive products are finally obtained [107, 112].



Scheme 1.13. Complementary Mechanisms Involving Hydroquinones and its Oxidation Products

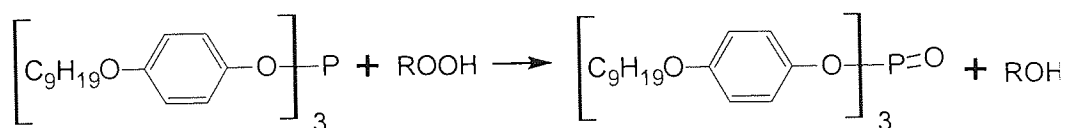
Some chain-breaking antioxidants have the ability to alternate between the oxidised and the reduced state and hence they exhibit regenerative behaviour under conditions where both alkyl and alkylperoxyl radicals are present. The stable phenoxyl radical galvinoxyl was shown to be very effective melt stabiliser for

polypropylene. It does not become chemically bound to the polymer during processing but is converted to hydrogalvinoxyl (see Scheme 1.14) [107, 112].



Scheme 1.14. Regeneration of Galvinoxyl Used in Polypropylene Stabilisation

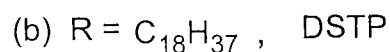
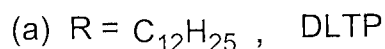
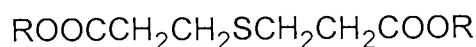
The main requirement of compounds falling into the class of peroxide decomposition mechanism is that they should substantially reduce hydroperoxides to alcohols without the substantial formation of free radicals. The most widely used PD-S antioxidants are the phosphite esters of which tris-nonyl phenylphosphite is a typical commercial stabiliser, stoichiometrically reduces hydroperoxides to alcohols (see Scheme 1.15) [119, 120].



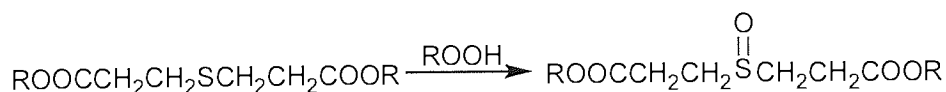
Scheme 1.15. Stabilisation Reaction by Tris-nonyl Phenylphosphite

Of much more general applicability is the class of sulfur compounds that destroy hydroperoxides by a catalytic mechanism (PD-C). Acidic species (e.g. sulfur acids) are very effective antioxidants in model substrates but cannot normally be used in polymers due to their insolubility in organic media and their corrosive tendencies. However, a number of sulfur compounds give acidic species on oxidation with hydroperoxides and therefore act as reservoirs for the peroxidolytic species [112, 121].

Of particular importance because they are the basis of most thermal antioxidant systems for thermoplastic hydrocarbon polymers, are the dialkyl-thiodipropionates [107].



The oxidation chemistry of dialkyl-thiodipropionates is quite complex. Its oxidation to sulfoxide is a stoichiometric reaction (see Scheme 1.16). At temperatures above 60°C, the sulfoxide undergoes a series of reactions with hydroperoxides and forms different types of acidic species. As reaction products, all the sulfur acids can readily inhibit oxidation initiated by alkylperoxyl radicals in the presence of oxygen [107].



Scheme 1.16. Reaction of Dialkyl-thiodipropionates with Hydroperoxide

However, compared with hindered phenols or arylamines, sulfur compounds are not powerful CB-D antioxidants. The sulfinic and sulfonic acids are however also

powerful catalysts for the decomposition of hydroperoxides and consequently effectively inhibit oxidation by interrupting the B-cycle in Scheme 1.9 (PD-C mechanism) [107].

1.3.3. Stabilisation of Polyethylene during Melt Processing

Stabilisation of polyethylene during processing is not only important to the converter, but it is basic to the subsequent service performance of the polymers. As a result, the inhibition of thermal oxidative degradation of polyethylene is a key issue for the plastics industry [122]. From a processing point of view, the primary objective is to maintain the viscosity of the polymer constant when it is in the barrel of a screw extruder. It was shown previously that shearing of the polymer chain, followed by the subsequent formation of peroxides which initiate radical processes (crosslinking or chain scission), are the primary causes of the rheological characteristic changes in polyethylene melt. Both removal of the macro-radicals and destruction of hydroperoxides should therefore be effective melt-stabilising processes [123]. Inhibition of polyethylene oxidation can therefore be achieved by incorporating antioxidants into the polymer matrix before or during the processing stage.

The effectiveness of antioxidants is a product of a complex relationship between all the chemical and physical factors; chemical structure of the antioxidant, thermal stability of both the parent antioxidant and of its transformation products, and their physical behaviour e.g. solubility and their interactions with the polymer substrate with due account to chemical and morphological features. Some times, the commercial success of antioxidants depends not only on their inherent chemical effectiveness and physical persistence in the polymer but also on their toxicological behaviour and cost considerations [124].

It is known that many antioxidants are converted to higher molecular weight transformation products during their function as antioxidants. In the case of aromatic

amines, intensely coloured poly-conjugated products of high molecular weight and low volatility are produced. Many of these transformation products are themselves antioxidants that contribute to the high efficiency of aromatic amines as heat stabilisers for polymers. However, most are also very highly coloured and result in discolouration of polymers, hence, aromatic amines are rarely used in polyethylene. Similarly, hindered phenols subjected to high temperature conditions result in transformations to poly-phenols and derived quinones, which are themselves effective antioxidants. Antioxidants that deactivate hydroperoxides such as alkyl phosphites have generally poor hydrolytic stability. The hydrolysis of phosphorous stabilisers in polyethylene leads to a loss in effectiveness as a processing stabiliser and presents difficulties in handling the additives [108].

The intrinsic chemical activity of antioxidants is a function of their molecular structure. However, use of the chemical activity alone as an indicator can lead to unreliable predictions of the efficiency of antioxidants in polymers under practical conditions owing to the dominating influence of physical factors under certain conditions. For example, the hindered phenol BHT is amongst the most efficient antioxidants known for liquid hydrocarbons but is ineffective in protecting polyolefin because of its rapid depletion through volatilisation from the polymers. The physical behaviour of antioxidants is a major factor affecting their durability, efficiency and acceptability. Physical factors, which control the effectiveness and permanence of antioxidants, include distribution, solubility, diffusivity, volatility and leachability [125].

Effective stabilising packages, for readily oxidisable polymers such as polyethylene, may contain several antioxidants, acting by different mechanisms. It is increasingly important in modern polymer-additive technology to develop the most effective multi-component stabiliser packages. Hence the important considerations including processing conditions, chemical and physical properties of antioxidants, end-use properties of the polymer as well as the cost, all must be taken into account when developing effective stabiliser systems for polyethylene processing [126].

In practice, melt stabilisation of polyethylene is fairly readily achieved using a hindered phenol (CB-D) antioxidant. For example, Irg1076, is the most commonly used antioxidant in polyethylene because it is quite cheap and relatively efficient. Phenolic antioxidants and phosphite or phosphonite stabilisers are effective in preventing the reactive groups from oxidative reactions. Blends of phenolic antioxidants and phosphites exhibit synergism of stabilisation during polyethylene processing [127, 128, 129]. However, although polyethylene is almost always protected against oxidation by antioxidants in industrial processing, the primary steps of thermal oxidation cannot be fully avoided by the use of stabilizers. Even in a system protected by antioxidants, the following processes should be reckoned with [74]:

- (1) The primary process of oxidation; thus a slight structural change of the polymer is inevitable.
- (2) Gradual stabiliser consumption in the primary process; the protection is, therefore, transitional. (The stabiliser system should be chosen after a careful analysis of the demand and of the requested lifetime.)
- (3) Unexpected local deterioration due to the inhomogeneous distribution of the antioxidants even in an optimally designed composition. Homogeneous distribution, on the other hand, is not easily achieved in a semicrystalline polyethylene such as LLDPE with inhomogeneous structure. This problem is of great practical importance.
- (4) In the case of polyethylene based blends and composites the oxidative stability will highly depend on the other ingredients.

1.4. AIMS AND OBJECTIVES OF PRESENT WORK

The overall aim of this research work was two fold, firstly, to investigate the thermal oxidative degradation mechanisms of different grades of metallocene-based LLDPE having different co-monomer content (hence different densities) but close melt

indices, which occur under different processing conditions and to compare those mechanisms identified for the m-LLDPE polymers with the degradation mechanisms of a Zeigler type polyethylene (z-LLDPE) analogue. Secondly, to examine the effects of some commercial stabilisers on the stability of the different grades of m-LLDPE and to compare their performance with a z-LLDPE during melt extrusion.

The main objectives of this work were:

1. To characterise each of the polymers provided, in term of their molecular structure and melt rheology.
2. To examine the effects of processing variables such as processing time, temperature, on the thermal oxidation of different LLDPE, using an internal mixer and twin-screw extruder.
3. To investigate the molecular (functional group concentrations, unsaturation type and content, carbonyls, chain branching, co-monomer content) and rheological (MI, HMI, MWD, rheometry) characteristics of the polymer samples processed under different conditions. The aim is to identify the differences in the oxidation mechanisms of the different polymers and to understand the effect of the molecular structure on the oxidation mechanism.
4. To study the role of certain commercial antioxidants on the thermal stability of the polymers during melt extrusion.

CHAPTER 2. EXPERIMENTAL TECHNIQUES AND METHODOLOGIES

2.1. MATERIALS

The different grades of linear low density polyethylene used in this work were based on ethylene/1-octene copolymers as pellets donated by Dow Chemical Company in Spain. Their detailed characteristics are shown in Table 2.1 and the FTIR spectra of z-LLDPE and one of the m-LLDPE are displayed in Figures 2.1 and 2.2. These polymers were selected based on similarity in their melt indices (MI) but differences in their comonomer contents and densities with the exception of polymer EG8150 (based on the data provided by manufacturer). Some characteristics of these LLDPE were also examined in the PPP Labs and the results are listed in Table 2.2. According to the polymer supplier, a limited amount of commercial antioxidants were originally contained in all of these polymers to provide basic stability during transportation and storage. The polymers were always kept in a freezer room at -20°C to prevent degradation. When required, they were taken out to thaw at room temperature (in the dark) for at least 24 hours before use.

The following commercial solid antioxidants (see Table 2.3), Irganox 1076, Irganox HP136, Irgafos 168, Irgafos P-EPQ, Irganox HP 2921 (2: 4: 1, w/w ratio of Irganox 1076: Irgafos 168: Irganox HP136 respectively, as specified by the manufacturer) and Irganox XP 490 (3: 2: 1, w/w ratio of Irganox 1076: Irgafos P-EPQ: Irganox HP136 respectively, as specified by the manufacturer) were donated by Ciba Specialty Chemicals (Switzerland). Ultrinox 626 was donated by GE Specialty Chemicals (the Netherlands). All the solid antioxidants were used directly without further purification. Irganox E 201 (Ciba Specialty Chemicals, Switzerland) and Weston 399 (GE Specialty Chemicals, the Netherlands), the two liquid antioxidants were also used directly without further purification. Once used, the liquid

antioxidants were stored under nitrogen in freezer. FTIR and UV-VIS spectra of each single antioxidant are displayed in Appendix from Figure A2.1 to A2.14.

Trimethylolpropane ethoxylate (TMP, 20/3 EO/OH)), dichloromethane (spectrophotometric grade, 99.6%), 1,2,4-trichlorobenzene (GC grade, 99⁺%) and deuterated 1,4-dichlorobenzene-d₄ were all supplied by Aldrich Chemical Company Inc. (see Table 2.4). These chemicals were used directly without further purification.

2.2. POLYMER PROCESSING AND SAMPLE PREPARATION

2.2.1. Processing Using an Internal Mixer (Torque Rheometer)

Both metallocene and Ziegler polymers were processed using an internal mixer, RAPRA-Hampden Torque Rheometer (TR) under specified conditions. This mixer operates with an oil heater running up to 300°C and is equipped with a mixing chamber with a pair of counter rotating rotors, a TR ram which can be lowered down to form a closed system, a digital torque displaying unit and heating oil pipes. To simulate the processing conditions in oxygen-deficient extruder, most of the processing was carried out at lower speed of 60rpm [52], oxygen deficient conditions (closed mixer) and varying temperatures of 220°C, 250°C, 270°C and 290°C for a period of 10 minutes (see Scheme 2.1).

Before processing, the mixing chamber was flushed with nitrogen for half a minute prior to feeding in the polymer. Normally, about 35g of polymer can be processed each time and only the polymer around the centre of the chamber was collected after processing. The processed polymer samples were quenched in cold water, dried, and kept in a freezer for further use. The torque rheometer head was cleaned thoroughly after each processing operation using general-purpose polystyrene. All processed polymer samples were further treated before characterisation. They were granulated using a bench-top laboratory electrical granulator and kept in a freezer until required.

2.2.2. Processing Using Twin-Screw Extruder (TSE)

All m-LLDPE and z-LLDPE polymers were extruded in a Betol co-rotating twin-screw extruder (TSE), comprising a barrel divided into eight zones, in which two co-rotating intermeshing screws ($L/D=33$) are contained (see Figure 2.3 for the screw configurations). Figure 2.4 shows the TSE line which also has a single lace die with 4mm internal diameter, a feeding system (a Churchill Single Auger screw feeder, for pellets, and a K-Tron twin-screw feeder for granules), a motor and gear box; heat sensitive thermocouples assembled in each zone of the barrel and the die; electric heating and control system; cooling water system and an on-line 1 meter long Prism water bath with two air knives and pelletiser.

Individually, the two co-rotating screws, made of high-grade steel, generally rotate at a fixed speed that can be varied between 50 to 200rpm, capable of running at a high torque rating. The die, which determines the shape of the polymer extrudate, is simply a circular shaped hole (4mm diameter) made of hardened steel and set at a fixed temperature when the machine is running. The feeders are electrically driven by a Churchill control console, which controlled the flow rate of feeding materials. Each feeder delivers the required amounts of polymers, granules or pellets, directly into the hopper above the TSE barrel. The power to rotate the screw was controlled by a variable speed electric motor and exported through the gear box. Heat sensitive thermocouples are connected to gauges on the control panel and switched the heaters on and off as necessary to control the temperature of each zone. The barrel heaters are also equipped with a water-cooling circulatory system to control the temperature more effectively. The Prism water bath is 1 meter in length and the temperature of the cooling water in the bath is at about 10~20°C.

The polymer was extruded through the die at a given temperature profile and the extrudate lace was quenched into the cooling water using the on-line Prism water bath by wrapping the polymer lace twice across the length of the bath, this was followed by drying with the two air knives and pelletisation using the Prism on-line

pelletiser at a fixed speed (generally 500~800 rpm). The twin-screw extruder processing line is shown in Figure 2.4 and the basic operation of the TSE extrusion is schematically illustrated in Scheme 2.2.

After the die and all the zones were pre-heated to the setting temperatures and before the formal extrusion of each polymer sample was carried out, the extruder was “washed” by extruding about 1kg z-LLDPE granules (from Exxon) to clean away the polymers remained in the barrel in last extrusion (they may be burnt or seriously degrade during the pre-heating). To compare the extent of oxidative degradation of the extruded polymers, the screw speed was always fixed at 100rpm and the output rates were kept consistent for samples processed at the same temperature profile but different extrusion passes (see Table 2.5). The determination of the output rates for different temperature profile was based on the previous work achieved by other researchers in PPP Labs [130]. The extrusions of LLDPE carried out under these conditions generally produce a uniform lace (not starve fed) and maintain lower pressure fluctuation (within $\pm 5\%$) and similar current. The output rates were measured by weighing an extruded polymer leaving the die during a fixed time period (e.g. 30seconds) and controlled by adjusting the feeding speed of the feeder. The actual melt temperature of the polymer extrudate at the die exit was measured using a THI-500 non-contact infrared thermometer. The temperatures of the die and the melt, output rate, melt pressure (at the die), current as well as the appearance of the polymer lace were recorded for each sample (see Table 2.6 as typical example). The power consumption per kg of polymer extruded was calculated according to Equation 2.1 [130]:

$$P = P_m \times (I / I_{\max}) \times (S / S_{\max}) \times 1/F \quad (2.1)$$

Where:

P is the power consumption per kg of polymer extruded (kW.h/kg)

P_m is the maximum power of the motor (7.5 kW)

I is the current during extrusion (A)

I_{\max} is the maximum current (28A)

S is the screw speed during extrusion (rpm)

S_{\max} is the maximum screw speed (220rpm)

F is the output rate (kg.h^{-1})

During extrusion, any gases produced, i.e. steam or volatile solvents (during the compounding step) were removed from the extruder with the aid of a vent connected to a vacuum pump (see Figure 2.4). The vent zone was positioned along the barrel where the polymer experienced least pressure (otherwise the melt would simply discharge out).

(a) Twin-screw Extrusion of “Virgin” LLDPE (with no added antioxidants)

Five extrusion passes were carried out at one (the same) temperature profile for all the polymers with four different temperature profiles examined ($T_2 \sim T_5$, see Table 2.5) used in different experiments throughout the extrusion work. 4kg virgin polymer (with no added antioxidants) was typically extruded for first pass (Pass1) at 100rpm screw speed under atmospheric conditions. After the first extrusion pass, the extruded polymer pellets were collected and continuously re-processed for four further times (multi-pass extrusion, i.e. passes 2 to 5) under the same extrusion conditions. Scheme 2.3 shows the procedure of multi-pass extrusion for LLDPE at a fixed temperature profile.

(b) Twin-screw Extrusion of LLDPE in the Presence of Antioxidants (AO)

A compounding step in which the antioxidants are homogenised with the polymer is referred to here as extrusion pass zero (P_0). Both m-LLDPE and z-LLDPE polymer samples were stabilised by homogenising the antioxidants with polymers under mild processing conditions during a P_0 extrusion step in the TSE. This P_0 step was conducted under nitrogen at a screw speed of 100rpm and die temperature of 210°C (the temperature profile used from zone 8 to zone 1 was: 210, 205, 200, 195, 190, 185, 180, 175°C).

The solid antioxidants, e.g. Irganox 1076, were added to the virgin polymer pellets and tumble mixed in a closed container on a roll mill for 24 hours before extrusion. The mixture of polymer pellets containing “blended-in” solid antioxidants was fed into the TSE *via* the Churchill Single Auger screw feeder during P₀ extrusion step (see Figure 2.4). To form a target antioxidant concentration, the amount of a solid AO added into a given amount of polymer is given in Equation 2.2:

$$\text{Amount of Solid AO (g)} = \frac{\text{Target Concentration(ppm)} \times \text{Polymer Amount (g)}}{1 \times 10^6} \quad (2.2)$$

In the case of liquid antioxidants, they were diluted in spectrophotometric grade (99.6%) dichloromethane (DCM) to form a solution. Typically, 50ml solution was prepared for each compounding extrusion step. During P₀ extrusion, the AO solution was fed by drop-wise addition to the polymer at a fixed flow rate of 0.25ml/min, using a peristaltic liquid pump through a port under the hopper (with a continuous nitrogen purging of the port), directly into the extruder. The employment of this particular flow rate is based on running-in of the pump during polymer extrusion. It is shown that the pump running at this flow rate can provide stable and moderate flux of AO solution and well match the general feeding speed of the polymers. The concentration of AO solution was determined according to the following calculation:

$$C = A \cdot R \cdot 10^{-6} / F \quad (2.3)$$

Where,

C is the concentration of antioxidant in DCM solution (g/ml)

A is the target AO concentration in stabilised polymer (ppm)

R is the output rate of polymer during P₀ extrusion (66.7g/min)

F is the flow rate of the antioxidant-DCM solution (0.25ml/min)

For example, to add a liquid antioxidant at a target concentration of 2000ppm to one of the LLDPE polymers at a speed of 100rpm, with a die extrusion temperature of

210°C (under nitrogen conditions) and output rate of 4.0kg/hr (66.7g/min), the concentration of the antioxidant in DCM solution should be:

$$C_{AO} = (2000 \times 10^{-6} \times 66.7) / 0.25 = 0.534 \text{ g/ml}$$

Liquid phosphite antioxidants are hydrolytically unstable, hence special precautions were taken to avoid any contact with moisture in the air (the phosphite antioxidants being stored and sealed under nitrogen). Furthermore, Weston 399 and Irganox E201 were continuously purged with nitrogen in a sealed container, during their use in the P_0 extrusion step. All stabilised polymer samples (after P_0 extrusion) were stored in a freezer room at -20°C until required for further processing and characterisation.

The stabilised polymers after the compounding step were then subjected to multiple extrusions at temperature of 265°C under atmospheric conditions (see Scheme 2.3 for detailed method). Table 2.7 shows the antioxidant packages used for stabilising polymers and the extrusion conditions used for all P_0 and multi-pass extrusion experiments throughout this work. These stabilised and multi-extruded polymers were then characterised by a number of techniques which were described in details in the following sections.

2.2.3. Preparation of Polymer Films and Plaques by Compression Moulding

2.2.3.1. Preparation of Polymer Films for FTIR Analysis

Both virgin and processed LLDPE samples were pressed to thin films for infrared analysis. The films were prepared by compression moulding, using a SPECAC electric heating press. First of all, two pieces of round aluminium foil with 4cm diameter were shaped into a pair of covers using a specific manual mould. The machine was preheated to 150°C and a metal gap ring of 0.25mm thickness was used. About 6~8 pellets of polymer samples were used for each press (depending on the size of pellets) and placed between the two aluminium foil covers. The resulting

preparation was placed between the two metal pressing plates, which were very smooth and thoroughly cleaned before use. The polymer sample was first heated for 3min without pressure at 150°C and then a pressure of 2tons was applied for 1.5min. Finally, the sample was cooled down to 100°C under full pressure using cold running water, before taking it out. Films of about 0.20mm thickness were obtained and directly used for infrared analysis.

2.2.3.2. Preparation of Polymer Plaques for Colour Analysis

Virgin and TSE extruded LLDPE polymers (both unstabilised and stabilised samples) were pressed into plaques for colour analysis [131]. The plaques were prepared by compression moulding using an electric Daniels press machine. Approximately 7 g of processed LLDPE polymer samples were placed in each of the 8 compartments of a mould which were each 5×5 cm² and 3 mm in depth. The whole mould was wrapped in a special high temperature grade cellophane film and placed between two stainless steel metal plates (thoroughly cleaned before to ensure a smooth surface). The whole preparation was then placed in the Daniels press set at 160°C and the polymer was preheated for 3.5min without applying any pressure. The samples were then subjected to full pressure (120 kg.cm²) for 1.5min, followed by cooling to 100°C at the full pressure and finally by quenching of the polymer in cold water. Two plaques were prepared for each polymer sample and stored in a cool dark place.

2.3. POLYMER CHARACTERISATION

Both unprocessed and processed polymers were characterised utilising a number of techniques to examine the changes of their rheological and structural properties after processing under different conditions. The rheological behaviour of the polymers was evaluated using melt flow index and capillary rheometer. Whereas ¹³C-NMR and FTIR spectroscopy were used to quantify the branching amount, unsaturation and carbonyl contents present in the polymers. In addition, FTIR was also applied to

determine the amount of antioxidants contained in the polymers after the compounding step, and spectrophotometry was used for measuring the discolouration of polymer plaques.

2.3.1. Rheological Measurements

2.3.1.1. Melt Index (MI) and High Load Melt Index (HMI)

Based on ASTM standard D 1238-95 [106], the melt flow index (MI) is defined as the mass (g) of the molten polymer extruded through a die of a specified length and diameter in a given time (normally 10minutes) under prescribed conditions of temperature, load and piston position in the barrel. As an approximate relationship, the melt viscosity of a polymer is inversely proportional to molecular weight, thus MI gives an indication of the extent of degradation after processing, i.e. melt stability. The MI of virgin, stabilised and unstabilised processed LLDPE samples were examined. About 2g of each of the polymer samples were measured on a Davenport melt flow indexer, (see Figure 2.5) at a constant temperature of $190^{\circ}\text{C} \pm 0.1^{\circ}\text{C}$. The barrel of the indexer was charged with the material using a charging tool to exclude air and, at that moment, the stopwatch was started ($t = 0\text{min}$). The charging time should not take more than one minute. A piston was placed on top of the sample and a load of 2.16kg (low load melt index, MI) or 21.6kg (high load melt index, HMI) was then placed on top of the piston and lowered until it reached the metal block. When high load measurements were carried out, the piston with the guide bush was used. The polymer sample was left to reach an equilibrium temperature for a total of five minutes ($t = 5\text{min}$). After that, the metal block was removed and the molten polymer was left to extrude through the die (internal diameter of $2.0955\text{mm} \pm 0.0051\text{mm}$) until the lower mark of the piston coincided with the top of the barrel (see Figure 2.5). The time interval for cut-off of the each first extrudate was 120 or 5 seconds for MI and HMI, respectively. The first extrudate was discarded and then followed by five or three successive cut-offs each after 120 or 5 seconds for MI and HMI, respectively. All extrudates were weighed

after cooling down fully and an average MI or HMI was calculated from the amount of polymer melt (in grams), which passed through the die within a set period, i.e. 2 minutes or 5 seconds, using Equation 2.4. The melt flow rate (MFR) and percentage change in MI, HMI and MFR were calculated using Equations 2.5 and 2.6. It is important to note here that a more negative value of MI or HMI percentage change would reflect a higher extent of crosslinking of the polymer (during processing), whereas, a more positive value would indicate an overall chain scission.

$$\text{MI or HMI} = 10 \cdot m / t \text{ (g/10min)} \quad (2.4)$$

$$\text{MFR} = \text{HMI} / \text{MI} \quad (2.5)$$

MI (HMI, MFR) Percentage Change (%)

$$= \frac{\text{MI of Processed Polymer} - \text{MI of Virgin Unprocessed Sample}}{\text{MI of Virgin Sample}} \times 100\% \quad (2.6)$$

Where:

m is the average weight of the extrudates (g)

t is the time interval of extrusion (min)

MI is the low load melt flow index (g/10min)

HMI is the high load melt flow index (g/10min)

MFR is the melt flow rate

In MI and HMI measurement, if the difference between the weight of an individual extrudate and the average weight of all extrudates is 10% of the average value, that means an un-negligible error has been involved and the measurement was repeated.

Experimental error, which is generally caused by analytical system and individual operation, is always shown as scatter, or the spread of the values of experimental results. In this work, the deviation of characterisation was determined based on

statistics derived from the replicate measurements of representative samples [132]. The processing variability was determined based on statistics derived from replicate processing runs of representative samples. The reproducibility of MI and HMI measurements was also determined and the results are shown in Table 2.8 and 2.9.

Where,

$$X = \text{arithmetic mean} = \sum X_i / N \quad (2.7)$$

$$X_i = \text{numerical result of the } i^{\text{th}} \text{ run} \quad (2.8)$$

$$\text{Standard deviation} = S = [\sum (X_i - X)^2 / N]^{1/2} \quad (2.9)$$

$$N = \text{total number of runs} \quad (2.10)$$

$$\text{RSD (\%)} = \text{relative standard deviation} = (S / X) \cdot 100\% \quad (2.11)$$

$$95\% \text{ CL} = 95\% \text{ confidence limit} = S \cdot [t / N^{1/2}] \quad (2.12)$$

t is a factor which varies with the confidence limit and the value of N

For 2 measurements, $[t / N^{1/2}] = 8.99$

For 3 measurements, $[t / N^{1/2}] = 2.48$ [132]

2.3.1.2. Rheological Properties Measured Using a Capillary Rheometer

The rheological characteristics of virgin and TSE extruded metallocene and Ziegler LLDPE pellets were measured in a Rosand RH2000 twin-bore capillary rheometer (see Figure 2.6) controlled by computer software (Version 1.0.24) [133]. All test parameters including the type of test, barrel temperature, configuration of dies and shear rate range were entered *via* the computer interface. Before test, the two transducers (P_{left} and P_{right}) were calibrated at full scale (68.948Mpa for the P_{left} and 10.340Mpa for P_{right}), 1.0000 gain value and 80% calibration resistor. Dies for the two barrels: (1) long die on the left, 16mm length with a 1mm diameter, (2) zerolength die on the right, 0mm length, 1mm diameter, were used for the Bagley correction. The Bagley correction takes account of the pressure drops at the entry and exit from a capillary die [133]. The procedure of carrying out rheological test using the twin-bore capillary rheometer is shown in Scheme 2.4.

Useful information for assessing the stability and processability of polymers can be obtained by running capillary rheological test. The values of the pressures at the long die (P_1) and at the zero length die (P_0), the shear stress (σ_s), shear rate ($\dot{\gamma}$), extensional stress (σ_E), elongational viscosity (η_E) and power law index (n) for each shear rate were calculated automatically by the Rosand software, according to Equations 2.13 to 2.17. The value “ n ” is an index of the degree of non-Newtonian behaviour of the polymer melt. If $n < 1$, it indicates the level of pseudoplasticity exhibited by the polymer (otherwise, $n > 1$, it indicates the fluid is in a dilatant flow). The smaller the n is, the more pseudoplastic the polymer behaves, i.e. the viscosity is more dependant on shear rate and is more shear thinning. Normally the rheometer calculates extrudate shear rate from the volume flow rate and die dimensions by assuming that the velocity of the extrudate at the die wall is zero. This calculation is invalid if for some reason the velocity is non-zero, but with an appropriate choice of dies, the results can be automatically corrected by the Rosand software.

$$\text{Apparent Shear rate } \dot{\gamma} = \frac{4Q}{\pi r^3} \quad (2.13)$$

$$\text{Shear stress } \sigma_s = \frac{(P_1 - P_0)r}{2L} \quad (2.14)$$

$$\text{Shear viscosity } \eta = \frac{\sigma_s}{\dot{\gamma}} \quad (2.15)$$

$$\text{Extensional stress } \sigma_E = \frac{3}{8}(n+1)P_0 \quad \text{with } \sigma_s \propto \dot{\gamma}^n \quad (2.16)$$

$$\text{Elongational viscosity } \eta_E = \frac{9}{32} \frac{(n+1)^2}{\eta} \left(\frac{P_0}{\dot{\gamma}} \right)^2 \quad (2.17)$$

Where:

Q is the volume flow rate of the polymer (cm^3/s)

r is the radius of the long and short die (0.5mm)

P_1 is the pressure measured at the long die (16mm length, 1mm diameter)

P_0 is the pressure measured at the zero length die (0mm length, 1mm diameter).

L is the length of the long die (capillary, 16mm)

η is the shear viscosity at a specific shear rate.

N is the power law index.

The capillary rheometer was used to determine the changes in shear and elongational viscosity of virgin and extruded un-stabilised m-LLDPE and z-LLDPE pellets. All the experiments were carried out in the shear rate range of $80\text{-}3000\text{s}^{-1}$, and at temperatures of 210, 235, 265 and 285°C , simulating the conditions experienced by polymers during TSE processing. Ascending and descending shear rates during a test-run provided information as to the melt stability of the polymer during the analysis. Hence, the more stable the material during the test, the better the hysteresis loop. All the polymers were tested in the following shear rate stages and orders (ramp up and down).

Constant Shear Rate Test: 80-140-200-300-450-650-1000-1400-2000-3000-2000-1400-1000-650-450-300-200-140-80 s^{-1}

Using material degradation test, the rheological characteristics (corrected shear stress, shear and extensional viscosity) of virgin LLDPE polymers were evaluated with the aid of the RH2000 capillary rheometer at 265°C . The material degradation test involved five degradation cycles with ascending shear rates ranging from 200-300-400-500-700-900-1200-1600 s^{-1} (ramp up) in each cycle and ten minute waiting time intervals (see Figure 2.7).

2.3.2. Characterisation of the Molecular Structure of LLDPE

2.3.2.1. Fourier Transform Infrared Spectroscopy (FTIR)

The concentrations of double bonds (trans-vinylene, vinyl and vinylidene) and carbonyl compounds contained in original and processed polymers were determined using a Nicolet 5DXC Fourier Transform Infrared Spectrometer. All polymer samples were analysed as thin films which were pressed using an electric press (see Section 2.2.3.1). Infrared spectroscopy was carried out at room temperature with 16 scans and a resolution of 1 cm^{-1} . The FTIR spectra were obtained over the range of 4000cm^{-1} to 400cm^{-1} .

(a) Determination of Unsaturated Group Concentrations

The determination of double bonds was based on their peak areas of the FTIR spectrum at 965cm^{-1} (trans-vinylene), 908cm^{-1} (vinyl) and 889cm^{-1} (vinylidene) respectively [54]. The FTIR absorption spectra of z-LLDPE and one of the m-LLDPE in this region are shown in Figures 2.8 and 2.9.

The relative concentrations of all double bonds in TR-processed polymers were calculated from their peak area absorbance compared to that of a reference peak in the spectrum region of $1979\sim 2113\text{ cm}^{-1}$ [134]. The relative concentrations are defined as the ratio of the integral of an absorbance peak area of a given functional group to that of the absorbance area of the reference peak (absorption area index, see Equations 2.18 to 2.20).

$$[\text{-CH=CH-}]_{\text{Relative}} = \frac{\text{Integral of the Area of IR Absorption Peak at } 965\text{ cm}^{-1}}{\text{Integral of the Area of Reference Absorption Peak (1979~2113 cm}^{-1})} \quad (2.18)$$

$$[\text{-CH=CH}_2]_{\text{Relative}} = \frac{\text{Integral of the Area of IR Absorption Peak at } 908\text{ cm}^{-1}}{\text{Integral of the Area of Reference Absorption Peak (1979~2113 cm}^{-1})} \quad (2.19)$$

$$[\text{>C=CH}_2]_{\text{Relative}} = \frac{\text{Integral of the Area of IR Absorption Peak at } 889\text{ cm}^{-1}}{\text{Integral of the Area of Reference Absorption Peak (1979~2113 cm}^{-1})} \quad (2.20)$$

For the TSE processed LLDPE, the concentrations of double bonds were determined quantitatively via the integral of peak areas in the appropriate IR absorption region and the IR extinction coefficients of the individual unsaturated groups. The IR extinction coefficients applied were taken from the literature values [46, 135] and are shown in Table 2.10; the calculation is based on the Equation 2.22.

$$I = \epsilon \cdot C \cdot L \longrightarrow C = I / (\epsilon \cdot L) \quad (2.22)$$

Where,

C — Concentration of a Given Functional Group (mol/L)

I — Integral of the Absorption Peak Area in IR Absorption Spectrum

ϵ — IR Extinction Coefficient of the Corresponding Functional Group
(L/mol.cm) – from literature values

L — Thickness of the Sample Film (cm)

The definition and calculation of percentage change of each double bond concentration are similar to that used for MI (see Equation 2.6). The experimental error and deviation of results derived from processing and measurement has been evaluated according to the same method as MI measurement and the outcome is shown in Tables 2.11 and 2.12.

(b) Determination of Concentrations of Carbonyl Containing Compounds

The concentration of carbonyl containing compounds in both virgin and processed LLDPE can also be determined from FTIR spectroscopy. Since the characteristic peaks of most carbonyl compounds appear at a quite narrow region in the FTIR spectrum, and in most cases some of them may overlap, the peaks in this region (1782~1682 cm^{-1}) were taken into account as a whole when quantitative calculation was carried out.

Similar to the double bond measurement, the carbonyl concentrations of TR-processed polymers were determined by measuring carbonyl absorption area index with referring to a reference peak at 1979~2113 cm^{-1} according to Equation 2.23. Figures 2.10 and 2.11 show the carbonyl region in FTIR spectra of unprocessed z-LLDPE and one of m-LLDPE (the reference peak is shown in Figure 2.11). The determination of carbonyl concentrations of TSE processed LLDPE samples were done on the base of IR-extinction coefficient of the maximum peak at the carbonyl region (see Table 2.10) and the integral of all the peak areas at 1782~1682 cm^{-1} (see Equation 2.22).

$$[>\text{C}=\text{O}]_{\text{relative}} = \frac{\text{Integral of the Absorption Peak Area Between 1782 and 1682 } \text{cm}^{-1}}{\text{Integral of the Area of Reference Absorption Peak (1979~2113 } \text{cm}^{-1})} \quad (2.23)$$

The percentage change of carbonyl concentration is also defined according to Equation 2.6. Experimental error and deviation of the carbonyl quantification are calculated using the same statistical methods detailed in Section 2.3.1 and the results are shown in Table 2.13.

2.3.2.2. ^{13}C -NMR Spectroscopy for Quantification of the Level of Branching

The amount of branching (1-octene content) of the virgin LLDPE and some TSE processed polymers was determined using ^{13}C -NMR according to ASTM standard D5017-91 [43]. The analytical samples were prepared by heating a 10mm diameter NMR sample tube containing mixture of 1g polymer and 2.3 ml 1,2,4-trichlorobenzene (TCB) in an oil bath at 150°C for about 2~3 hours. Then a 3 mm diameter small tube containing 1g deuterated 1,4-dichlorobenzene (d-DCB), which was used as internal lock material, was inserted into the molten sample until it touches the bottom of sample tube. The sample tube was heated again at 150°C for another 1~2 hours (see Figure 2.12). After that, it was taken out of the oil bath and kept in an oven at 130°C to equilibrate for 3 hours, followed by ^{13}C -NMR analysis at 130°C.

The two parameters that must be determined for quantitative analysis by ^{13}C -NMR spectroscopy are the spin lattice relaxation time (T_1) and the nuclear overhauser enhancement (NOE) factor of the carbons used for quantitative analysis. The T_1 value of 10 seconds was applied in this measurement and at least 5000 scans were accumulated in order to achieve adequate signal-to-noise. Meanwhile, the NOE factor was kept full and constant for all carbons of the copolymers [42, 43]. The ^{13}C -NMR was carried out at 130 °C using a Bruker AC300 spectrometer. The samples were scanned with complete broadband decoupling using the parameters shown below, and the spectrum as well as the accurate full scale integral from 10 to 50 ppm was recorded. Figure 2.13 shows the ^{13}C -NMR spectrum of a high branching m-LLDPE sample (EG8150) obtained under the following analytical conditions:

1. 10s delay between pulses
2. Pulse angle of 90°
3. Complete proton decoupling mode
4. Minimum signal-to-noise, 5000:1
5. Sweep width, 175ppm
6. Transmitter frequency (F_1), 50-55 ppm
7. The apodisation is exponential, 2 Hz broadening
8. Pulse width, $< [4 \times \text{sweep width Hz}]^{-1}$
9. Nuclear overhauser enhancement (NOE) for the carbons used for quantitative analysis is full
10. The resonance of isolated methylenes is assigned to 30.0 ppm

The polymer branching can be quantitatively measured and calculated through the integration of different carbons in the NMR spectrum when experimental parameters were properly set. A typical calculation is shown below based on the ^{13}C -NMR spectrum in Figure 2.13 [43]. The percentage change of branching amount of TSE processed polymers is also defined as shown in Equation 2.6 and the experimental error has been estimated (see Table 2.14).

Sample Calculation for an Ethylene–1-Octene Copolymer (EG8150):

| Area | Region (ppm) | Integral |
|-------|--------------|----------|
| A | 41.5 to 40.5 | 0.8 |
| B | 40.5 to 39.5 | 1.2 |
| C | 39.5 to 37.0 | 15.4 |
| D | Peak at 35.8 | 0.0 |
| D+E | 36.8 to 33.2 | 63.6 |
| F+G+H | 33.2 to 25.5 | 309.5 |
| H | 28.5 to 26.5 | 48.9 |
| I | 25.0 to 24.0 | 2.0 |
| P | 24.0 to 22.0 | 21.8 |

$$O_1 = \text{CH (br) carbons} = (A+2C+2D)/2 = (0.8+30.8+0.0)/2 = 15.8$$

$$O_2 = \alpha\text{-carbons} = [1.5A+2B+(D+E)-D]/3 = [1.2+2.4+63.6-0.0]/3 = 22.4$$

$$O' = \text{average moles 1-octene} = (O_1+O_2)/2 = (15.8+22.4)/2 = 19.1$$

$$\begin{aligned} E' = \text{moles ethylene} &= \{[(F+G+H)-(3A+3B+H+P+I)]/2\} + O' \\ &= \{[309.5-(2.4+3.6+48.9+21.8+2.0)]/2\} + O' \\ &= 115.4+19.1 = 134.5 \end{aligned}$$

$$\text{Mole \% 1-Octene} = O'/(O'+E') \times 100\% = 19.1/(19.1+134.5) \times 100\% = 12.4\%$$

$$\begin{aligned} \text{Weight \% 1-Octene} &= \frac{112(\text{Mole \% 1-Octene})}{112(\text{Mole \% 1-Octene}) + 28 (1 - \text{Mole \% 1-Octene})} \times 100\% \\ &= 13.9/(13.9+24.5) \times 100\% = 36.2\% \end{aligned}$$

Where,

112 and 28 are the molecular weights of 1-octene and ethylene, respectively.

2.3.3. Determination Of Antioxidant Concentration in LLDPE

Since the antioxidants contained in polymers play a very important role when the polymer is subject to thermal oxidation, the concentrations of antioxidants added in polymers must be properly controlled to obtain the optimum results of stabilisation. In order to assess the actual antioxidant concentration after processing compared to the target concentration, some of the stabilised P₀ LLDPE were analysed using FTIR

spectroscopy to examine the exact concentrations of some antioxidants that were actually left in the polymer after the compounding step (P_0 extrusion). First, several series of standard solutions (in spectrophotometric grade solvent) of pure antioxidants were prepared and the IR absorbance for specific groups in these antioxidants were determined by means of the integral of absorption peak area, the calibration curves of IR absorbance *via* AO concentration can then be obtained. Finally, the concentrations of antioxidants in stabilised polymers can be measured based on their calibration curves and the IR absorbance of corresponding groups in polymers (see Figures A2.15 to A2.26 in Appendix for the FTIR spectra in the regions containing the specific groups of different antioxidants in standard solutions and polymers as well as calibration curves).

2.3.3.1. Calibration of Standard Antioxidant Solutions

The standard solutions were prepared by fully dissolving the antioxidant in dichloromethane (DCM, spectrophotometric grade) at room temperature. A thoroughly clear and transparent solution can ensure the complete solubility of the antioxidant. 25 ml high concentration (10000ppm) stock solution was first made according the calculation in Equation 2.24.

$$W_s = 10,000 \cdot 10^{-6} \cdot \rho \cdot V \quad (2.24)$$

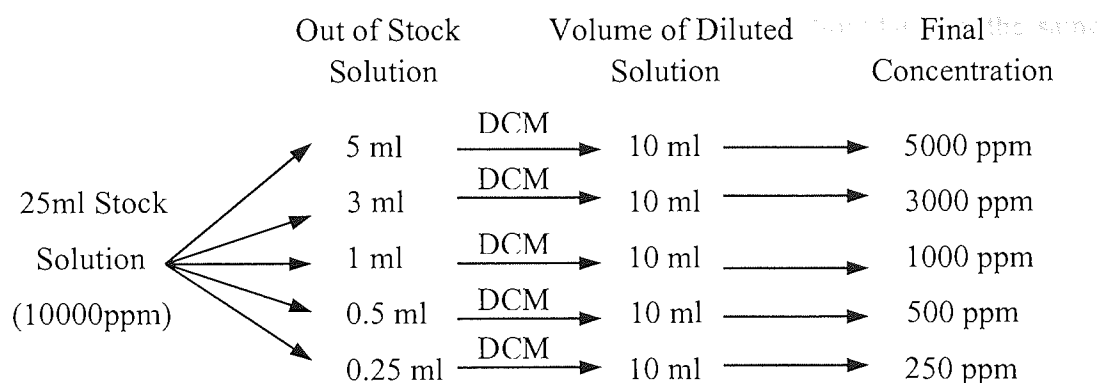
Where,

W_s is the weight of antioxidant dissolved in stock solution

ρ is the specific gravity of dichloromethane (1.325g/ml)

V is the volume of stock solution (25ml)

Different amounts of stock solution were diluted down to 10ml using DCM forming a series of standard solutions with antioxidant concentrations of 5000, 3000, 1000, 500, 250ppm respectively. The detailed preparation of antioxidant standard solution is shown below:



The standard solutions of antioxidant were analysed using FTIR spectroscopy. The difference in concentrations is reflected in the significant changes in absorption peak of the specific group under examination in the IR spectrum. The IR absorption peaks of antioxidants used for calibration are: Irganox1076 — ester group at 1735 cm^{-1} , IrganoxHP136 — lactone group at 1780 cm^{-1} , Irgafos168 — C-O group at 1080 cm^{-1} , IrgafosP-EPQ — C-O group at 1080 cm^{-1} (see Figures A2.15, A2.17, A2.19 and A2.21 in Appendix for the FTIR spectra). A calibration curve of the individual antioxidants can then be made on the bases of the concentrations of standard solutions and the corresponding IR absorbance (measured in IR-KBr liquid cell with spacer of 1 mm thickness) of the characteristic peak (see Figures A2.23 to A2.26 in Appendix).

2.3.3.2. Determination of Antioxidant Concentration in Polymers

The P_0 polymer samples used for examination of the antioxidant concentrations were the same films as those used for measurements of double bond and carbonyl using FTIR. The FTIR analysis for these P_0 samples was carried out (16 scans, 4 cm^{-1} resolution, air background) and the absorbance of specific peaks was recorded (see Figures A2.16, A2.18, A2.20 and A2.22 in Appendix for the FTIR spectra). It is shown that the virgin polymer (PL-1840) also has smaller absorption in the regions where the characteristic peaks of antioxidants are located and examined. Thus, the integral used for AO determination is the value of subtraction of IR absorption peak

area of virgin polymer from that of the specific groups of antioxidants in the same region.

As there are differences between the thickness of sample films and the standard solutions (determined via a spacer for liquid sample in the IR analysis), the specific IR absorbance of the antioxidants in individual sample films were all transformed to standard absorbance compared to the corresponding absorbance of the same antioxidant dissolved in a standard solution as shown in Equation 2.25.

$$A_f = \frac{A_s \cdot L_f}{L_s} \quad (2.25)$$

Where,

A_s is IR standard absorbance of individual antioxidant

A_f is actual IR absorbance of antioxidant in P_0 sample film

L_s is the thickness of spacer used for standard solution (1.067mm)

L_f is the thickness of P_0 sample film

The concentrations of some of the used antioxidants in P_0 polymer samples were determined based on the IR standard absorbance of specific peaks and the calibration curves. Due to some difficulties, e.g. poor solubility in solvent, serious overlap of FTIR peaks, the actual concentrations of some antioxidants such as Ultrinox626, IrganoxE201 were not examined by this method.

2.3.4. Spectrophotometry for Colour Measurements of Polymer Plaques

Polymer plaques (see Section 2.2.3.2) were analysed for colour using a Minolta CM5081 spectrophotometer, according to the ASTM 1925 method [136], with the settings as illuminate C and an observer angle of 2°. Before any colour measurement, white calibration was performed under the same conditions as the following sample measurements using a white calibration cap provided by the manufacturer. All the colour measurements of polymer samples were carried out and

targeted against a white background. Three-time measurements were always taken for each polymer sample by simply rotating the sample to change the measurement position. Each measurement of the same polymer was in itself an average of consecutive measurements of two different plaque samples. The YI (Yellow index) measurement was first taken for virgin polymers as reference standards (YI_0), and then the measurements of yellow indices of processed samples were followed (YI). The differences between the average YI and YI_0 of each polymer were also calculated by the following equation.

$$\Delta YI = YI - YI_0 \quad (2.26)$$

The experimental error and deviation of YI measurement caused by processing were estimated and the results are shown in Table 2.15.

Table 2.1. Characteristics of LLDPE Used in This Study (as specified by the manufacturer, Dow Chemical Company)

| Polymer Code | Comments | MI (g/10min) | Density (g/cm ³) | M _w (kg) | M _n (kg) | M _w /M _n | 1-octene Wt. % |
|---------------|---|--------------|------------------------------|---------------------|---------------------|--------------------------------|----------------|
| FM-1570 | Affinity Polymers, Metallocene-LLDPE Based on Insite® Technology with 1-octene Co-monomer | 0.94 | 0.916 | 78.1 | 35.7 | 2.19 | 11.0 |
| PL-1840 | | 1.01 | 0.911 | 77.1 | 34 | 2.26 | 13.9 |
| PL-1880 | | 1.09 | 0.903 | 84.9 | 37.2 | 2.28 | 19.1 |
| VP-8770 | | 1.07 | 0.886 | 100 | 46.6 | 2.15 | 30.9 |
| EG-8100 | | 0.92 | 0.871 | 108 | 53.8 | 2 | 38.7 |
| EG 8150 | | 0.55 | 0.869 | 120 | 59 | 2.04 | 40.0 |
| Dowlex 2045-E | Ziegler-LLDPE with Same Co-monomer | 1 | 0.92 | — | — | — | — |

Table 2.2. Characteristics of Unprocessed LLDPE (as received) (measured in Aston's PPP Labs)*

| Polymer | 1-octene SCB Wt% | MI (g/10min) | MFR | t-Vinylene (mol/L) | Vinyl (mol/L) | Vinylidene (mol/L) | Total Double Bond (mol/L) | Carbonyl (mol/L) |
|--------------------------|------------------|--------------|------|--------------------|---------------|--------------------|---------------------------|------------------|
| FM-1570 | 11.6 | 1.43 | 38.6 | 0.24 | 0.09 | 0.22 | 0.55 | 0.04 |
| PL-1840 (Old) | 13.4 | 1.16 | 37.7 | 0.27 | 0.03 | 0.22 | 0.52 | 0.04 |
| PL-1840 (New) | - | 1.34 | 37.9 | 0.18 | 0.04 | 0.15 | 0.37 | 0.05 |
| PL-1880 | 17.1 | 1.10 | 33.8 | 0.24 | 0.03 | 0.20 | 0.47 | 0.04 |
| VP-8770 (Old) | 28.2 | 1.04 | 29.7 | 0.33 | 0.03 | 0.21 | 0.57 | 0.03 |
| VP-8770 (New) | - | 1.35 | 28.5 | 0.33 | 0.02 | 0.22 | 0.57 | 0.03 |
| EG8100 | 34.5 | 1.11 | 29.4 | 0.48 | 0.02 | 0.25 | 0.75 | 0.03 |
| EG8150 | 36.2 | 0.58 | 28.3 | - | - | - | - | - |
| Dowlex2045-E (Old Batch) | 10.5 | 1.21 | 35.9 | 0.06 | 0.25 | 0.08 | 0.39 | 0.01 |
| Dowlex2045-E (New Batch) | 9.6 | 1.15 | 29.5 | 0.06 | 0.19 | 0.07 | 0.32 | 0.02 |

* Refer to Sections 2.3.1.1, 2.3.2.1 and 2.3.2.2 of this Chapter for details of the measurements (the concentrations of double bonds and carbonyl groups were determined by FTIR based on literature values of extinction coefficients)

Table 2.3. Details of Antioxidants Used in this Work

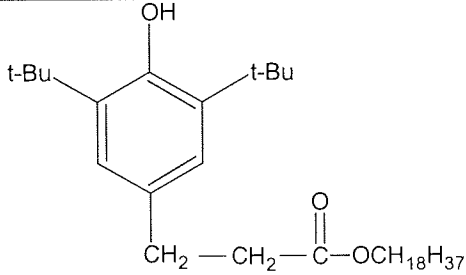
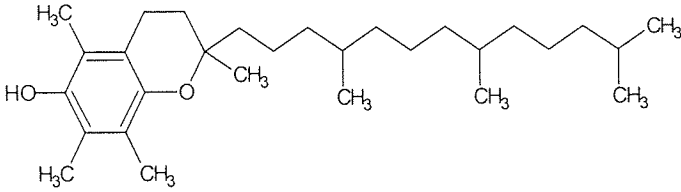
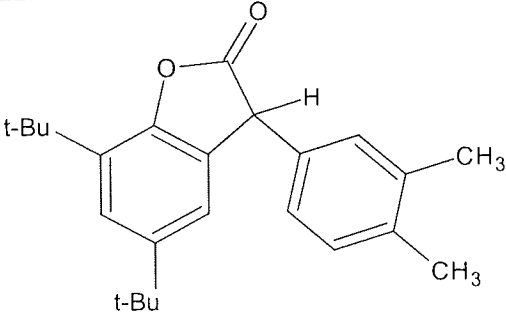
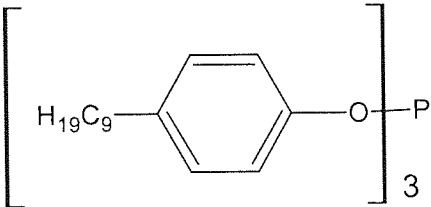
| Commercial Name | Chemical Structure and Name | Physical Properties | Supplier |
|-----------------------------|---|--|--------------------------------|
| Irganox 1076 (Irg 1076) |  <p>n-Octadecyl-3-(3',5'-di-t-butyl-4'-hydroxy- phenyl) propionate</p> | White Powder, Mw = 531 m.p. = 50~55°C | Ciba Specialty Chemicals |
| Irganox E 201 (Irg E201) |  <p>6-hydroxy-2,5-dimethyl-2-phytyl-7,8-benzochroman</p> | Brown Viscous Liquid, Mw = 431 | Ciba Specialty Chemicals |
| Irganox HP136 (HP136) |  <p>3-Aryl benzofuran-2-one</p> | White with Light Yellow Powder, Mw = 351 m.p. = 97~130°C | Ciba Specialty Chemicals |
| Weston 399 (W399) |  <p>Tris-(nonylphenyl) phosphite</p> | Clear Viscous Liquid, Mw = 688 | GE Specialty Chemicals |

Table 2.3, Continued ...

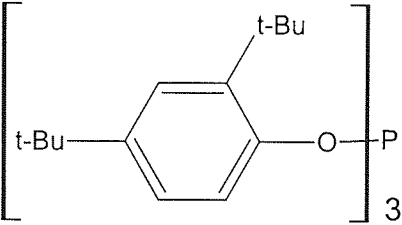
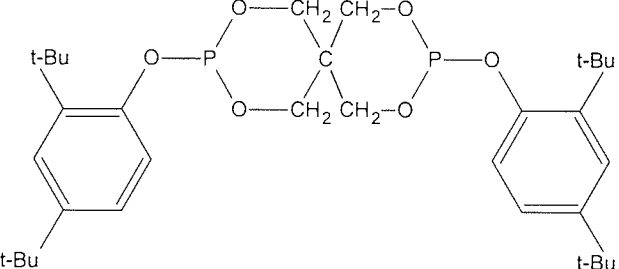
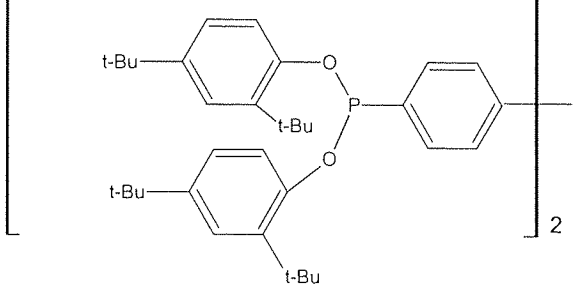
| | | | |
|--------------------------------------|---|---|---|
| <p>Irgafos 168 (Irg 168)</p> |  <p><i>Tris</i>-(2,4-di-tert-butylphenyl) phosphite</p> | <p>White Powder, Mw = 647 m.p. = 180~186°C</p> | <p>Ciba Specialty Chemicals</p> |
| <p>Ultranox 626 (Ultr626)</p> |  <p><i>bis</i>-(2,4-di-t-butylphenyl) pentaerythritol diphosphite</p> | <p>White Powder, Mw = 604 m.p. = 160~175 °C</p> | <p>GE Specialty Chemicals</p> |
| <p>Irgafos P-EPQ (Irg P-EPQ)</p> |  <p>Phosphorous acid, [1,1'-biphenyl]-4,4'-diyl<i>bis</i>-tertarkis-[2,4-<i>bis</i>(1,1-dimethylethyl) phenyl] ester</p> | <p>Off-white Pellet Mw = 991 m.p. = 85~110 °C</p> | <p>Ciba Specialty Chemicals</p> |

Table 2.4. Details of Chemicals Used in this Work

| Name & Purity | Formula | Physical Properties | Supplier |
|---|--|--|----------|
| Trimethylolpropane ethoxylate (TMP) | $C_2H_5C[CH_2(OCH_2CH_2)_nOH]_3$ EO/OH = 20/3 | Liquid, Mn = 1014 d = 1.10 g/cm ³ | Aldrich |
| Dichloromethane (DCM, spectrophotometric) | CH ₂ Cl ₂ | Liquid, b.p. = 40°C d = 1.325 g/cm ³ | Aldrich |
| 1,2,4-trichlorobenzene (TCB, GC grade, 99 ⁺ %) | C ₆ H ₃ Cl ₃ | Liquid, b.p. = 214 °C d = 1.454 g/cm ³ | Aldrich |
| Deuterated 1,4-Dichlorobenzene (DCB-d ₄) | C ₄ D ₄ Cl ₂ | Liquid, Mw = 127 m.p. = 54~56 °C | Aldrich |

Table 2.5. Different Temperature Profiles Used for the Twin-Screw Extrusions of LLDPE
(Profiles of T₂~T₅ were used respectively for all five extrusion passes for each polymer)

| Profile Number | Die Temp. (°C) | Zone Temperature (°C) | | | | | | | | Output Rate (kg/hr) | Atmosphere & Extrusion Passes |
|---|----------------------|-----------------------|-----|-----|-----|-----|-----|-----|-----|---------------------------|--|
| | Die | 8 | 7 | 6 | 5 | 4 | 3 | 2 | 1 | | |
| Profile for Pass-zero (P ₀) Stabilisation | | | | | | | | | | | |
| T ₁ | 210 | 210 | 205 | 200 | 195 | 190 | 185 | 180 | 175 | 4.0 | Nitrogen |
| Profile for Multi-pass Extrusions | | | | | | | | | | | |
| T ₂ | 210 | 210 | 205 | 200 | 195 | 190 | 185 | 180 | 175 | 4.0 | Air, P1~P5 |
| T ₃ | 235 | 235 | 225 | 215 | 210 | 200 | 190 | 180 | 175 | 4.8 | Air, P1~P5 |
| T ₄ | 265 | 265 | 250 | 235 | 220 | 210 | 200 | 190 | 175 | 4.8 | Air, P1~P5 |
| T ₅ | 285 | 285 | 270 | 255 | 240 | 225 | 210 | 190 | 175 | 4.8 | Air, P1~P5 |

Table 2.6. A Typical Example Showing the Characteristics of TSE Extrusion for LLDPE Polymers

| TSE Zone Temperature (°C) | | | | | | | | |
|---------------------------|-----|------------------|-------------|---------------------|-------------|----------------|----------------|----------------------|
| Die | 8 | 7 | 6 | 5 | 4 | 3 | 2 | 1 |
| 265 | 265 | 250 | 235 | 220 | 210 | 200 | 190 | 175 |
| Polymer Code | | Extrusion Passes | Screw Speed | Output Rate (kg/hr) | Current (A) | Pressure (psi) | Melt Tem. (°C) | Extrudate Appearance |
| PL -1840 | | 1 | 100rpm | 4.8 | 11.2 | 530+ <u>25</u> | 261.6 | Uniform |
| | | 2 | 100rpm | 4.8 | 11.2 | 510+ <u>25</u> | 261.7 | Uniform |
| | | 3 | 100rpm | 4.8 | 11.5 | 530+ <u>20</u> | 262.0 | Uniform |
| | | 4 | 100rpm | 4.8 | 11.8 | 550+ <u>20</u> | 263.0 | Uniform |
| | | 5 | 100rpm | 4.8 | 11.8 | 550+ <u>30</u> | 263.2 | Uniform |
| TSE Zone Temperature (°C) | | | | | | | | |
| Die | 8 | 7 | 6 | 5 | 4 | 3 | 2 | 1 |
| 265 | 265 | 250 | 235 | 220 | 210 | 200 | 190 | 175 |
| Polymer Code | | Extrusion | Screw | Output | Current | Pressure | Melt | Extrudate |
| | | Passes | Speed | Rate (kg/hr) | (A) | (psi) | Tem. (°C) | Appearance |
| Dowlex2045-E | | 1 | 100rpm | 4.8 | 11.0 | 640+ <u>30</u> | 263.2 | Uniform |
| | | 2 | 100rpm | 4.8 | 11.5 | 650+ <u>20</u> | 266.0 | Uniform |
| | | 3 | 100rpm | 4.8 | 11.5 | 650+ <u>20</u> | 266.5 | Uniform |
| | | 4 | 100rpm | 4.8 | 12.0 | 670+ <u>20</u> | 267.4 | Uniform |
| | | 5 | 100rpm | 4.8 | 12.5 | 700+ <u>20</u> | 268.1 | Uniform |

Table 2.7. Twin-Screw Extrusion of LLDPE with Antioxidants (100rpm)

| Antioxidant Composition [ppm] | Polymer Code | Compounding | | Multiple Extrusion | |
|--|--------------------|----------------|---------------|--------------------|---------------|
| | | Pass | Die Tem. (°C) | Pass | Die Tem. (°C) |
| Irg1076 [900] | FM-1570 | P ₀ | 210 | P1~P5 | 265 |
| | PL-1840 | P ₀ | 210 | P1~P5 | 265 |
| | VP-8770 | P ₀ | 210 | P1~P5 | 265 |
| | Dowlex2045-E | P ₀ | 210 | P1~P5 | 265 |
| HP136 [500] | FM-1570 | P ₀ | 210 | P1~P5 | 265 |
| | PL-1840 | P ₀ | 210 | P1~P5 | 265 |
| | VP-8770 | P ₀ | 210 | P1~P5 | 265 |
| | Dowlex2045-E (New) | P ₀ | 210 | P1~P5 | 265 |
| Ultranox626 [1000] | FM-1570 | P ₀ | 210 | P1~P5 | 265 |
| | PL-1840 | P ₀ | 210 | P1~P5 | 265 |
| | VP-8770 | P ₀ | 210 | P1~P5 | 265 |
| | Dowlex2045-E (New) | P ₀ | 210 | P1~P5 | 265 |
| IrganoxE201 [300] | FM-1570 | P ₀ | 210 | P1~P5 | 265 |
| | PL-1840 | P ₀ | 210 | P1~P5 | 265 |
| | VP-8770 | P ₀ | 210 | P1~P5 | 265 |
| | Dowlex2045-E (New) | P ₀ | 210 | P1~P5 | 265 |
| Irg1076:Irgafos168 [500:1250] | PL-1840 | P ₀ | 210 | P1~P5 | 265 |
| Irg1076:Irg168:HP136 [500:1250:250] | PL-1840 | P ₀ | 210 | P1~P5 | 265 |
| Irg1076:Ultra626 [500:600] | PL-1840 | P ₀ | 210 | P1~P5 | 265 |
| Irg1076:Ultra626:HP136 [500:600:250] | PL-1840 | P ₀ | 210 | P1~P5 | 265 |
| Irg1076:IrgafosP-EPQ [500:1000] | PL-1840 | P ₀ | 210 | P1~P5 | 265 |
| Irg1076:P-EPQ:HP136 [500:1000:250] | PL-1840 | P ₀ | 210 | P1~P5 | 265 |
| Irg1076:Weston399 [500:1330] | PL-1840 | P ₀ | 210 | P1~P5 | 265 |
| Irg1076:W399:HP136 [500:1330:250] | PL-1840 | P ₀ | 210 | P1~P5 | 265 |
| IrgE201:Ultra626 [300:600] | PL-1840 | P ₀ | 210 | P1~P5 | 265 |
| IrgE201:Ultr626:HP136 [300:600:250] | PL-1840 | P ₀ | 210 | P1~P5 | 265 |
| IrgE201:Ultr626:TMP [300:600:450] | PL-1840 | P ₀ | 210 | P1~P5 | 265 |
| Irg XP 490 [1500] (Irg1076: Irgfos P-EPQ: HP136 = 3: 2: 1) | PL-1840 | P ₀ | 210 | P1~P5 | 265 |
| | VP-8770 | P ₀ | 210 | P1~P5 | 265 |
| | Dowlex2045-E (New) | P ₀ | 210 | P1~P5 | 265 |
| Irg HP 2921 [1750] (Irg1076: Irgfos 168: HP136 = 2: 4: 1) | PL-1840 | P ₀ | 210 | P1~P5 | 265 |
| | VP-8770 | P ₀ | 210 | P1~P5 | 265 |
| | Dowlex2045-E (New) | P ₀ | 210 | P1~P5 | 265 |

Table 2.8. Deviation in MI and HMI Measurements Determined from Replicate Measurements of Representative Polymer Samples

| Deviation of MI | | | | | | | | |
|---|-----------------|------|----------------|-----------------------|-----------------------|------------|-----------|----------------|
| Polymer | Processing | No.* | MI (g/min) | Mean (X) (g/10min) | Standard Deviation | RSD (%) | 95% CL | Value Range |
| Virgin PL-1840 | TR, 10min | 1 | 1.23 | 1.23 | 0.01 | 0.81% | 0.02 | 1.23± 0.02 |
| | 220°C | 2 | 1.23 | | | | | |
| | 60rpm | 3 | 1.22 | | | | | |
| Virgin FM1570 | TSE, 100rpm | 1 | 1.42 | 1.42 | 0.01 | 0.71% | 0.02 | 1.42± 0.02 |
| | 265°C, 4.8kg/hr | 2 | 1.44 | | | | | |
| | P1 | 3 | 1.41 | | | | | |
| Stabilized VP-8770 Irg1076 (900ppm) | TSE, 100rpm | 1 | 0.89 | 0.87 | 0.02 | 2.30% | 0.04 | 0.87± 0.04 |
| | 265°C, 4.8kg/hr | 2 | 0.88 | | | | | |
| | P3 | 3 | 0.85 | | | | | |
| Deviation of HMI | | | | | | | | |
| Polymer | Processing | No.* | HMI (g/min) | Mean (X) (g/10min) | Standard Deviation | RSD (%) | 95% CL | Value Range |
| Virgin PL-1840 | TR, 10min | 1 | 45.5 | 45.3 | 0.14 | 0.31% | 0.3 | 45.3 ± 0.3 |
| | 220°C | 2 | 45.2 | | | | | |
| | 60rpm | 3 | 45.2 | | | | | |
| Virgin FM-1570 | TSE, 100rpm | 1 | 56.1 | 56.4 | 0.29 | 0.51% | 0.7 | 56.4 ± 0.7 |
| | 265°C, 4.8kg/hr | 2 | 56.8 | | | | | |
| | P1 | 3 | 56.3 | | | | | |
| Stabilised VP-8770 Irg1076 (900ppm) | TSE, 100rpm | 1 | 31.6 | 31.3 | 0.25 | 0.80% | 0.6 | 31.3 ± 0.6 |
| | 265°C, 4.8kg/hr | 2 | 31.2 | | | | | |
| | P3 | 3 | 31 | | | | | |

* The numbers 1, 2, 3 are three replicate measurements for the same representative sample

Table 2.9. Deviation of MI and HMI Measurements Determined from Repeat Processing of Representative Polymer Samples under the Same Conditions

| Deviation of MI | | | | | | | | |
|--|--------------------------------------|------|----------------|-----------------------|-----------------------|------------|-----------|----------------|
| Polymer | Processing | No.* | MI (g/min) | Mean (X) (g/10min) | Standard Deviation | RSD (%) | 95% CL | Value Range |
| Virgin VP-8770 | TR, 10min 270°C 60rpm | 1 | 0.94 | 0.93 | 0.01 | 1.08% | 0.03 | 0.93 ± 0.03 |
| | | 2 | 0.92 | | | | | |
| | | 3 | 0.94 | | | | | |
| Virgin Dowlex2045-E | TSE, 100rpm 210°C, 4.0kg/hr P3 | 1 | 0.41 | 0.42 | 0.01 | 2.38% | 0.09 | 0.42 ± 0.09 |
| | | 2 | 0.43 | | | | | |
| PL-1840 IrgE201: U626= 300:600 (ppm) | TSE, 100rpm 265°C, 4.8kg/hr P3 | 1 | 1.19 | 1.17 | 0.02 | 1.71% | 0.18 | 1.17 ± 0.18 |
| | | 2 | 1.15 | | | | | |
| Deviation of HMI | | | | | | | | |
| Polymer | Processing | No.* | HMI (g/min) | Mean (X) (g/10min) | Standard Deviation | RSD (%) | 95% CL | Value Range |
| Virgin VP-8770 | TR, 10min 270°C 60rpm | 1 | 34.5 | 34.2 | 0.17 | 0.50% | 0.4 | 34.2 ± 0.4 |
| | | 2 | 34.1 | | | | | |
| | | 3 | 34.1 | | | | | |
| Virgin Dowlex2045-E | TSE, 100rpm 210°C, 4.0kg/hr P3 | 1 | 32.0 | 31.9 | 0.16 | 0.50% | 1.4 | 31.9 ± 1.4 |
| | | 2 | 31.7 | | | | | |
| PL-1840 IrgE201: U626= 300:600 (ppm) | TSE, 100rpm 265°C, 4.8kg/hr P3 | 1 | 49.6 | 49.6 | 0.1 | 0.20% | 0.6 | 49.6 ± 0.6 |
| | | 2 | 49.5 | | | | | |

* The numbers 1, 2, 3 are the samples of the same polymer repeatedly processed under the same processing conditions

Table 2.10. IR-Extinction Coefficients of Double Bonds and Some Carbonyl Containing Compounds

| Group Type | Structure | IR Absorbance (cm^{-1}) | Extinction Coefficient from IR (L/mol.cm) | Reference |
|----------------|---------------------|---------------------------------------|--|-----------|
| Trans-vinylene | -CH=CH- | 965 | $\epsilon_{965} = 100 \pm 7$ (Olefin) | 46 |
| Vinyl | -CH=CH ₂ | 908 | $\epsilon_{908} = 122 \pm 7$ (Olefin) | 46 |
| Vinylidene | >C=CH ₂ | 889 | $\epsilon_{889} = 158 \pm 7$ (Olefin) | 46 |
| Carboxyl Acid | -COOH | 1713 | $\epsilon_{1713} = 710$ (Lauric acid) | 135 |
| Ketone | -CO- | 1720 | $\epsilon_{1720} = 275$ (2-undecanone) | 135 |
| Ester | -COO- | 1735 | $\epsilon_{1735} = 340$ (Methyl butyrate) | 135 |

Table 2.11. Deviation of the Double Bond Concentrations Determined from the Measurements of Different Samples Taken out from the Same Processed Polymer

| Polymer | Type of Double Bond | No.* | Concentration** | Mean (X) | Standard Deviation | RSD (%) | 95% CL | Value Range |
|---|---------------------|------|-----------------|----------|--------------------|---------|--------|-------------------|
| TR-Processed FM-1570 270°C, 60rpm 10min | trans-Vinylene | 1 | 0.128 | 0.128 | 0.001 | 1.01% | 0.003 | 0.128 \pm 0.003 |
| | | 2 | 0.129 | | | | | |
| | | 3 | 0.126 | | | | | |
| | Vinyl | 1 | 0.020 | 0.018 | 0.002 | 9.62% | 0.004 | 0.018 \pm 0.004 |
| | | 2 | 0.017 | | | | | |
| | | 3 | 0.016 | | | | | |
| | Vinylidene | 1 | 0.215 | 0.213 | 0.004 | 1.67% | 0.009 | 0.213 \pm 0.009 |
| | | 2 | 0.208 | | | | | |
| | | 3 | 0.216 | | | | | |
| TSE Processed PL-1840 265°C, 100rpm 4.8kg/hr P3 | trans-Vinylene | 1 | 0.199 | 0.192 | 0.005 | 2.84% | 0.012 | 0.192 \pm 0.012 |
| | | 2 | 0.186 | | | | | |
| | | 3 | 0.190 | | | | | |
| | Vinyl | 1 | 0.013 | 0.011 | 0.001 | 11.74% | 0.003 | 0.011 \pm 0.003 |
| | | 2 | 0.011 | | | | | |
| | | 3 | 0.010 | | | | | |
| | Vinylidene | 1 | 0.206 | 0.212 | 0.005 | 2.33% | 0.012 | 0.212 \pm 0.012 |
| | | 2 | 0.213 | | | | | |
| | | 3 | 0.218 | | | | | |
| TSE Processed PL-1840 (900ppm Irg1076) 265°C, 100rpm 4.8kg/hr, P3 | trans-Vinylene | 1 | 0.257 | 0.254 | 0.002 | 0.94% | 0.006 | 0.254 \pm 0.006 |
| | | 2 | 0.252 | | | | | |
| | | 3 | 0.252 | | | | | |
| | Vinyl | 1 | 0.014 | 0.015 | 0.001 | 6.67% | 0.003 | 0.015 \pm 0.003 |
| | | 2 | 0.016 | | | | | |
| | | 3 | 0.016 | | | | | |
| | Vinylidene | 1 | 0.222 | 0.219 | 0.002 | 0.95% | 0.005 | 0.219 \pm 0.005 |
| | | 2 | 0.217 | | | | | |
| | | 3 | 0.219 | | | | | |

* The number is that of a different IR sample of the same representative processed polymer

** The value is absorption area index based on a reference peak for TR processed sample; the value is absolute concentration (mol/L) based on IR extinction coefficients for TSE processed samples

Table 2.12. Deviation of the Double Bond Concentrations Determined from the Samples of Repeat Processing of Representative Polymer Samples under the Same Conditions

| Polymer | Type of Double Bond | No.* | Concentration** | Mean (X) | Standard Deviation | RSD (%) | 95% CL | Value Range |
|--|---------------------|------|-----------------|----------|--------------------|---------|--------|---------------|
| TR Processed VP-8770 270°C, 60rpm 10min | trans-Vinylene | 1 | 0.213 | 0.205 | 0.007 | 3.65% | 0.019 | 0.205 ± 0.019 |
| | | 2 | 0.207 | | | | | |
| | | 3 | 0.195 | | | | | |
| | Vinyl | 1 | 0.058 | 0.061 | 0.004 | 6.50% | 0.01 | 0.061 ± 0.010 |
| | | 2 | 0.067 | | | | | |
| | | 3 | 0.058 | | | | | |
| | Vinylidene | 1 | 0.456 | 0.462 | 0.018 | 3.95% | 0.045 | 0.462 ± 0.045 |
| | | 2 | 0.486 | | | | | |
| | | 3 | 0.442 | | | | | |
| TSE Processed Dowlex2045-E 210°C, 100rpm 4.0kg/hr P3 | trans-Vinylene | 1 | 0.057 | 0.056 | 0.001 | 1.79% | 0.009 | 0.056 ± 0.009 |
| | | 2 | 0.055 | | | | | |
| | Vinyl | 1 | 0.240 | 0.238 | 0.003 | 1.07% | 0.023 | 0.238 ± 0.023 |
| | | 2 | 0.235 | | | | | |
| | Vinylidene | 1 | 0.070 | 0.072 | 0.002 | 2.20% | 0.014 | 0.072 ± 0.014 |
| | | 2 | 0.073 | | | | | |
| TSE Processed PL-1840 IrgE201:Ultr626 300:600 (ppm) 265°C, 100rpm 4.8kg/hr, P3 | trans-Vinylene | 1 | 0.245 | 0.247 | 0.002 | 0.64% | 0.014 | 0.247 ± 0.014 |
| | | 2 | 0.248 | | | | | |
| | Vinyl | 1 | 0.018 | 0.019 | 0.001 | 5.26% | 0.009 | 0.019 ± 0.009 |
| | | 2 | 0.020 | | | | | |
| | Vinylidene | 1 | 0.218 | 0.218 | 0.001 | 0.32% | 0.006 | 0.218 ± 0.006 |
| | | 2 | 0.217 | | | | | |

* The number is that of times of repeat processing for the same representative polymer

** The value is absorption area index based on a reference peak for TR processed samples; the value is absolute concentration (mol/L) based on IR extinction coefficients for TSE processed samples

Table 2.13. Deviation of the Carbonyl Concentration Determined from Different Samples of the Same Processed Polymer and from Repeat Processing of a Representative Polymers under the Same Conditions

| Deviation of Carbonyl Concentration from Different Samples | | | | | | | | |
|--|--------------------------------------|------|----------------------|-------------|-----------------------|------------|-----------|----------------|
| Polymer | Processing | No.* | Concen- tration** | Mean (X) | Standard Deviation | RSD (%) | 95% CL | Value Range |
| Virgin FM-1570 | TR, 10min 270°C 60rpm | 1 | 0.883 | 0.874 | 0.007 | 0.76% | 0.017 | 0.874 ± 0.017 |
| | | 2 | 0.868 | | | | | |
| | | 3 | 0.870 | | | | | |
| Virgin PL-1840 | TSE, 100rpm 265°C, 4.8kg/hr P3 | 1 | 0.061 | 0.063 | 0.001 | 2.05% | 0.003 | 0.063 ± 0.003 |
| | | 2 | 0.063 | | | | | |
| | | 3 | 0.064 | | | | | |
| Stabilised PL-1840 Irg1076 (900ppm) | TSE, 100rpm 265°C, 4.8kg/hr P3 | 1 | 0.116 | 0.117 | 0.001 | 1.21% | 0.004 | 0.117 ± 0.004 |
| | | 2 | 0.119 | | | | | |
| | | 3 | 0.116 | | | | | |
| Deviation of Carbonyl Concentration — Replicate Processing | | | | | | | | |
| Polymer | Processing | No.* | Concen- tration** | Mean (X) | Standard Deviation | RSD (%) | 95% CL | Value Range |
| Virgin VP-8770 | TR, 10min 270°C 60rpm | 1 | 1.119 | 1.122 | 0.005 | 0.40% | 0.011 | 1.122 ± 0.011 |
| | | 2 | 1.128 | | | | | |
| | | 3 | 1.118 | | | | | |
| Virgin Dowlex2045-E | TSE, 100rpm 210°C, 4.0kg/hr P3 | 1 | 0.030 | 0.031 | 0.001 | 2.28% | 0.006 | 0.031 ± 0.006 |
| | | 2 | 0.031 | | | | | |
| PL-1840 IrgE201: U626= 300:600 (ppm) | TSE, 100rpm 265°C, 4.8kg/hr P3 | 1 | 0.048 | 0.051 | 0.003 | 5.88% | 0.027 | 0.051 ± 0.027 |
| | | 2 | 0.054 | | | | | |

* The number is that of different IR samples of the same processed polymer, or the times of repeat processing for the same representative polymer under the same conditions

** The value is absorption area index based on a reference peak for TR processed samples; the value is absolute concentration (mol/L) based on IR extinction coefficients for TSE processed samples

Table 2.14. Deviation of the Branching Amount Determination Derived from Repeat Integration of the Same Sample and from Different Samples of the Same Representative Polymers

| Deviation of Branching Amount from Repeat Integration | | | | | | | | |
|---|-----------------|-------|------------------------|-------------|-----------------------|------------|-----------|----------------|
| Polymer | Processing | No.* | Content of SCB (w%) | Mean (X) | Standard Deviation | RSD (%) | 95% CL | Value Range |
| Virgin FM-1570 | Un-processed | 1 | 11.68 | 11.62 | 0.05 | 0.39% | 0.11 | 11.62 ± 0.11 |
| | | 2 | 11.62 | | | | | |
| | | 3 | 11.57 | | | | | |
| Virgin PL-1840 | TSE, 100rpm | 1 | 13.69 | 13.68 | 0.05 | 0.36% | 0.12 | 13.68 ± 0.12 |
| | 265°C, 4.8kg/hr | 2 | 13.74 | | | | | |
| | P3 | 3 | 13.62 | | | | | |
| Stabilised VP-8770 Irg1076 (900ppm) | TSE, 100rpm | 1 | 26.50 | 26.56 | 0.05 | 0.17% | 0.11 | 26.56 ± 0.11 |
| | 265°C, 4.8kg/hr | 2 | 26.61 | | | | | |
| | P3 | 3 | 26.57 | | | | | |
| Deviation of Branching Amount from Different Samples of The Same Polymer | | | | | | | | |
| Polymer | Processing | No.** | Content of SCB (w%) | Mean (X) | Standard Deviation | RSD (%) | 95% CL | Value Range |
| Virgin VP-8770 | Un-processed | 1 | 28.33 | 28.25 | 0.06 | 0.21% | 0.15 | 28.25 ± 0.15 |
| | | 2 | 28.23 | | | | | |
| | | 3 | 28.19 | | | | | |

* The number is that of repeat integration for the same ^{13}C -NMR spectrum

** The number is that of different ^{13}C -NMR samples for the same representative polymer

Table 2.15. Deviation of the Yellow Index Determined from Different Samples and Replicate Processing for the Representative Polymers

| Deviation of Yellow Index (YI) from Different Samples | | | | | | | | |
|---|-----------------|-------|------|-------------|-----------------------|------------|-----------|----------------|
| Polymer | Processing | No.* | YI | Mean (X) | Standard Deviation | RSD (%) | 95% CL | Value Range |
| VP-8770 Virgin | TSE, 210°C | 1 | 7.50 | 7.46 | 0.05 | 0.61% | 0.41 | 7.46 ± 0.41 |
| | P3 | 2 | 7.41 | | | | | |
| PL-1840 lrg1076 (900ppm) | TSE, 265°C | 1 | 5.33 | 5.36 | 0.03 | 0.48% | 0.23 | 5.36 ± 0.23 |
| | P5 | 2 | 5.38 | | | | | |
| PL-1840 lrg1076:lrg168 = 500:1250 (ppm) | TSE | 1 | 3.71 | 3.73 | 0.02 | 0.54% | 0.18 | 3.73 ± 0.18 |
| | 265°C P5 | 2 | 3.75 | | | | | |
| Deviation of Yellow Index (YI) from Repeat Processing | | | | | | | | |
| Polymer | Processing | No.** | YI | Mean (X) | Standard Deviation | RSD (%) | 95% CL | Value Range |
| Dowlex2045-E Virgin | TSE, 210°C | 1 | 7.91 | 7.86 | 0.05 | 0.64% | 0.45 | 7.86 ± 0.45 |
| | P3 | 2 | 7.81 | | | | | |
| PL-1840 lrgE201: U626 = 300:600 (ppm) | TSE | 1 | 7.36 | 7.46 | 0.10 | 1.28% | 0.86 | 7.46 ± 0.86 |
| | 265°C P3 | 2 | 7.55 | | | | | |

* The number is that of different plaque samples for the same processed polymer

** The number is that of plaque samples of repeat extrusion for the representative polymer under the same conditions

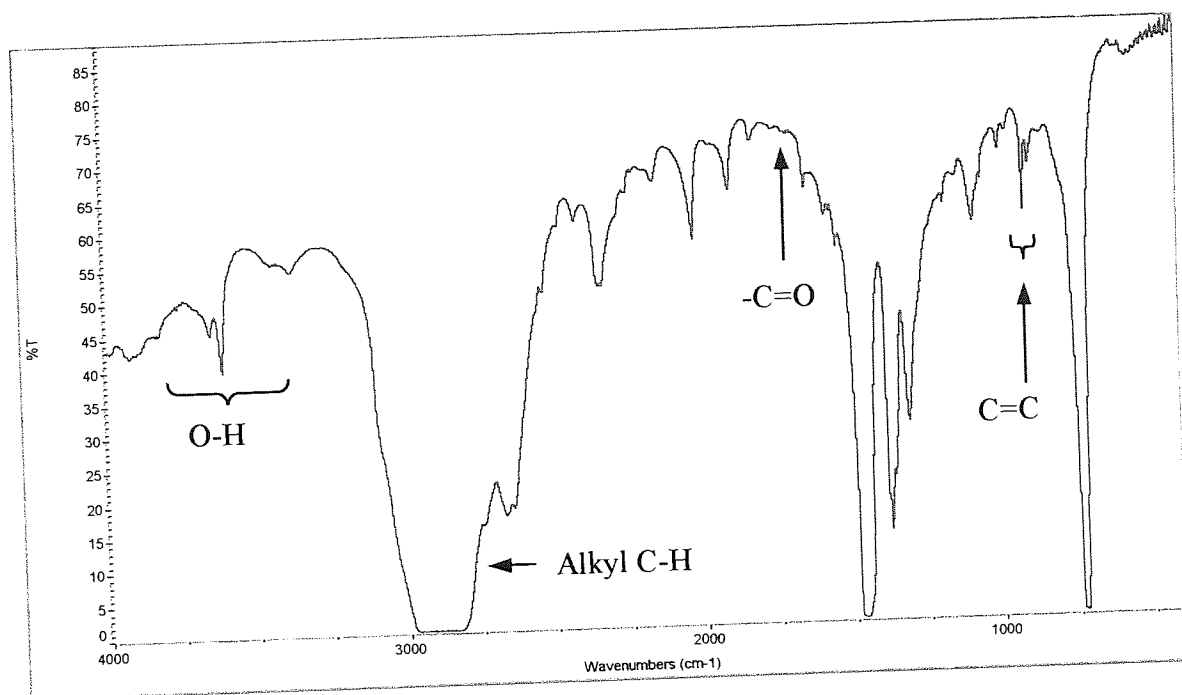


Figure 2.1. FTIR Spectrum of Virgin Dowlex2045-E (z-LLDPE)

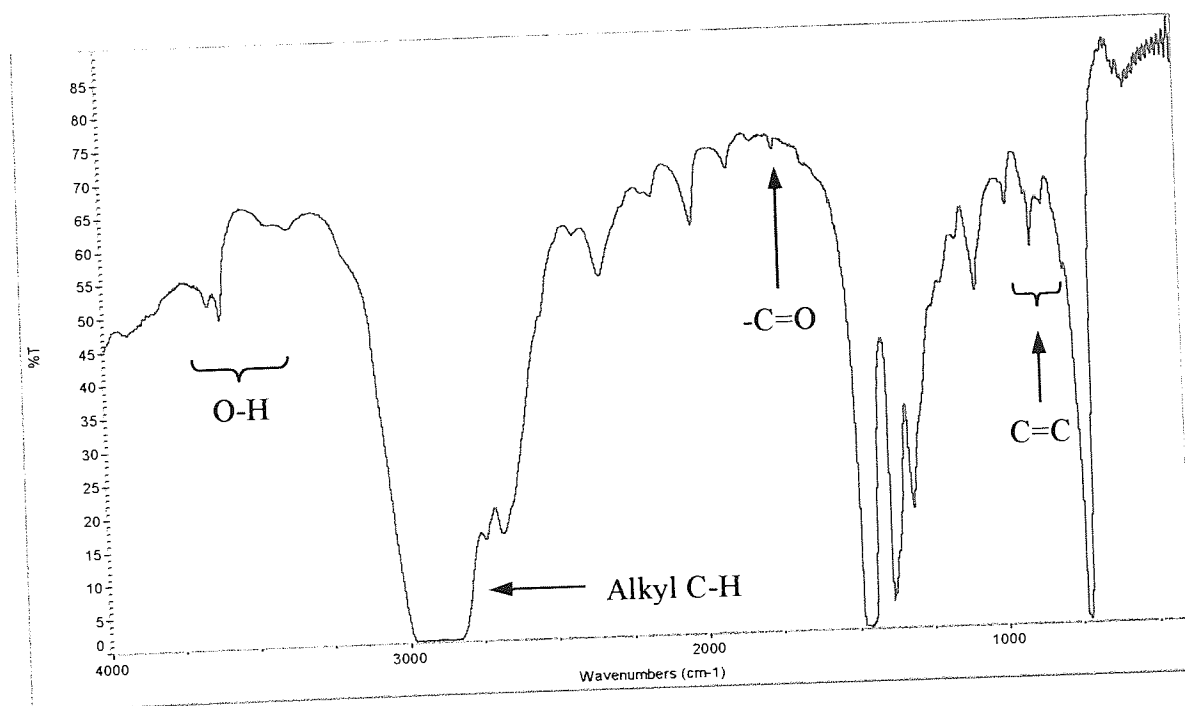


Figure 2.2. FTIR Spectrum of Virgin VP-8770 (m-LLDPE)

Twin Screw Configuration for Betol TSE

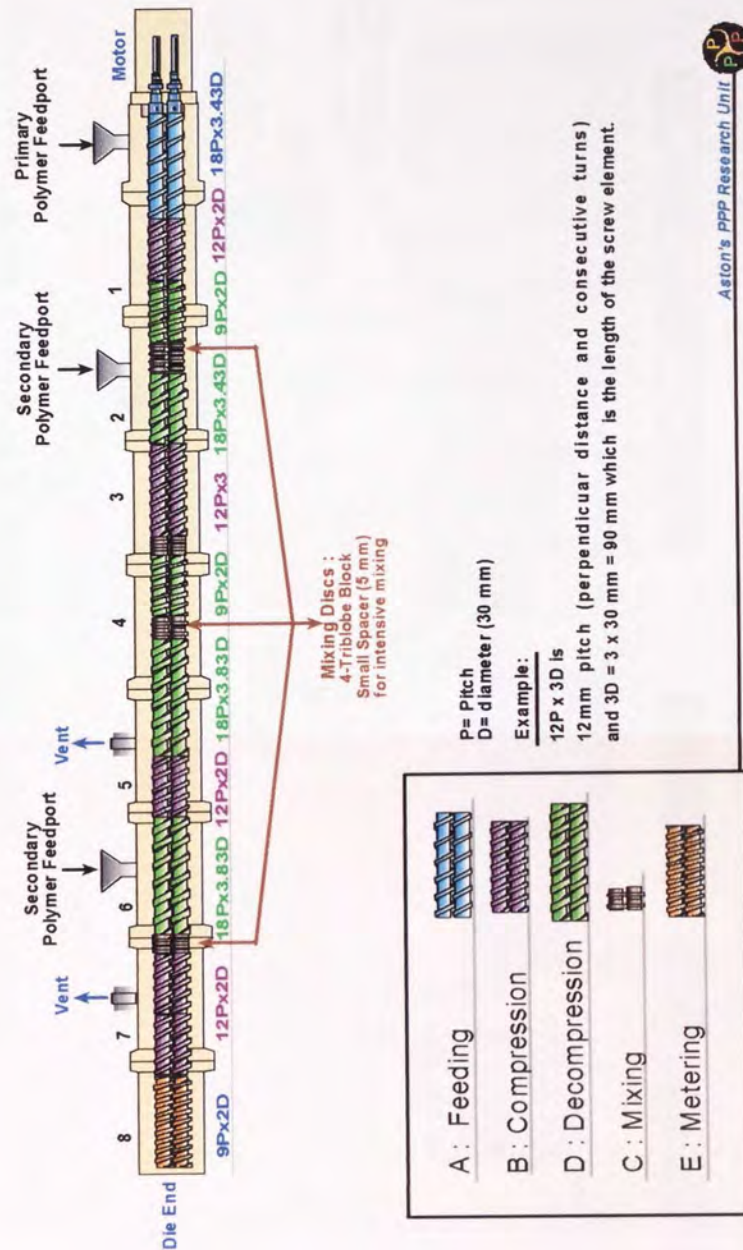


Figure 2.3. The Screw Configurations of the Co-rotating Screw in the BETOL 30mm Twin-Screw Extruder

PPP Res Unit's Twin Screw Extrusion Line

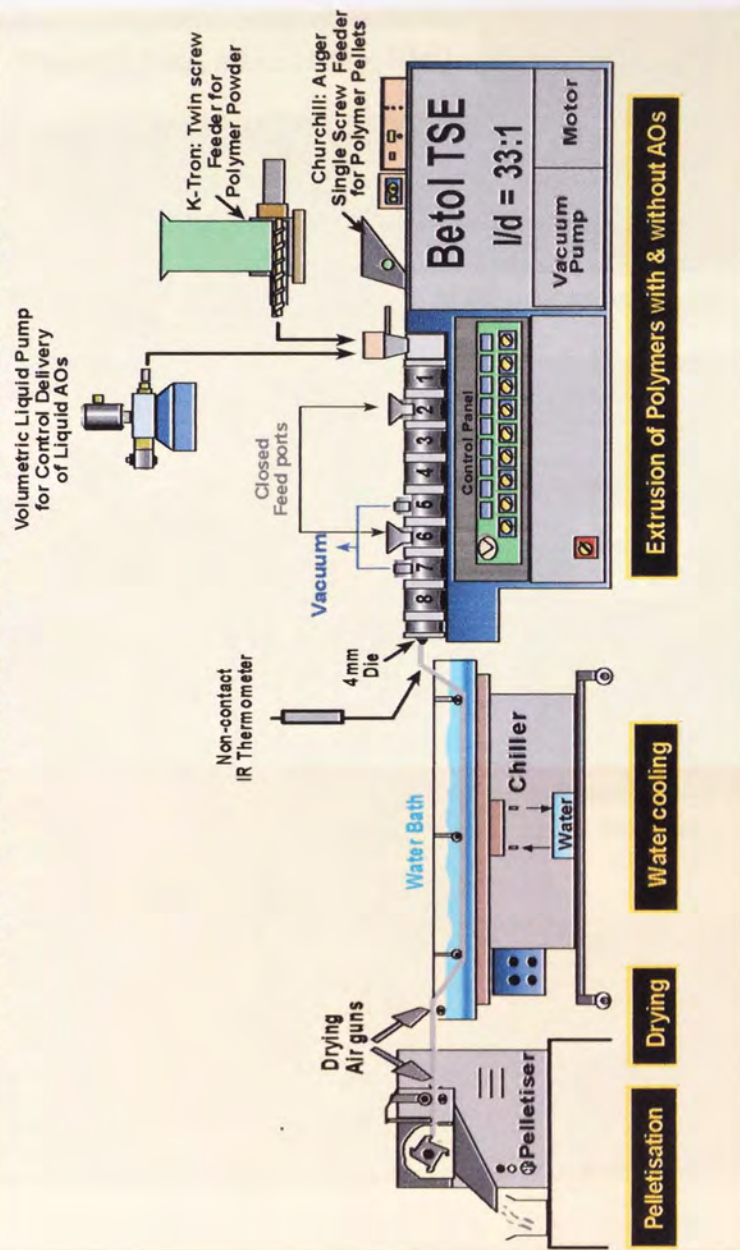


Figure 2.4. Twin-Screw Extruder Line and Arrangements Shown for P₀ Compounding and Multi-pass Extrusion

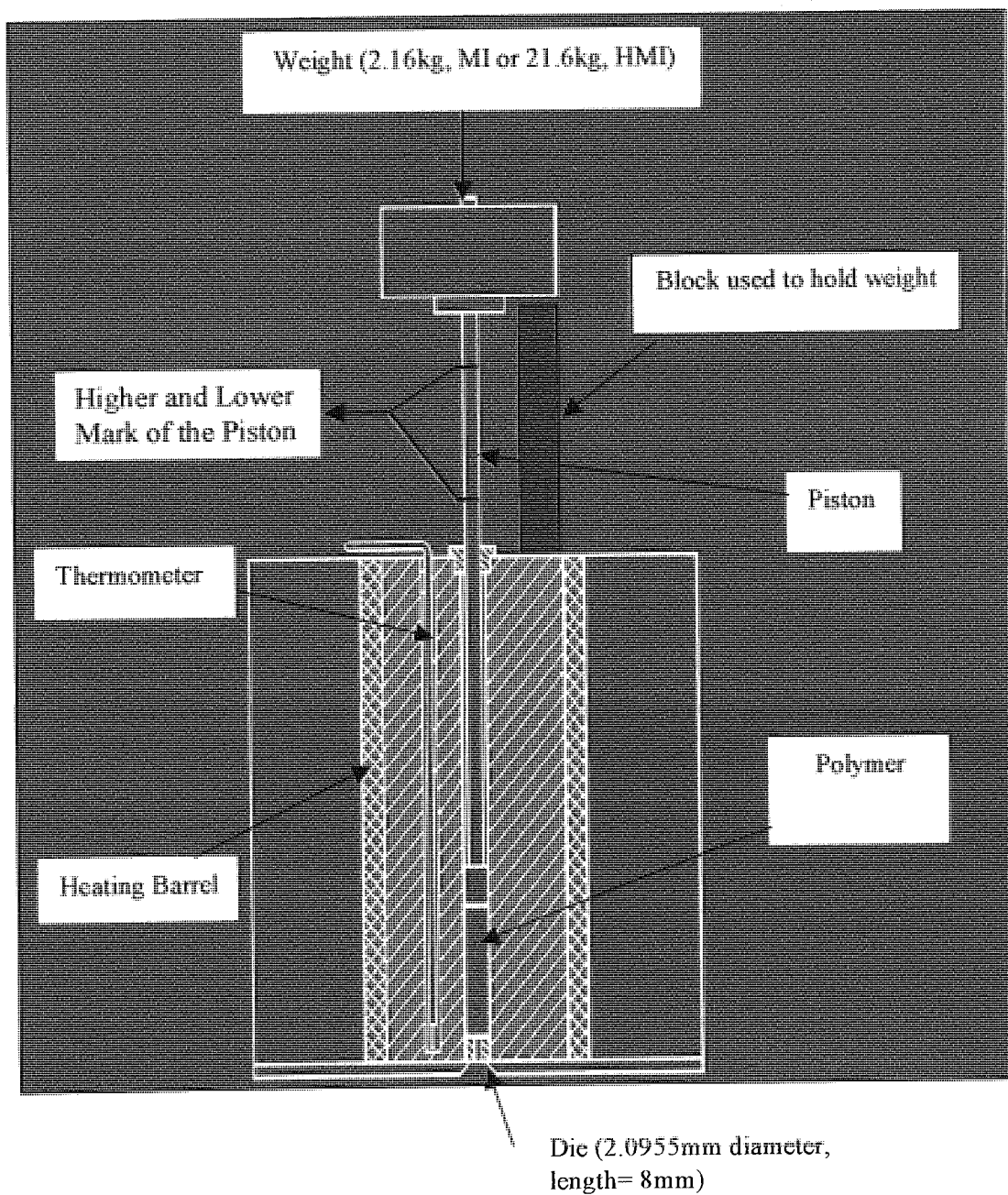


Figure 2.5. Schematic Diagram of the Davenport Melt Flow Indexer

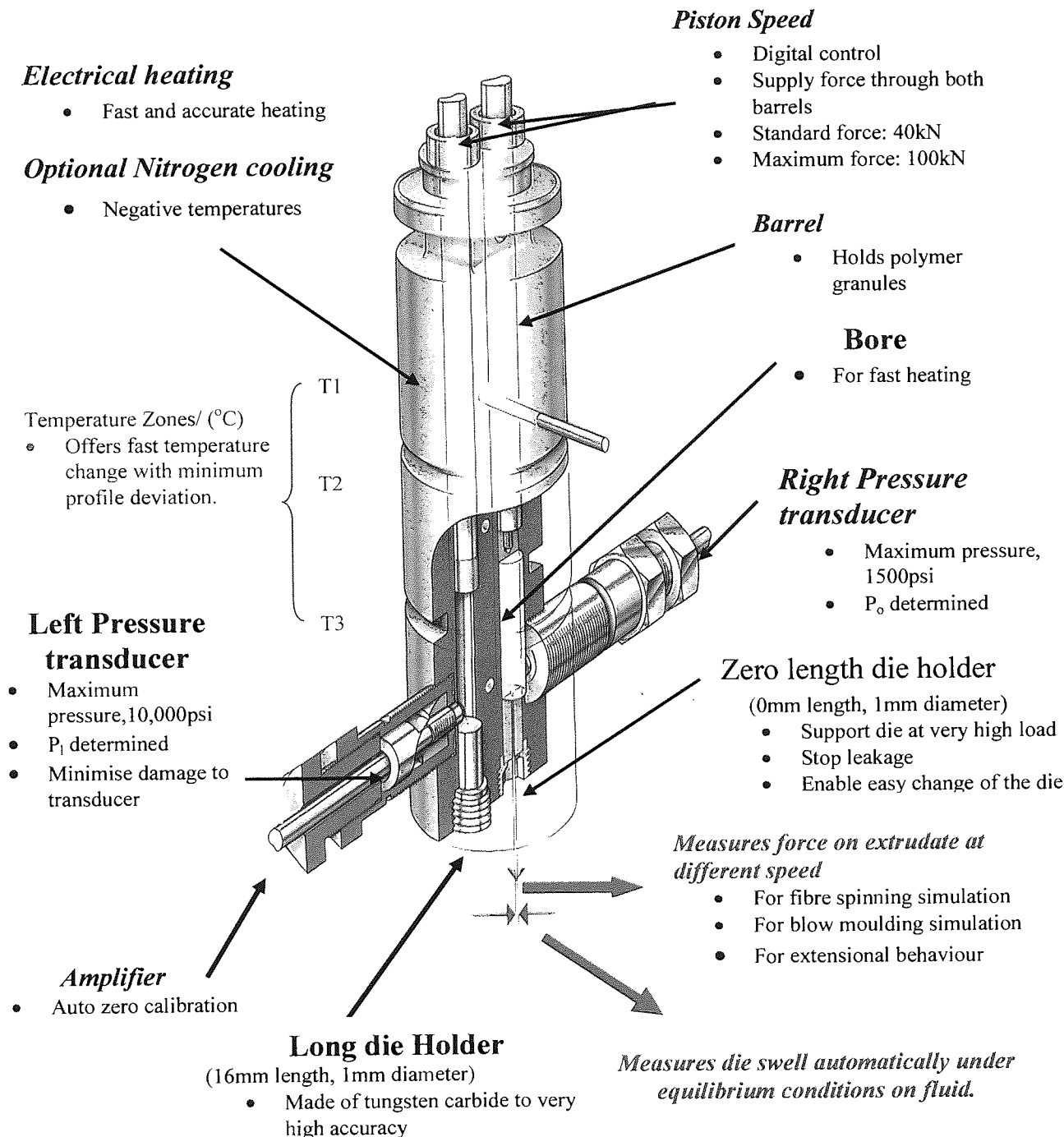


Figure 2.6. Schematic Diagram of the Rosand RH2000 Twin-Bore Capillary Rheometer. The schematic diagram is taken from Rosand on-line manual.

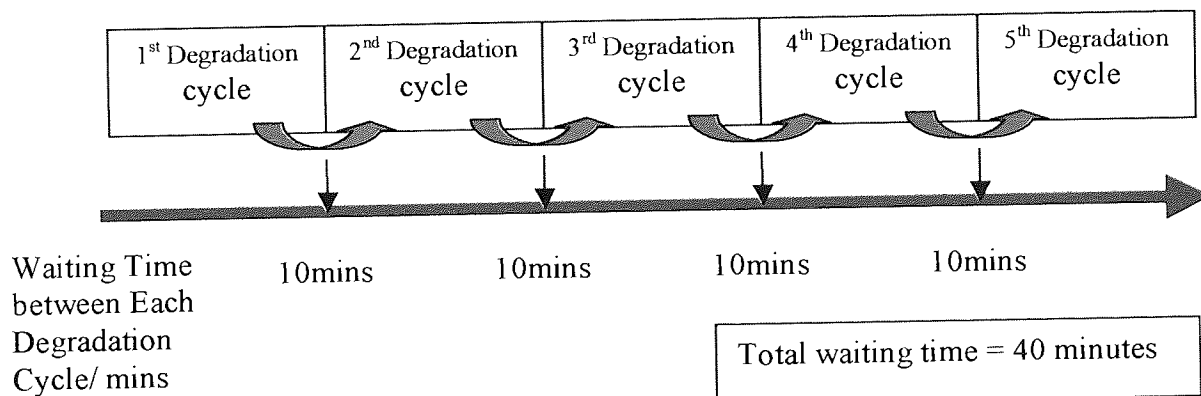
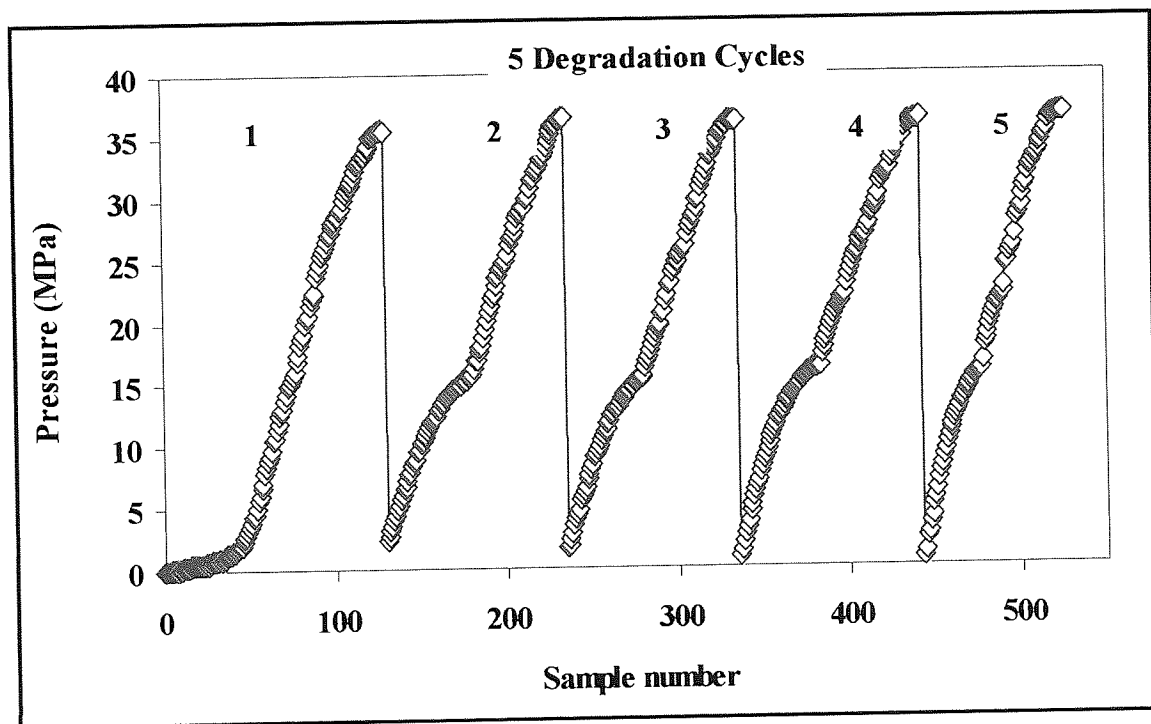


Figure 2.7. Outline of the Material Degradation Test of Virgin LLDPE Polymers Using the Rosand Twin-Bore Capillary Rheometer

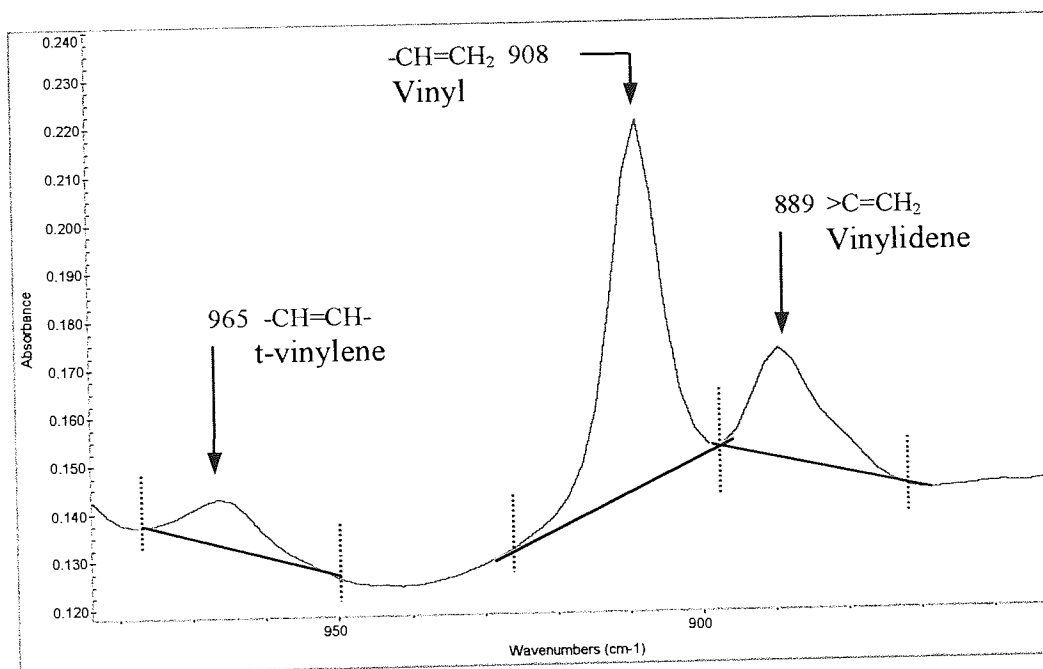


Figure 2.8. FTIR Spectrum of Virgin Dowlex2045-E (z-LLDPE) at the Region of Unsaturation

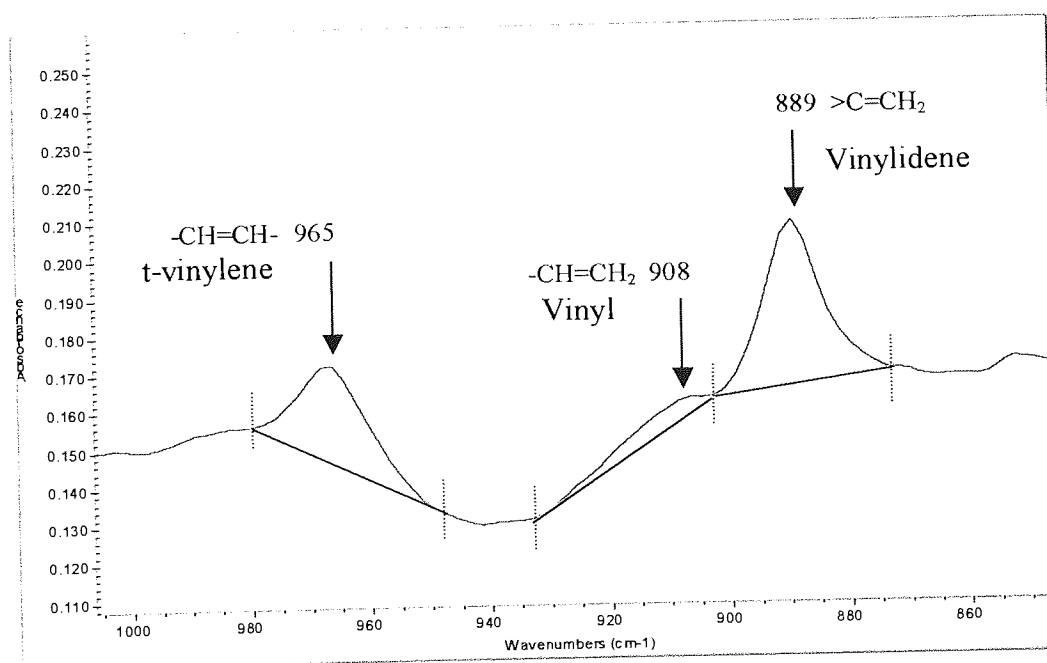


Figure 2.9. FTIR Spectrum of Virgin VP-8770 (m-LLDPE) at the Region of Unsaturation

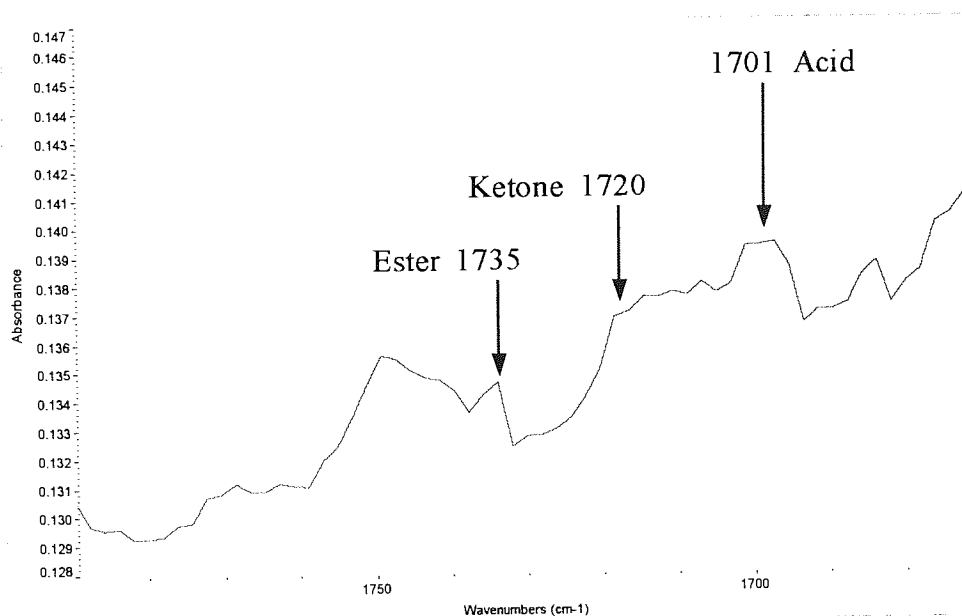


Figure 2.10. FTIR Spectrum of Virgin Dowlex2045-E (z-LLDPE) at Carbonyl Region

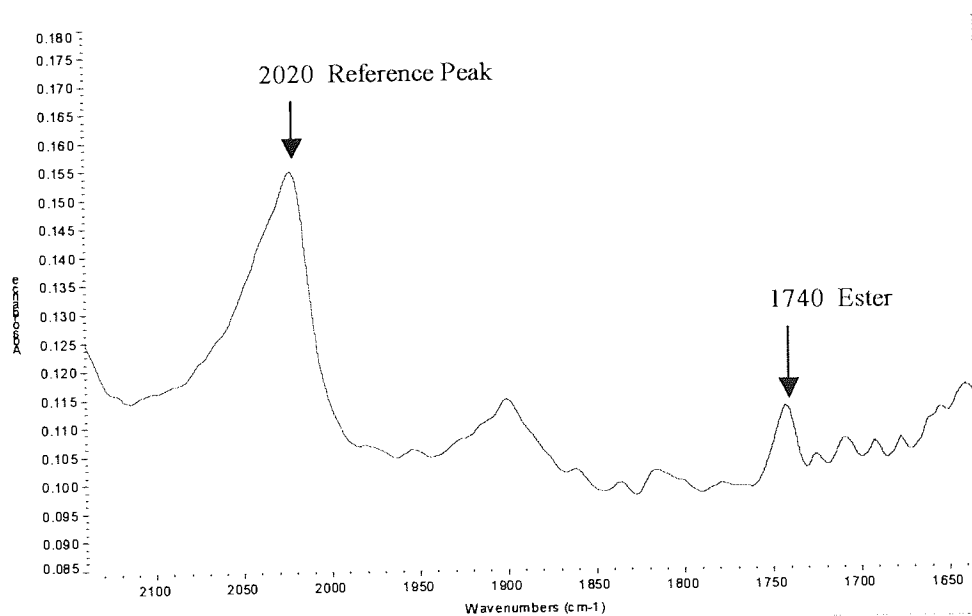


Figure 2.11. FTIR Spectrum of Virgin VP-8770 (m-LLDPE) at Carbonyl Region

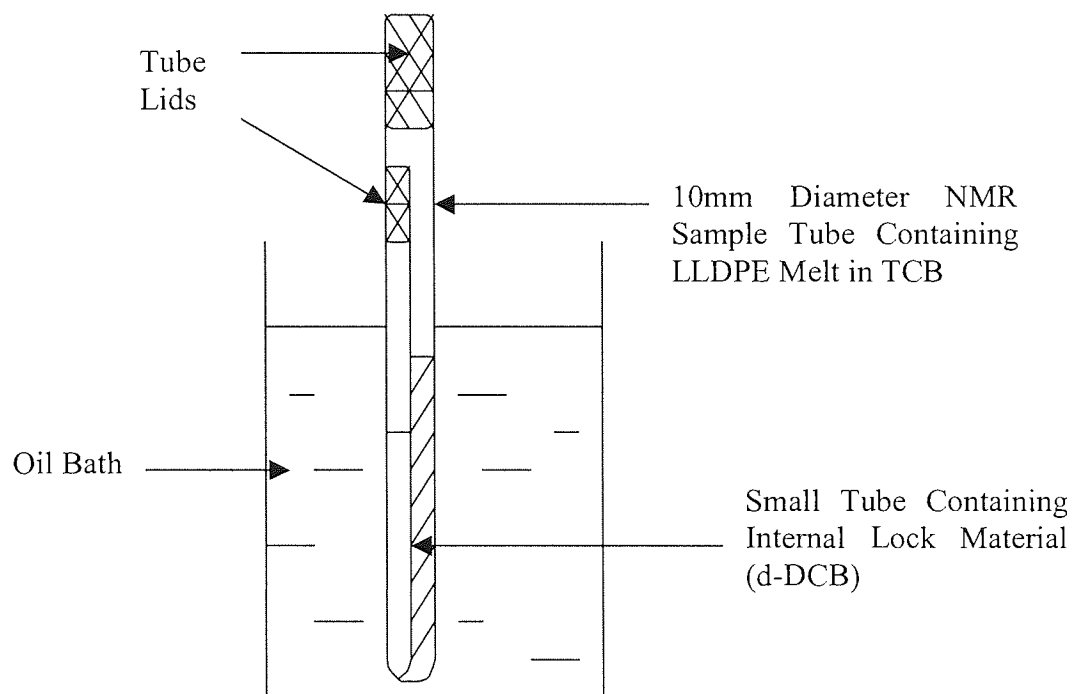


Figure 2.12. Schematic Diagram of Sample Preparation for ^{13}C -NMR Analysis

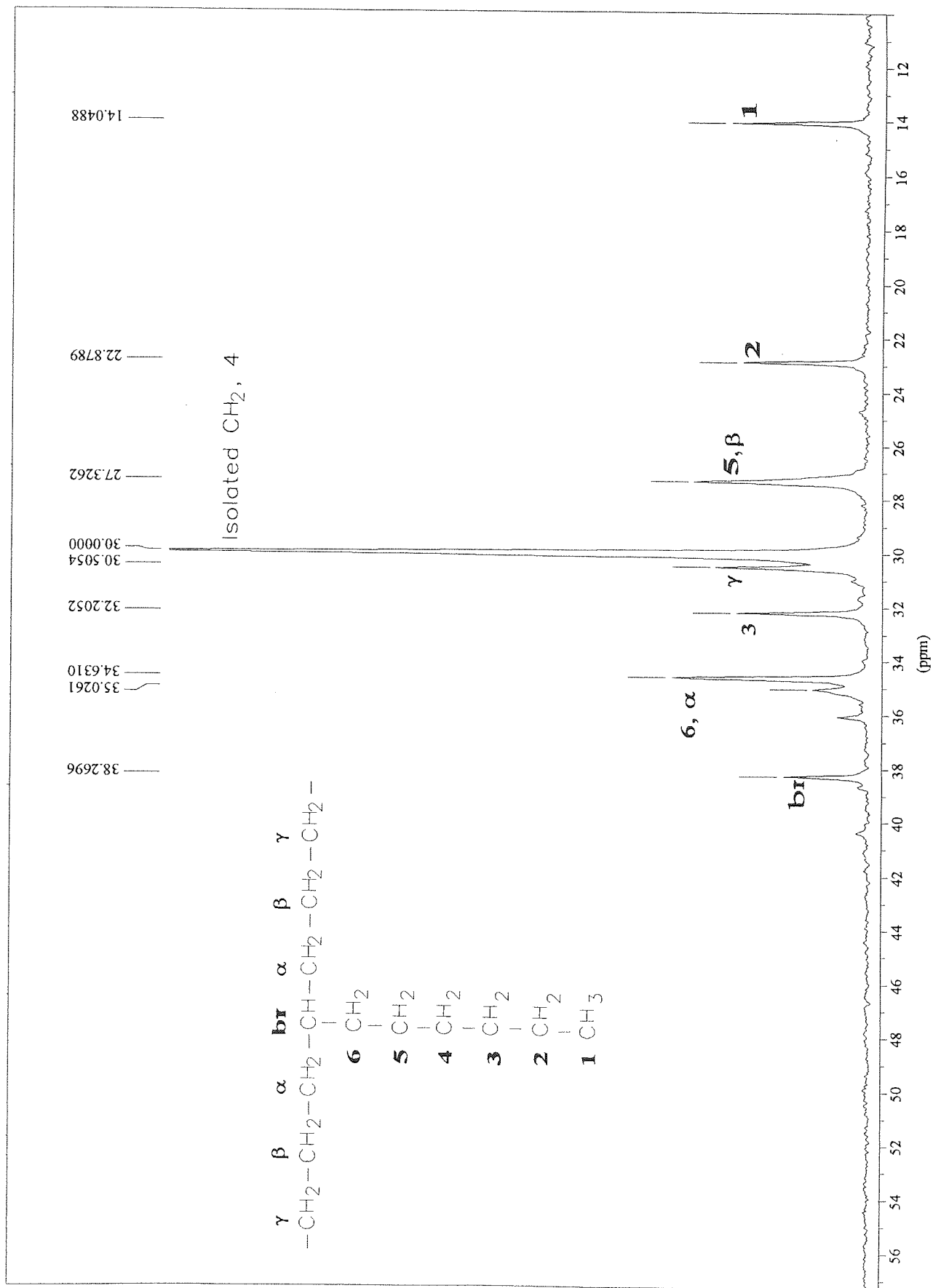
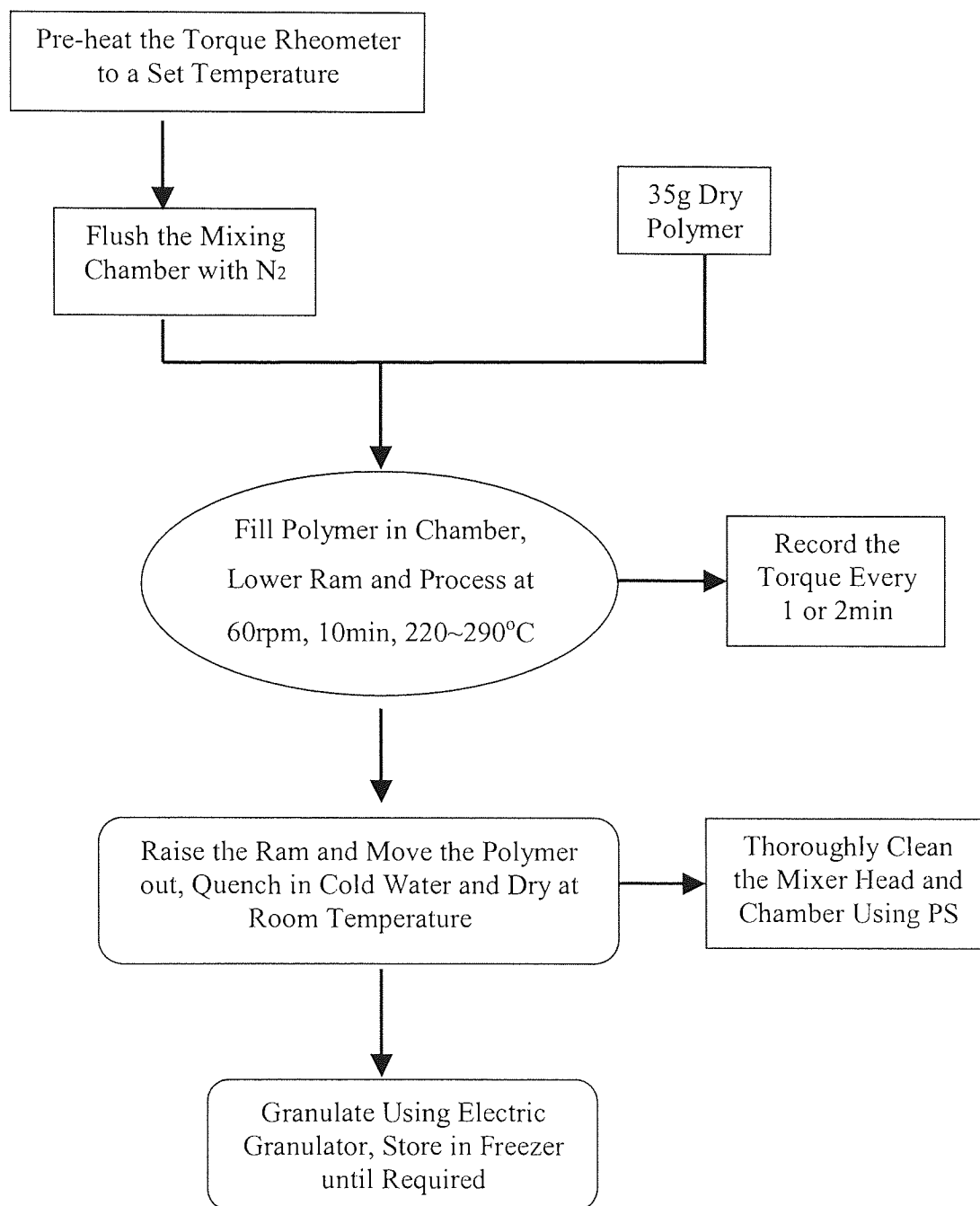
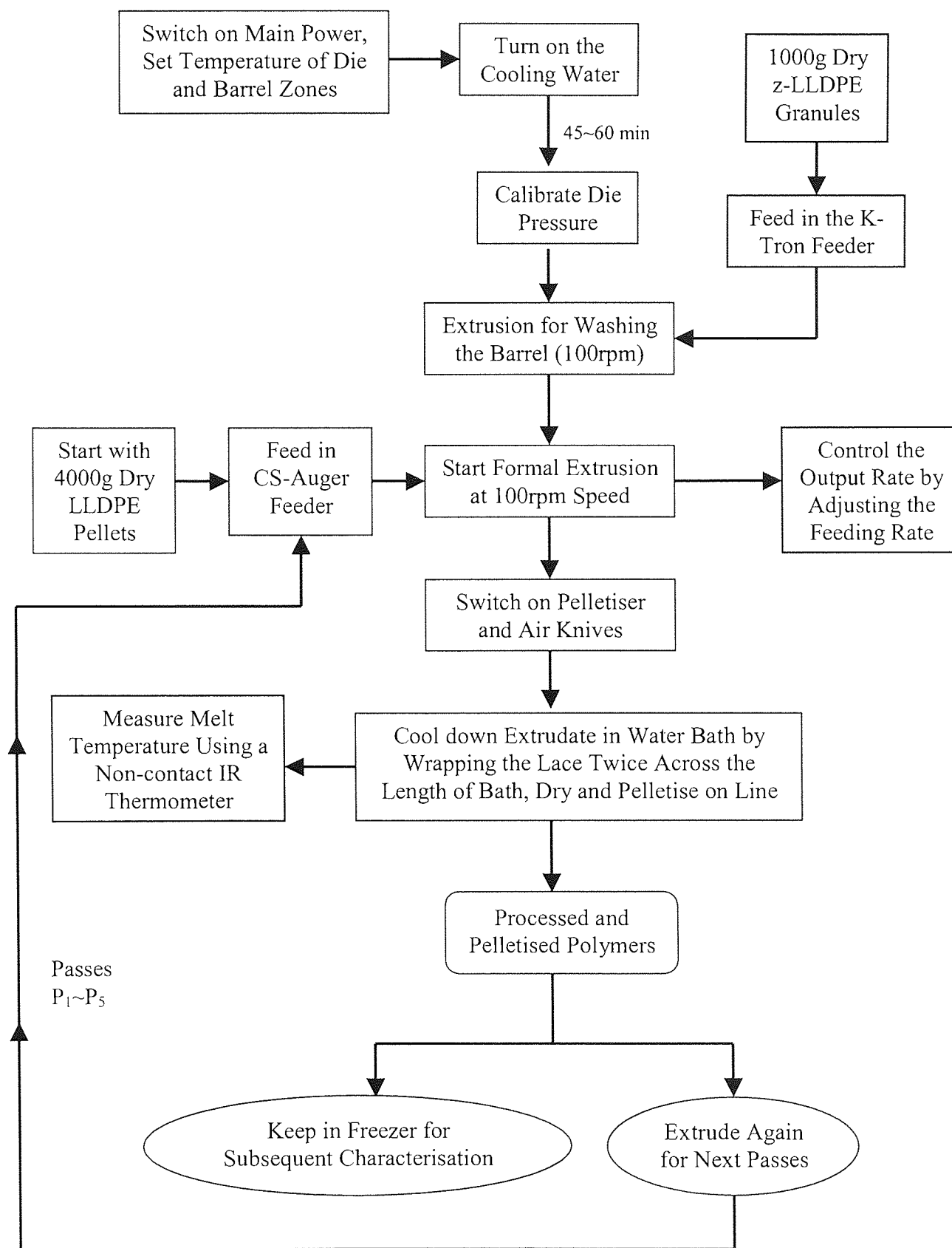


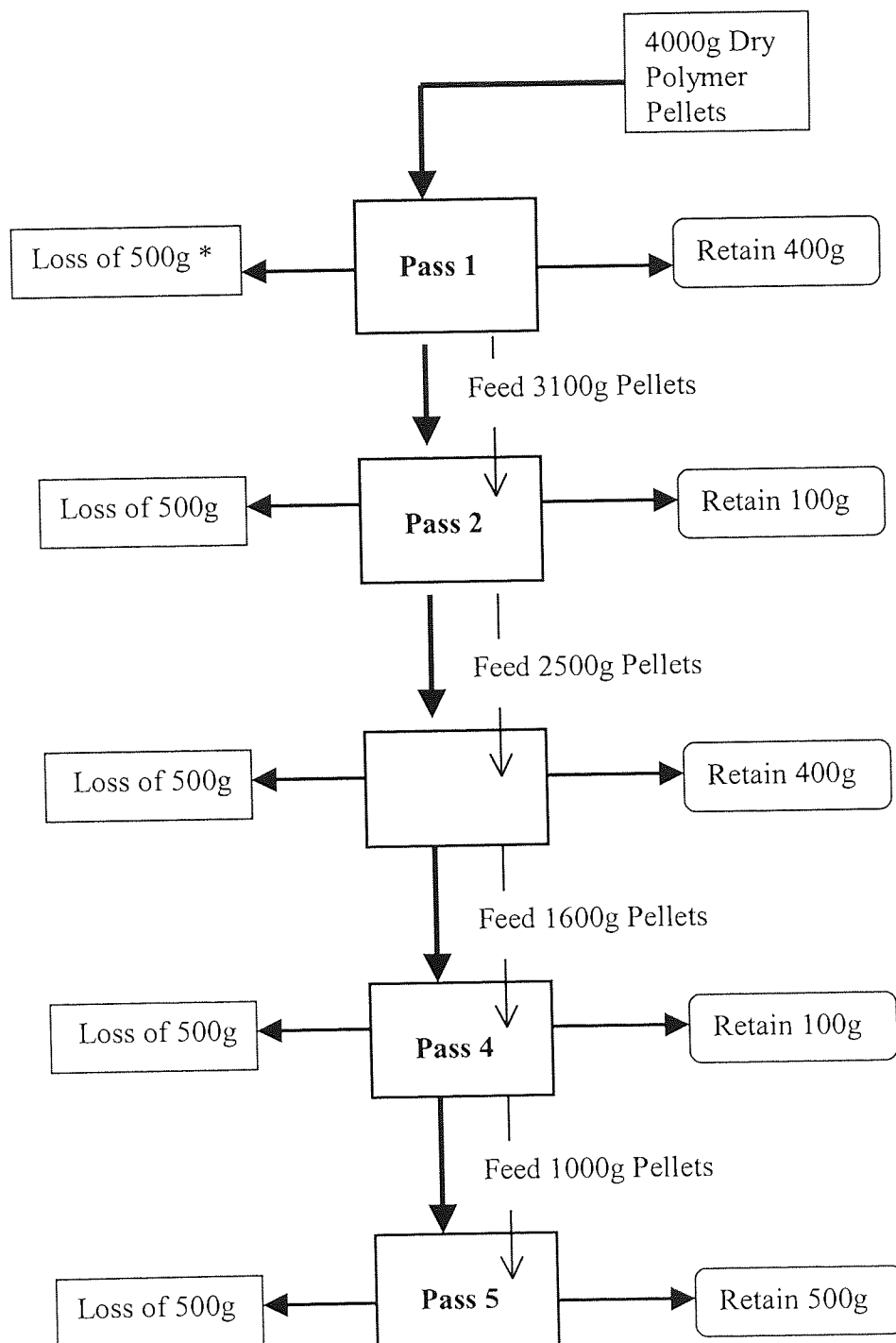
Figure 2.13. ¹³C-NMR Spectrum of Virgin EG8150 (m-LLDPE)



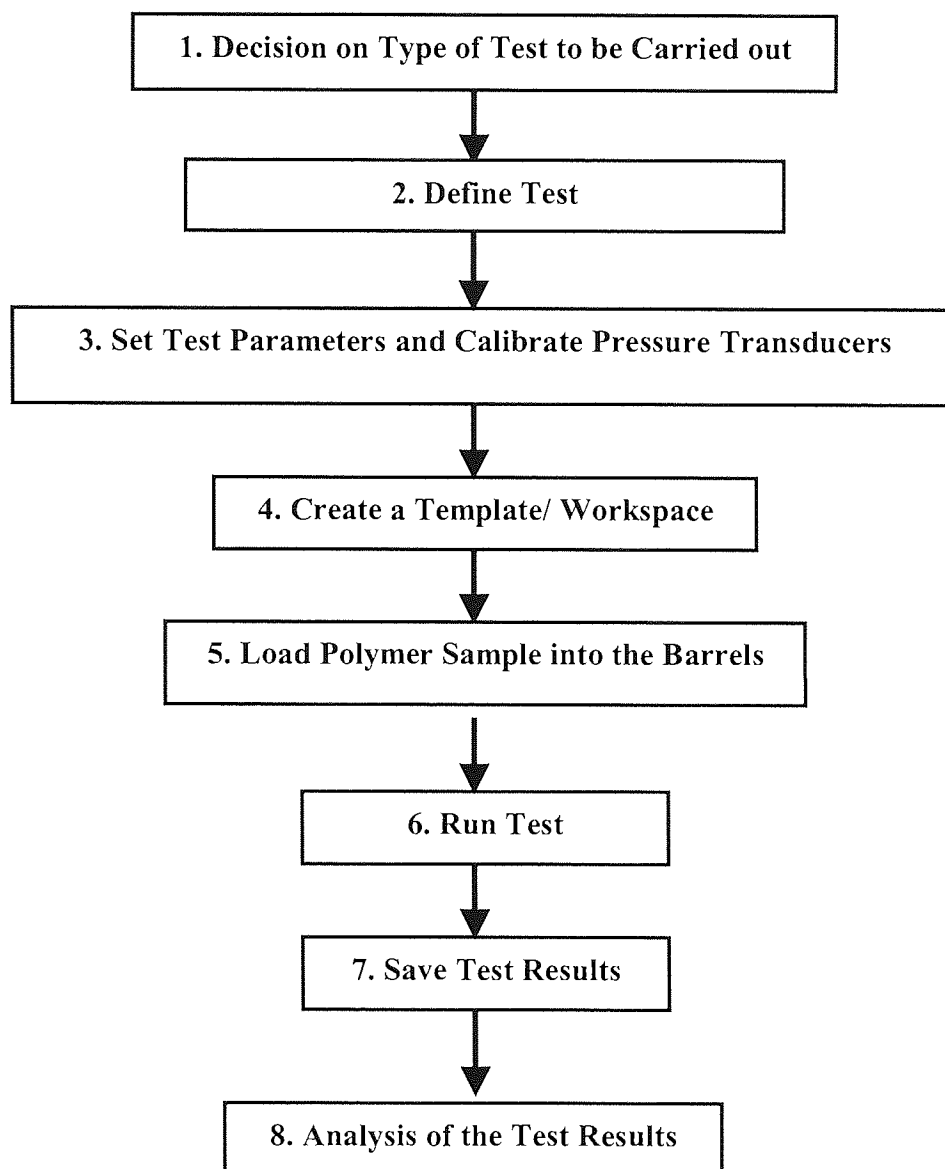
Scheme 2.1. Flow Chart of the Procedure Used to Process Polymers in Torque Rheometer



Scheme 2.2. Basic Operation of Twin-Screw Extruder for LLDPE Processing



Scheme 2.3. The Amount of Polymers Used During a Typical 5-Multi-pass Extrusions of LLDPE at 100rpm Speed Using BETOL Twin-Screw Extruder
 (* Loss due to collection of “middle-cut” only, i.e. discarding first and last fractions of extrudate for sampling consistency)



Scheme 2.4. Flow Diagram of the General Procedure of Rheological Test Using the Rosand Twin-Bore Capillary Rheometer

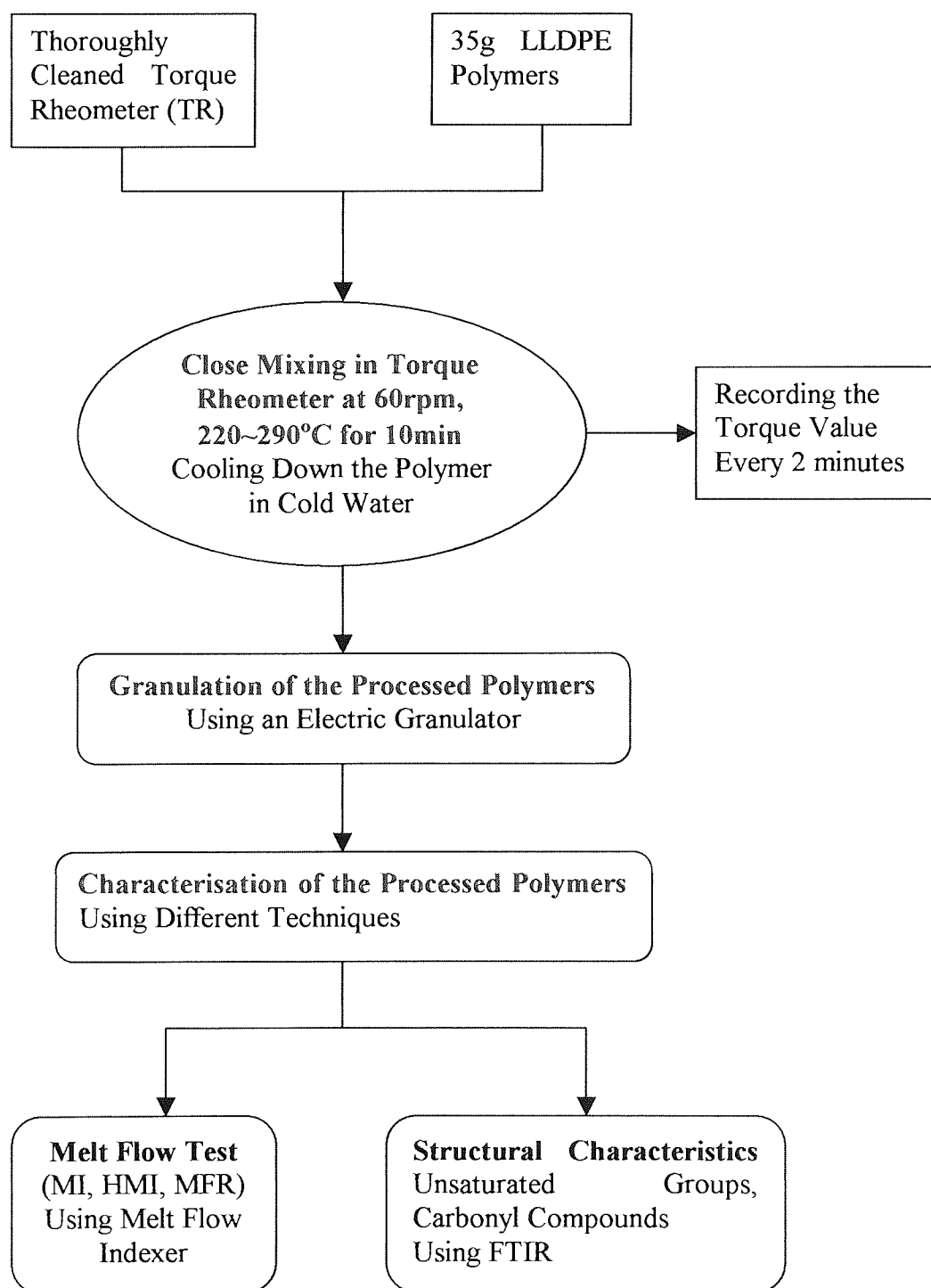
CHAPTER 3. THERMAL OXIDATION OF LLDPE DURING PROCESSING USING AN INTERNAL MIXER (TORQUE RHEOMETER, TR)

3.1. OBJECTIVES AND METHODOLOGY

The use of metallocene catalysts in the polymerisation of a new generation polyolefins has led to faster commercialisation of metallocene-based linear low density polyethylene (m-LLDPE) and has opened up new markets and opportunities. The type of the manufacturing process, the reaction conditions and the catalyst type are the main controlling factors for the molecular structure of these polymers. In turn, the molecular structure governs their processibility and oxidation behaviour during melt processing, hence the ultimate properties of products. The primary objectives of this part of work were to establish a basic understanding of the oxidative degradation of different grades of m-LLDPE (containing different amounts of 1-octene comonomer) made by Dow Chemical Company using “in-site” technology [59, 60] during processing in an internal mixer (torque rheometer, TR). Meanwhile, a Ziegler catalysed LLDPE analogue (z-LLDPE) was chosen to compare its degradation mechanisms with those of the metallocene-based polymers.

The metallocene and Ziegler-based LLDPE polymers were processed using an internal mixer (torque rheometer) under closed mixing conditions at different temperatures. The rheological (MI, HMI, MFR) and structural (content of unsaturated groups, concentration of carbonyl compounds) characteristics of both virgin and processed polymers were examined. The MI and HMI measurements were carried out using a melt flow indexer at 190°C with 2.16kg load and 21.6kg load respectively. The amounts of unsaturation and carbonyl compounds (relative concentration) were determined from absorption area index of their FTIR spectra (i.e. the absorption area of functional groups over the absorbance of a polymer reference peak, see Section 2.3.2.1 in Chapter 2). The SCB content in the virgin polymers was also quantified using ^{13}C -NMR. The effects of processing variables on the characteristics of TR processed LLDPE

polymers were investigated and the overall methodology used in the work is summarised in Scheme 3.1.



Scheme 3.1. Methodology Used in the Investigation of Oxidative Degradation of LLDPE Polymers During TR Processing

3.2. RESULTS

3.2.1. Effects of TR Processing on Characteristics of the Polymer Melt

3.2.1.1. Effects of Processing on the Changes in Torque

The experiments initially utilised a torque rheometer as an internal mixer to test the processing stability of different types and grades of LLDPE polymers. It has been reported [52] that, lower rotor speeds (50~60rpm) applied in TR processing may give better simulation of the oxygen-deficient conditions in an extruder. In addition, lower speed torque measurements are rheologically more sensitive to viscosity changes of LLDPE due to crosslinking [52]. Thus, all the polymers were processed at 60rpm speed in a closed chamber of the torque rheometer.

Figure 3.1 shows that the torque values of all the LLDPE polymers generally decrease with time at the start of processing at all temperatures. However, the torque tended to increase after processing for 6~8 minutes for most of the polymers, suggesting the occurrence of structural changes due to oxidative degradation. The overall change in torque is the result of competition of crosslinking and chain scission reactions during processing, with an increase in torque reflecting dominance of crosslinking reactions.

It is also clear from Figure 3.1 that in the case of m-LLDPE polymers, those containing higher concentration of comonomer show higher overall torque values during TR processing. This is almost certainly attributed to the higher original viscosities (lower MI values) presented by the corresponding virgin polymers (see Table 3.1). Due to the significant influences of processing temperature on the melt viscosity of LLDPE polymers, and in turn the torque values during processing, it is difficult to investigate the effects of processing temperature on the oxidative degradation of LLDPE polymers based only on observation of their torque changes.

3.2.1.2. Effects of Processing on Melt Flow Properties

In order to make a clear comparison with the virgin polymers, percentage change of individual rheological characteristics was calculated. For example, for the MI value, its percentage change is defined as the MI difference between processed and virgin polymer divided by the MI of virgin polymer times 100%. Figures 3.2 and 3.3 show that both MI and HMI decrease with increasing temperature for the metallocene polymers having relatively low comonomer content (FM-1570 and PL-1840); while, the m-LLDPE containing more amount of comonomer (VP-8770 and EG 8150) present a very contrary tendency in MI and HMI changes when the processing temperature was increased higher than 250°C (also see Table 3.1). It also clear that the percentage changes in MI and HMI of z-LLDPE (Dowlex2045-E) are always negative values. Furthermore, the MI and HMI of this polymer exhibit much larger extents of decrease after TR processing compared to that of metallocene-based polymers.

Figure 3.4 illustrates that the percentage change in MFR of all the polymers after TR processing is generally positive, indicating a broadening of molecular weight distribution (MWD), and their MFR values increase with increasing temperature within the range of 220°C to 270°C (also see Table 3.1). However, a slight decrease in MFR can be observed for the more comonomer containing m-LLDPE (VP-8770 and EG 8150), as well as the Ziegler-based polymer, Dowlex2045-E (see Table 3.1), when the processing temperature was higher than 270°C. Moreover, it is also shown from Figure 3.4 that z-LLDPE results in much greater extent of increase in its MFR percentage change when compared to the values of the metallocene polymers.

3.2.2. Effects of TR Processing on Structural Characteristics of LLDPE

3.2.2.1. Effects of Processing on the Type and Extent of Unsaturation

Both virgin and the TR Processed LLDPE samples were analysed by FTIR to examine the relative concentrations of different unsaturated groups. The concentrations of unsaturated groups that exist in virgin LLDPE substrate vary

greatly depending on the comonomer content and the catalyst system (metallocene or Ziegler) used in polymerisation (see Tables A3.1 in Appendix). Generally, the m-LLDPE with higher comonomer content has overall higher level of unsaturation (total double bond concentration) in the virgin polymers. In contrast to m-LLDPE, the virgin z-LLDPE contains much more vinyl group which is the predominant group out of all unsaturated groups in both virgin and processed Ziegler polymers (see FTIR spectra in Figures A3.1 to A3.3 in Appendix).

Figure 3.5 indicates that the relative concentration of trans-vinylene in all the LLDPE polymers tends to increase (relative to the corresponding virgin polymers) with increasing temperature. Meanwhile, more trans-vinylene groups were produced in the TR-processed polymers with the exceptions of m-LLDPE with higher comonomer content (VP-8770 and EG 8150) processed at lower temperatures. It is shown in Figure 3.6 that the vinyl concentration in all the m-LLDPE decreases after processing (compared to virgin m-LLDPE) at all temperatures, the more comonomers are contained, the less extent of decrease in vinyl content the polymer has. However, the amount of vinyl group in processed z-LLDPE shows a considerable increase compared to that in the corresponding virgin Ziegler polymer. It is also worth noting that an increasing tendency in vinyl concentration was observed with all the LLDPE polymers after processing at higher temperatures (270~290°C). Figure 3.7 shows that the relative concentration of vinylidene group always increases after TR processing for all the polymers examined (also see Table 3.2), and basically, in all cases more vinylidene groups were formed when polymers were processed at higher temperature.

3.2.2.2. Effects of Processing on the Concentration of Carbonyl Compounds

Carbonyl compounds present in both virgin and processed LLDPE polymers can also be semi-quantified (as a whole) using FTIR absorption area index of carbonyl region with respect to a polymer reference peak (see Table 3.2). Figure 3.8 shows the relative carbonyl concentration in both metallocene and Ziegler-based polymers has a great enhancement after TR processing. For m-LLDPE,

larger extent of increase in carbonyl concentration can be found in the polymers containing more comonomers (VP-8770 and EG 8150), while the processed z-LLDPE presents much higher increase in carbonyl concentration compared to metallocene polymers processed under the same conditions. It is also clear that the relative carbonyl concentration in all the LLDPE polymers increases with elevated processing temperature.

From the FTIR spectra in carbonyl region, it can be clearly found that the composition of carbonyl compounds (e.g. ketone, acid, ester...) varies with the polymer type, comonomer content and the processing conditions (see Figures 3.9 to 3.13). The major carbonyl compound in virgin LLDPE polymers is ester, and it is still the major part in the carbonyl composition of m-LLDPE processed at lower temperatures. However, when the processing temperature was increased higher than 250°C, ketone and carboxylic acid become to be predominant in the processed m-LLDPE. For z-LLDPE, the carbonyl compounds in the processed polymer mainly consist of ketone and carboxyl acid.

3.3. DISCUSSION

The experimental results shown in Section 3.2.1 make it clear that the catalyst system and comonomer content in LLDPE polymers have great impact on their melt stabilities during processing in TR. In the percentage change of MI values (change relative to virgin polymer), a positive value relates to chain scission, whereas a more negative value reflects a higher extent of crosslinking. Figure 3.2 shows that chain scission predominates for all the metallocene polymers when processed at 220°C (the lowest temperature used). However, at higher temperatures (e.g. 250°C), crosslinking becomes the predominant reaction but the extent of this crosslinking decreases with further increase in processing temperature, particularly in the case of m-LLDPE containing higher comonomers (e.g. VP-8770 and EG8150) due to increased competition from chain scission reactions at these higher temperatures (270~290°C). In contrast to m-LLDPE, crosslinking is shown to be always the dominant reaction for z-LLDPE (Dowlex2045-E) under all processing temperatures (220~290°C; much higher negative values), paralleled by a much higher increase in MFR value

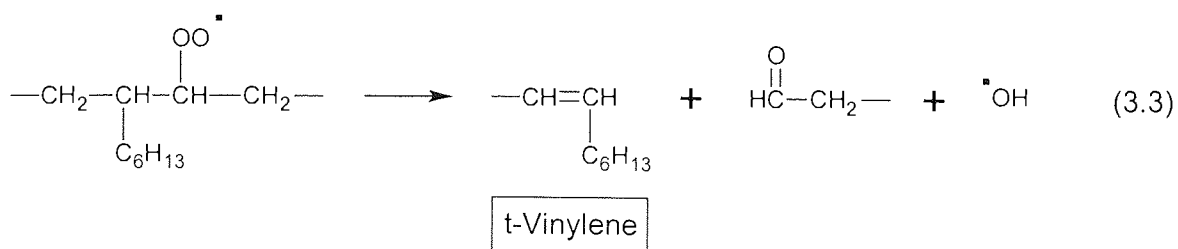
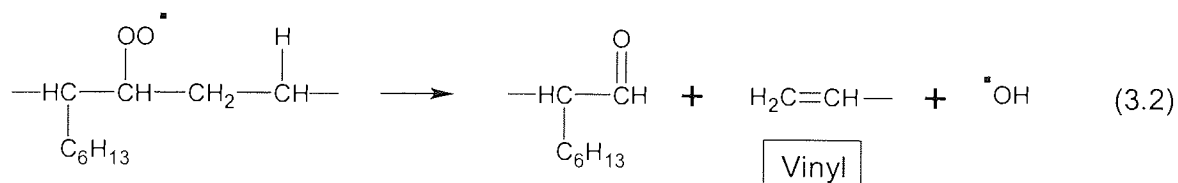
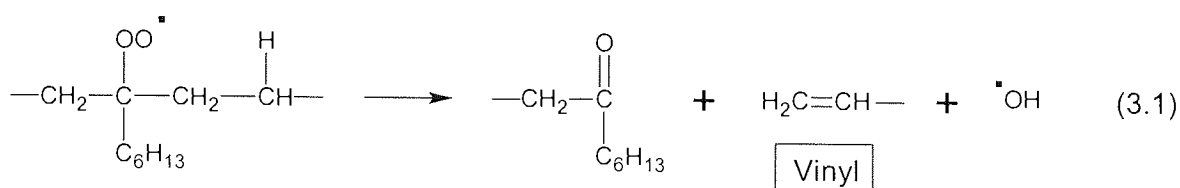
indicating a much higher extent of broadening in molecular weight distribution (see Figure 3.4) [80].

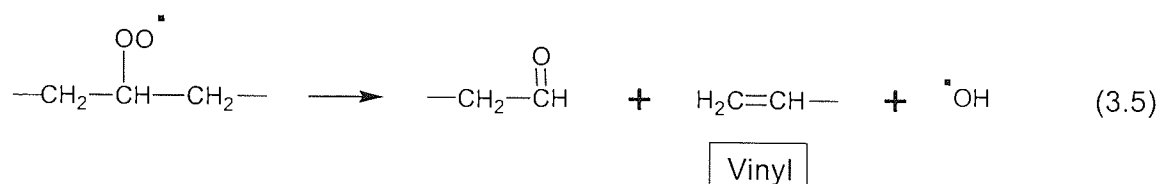
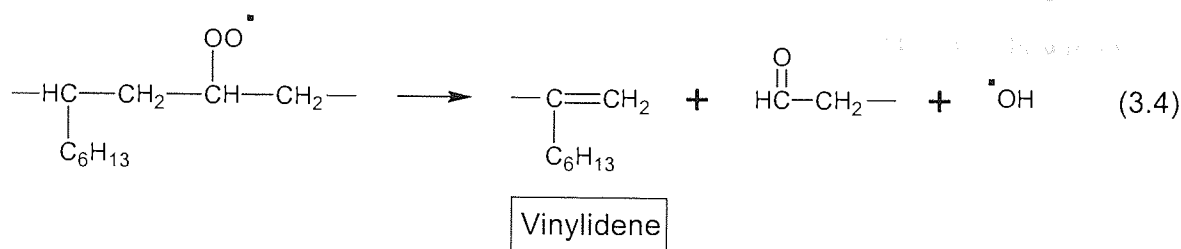
The observed changes in MI and HMI results are directly related to the outcome of the competition between chain scission and crosslinking during polymer processing, leading to the production of both lower molecular weight (MW) fractions as well as branched polymer chains. When the processed polymer was subjected to higher shear rates (e.g. HMI measurement), the low MW molecules may act as plasticisers whereas the branched polymer chains may orient themselves along the shear direction. As a result, the melt viscosity of the processed polymer decreases under higher shear rate and its percentage change in HMI tends to be less negative or more positive compared to the change of MI value (see Figures 3.2 and 3.3). This inference has been evidently confirmed by Figure 3.4, whereby the MFR values suggest broadening of MWD of all processed LLDPE polymers under all processing conditions as a result of oxidative degradation of the polymers [97].

The occurrence of chain scission and crosslinking in LLDPE polymers are generally caused by oxidative degradation during melt processing. At the beginning of TR processing, the small concentration of oxygen that is present in the mixer must be taken into account, it can react with the polymer melt to form peroxy radicals and hydroperoxides, their further decomposition can contribute to the production of alkoxy radicals, olefinic unsaturation and carbonyl compounds [93]. At this stage, the chain scission reactions are mainly the β -scissions of peroxy (and alkoxy) radicals (see Reactions 3.1 to 3.5) [99]. The evident chain scission that occurs in the m-LLDPE with high comonomer content (e.g. EG 8150) during TR processing at higher temperature (270~290°C), see Figures 3.2 and 3.3, is most likely attributed to the β -scission reaction of tertiary alkyl-peroxy radicals (see Reaction 3.1). Since more tertiary carbons are contained in the backbone of the LLDPE polymer like EG 8150 and the formation of peroxy radicals takes place preferentially at the branching point [74], more peroxy and alkoxy (yield from the decomposition of hydroperoxide) radicals are most likely produced in the polymer during melt processing and most of them would be of a tertiary alkyl-peroxy or alkoxy radical type. Higher

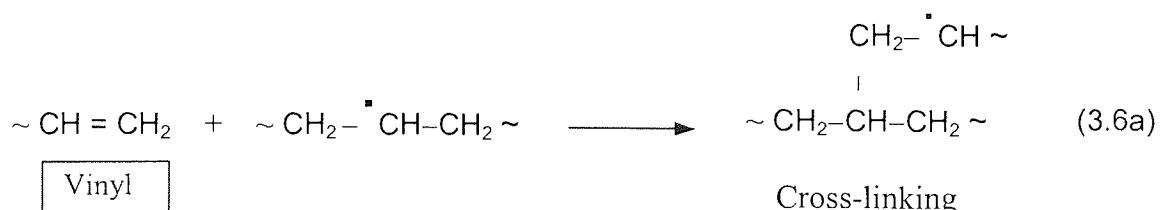
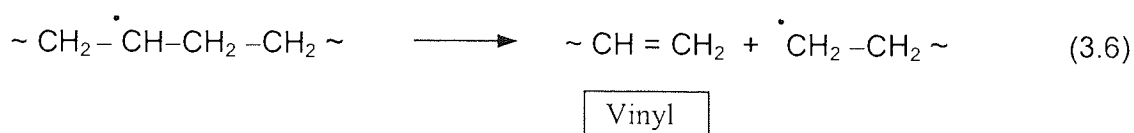
processing temperature favours the decomposition of alkyl-peroxyl and alkoxyl radicals and lead to relatively larger extent of chain scission. Therefore, the decomposition of tertiary oxygen-containing radicals in m-LLDPE with higher comonomer concentration is closely related to the extent of polymer chain scission observed during TR processing.

Although Reaction 3.1 results in the production of vinyl groups, it is clear that in all m-LLDPE polymers, there is an overall decrease in vinyl concentration relative to its concentration in the corresponding virgin polymers (see Figure 3.6), which must be due to competition between oxidative reactions leading to formation of vinyl (e.g. Reaction 3.1) against those responsible for their destruction (e.g. Reaction 3.6a). However, EG8150 (m-LLDPE having the highest comonomer content) does show the least extent of reduction in its vinyl concentration (compared to other metallocene polymers, see Figure 3.6) confirming the relative predominance of chain scission when processed in TR at higher temperature.





As oxygen is generally deficient while the processing is carried out in a closed mixer, the β -scission of alkyl radicals becomes an important reaction contributing to chain scission (see Reaction 3.6). It can be clearly found from Figures 3.2 and 3.3 that all the m-LLDPE processed at the lowest temperature (220°C) show small extents of chain scission. This is most likely a consequence of the high shear forces caused by higher melt viscosity when processing at lower temperature. The high melt viscosity prevents the active groups (e.g. alkyl radicals, vinyl groups) from crosslinking reactions to some extents. As a result, a large amount of alkyl radicals undergo β -scission leading to the break up of polymer chains.



On the one hand, the β -scission of peroxy, alkoxy and alkyl radicals can lead to the scission on polymer backbone. On the other hand, crosslinking between macromolecules can occur through both the addition reactions of alkyl radicals

with vinyl group (destruction of vinyl concentration in polymers, see Reaction 3.6a) and the recombination of two macro-alkyl radicals [74]. As shown in Figure 3.6, the vinyl concentration in all the m-LLDPE decreases after TR processing at all the examined temperatures compared to the virgin polymers, this indicates that part of the vinyl groups originally presented in the virgin m-LLDPE has been consumed *via* such crosslinking reactions [99].

The change of vinyl concentration in z-LLDPE displayed in Figure 3.6 is very different from that in metallocene polymers. This polymer is much more susceptible to crosslinking than are the m-LLDPE polymers as clearly shown in Figures 3.2 and 3.3, however, the vinyl content in the processed Dowlex2045-E always increases compared to the virgin sample. The recombination of macro-alkyl radicals is considered to play a more important role in the total crosslinking reactions of z-LLDPE. Meanwhile, the higher vinyl group concentration produced in z-LLDPE (see Figure 3.6) must result from some degradation reactions during processing such as Reaction 3.6.

As many thermo-oxidative degradation reactions during melt processing of polyolefins involve olefinic unsaturated groups, the changes in the various unsaturated groups in processed polymers could be related to the characteristic differences in the various grades of LLDPE polymers and their interrelation with their degradation behaviour [93]. In general, the changes in vinyl group concentration are closely related to the melt stability of LLDPE polymers (crosslinking or chain scission) during processing. Other unsaturated groups (e.g. trans-vinylene and vinylidene) are suggested to be relatively stable and changes in their amounts can be used to characterise some radical reactions involving them during polymer oxidation [99]. Besides the β -scission of peroxy, alkoxy and alkyl radicals, the disproportionation reaction of alkyl radicals is suggested to be another major contributor to the yield of double bonds according to Reactions 3.7 to 3.11 [99]. Under the condition of lower oxygen pressure (close mixing), alkyl radical plays a dominating role in the production of unsaturated groups during processing of LLDPE polymers.

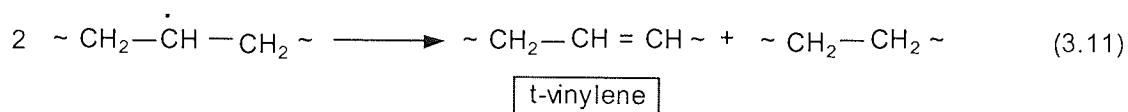
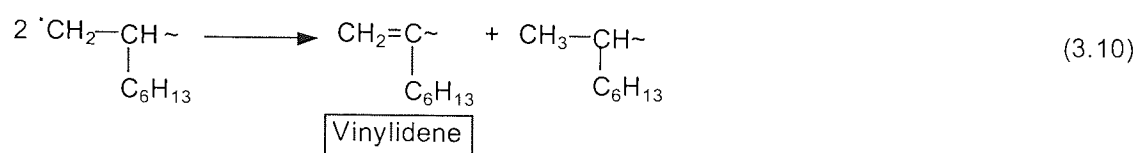
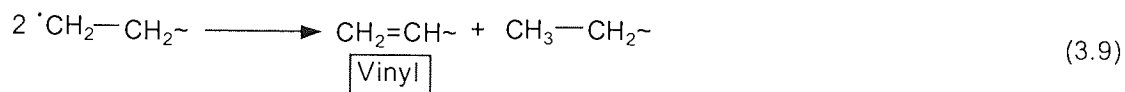
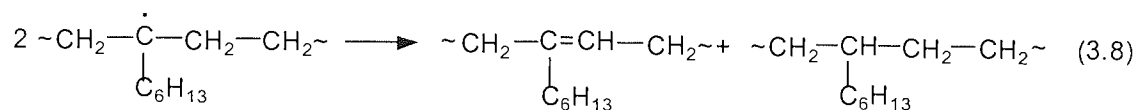
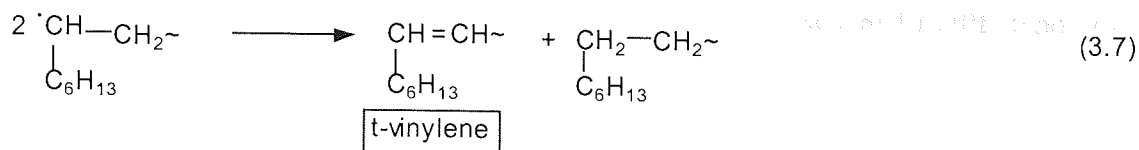
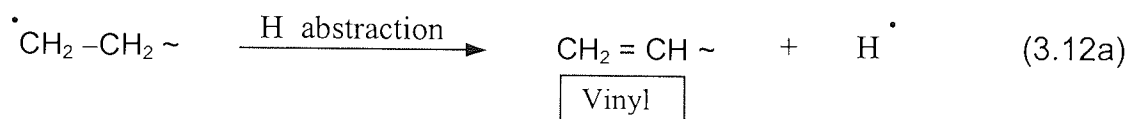
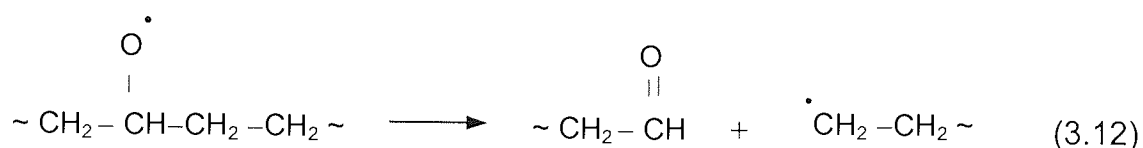


Figure 3.5 has shown that the concentrations of trans-vinylene group in z-LLDPE and m-LLDPE with lower comonomer content increase greatly after TR processing and show a rising tendency with elevated temperatures. Since all these polymers contain less comonomers, secondary alkyl radicals would be expected to predominate as a consequence of their thermal oxidation. The disproportionation reaction of secondary alkyl radicals is considered to make an important contribution to the increase of trans-vinylene concentration (see Reaction 3.11). Whereas, the amount of trans-vinylene group in the processed m-LLDPE with higher comonomer content (e.g. EG 8150) generally reduces, although a similar tendency of temperature dependent increase has also been observed. This reveals that there is a smaller chance for this grade of m-LLDPE polymer to form trans-vinylene while undergoing thermal oxidation. In this polymer, some degradation reactions that lead to a decrease in trans-vinylene concentration must be occurring to certain extents during their processing.

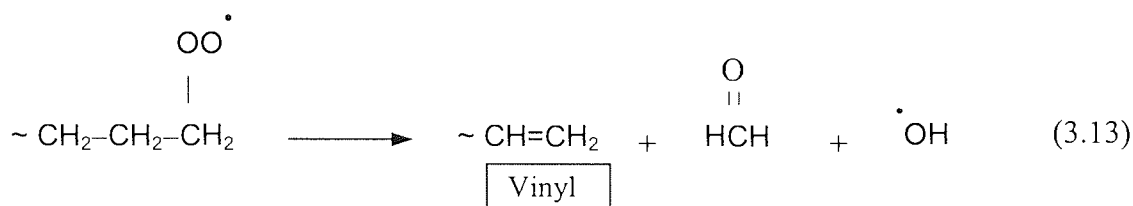
It is clear from Figure 3.6 that the vinyl concentration in all the m-LLDPE decreases after TR processing and this corresponds well with the predominance

of crosslinking in most of the polymers. However, when the processing temperature was raised, the vinyl content in the processed m-LLDPE tends to increase, especially for the polymers containing more comonomers. The cleavage of peroxy radicals derived from both tertiary (branching point) and secondary alkyl radicals, which is much favoured at higher temperature, could mainly account for the production of vinyl group (see Reactions 3.1 and 3.5). Meanwhile, the β -scission of secondary alkyl radical itself (see Reaction 3.6) and the derived secondary alkoxy radicals can all make contributions to the increase of vinyl group amount (see Reactions 3.12 and 3.12a) [74].

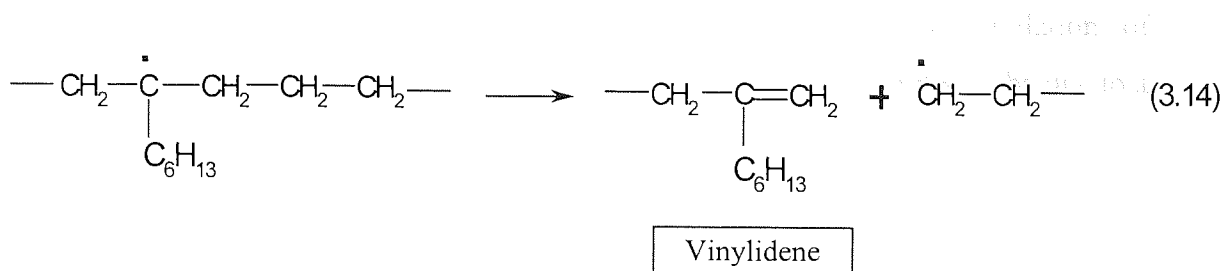


It can be found that most of the reactions involving the formation of vinyl group lead to polymer chain scission, and this is the main reason for the predominance of chain scission in EG 8150 (m-LLDPE with the highest comonomer content) processed at higher temperatures (see Figures 3.2 and 3.3). However, crosslinking is generally the dominant reaction in melt oxidation of m-LLDPE with lower comonomer content. The overall decrease of vinyl concentration in all processed metallocene-based polymers suggests the importance of the addition reactions of alkyl radicals to vinyl group in crosslinking of these polymers. It is evident that the competition between the R^\bullet addition reaction and the ROO^\bullet decomposition reaction, in other words, the ratio between the amounts of R^\bullet and ROO^\bullet radicals may to some extent, determine the melt stability of LLDPE polymers, i.e. overall balance between crosslinking and chain scission reactions [74, 99].

Crosslinking has been shown to predominate in z-LLDPE during processing (see Figures 3.2 and 3.3). However, the vinyl concentrations in the processed polymers are found to increase (see Figure 3.6). It is reasonable to suppose that the increase of vinyl group in processed z-LLDPE is most likely to be due to some reaction that yield vinyl group and meanwhile, does not lead to polymer chain scission. Thus, more $\cdot\text{CH}_2\text{-CH}_2\sim$ radicals are suggested to be produced in the initiation stage of thermal oxidation due to the catalyst system used for the polymerisation (Ziegler-Natta catalyst). Both the disproportionation of these radicals (see Reaction 3.9) and the breakdown of peroxy radicals derived from them (see Reaction 3.13) can contribute to the enhancement of vinyl group concentration during processing. Even though the re-combination of macro-alkyl radicals is considered to play a more important role in the crosslinking of z-LLDPE, the contribution of the addition reaction (alkyl radical with vinyl group) to the polymer crosslinking cannot be ignored because of the large amount of vinyl groups originally presented in this polymer.



As shown in Figure 3.7, the vinylidene concentration in all processed polymers shows a considerable increase, and it becomes higher when the processing temperature was raised. The overall increase in the amount of vinylidene is partially due to the relatively higher stability of this unsaturated group and thus, there is very little loss after its formation. The yield of vinylidene group is generally through some reactions involving short chain branches (SCB) as shown in Reactions 3.4, 3.10 and 3.14. That is why the m-LLDPE with higher comonomer content basically contains more vinylidene groups after TR processing (see Table 3.2). The increasing tendency of vinylidene concentration at elevated temperatures also implies that high temperature is favourable to the occurrence of these reactions during melt processing.



It can be clearly found from Figure 3.8 that TR processing caused great extents of enhancement in the amounts of carbonyl compounds in all examined polymers, especially in z-LLDPE. The increase in carbonyl concentration with processing temperature is indicative of increased extents of thermal oxidation and polymer chain scission. Furthermore, there are generally more carbonyls produced in m-LLDPE with higher comonomer content compared to lower comonomer containing polymers, indicating the important effect of short branching on the formation of carbonyl compounds [93].

The composition of carbonyl compounds in processed polymers changes differently with temperature for different types of LLDPE polymers (see Figures 3.9 to 3.13). Ester is normally the major carbonyl product when m-LLDPE is processed at lower temperature. The β -scission of both secondary and primary oxygen containing radicals (peroxyl and alkoxy radicals, see Reaction 3.2 to 3.5, 3.12 and 3.13), which are the major intermediates of melt oxidation in the LLDPE polymers, can lead to the formation of aldehydes and then carboxylic acids followed by further oxidation. As a result, esters are produced by the combination of carboxylic acids and alcohols transformed from alkoxy radicals [93, 94].

The major carbonyl compounds become ketones and carboxylic acids when m-LLDPE is processed at higher temperature. The greatly increasing production of ketones indicates that the decompositions of tertiary peroxyl and alkoxy radicals play very important role in m-LLDPE melt oxidation at higher processing temperature, as their cleavage is a major route for the yield of ketones (see Reaction 3.1) [102]. The larger extent of increase in carbonyl concentration in more comonomer containing m-LLDPE (i.e. VP-8770, EG8150) after processing at higher temperature is most probably due to the β -scission of tertiary oxygen

containing radicals. The most important reason for the accumulation of carboxylic acids in the processed metallocene polymers is assumed to be due to a more favourable cleavage of alkoxyl radicals rather than the abstraction of hydrogen from polymer chain (to forming alcohol) at higher temperatures. As a result, there are not enough alcohols to react with the carboxylic acids, which are produced and left in the processed polymer as final oxidation products.

Compared with m-LLDPE polymers, the Ziegler LLDPE polymer has generally a similar composition of carbonyl compounds after TR processing (see Figure 3.13). The small difference is ketones and carboxylic acids are always the dominant carbonyl products in processed z-LLDPE no matter what temperature was used. This indicates that the alkoxyl radicals are more susceptible to cleavage in z-LLDPE than in the metallocene catalogues. The formation of carboxylic acids in z-LLDPE is considered to be through the same reactions as those that occur in m-LLDPE. However, due to the lower comonomer content in this polymer, the production of large amount of ketones in z-LLDPE processed at higher temperature is attributed, at least partially, to some reactions not involving tertiary peroxy or alkoxyl radicals.

Table 3.1. MI, HMI and MFR of TR Processed LLDPE Polymers

| Melt Flow Measurement | Processing Temperature (°C) | Polymer Code | | | | |
|-----------------------|-----------------------------|--------------|---------|---------|---------|---------------|
| | | FM-1570 | PL-1840 | VP-8770 | EG 8150 | Dowlex 2045-E |
| MI (g/10min) | Virgin | 1.43 | 1.16 | 1.04 | 0.58 | 1.21 |
| | 220 | 1.47 | 1.23 | 1.09 | 0.61 | 0.70 |
| | 250 | 1.31 | 1.02 | 0.92 | 0.56 | 0.56 |
| | 270 | 1.20 | 0.79 | 0.94 | 0.61 | 0.51 |
| | 290 | 1.16 | 0.71 | 1.01 | 0.67 | 0.49 |
| HMI (g/10min) | Virgin | 55.2 | 43.7 | 30.9 | 16.4 | 43.8 |
| | 220 | 56.0 | 45.3 | 32.9 | 17.5 | 38.1 |
| | 250 | 55.0 | 44.6 | 32.4 | 18.4 | 34.4 |
| | 270 | 54.2 | 39.5 | 34.5 | 22.2 | 33.3 |
| | 290 | 54.2 | 41.0 | 36.6 | 23.4 | 31.5 |
| MFR (HMI/MI) | Virgin | 39 | 38 | 30 | 28 | 36 |
| | 220 | 38 | 37 | 30 | 29 | 54 |
| | 250 | 42 | 44 | 35 | 33 | 61 |
| | 270 | 46 | 50 | 37 | 36 | 65 |
| | 290 | 47 | 58 | 36 | 35 | 64 |

Table 3.2. Relative Concentrations (from IR absorption area indeces) of Unsaturated and Carbonyl Groups Contained in Virgin and TR Processed LLDPE Polymers

| Unsaturated Group | Processing Temperature (°C) | Polymer Code | | | | |
|--|-----------------------------|------------------------|---------|---------|---------|---------------|
| | | FM-1570 | PL-1840 | VP-8770 | EG 8150 | Dowlex 2045-E |
| | | Relative Concentration | | | | |
| t-Vinylene –CH=CH– 965 cm ⁻¹ | Virgin | 0.069 | 0.095 | 0.211 | 0.255 | 0.028 |
| | 220 | 0.088 | 0.107 | 0.173 | 0.212 | 0.030 |
| | 250 | 0.148 | 0.160 | 0.205 | 0.250 | 0.035 |
| | 270 | 0.145 | 0.163 | 0.205 | 0.238 | 0.034 |
| | 290 | 0.160 | 0.166 | 0.236 | 0.253 | 0.048 |
| Vinyl –CH=CH ₂ 908 cm ⁻¹ | Virgin | 0.062 | 0.034 | 0.043 | 0.029 | 0.143 |
| | 220 | 0.019 | 0.013 | 0.023 | 0.016 | 0.173 |
| | 250 | 0.017 | 0.011 | 0.023 | 0.015 | 0.181 |
| | 270 | 0.018 | 0.013 | 0.025 | 0.019 | 0.178 |
| | 290 | 0.019 | 0.016 | 0.030 | 0.021 | 0.189 |
| Vinylidene >C=CH ₂ 889 cm ⁻¹ | Virgin | 0.128 | 0.157 | 0.282 | 0.488 | 0.061 |
| | 220 | 0.169 | 0.175 | 0.399 | 0.492 | 0.067 |
| | 250 | 0.193 | 0.183 | 0.425 | 0.607 | 0.081 |
| | 270 | 0.213 | 0.191 | 0.462 | 0.611 | 0.080 |
| | 290 | 0.212 | 0.192 | 0.465 | 0.614 | 0.084 |
| All Carbonyl Compounds –C=O 1682~1782 cm ⁻¹ | Virgin | 0.081 | 0.078 | 0.068 | 0.080 | 0.046 |
| | 220 | 0.099 | 0.102 | 0.085 | 0.108 | 0.156 |
| | 250 | 0.174 | 0.136 | 0.190 | 0.244 | 0.222 |
| | 270 | 0.199 | 0.184 | 0.263 | 0.334 | 0.286 |
| | 290 | 0.267 | 0.237 | 0.310 | 0.371 | 0.297 |

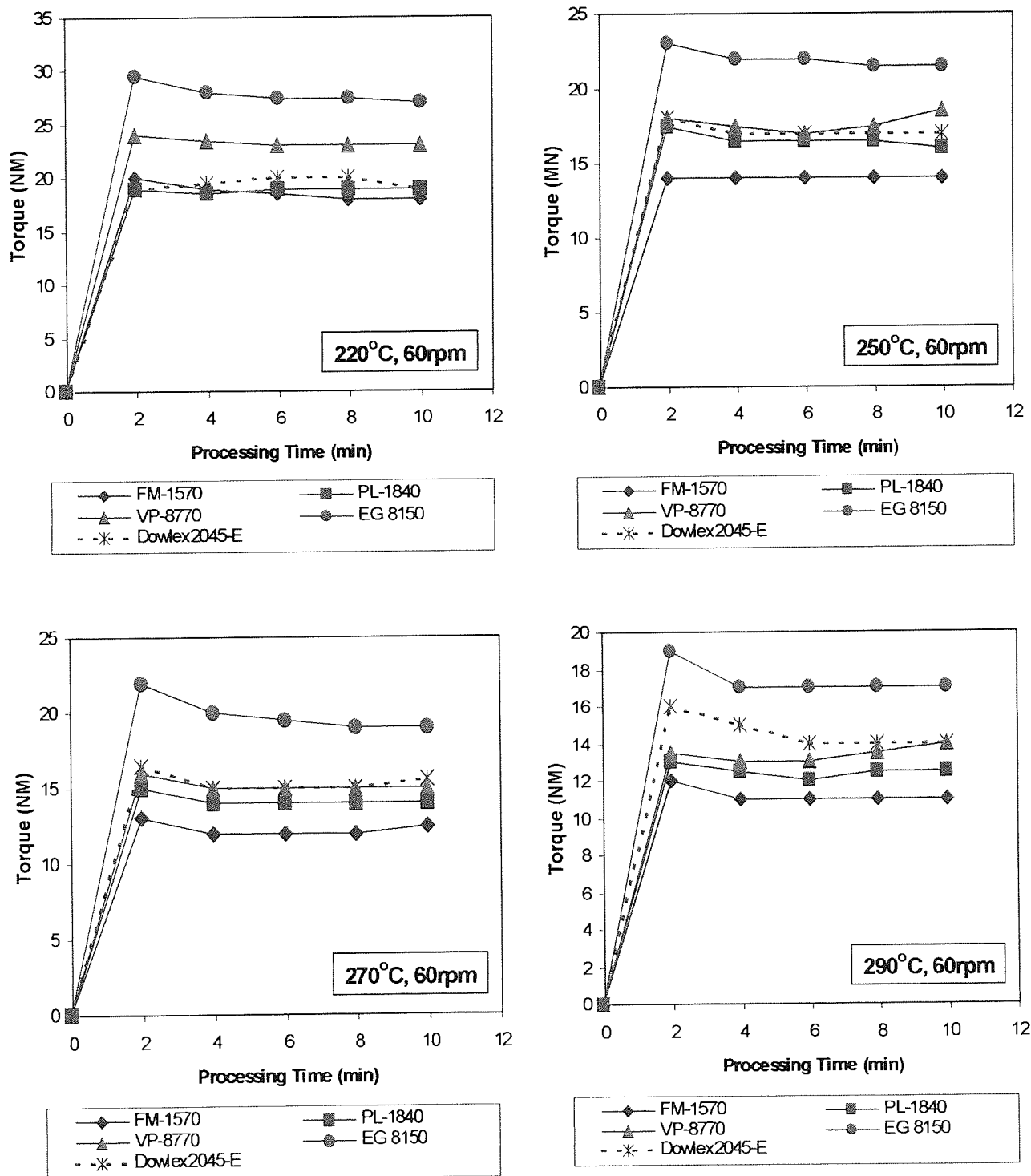


Figure 3.1. Torque Changes of LLDPE Polymers During TR Processing.

The Comonomer Contents of These Polymers are as Follows (see Table 2.2 in Chapter 2)

| Polymer | FM-1570 | PL-1840 | VP-8770 | EG 8150 | Dowlex2045-E |
|-------------|---------|---------|---------|---------|--------------|
| w% 1-Octene | 11.6 | 13.4 | 28.2 | 36.2 | 10.5 |

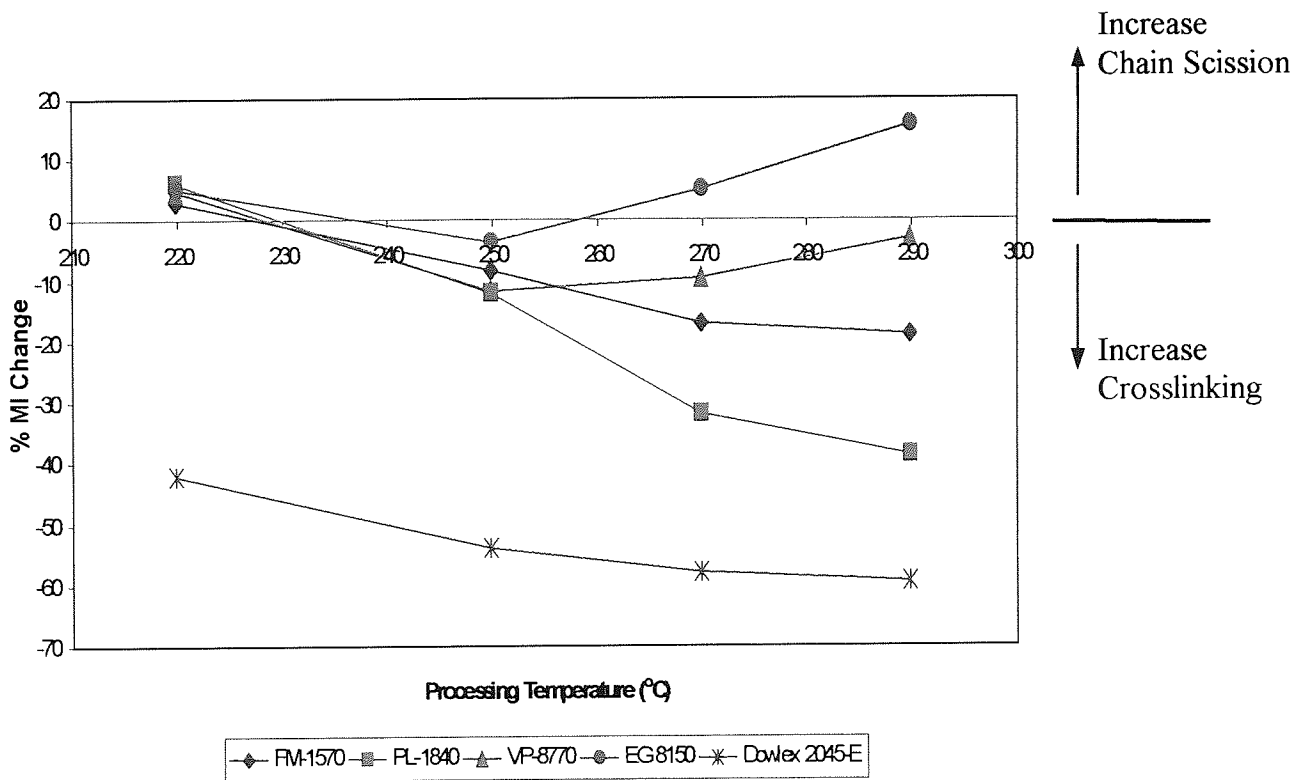


Figure 3.2. Percentage MI Change of TR Processed LLDPE Polymers

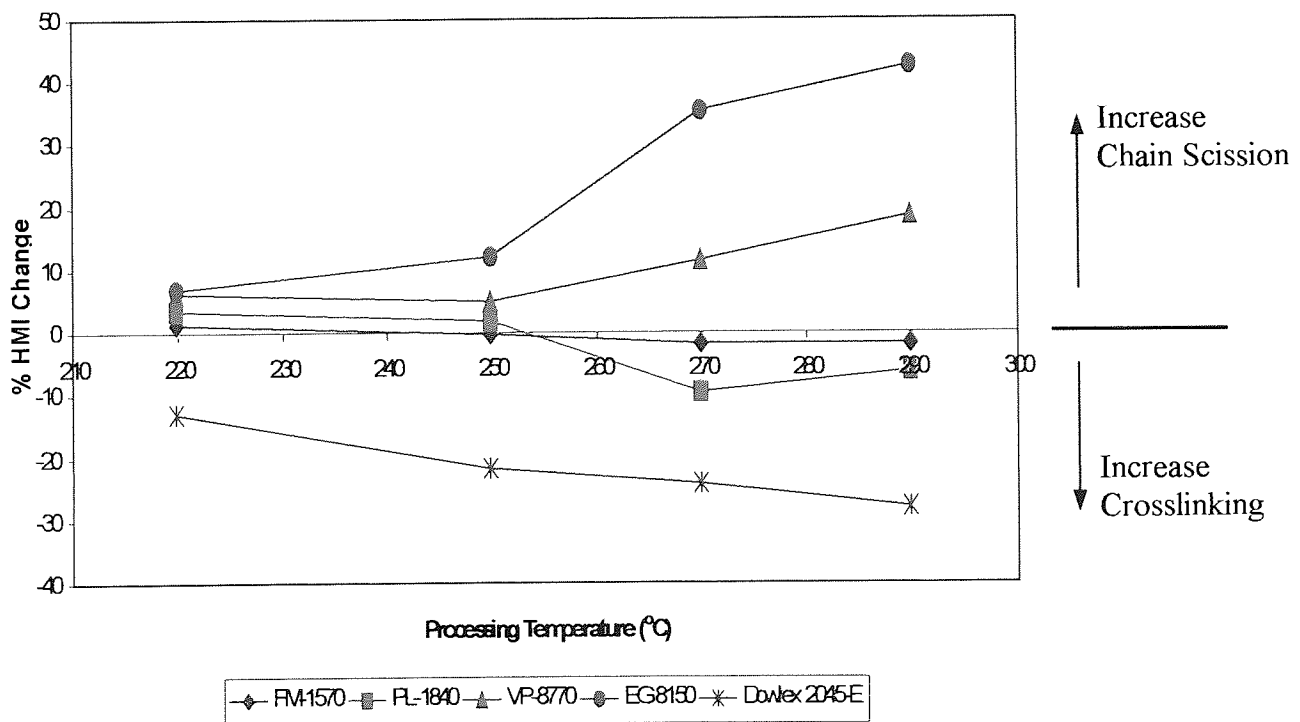


Figure 3.3. Percentage HMI Change of TR Processed LLDPE Polymers

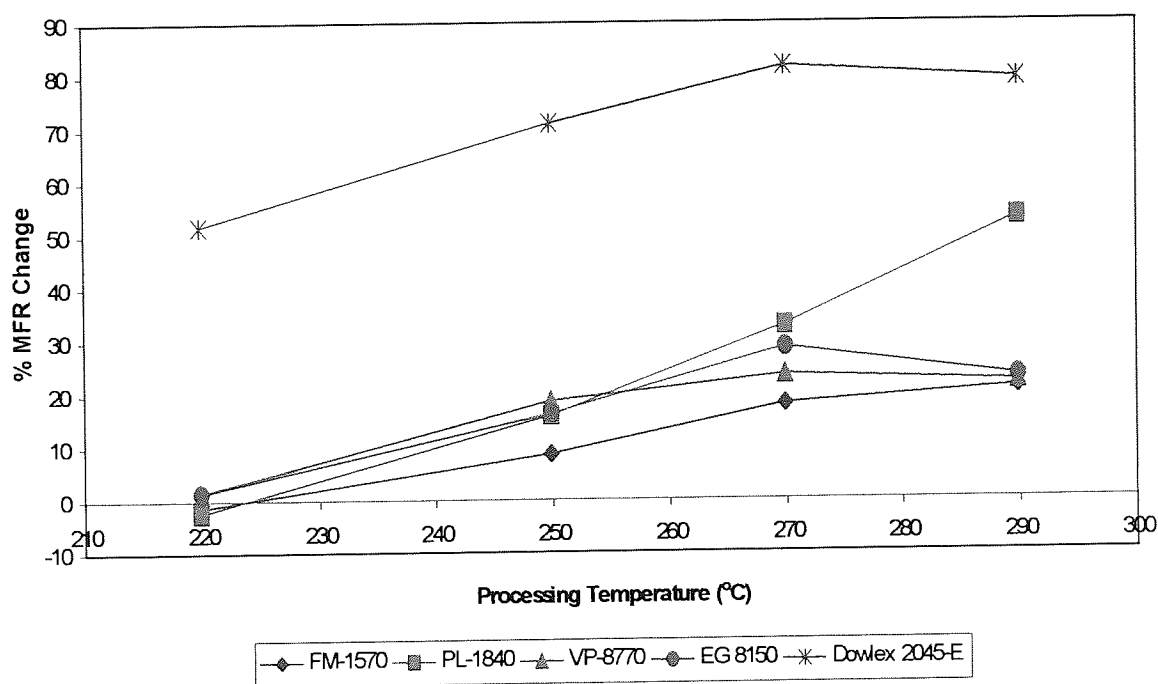


Figure 3.4. Percentage MFR Change of TR Processed LLDPE Polymers

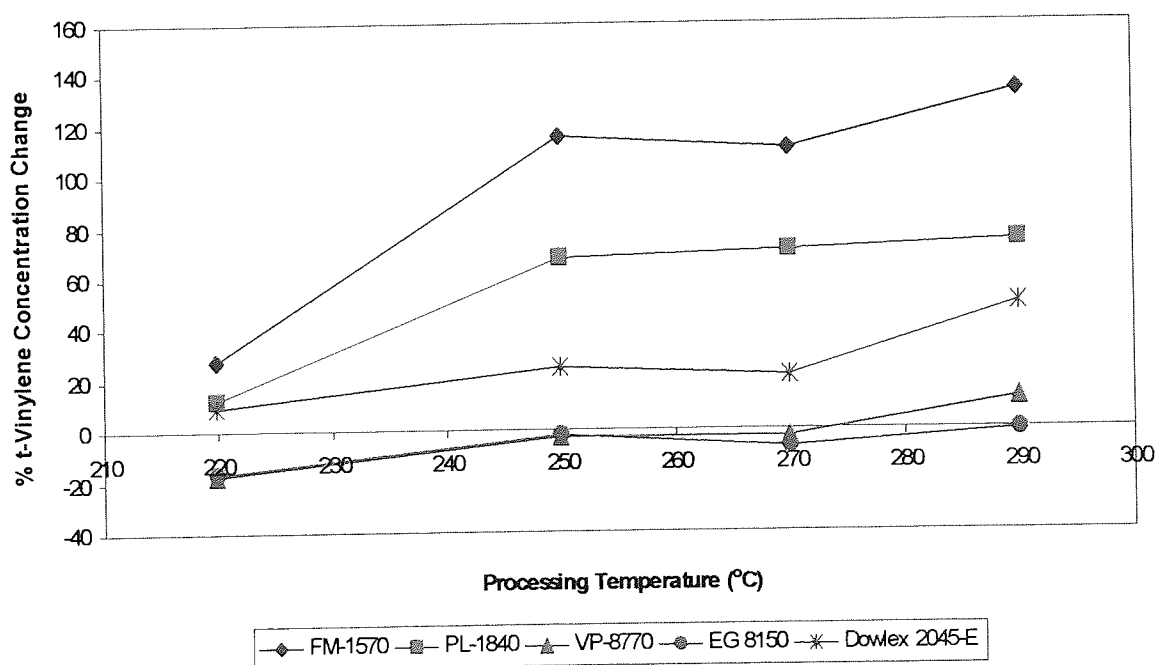


Figure 3.5. t-Vinylene Relative Concentration Change of TR Processed LLDPE Polymers

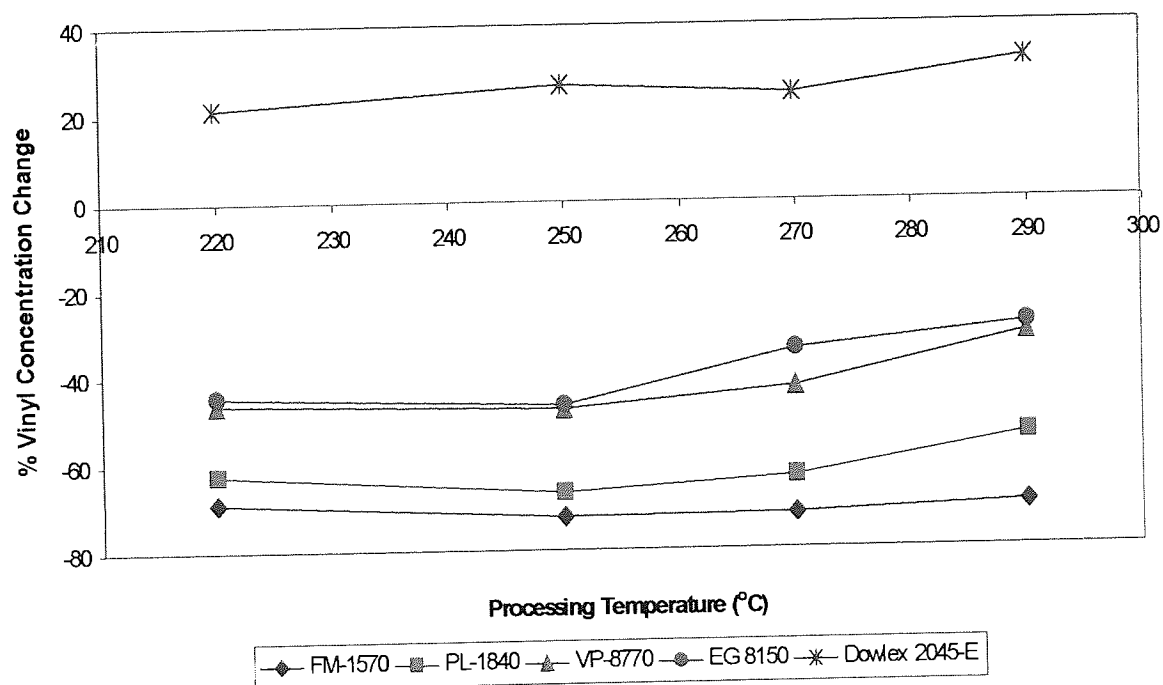


Figure 3.6. Vinyl Relative Concentration Change of TR Processed LLDPE Polymers

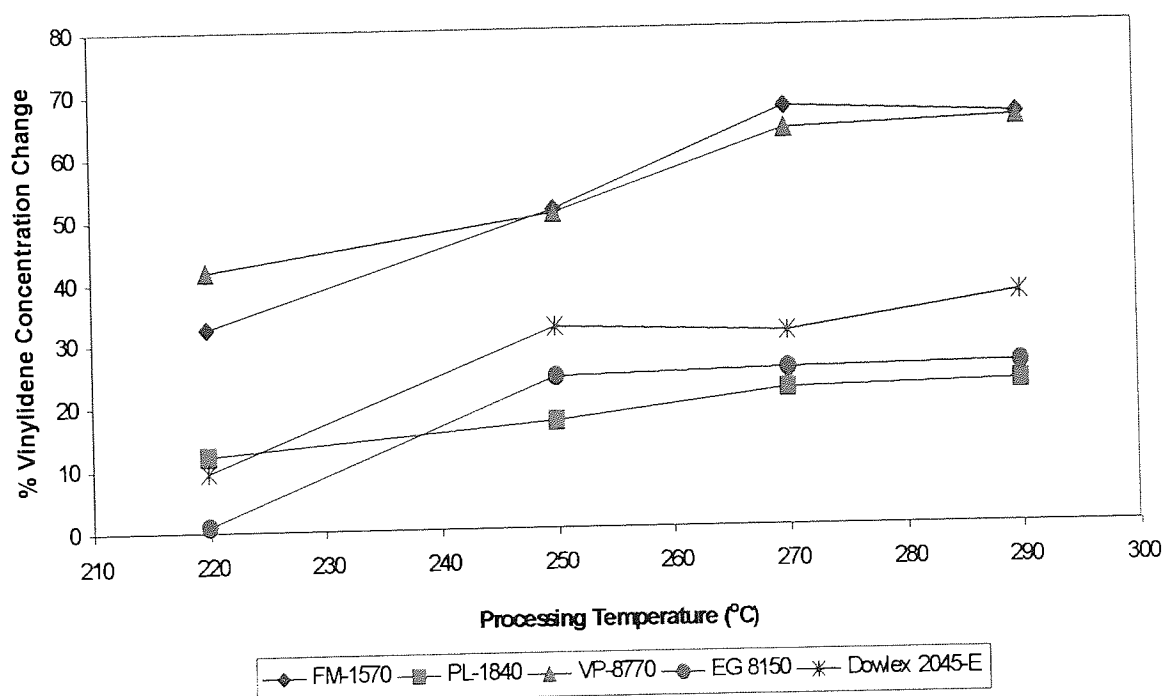


Figure 3.7. Vinylidene Relative Concentration Change of TR Processed LLDPE Polymers

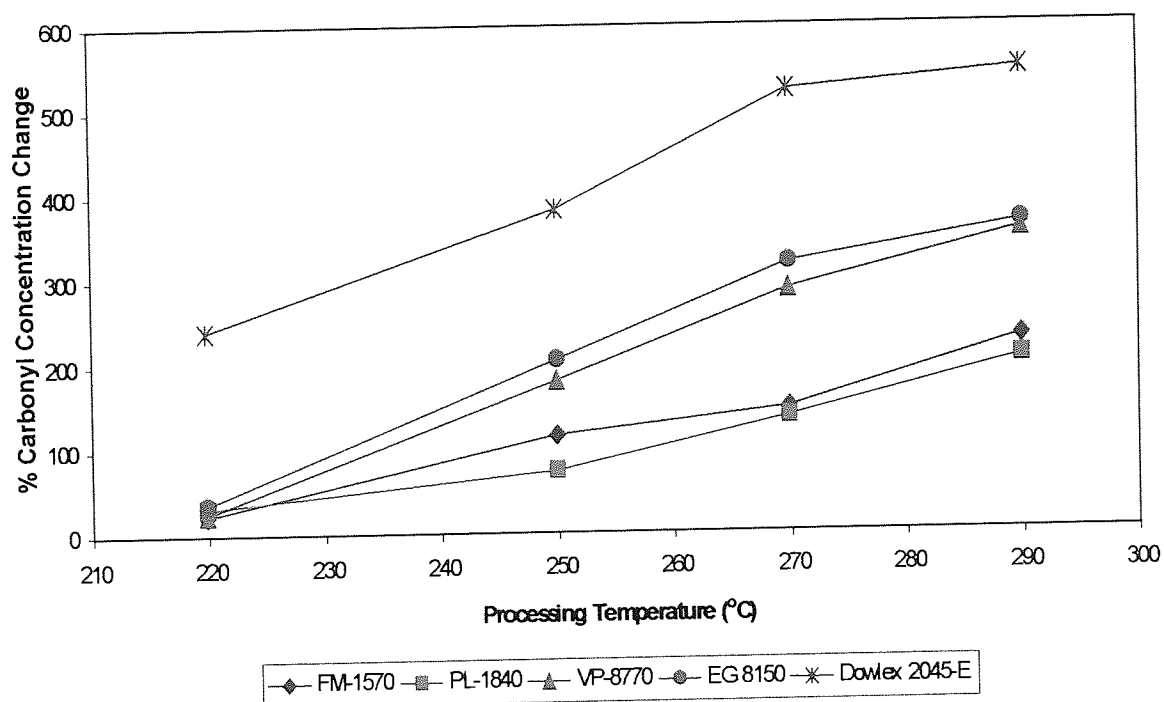


Figure 3.8. Percentage Changes of Relative Carbonyl Concentrations in TR Processed LLDPE Polymers

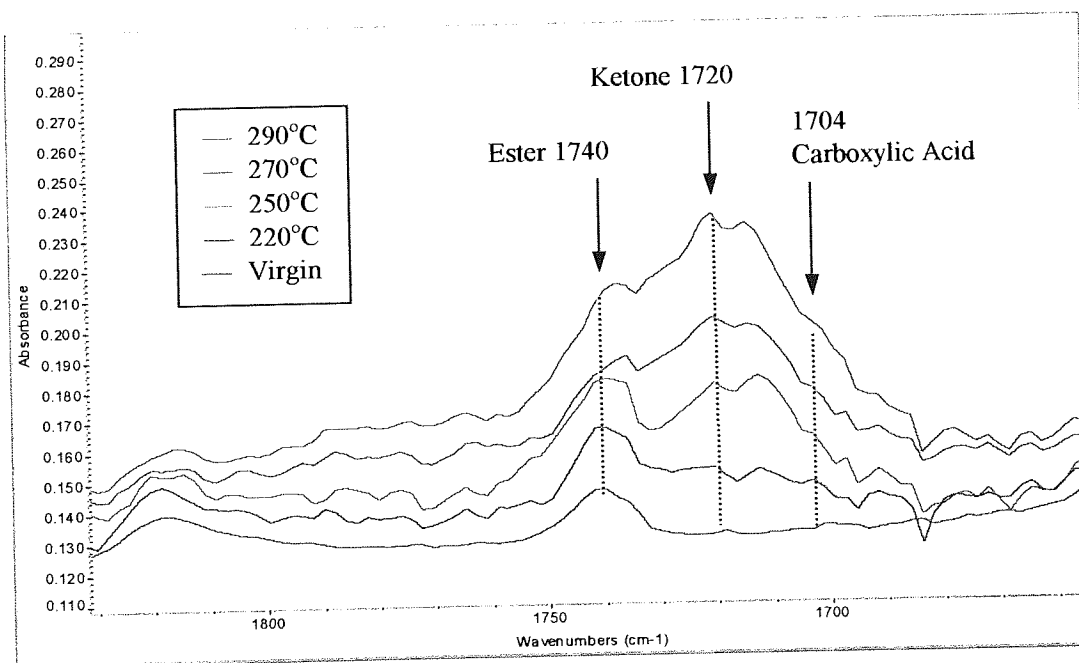


Figure 3.9. FTIR Spectra in the Carbonyl Region of TR Processed FM-1570 (60rpm, 10min)

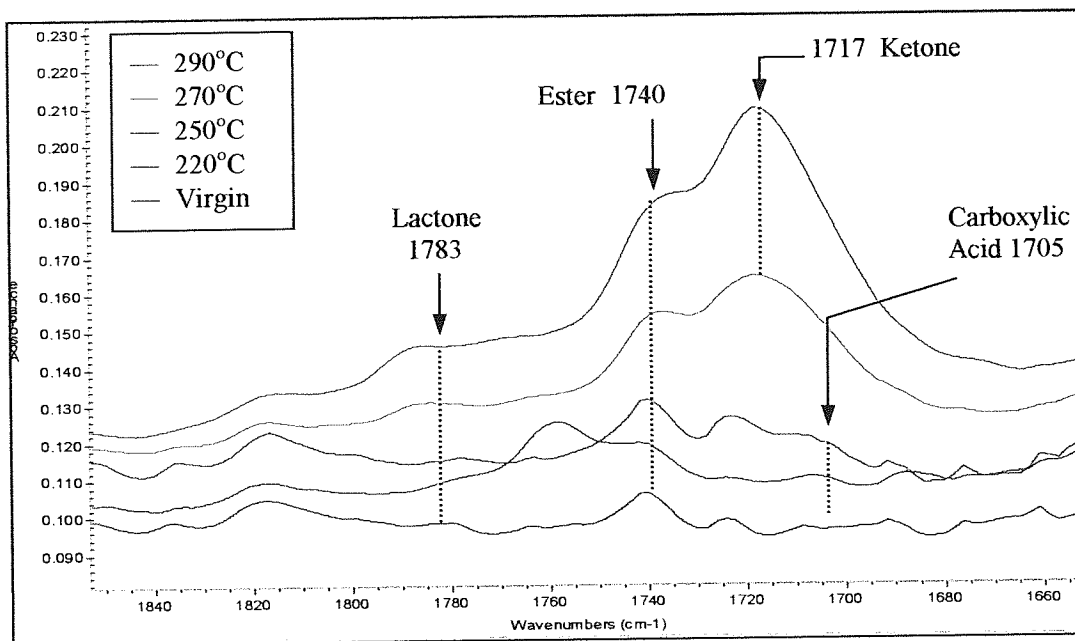


Figure 3.10. FTIR Spectra in the Carbonyl Region of TR Processed PL-1840 (60rpm, 10min)

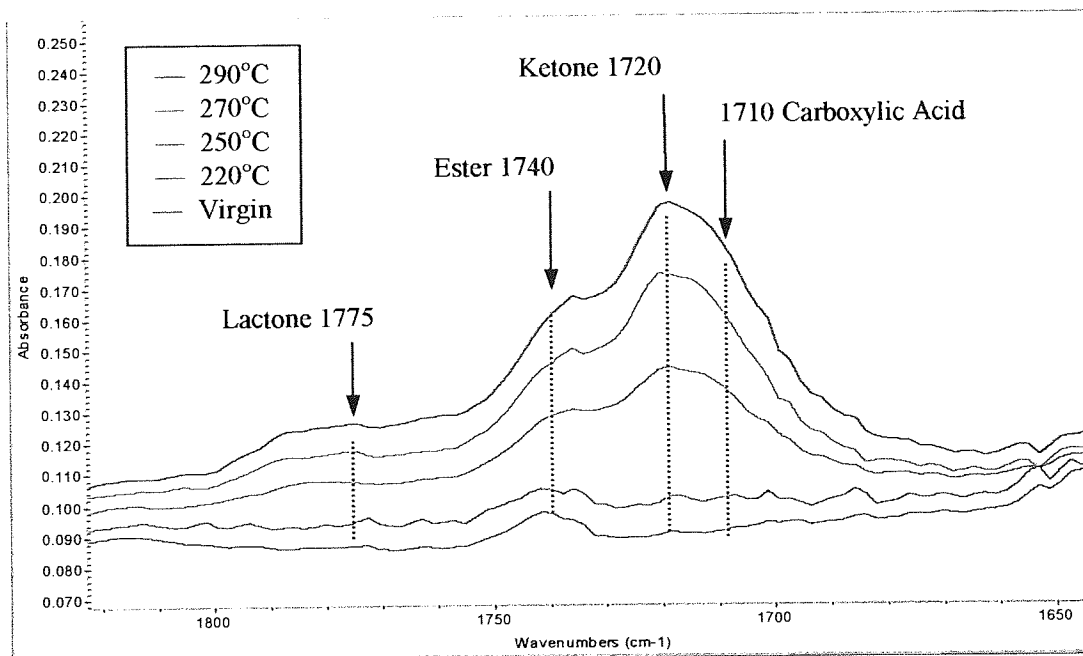


Figure 3.11. FTIR Spectra in the Carbonyl Region of TR Processed VP-8770 (60rpm, 10min)

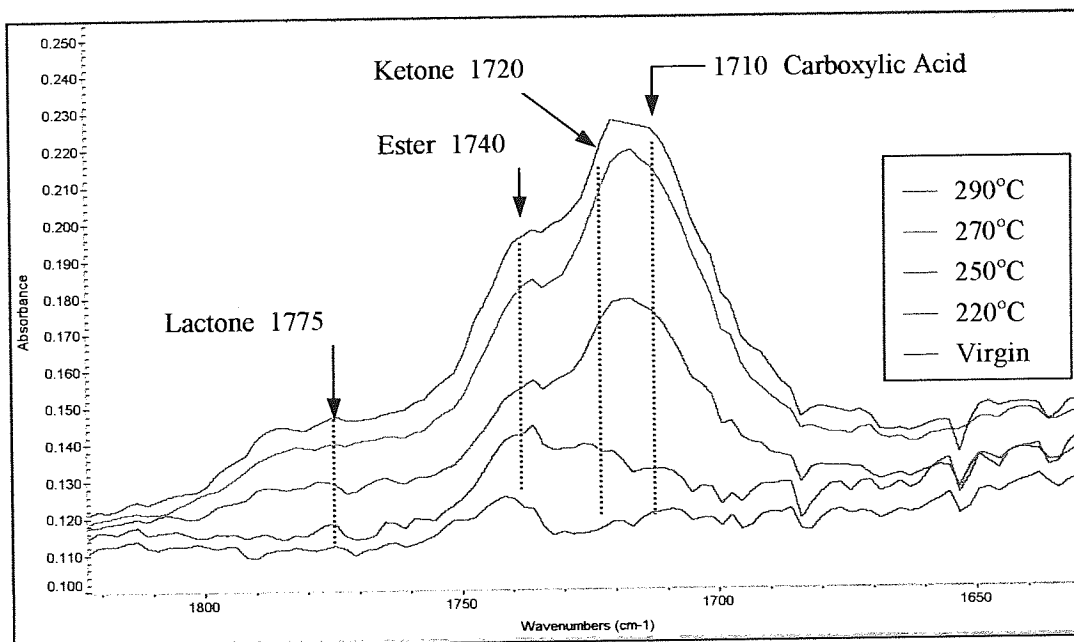


Figure 3.12. FTIR Spectra in the Carbonyl Region of TR Processed EG8150 (60rpm, 10min)

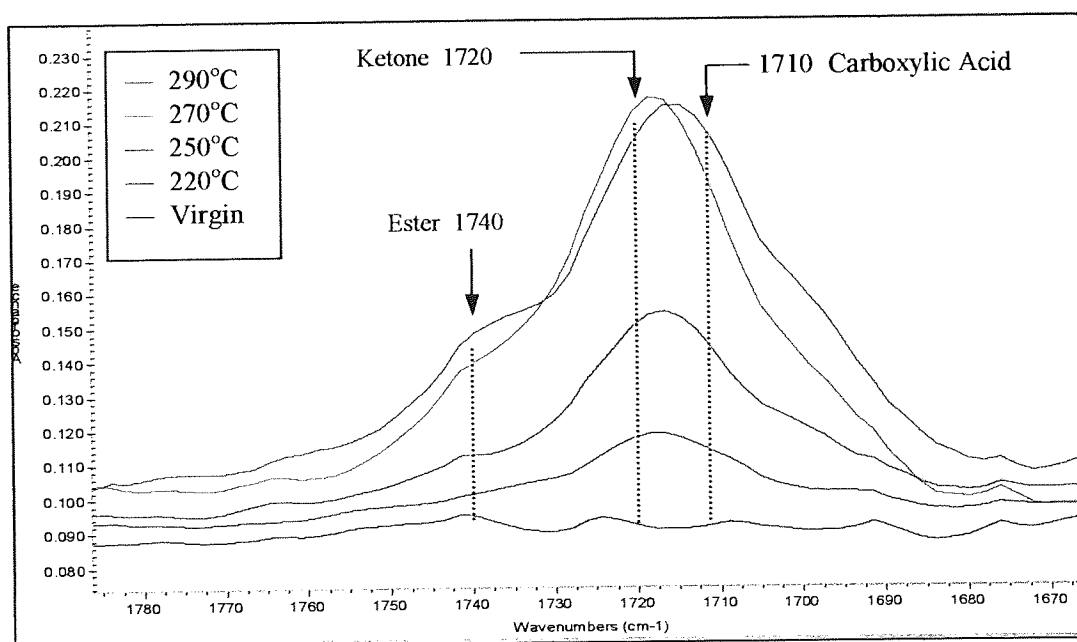


Figure 3.13. FTIR Spectra in the Carbonyl Region of TR Processed Dowlex2045-E (60rpm, 10min)

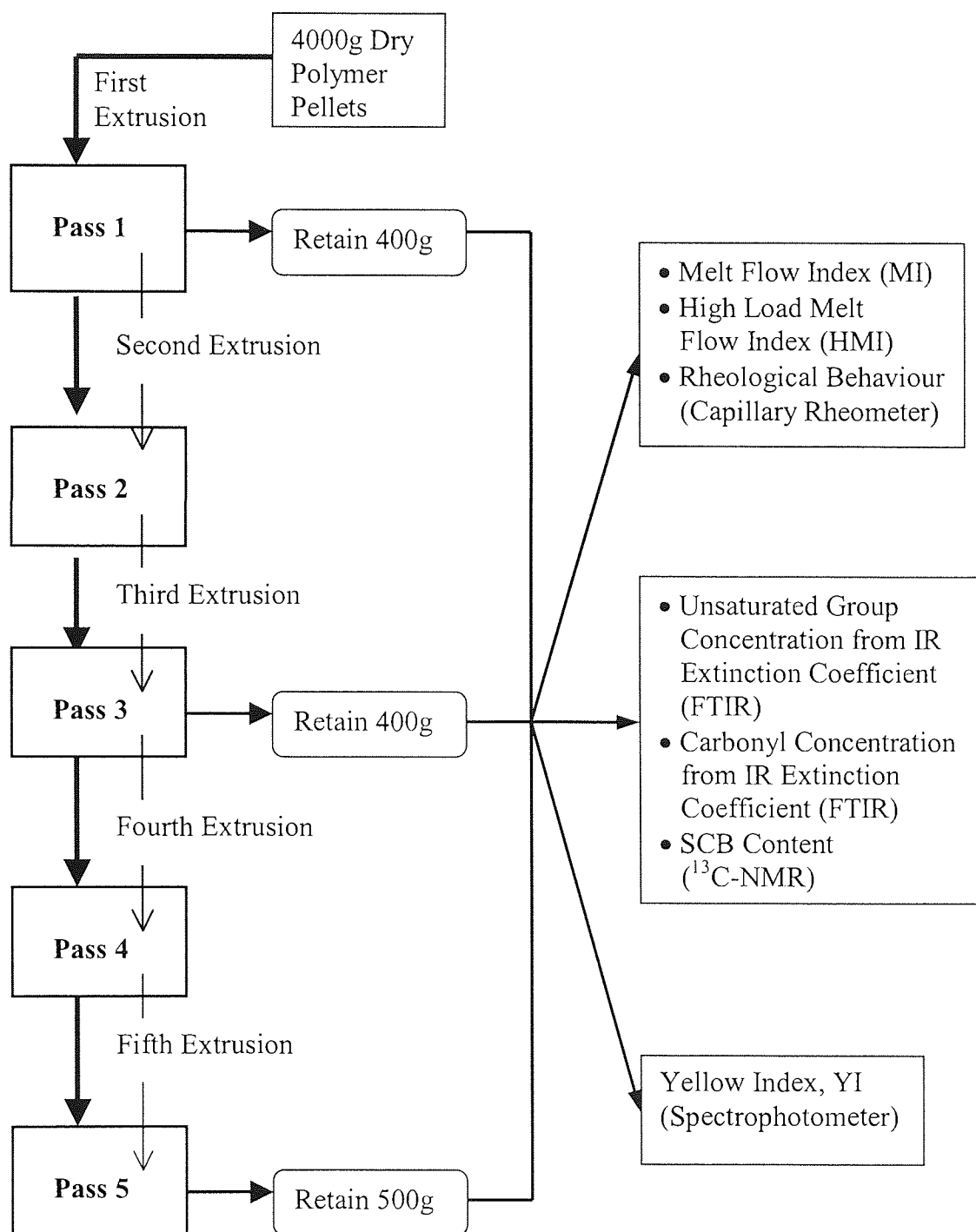
CHAPTER 4. THERMAL OXIDATION OF LLDPE DURING PROCESSING USING A TWIN-SCREW EXTRUDER (TSE)

4.1. OBJECTIVES AND METHODOLOGY

Linear low density polyethylene (LLDPE) has in recent years dominated the productions of extruded films for packaging applications. Twin-screw extruder (TSE) is commonly used in industry to manufacture LLDPE into useful products at elevated temperatures. A combination of high shear, high temperatures and considerable concentrations of oxygen can result in prominent changes in polymer structure due to thermal oxidative degradation, thereby significantly affecting the physical and mechanical properties of the final articles. In this part of the work, the effects of extrusion variables on the rheological and structural characteristics of different grades of unstabilised metallocene-based LLDPE polymers (having different comonomer content) and a selected Ziegler type LLDPE analogue were investigated. The main objectives were to identify the differences in the oxidation mechanisms during melt extrusion of different LLDPE polymers and to understand the effects of the molecular structure and extrusion conditions on the oxidation mechanism of the polymers.

Unstabilised m-LLDPE and z-LLDPE polymer pellets were extruded using a Betol twin-screw extruder. The extrusions of each polymer were conducted at different die temperatures (210-285°C) with a fixed screw speeds (100rpm). Five extrusions were carried out at each temperature and the extruded polymer samples after one, three and five passes were characterised using a range of analytical techniques. The rheological properties were investigated using a melt flow indexer and a Rosand twin-bore capillary rheometer. The structural characteristics were determined by FTIR (unsaturated groups and carbonyl compounds were quantified using the corresponding IR extinction coefficients) and ^{13}C -NMR (extent of short chain branching, SCB) respectively. Moreover, colour measurements were also carried out on both the virgin and the extruded LLDPE polymers using a Minolta CM-508i spectrophotometer (see Scheme 4.1

for the methodology used in polymer extrusion and characterisation). It is important to point out here that for the figures having percentage change in property in the Y-axis, the percentage change is with respect to the virgin unprocessed polymers and the zero point on the number of extrusion passes, X-axis, refers to virgin unprocessed polymer.



Scheme 4.1. Methodology Used in Investigation of Unstabilised LLDPE Oxidation during Melt Extrusion

4.2. RESULTS

4.2.1. Extrusion Parameters of Processed LLDPE Polymers

Extrusion conditions must be carefully determined based on the type of polymer and its grade in order to ensure that a stable extrusion process with minimum melt fracture is achieved. The extrusion conditions chosen for both Ziegler and metallocene LLDPE are based on conditions which were previously established in similar work in the PPP Research Unit [130, 133]. The variation of extrusion parameters can reflect, to a certain extent, changes in structural and rheological characteristics of the polymer.

The actual melt temperature of the polymer extrudate at the die exit was measured using an infrared thermometer (THI-500). Table 4.1 shows that when the LLDPE polymers were extruded at lower die temperatures (210, 235°C), their actual melt temperatures were higher than that of the die; whereas, the melt temperatures were lower than the die temperatures when the latter was fixed at higher processing temperatures (265, 285°C). The difference between the die temperature and the actual melt temperature (see Figure 4.1) indicates differences in the physical and chemical behaviour of the polymer melts, though the extents of these changes seem to be similar for the different types and grades of LLDPE used in this work.

Table 4.1 and Figure 4.2 also show that the melt pressure of all the polymers decreases with increasing extrusion temperature. This is mainly due to the reduction of the shear viscosity of the polymer melt at higher processing temperatures. Under conditions of similar die temperature and output rate, the m-LLDPE with highest comonomer content (VP-8770) presents higher melt pressure during extrusion (see Figure 4.2). Generally, the more comonomer the polymer contains (higher branching), the lower is its density (see Table 2.1 in Chapter 2). In order to keep the same extrusion output rate and to achieve comparable extent of screw fill, higher feeding rate was required for the lower density polymers (see Figure 4.3, a). As a result, more of the lower density

polymers were fed in a given volume for the same output rate leading to the observed increase of melt pressure (see Figure 4.3, b). In comparison with the metallocene-based polymers, the z-LLDPE analogue has higher melt pressure (see Figure 4.2) and lower feeding rate (see Figure 4.3, a) under the same extrusion conditions. The high shear viscosity of LLDPE polymers contributes towards their degradation during melt processing. The higher melt pressures (corresponding to higher shear viscosity) seen for the m-LLDPE containing higher comonomer (e.g. VP-8770), and for the z-LLDPE, indicate that, these LLDPE polymers may be more susceptible to mechanical and chemical degradation during melt extrusion, in the presence of shear, oxygen and heat.

The power consumption per kg of polymer extruded reflects the processability of polymers and is a function of the output rate, screw speed and electric current during extrusion. Table 4.1 shows that there is only small difference in the power consumption for the different types of LLDPE examined under various extrusion conditions.

4.2.2. Rheological Characteristics of Extruded LLDPE Polymers

4.2.2.1. Effects of TSE Processing on Melt Flow Behaviour Measured from Melt Flow Index

The melt flow behaviour of extruded LLDPE was examined under different loading weights (see Table A4.1). Figures 4.4 and 4.5 show the variation of percentage change in MI (with respect to the corresponding virgin polymers) with extrusion passes at different temperatures. A negative value in the percentage change in melt flow property indicates that the processed polymer undergoes crosslinking with respect to the virgin (unprocessed) analogue, whereas a positive value indicates chain scission. At the lowest extrusion temperature of 210°C, there is little change in melt flow behaviour of metallocene-based polymers (especially for those containing lower SCB content) with passes, whereas at higher extrusion temperature, there is a persistent negative change which increases with increasing extrusion temperatures, indicating increasing extent of crosslinking (see Figure 4.4). However, it is clear

from Figure 4.4 that the changes in melt rheological property of the z-LLDPE (Dowlex2045-E) occurs always to a higher negative values with passes at all extrusion temperatures, indicating higher extent of crosslinking compared to the m-LLDPE analogues.

The percentage changes in melt flow index of the individual LLDPE polymers after multiple extrusions are shown in Figure 4.5. The MI value of m-LLDPE with lower comonomer contents (FM-1570, PL-1840 and PL-1880) undergoes similar changes with increasing extrusion passes and temperatures. However, the MI change of m-LLDPE with the highest comonomer content (e.g. VP-8770) tends to show a lower extent of its negative values (less crosslinking) at increasing temperatures higher than 235°C upon multi-pass extrusions (see also Figure 4.4). It can also be found from Figure 4.5 that the MI change of extruded z-LLDPE always tends to be of a higher negative value with more extrusion passes; but the differences in MI change at the different temperatures are much less significant when the polymer was extruded for five passes.

Changes in MFR give an indication of changes in MWD of the polymer; the higher the percentage MFR change, the broader is the MWD. Figure 4.6 shows clearly that the Ziegler polymer gives much larger increase in MFR after multi-pass extrusions at all temperatures when compared to the changes observed in all the metallocene-based polymers, which show a relatively small increase in their MFR values with the VP-8770 (containing the highest comonomer content) generally giving the largest increase in MFR. Figure 4.7 indicates further that the MFR change in different grades of m-LLDPE polymers shows similar tendency after multiple extrusions.

Comparison of the effects of extrusion temperature for z-LLDPE with that for the metallocene polymers during multi-pass extrusions on the melt rheological properties is clearly illustrated in Figures 4.8 to 4.10. The much higher extent of negative change in MI and HMI for the Ziegler polymer at all temperatures (with higher extent of change at higher temperatures) clearly contrasts the much lower change observed in the case of the metallocene polymers, particularly at the lower extrusion temperatures. All the m-LLDPE show continuous gentle

decrease in their percentage MI change with temperature at all passes with the exception of the VP-8770 containing the highest comonomer content which gives rise to an initial fast negative decrease when extrusion temperature is increased from 210°C to 235°C, followed by a relative increase (though still negative values in % MI change) on further increase in processing temperature up to 285°C, see Figure 4.8. Similar tendency can also be observed from the percentage HMI change of the extruded LLDPE polymers with extrusion temperature (see Figure 4.9), but the HMI change of VP-8770 tends to be more positive when extruded higher than 265°C at all passes. Furthermore, the z-LLDPE shows a much larger increase in MFR value at all temperatures and extrusion passes compared to the different metallocene polymers that show relatively small changes, see Figure 4.10. Meanwhile, a generally similar change in MFR with increasing extrusion temperature can be observed for all the grades of m-LLDPE and VP-8770 always shows the biggest change.

4.2.2.2. Effects of Melt Processing on Rheological Properties Measured Using a Twin-bore Capillary Rheometer

The conversion of LLDPE matrix (granule or pellet) into useful final articles requires an operation of melt processing at high temperature (180~300°C) using for example extruders. The structural characteristics of LLDPE polymers (MW, MWD, SCB, SCBD) have great impact on their processability and also the processing conditions can significantly affect their rheological and molecular characteristics due to thermal oxidation that occur during melt processing. Rheological test of the virgin polymers using a capillary rheometer can provide valuable information that is directly related to their processability. Additionally, the differences of rheological performance for different processed LLDPE polymers can help us have a better understanding on their structural variation caused by oxidative degradation. The work on capillary rheometry of some virgin and processed LLDPE samples was conducted as part of undergraduate projects [137, 138]. The results were analysed and linked up with the processing stability through the comparison of rheological properties of virgin and processed polymers.

As polymer melts are non-Newtonian liquids, their shear viscosity is dependent on shear rate. While a shear stress is employed on polymer melt, the entanglement of the polymer chain is reduced and some kind of structural deformation and molecular orientation along the flow direction will occur. As a result, the polymer chains become more ordered and the increase of shear stress is slower than that of the shear rate, i.e. the shear viscosity decreases with increasing shear rates, which is so-called shear thinning. Most of the polymer melts show shear thinning during flow and the relationship between shear rate and stress can, to some extent, reflect their structural properties. The rheological behaviour of virgin LLDPE were first tested using a twin-bore capillary rheometer at different temperatures and a range of shear rates, which simulated the extrusion conditions carried out in TSE extruder.

Figures 4.11 to 4.12 show that both virgin m-LLDPE and z-LLDPE polymer melts exhibit shear thinning behaviour and so they all demonstrate pseudoplastic flow. At lower testing temperature (210°C), there is not much difference in the rheological performance of m-LLDPE polymers and the z-LLDPE (Dowlex2045-E) and all display excellent hysteresis (see Figure 4.11) corresponding to a good processing stability under this condition. Meanwhile, the increase of shear stress for z-LLDPE is very small after the shear rate reaches about 2000s⁻¹ at 210°C and significant shear thinning can be observed. The lower comonomer content and broader MWD are expected to be the main reasons for this phenomenon, because chain disentanglement would be expected to be easier for a polymer with less SCB. Moreover, the fraction of lower molecular weight polymer chains may perform as plasticiser molecules during the flow of polymer melt. However, when the testing temperature was increased to 265°C, some considerable changes in the rheological performance of LLDPE polymer melts could be clearly seen from Figures 4.11 and 4.12. Compared to the results obtained at 210°C, at the higher temperature of 265°C, the shear stresses of all m-LLDPE polymers showed a substantial decrease; VP-8770 polymer presented the lowest shear stress at high shear rates but also showed the best hysteresis cycle suggesting good processing stability. Moreover, unlike the situation at 210°C, the shear stress of Dowlex2045-E (z-LLDPE) increased continuously with shear rate when testing at 265°C (see Figure 4.12). These results imply that,

in addition to the effects of temperature on the viscosity of LLDPE melts, the changes in molecular structure of the polymers during extrusion in a capillary rheometer must be considered.

Figure 4.13 compares the shear viscosity changes with shear rate for individual virgin polymer samples tested at different temperatures. It can be seen that the shear viscosity of both m-LLDPE and z-LLDPE decreases with increasing testing temperature and this is paralleled by the observed decrease in melt pressure of LLDPE polymers during TSE extrusions at higher extrusion temperatures (see Figure 4.2). Figure 4.14 shows that the m-LLDPE containing higher comonomer content (VP-8770) gives higher shear viscosity when compared to the metallocene polymer having lower comonomer content (FM-1570). In most cases, the z-LLDPE showed higher viscosity compared to the m-LLDPE with similar comonomer content, i.e. FM-1570.

The shear viscosity changes with shear rate for TSE extruded LLDPE polymers tested by capillary rheometer are shown in Figures 4.15 and 4.16. Compared with the virgin polymers examined under the same conditions (see Figures 4.13 and 4.14), it is clear that the shear viscosity of both metallocene and Ziegler LLDPE has increased after TSE extrusion at 265°C (see Figure 4.16). The increase in shear viscosity in the extruded polymers is evidence of the occurrence of crosslinking for all the LLDPE samples tested. This is paralleled by a negative percentage MI changes after TSE processing (see Figure 4.4). Among all polymers examined, it is clear that VP-8770 polymer exhibited the largest extent of increase in shear viscosity at high shear rates (see Figures 4.16 and 4.19). This may be attributed to the higher SCB content and the higher extent of crosslinking during TSE extrusion, both of these factors can significantly restrict the movement of polymer chains, leading to the observed increase of shear viscosity during the polymer melt flow. Similar results can also be observed from the shear stress changes with shear rate shown in Figures 4.17 and 4.18. Furthermore, it is indicated in Figures 4.16, 4.18 and 4.19 that the number of extrusion passes does not significantly affect the rheological behaviour of the extruded m-LLDPE tested in a capillary rheometer, and the TSE extrusions generally have less effect on the rheological properties of z-

LLDPE (Dowlex2045-E), especially at high shear rates. The much broader MWD caused by TSE processing of the z-LLDPE polymer (see Figure 4.6) is suggested here to be one of the main reasons for the observed lower extent of increase in both shear viscosity and shear stress.

Extensional flow behaviour of polymer melts was also examined using the twin-bore capillary rheometer. As an important rheological parameter, extensional viscosity provides useful information on polymer melt elasticity. Polymers with a high extensional viscosity generally present high melt elasticity. Extensional viscosity involves the stretching of polymer melt during flow and is essentially a reflection of tensile deformation [133]. Furthermore, extensional viscosity is extremely sensitive to molecular weight distribution (MWD) and the degree of chain branching of the polymer. It is shown in Figure 4.20 that the polymer melts present tension thinning behaviour for both types of polymers as their extensional viscosities tended to decrease with increasing extensional stress. Meanwhile, the more significant decrease in extensional viscosity of VP-8770 (m-LLDPE containing the highest SCB amount) tested at 265°C illustrates the occurrence of larger extent of chain scission compared to other m-LLDPE polymers when extruded at higher temperatures using the capillary rheometer. The generally wider changing range of extensional viscosity exhibited by Dowlex2045-E (z-LLDPE) proposes that the extrusion in capillary rheometer results in broader MWD in z-LLDPE compared to metallocene polymers. Figure 4.21 shows the variations of extensional viscosity with extensional stress for virgin m-LLDPE and z-LLDPE polymers tested at 210°C and 265°C. It can be seen that the extensional viscosity of z-LLDPE is always higher than that of the metallocene polymers when tested at 265°C compared to its lower extensional viscosity measured at 210°C. This result indicates the higher melt elasticity of z-LLDPE when flowing at 265°C and it is mainly due to the occurrence of larger extent of crosslinking in z-LLDPE melt during extrusion in capillary rheometer. The relatively lower extensional viscosity exhibited by VP-8770 melt amongst the m-LLDPE polymers suggests again, that for this polymer a greater extent of chain scission occurs during the capillary extrusion at both temperatures, but more so at higher temperatures.

The extensional flow behaviours of TSE processed LLDPE polymers (265°C, P3) were also examined using capillary rheometer at 265°C and the results are shown in Figure 4.22. Comparison of Figure 4.21 (for virgin polymers) and Figure 4.22 (for extruded polymers) illustrates clearly that the extensional viscosity of all examined LLDPE polymers is much larger in the case of extruded polymers. It is evident that overall crosslinking reactions predominate in both types of polymers during TSE multiple extrusions at 265°C. It is also shown from Figure 4.22 that the extensional viscosity of the TSE extruded z-LLDPE decreases more steeply with increasing extensional stress compared to that of m-LLDPE polymers, indicating a greater extent of broadening in MWD for z-LLDPE during TSE extrusion under the same conditions. Meanwhile, the larger extent of increase in extensional viscosity for extruded VP-8770 (m-LLDPE containing the highest comonomer content) compared to other LLDPE polymers suggests the more significant effect of crosslinking on the rheological property of this polymer.

The results of degradation test using capillary rheometer at 265°C for virgin LLDPE polymers are illustrated in Figure 4.23. Each set of shear tests between interval times (10 minutes) was done to simulate an extrusion pass in the extruder, and all the polymers generally show an increasing trend in shear stress with degradation time, again suggesting that crosslinking reactions are predominant in this test. Among the degradation curves of LLDPE polymers, fluctuation can be observed for FM-1570 and VP-8770 (see Figure 4.23), indicating the complicated effects of crosslinking, chain scission, branching and orientation during the degradation test of polymer melts.

4.2.3. Structural Characteristics of Extruded LLDPE Polymers

The oxidative degradation of LLDPE polymers during twin-screw extrusion can lead to significant changes in their molecular structures. Thus, to have a comprehensive understanding of the oxidation mechanisms during TSE processing, the structural characteristics of LLDPE polymers after extrusion must be analysed. Generally, the most important effects of thermal oxidation on

the LLDPE structure are manifested in the variations of concentrations of their unsaturated groups, carbonyl compounds and extent of short chain branches. These structural characteristics of extruded polymers were examined using different analytical techniques and their changes are discussed in the following sections.

4.2.3.1. Effects of Extrusion on the Extent and Nature of Unsaturation Determined by FTIR

The quantification of the amount of double bonds contained in both virgin and the TSE-processed LLDPE polymers was carried out using FTIR (from corresponding IR extinction coefficient, see Section 2.3.2.1 in Chapter 2) and the results are displayed in Figure 4.24 and Tables A4.2 to A4.6. It can be clearly seen from these Tables that the trans-vinylene concentration in all the polymers tends to decrease with more extrusion passes at 210°C. At higher processing temperature (235~285°C), however, the more extrusion passes the polymers experienced, the more trans-vinylene were produced during the extrusions. It is clear from Figure 4.25 that the VP-8770 (m-LLDPE with the highest SCB content) contains the highest concentration of trans-vinylene after extrusion under all conditions; while, z-LLDPE has the lowest concentration of this double bond (similar to the situation of virgin polymers, see Figure 4.24). Figure 4.26 also shows that relative to the virgin polymers, the trans-vinylene concentration reduces in all the m-LLDPE after TSE extrusion under most processing conditions. However, there is generally an enhancement of trans-vinylene amount in z-LLDPE after TSE extrusions and an evident increase in trans-vinylene concentration with increasing temperature can also be observed upon multi-pass extrusions.

It is shown in Figure 4.27 that the vinyl content in z-LLDPE (Dowlex 2045-E) is much higher than that in m-LLDPE for both virgin and extruded polymers, and it reduces with more extrusion passes at all temperatures (see Tables A4.2 to A4.6). Meanwhile, the amount of vinyl group contained in different grades of extruded m-LLDPE varies within only a small range. Figure 4.28 indicates further that relative to the virgin polymers, the vinyl concentrations in all the

processed LLDPE polymers decrease under most conditions. However, a relative rise in vinyl concentration can also be observed for all the polymers when the extrusion temperature was increased to 285°C.

Generally, the vinylidene concentration in all the LLDPE polymers tends to increase (relative to virgin polymers) with more extrusion passes as well as increasing temperature (see Tables A4.2 to A4.6 and Figure 4.29). Similar to the situation of virgin polymers, the VP-8770 has the highest and the Dowlex2045-E (z-LLDPE) has the lowest vinylidene concentrations after TSE extrusion under all conditions. It is also clear from Figure 4.30 that the amount of vinylidene group in all the m-LLDPE increase after TSE processing, but the vinylidene concentration in z-LLDPE basically shows no substantial changes after extrusions.

Figure 4.31 shows that similar to the case of virgin polymers (see Figure 4.24), the m-LLDPE with the highest SCB content (VP-8770) has the highest amount of total double bonds and in most cases, z-LLDPE contains less total double bonds than m-LLDPE after TSE extrusions. Furthermore, Figure 4.32 indicates that the overall content of double bonds in extruded z-LLDPE generally decreases after processing under all conditions compared to the virgin polymer. The amount of total double bond decreases (with respect to the virgin polymers) for most of the m-LLDPE after one pass extrusion, with the exception of extrusion temperature of 285°C, and generally increases with increasing temperature for the m-LLDPE after five extrusion passes. The total double bond concentration increased at the highest extrusion temperature (285°C) for all the metallocene polymers.

4.2.3.2. Effects of Extrusion on the Type and Level of Carbonyl Containing Compounds Determined by FTIR

The concentration of carbonyl compounds in all the LLDPE polymers increased with more extrusion passes at all processing temperatures (see Table A4.7 in Appendix). Moreover, the higher extrusion temperature, the higher was the increases in carbonyl concentration. It is also shown in the Table that the carbonyl content in the z-LLDPE increases to a much greater extent with

extrusion passes at all temperatures compared to m-LLDPE, especially at lower extrusion temperatures. Figure 4.33 reveals further that the m-LLDPE with the highest SCB content (VP-8770) contains lower amount of carbonyl compounds than other metallocene polymers when only one pass extrusion was carried out. However, after five-pass extrusions, VP-8770 becomes the polymer containing the highest amount of carbonyl compounds.

Figure 4.34 shows that the change (with respect to the virgin polymers) in carbonyl compounds in LLDPE polymers increases after TSE extrusion under most conditions and the extent of increase in the z-LLDPE is much more significant than the metallocene-based polymers. Furthermore, the carbonyl concentration in all the m-LLDPE increases at higher temperatures after multi-pass extrusions with the VP-8770 (having the highest comonomer content) generally forming more carbonyl compounds compared with the other m-LLDPE polymers.

Figure 4.35 shows the FTIR spectra of one-pass and five-pass extruded FM-1570 (m-LLDPE with lower SCB content) in the carbonyl region. It is clear that the major carbonyl compound contained in this metallocene polymer is ester after one-pass extrusion at all temperatures and traces of ketone and carboxylic acid can also be observed. When five-pass extrusions were carried out, the ketone content increased greatly particularly at higher extrusion temperatures and aldehyde became dominant group out of all carbonyl compounds in FM-1570 extruded at higher temperatures (265°C and 285°C). Figure 4.36 shows the FTIR spectra of FM-1570 extruded at different temperatures (235°C and 285°C). It can be found that the amount of ketone increases remarkably when more extrusion passes were carried out at 235°C, although ester is still the predominant carbonyl compounds. Some differences can be observed from the FTIR spectra of FM-1570 extruded at higher temperature, i.e. 285°C (see Figure 4.36). The spectra show that multi-pass extrusions lead to greater extent of increase in the ketone content. Meanwhile, the aldehyde peak becomes the strongest in carbonyl region after multiple extrusions of this metallocene polymer.

The composition of carbonyl compounds in m-LLDPE with higher comonomer content (VP-8770) after multiple extrusions is shown in Figures 4.37 and 4.38. It can be seen from Figure 4.37 that esters are again the predominant compounds after one-pass extrusion at all temperatures. Additionally, considerable increases of lactone, ketone and carboxyl acid content can also be observed in the polymer extruded at 210 and 285°C. After five-pass extrusions, the majority of carbonyl compounds changes from ester to ketone when the extrusion temperature was increased from 210°C to 235°C or higher. There are no great differences in the amounts of lactone and carboxyl acids when VP-8770 was subjected to five extrusion passes at different temperatures. Figure 4.38 indicates the changes in FTIR spectra of VP-8770 extruded at 235°C and 285°C. It is important to note that when the polymer was processed at lower temperature (235°C), ester was still the major component of the carbonyl compounds after one-pass and three-pass extrusions, but ketone content kept increasing with more extrusion passes and finally became the dominant group after five-pass extrusions of VP-8770. When the temperature was increased to 285°C, esters were still the dominant group in the carbonyl region in VP-8770 extruded for one pass; while, ketone becomes the major component after multi-pass extrusions.

Figure 4.39 shows very different changes in the FTIR spectra (in carbonyl region) of z-LLDPE (compared to that of the m-LLDPE) extruded at different temperatures for one and five passes. In this case, the ketones and/or carboxylic acids rather than esters are seen to dominate the carbonyl composition after one-pass extrusion at all temperatures. The concentrations of both ketone and carboxylic acids tended to increase with the extrusion temperature; meanwhile, the content of another major carbonyl compound, aldehyde, is relatively low and shows little difference after extrusions at different temperatures. The FTIR spectra of z-LLDPE extruded for five passes indicate that there is always a great extent of rise in the amount of carbonyl compounds after five-pass extrusions. It is clear from Figure 4.39 that ketone is the dominant carbonyl compound in z-LLDPE after five-pass extrusions, although great amounts of aldehydes can also be observed. Figure 4.40 illustrates the changes of FTIR spectra in carbonyl region for z-LLDPE extruded at 235°C and 285°C. It can be clearly found that ketone is always the major carbonyl compound in the extruded polymer no

matter how many passes were carried out. Meanwhile, aldehyde evidently presents in the FTIR spectra and more extrusion passes is generally favourable to its formation.

4.2.3.3. Effects of Extrusion on the Extent of Branching Determined by ^{13}C - NMR

Tables 4.2 and 4.3 show the extent of short branching in LLDPE polymers extruded under different conditions. It can be seen that the extrusion temperature (after one-pass extrusion) has no significant impact on the SCB content (w%) in the extruded polymers (see Table 4.2). Table 4.3 highlights the effects of multi-pass extrusions at 265°C on the extent of branching in the processed polymer samples. Similarly, there is no evident change in the SCB content after different extrusion passes for all the polymers examined.

Figures 4.41 and 4.42 show the percentage changes in SCB content of LLDPE polymers after TSE extrusion and illustrate that the SCB content in FM-1570 (m-LLDPE containing the lowest amount of comonomer) always increases after one-pass extrusion at all temperatures. While, other m-LLDPE and z-LLDPE give a lower SCB content after one-pass extrusion compared with the virgin polymers. Figure 4.42 indicates that VP-8770 (m-LLDPE containing the highest amount of comonomer) is the only polymer in which the SCB content decreases after extrusion for all passes at 265°C.

4.2.4. Effects of Extrusion on Discoloration (Yellowing) of the TSE Processed Polymers

Typically, melt processing can lead to discoloration and the occurrence of yellowing in LLDPE polymers. The change in yellow index (YI) has been proved very useful in the evaluation of plastics degradation during processing [136]. By measuring the YI, a positive value describes the presence and magnitude of yellowness; a specimen with a negative YI will appear bluish.

Table 4.4 gives the YI results of LLDPE extruded under different conditions. It is very clear that the yellow index of all m-LLDPE increases with the pass of

extrusion at all processing temperatures, indicating more intensive yellowing and the formation of more coloured oxidative products in the polymers when subjected to multi-pass extrusions. In contrast, the YI values of z-LLDPE basically fluctuate with the pass of extrusion within a quite small range.

The variation of yellow index with extrusion temperature is shown in Figure 4.43. After one-pass extrusion, FM-1570 and PL-1840 (m-LLDPE containing less SCB) present negative YI, while VP-8770 (m-LLDPE with higher SCB content) and Dowlex2045-E exhibit positive YI value at all temperatures. The yellow index of both FM-1570 and PL-1840 tends to become more positive when subjected to more extrusion passes and at most temperatures after five-pass extrusions. Similar to the virgin polymers (see Table 4.4), the extruded z-LLDPE generally has higher YI value than m-LLDPE.

The YI difference between the virgin and processed polymer (Δ YI) indicates the change in polymer discolouration after TSE processing. Figure 4.44 shows the changes of Δ YI with temperature after multiple extrusions. In which, positive value of Δ YI indicates the increased yellowness and negative Δ YI indicates the decreased yellowness or increased blueness. It can be seen that, with the exception of PL-1840, all other polymers show positive Δ YI after extrusion at all conditions. Among them, z-LLDPE generally presents the highest Δ YI and VP-8770 exhibits the largest extent of increase in yellowness in m-LLDPE. Further, the Δ YI of metallocene polymers tends to increase with more extrusion passes and becomes close to that of z-LLDPE, especially for FM-1570 and VP-8770.

4.3. DISCUSSION

Thermal oxidation of LLDPE polymers during melt extrusion proceeds accompanied with significant changes in polymer structure and formation of numerous oxidation products. The oxidative degradation mechanisms of these polymers vary greatly depending on SCB amount, catalyst system as well as the processing conditions. Thus, the effects of thermal oxidation on the molecular

structures of different types and grades of LLDPE polymers are investigated respectively in this work.

4.3.1. Melt Stabilities of LLDPE Polymers during TSE Extrusion

The thermal oxidation of LLDPE during melt processing is reflected from changes in the melt flow behaviour of extruded polymers as a result of crosslinking or chain scission reactions. The MI changes described in Section 4.2.2.1 (see Figure 4.4) indicate that metallocene LLDPE generally tends to cross-link with more extrusion passes. In the case of extrusion at lower temperature (210°C), however, chain scission is found to dominate for some m-LLDPE. It is very interesting to point out that VP-8770, the metallocene-based polymer with the highest comonomer content, basically shows larger extent of crosslinking amongst the m-LLDPE after multi-pass extrusions at lower temperatures (210, 235°C), but the extent of crosslinking decreases when the extrusion temperature is increased to above 265°C. The significant drops of melt pressure with more passes during extrusion of VP-8770 at higher temperatures (compared with other metallocene polymers, see Table 4.1 and Figure 4.2) can also confirm this change in crosslinking, as the decrease in the extent of crosslinking leads to the reduction in polymer melt viscosity, hence the drop in melt pressure. Meanwhile, the MI performance of VP-8770 individually shown in Figure 4.5 reveals that the crosslinking extent of the polymer extruded at higher temperature (above 235°C) decreases definitely compared to that of the polymer extruded at 235°C. Other metallocene-based polymers show very similar curves of melt flow behaviour (see Figure 4.4), thus similar changing tendency in crosslinking or chain scission under all extrusion conditions, especially at higher temperatures. Furthermore, the difference of extrusion temperature has little effects on the MI changes of m-LLDPE with lower comonomer content when they were extruded at higher temperatures (265 and 285°C, see Figure 4.5). However, there is no evident correspondence between the melt flow index and the comonomer content for these extruded m-LLDPE (FM-1570, PL-1840 and PL-1880, the original SCB contents are 11.6 w%, 13.4 w% and 17.1 w% respectively). Based on the melt flow behaviour it can be assumed that there is a limiting comonomer content (e.g. ~20 wt%) in m-LLDPE

so that polymers containing comonomer within this limit generally show similarity in their oxidative degradation during extrusion, and the differences in oxidative performance are most likely caused by other factors such as the amount of catalyst residue rather than the difference in comonomer content. A polymer, which has a comonomer content higher than this limit, e.g. VP-8770 (SCB content 28.2 wt%), shows totally different and more complicated thermal oxidation characteristics during TSE extrusion.

It can be clearly found from Figure 4.4 that z-LLDPE always shows serious crosslinking after extrusion, especially at higher temperatures, and the extent of crosslinking tends to be greater when more extrusion passes were carried out. Additionally, z-LLDPE shows much higher degree of crosslinking compared to m-LLDPE under the same extrusion conditions. The totally different catalyst system used to produce these two types of polymer is suggested here to be the main reason for their different oxidation behaviour. Although z-LLDPE presents a very strong tendency of crosslinking during extrusion and shows greater extent of crosslinking at higher extrusion temperatures or under multi-pass extrusions, there seems to be a limitation of crosslinking for this polymer, which can be observed from Figure 4.5. This figure shows the extents of crosslinking of five-pass extruded z-LLDPE at different temperatures are very close and the curves of MI changes tend to level off.

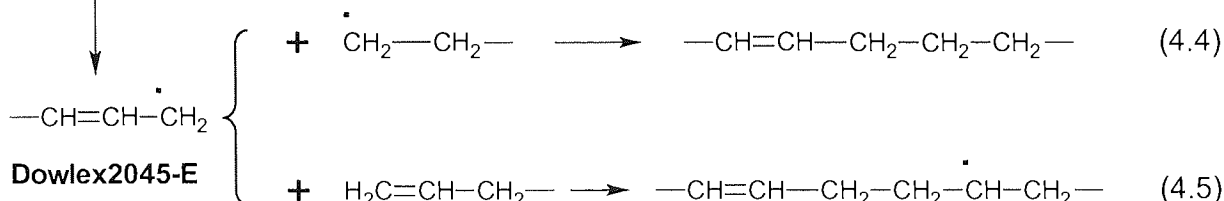
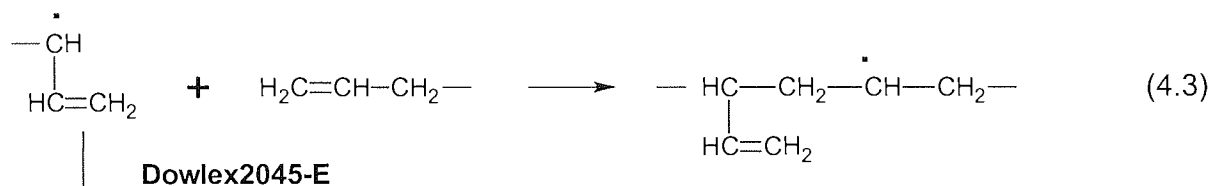
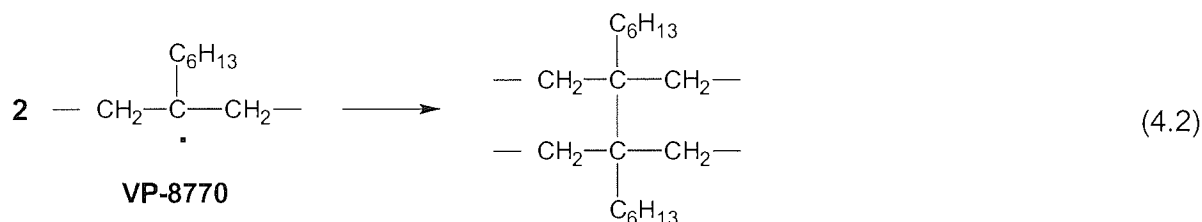
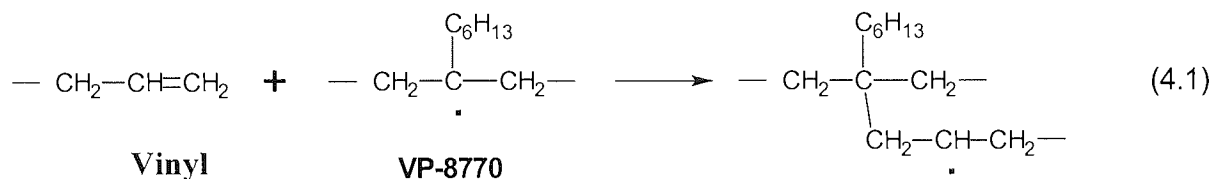
The MFR changes illustrated in Figure 4.6 indicate that the molecular weight distribution of most of the LLDPE tends to be broader with more extrusion passes as well as extrusion temperature (see Figure 4.7). An exception can be found for VP-8770 extruded under the conditions of 285°C, five passes. Relating to its MI changes after extrusion under the same conditions, this result indicates that a considerable chain scission occurs in this polymer leading to a narrower molecular weight distribution after extrusion. The very similar MFR changes for other m-LLDPE correspond well with their melt flow behaviour (see Figures 4.8 to 4.10). Conclusion can be made from the much greater increase of MFR for extruded z-LLDPE that, the molecular weight distribution of z-LLDPE becomes much broader than that of m-LLDPE if they are extruded under the same conditions. A further comparison of the relationship between MI and MFR

reveals that no matter what type of LLDPE polymer, the more MI changes (compared to the virgin polymer) after the extrusion, the higher is the MFR, and hence the broader is the molecular weight distribution.

The results come from the analysis of the rheological behaviour of LLDPE measured by a capillary rheometer correspond well with the observation from the TSE extrusion as well as the outcome of MI measurements, and further confirm that all the polymers undergo mainly crosslinking during melt extrusion (see Section 4.3.2). Moreover, the rheological measurement shows more clearly that the m-LLDPE containing the highest comonomer content (VP-8770) undergoes chain scission (to some extent) when it was extruded in the capillary rheometer (equal to TSE extrusion P₁, see Figures 4.11 and 4.12) at a higher temperature (265°C). In addition, Figures 4.13 and 4.14 show that the testing temperature generally has more significant effect on the rheological behaviour of LLDPE polymers than the structural variation (chain scission or crosslinking) during extrusion in a capillary rheometer. The exception presented by VP-8770 tested at higher temperatures (e.g. 265°C and 285°C, see Figures 4.13 and 4.14) indicates that both chain scission and crosslinking reactions occurred to a larger extent and they can greatly affect the rheological performance of this polymer at high shear rates.

It is shown from Figures 4.15 and 4.17 that the TSE extruded z-LLDPE generally exhibits lower shear viscosity and shear stress (compared to the m-LLDPE polymers) at high shear rates, although it shows a much larger extent of crosslinking (from MI measurement, see Figure 4.4) after multi-pass extrusions. Meanwhile an overall crosslinking can be observed from the considerable increase of shear viscosity and shear stress for all the extruded LLDPE polymers compared to the corresponding virgin polymer (see Figures 4.16 and 4.18). Figure 4.19 shows the TSE processed VP-8770 (m-LLDPE with higher comonomer content) gives the highest increase in shear stress (compared to virgin polymers), while z-LLDPE presents the lowest extent of increase in shear stress when tested at high shear rate. The rheological properties of these two extruded polymers suggest that although crosslinking predominates for both polymers during TSE extrusions, there must be some important differences in

their oxidative reactions. The related crosslinking reactions that are suggested to contribute to the different rheological behaviour observed for these two polymers are shown below in Reactions 4.1 to 4.5.



The formation of alkyl radicals takes place preferentially at the branching points (e.g. on the tertiary carbon atoms) [66, 76]; on the other hand, the primary initiation of oxidation occurs mainly at allylic C-H bonds [74], meanwhile, the vinyl group plays the most important role in crosslinking *via* addition to an alkyl radical [99]. Since the more comonomer containing metallocene-based polymer (VP-8770) has much more SCB than the other m-LLDPE examined here, it generally undergoes long-chain branching and “side-to-side” crosslinking according to Reactions 4.1 and 4.2. These kinds of crosslinking reactions can greatly enhance the entanglement of polymer chain and seriously restrict the

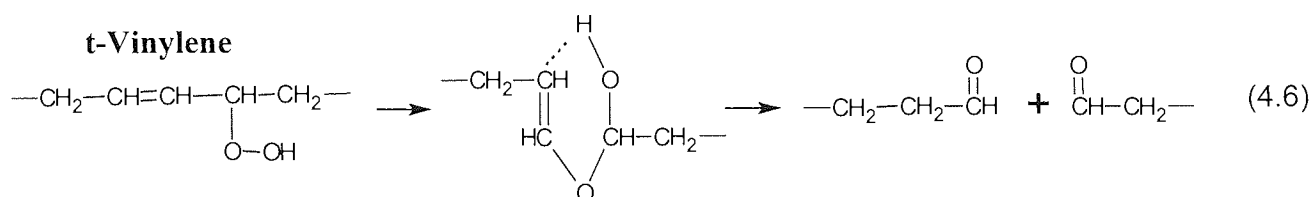
movement of polymer melt, even though the extent of crosslinking may be relatively small. The z-LLDPE has the lowest comonomer content and the greatest amount of vinyl groups (much more than that in all m-LLDPE, see Figure 4.24). As a result, the crosslinking reactions that occur during melt extrusion are primarily short-chain branching and “head-to-head” crosslinking (see Reactions 4.3 to 4.5) [46], leading to linear enlargement of the molecular chains. The effects of crosslinking by these reactions on the rheological performance of polymer melt are significant when lower pressure is applied (i.e. MI measurement). However, in the case of high-pressure measurement (i.e. using capillary rheometer), especially at higher shear rates, the cross-linked polymer chain can undertake molecular orientation to a greater extent along the stress direction thus reducing remarkably the chain entanglement, and hence the melt viscosity, even if the polymer undergoes a high degree of molecule enlargement and short chain branching. Comparing the results of extension measurement between the virgin and TSE extruded LLDPE polymers (265°C, 100rpm, P3) as shown in Figures 4.21 and 4.22, the greater extent of increase in extensional viscosity for three-pass extruded VP-8770 (compared to the extruded z-LLDPE) indicates further that the crosslinking caused by TSE extrusion has more significant effect on the rheological performance of VP-8770 (high comonomer containing m-LLDPE) than that of Dowlex2045-E (z-LLDPE)

4.3.2. Changes in Micro-structure of m-LLDPE with Lower SCB Content

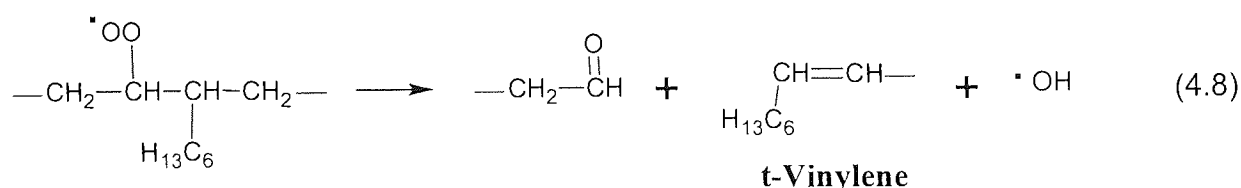
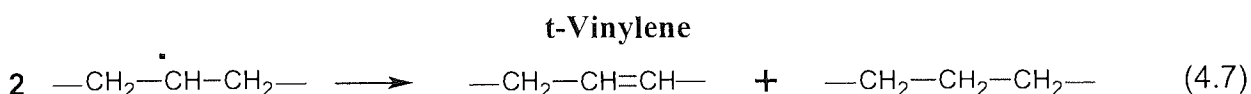
The virgin (unprocessed) metallocene-based polymers containing relatively lower amount of comonomer (FM-1570, PL-1840 and PL-1880) have generally similar content of unsaturated groups (see Figure 4.24). The variation of double bond concentrations for these virgin m-LLDPE polymers seems to have no direct relation to the SCB content and is most likely dependent on the composition of catalyst system used for polymerisation. Further, the carbonyl concentrations originally contained in these polymers show almost no difference.

It is evidently shown in Figure 4.25 that no matter what type of LLDPE, the polymer originally containing more amount of trans-vinylene normally has higher trans-vinylene concentration after TSE extrusion under all conditions

(refer to Figure 4.24). That means the variation of trans-vinylene caused by melt extrusion is quite limited and has no substantial effect on the overall trans-vinylene content. However, as shown in Figure 4.26, the trans-vinylene content in the m-LLDPE polymers containing lower extent of branching decreased after TSE processing, although there is a trend of increase with temperature when the polymers were subjected to multi-pass extrusion. As trans-vinylene is basically not involved in addition reaction with alkyl radicals [93, 99], its decrease is assumed to be due to the decomposition of allylic hydroperoxides that are formed on oxidation of these m-LLDPE [101].



The cleavage of allylic hydroperoxides shown above is normally an acid-catalysed reaction, leading to chain scission and formation of two aldehyde groups [101]. In spite of the reduction of trans-vinylene concentration after TSE processing, reactions leading to the formation of trans-vinylene have also been recognized as competing with Reaction 4.6, this can be observed from the increase of trans-vinylene amount in extruded z-LLDPE as well as the evident increasing tendency of trans-vinylene for the processed m-LLDPE polymers subjected to multi-pass extrusion at higher temperatures (see Figure 4.26). The formation of trans-vinylene is proposed as a result of disproportionation of secondary alkyl radicals and β -scission of α,β -branch-peroxy radicals which are shown in Reactions 4.7 and 4.8 [96, 99].



Although some reactions that result in the variation of trans-vinylene amount can lead to polymer chain scission (i.e. Reactions 4.6 and 4.8), crosslinking is still predominant for lower branching m-LLDPE as a consequence of multi-pass extrusion at higher temperature (see Figure 4.4). The vinyl group is the most important unsaturated structural unit affecting crosslinking in LLDPE [93, 99]. The addition of alkyl (or perhaps alkoxy or alkylperoxy) radicals to the vinyl group is the most important mode of crosslinking in LLDPE thermal oxidation. This can well explain the dominance of crosslinking in FM-1570 (originally having the highest content of vinyl groups in the three lower branching m-LLDPE) extruded at 210°C, while chain scission is predominant for PL-1840 and PL-1880 during extrusion under the same conditions. In most cases, the radicals involved in the addition reactions of low branching m-LLDPE are secondary radicals (see Reaction 4.9).

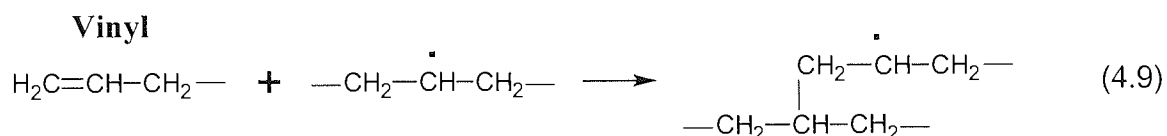
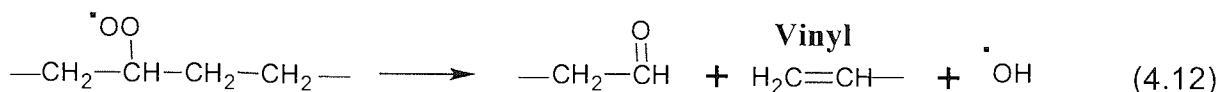
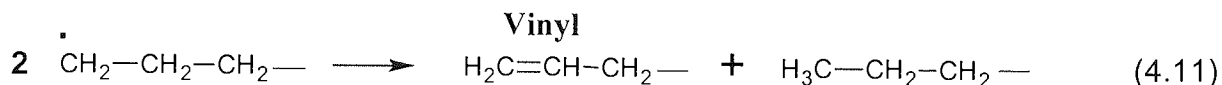
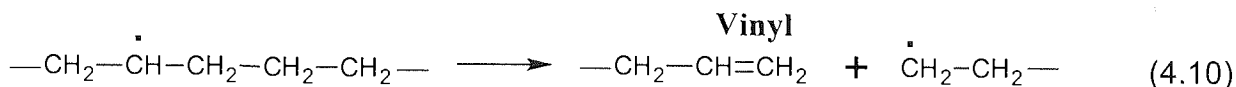
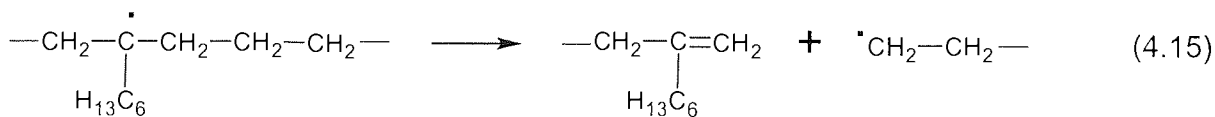
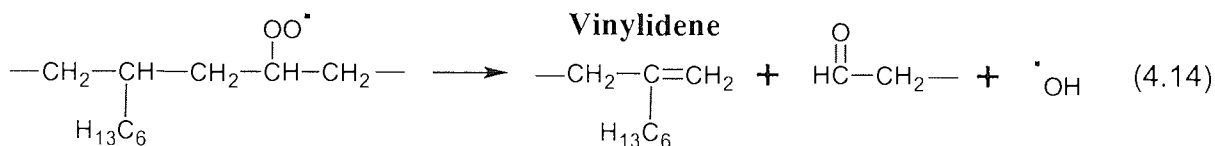
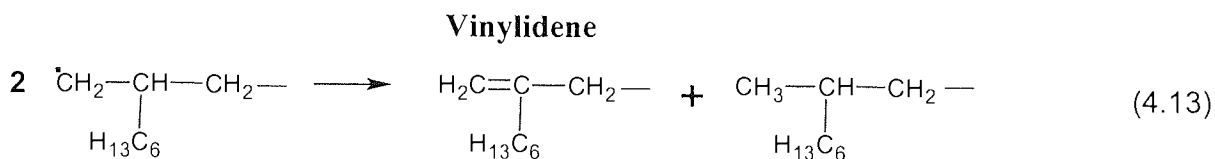


Figure 4.28 shows that the vinyl concentrations of all the m-LLDPE with lower comonomer content decrease to a great extent after TSE extrusion, confirming the fact that vinyl groups were consumed in the addition reactions leading to crosslinking. However, it is also very clear that the vinyl concentrations of these polymers tend to increase with extrusion temperature and do not drop down corresponding to the enhancement of crosslinking extents shown in Figure 4.4. On the one hand, it is indicated that some reactions that yield vinyl groups must also occur during melt extrusion, especially at higher temperatures (see Reactions 4.10 to 4.12); on the other hand, other reactions that result in crosslinking such as recombination of alkyl radicals with each other, with alkoxy or alkylperoxy radicals seems to be involved, and high temperature is more favourable to these reactions as it is much easier for the radicals to escape out of the “cage” and recombine or disproportionate.



Both trans-vinylene and vinylidene are relatively stable groups but are nevertheless important unsaturation for elucidation of the mechanisms of LLDPE thermal oxidation. It can be found from Figure 4.29 that the vinylidene concentrations of the three lower SCB containing m-LLDPE polymers are very close and exhibit a trend of increase with extrusion temperature. Figure 4.30 shows further that more vinylidene groups were formed after TSE extrusion of these polymers. The vinylidene groups is suggested to be mainly formed *via* disproportionation of alkyl radicals and β -cleavage of alkyl or peroxy radicals adjacent to SCB (see Reactions 4.13 to 4.15) [99].



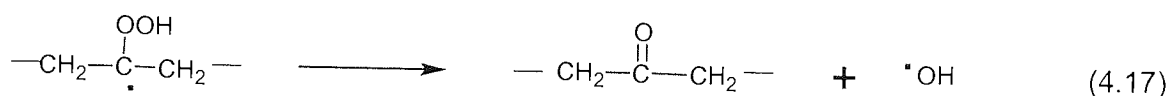
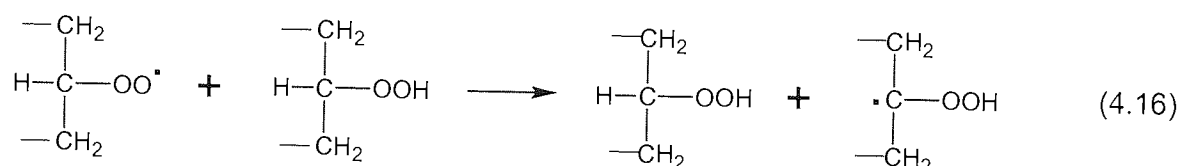
It is worth noting that the reactions producing vinylidene groups normally involve some structural units containing SCB, and the vinylidene groups resulted

from different reactions have the same structure, i.e. they are all formed by the transformation of a σ -bond attached to the branching point to a π -bond. Accordingly, the SCB structure plays a very important role in the formation of vinylidene groups. It can be seen from Figure 4.24 that PL-1840 contains the highest amount of vinylidene before any extrusion. However, Figure 4.30 shows after extrusion under all conditions, the increase of vinylidene content in PL-1840 is much smaller compared with that in the other two lower branching m-LLDPE polymers. This suggests that for the m-LLDPE having lower comonomer content, if a polymer originally contains more vinylidene groups, that means more SCB are distributed on the end of polymer chains and as a result, there are less SCB on the chains to provide tertiary carbon atom for the formation of vinylidene groups during thermal oxidation.

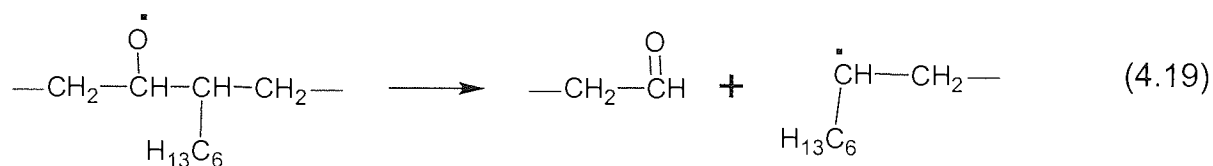
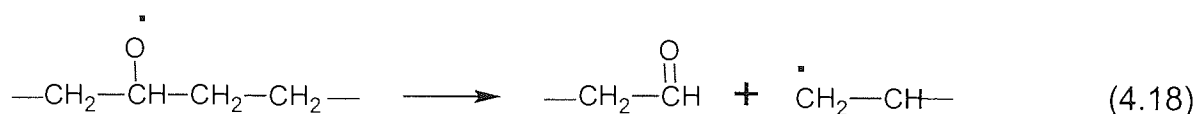
The carbonyl concentrations of the three lower branching metallocene-based polymers are very close and their changes after TSE extrusion are also very similar (see Figures 4.33 and 4.34). It was found that the carbonyl concentrations of the extruded m-LLDPE become higher compared to the virgin polymers and they steadily increase with temperature when multi-pass extrusions were carried out. Associated with the FTIR spectra of the representative polymer (FM-1570) shown in Figures 4.35 and 4.36, it has been indicated that carbonyl compounds were formed as a result of thermal oxidation during extrusion and the carbonyl composition varies depending on the processing conditions.

The FTIR spectra of FM-1570 in carbonyl region (see Figure 4.35) show that there are no significant changes for the spectra in this region after one pass extrusion at different temperatures, only a little increase on the peak of ketone can be observed with raising the temperature. However, when five-pass extrusions were carried out, large differences in the FTIR spectra were obtained at different temperatures. The main feature in the spectra of the extruded polymer at higher temperatures is the large increase of ketones. The hydroperoxide decomposition shown in Reactions 4.16 and 4.17 is considered especially important to the formation of the ketone groups because the tertiary hydrogen atom in α -position to the hydroperoxide group is rather labile to free

radical attack [95, 101]. Since most hydroperoxides formed in the lower branching m-LLDPE are secondary ones, it is assumed that ketones are produced in the decomposition of secondary hydroperoxide attacked by secondary peroxy radicals within the "cage" [100,102].



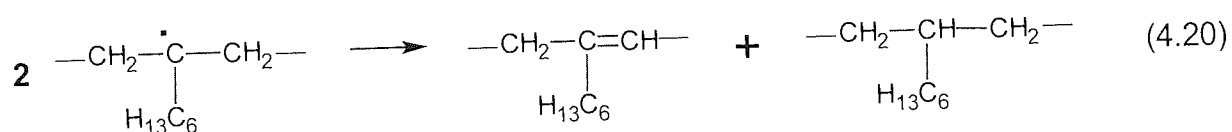
Compared to the FTIR spectra of virgin (unprocessed) FM-1570, a major change in the spectra of the same polymer when extruded at higher temperatures and more extrusion passes (see Figures 4.35 and 4.36) centres around the formation of peaks at 1730cm^{-1} and 1718cm^{-1} attributed to aldehydes and ketones [139]. Aldehydes can be formed *via* several routes (see Reactions 4.6, 4.8, 4.12 and 4.14), but mainly from the breakdown of secondary peroxy radicals accompanied with the yield of different types of unsaturated groups, as well as the β -scission of secondary alkoxy radicals described in Reactions 4.18 and 4.19. Higher temperatures are especially favourable for the decomposition of both peroxy and alkoxy radicals, because they all need energy to break σ -bonds and form π -bonds [99]. Although aldehydes are not usually stable in polyethylene during extrusion, the high viscosity of LLDPE polymers may prevent aldehydes from further oxidation by restricting the availability of oxygen. In addition, most of the decomposition reactions of oxygen containing (peroxy and alkoxy) radicals in LLDPE lead to the formation of aldehydes. As a result, aldehydes could be produced continuously and accumulated in the extruded LLDPE polymers.



As shown by the FTIR spectra of FM-1570, although ester is the dominant carbonyl compound in unprocessed (virgin) polymer, its change after TSE extrusion is quite small no matter what processing conditions were applied. Additionally, the variations of the contents of other carbonyl compounds (except for ketones and aldehydes) are not evident either after melt extrusion, despite the fact that a little increase of lactones and carboxylic acids can be observed in the polymer extruded under certain conditions. Meanwhile, the accumulation of aldehydes clearly found in the FTIR spectra of extruded FM-1570 polymers (higher temperature, multiple passes) also suggest that the further oxidation of aldehydes to carboxylic acids, which has been discussed in literatures [101, 139], are not very important for the m-LLDPE with lower SCB content under the extrusion conditions chosen for this work due to the restriction of oxygen. Thus, the esterification through reaction of carboxylic acids with alcohols, which is supposed to make the most significant contribution to the formation of ester [94], has less chance to occur during the extrusion of these polymers, their ester concentration remains almost unchanged.

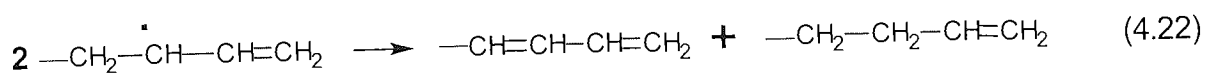
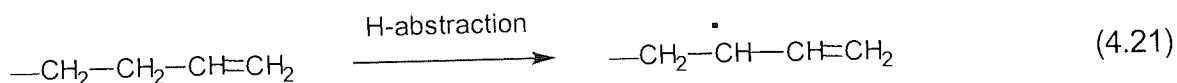
The alteration of SCB amount in extruded FM-1570 and PL-1840 (m-LLDPE with lower comonomer content) was examined. The results (see Tables 4.2 and 4.3) show that the changes of short branching are very small for these two polymers after TSE extrusion at most chosen conditions. That means the melt extrusion has no significant effects on the total amount of branches in these m-LLDPE; in other words, the changes in branching caused by melt extrusion are too small compared to the original SCB amount and are within the range of experimental error. However, the melt flow measurements and structural

analysis of the extruded polymers indicated that thermal oxidation involved changes in the branching, at least to some extent, during the extrusion. Two main factors are considered to account for the inconsistency between the results on extent of branching and other measurements. The first is the position of the branches produced or lost in the polymer chains (middle or near to the end). Since the changes of branching normally accompany crosslinking or chain scission, the branching point position will greatly affect the melt flow behaviour of the polymer. Another factor is the method utilized to quantify the branching amount. Based on the ^{13}C -NMR technique used for branching determination in this work [42, 43], it is impossible to correctly measure the SCB attached near to other groups, e.g. the branch adjacent to double bond formed in Reaction 4.20.

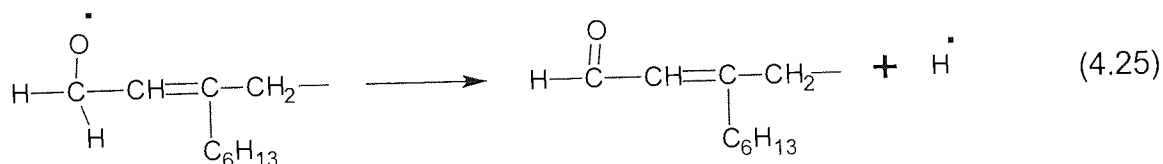
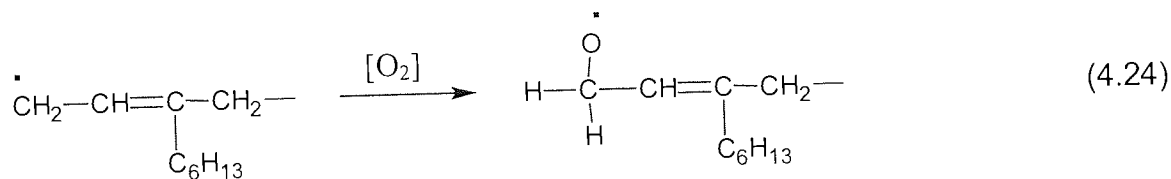
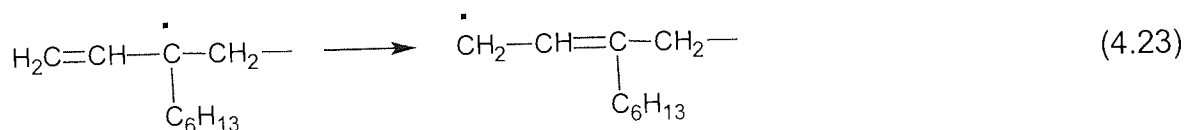


Although it seems unsuccessful to analyse oxidative degradation of LLDPE polymers by means of measuring the branching amount, it is still useful in the evaluation of oxidation behaviour of m-LLDPE. As shown in Figure 4.41, the increase of branching amount in FM-1570 after one-pass extrusion at 210°C further confirms the dominance of crosslinking which has been indicated in melt flow measurement (see Figures 4.4 and 4.5).

The results from colour measurement of TSE extruded LLDPE (see Figures 4.43 and 4.44) show that FM-1570 exhibits higher yellow index (YI) as well as more positive YI changes compared to other m-LLDPE containing lower SCB content (e.g. PL-1840). The generally larger amount of carbonyl compounds yielded in FM-1570 during thermal oxidation (see Figure 4.33) is a reason for its more serious yellowing. Meanwhile, FM-1570 originally contains much more amounts of vinyl groups than PL-1840 (see Tables A4.2 and A4.3), the vinyl groups are suggested to perform some kinds of transformation through thermal oxidation within the "cage", leading to the formation of conjugated sequences, which are believed to be another primary factor causing discolouration (see Reactions 4.21 and 4.22) [93].



In addition, the melt flow behaviour of TSE processed polymers shown in Figure 4.4 indicate that FM-1570 overall undergoes greater extent of crosslinking compared to PL-1840 under the same extrusion conditions; overall less extent of chain scission occurred in FM-1570 under the same extrusion conditions. As branching points (tertiary carbon atoms) play very important role in propagation of LLDPE thermal oxidation, their position on the chain can greatly affect the properties of chain scission. The breakdown of branches in the middle of polymer chains has much more effect on the changes in melt flow performance than those near to the end of chains. Based on this analysis, relatively more amounts of SCB in FM-1570 is proposed here to be attached to the carbon atom adjacent to a vinyl group (near to the end of the polymer chain), and Reactions 4.23, 4.24 and 4.25 are suggested to occur in the thermal oxidation, leading to the formation of both carbonyl compounds and conjugated systems that cause more substantial discolouration [93].

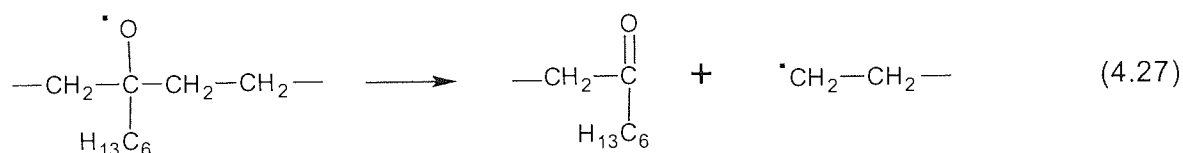
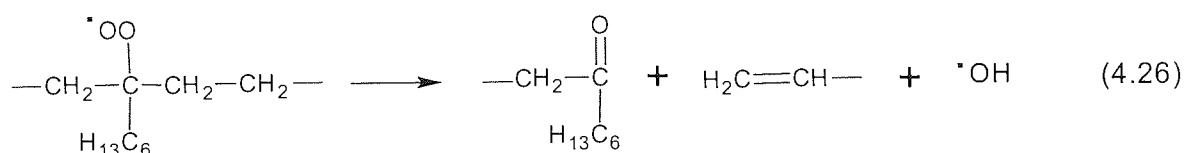


4.3.3. Changes in Micro-structure of m-LLDPE with Higher SCB Content

By comparison with the metallocene polymers having lower amount of comonomer, VP-8770, the m-LLDPE containing much higher comonomer content, has shown some similarities in the variation of unsaturated groups (see Figures 4.25 to 4.30) and carbonyl composition (see Figures 4.35 to 4.38) after melt extrusion. On the other hand, the higher content of SCB in this polymer (more tertiary carbon atoms presented in the polymer chains) has substantial effects on its oxidative behaviour when subjected to multiple extrusions.

It can be seen from Figures 4.25 to 4.32 that the extruded VP-8770 has always the highest concentrations of trans-vinylene, vinylidene and total double bond compared to other m-LLDPE, corresponding well with the original content of these unsaturated groups in the virgin polymers (see Figure 4.24). However, the vinyl concentrations in processed VP-8770 are the lowest and in most cases they have the largest extent of decrease after extrusion among the metallocene-based polymers. In addition to the consumption of vinyl groups in the addition reactions with alkyl radicals, due to the presence of relatively large amounts of SCB in VP-8770, vinyl groups are more likely to be attached to branching points and undergo isomerisation as shown in Reaction 4.23, leading to the decrease of vinyl concentration without crosslinking (See Figure 4.4).

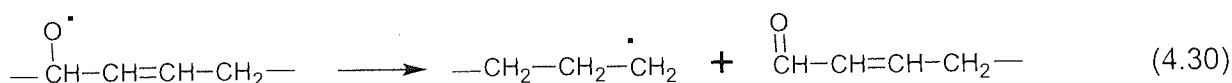
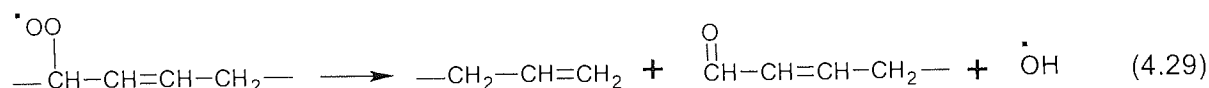
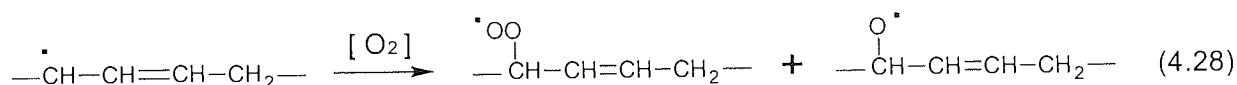
Figures 4.33 and 4.34 show that VP-8770 contains less carbonyl compounds than other lower branching m-LLDPE after one pass extrusion, but its carbonyl contents become higher than that of other metallocene-based polymers after multi-pass extrusions, especially at higher temperatures. As VP-8770 has much more comonomer it will have a great number of tertiary radicals produced in the propagation step of the oxidative degradation, Reactions 4.26 and 4.27 are considered to make the most significant contribution to the formation of carbonyl compounds in the thermal oxidation of this polymer at higher temperatures.



The decomposition of tertiary peroxy and alkoxy radicals leads to chain scission and that is one of the main reasons for the increasing tendency of melt flow index for VP-8770 extruded at higher temperatures (see Figure 4.5). Figure 4.28 also shows that the vinyl concentrations in VP-8770 after multi-pass extrusions present an evident tendency of increase with temperature. The production of vinyl groups through Reaction 4.26 and disproportionation reaction of primary alkyl radicals formed in Reaction 4.27 (See Reaction 4.11) would be a reasonable explanation. Meanwhile, since VP-8770 originally contains less amounts of vinyl groups, the recombination of tertiary alkyl, alkoxy and peroxy radicals produced in thermal oxidation at lower temperatures is assumed to play an important role in the formation of higher extents of crosslinking (compared to other m-LLDPE, see Figure 4.4) found after multi-pass extrusions at 210 and 235°C.

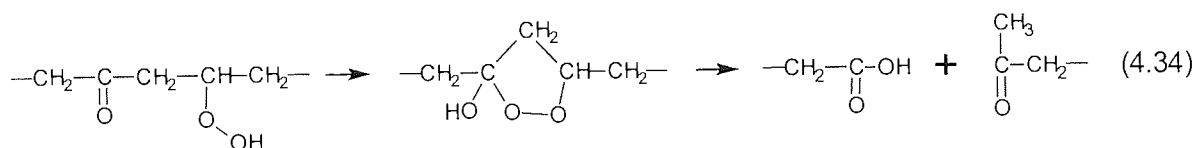
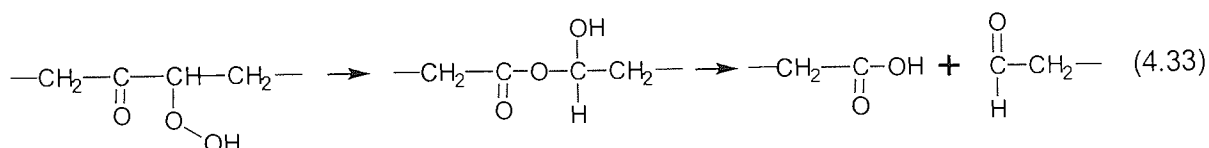
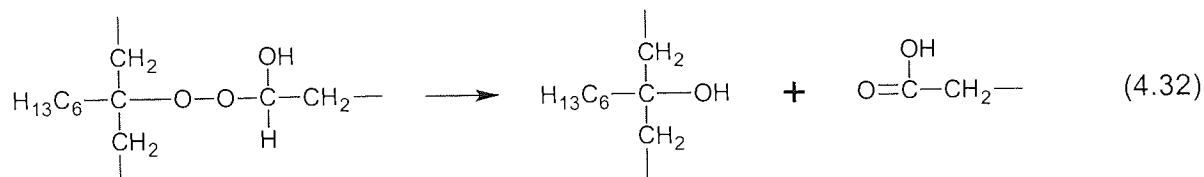
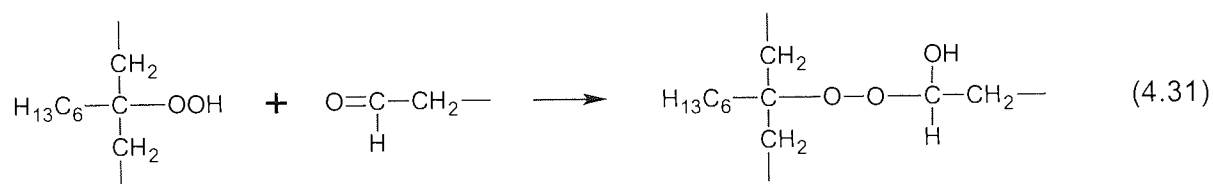
Virgin VP-8770 has ester groups as the main carbonyl compound and its content is shown not to change after TSE extrusion under most conditions (see Figures 4.37 and 4.38). Ketones were formed and accumulated in the processed polymer and became the dominant carbonyl compounds after multi-pass extrusions at higher temperatures. Ketones in VP-8770 are mainly produced through the monomolecular decomposition of α -alkyl-hydroperoxy radicals shown in Reactions 4.16 and 4.17 [102], as well as the β -scission of tertiary alkoxy and peroxy radicals shown in Reactions 4.26 and 4.27 [99]. During the melt extrusion of high branching LLDPE like VP-8770, the latter is assumed to be more important for the formation of ketones in thermal oxidation.

The peak of aldehydes can also be found from the FTIR spectra of TSE extruded VP-8770, and more amounts of aldehydes are formed in the polymer when subjected to multi-pass extrusions at higher temperatures. The major routes of aldehyde production are also assumed to be the decompositions of secondary peroxy and alkoxy radicals (e.g. Reactions 4.14, 4.19). In addition, unsaturated aldehydes could be produced through the reactions involving trans-vinylene. As the VP-8770 originally contains relatively high content of trans-vinylene and the primary initiation of oxidation preferentially occurs at allylic C-H bonds [93], the cleavage of the further oxidised products (peroxy and alkoxy radicals) will lead to the formation of unsaturated aldehydes (see Reactions 4.28 to 4.30).

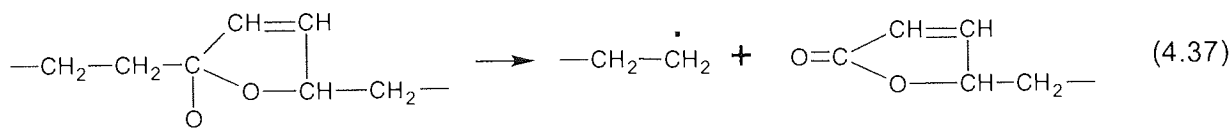
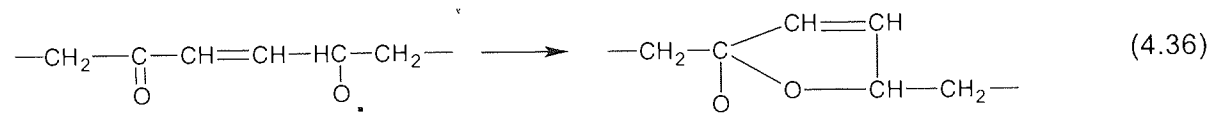
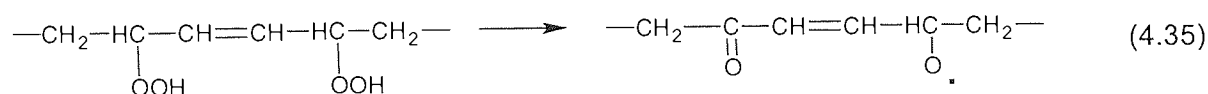


There are also some differences in the FTIR spectra of VP-8770 compared to that of FM-1570 (see Figures 4.35 to 4.38). Carboxylic acids can be clearly observed in the extruded VP-8770 samples under most processing conditions. The oxidation of aldehydes by tertiary hydroperoxides through “cage” reaction has been considered to make a great contribution to the production of carboxylic acids (see Reactions 4.31 and 4.32) [101]. Additionally, since significant amount of ketones has been shown to be accumulated in the extruded polymers, the formation of some hydroperoxides with special structures such as α -keto-hydroperoxides and α,γ -keto-hydroperoxides are expected to become important and these special structures are also suggested to be involved in the production of carboxylic acids. Their decompositions are generally acid-catalysed reactions, leading to the formation of carboxylic acids with simultaneous occurrence of chain scission (see Reactions 4.33 and 4.34) [101]. The accumulation of

carboxylic acids reveals that alcohols may not be the major products in the thermal oxidation of VP-8770 and thus no more esters can be yielded through the combination of carboxylic acids and alcohols.



Another feature that can be observed from the FTIR spectra of extruded VP-8770 is the notable absorbance of γ -lactones at 1772cm^{-1} . The formation of γ -lactone normally involves several reactions steps and requires the presence of oxygen containing groups in 1,4-position. Therefore, the mechanisms are quite complicated and strongly dependent on the extrusion conditions. However, due to the great amount of trans-vinylene originally contained in VP-8770, it becomes much easier for this polymer to get some reactive groups attached to the α position on both sides of trans-vinylene group. Reactions 4.35 to 4.37 give the basic mechanisms that are proposed to be important for yielding α -vinylene- γ -lactones from 1,4-bi-hydroperoxides in the “cage” [96].



In addition to the carbonyl compounds commonly found in the products of LLDPE thermal oxidation, unsaturated ketones, which normally contribute to the absorption in the range of 1680 to 1695 cm^{-1} [93, 139], can also be observed in the FTIR spectra of VP-8770 extruded under most conditions. Since VP-8770 contains the highest amounts of vinylidene groups among the LLDPE chosen for this work (see Figure 4.24), the formation of unsaturated ketones is proposed to form *via* the decomposition of the α -vinylidene hydroperoxide groups under the catalysis of acids, leading to the yield of α -vinylidene ketones during extrusion (see Reaction 4.38) [93,101].

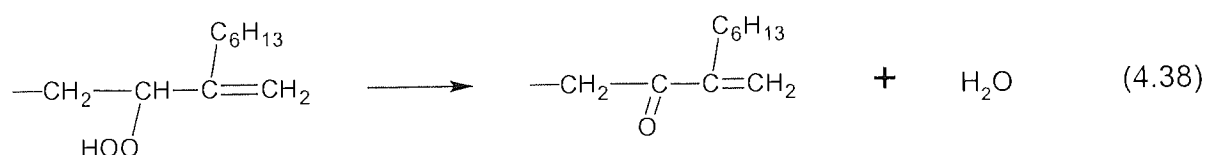
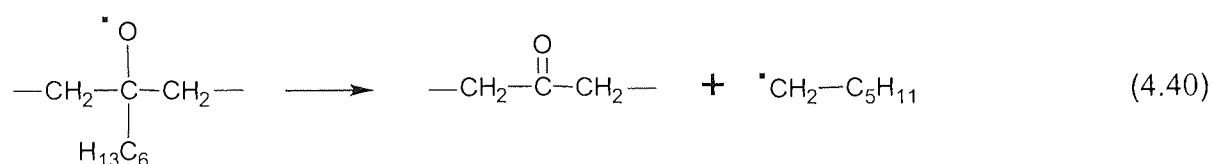
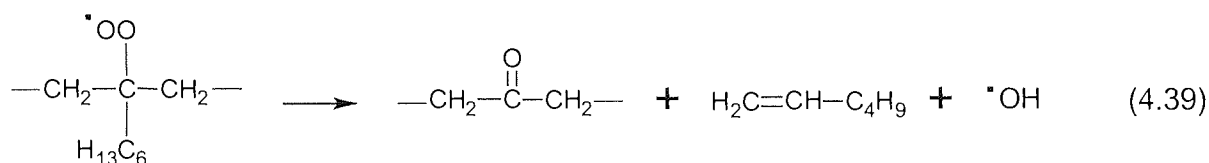


Figure 4.41 shows that compared with the virgin polymer, the SCB content in VP-8770 reduces after one-pass extrusion and has a trend of decreasing with the processing temperature. This result is in good agreement with the melt flow behaviour of the extruded polymers shown in Figure 4.8. Chain scission is predominant for one-pass extruded VP-8770 and the extent becomes greater when raising the extrusion temperature. Correspondingly, the SCB amount in extruded VP-8770 drops down with temperature, because most of the chain scission reactions involve the breakdown of branches based on the mechanism analysis of LLDPE thermal oxidation. Meanwhile, it can be seen from Figure 4.42 that the SCB content in VP-8770 always reduces after extrusion at 265°C

and has the most significant extent of decrease compared to that of other m-LLDPE. However, the results of melt flow measurements (see Figure 4.5) show that crosslinking still dominates in VP-8770 extruded at this temperature, even though there is an evident tendency of chain scission, which has not been found for the lower branching m-LLDPE, when multi-pass extrusions were carried out. On one hand, the fairly contradictory results from melt flow measurement and branching determination further imply that a considerable part of crosslinking in VP-8770 is achieved by "side-to-side" recombination of tertiary radicals (i.e. alkyl, alkoxy and peroxy radicals), which can not be correctly measured by the method adopted in this work. On the other hand, the SCB may be lost by the decomposition of tertiary alkoxy or peroxy radicals, leading to the decrease of branching amount without polymer chain scission (see Reactions 4.39 and 4.40). Overall, it is believed that the SCB in m-LLDPE makes the polymer more reactive in thermal oxidation and more susceptible to chain scission during melt processing, especially at higher temperature [105].



It is very clear from the yellow index shown in Figures 4.43 and 4.44 that VP-8770 has the highest YI values among m-LLDPE after TSE extrusion under all conditions (its original YI is also the highest). The results confirm that more products causing discolouration like carbonyl compounds and conjugated systems were formed during extrusion of VP-8770. However, comparing with the carbonyl content given in Figure 4.33, it can be found that only after multi-pass extrusions at higher temperatures, VP-8770 contains more amounts of carbonyl compounds than other m-LLDPE, but not significantly. The suggestion is therefore reasonable that some special structures like conjugated sequences

make more contribution to the discolouration of extruded VP-8770 under certain circumstances. Theoretically, all the types of unsaturated groups in LLDPE can be transformed into some kinds of conjugated structures in thermal oxidation (see Reactions 4.22, 4.25, 4.29, 4.30 and 4.38), depending on the specific polymer structure and processing conditions. Due to the existence of a large amount SCB, relatively more vinyl-attached branching points is considered to be contained in virgin VP-8770, their decomposition in the thermal oxidation can produce both carbonyl compounds and conjugated structures leading to more substantial discolouration (see Reactions 4.23 to 4.25). Additionally, it is well known that the hydrogen atom on the α -carbon atom adjacent to a vinylidene group is less stable than that on α -position to any other unsaturated groups. As a result, vinylidene group is easier to be initiated in oxidative reactions and transformed into conjugated structures (see Reaction 4.38). As VP-8770 originally contains the highest amounts of total unsaturated groups as well as the highest amount of trans-vinylene and vinylidene groups in LLDPE polymers chosen for this work, the discolouration of extruded VP-8770 is to a great extent attributed to the formation of conjugated systems during thermal oxidation.

4.3.4. Changes in Micro-structure of z-LLDPE

As an analogue of metallocene-based LLDPE, the structural characteristics of Ziegler-Natta catalysed polymer, Dowlex2045-E, have also been examined after TSE extrusion. This z-LLDPE (older batch) contains very low amount trans-vinylene groups in both virgin and extruded polymers compared to m-LLDPE (see Figures 4.24 and 4.25). However, in contrast to the m-LLDPE polymers, the z-LLDPE polymer yields more trans-vinylene groups after extrusion under most conditions, and presents a trend of increase with temperature when multiple passes were carried out (see Figure 4.26). Since the SCB incorporated in z-LLDPE is less than that in any of the m-LLDPE, the production of trans-vinylene in this polymer is mainly from the disproportionation of secondary alkyl radicals (see Reaction 4.7). The catalyst residues in z-LLDPE are envisaged to play a role of facilitating this reaction. Additionally, the isomerization of α -vinyl alkyl radicals as well as the further reactions (see

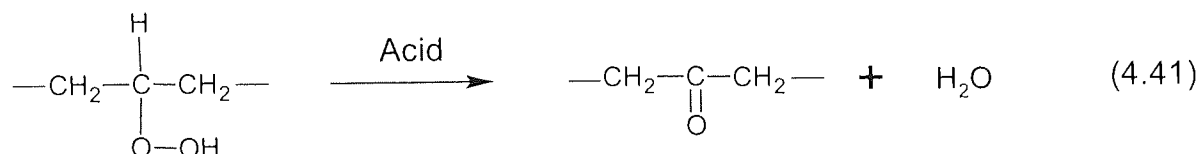
Reactions 4.4 and 4.5) can all make contribution to the formation of trans-vinylene groups.

The much higher original content of vinyl groups (compared to m-LLDPE) is a very specific feature of this z-LLDPE. It is very interesting to note that there is no significant decrease of vinyl amount in the extruded z-LLDPE (see Figures 4.27 and 4.28), although this polymer does undergo much greater extent of crosslinking than m-LLDPE under all extrusion conditions (see the results of MI measurement in Figure 4.8). It is suggested that the highly predominant crosslinking in extruded z-LLDPE is still attributed mainly to the addition reactions of vinyl group with alkyl radicals due to the high availability of vinyl in this polymer. Furthermore, specific oxidative reactions leading to the formation of the vinyl groups (see Reactions 4.10, 4.11, 4.12, 4.26, 4.29 and 4.39) may be favoured under certain conditions, some of them have considerable effect on the melt flow behaviour of the polymer and result in the noticeable variation in the correlation between crosslinking degree and vinyl content in extruded z-LLDPE.

The change of vinylidene in extruded z-LLDPE is similar to the situation of trans-vinylene (see Figures 4.29 and 4.30). The vinylidene content in the extruded z-LLDPE is lower than that in the metallocene polymers. Moreover, there is no significant alteration but a small range of fluctuation for vinylidene amount after TSE extrusion at different temperatures. So it can be assumed that the oxidative reactions involving vinylidene groups are less important for the structural changes during melt extrusion of this polymer.

Dowlex2045-E (z-LLDPE) contains the lowest amount of carbonyl compounds in the virgin polymers examined (see Table A4.7). After TSE extrusion, the carbonyl content in z-LLDPE has a great increase and it is even higher than that in m-LLDPE depending on the extrusion conditions (see Figure 4.33). It is clear from Figure 4.34 that compared to m-LLDPE, carbonyl amount in z-LLDPE shows a much greater extent of increase after extrusion under all conditions and more carbonyl compounds are produced when more extrusion passes were carried out.

There are also some differences in carbonyl composition between the TSE extruded z-LLDPE and m-LLDPE, especially for the polymers after only one-pass extrusion (see FTIR spectra in Figure 4.39). The major carbonyl product in one-pass extruded Dowlex2045-E is ketone rather than the esters in m-LLDPE. Meanwhile, considerable absorbance of carboxylic acids and aldehydes can also be found from the FTIR spectra. When five-pass extrusions were carried out, ketone is still the dominant carbonyl compound, just like the situation of m-LLDPE (see FTIR spectra in Figure 4.39), and aldehydes become secondary carbonyl products of thermal oxidation. Since great extent of crosslinking occurred in z-LLDPE after extrusions under most conditions (see Figure 4.8), the monomolecular decompositions of α -alkyl-hydroperoxy radicals (see Reactions 4.16 and 4.17) and secondary alkyl hydroperoxides (see Reaction 4.41) [101], which do not lead to polymer chain scission, are proposed to be the most important reactions that contribute to the accumulation of ketones in the extruded z-LLDPE. Further, the decompositions of α -keto-hydroperoxides and α,γ -keto-hydroperoxides that simultaneously form aldehydes/ketones and carboxylic acids (see Reactions 4.33 and 4.34) are considered to play important roles in the production of carbonyl compounds.



Similarly, ketones are found to be the dominant carbonyl compounds when z-LLDPE was multi-extruded at both 235°C and 285°C (see in Figure 4.40). Two factors are considered to lead to the predominance of ketones in multi-pass extruded Dowlex2045-E. The first is the production of ketones through Reaction 4.41 catalysed by acids (e.g. hydroperoxides) formed in the previous extrusions. In addition, the multiple extrusions can yield more amounts of secondary hydroperoxides and hydroperoxy radicals and they can produce ketones through Reactions 4.16 and 4.17.

Aldehydes are also observed in the FTIR spectra of z-LLDPE extruded under most conditions, especially at higher temperatures and more extrusion passes.

Since the formation of aldehydes is normally accompanied by polymer chain scission, the accumulation of aldehydes in this extruded polymer would be correlated to a decrease in molecular weight. However, crosslinking that leads to the increase of MW always predominates in z-LLDPE during melt extrusion, thus the molecular weight distribution of z-LLDPE becomes broader after extrusion (especially at higher temperatures with more extrusion passes) and this has been observed from the significant increase of MFR values of extruded Dowlex2045-E polymers (see Figure 4.6).

Other carbonyl compounds can also be found from the FTIR spectra of extruded z-LLDPE samples (see Figures 4.39 and 4.40). Unsaturated ketones (at about $1690\sim1680\text{ cm}^{-1}$) are produced under most extrusion conditions from the acid-catalysed decomposition of allylic hydroperoxides as shown in Reaction 4.38. Due to higher content of vinyl group in virgin (unprocessed) Dowlex2045-E, the major part of unsaturated ketones in extruded z-LLDPE are proposed to be formed by the breakdown of secondary hydroperoxides connected to vinyl groups (similar to Reaction 4.38) and correspond to the absorption at 1684 cm^{-1} in FTIR spectra. Relatively weak absorptions of γ -lactones can be observed in the FTIR spectra of some extruded z-LLDPE samples and the route of γ -lactones formation is considered to be similar to that in m-LLDPE.

It is shown in Figure 4.41 that the branching amount in Dowlex2045-E decreases slightly after one-pass extrusion at all temperatures. However, the melt flow measurement indicates that crosslinking is predominant for this polymer extruded under the same conditions (see Figure 4.8). The only explanation for the results is, the “crosslinking” in the thermal oxidation of z-LLDPE is mainly the linear enlargement of polymer chains through addition reactions of vinyl groups with primary radicals (head-to-head addition), and this would not make any contribution to SCB formation (see Reaction 4.5). Meanwhile, the oxidative reactions involving SCB in most cases lead to its decomposition. The linear addition reactions in z-LLDPE produce secondary alkyl radicals and their disproportionation can result in the formation of trans-vinylene groups (see Reaction 4.7). The general tendency of increase in trans-vinylene in extruded z-

LLDPE (see Figure 4.26) confirms the occurrence of the specific crosslinking in this polymer after one-pass extrusion. Figure 4.42 reveals an increasing tendency of branching amount with extrusion passes when z-LLDPE was processed at 265°C. It can be seen that the branching content still reduces after extrusion for one or three passes, while it increases when five-pass extrusions were carried out. More secondary alkyl radicals may be produced under this condition (265°C, five passes) and they undergo addition reactions with vinyl groups (see Reaction 4.9), leading to the yield of branches and simultaneous crosslinking. This can also be confirmed by the great extent of enhancement in trans-vinylene in z-LLDPE extruded at 265°C for five passes (see Figure 4.26).

The results of colour measurement in Figures 4.43 and 4.44 show that z-LLDPE generally has the highest YI value as well as the extent of YI increase after TSE extrusion compared to most m-LLDPE. The existences of carbonyl compounds and conjugated systems are proposed to be the main reasons for the discolouration of LLDPE [93]. Figure 4.33 shows the carbonyl content in Dowlex2045-E is less than that in any m-LLDPE when the polymers were subjected to one-pass extrusion (at any temperatures). The much higher YI value presented by the extruded z-LLDPE can only be attributed to the formation of more amounts of conjugated structures in thermal oxidation (see Reactions 4.22, 4.25, 4.29, 4.30 and 4.38), and the transformation of vinyl groups to conjugated systems is proposed to play a more important role. Figure 4.44 compares the YI changes of LLDPE after extrusion for different passes. It can be seen that the increase of YI values has no significant changes when Dowlex2045-E was extruded for different passes at any temperature. However, the carbonyl content changes shown in Figure 4.34 illustrate that the carbonyl amount in extruded z-LLDPE is enhanced with more extrusion passes. Thus, a conclusion can be drawn that the carbonyl compounds produced in LLDPE thermal oxidation make less contribution to the discolouration of extruded polymers compared to conjugated structures.

4.3.5. Relationship between the Concentrations of Carbonyl Compounds and Unsaturated Groups in TSE Extruded LLDPE Polymers

The relationships between the concentrations of carbonyl compounds and different unsaturated groups in TSE extruded LLDPE polymers are shown in Figure 4.45. It has been observed that linear relationships exist between the concentrations of carbonyl and all individual unsaturated groups according to the type (metallocene or Ziegler-based) and grade (comonomer content) of LLDPE, rather than only the correlation between carbonyl and trans-vinylene that has been described in the literatures [52, 93]. Generally, the carbonyl groups–unsaturation correlation curves for different grades of metallocene-based polymers are quite similar and their positions are mainly determined by the amounts of unsaturated groups originally contained in the virgin polymers. The correlation lines for z-LLDPE always have very small slopes indicating the relatively small changes of unsaturated groups with the degree of thermal oxidation (increase of carbonyl amount). The carbonyl groups–unsaturation linear relationships for extruded LLDPE found in this work make it possible to approximately assess the extent of LLDPE thermal oxidation by simply measuring the content of a proper type of double bond.

4.4. OVERVIEW OF THE OXIDATIVE DEGRADATION OF LLDPE POLYMERS IN MELT PROCESSING (TR AND TSE)

4.4.1. Comparison of the Oxidative Degradation of LLDPE Polymers Processed by TR and TSE

Based on the analysis of the mechanisms of LLDPE thermal oxidation during melt processing in both twin-screw extruder (TSE) and torque rheometer (TR), further understanding of the oxidation behaviour of m-LLDPE and z-LLDPE may be reached through comparison of the results obtained from TSE and TR processing. Since each TSE processed polymer was subjected to extrusion for a total of five passes, generally the characteristics of one-pass extruded samples are taken to compare with that of the TR processed polymers.

The melt flow measurement showed very similar results for TR and TSE processed LLDPE. The m-LLDPE polymers underwent mainly chain scission when processed at lower temperatures (210~220°C), while crosslinking became the predominant reaction when higher processing temperatures were applied; the more SCB the polymer contained, the more it became susceptible to chain scission. On the other hand, crosslinking always dominated in z-LLDPE and its extent increased greatly with processing temperatures (see Figures 4.8 and 4.9 as well as Figures 3.2 and 3.3 in Chapter 3). The MFR values examined for both TR and TSE processed polymers presented an increasing tendency after processing, corresponding to broadening of molecular weight distribution, and the MFR changes tended to increase with increasing temperatures. Among all the polymers, z-LLDPE showed much more MFR increase after processing compared to m-LLDPE (see Figure 4.10 and Figure 3.4 in Chapter 3). Some differences in the melt flow behaviour between TR and TSE processed polymers were identified, e.g. the m-LLDPE presented much greater extent of MI reduction and MFR enhancement after TR processing at higher temperatures compared to TSE extrusion at similar temperatures (see Figures 3.2 and 3.4 in Chapter 3 as well as Figures 4.8 and 4.10). It is proposed that the difference in oxidation degree caused by the different residence time in TR and TSE (TR = 10 min, TSE \approx 2 min) is the main reason responsible for the differences in the melt flow behaviour of metallocene LLDPE polymers processed by these two methods.

Unsaturation changes in the processed LLDPE can reveal some specific characters of the thermal oxidation process during TR and TSE processing. The trans-vinylene content in both m-LLDPE and z-LLDPE tended to increase after TR processing under most conditions (see Figure 3.5 in Chapter 3), especially at higher temperatures. On the contrary, the trans-vinylene concentration reduced in almost all the TSE extruded m-LLDPE, only small extents of increase was observed in z-LLDPE under some conditions (see Figure 4.26). As the formation of trans-vinylene is mainly attributed to disproportionation of alkyl radicals (see Reaction 4.7) and its consumption (see Reaction 4.6) as well as the further oxidation of alkyl radicals (see Reaction 4.24) normally involves oxygen, it is

concluded that the oxygen pressure in the closed mixing chamber of torque rheometer for the duration of the processing (10 minutes) is lower than that in the TSE extrusion barrel (residence time \approx 2 minutes). The oxygen deficient environment during TR processing is very favourable to the yield of trans-vinylene but not to its decomposition, leading to the accumulation of more trans-vinylene groups in the TR processed polymers.

The remarkable difference in the changes in vinyl concentration in z-LLDPE in TR and TSE processed samples is a contradictory tendency. The amount of vinyl groups in z-LLDPE increased after TR processing under all conditions (see Figure 3.6 in Chapter 3), while it reduced after TSE extrusion, especially at higher temperatures (see Figure 4.28). However, the results of MI measurement have shown that the TR processed z-LLDPE has overall undergone a greater extent of crosslinking than in the case with one-pass extruded (TSE processing) samples (compare Figure 3.2 in Chapter 3 with Figure 4.8). On the one hand, the crosslinking of TR processed polymer may be attributed to other reactions such as the recombination of two radicals and the esterification of carboxylic acids and alcohol. On the other hand, more vinyl groups may be produced in thermal oxidation during TR processing to compensate for its consumption in addition reactions with alkyl radicals leading to crosslinking. It has been noticed that [139] the β -cleavage of secondary alkyl radicals under lower oxygen pressure can produce both vinyl and primary alkyl radicals (see Reaction 4.10), the latter has been suggested [99, 139] to be one of the most important intermediates in thermal oxidation that contribute to the vinyl formation and crosslinking in TR processed z-LLDPE. From this point of view, it is reasonable to assume that more primary alkyl radicals are produced in z-LLDPE (except for the isomerisation of α -vinyl alkyl radicals as shown in Reaction 4.23) during TR processing compared to the situation in TSE extrusion.

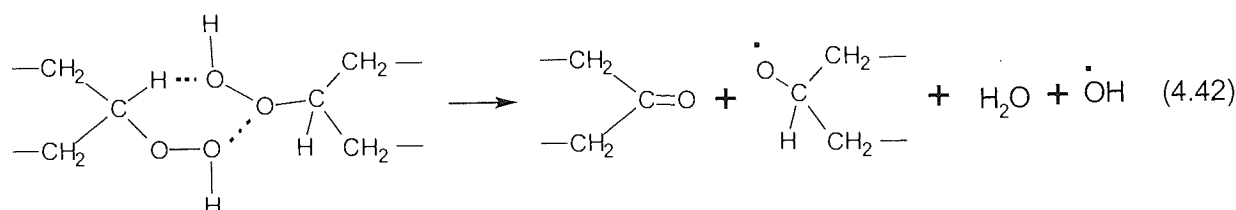
The variation of vinylidene content is quite similar for LLDPE processed in torque rheometer and twin-screw extruder, i.e. vinylidene groups were produced during the processing and their amount tended to increase with temperature (see Figure 3.7 in Chapter 3 and Figure 4.30). However, there is no evident increase

in vinylidene amount after extrusions of z-LLDPE at all temperatures (see Figure 4.30). The β -cleavage of branched tertiary alkyl radicals is considered to be the most important route for the yield of vinylidene groups (see Reaction 4.15) in z-LLDPE. Under the relatively higher oxygen pressure during TSE extrusion, the tertiary radicals are very susceptible to further oxidation into tertiary hydroperoxides, which cannot produce vinylidene group through decomposition in thermal oxidation. Thus, the difference of oxygen pressure is proposed to be the main reason for the different concentrations of vinylidene produced or consumed in z-LLDPE during TR and TSE processing.

Comparing the variations of carbonyl content in TR and TSE processed LLDPE, it can be seen that the changes are not too different when processing is carried out in TR and TSE (see Figure 3.8 in Chapter 3 and Figure 4.34). The carbonyl concentration in m-LLDPE generally became higher after melt processing and increased with increasing temperature. The z-LLDPE is suggested to be more susceptible to thermal oxidation than m-LLDPE due to the much higher increase in its carbonyl content after both TR and TSE processing. Meanwhile, the carbonyl content in z-LLDPE increased to a much greater extent after multi-pass extrusion compared to that in TR processed samples (see Figure 4.34 and Figure 3.8 in Chapter 3), confirming further that a higher oxygen pressure is maintained during TSE extrusion.

The differences in carbonyl composition of TR and TSE processed LLDPE can be observed from their FTIR spectra at carbonyl region (see Figures 3.9 to 3.11 in Chapter 3 and Figures 4.35 to 4.40). As the change in carbonyl content in TR processed polymers shows more similarity with that in multi-pass extruded samples, the FTIR spectra of LLDPE subjected to five-pass extrusions are chosen for comparison purpose. It was found that generally the variations of carbonyl composition with temperature were quite similar for TR and TSE processed m-LLDPE. The major carbonyl compounds change from esters at lower temperatures to ketones at higher temperatures. The essential difference is, in the formation of ketones, large amount of aldehydes were produced in m-LLDPE during TSE extrusion at higher temperatures. Since TSE extrusions were

carried out under a higher oxygen pressure, more hydroperoxides were produced in the polymers and they are more likely to undergo bimolecular decompositions as shown in Reaction 4.42 [95, 96, 100]. As a result, the oxidation of aldehydes through reactions with hydroperoxides (Reactions 4.31 and 4.32) had less chance to occur. Meanwhile, aldehydes can be produced constantly and accumulate in extruded polymers through the breakdown of secondary peroxy and alkoxy radicals (See Reactions 4.12 and 4.18). A similar situation can also be found for z-LLDPE, the only difference is even at lower temperature, aldehyde was formed to be the major carbonyl compound in the TSE processed polymers. In addition, the evident increases of ester absorption with temperature shown in the FTIR spectra of TR processed LLDPE polymers further confirm that esterification of carboxylic acids (mainly formed by aldehyde oxidation) and alcohol occurred during processing and made a contribution to the polymer crosslinking.



Overall, the oxygen pressure and residence time have the most important effects on the difference in oxidation behaviour of LLDPE polymers during TR and TSE processing.

4.4.2. Comparison of the Oxidative Degradation of Different LLDPE Polymers Processed by TSE

It is shown from the measurements of rheological properties of extruded LLDPE polymers that, the m-LLDPE having lower comonomer content (< 20 wt%, e.g. FM-1570 and PL-1840) generally present similar melt stabilities upon multiple extrusions (see Figures 4.4, 4.6, 4.16 and 4.18). They tended to crosslink to a greater extent with increasing processing temperature and more extrusion passes; meanwhile, their MWD increased correspondingly. Crosslinking was also the predominant reaction for the m-LLDPE containing higher comonomer content

(e.g. VP-8770). However, the extent of crosslinking in this polymer started to decrease when the extrusion temperature was increased higher than 265°C. Additionally, the VP-8770 polymer showed a broader MWD after TSE extrusions compared to the m-LLDPE incorporated with less comonomers (e.g. FM-1570 and PL-1840). In contrast, the extruded Ziegler-catalysed polymer, Dowlex2045-E, always showed much larger extent of crosslinking and much broader MWD compared to the metallocene-based analogues. As discussed in Section 4.3, the addition reaction of vinyl group with alkyl radicals is generally considered to be the most important route for crosslinking [93]. It can be seen from Figure 4.46 that the vinyl amount in z-LLDPE consumed during extrusions corresponds fairly well with the drop in MI (crosslinking) shown in Figure 4.4.

As shown in Figures 4.47 to 4.49, the changes of unsaturated groups in m-LLDPE polymers upon multiple extrusions are generally similar. The amounts of trans-vinylene and vinyl groups decreased in most cases; while, vinylidene was produced as a result of TSE extrusions. Compared to the metallocene polymers, the most significant difference in the variation of double bonds in z-LLDPE is the evident increase in trans-vinylene after extrusions, especially when more extrusion passes were carried out at higher temperatures (see Figure 4.50). Much more secondary alkyl radicals are assumed to be formed in z-LLDPE during TSE extrusions and their disproportionation is the major reason for the production of more trans-vinylene in z-LLDPE (see Reaction 4.7). Meanwhile, less vinylidene groups were formed in extruded z-LLDPE compared to m-LLDPE processed under the same conditions; and in some cases, the vinylidene concentration in extruded z-LLDPE even decreased with respect to that in the virgin polymer. The lower production of vinylidene in the Ziegler-based polymer is considered to be attributed to both the very low content of SCB (since most of the reactions leading to the formation of vinylidene involve radicals adjacent to SCB, see Reactions 4.13 to 4.15) and the effect of the catalyst residues.

The changes in the concentration of carbonyl compounds upon multiple extrusions are similar for all the LLDPE polymers examined (see Figures 4.47 to 4.50). The carbonyl content in the extruded polymers generally increased with more extrusion passes and elevated temperature, indicating the more serious

thermal oxidation occurred in the polymers. It is indicated that amongst the metallocene polymers, relatively more carbonyl compounds were produced in the higher comonomer containing m-LLDPE (e.g. VP-8770) when multi-pass extrusions were carried out at higher temperatures. The high SCB content in this polymer is closely relative to the production of more carbonyl compounds, as the branching point is more likely to be initiated for oxidative reactions. Moreover, much larger extent of increase in carbonyl concentration can be observed in extruded z-LLDPE compared to m-LLDPE polymers (see Figures 4.47 to 4.50). This suggests the production of more hydroperoxides in this polymer and its higher susceptibility to oxidative degradation during melt extrusions.

The composition of carbonyl compounds formed during TSE extrusions is also quite similar for different LLDPE polymers (see Figures 4.35 to 4.40). Ketone was generally the most important carbonyl product in all the extruded LLDPE samples. More aldehydes were produced in the polymers subjected to multi-pass extrusions at higher temperatures. Meanwhile, other carbonyl compounds, e.g. carboxylic acids, esters, γ -lactone, can also be found in some polymers after extrusions under certain conditions. Conjugated structures (e.g. unsaturated ketones) have been observed in extruded z-LLDPE and m-LLDPE with higher comonomer content (VP-8770), which are proposed to be the major oxidative products leading to the more intensive discolouration in these polymers after multiple extrusions.

Basically, the oxidative degradation behaviour of LLDPE polymers during melt extrusions depends significantly on the catalyst system used for their synthesis (Ziegler or metallocene) as well as their comonomer content. Meanwhile, the unsaturated groups originally contained in the polymer have also great effects on its melt stability, production of carbonyl compounds and extent of discolouration when subjected to multiple extrusions. Furthermore, high temperature and more extrusion passes can lead to larger extent of oxidative degradation for both metallocene and Ziegler-based LLDPE polymers.

Table 4.1. TSE Parameters Used for Processing LLDPE (screw speed fixed at 100rpm)

| Polymer Code | Extrusion Passes | Temperature of Die (°C) | Temperature of Melt (°C) | ΔT (°C) | Feeding Rate (rpm) | Current (A)+0.5 | Pressure (psi)+5% | Output Rate (kg/hr) | Power (kW.h/kg) |
|---------------|------------------|-------------------------|--------------------------|-----------------|--------------------|-----------------|-------------------|---------------------|-----------------|
| FM-1570 | P1 | 210 | 218 | 8 | 42 | 10.8 | 640 | 4.0 | 0.33 |
| | P3 | 210 | 217 | 7 | 244 | 10.0 | 630 | 4.0 | 0.30 |
| | P5 | 210 | 217 | 7 | 250 | 10.0 | 630 | 4.0 | 0.30 |
| | P1 | 235 | 238 | 3 | 43 | 10.5 | 530 | 4.0 | 0.32 |
| | P3 | 235 | 234 | -1 | 253 | 10.0 | 520 | 4.0 | 0.30 |
| | P5 | 235 | 236 | 1 | 233 | 9.5 | 540 | 4.0 | 0.29 |
| | P1 | 265 | 261 | -4 | 95 | 10.8 | 460 | 4.8 | 0.27 |
| | P3 | 265 | 261 | -4 | 343 | 11.1 | 480 | 4.8 | 0.28 |
| | P5 | 265 | 262 | -3 | 313 | 11.5 | 500 | 4.8 | 0.29 |
| | P1 | 285 | 280 | -5 | 81 | 10.3 | 370 | 4.5 | 0.28 |
| | P3 | 285 | 277 | -8 | 328 | 10.3 | 380 | 4.5 | 0.28 |
| | P5 | 285 | 278 | -7 | 276 | 10.3 | 400 | 4.5 | 0.28 |
| PL-1840 | P1 | 210 | 220 | 10 | 52 | 10.8 | 710 | 4.0 | 0.33 |
| | P3 | 210 | 219 | 9 | 273 | 10.8 | 710 | 4.0 | 0.33 |
| | P5 | 210 | 219 | 9 | 247 | 10.8 | 710 | 4.0 | 0.33 |
| | P1 | 235 | 239 | 4 | 59 | 10.6 | 580 | 4.0 | 0.32 |
| | P3 | 235 | 239 | 4 | 270 | 10.2 | 585 | 4.0 | 0.31 |
| | P5 | 235 | 239 | 4 | 265 | 10.2 | 610 | 4.0 | 0.31 |
| | P1 | 265 | 262 | -3 | 132 | 11.2 | 530 | 4.8 | 0.28 |
| | P3 | 265 | 262 | -3 | 400 | 11.5 | 530 | 4.8 | 0.29 |
| | P5 | 265 | 263 | -2 | 385 | 11.8 | 550 | 4.8 | 0.30 |
| | P1 | 285 | 278 | -7 | 117 | 10.8 | 430 | 4.5 | 0.29 |
| | P3 | 285 | 279 | -6 | 355 | 10.8 | 420 | 4.5 | 0.29 |
| | P5 | 285 | 280 | -5 | 344 | 11.0 | 440 | 4.5 | 0.30 |
| PL-1880 | P1 | 210 | 221 | 11 | 82 | 10.0 | 720 | 4.0 | 0.30 |
| | P3 | 210 | 220 | 10 | 227 | 10.0 | 710 | 4.0 | 0.30 |
| | P5 | 210 | 220 | 10 | 222 | 9.9 | 730 | 4.0 | 0.30 |
| | P1 | 235 | 239 | 4 | 62 | 10.0 | 640 | 4.0 | 0.30 |
| | P3 | 235 | 240 | 5 | 235 | 9.8 | 640 | 4.0 | 0.30 |
| | P5 | 235 | 240 | 5 | 236 | 10.2 | 670 | 4.0 | 0.31 |
| | P1 | 265 | 265 | 0 | 170 | 11.3 | 550 | 4.8 | 0.29 |
| | P3 | 265 | 264 | -1 | 342 | 11.5 | 560 | 4.8 | 0.29 |
| | P5 | 265 | 264 | -1 | 341 | 11.5 | 560 | 4.8 | 0.29 |
| | P1 | 285 | 281 | -4 | 134 | 10.8 | 480 | 4.5 | 0.29 |
| | P3 | 285 | 280 | -5 | 323 | 10.8 | 460 | 4.5 | 0.29 |
| | P5 | 285 | 281 | -4 | 311 | 10.5 | 450 | 4.5 | 0.28 |
| VP-8770 | P1 | 210 | 223 | 13 | 130 | 10.0 | 840 | 4.0 | 0.30 |
| | P3 | 210 | 223 | 13 | 199 | 9.8 | 810 | 4.0 | 0.30 |
| | P5 | 210 | 223 | 13 | 188 | 9.8 | 800 | 4.0 | 0.30 |
| | P1 | 235 | 241 | 6 | 124 | 9.8 | 690 | 4.0 | 0.30 |
| | P3 | 235 | 239 | 4 | 238 | 9.8 | 690 | 4.0 | 0.30 |
| | P5 | 235 | 241 | 6 | 233 | 9.8 | 690 | 4.0 | 0.30 |
| | P1 | 265 | 266 | 1 | 234 | 11.0 | 600 | 4.8 | 0.28 |
| | P3 | 265 | 263 | -2 | 355 | 11.0 | 560 | 4.8 | 0.28 |
| | P5 | 265 | 263 | -2 | 365 | 11.0 | 530 | 4.8 | 0.28 |
| | P1 | 285 | 280 | -5 | 219 | 10.8 | 490 | 4.5 | 0.29 |
| | P3 | 285 | 277 | -8 | 360 | 10.2 | 410 | 4.5 | 0.28 |
| | P5 | 285 | 277 | -8 | 344 | 9.5 | 360 | 4.5 | 0.26 |
| Dowlex 2045-E | P1 | 210 | 220 | 10 | 10 | 10.0 | 770 | 4.0 | 0.30 |
| | P3 | 210 | 218 | 8 | 97 | 10.0 | 750 | 4.0 | 0.30 |
| | P5 | 210 | 219 | 9 | 66 | 12.0 | 780 | 4.0 | 0.37 |
| | P1 | 235 | 238 | 3 | 18 | 11.0 | 710 | 4.5 | 0.30 |
| | P3 | 235 | 238 | 3 | 170 | 11.0 | 750 | 4.5 | 0.30 |
| | P5 | 235 | 238 | 3 | 80 | 11.0 | 760 | 4.5 | 0.30 |
| | P1 | 265 | 263 | -2 | 40 | 11.0 | 640 | 4.8 | 0.28 |
| | P3 | 265 | 267 | 2 | 150 | 11.5 | 650 | 4.8 | 0.29 |
| | P5 | 265 | 268 | 3 | 155 | 12.5 | 700 | 4.8 | 0.32 |
| | P1 | 285 | 281 | -4 | 24 | 10.0 | 530 | 4.5 | 0.27 |
| | P3 | 285 | 283 | -2 | 139 | 11.5 | 580 | 4.5 | 0.31 |
| | P5 | 285 | 285 | 0 | 130 | 12.5 | 650 | 4.5 | 0.34 |

Table 4.2. Branching Amount of TSE Processed Unstabilised LLDPE (P1) Measured by ^{13}C -NMR

| Extrusion Tem. ($^{\circ}\text{C}$) | SCB Content (wt%) | | | |
|--|-------------------|---------|---------|--------------|
| | FM-1570 | PL-1840 | VP-8770 | Dowlex2045-E |
| Virgin Polymer | 11.6 | 13.4 | 28.2 | 10.5 |
| 210 | 12.1 | 13.3 | 27.7 | 10.4 |
| 265 | 11.7 | 13.4 | 27.2 | 10.1 |
| 285 | 11.6 | 13.1 | 27.0 | 10.3 |

Table 4.3. Branching Amount of TSE Processed Unstabilised LLDPE (265 $^{\circ}\text{C}$) Measured by ^{13}C -NMR

| Extrusion Pass | SCB Content (wt%) | | | |
|-------------------|-------------------|---------|---------|--------------|
| | FM-1570 | PL-1840 | VP-8770 | Dowlex2045-E |
| Virgin Polymer | 11.6 | 13.4 | 28.2 | 10.5 |
| 1 | 11.7 | 13.4 | 27.2 | 10.1 |
| 3 | 10.7 | 13.7 | 25.2 | 10.4 |
| 5 | 11.7 | 13.4 | 27.0 | 10.8 |

Table 4.4. Yellow Index (YI) of TSE Processed LLDPE (unstabilised)

| Extrusion Temperature ($^{\circ}\text{C}$) | | | 210 | 235 | 265 | 285 |
|--|---------------------------|------|-------|-------|-------|-------|
| Polymer | Virgin (YI ₀) | Pass | YI | YI | YI | YI |
| FM-1570 | -2.72 | 1 | -2.25 | -1.13 | -0.39 | -1.91 |
| | | 3 | -1.30 | 2.22 | 2.47 | 2.15 |
| | | 5 | 0.72 | 4.81 | 4.84 | 5.67 |
| PL-1840 | -0.28 | 1 | -2.95 | -1.93 | -1.76 | -2.21 |
| | | 3 | -1.93 | -0.86 | -0.06 | 0.19 |
| | | 5 | -0.91 | 1.70 | 2.08 | 3.54 |
| VP-8770 | 2.80 | 1 | 3.58 | 5.21 | 6.15 | 5.68 |
| | | 3 | 7.46 | 8.23 | 8.47 | 9.21 |
| | | 5 | 8.48 | 9.72 | 10.79 | 11.51 |
| Dowlex2045-E | 3.44 | 1 | 8.92 | 10.00 | 9.54 | 11.27 |
| | | 3 | 7.86 | 8.90 | 10.22 | 9.69 |
| | | 5 | 8.81 | 11.17 | 12.07 | 11.27 |

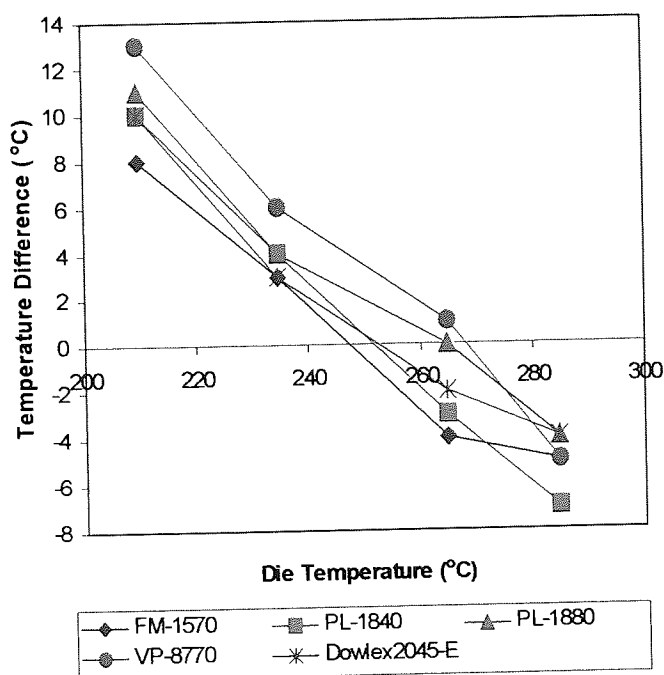


Figure 4.1. Change of Temperature Difference (between melt and die) with Die Temperature for LLDPE During Extrusion of Pass1

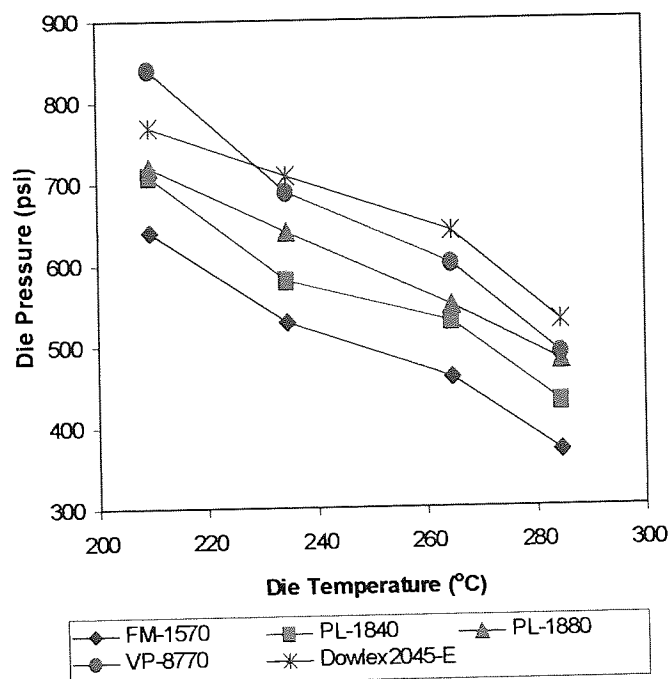


Figure 4.2. Change of Die Pressure with Die Temperature for LLDPE During Extrusion of Pass1

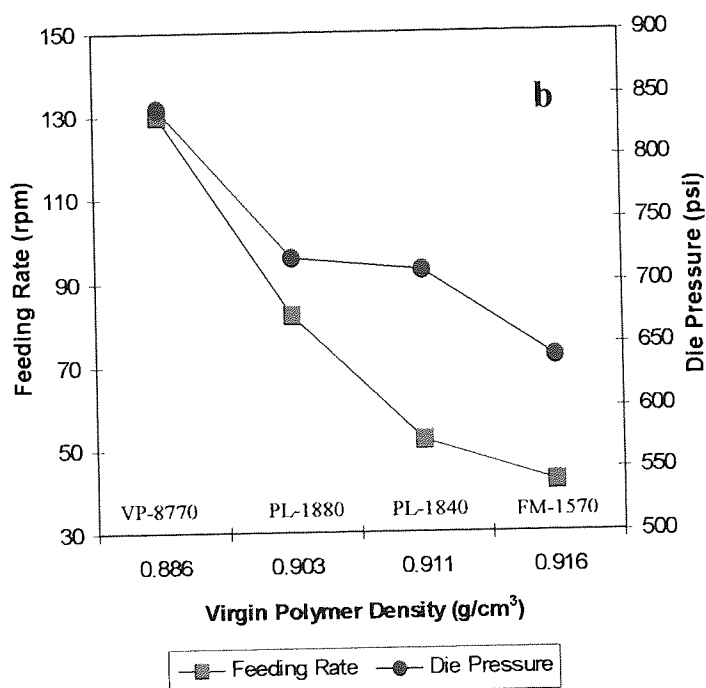
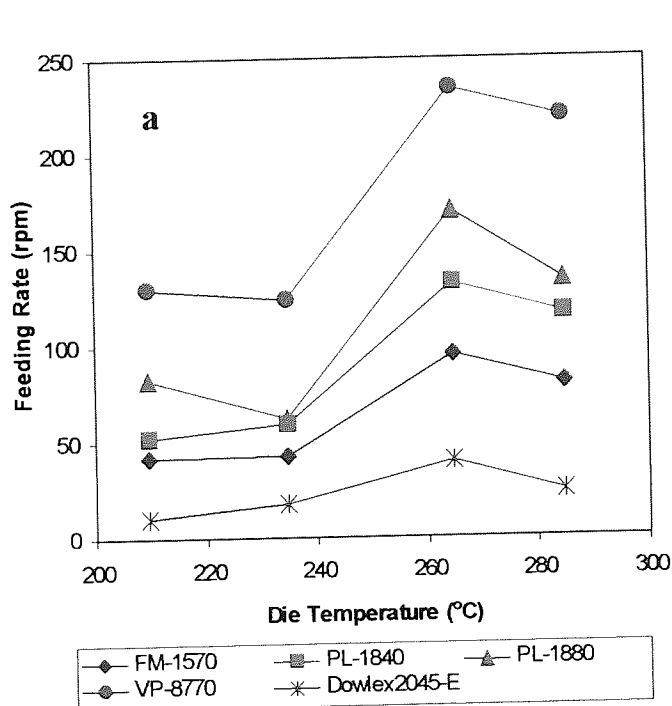


Figure 4.3. a: Change of Feeding Rate with Die Temperature for LLDPE During Extrusion of Pass1; b: Changes of Feeding Rate (Single Screw Feeder) and Die Pressure with the Density of Virgin m-LLDPE Polymers (210°C, Pass1)

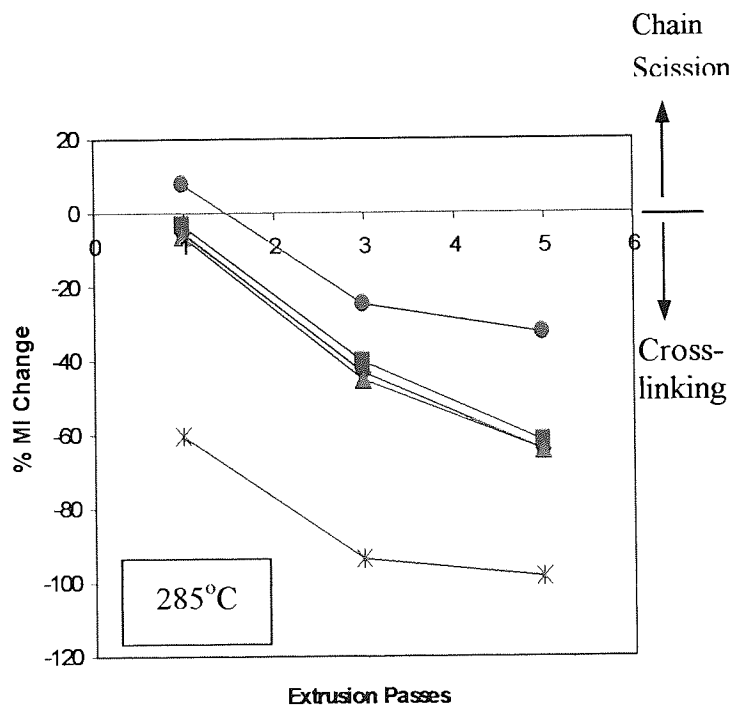
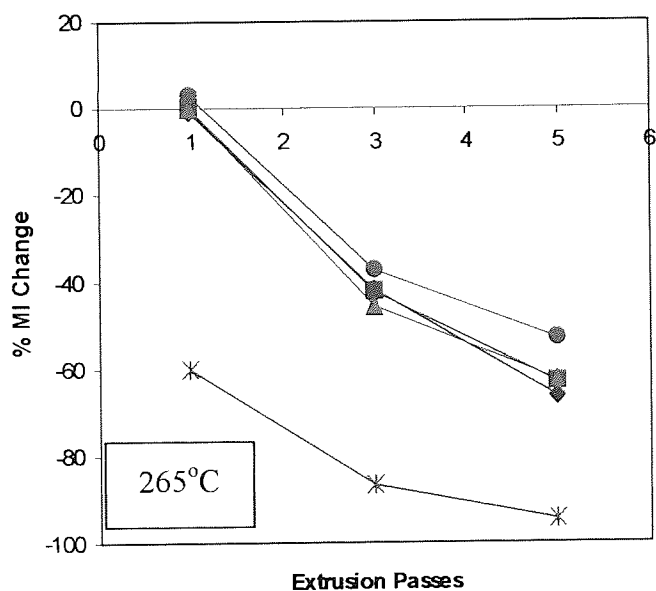
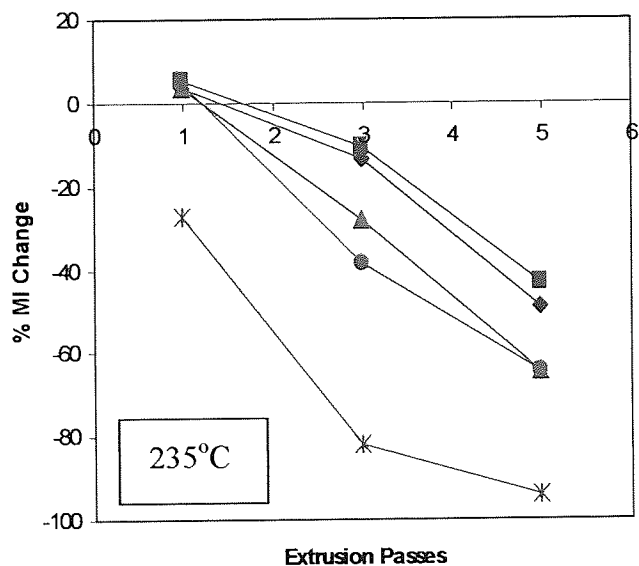
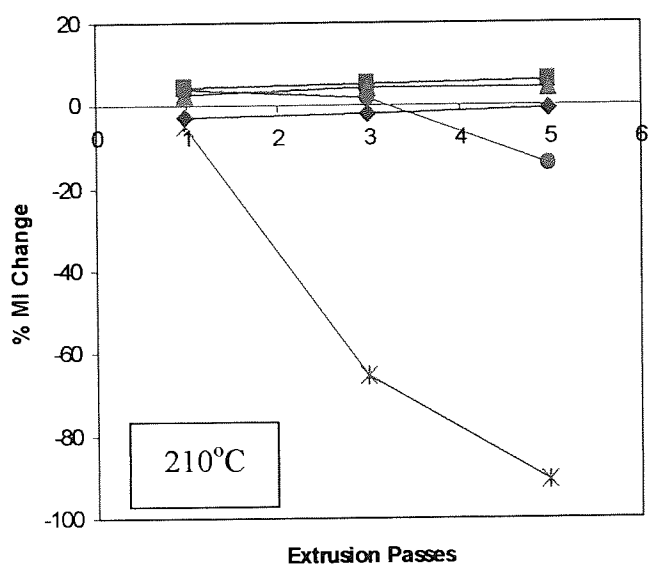


Figure 4.4. Changes in Melt Flow Index (MI) for Different LLDPE Polymers during Multiple Extrusions at Different Temperatures

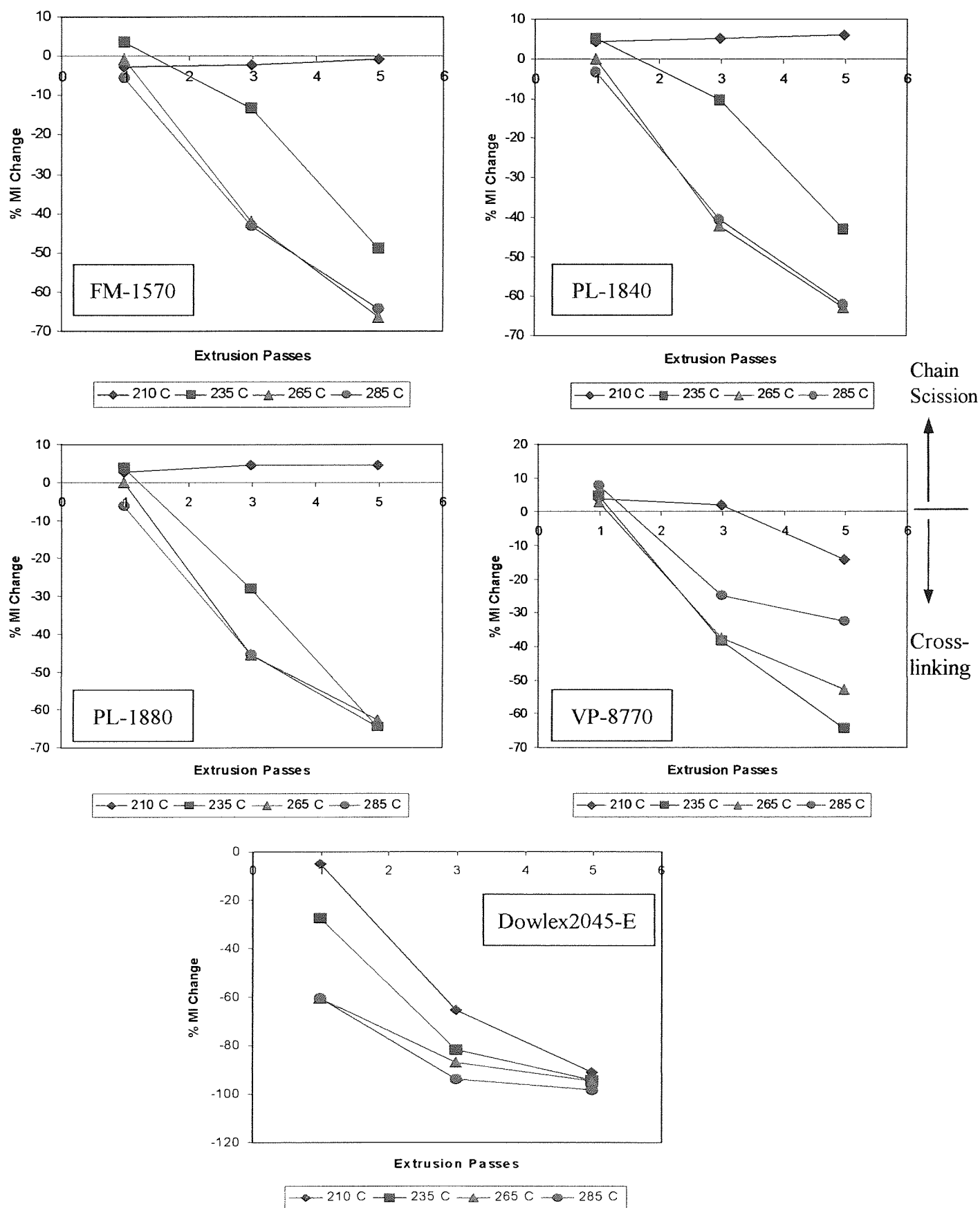


Figure 4.5. Changes in Melt Flow Index (MI) of Different LLDPE Polymers during Multiple Extrusions Each Compared at the Different Processing Temperatures

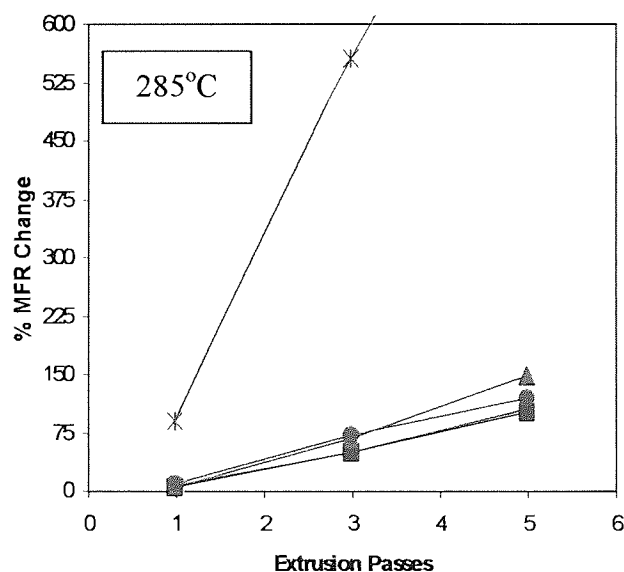
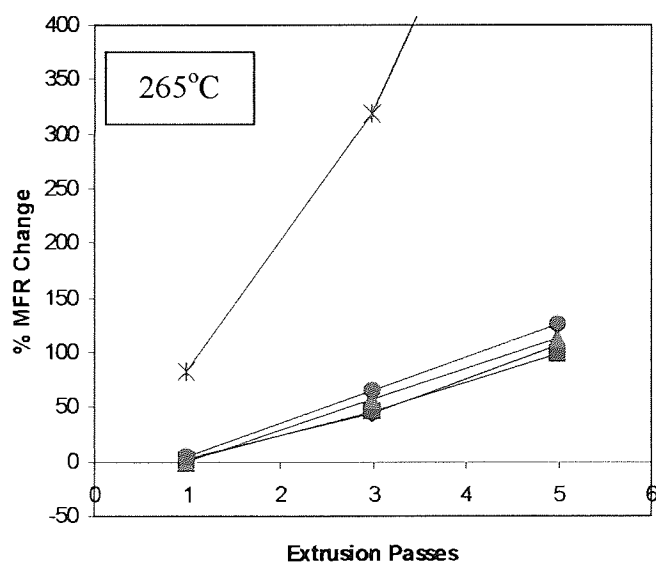
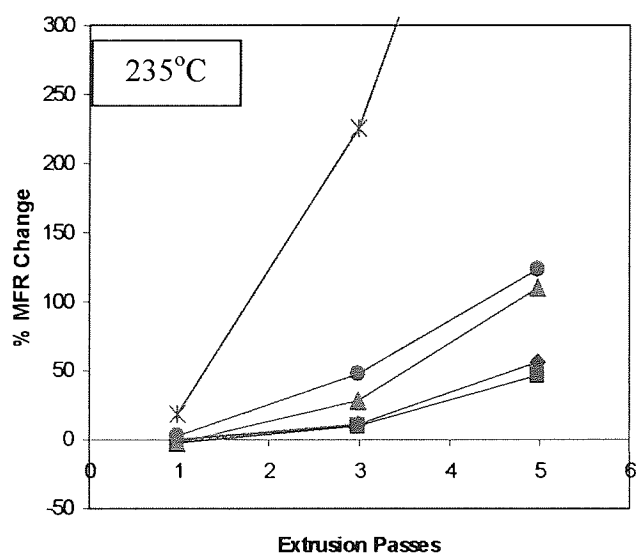
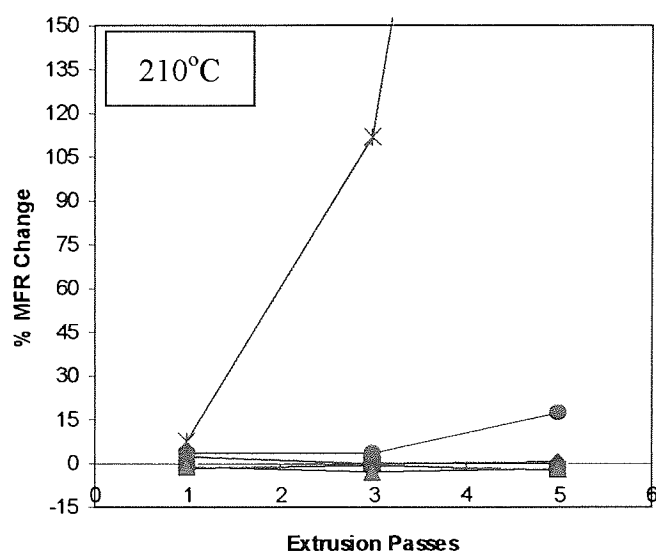


Figure 4.6. Changes in Melt Flow Rate (MFR) for Different LLDPE Polymers during Multiple Extrusions at Different Temperatures

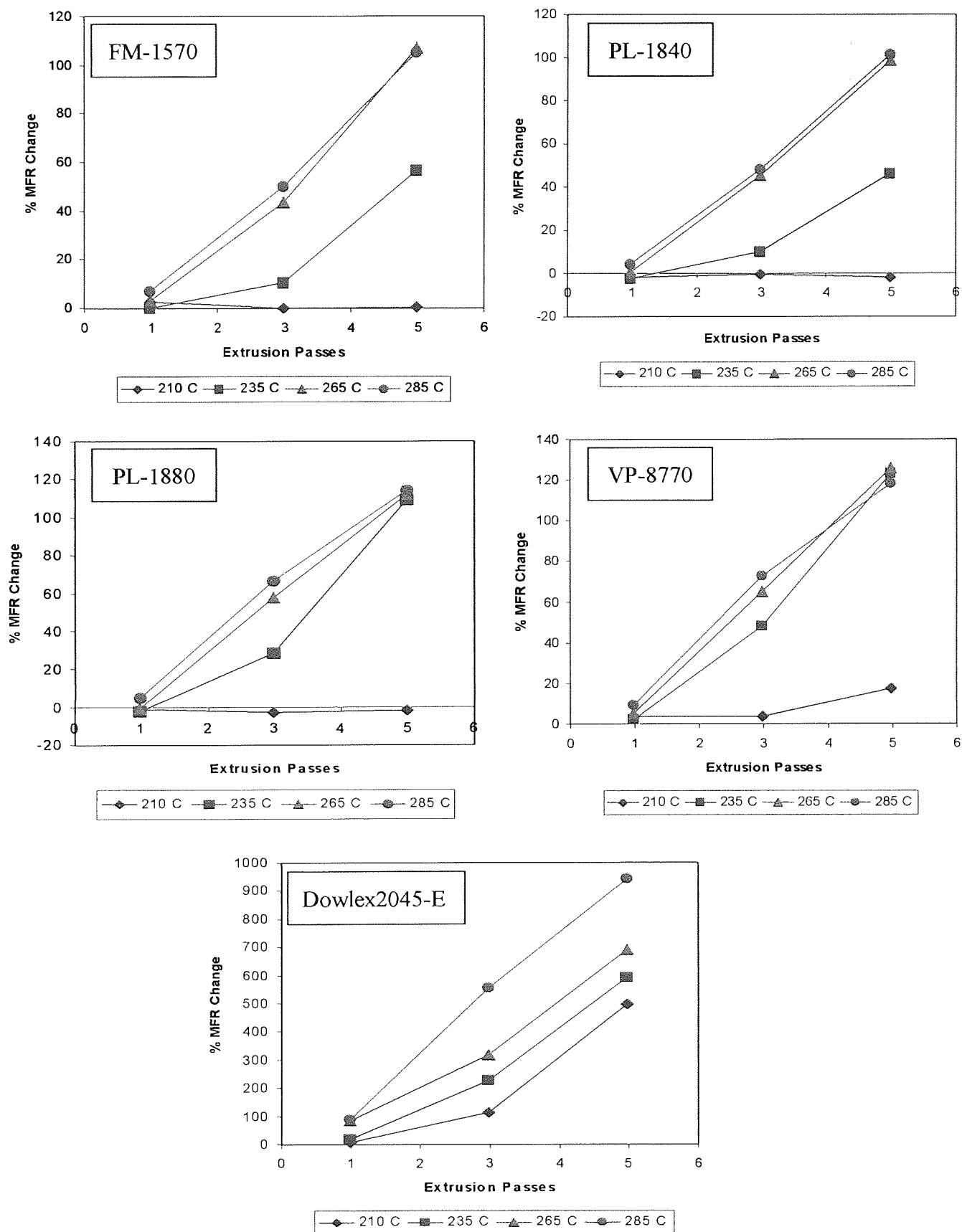


Figure 4.7. Changes in Melt Flow Rate (MFR) of Different LLDPE Polymers during Multiple Extrusions Each Compared at the Different Processing Temperatures

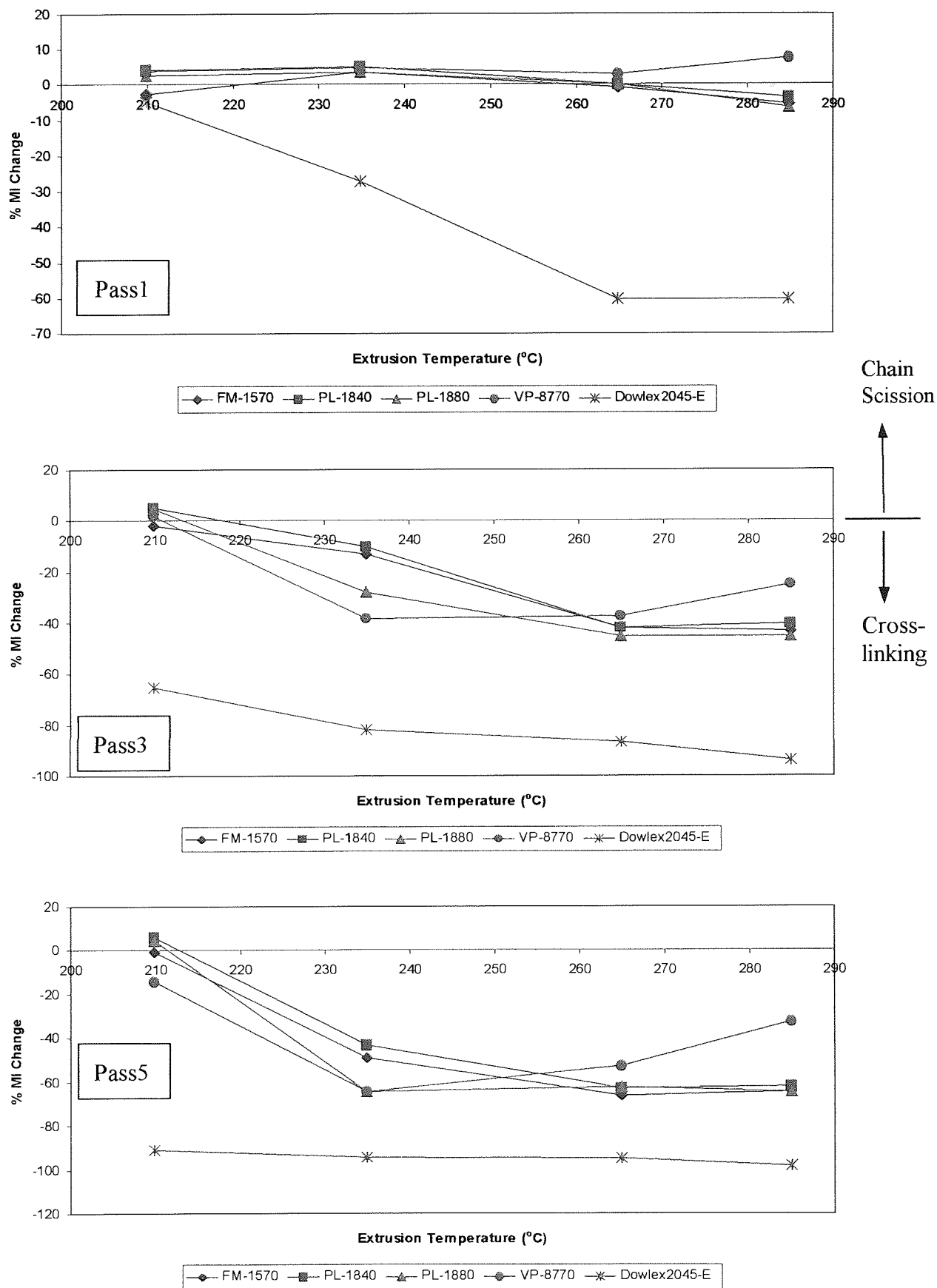


Figure 4.8. Changes in Melt Flow Index (MI) with Temperature for Different LLDPE Polymers after TSE Extrusion of Different Passes

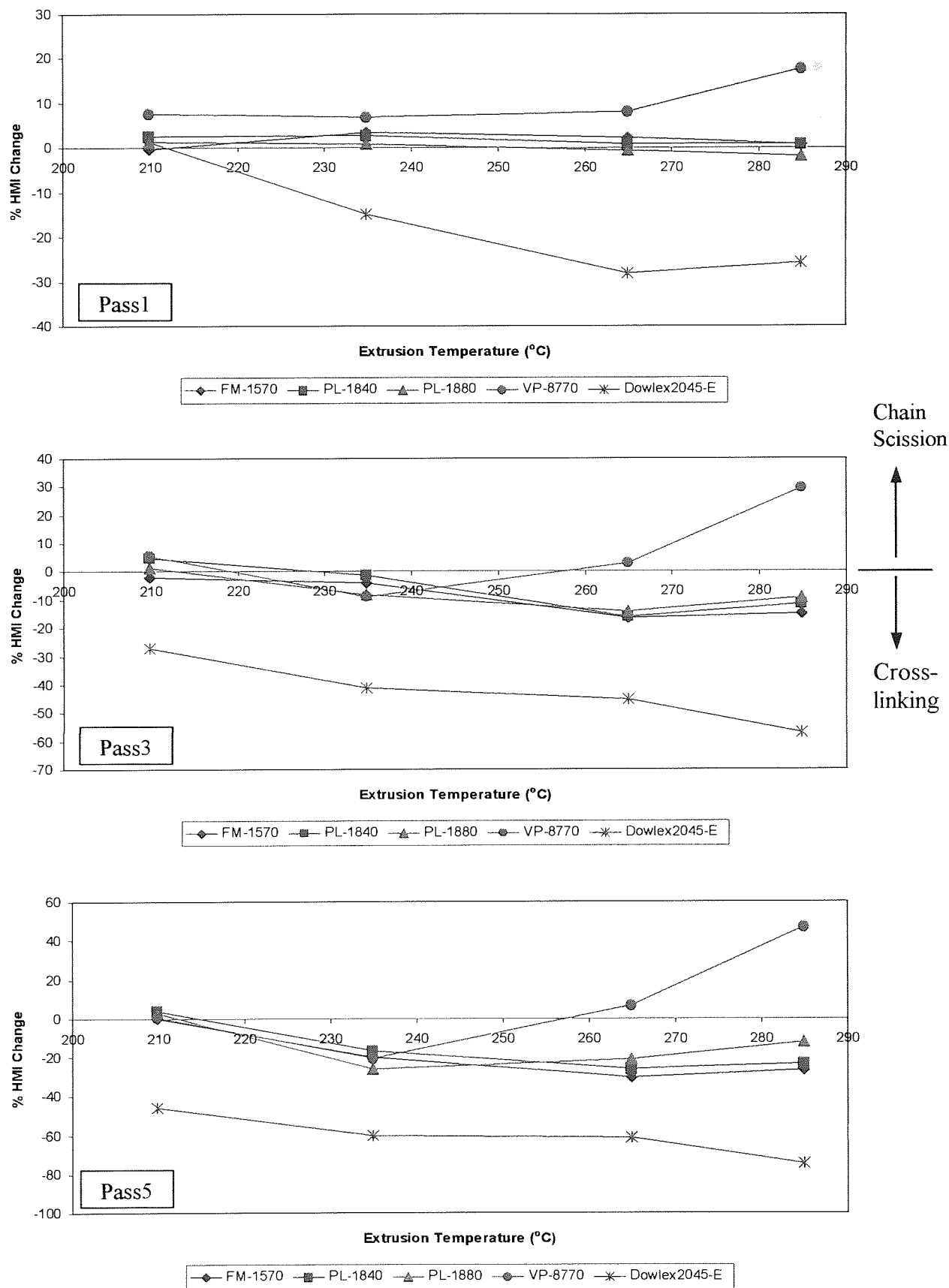


Figure 4.9. Changes in High Load Melt Flow Index (HMI) with Temperature for Different LLDPE Polymers after TSE Extrusion of Different Passes

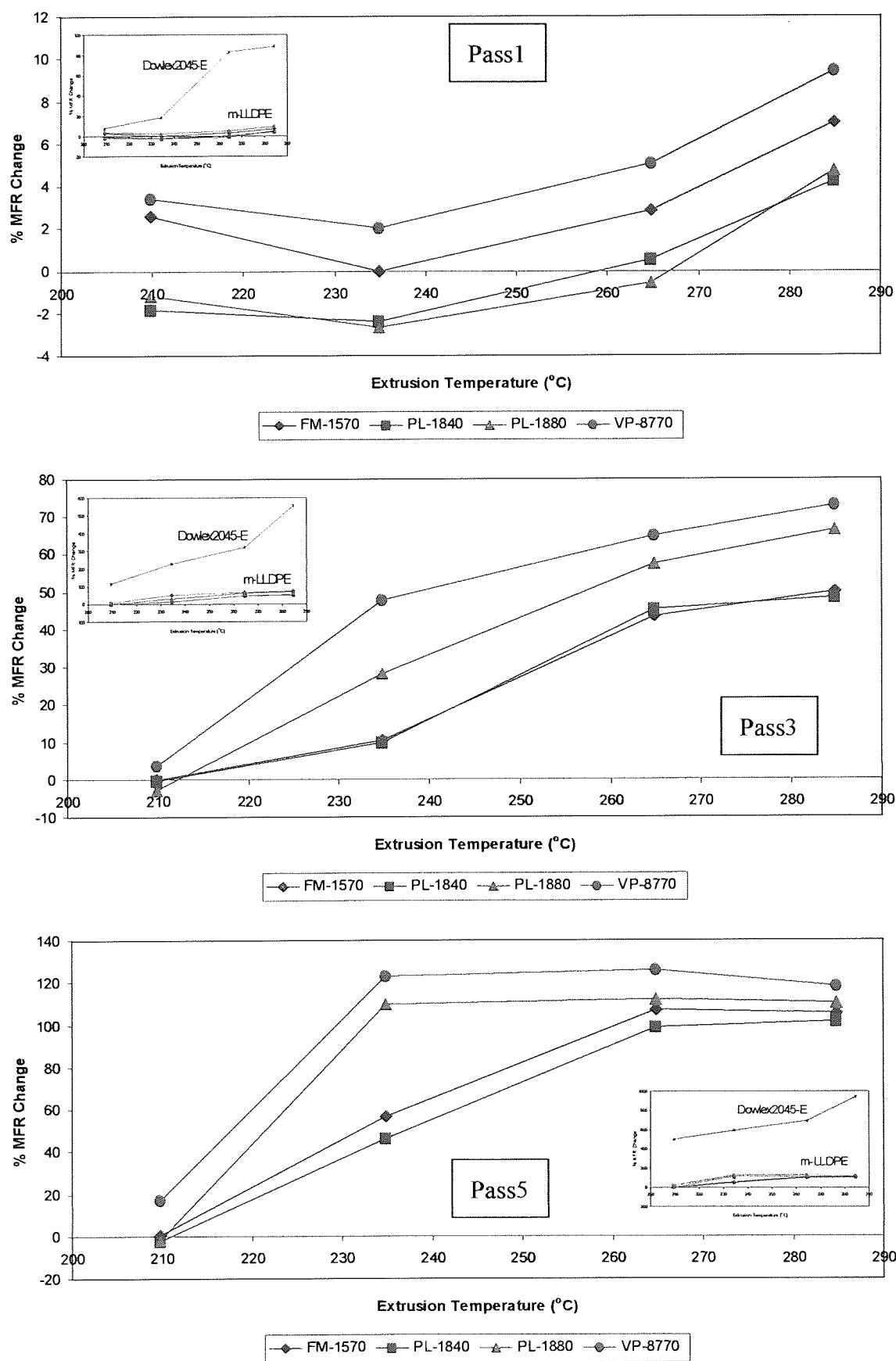


Figure 4.10. Changes in Melt Flow Rate (MFR) with Temperature for Different LLDPE Polymers after TSE Extrusion of Different Passes

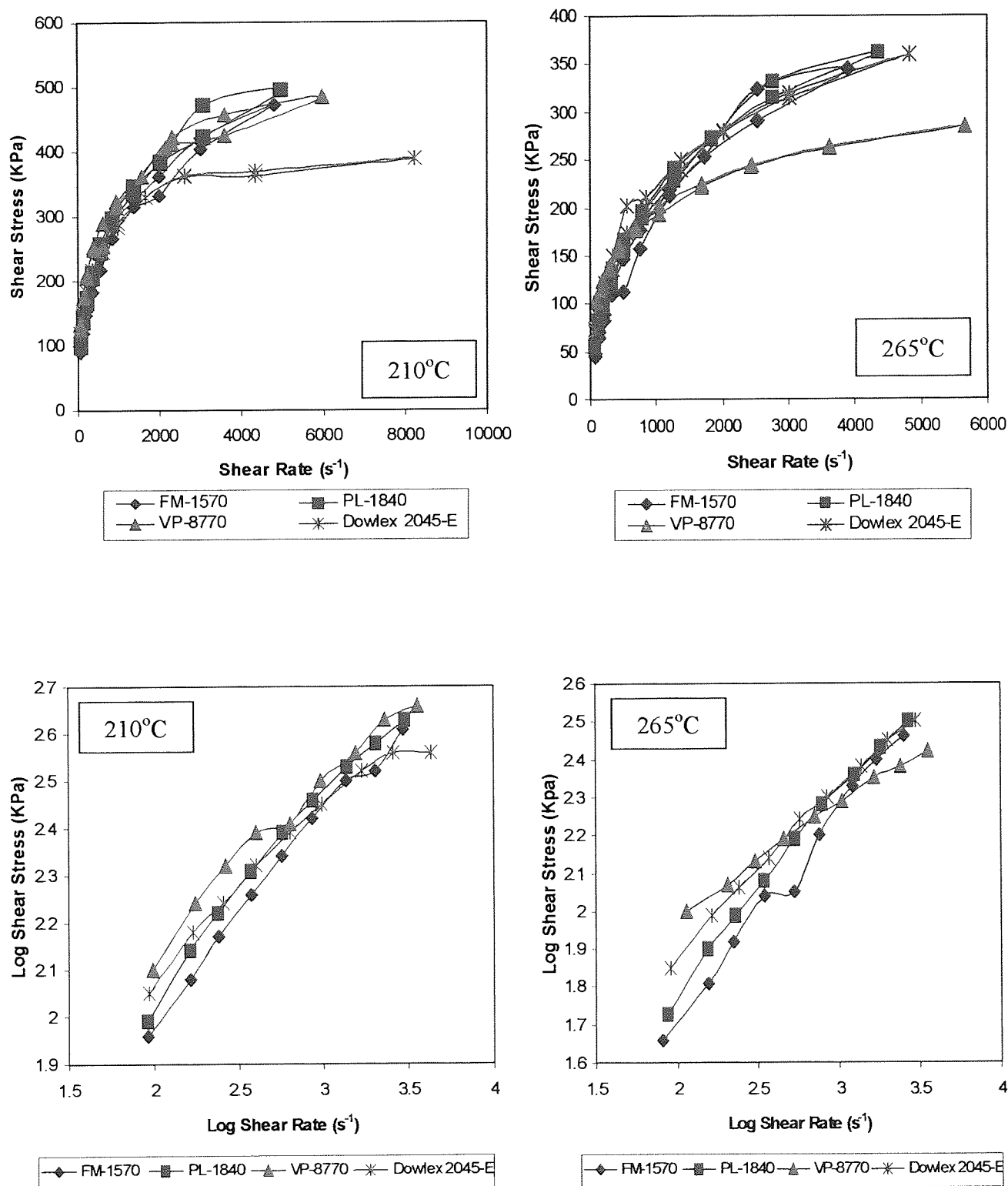


Figure 4.11. Rheological Behaviours of Different **Virgin LLDPE** Polymers Measured by a Rosand Capillary Rheometer at Different Temperatures

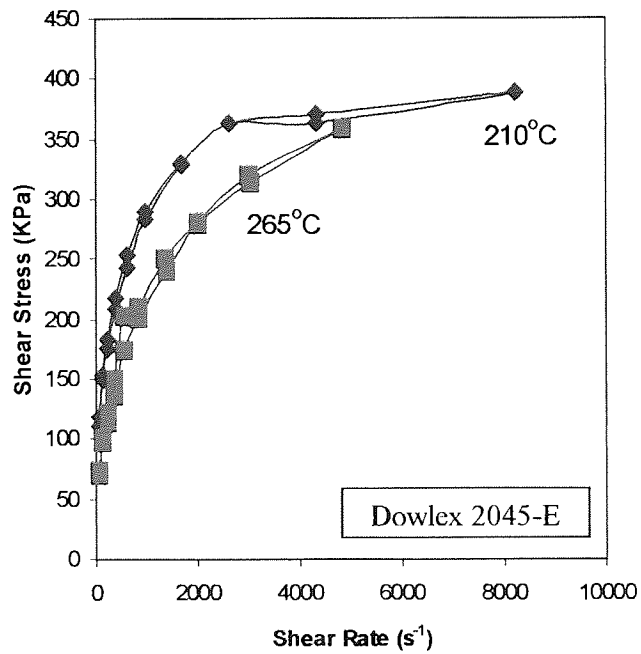
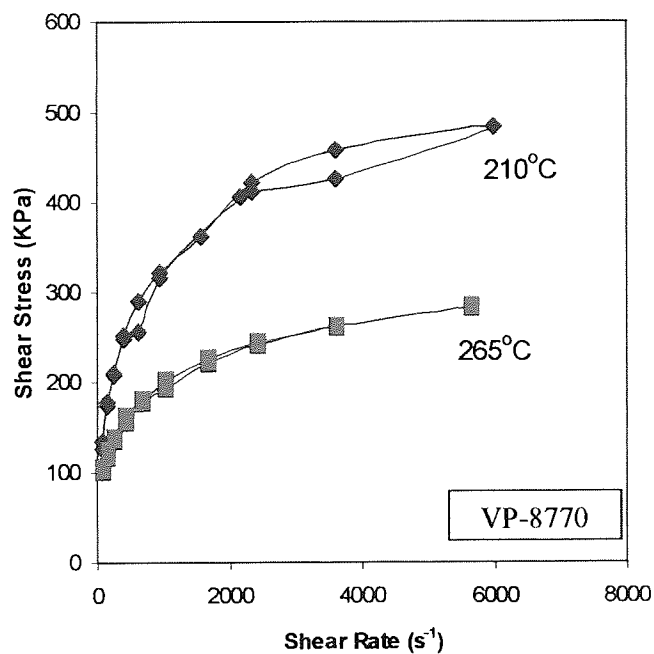
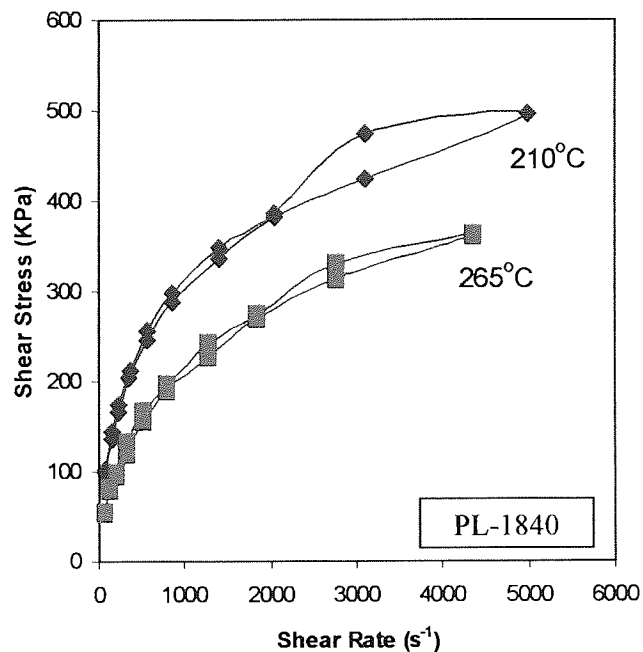
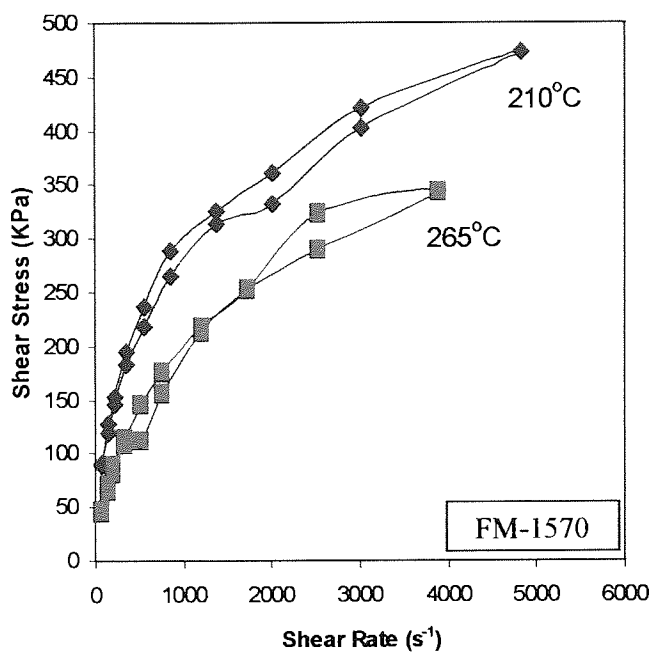


Figure 4.12. Comparison of Rheological Behaviours of Different **Virgin LLDPE** Polymers Tested by a Rosand Capillary Rheometer at 210°C and 265°C

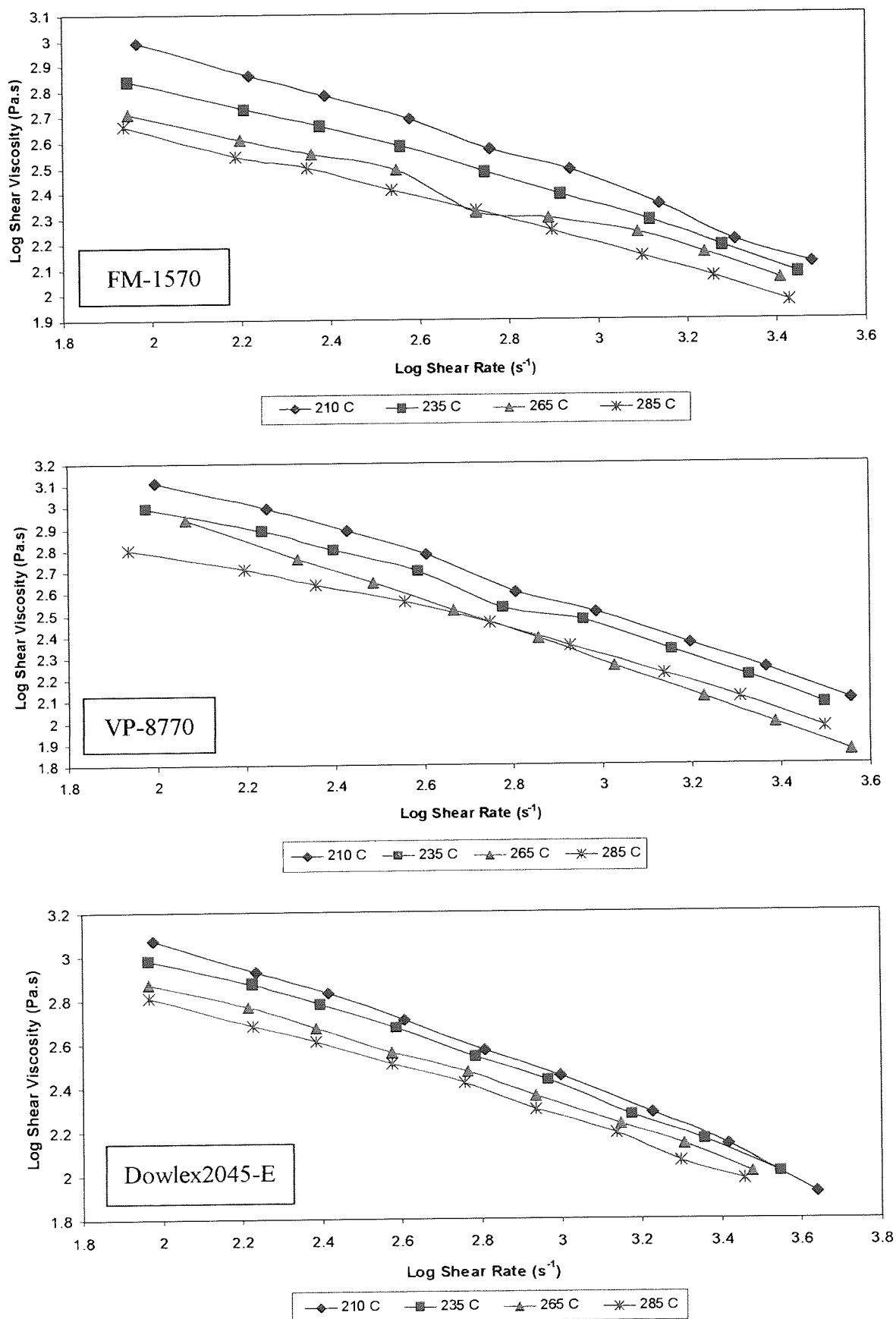


Figure 4.13. Rheological Behaviours of Different **Virgin LLDPE** Polymers Measured by a Rosand Capillary Rheometer, Each Polymer Compared at the Different Temperatures

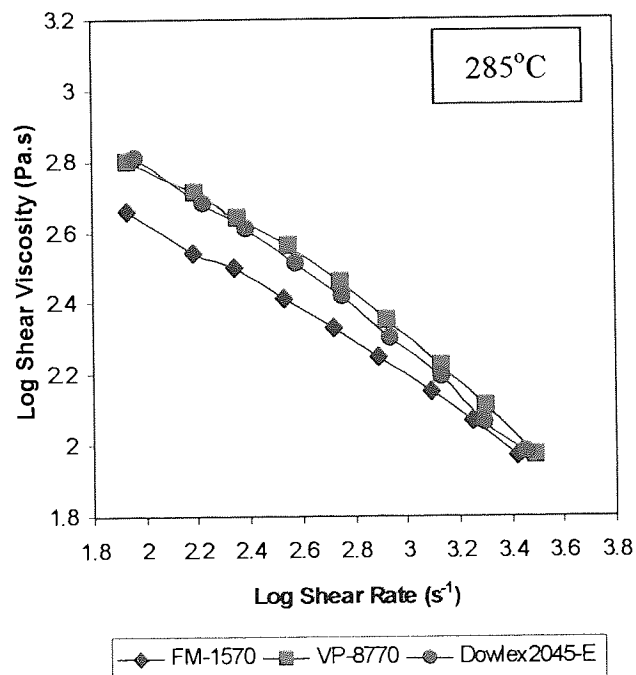
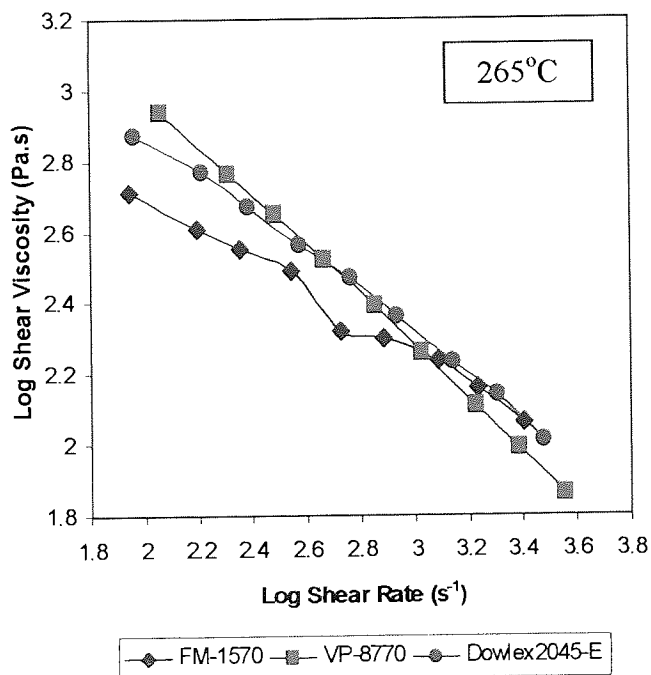
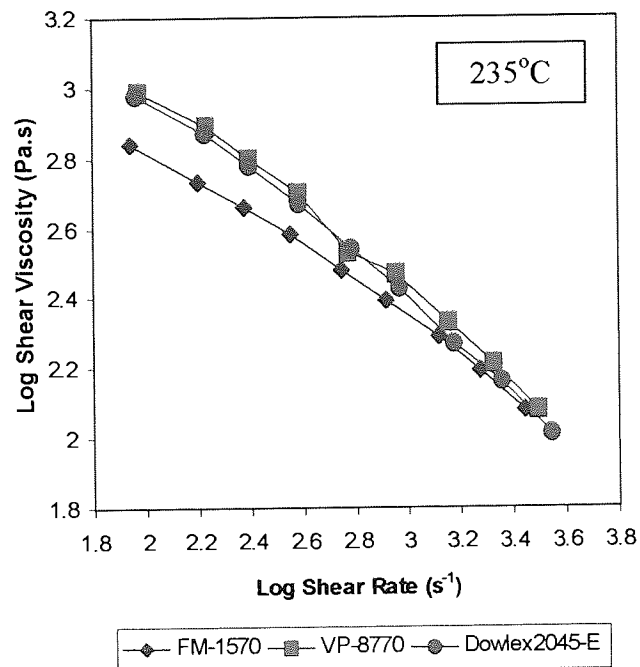
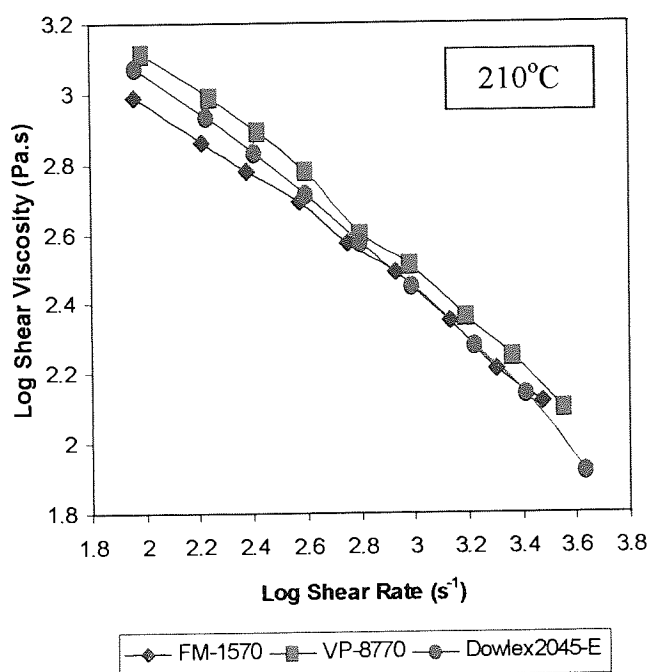


Figure 4.14. Comparison of Rheological Behaviours of Different **Virgin LLDPE** Polymers Tested by a Rosand Capillary Rheometer at Different Temperatures

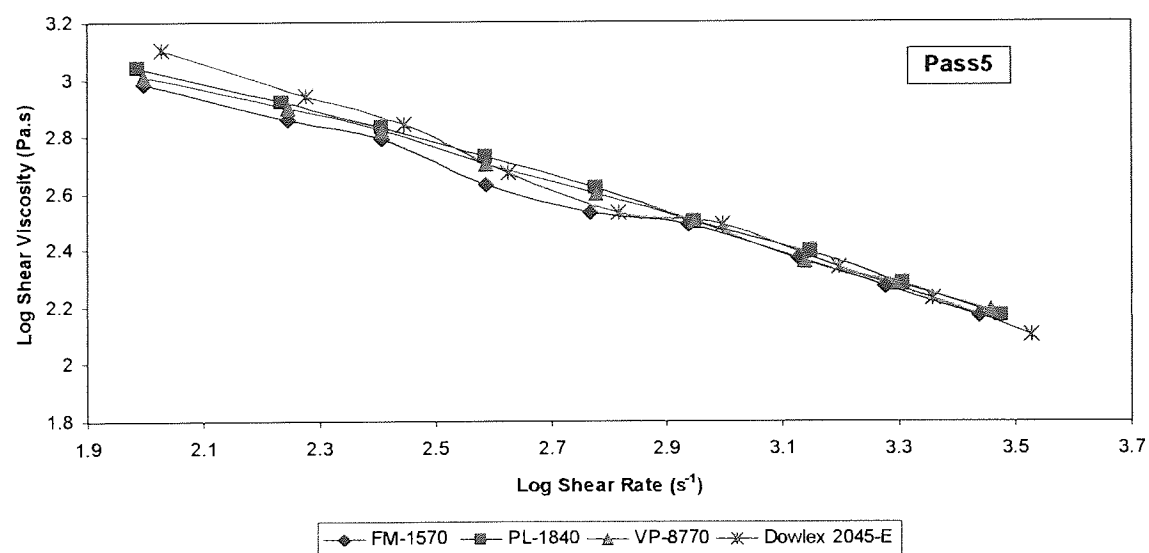
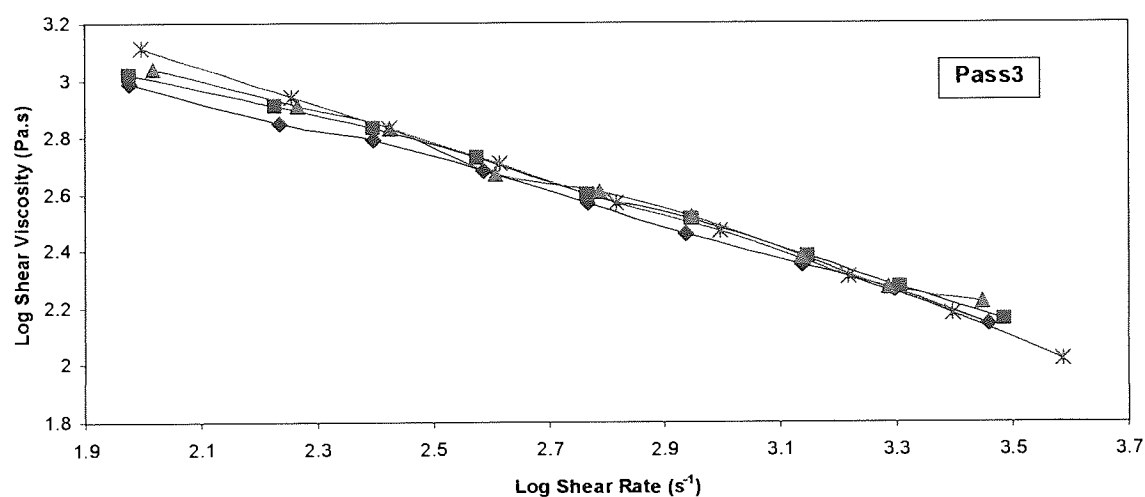
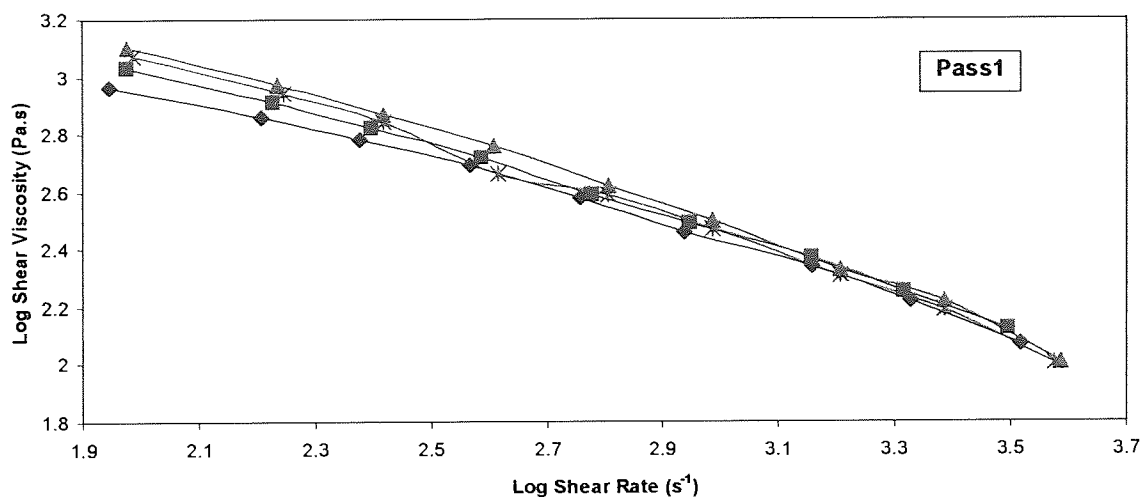


Figure 4.15. Shear Viscosity Changes with Shear Rate for Different **Extruded LLDPE** Polymers (under the conditions of 265°C, 100rpm) Measured by a Capillary Rheometer at 265°C

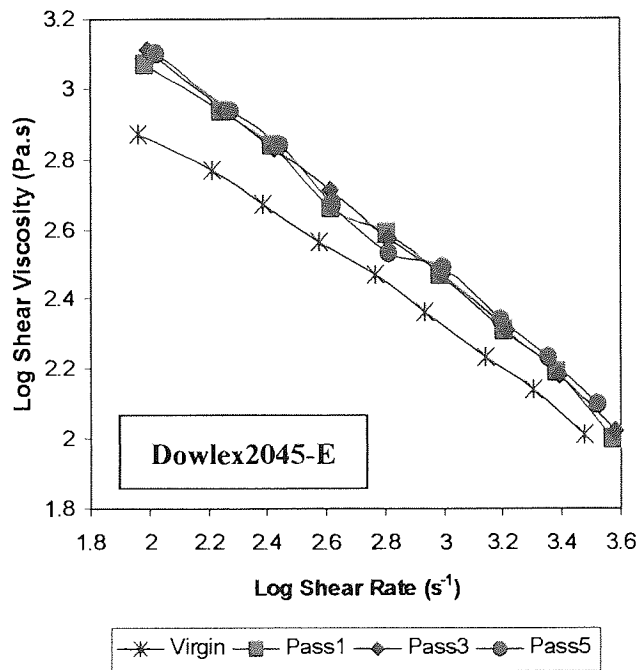
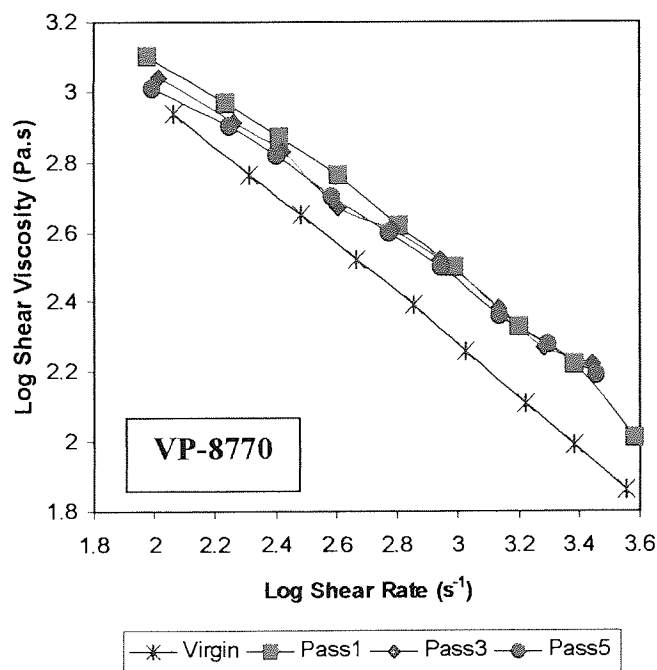
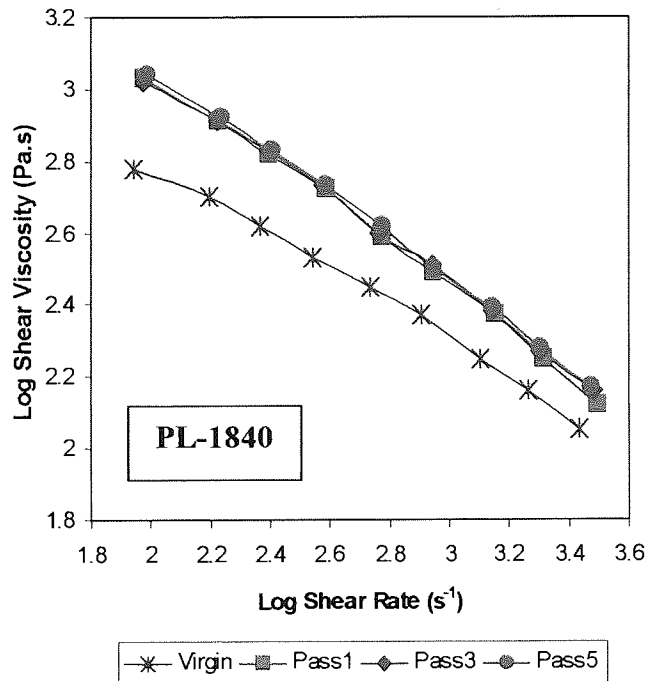
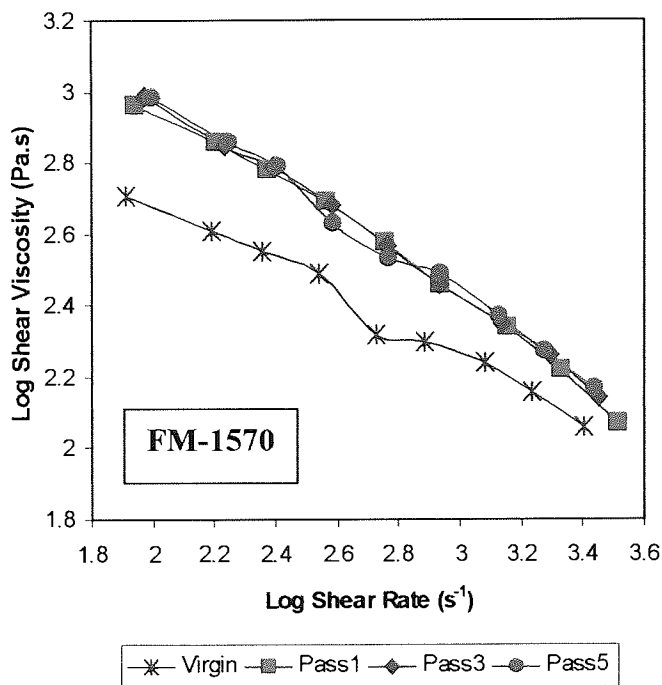


Figure 4.16. Shear Viscosity Changes with Shear Rate for Individual **Extruded LLDPE** Polymers (under the conditions of 265°C, 100rpm) Tested by a Rosand Capillary Rheometer at 265°C. The Rheological Properties of the Corresponding Virgin Polymers (as received not extruded) Tested in the Rheometer at 265°C (same testing conditions) Are also Shown

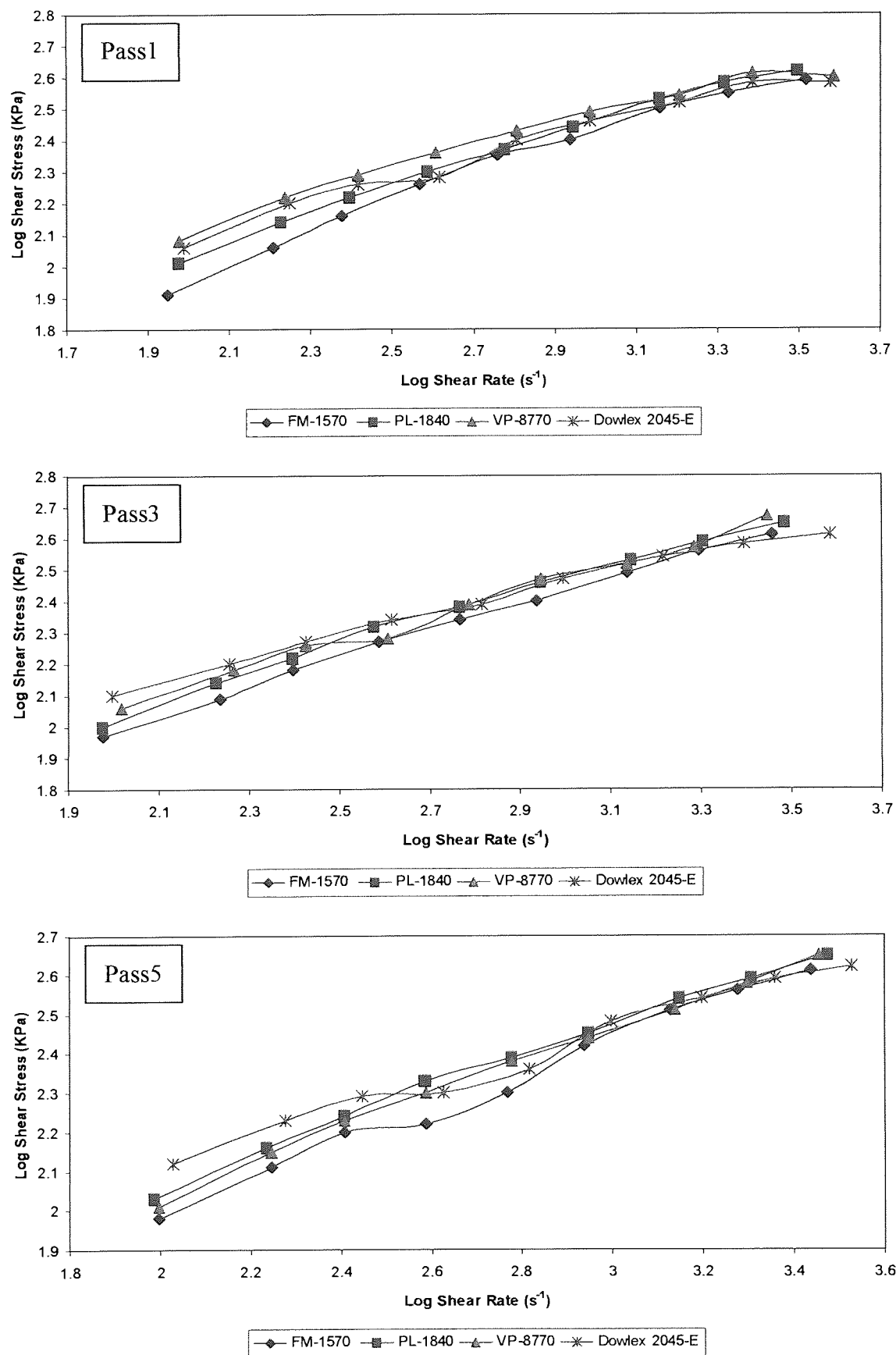


Figure 4.17. Shear Stress Changes with Shear Rate for Different **Extruded LLDPE** Polymers (under the conditions of 265°C, 100rpm) Measured by a Capillary Rheometer at 265°C

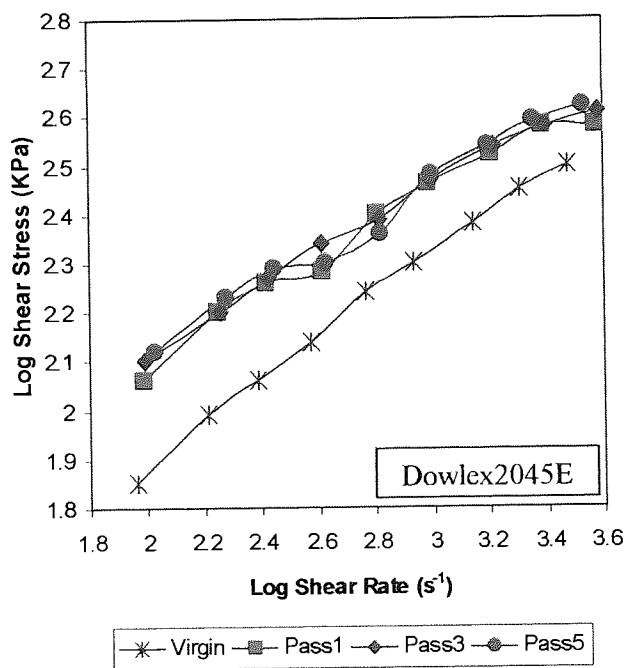
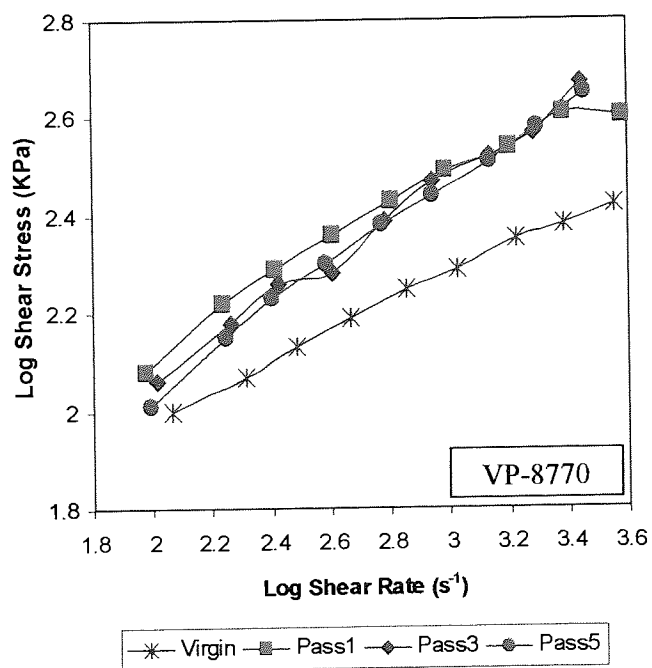
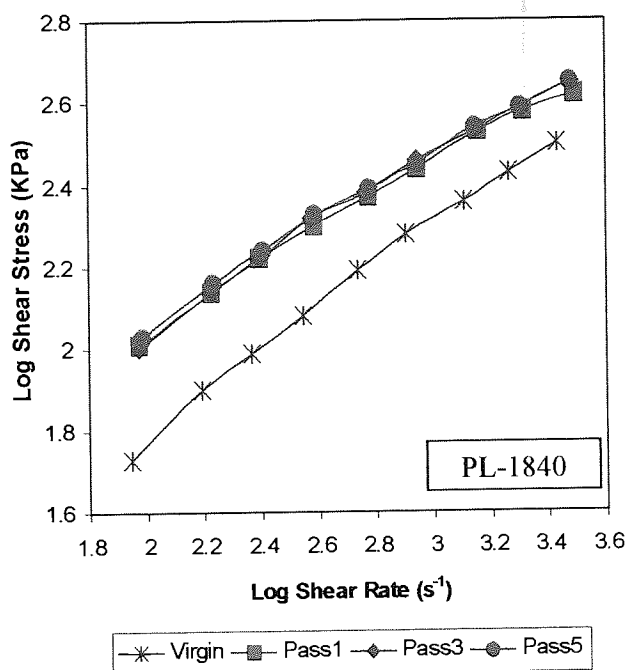
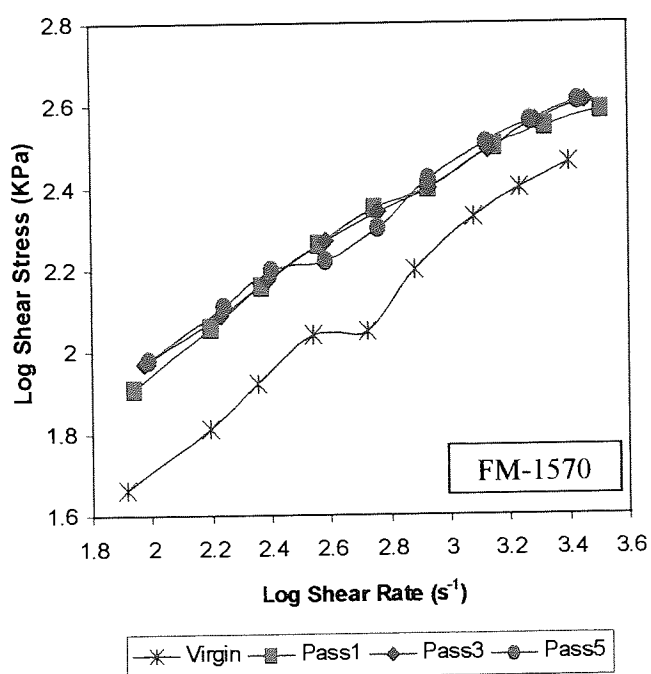


Figure 4.18. Shear Stress Changes with Shear Rate for Individual **Extruded LLDPE** Polymers (under the conditions of 265°C, 100rpm) Tested by a Rosand Capillary Rheometer at 265°C The Rheological Properties of the Corresponding Virgin Polymers (as received not extruded) Tested in the Rheometer at 265°C (same testing conditions) Are also Shown

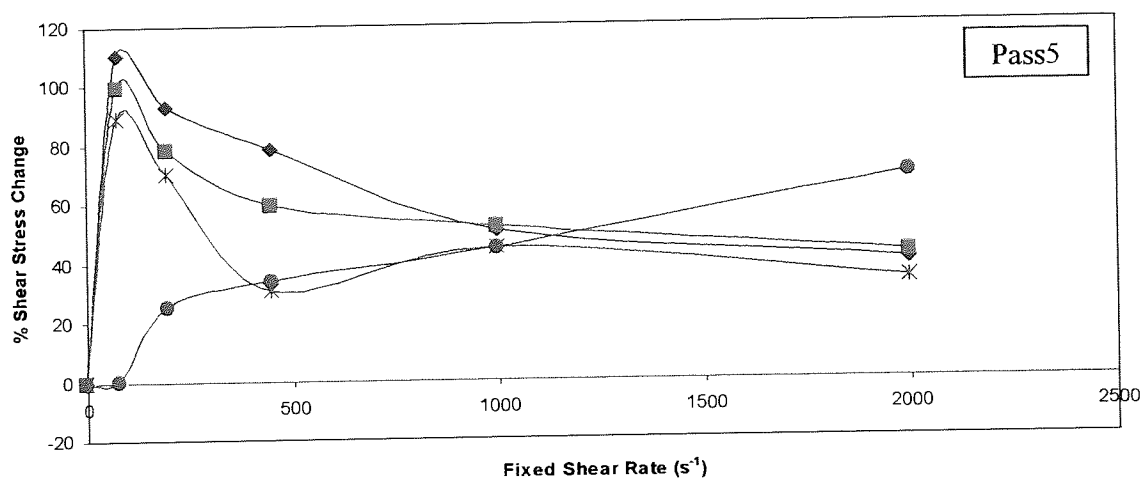
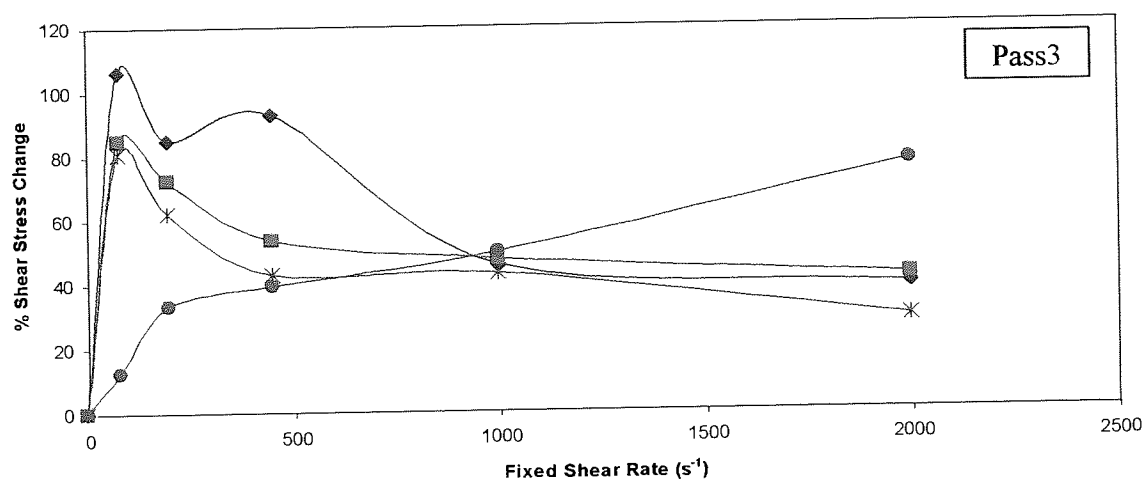
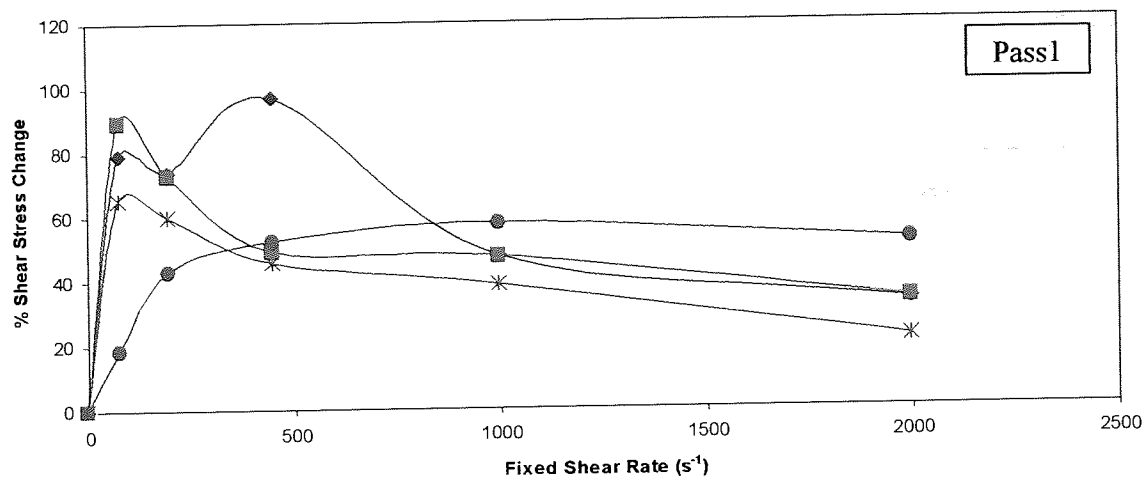


Figure 4.19. Changes of Shear Stress (compared with virgin polymers) at Fixed Shear Rate Values for Different **Extruded LLDPE** Polymers (under the conditions of 265°C, 100rpm) Measured by a Rosand Capillary Rheometer at 265°C

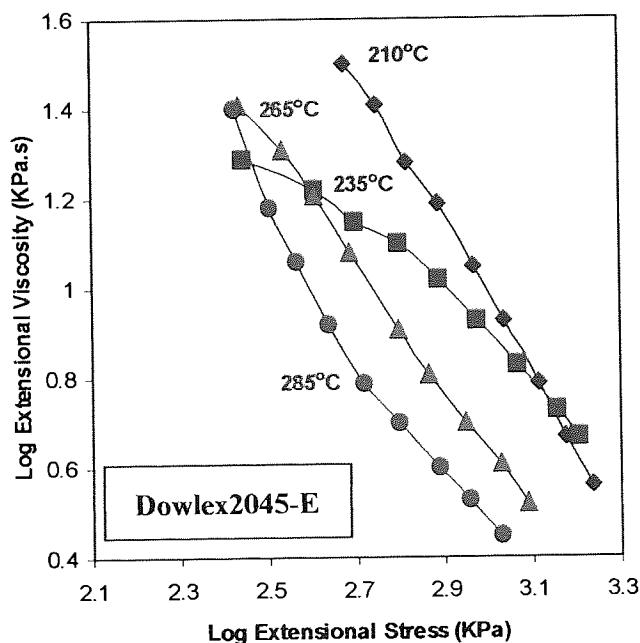
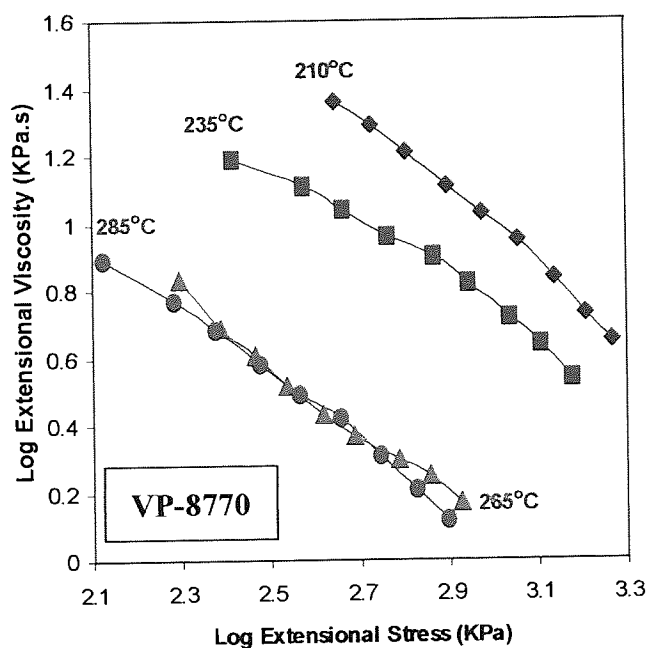
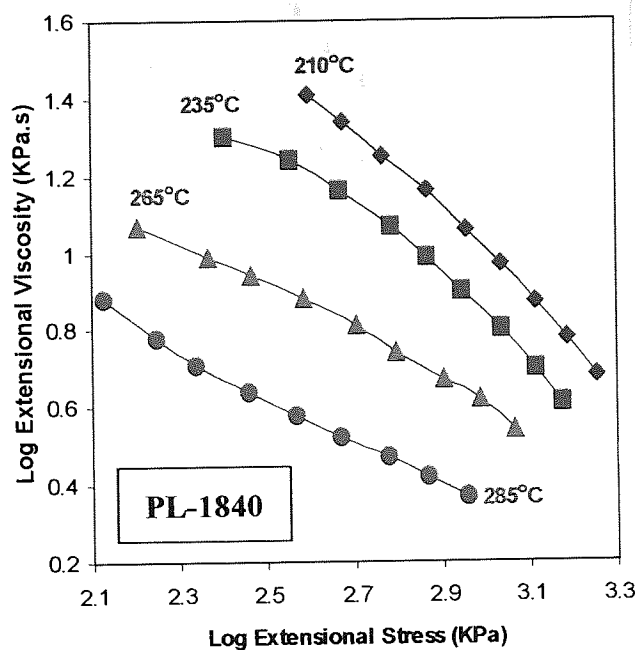
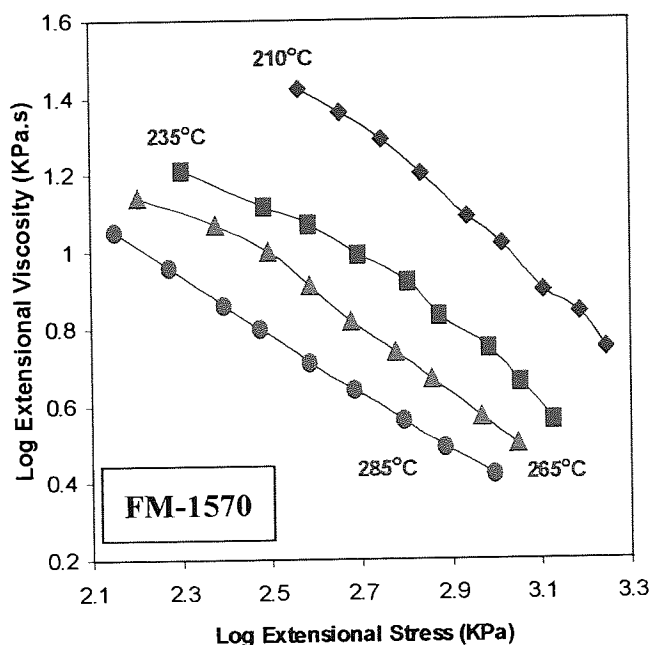


Figure 4.20. Extensional Viscosity versus Extensional Stress for Individual **Virgin LLDPE** Polymers Tested by a Rosand Capillary Rheometer at Different Temperatures

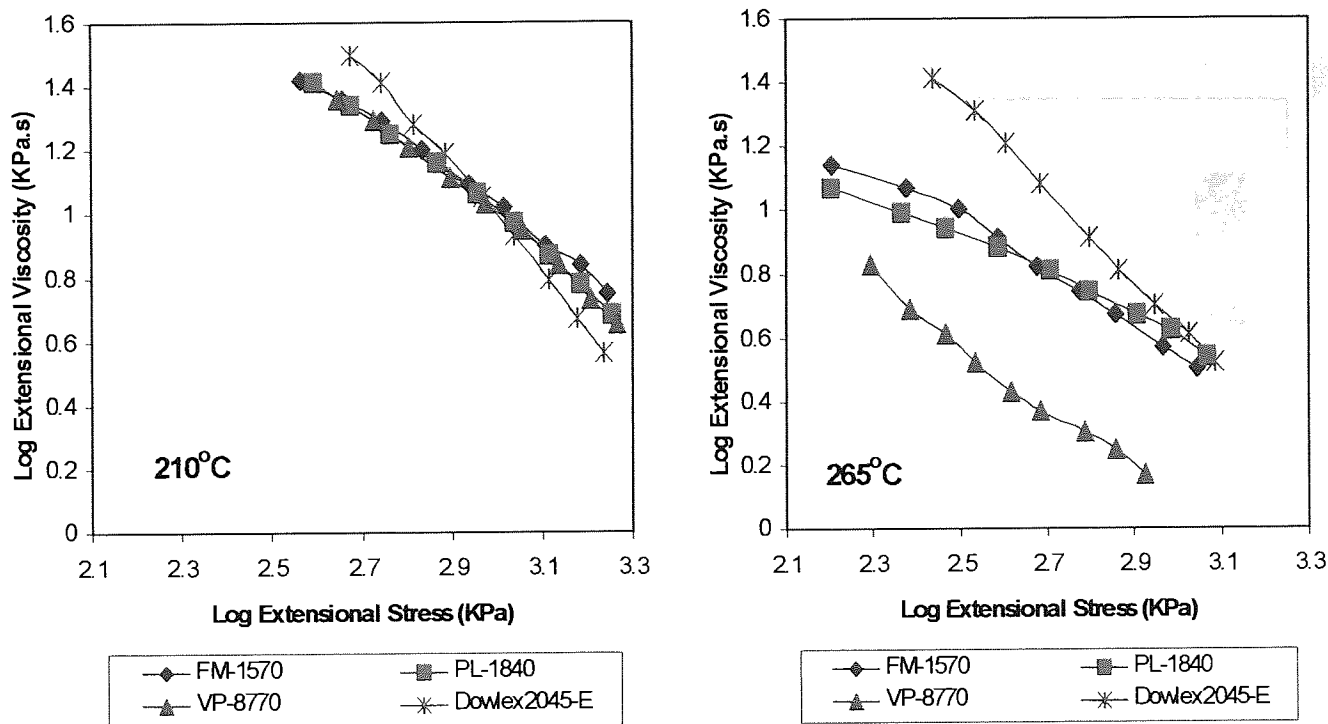


Figure 4.21. Extensional Viscosity versus Extensional Stress for Different **Virgin LLDPE** Polymers Measured by a Rosand Capillary Rheometer at Different Temperatures

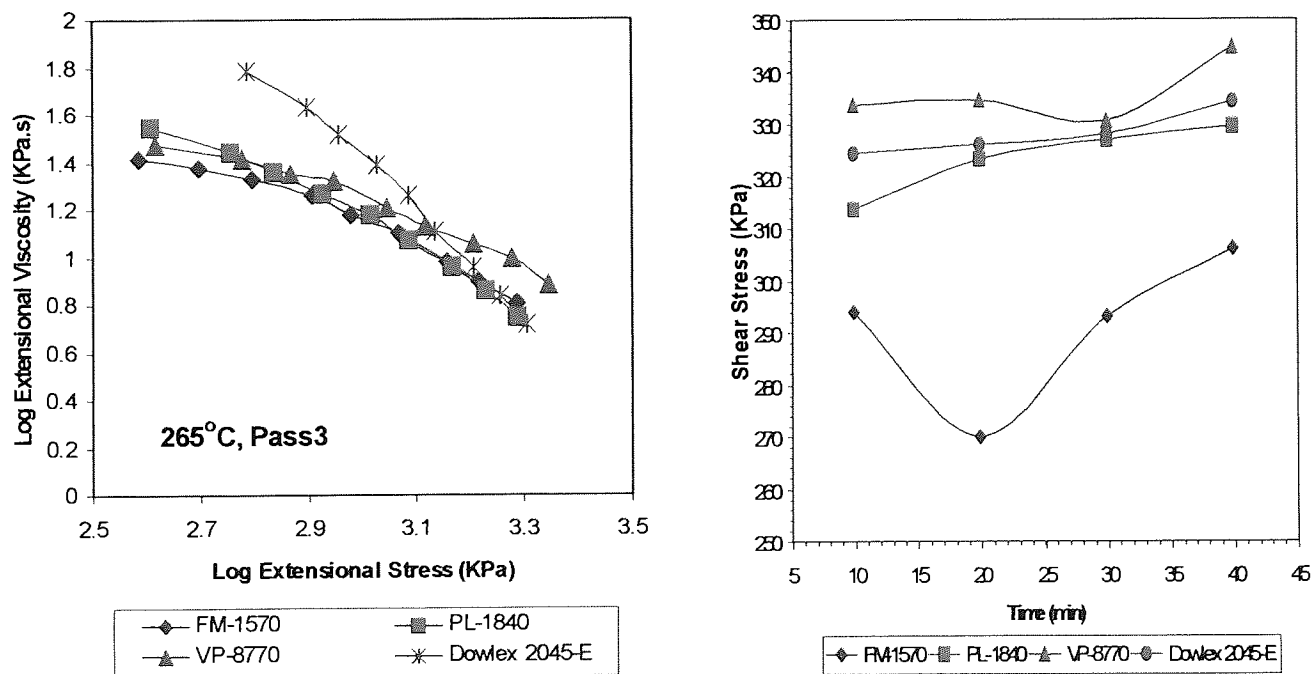


Figure 4.22. Extensional Viscosity versus Extensional Stress for **Extruded LLDPE** Polymers (265°C, Pass3) Measured by a Rosand Capillary Rheometer at 265°C

Figure 4.23. Shear Stress versus Time for Material Degradation Test of Different **Virgin LLDPE** Polymers Carried out in a Capillary Rheometer at 265°C

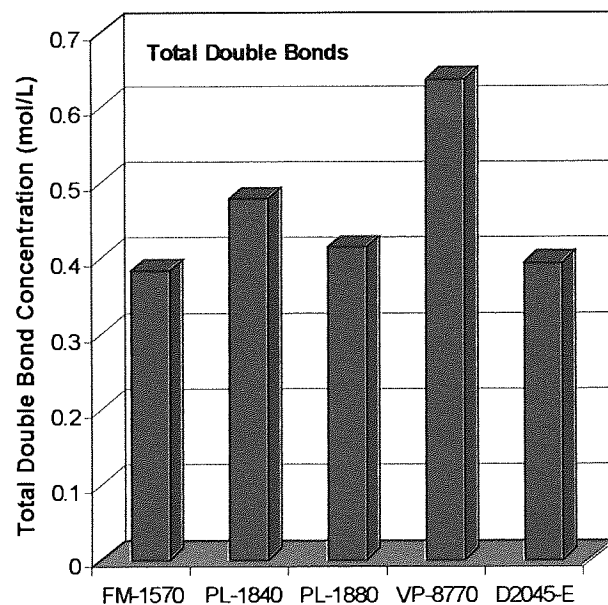
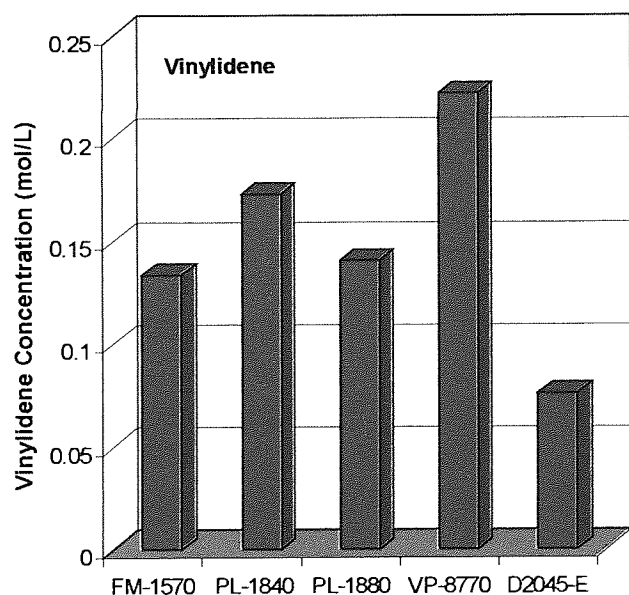
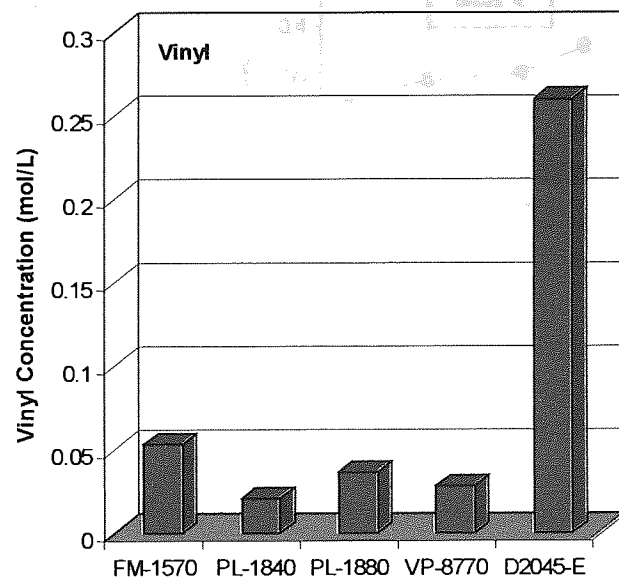
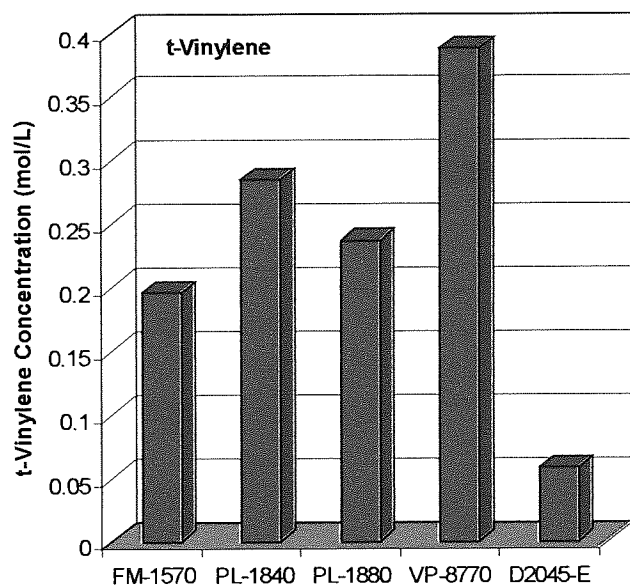


Figure 4.24. Concentrations of Double Bonds in Different **Virgin LLDPE** Polymers Measured by FTIR Based on Corresponding IR Extinction Coefficients

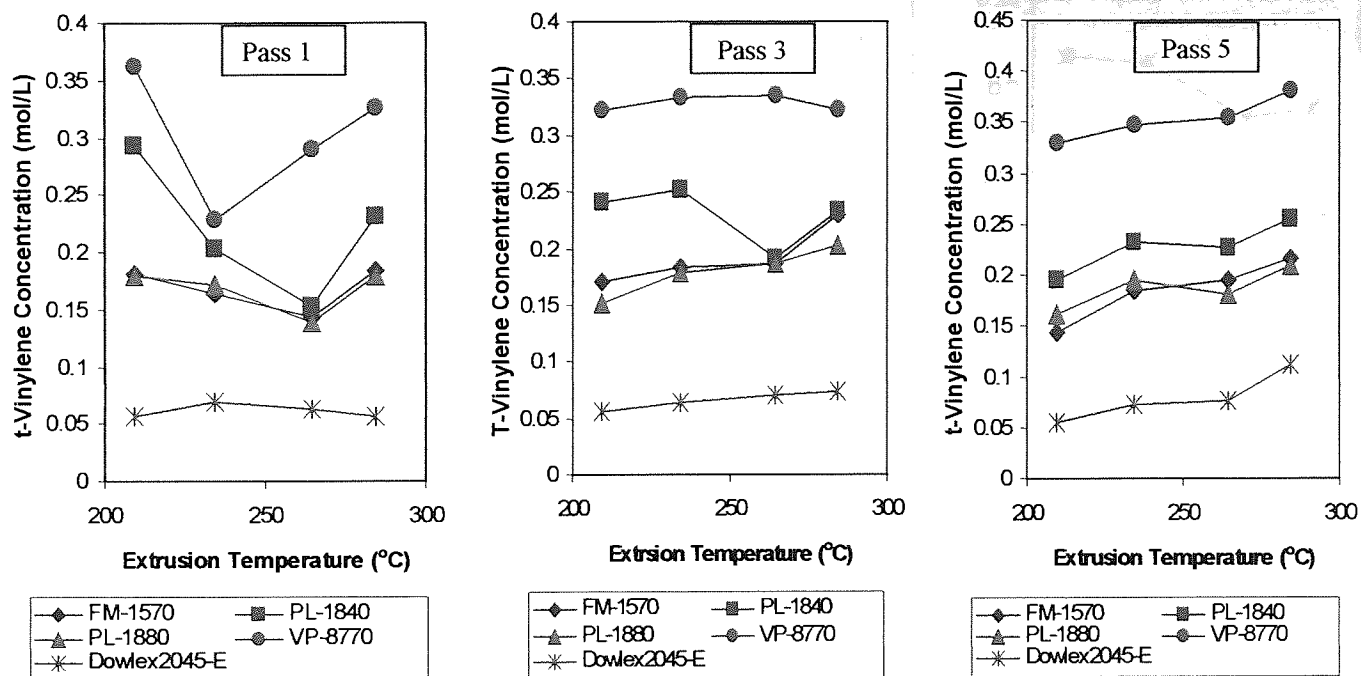


Figure 4.25. **trans-Vinylene** Concentration with Temperature Curves for Extruded LLDPE Polymers after Different Extrusion Passes

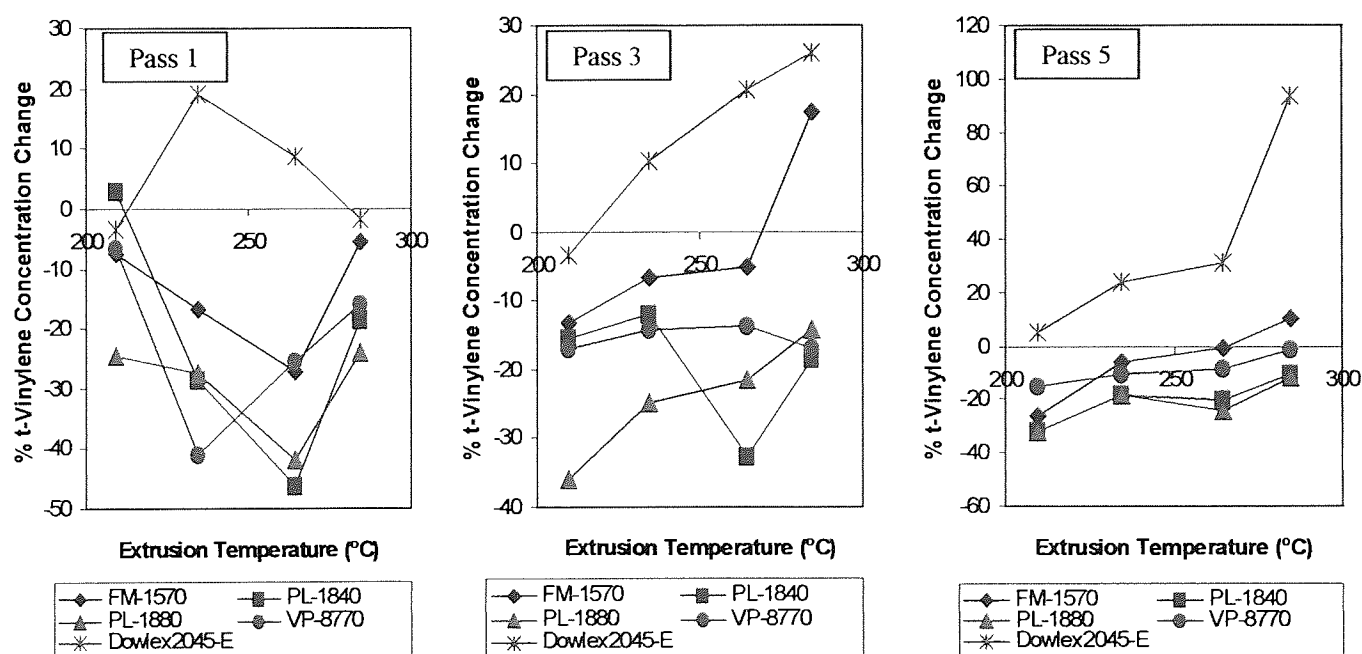


Figure 4.26. Percentage Changes of **trans-Vinylene** Concentration (compared to corresponding virgin polymers) with Temperature for Extruded LLDPE Polymers after Different Extrusion Passes

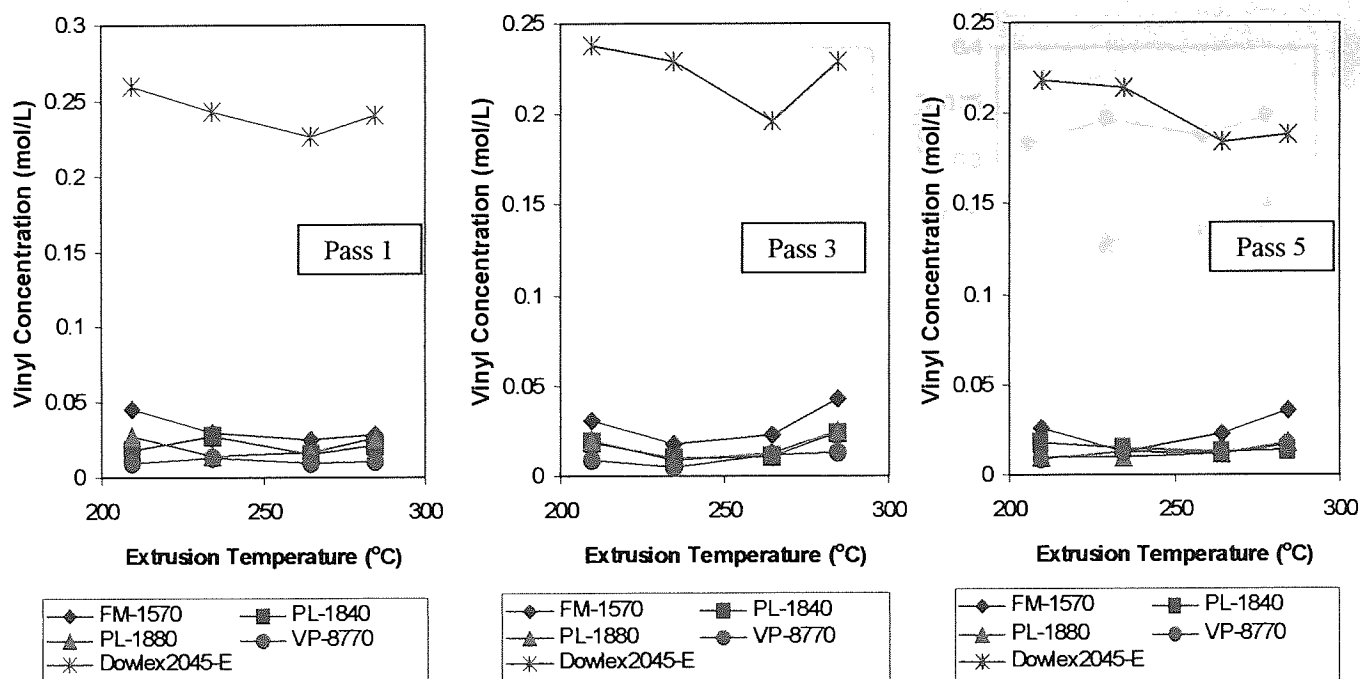


Figure 4.27. Vinyl Concentration with Temperature Curves for Extruded LLDPE Polymers after Different Extrusion Passes

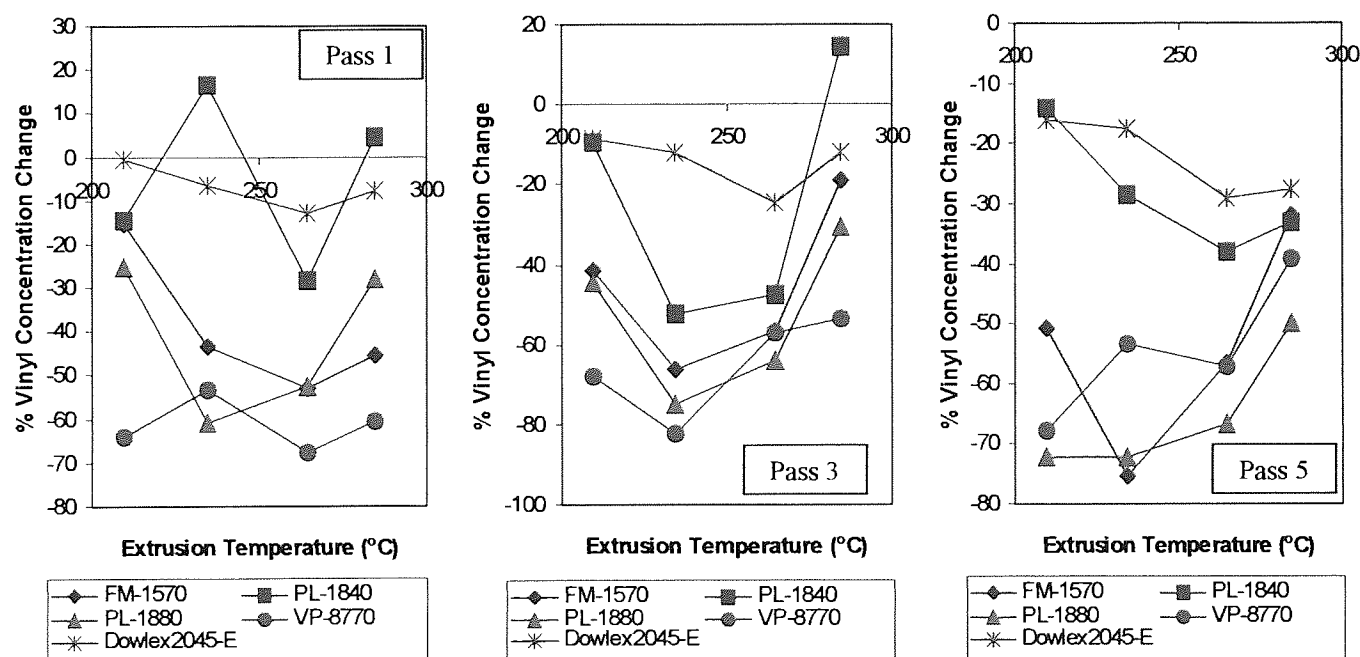


Figure 4.28. Percentage Changes of Vinyl Concentration with Temperature for Extruded LLDPE Polymers after Different Extrusion Passes

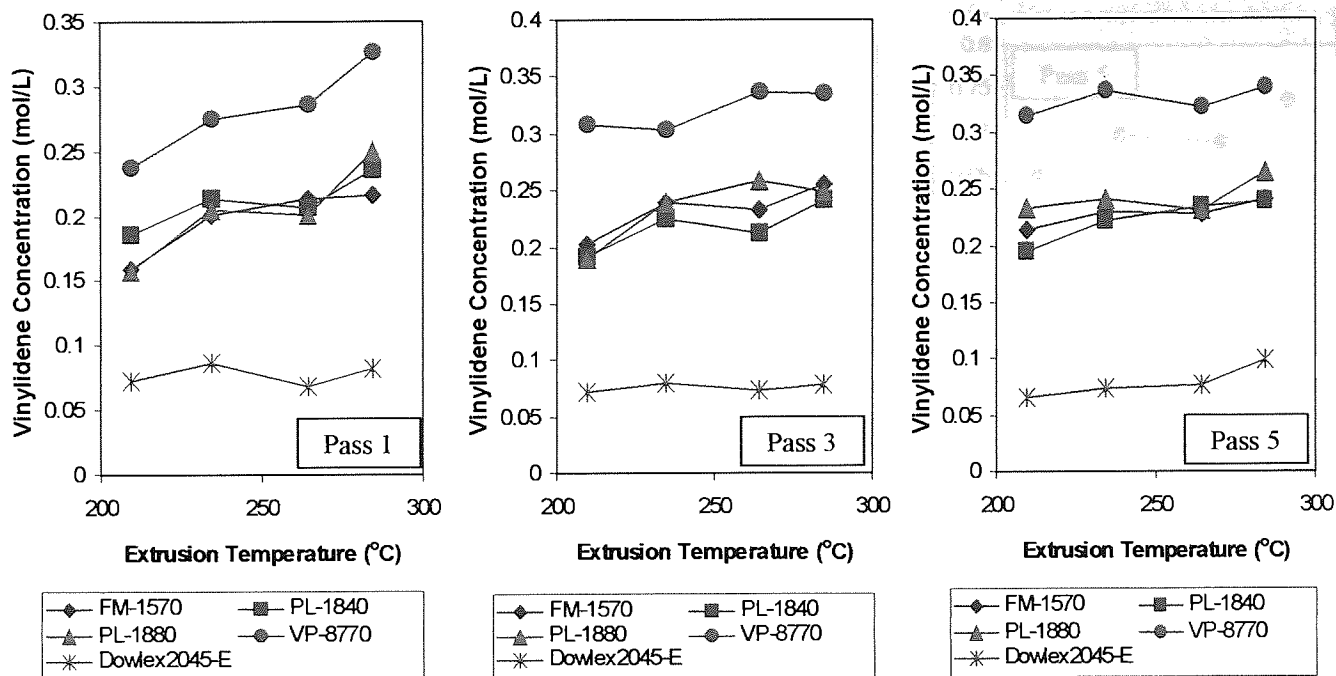


Figure 4.29. **Vinylidene** Concentration with Temperature Curves for Extruded LLDPE Polymers after Different Extrusion Passes

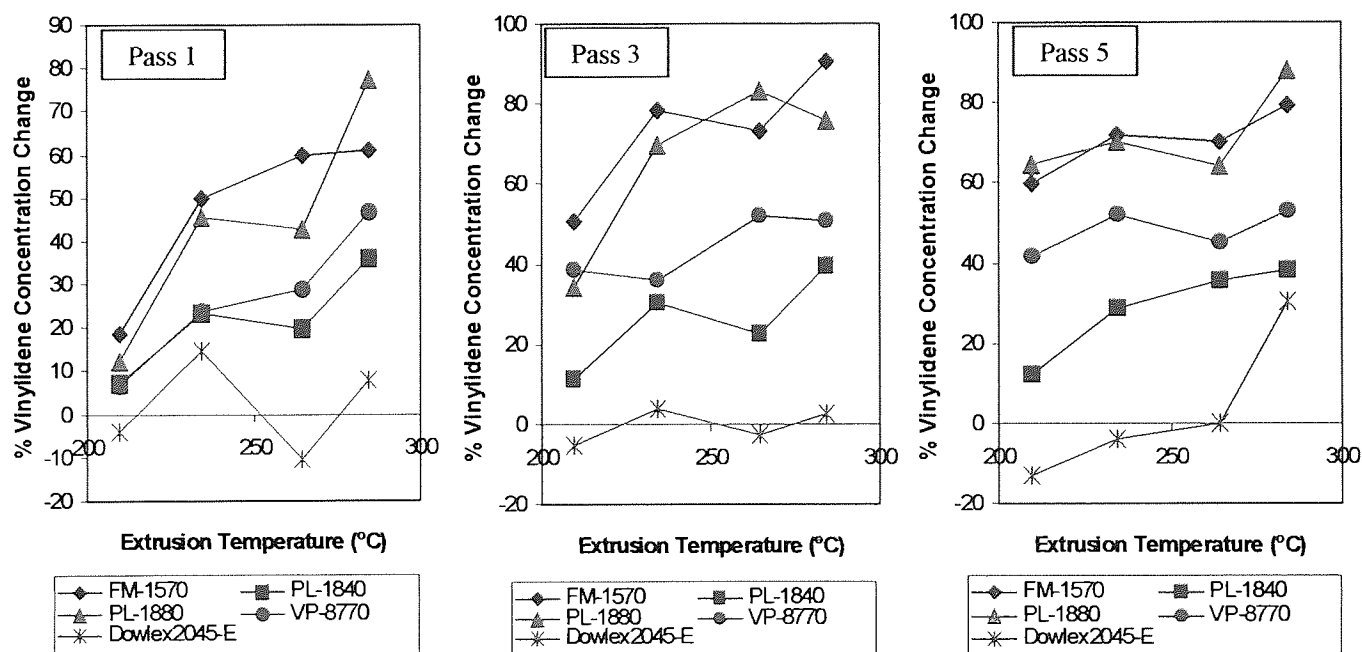


Figure 4.30. Percentage Changes of **Vinylidene** Concentration with Temperature for Extruded LLDPE Polymers after Different Extrusion Passes

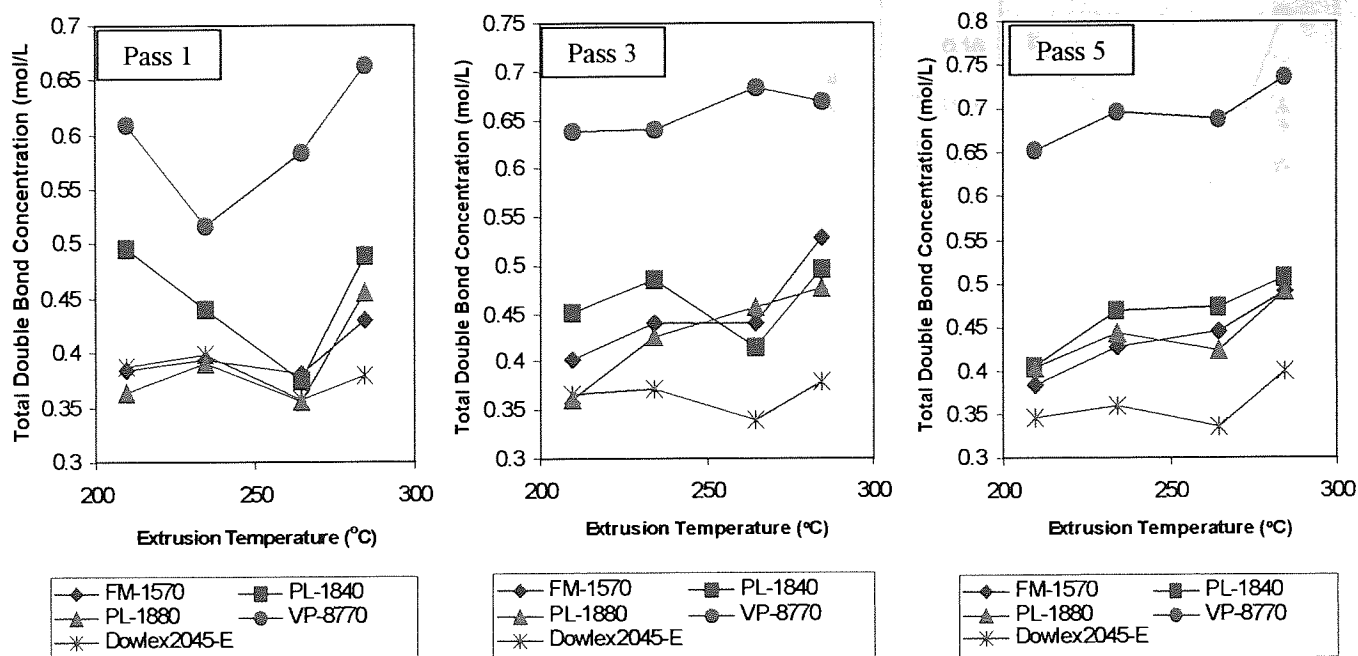


Figure 4.31. **Total Double Bond Concentration with Temperature Curves for Extruded LLDPE Polymers after Different Extrusion Passes**

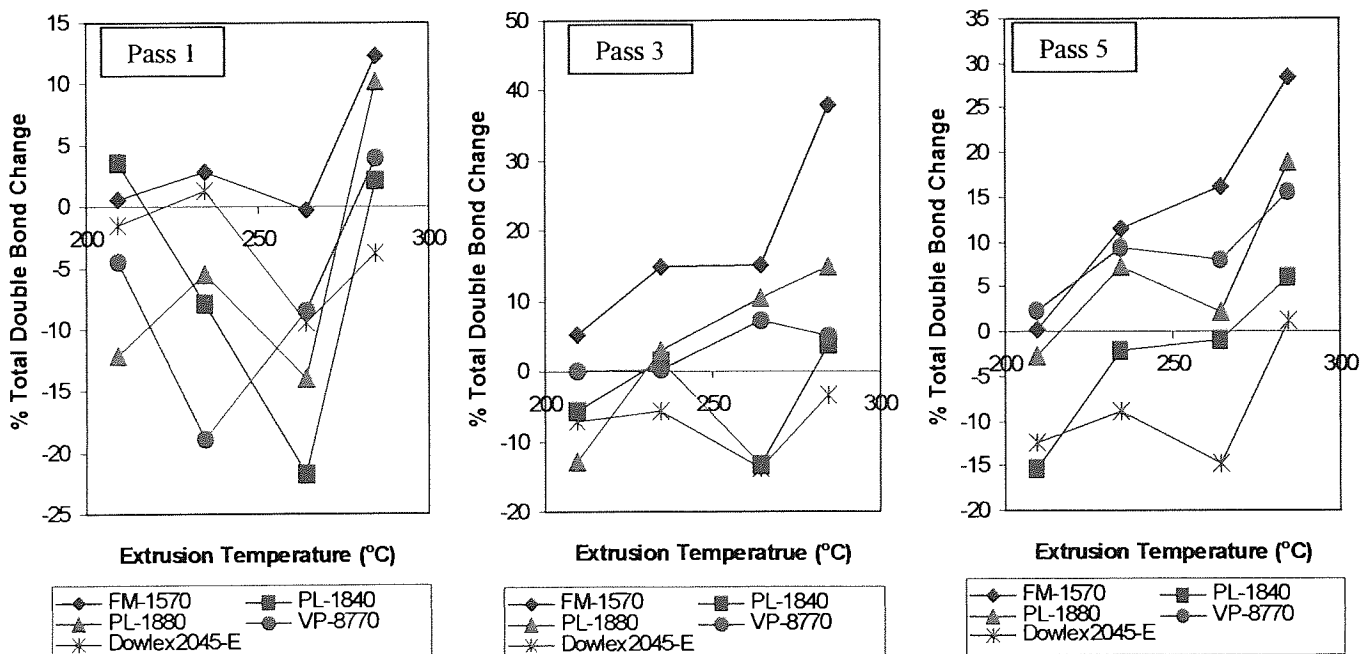


Figure 4.32. **Percentage Changes of Total Double Bond Concentration with Temperature for Extruded LLDPE Polymers after Different Extrusion Passes**

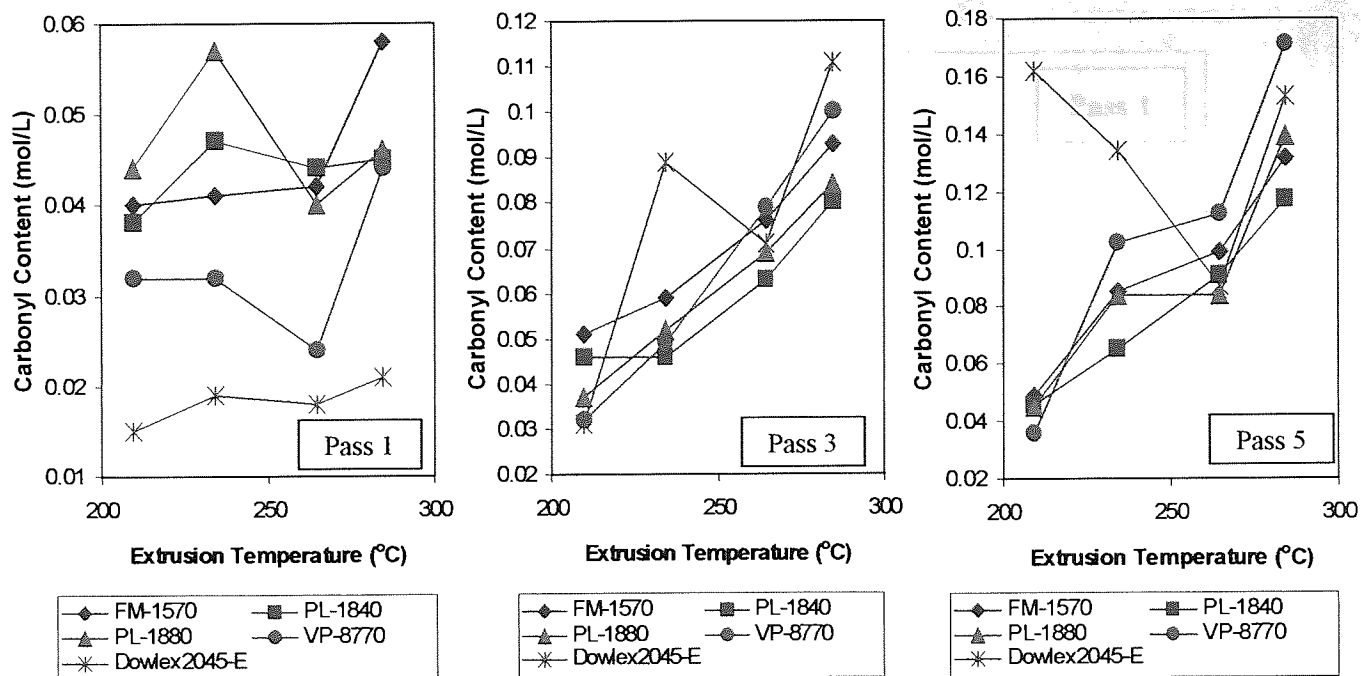


Figure 4.33. Carbonyl Group Concentration with Temperature Curves for Extruded LLDPE Polymers after Different Extrusion Passes

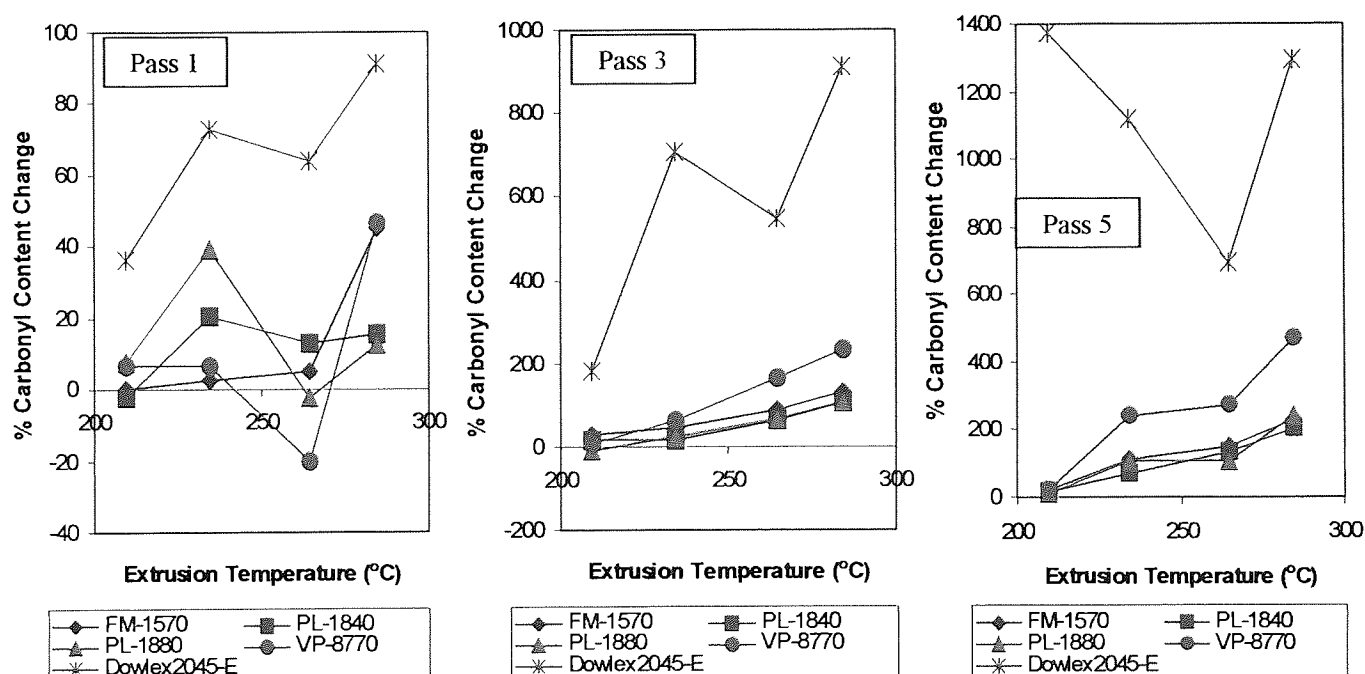


Figure 4.34. Percentage Changes of Carbonyl Group Concentration with Temperature for Extruded LLDPE Polymers after Different Extrusion Passes

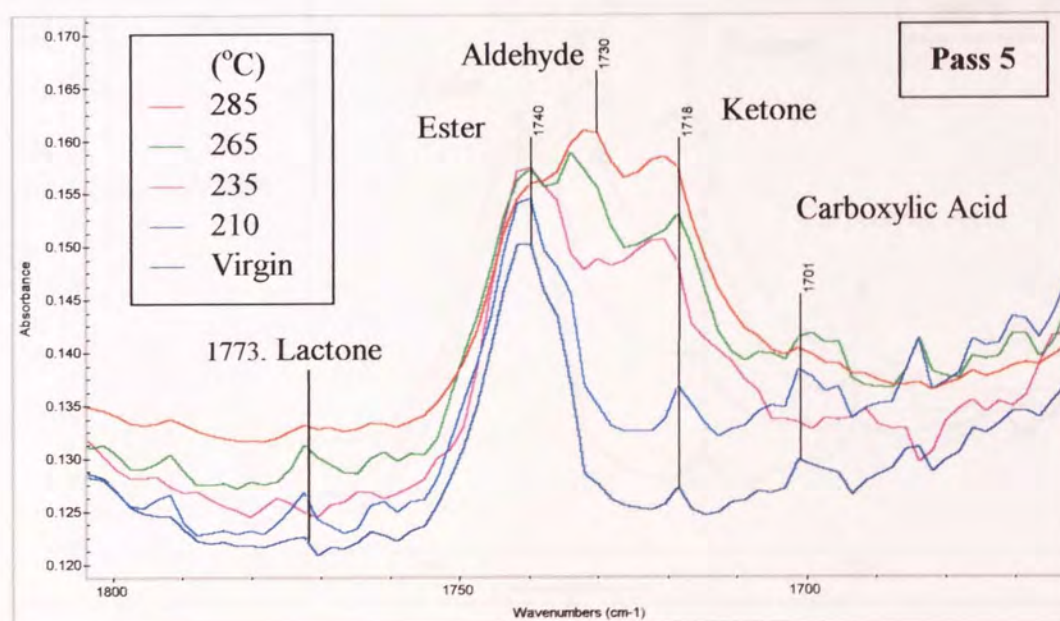
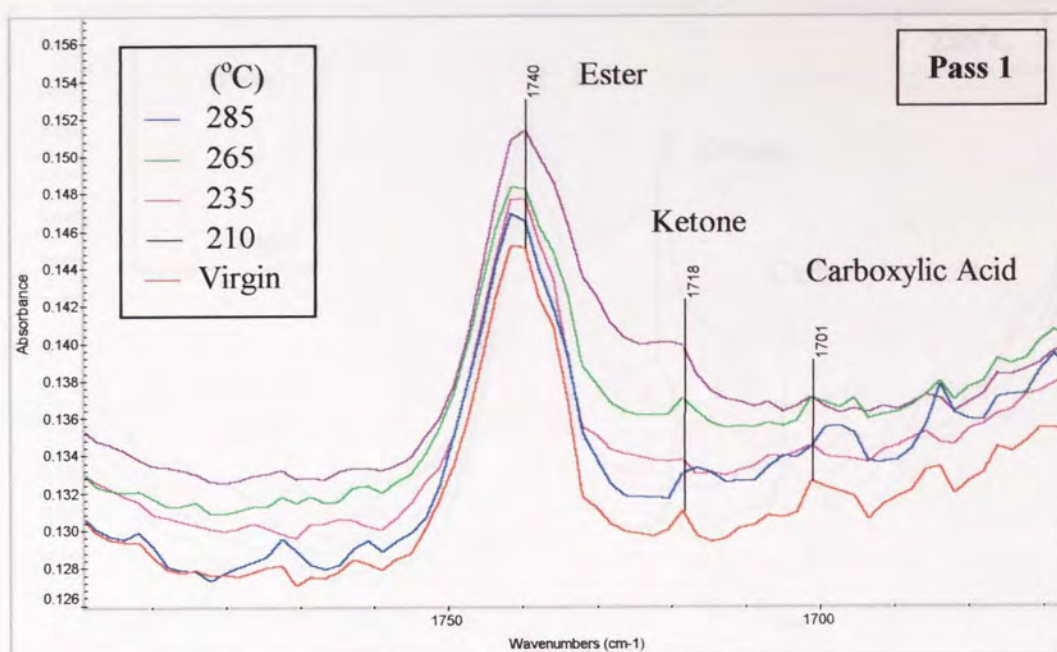


Figure 4.35. FTIR Spectra at Carbonyl Region for **FM-1570** Extruded at Different Temperatures for Different Passes

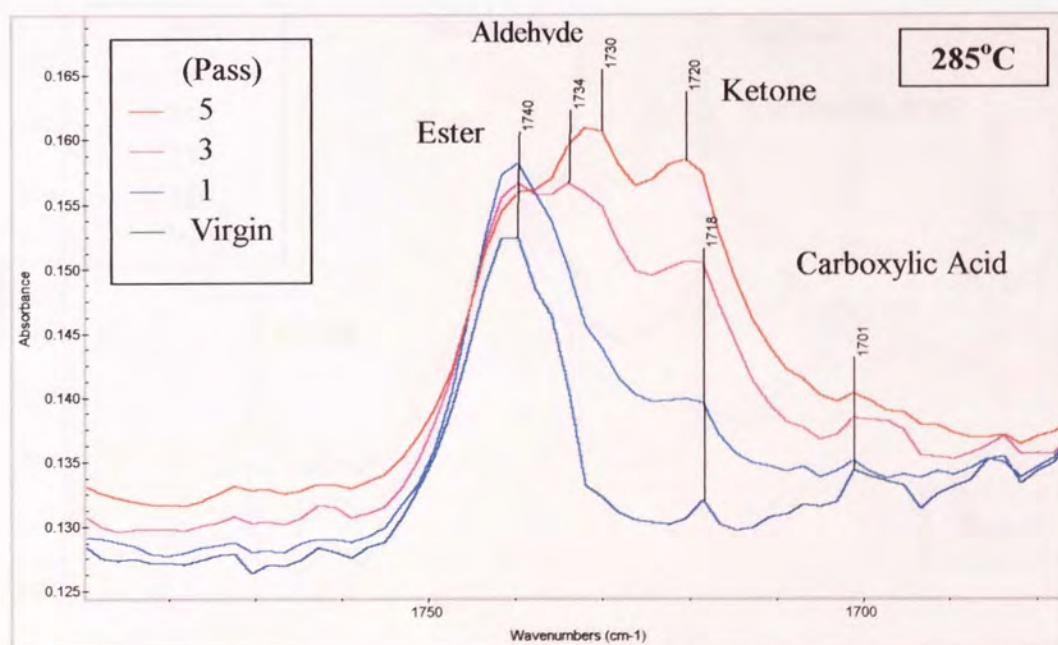
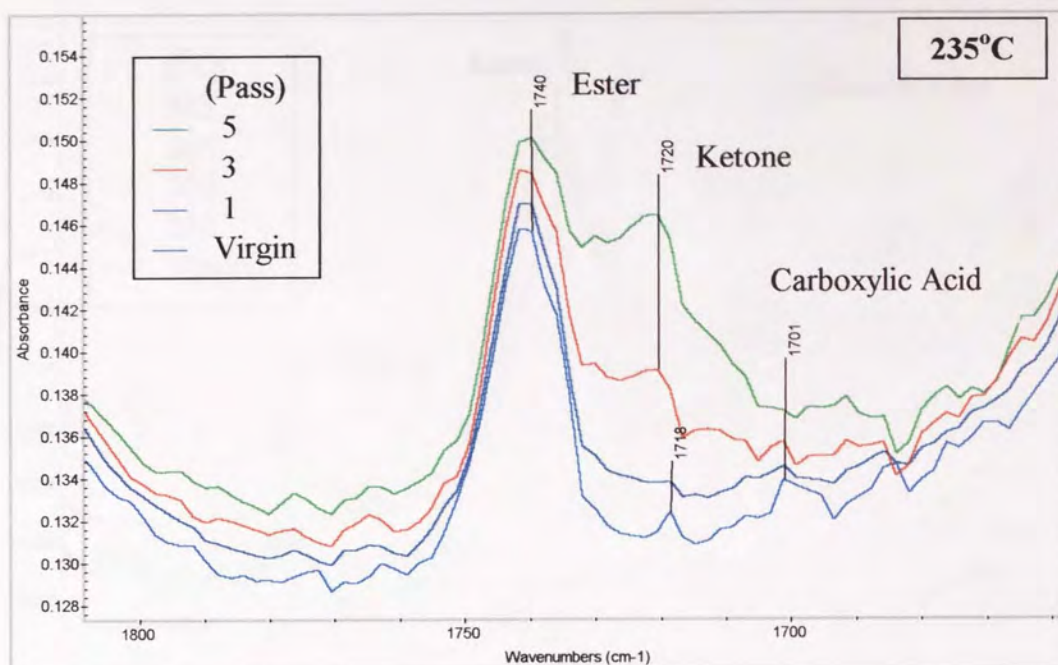


Figure 4.36. FTIR Spectra at Carbonyl Region for **FM-1570** after Different Extrusion Passes at Different Temperatures

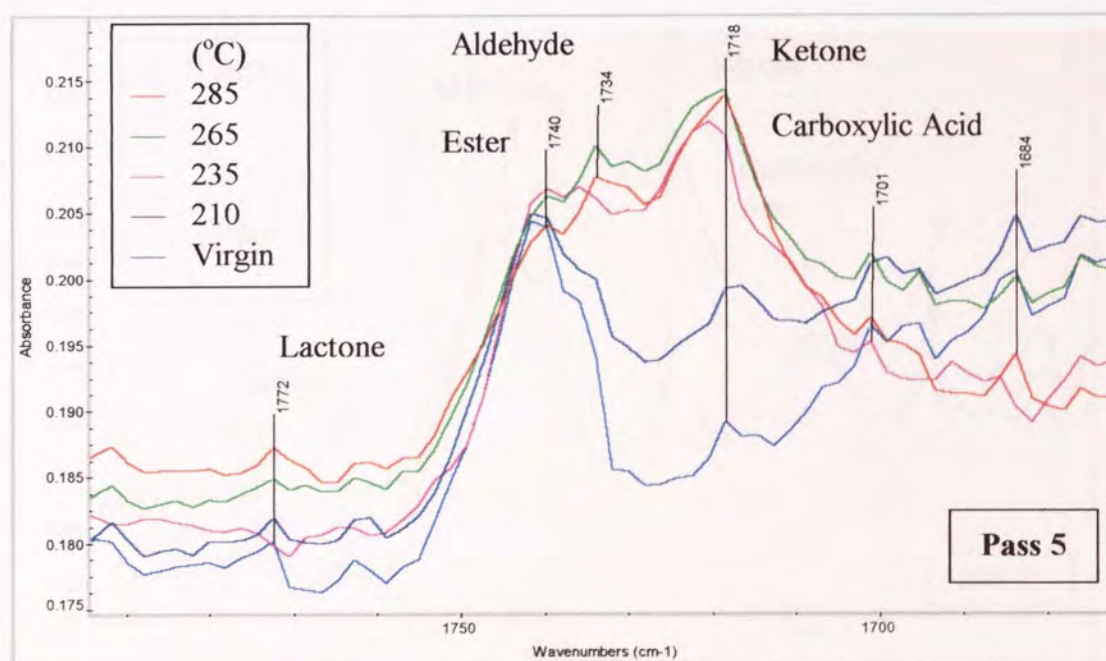
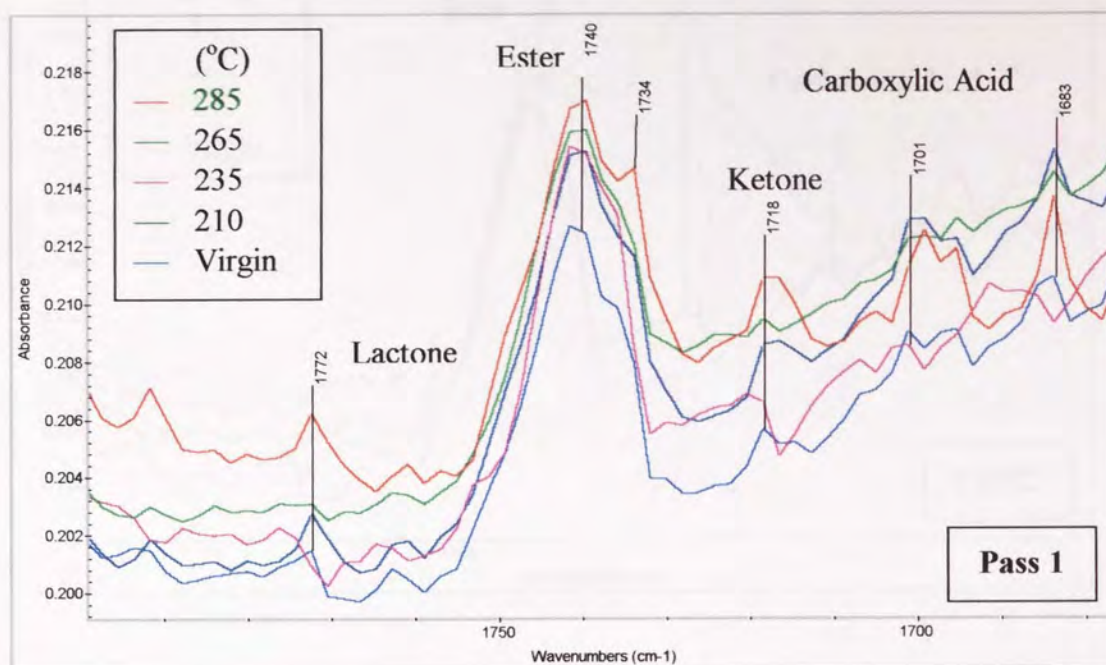


Figure 4.37. FTIR Spectra at Carbonyl Region for **VP-8770** Extruded at Different Temperatures for Different Passes

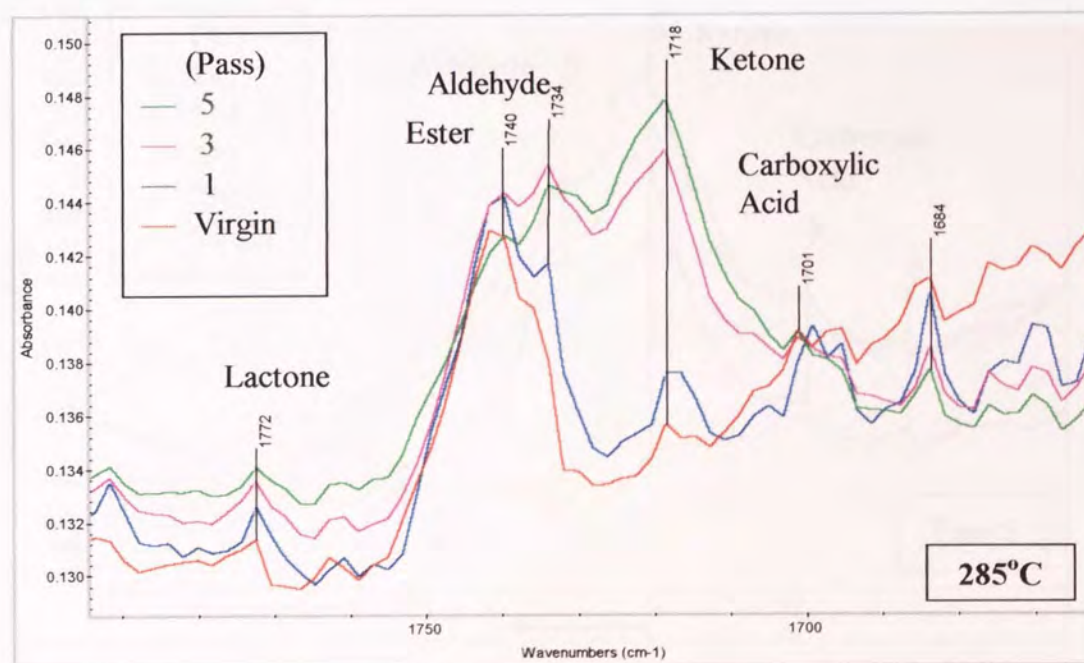
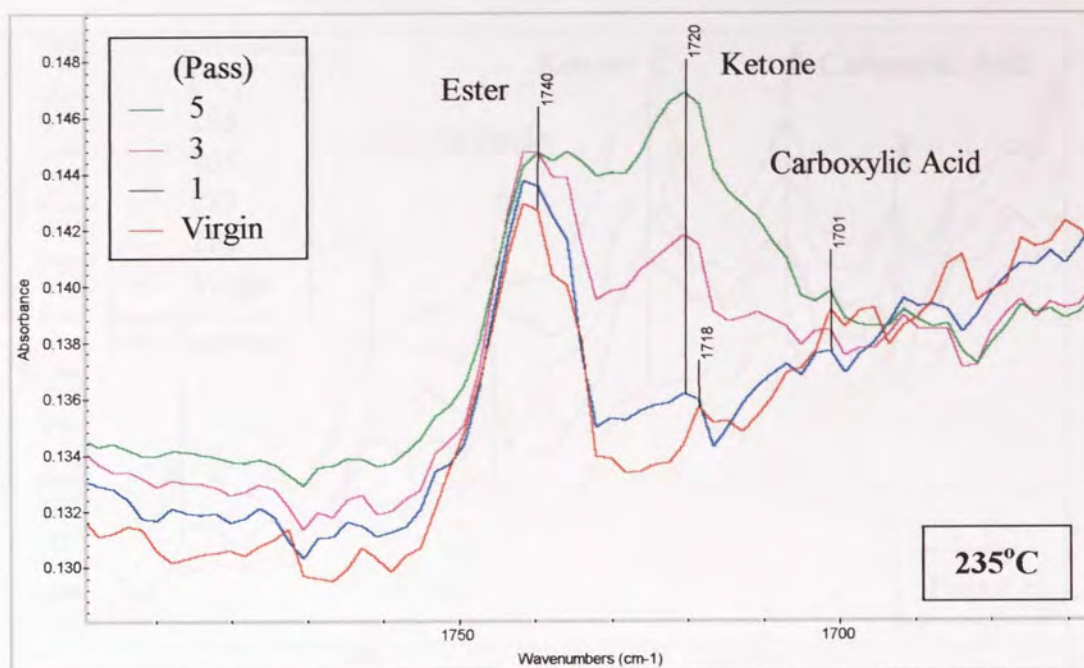


Figure 4.38. FTIR Spectra at Carbonyl Region for **VP-8770** after Different Extrusion Passes at Different Temperatures

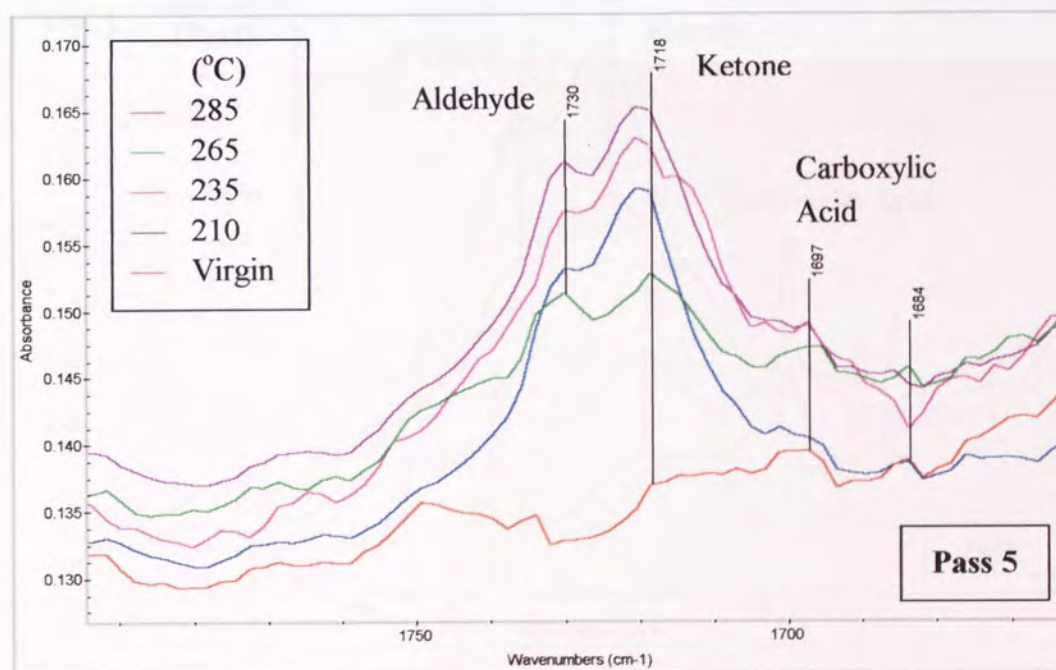
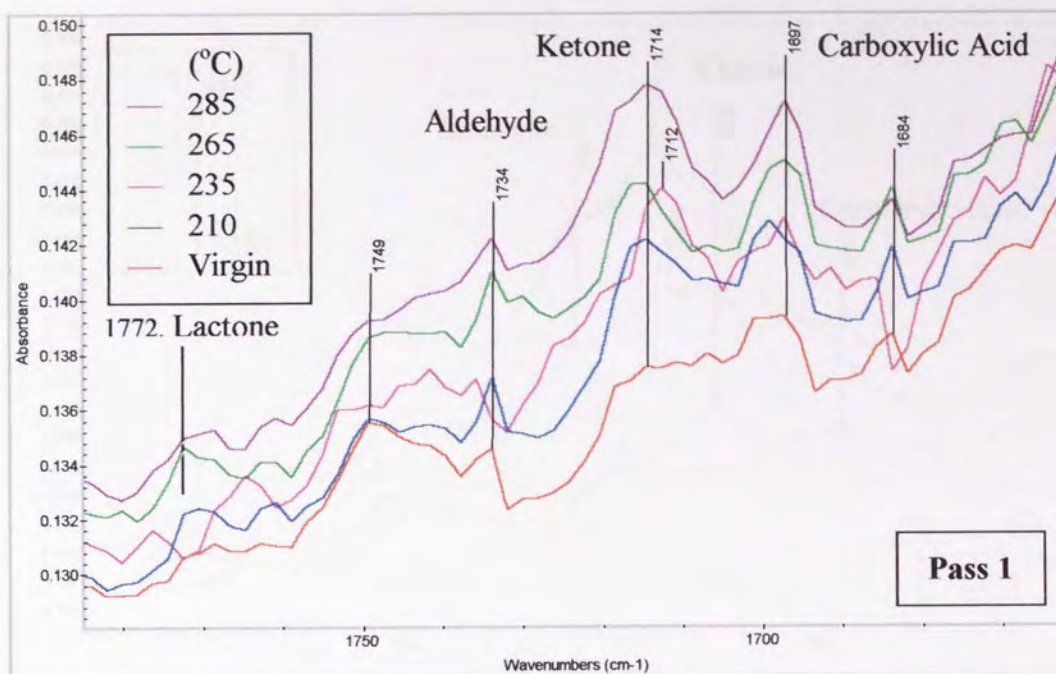


Figure 4.39. FTIR Spectra at Carbonyl Region for **Dowlex2045-E** Extruded at Different Temperatures for Different Passes

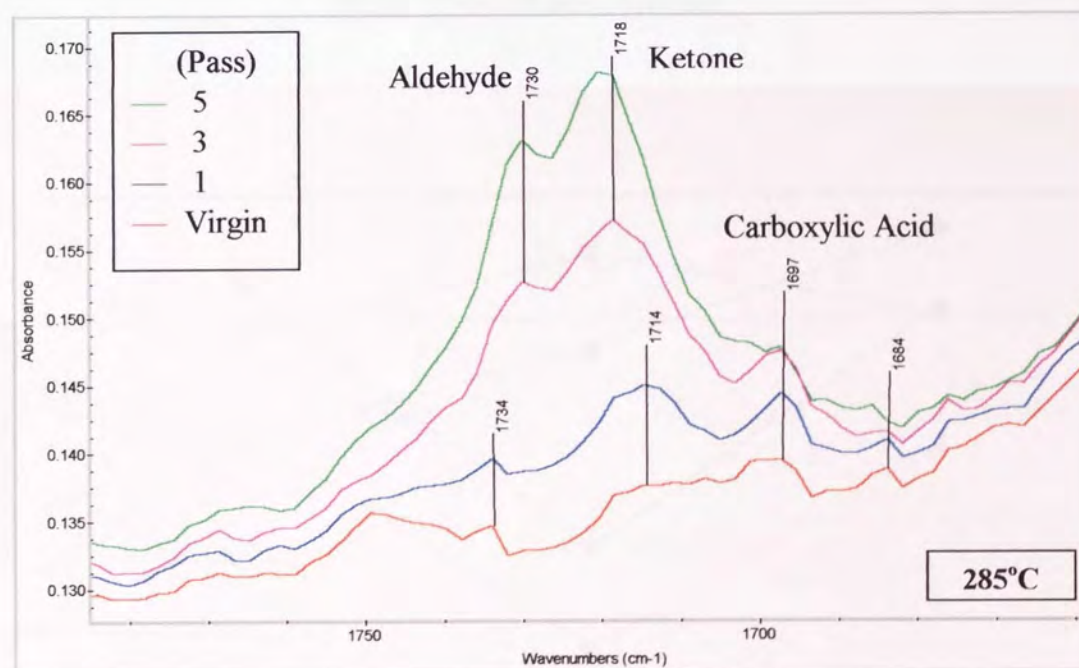
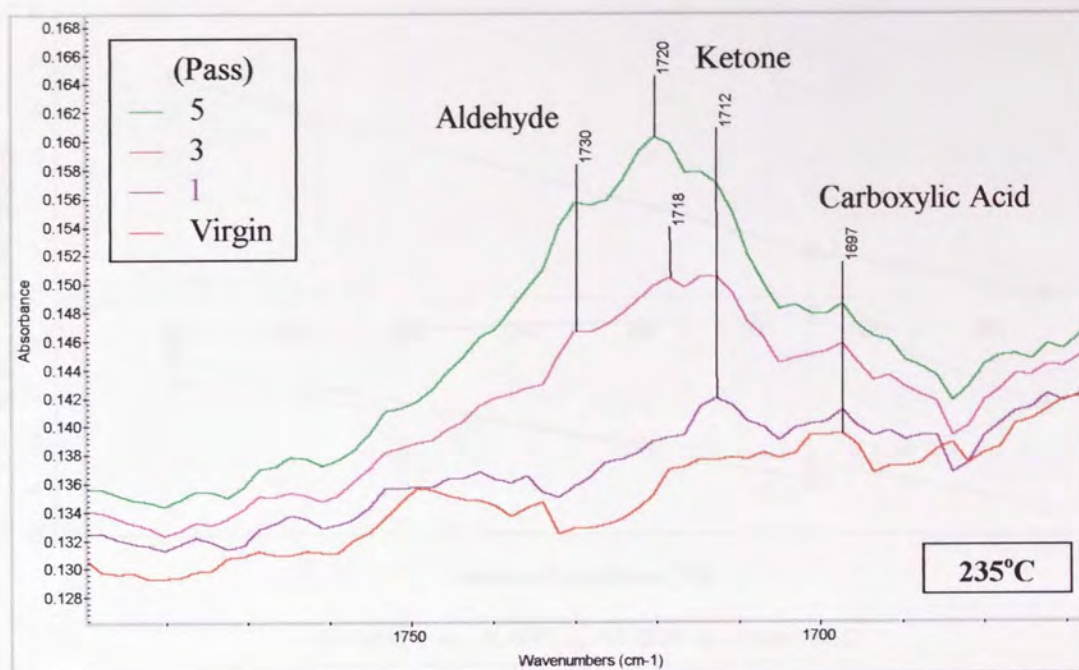


Figure 4.40. FTIR Spectra at Carbonyl Region for **Dowlex2045-E** after Different Extrusion Passes at Different Temperatures

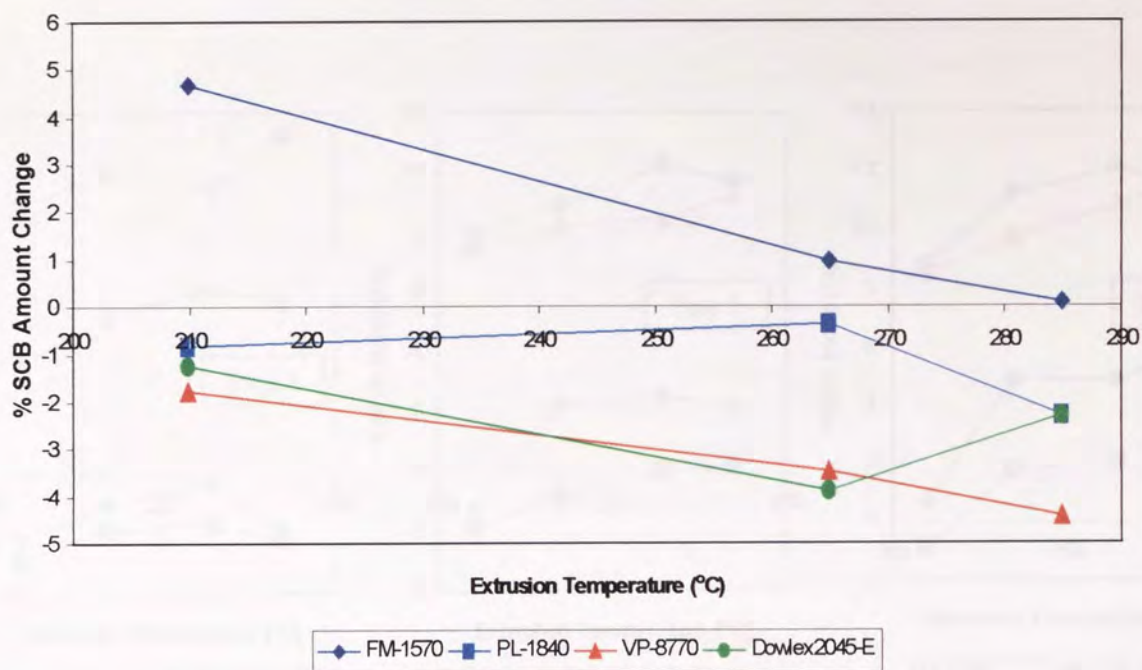


Figure 4.41. Percentage Change of **SCB Amount** (with respect to virgin polymer) with Extrusion Temperature for Different LLDPE Polymers after **One Pass** Extrusion (P1), from ^{13}C -NMR Measurement

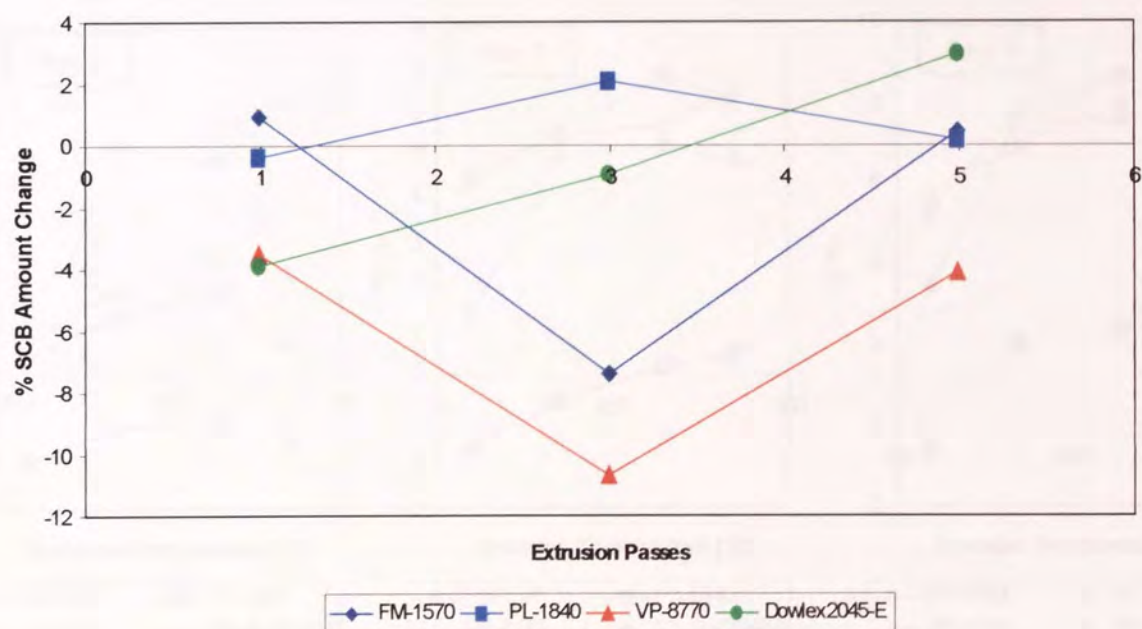


Figure 4.42. Percentage Change of **SCB Amount** with Extrusion Passes for Different LLDPE Polymers Extruded at **265°C**, from ^{13}C -NMR Measurement

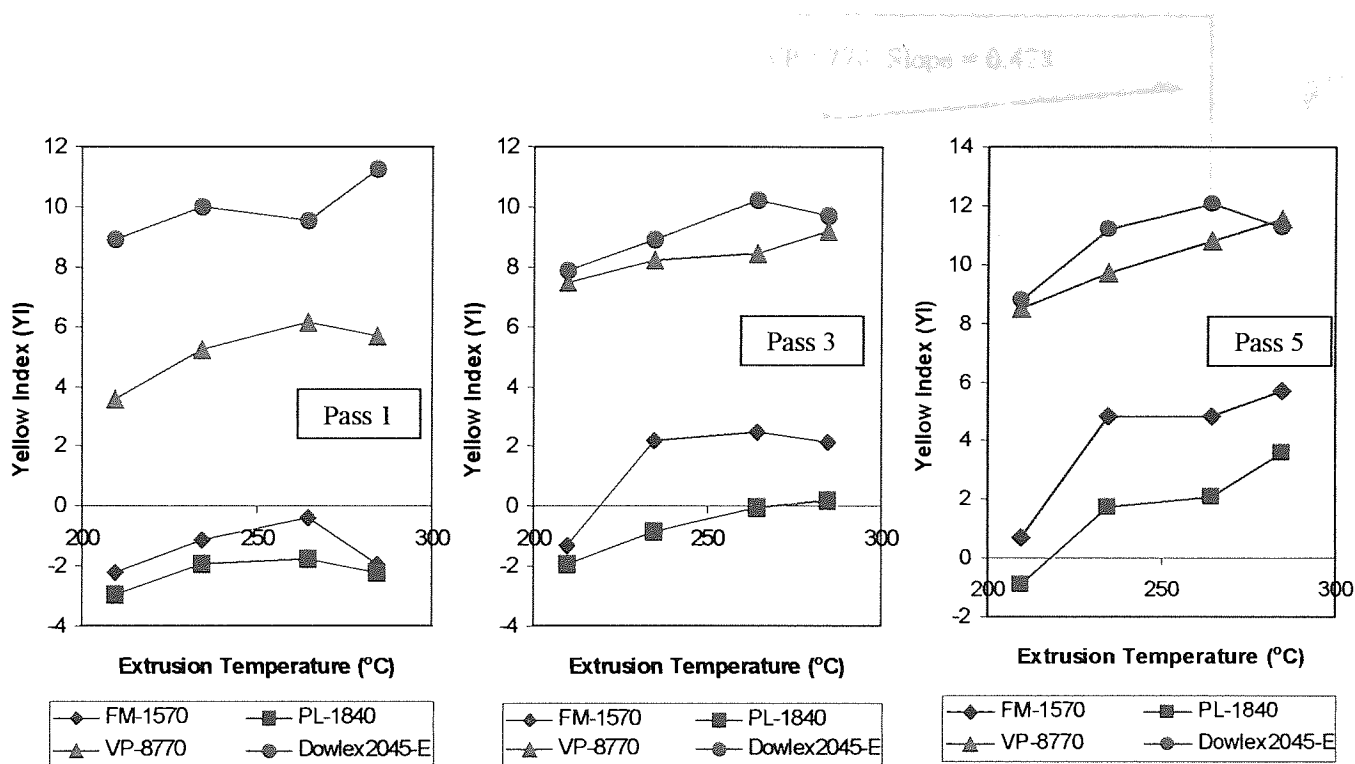


Figure 4.43. Variation of **Yellow Index (YI)** with Temperature for Extruded LLDPE Polymers after Different Extrusion Passes

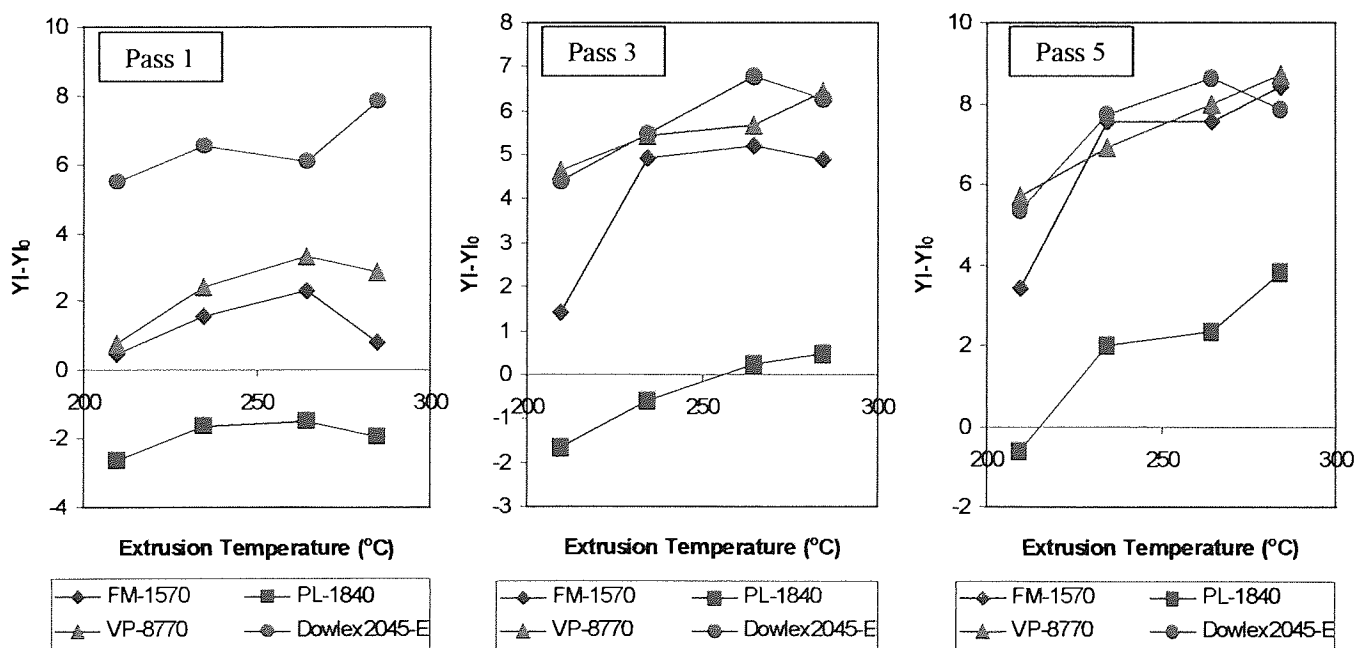


Figure 4.44. **Yellow Index Changes (YI-YI₀)**, with respect to virgin polymer) for Extruded LLDPE Polymers after Different Extrusion Passes

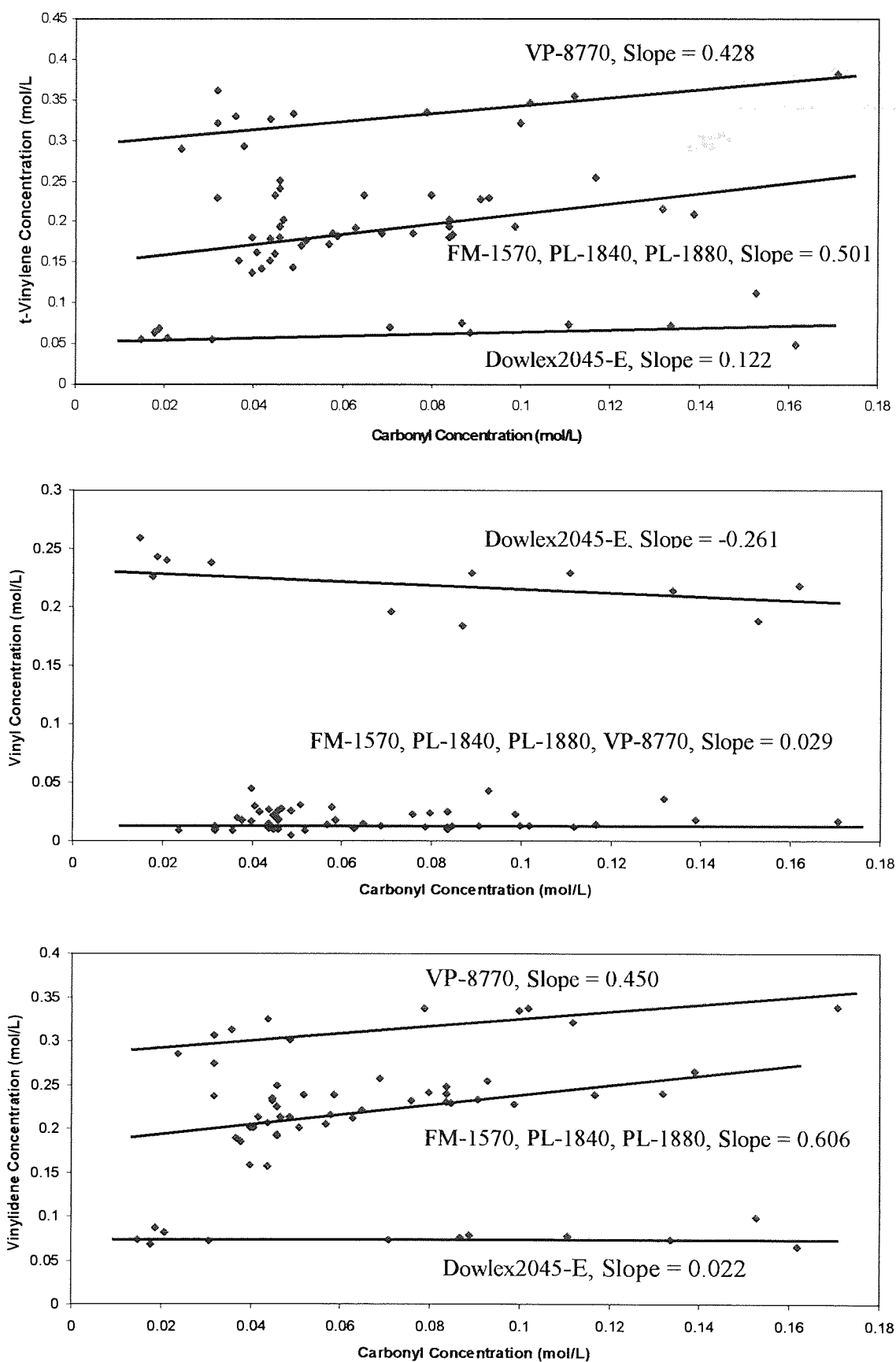


Figure 4.45. Relationship between the Concentrations of **Carbonyl** and Different **Double Bonds** (based on FTIR) for LLDPE Polymers Extruded under Different Conditions

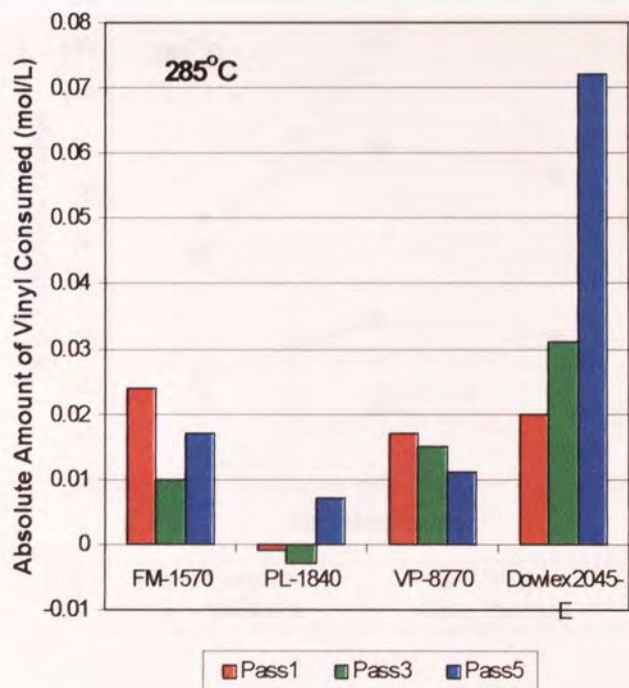
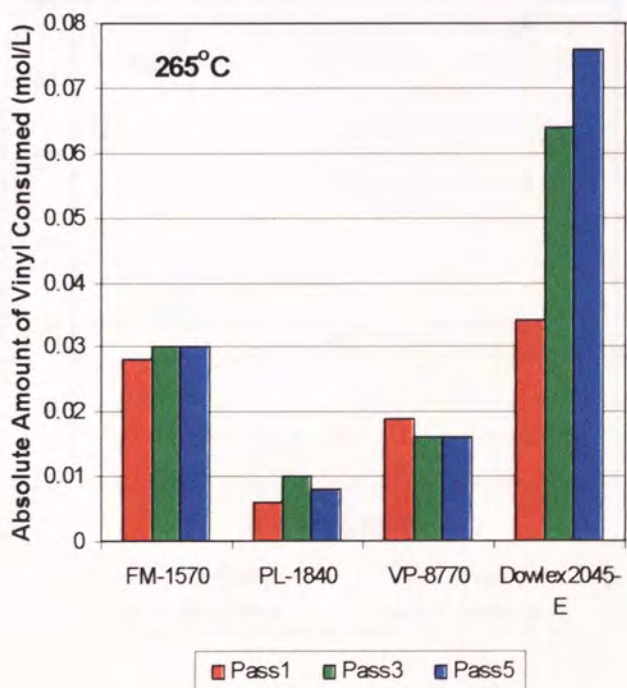
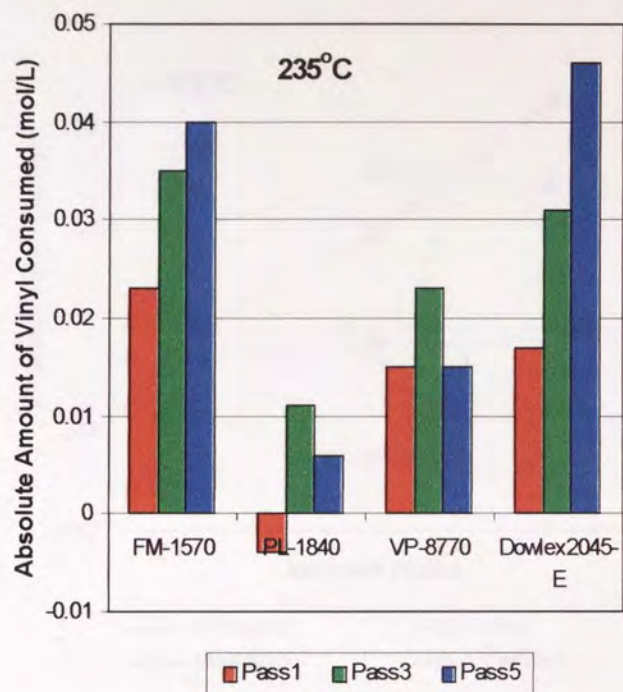
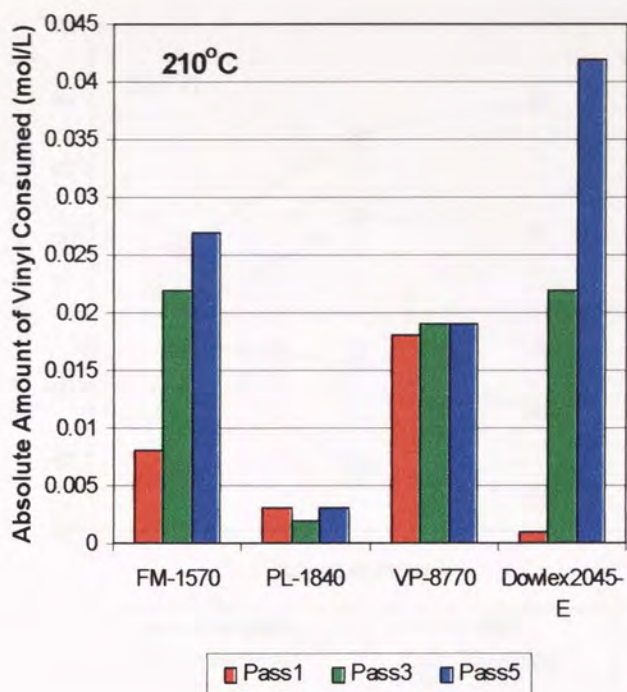


Figure 4.46. Absolute Amount of **Vinyl Group** Consumed in Different LLDPE Polymers during TSE Extrusions

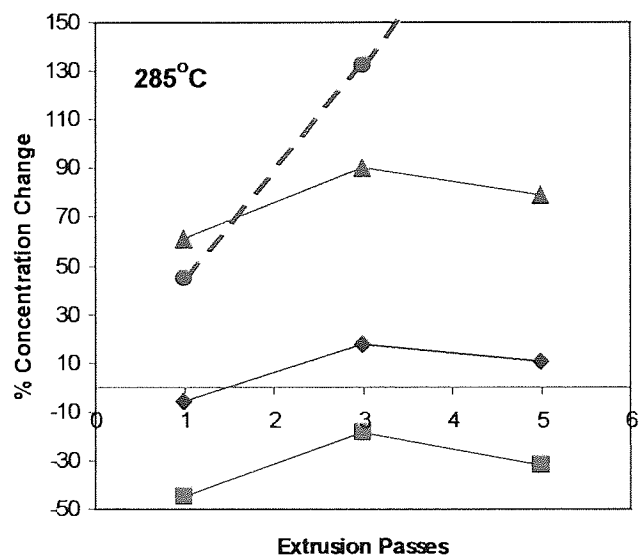
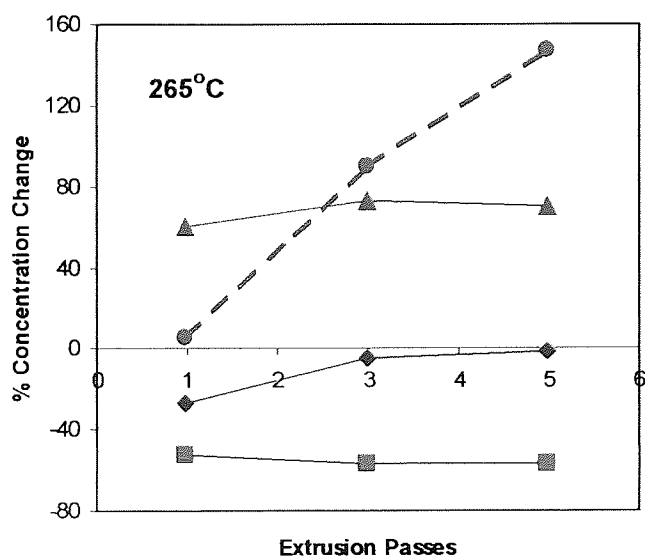
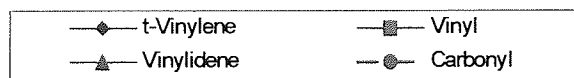
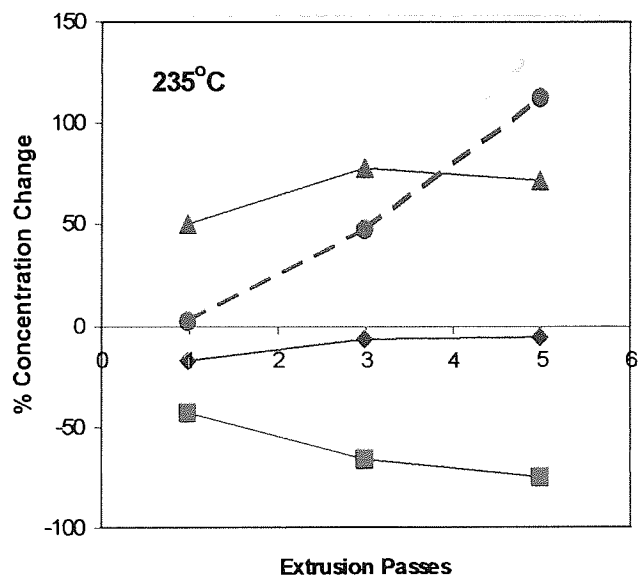
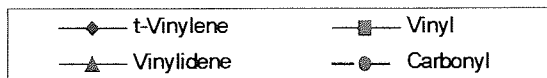
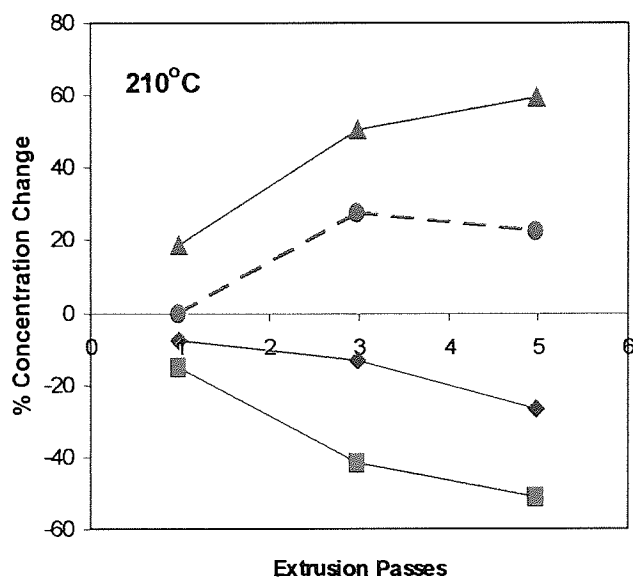


Figure 4.47. Comparison of the Percentage Changes of Double Bonds and Carbonyl Concentrations in **FM-1570** Polymer after TSE Extrusions at Different Temperatures

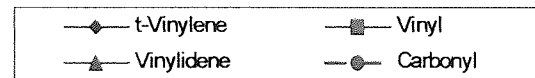
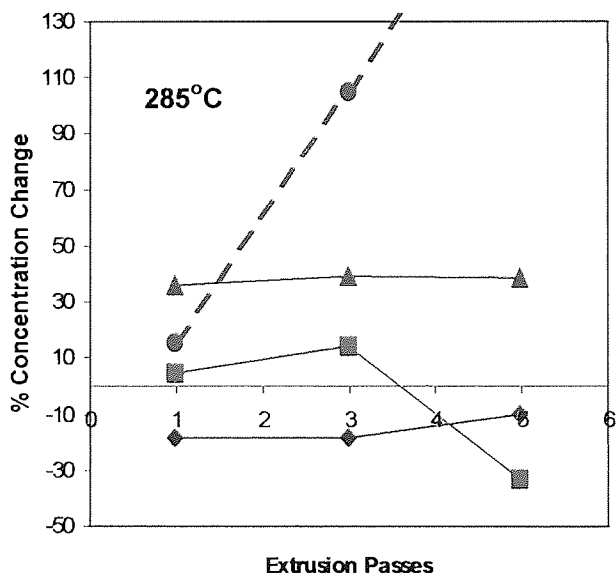
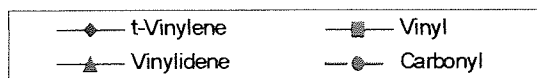
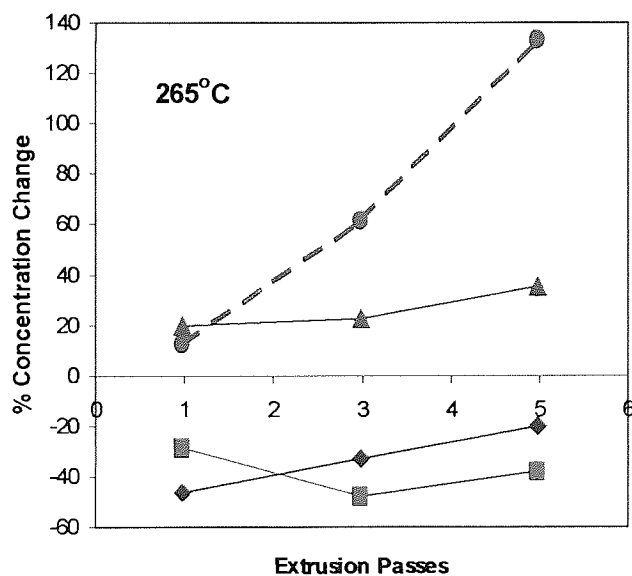
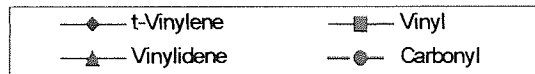
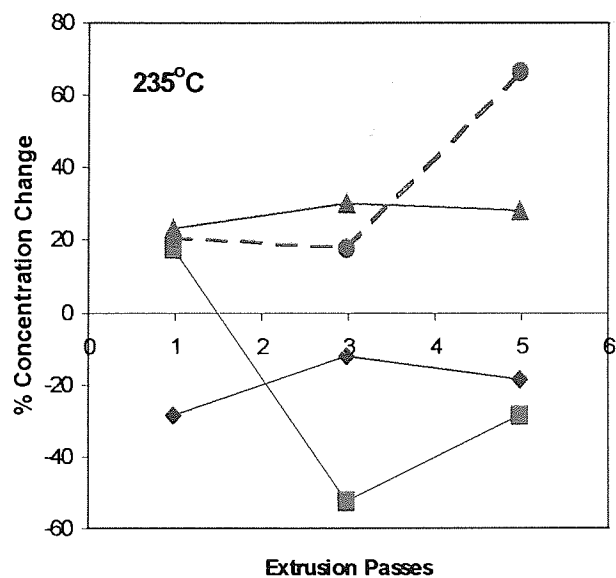
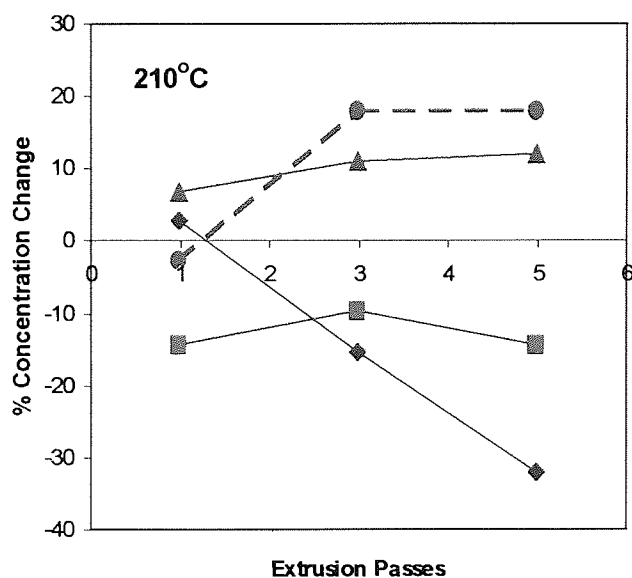


Figure 4.48. Comparison of the Percentage Changes of Double Bonds and Carbonyl Concentrations in **PL-1840** Polymer after TSE Extrusions at Different Temperatures

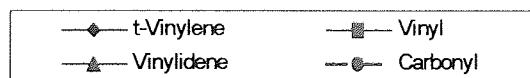
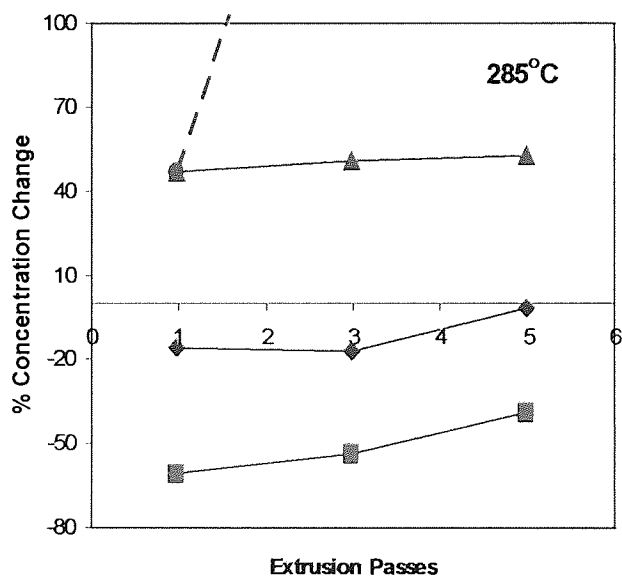
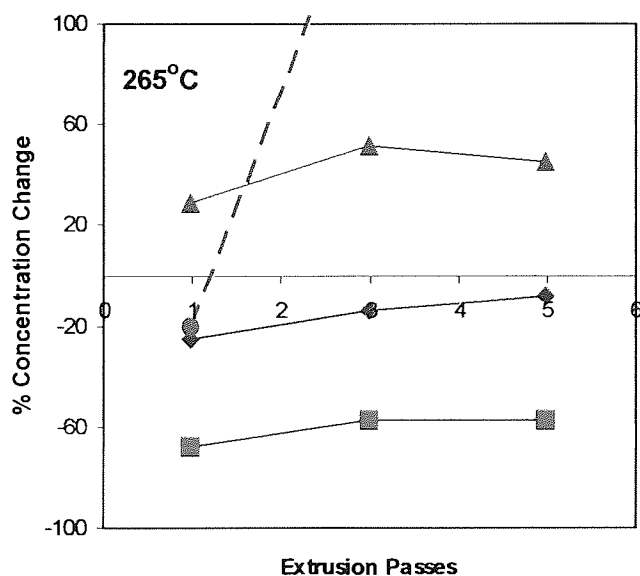
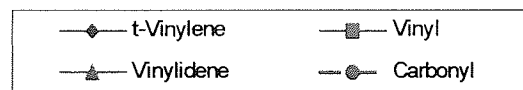
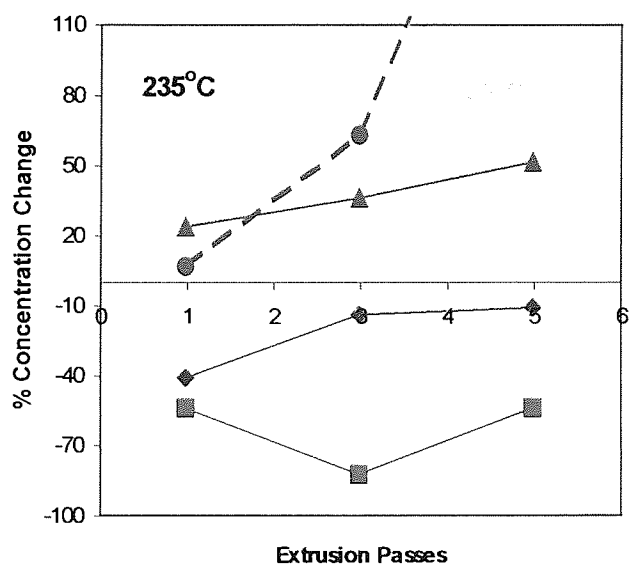
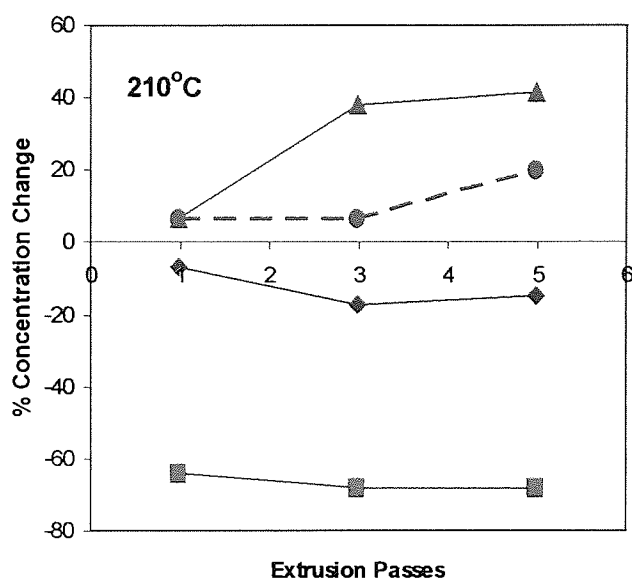


Figure 4.49. Comparison of the Percentage Changes of Double Bonds and Carbonyl Concentrations in **VP-8770** Polymer after TSE Extrusions at Different Temperatures

DIFFERENT CLASSES OF POLYMER STABILISATION

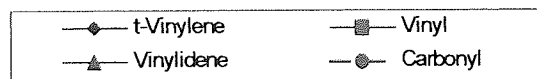
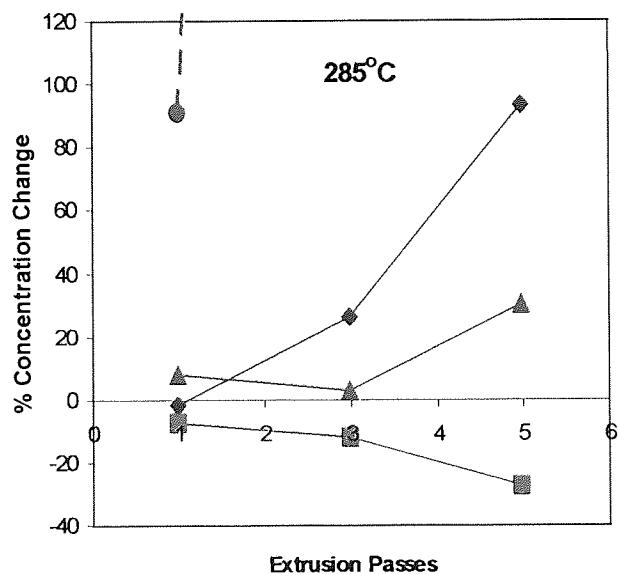
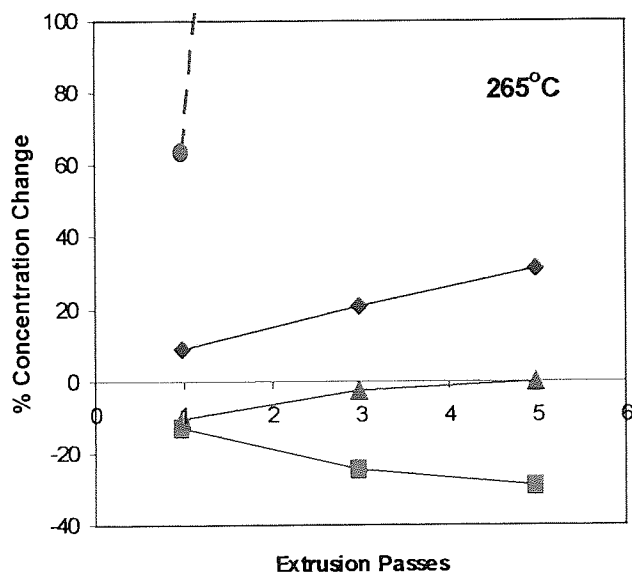
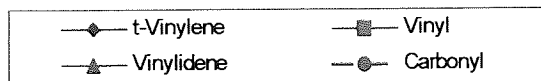
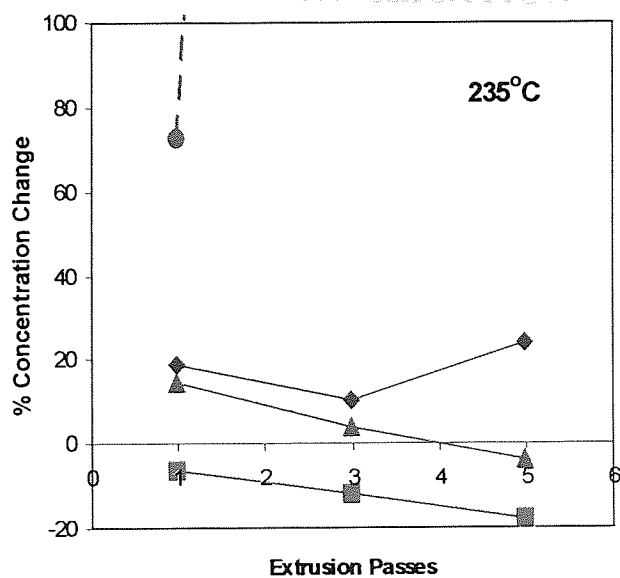
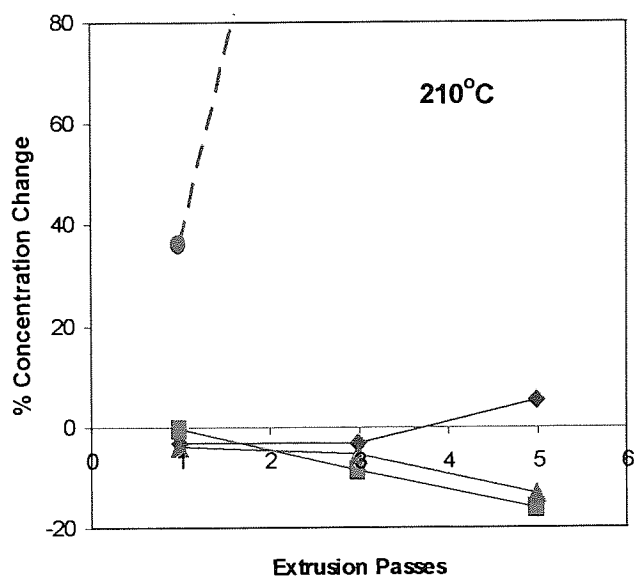


Figure 4.50. Comparison of the Percentage Changes of Double Bonds and Carbonyl Concentrations in **Dowlex2045-E** Polymer after TSE Extrusions at Different Temperatures

CHAPTER 5. EFFECTS OF DIFFERENT CLASSES OF ANTIOXIDANTS ON THE STABILISATION OF EXTRUDED LLDPE

5.1. OBJECTIVES AND METHODOLOGY

Characterisation of the melt oxidative stability of unstabilised LLDPE (see Chapter 4) has revealed that both metallocene and Ziegler catalysed polymers undergo oxidative degradation under all extrusion conditions examined with crosslinking reactions predominating under most extrusion conditions. However, some considerable differences were observed in the details of the thermal oxidation mechanisms (see Section 4.3 in Chapter 4) of polymers catalysed differently (metallocene and Ziegler) and of LLDPE grades having different extent of short chain branching (SCB). The addition of effective antioxidants during the polymer extrusion would, therefore, be expected to greatly reduce the extent of their thermal oxidative degradation. Accordingly, a number of commercially available antioxidants (AOs) that act by different stabilisation mechanisms were investigated and their AO role is discussed in this chapter. The performances of individual AO's, and their combinations, were examined by analysing the characteristics of the different types and grades of extruded LLDPE. The aim of this work was to establish a good understanding of the role of different AO classes in extruded metallocene-based LLDPE polymers.

The antioxidants used in this work include synthetic (Irganox1076) and biological (IrganoxE201) hindered phenols, a lactone (IrganoxHP136) and phosphites (Irgafos168, Ultrinox626, IrgafosP-EPQ, Weston399), see Table 2.3 in Chapter 2 for chemical structures. Fixed concentrations of AO were initially compounded with the polymer during extrusion (P_0) using a die temperature of 210°C and screw speed of 100rpm under nitrogen in a twin-screw extruder (TSE) (see Section 2.2.2, Chapter 2 for a detailed description). The stabilised (compounded) LLDPE samples were subsequently subjected to multiple extrusions for a total of five passes using the TSE at an extrusion temperature of 265°C and screw speed of 100rpm, under atmospheric conditions. Tables 5.1 and

5.2 give detailed information of the extruded LLDPE samples containing single and combined antioxidants. Table 5.3 compares the target and actual antioxidant concentrations in some of the AO mixtures determined by FTIR (see Section 2.3.3 in Chapter 2 for detailed method). The results indicate that the differences between the actual and target concentrations for all the examined antioxidants are acceptable, confirming the method used in the compounding step is reliable. The melt flow, structural and colour characteristics of all extruded polymers were analysed after the first, third and fifth passes (multi-pass extrusion). Scheme 5.1 summarises the methodology used in this work. It is important to point out here that figures in this chapter having extrusion passes in their X-axis have the zero pass (Pass0) referring to the compounding (with AO's) step, and where a percentage change in property is plotted on the Y-axis of figures, this refers to change with respect to the virgin unprocessed polymers.

Table 5.1. TSE Extrusion of LLDPE Samples Containing Single Antioxidants

| Polymer | SCB Cont. (w%) | Antioxidant | AO Target Conc. (ppm) | Extrusion Temp. (°C) * | Extrusion Speed (rpm) | Extrusion Pass |
|-------------------------------|-------------------|-------------|--------------------------|---------------------------|--------------------------|---|
| FM-1570 (m-LLDPE) | 11.6 (MI=1.43) | Irganox1076 | 900 | 265 | 100 | P ₀ , P ₁ ~P ₅ |
| | | HP136 | 500 | 265 | 100 | P ₀ , P ₁ ~P ₅ |
| | | Ultranox626 | 1000 | 265 | 100 | P ₀ , P ₁ ~P ₅ |
| | | IrganoxE201 | 300 | 265 | 100 | P ₀ , P ₁ ~P ₅ |
| PL-1840 (m-LLDPE) | 13.4 (MI=1.16) | Irganox1076 | 900 | 265 | 100 | P ₀ , P ₁ ~P ₅ |
| | | HP136 | 500 | 265 | 100 | P ₀ , P ₁ ~P ₅ |
| | | Ultranox626 | 1000 | 265 | 100 | P ₀ , P ₁ ~P ₅ |
| | | IrganoxE201 | 300 | 265 | 100 | P ₀ , P ₁ ~P ₅ |
| VP-8770 (m-LLDPE) | 28.2 (MI=1.04) | Irganox1076 | 900 | 265 | 100 | P ₀ , P ₁ ~P ₅ |
| | | HP136 | 500 | 265 | 100 | P ₀ , P ₁ ~P ₅ |
| | | Ultranox626 | 1000 | 265 | 100 | P ₀ , P ₁ ~P ₅ |
| | | IrganoxE201 | 300 | 265 | 100 | P ₀ , P ₁ ~P ₅ |
| Dowlex- 2045E (z-LLDPE) | 10.5 (MI=1.21) | Irganox1076 | 900 | 265 | 100 | P ₀ , P ₁ ~P ₅ |
| | | HP136 | 500 | 265 | 100 | P ₀ , P ₁ ~P ₅ |
| | | Ultranox626 | 1000 | 265 | 100 | P ₀ , P ₁ ~P ₅ |
| | | IrganoxE201 | 300 | 265 | 100 | P ₀ , P ₁ ~P ₅ |

* The temperature shown in the table was used for P₁~P₅ extrusions, the P₀ extrusions were carried out at 210°C under N₂.

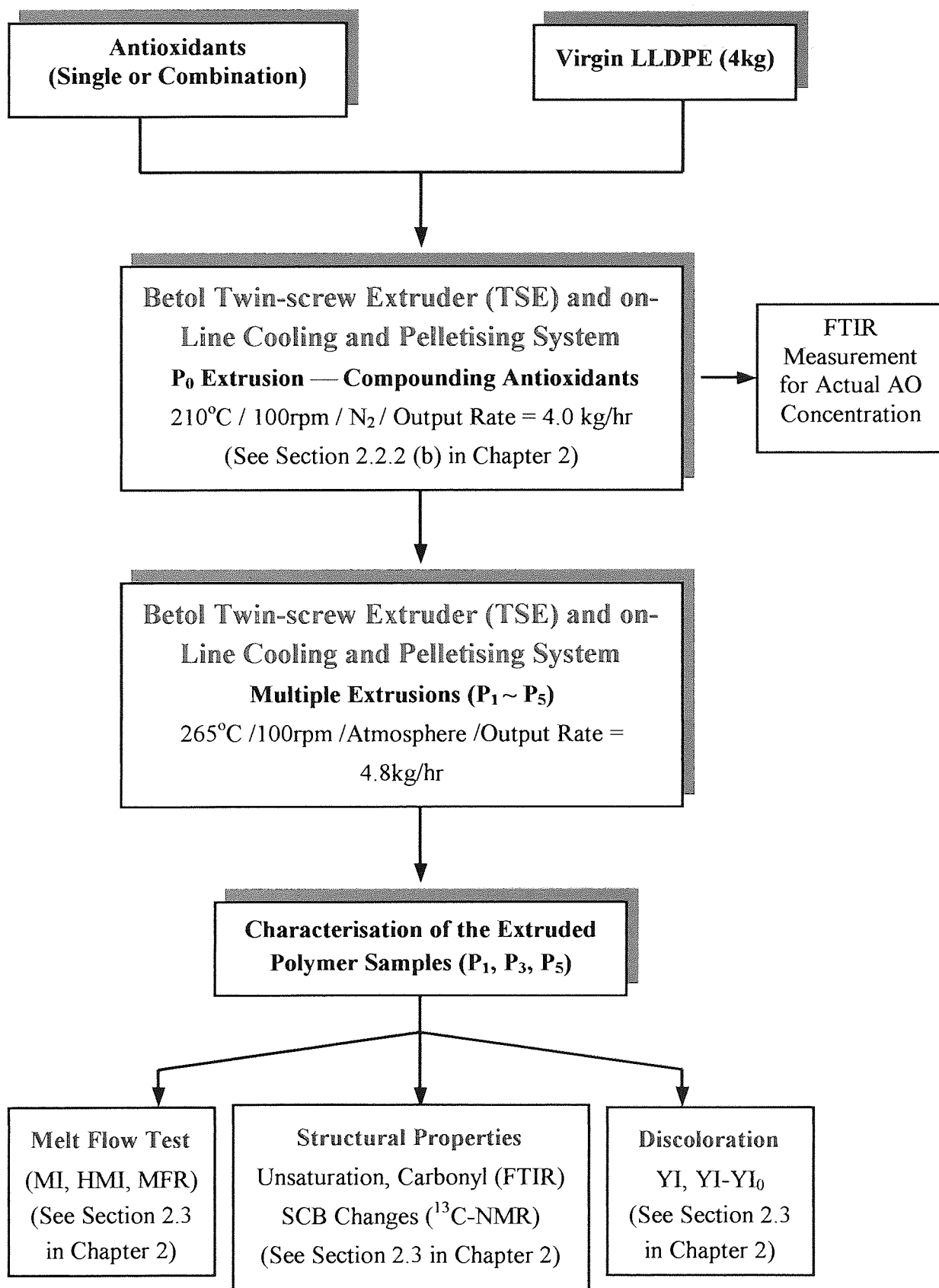
Table 5.2. TSE Extrusion of LLDPE Containing Antioxidant Mixture (265°C, 100rpm, 4.8kg/hr)

| Antioxidant Composition (ppm) | Total AO Concentration (ppm) | Antioxidant Mixture Code | Polymer * | Phosphorus Concentration (w%) | Extrusion Pass ** |
|--|------------------------------|--------------------------|-------------|-------------------------------|--|
| Irg1076: Irg168 500: 1250 | 1750 | AO-A1 | PL-1840 | 0.006 | P ₀ P ₁ ~P ₅ |
| Irg1076: Irg168: HP136 500: 1250: 250 | 2000 | AO-A2 | PL-1840 | 0.006 | P ₀ P ₁ ~P ₅ |
| Irg1076: Ultra626 500: 600 | 1100 | AO-B1 | PL-1840 | 0.006 | P ₀ P ₁ ~P ₅ |
| Irg1076: Ultra626: HP136 500: 600: 250 | 1350 | AO-B2 | PL-1840 | 0.006 | P ₀ P ₁ ~P ₅ |
| Irg1076: IrgP-EPQ 500: 1000 | 1500 | AO-C1 | PL-1840 | 0.006 | P ₀ P ₁ ~P ₅ |
| Irg1076: IrgP-EPQ: HP136 500: 1000: 250 | 1750 | AO-C2 | PL-1840 | 0.006 | P ₀ P ₁ ~P ₅ |
| Irg1076: Weston399 500: 1330 | 1830 | AO-D1 | PL-1840 | 0.006 | P ₀ P ₁ ~P ₅ |
| Irg1076: W399: HP136 500: 1330: 250 | 2080 | AO-D2 | PL-1840 | 0.006 | P ₀ P ₁ ~P ₅ |
| IrgE201: Ultra626 300: 600 | 900 | AO-E1 | PL-1840 | 0.006 | P ₀ P ₁ ~P ₅ |
| IrgE201: Ultra626: HP136 300: 600: 250 | 1150 | AO-E2 | PL-1840 | 0.006 | P ₀ P ₁ ~P ₅ |
| IrgE201: Ultra626: TMP 300: 600: 450 | 1350 | AO-E3 | PL-1840 | 0.006 | P ₀ P ₁ ~P ₅ |
| IrgXP490 = 1500 (Irg1076: IrgP-EPQ: HP136 3: 2: 1) | 1500 | AO-F | PL-1840 | 0.003 | P ₀ P ₁ ~P ₅ |
| | | | VP-8770 | 0.003 | |
| | | | Dowlex2045E | 0.003 | |
| IrgHP2921 = 1750 (Irg1076: Irg168: HP136 2: 4: 1) | 1750 | AO-G | PL-1840 | 0.005 | P ₀ P ₁ ~P ₅ |
| | | | VP-8770 | 0.005 | |
| | | | Dowlex2045E | 0.005 | |

* The LLDPE used were all new batch polymers whose characteristics are recorded in Table 2.2 in Chapter 2.

** P₀ extrusions were carried out at 210°C, 4.0kg/hr under N₂Table 5.3. Comparison of the Target and Actual AO Concentrations in m-LLDPE Measured in P₀ Processed PL-1840 (determined from IR spectroscopy and calibration curves, see Section2.3.3 in Chapter2 and v in the table)

| Polymer | Processing | Antioxidant Concentration (ppm) | | | | | | | |
|---------|---------------------|--|--------|---|--------|---|--------|---|--------|
| | | Irganox 1076 $\nu = 1735 \text{ cm}^{-1}$ | | Irgafos 168 $\nu = 1082 \text{ cm}^{-1}$ | | Irgafos P-EPQ $\nu = 1084 \text{ cm}^{-1}$ | | Irganox HP136 $\nu = 1800 \text{ cm}^{-1}$ | |
| | | Target | Actual | Target | Actual | Target | Actual | Target | Actual |
| PL-1840 | TSE, P ₀ | 500 | 450 | 1250 | 1100 | — | — | — | — |
| PL-1840 | TSE, P ₀ | 500 | 400 | 1250 | 1200 | — | — | 250 | 205 |
| PL-1840 | TSE, P ₀ | 500 | 450 | — | — | 1000 | 850 | — | — |
| PL-1840 | TSE, P ₀ | 500 | 410 | — | — | 1000 | 1050 | 250 | 220 |



Scheme 5.1. Overall Methodology Used in the Stabilisation of LLDPE Using Single and Combined Antioxidants

5.2. RESULTS

5.2.1. Extrusion Characteristics of Stabilised LLDPE

The changes in extrusion characteristics of LLDPE containing both single antioxidants and different AO mixtures have been monitored throughout the extrusion processes. These changes are considered to be a direct manifestation of the antioxidant effectiveness during the polymer extrusion process. The output rate and temperature profiles for the compounding step (P_0) and multiple extrusions ($P_1 \sim P_5$) were chosen on the basis of results of similar work carried out by former researchers in the PPP group [134]. It was shown [133, 134] that the extrusions of m-LLDLE in the Betol TSE resulting in minimum melt fracture and pressure variation can be achieved at 210°C, 4.0kg/hr for P_0 and 265°C, 4.8kg/hr output rate for $P_1 \sim P_5$ extrusion passes.

5.2.1.1. Extrusion Characteristics of LLDPE Containing Single Antioxidants

Table 5.4 shows that there are only minor differences in the characteristics of the compounding step (P_0) for the same polymer containing different single antioxidants (with the exception of Dowlex2045E containing Irg1076, since a different (older) batch was used in this experiment). Similar characteristics of multiple extrusions ($P_1 \sim P_5$) of the same polymer containing different single AOs are also clear from Table 5.5. Moreover, a comparison of the extrusion characteristics of unstabilised m-LLDPE during P_1 at 210°C (see Table 4.1 in Chapter 4) with those of the polymers stabilised with single antioxidants during the compounding step (P_0) shows that there is only a little difference in the characteristics after the first extrusions, e.g. an unstabilised PL-1840 polymer shows a melt pressure value of 710 psi at 210°C, 100 rpm, 4.0 kg/hr (for P_1); whereas that of the same polymer containing Irganox1076 was 720 psi at 210°C, 100 rpm, 4.0 kg/hr (for P_0).

Figure 5.1 shows the variation in power consumption with extrusion passes for LLDPE containing different single antioxidants. There are no significant changes

of power consumption for all the polymers during multiple extrusions. On the other hand, it is clear that no matter what antioxidant is used, the m-LLDPE polymers generally consume less power during multiple extrusions compared to their corresponding compounding steps (P_0), while the reverse is true for the z-LLDPE. It is also evident from Figure 5.2 that the differences in melt pressure at the die are small for all the polymers stabilised by different single antioxidants during multiple extrusions. On the other hand, metallocene polymers that contain higher levels of comonomer (e.g. VP-8770) as well as the z-LLDPE show generally a higher die pressure during extrusions; similar to the case of unstabilised polymers (see Table 4.1 in Chapter 4).

5.2.1.2. Extrusion Characteristics of LLDPE Containing Antioxidant Mixtures

The P_0 extrusion characteristics of LLDPE (PL-1840 was used in most cases) containing AO mixtures are also given in Table 5.4. It can be seen that the differences in power consumptions between the same polymers stabilised by different antioxidants are very small. However, PL-1840 containing TMP (AO-E3) shows lower power consumption compared to those stabilised by other AO systems (see Table 5.4), indicating the plasticising function of this additive. It is also evident that there are only minor differences in melt pressure of PL-1840 stabilised by different AO mixtures. Additionally, it is interesting to note that the melt pressures in the compounding step of PL-1840 containing combined antioxidants are considerably lower than that of the polymers containing single antioxidants. Table 5.6 shows the multi-pass extrusion characteristics of LLDPE stabilised by AO mixtures. Similar to the P_0 extrusion of PL-1840, the differences in extrusion characteristics between different passes as well as different AO systems are all very small, and the melt pressures are relatively lower compared to that of the polymers stabilised by single antioxidants (see Table 5.5).

Figures 5.3 and 5.4 compare the power consumptions of extruded LLDPE containing AO mixtures (mixed in the Lab) and commercially combined-antioxidant blends. In addition to the similarity of changes in power consumption for the same polymers stabilised by different AO systems (e.g. PL-1840), it is

worth noting that the power consumption of multiply extruded z-LLDPE stabilised with commercial AO- mixtures, is lower than that of the polymer stabilised with most single antioxidants. It can be suggested that the commercial combined-antioxidant blends are more effective in decreasing the extent of polymer crosslinking during thermal oxidation compared to single antioxidants. It has been also clearly shown from Figures 5.5 and 5.6 that the die pressures for the same polymers containing different AO mixtures are very similar. Just like the case of polymers containing single antioxidants, z-LLDPE and m-LLDPE having higher comonomer content show generally higher melt pressures in both compounding and multi-pass extrusions (see Figure 5.5).

5.2.2. Effects of Single Antioxidants on the Extent of LLDPE Stabilisation

In this part of work, both z-LLDPE and different grades of m-LLDPE (containing different amounts of comonomer) were singly combined with some of the most frequently used commercial antioxidants through compounding step (P_0 extrusion). The variations of MFI, unsaturation, carbonyl compounds and short chain branches (SCB) of the stabilised polymers were then investigated.

5.2.2.1. Effects on the Melt Stability

The melt flow index (MFI), melt flow rate (MFR) as well as their changes (compared to that of virgin unprocessed polymers) for LLDPE stabilised by different single antioxidants are given in Tables A5.1 and A5.2 (see Appendix). It has been shown that both MI and MFR values for LLDPE polymers after compounding with AO's (extrusions P_0) are only slightly different compared to that of their corresponding virgin polymers for all the antioxidants examined. Based on this result, it can be considered that the compounding step has no significant impact on the rheological properties of LLDPE under the conditions chosen for this work.

Figure 5.7 shows clearly that the hindered phenols (Irgnox1076 and IrgnoxE201) and γ -lactone (Irganox HP136) give higher overall melt stabilisation to all the different m-LLDPE polymers examined here compared to their effects on the z-

LLDPE polymer. However, these stabilisers, when used as single AO's, offer higher melt stabilisation to the metallocene polymers with the highest MI (1.43) and lowest extent of short chain branching (11.6 w% 1-octene), the FM-1570 grade. Figure 5.8 compares the stabilising performance of different AO's on rheological properties of each polymer. The lower extent of MI changes of m-LLDPE having lower levels of comonomer content (FM-1570 and PL-1840) containing IrganoxHP136, indicate the stronger stabilisation ability of lactone antioxidant for these grades of polymers. Meanwhile, the lactone (IrganoxHP136) also exhibits higher effectiveness in melt stabilisation of z-LLDPE during multi-pass extrusions, but hindered phenols are more effective on melt stabilisation of m-LLDPE with higher SCB content (VP-8770, 28.2 w% 1-octene).

The MFR results, Figure 5.9, support the above findings and show that all the metallocene type polymers undergo less change in their molecular weight distribution (MWD) as reflected by a smaller change in MFR values compared to the z-LLDPE polymer. Furthermore, the metallocene polymer FM-1570 shows the lowest change in MFR in all cases. The phosphite antioxidant, Ultrinox626, when used alone offered relatively lower stability to all the polymers examined here. This can be expected since phosphites generally operate as stoichiometric peroxide decomposers (PD-C) and thus are normally used in combination with other AO's, normally hindered phenols [112]. The MFR changes of each polymer stabilised by different single antioxidants (see Figure 5.10) show very similar results as obtained from the MI changes (see Figure 5.8). IrganoxHP136 provides generally the highest melt stability to FM-1570, PL-1840 (m-LLDPE) and Ziegler polymer, but hindered phenols have a better performance in the melt stabilisation of VP-8770 (m-LLDPE containing higher SCB).

5.2.2.2. Effects on the Degree of Unsaturation

In order to make a comparison, the percentage concentration change of unsaturated and carbonyl groups in unstabilised polymers extruded at the same temperature (265°C) is shown in Figure 5.11. Figures 5.12, 5.14 and 5.16 display the concentrations of different unsaturated groups in LLDPE containing single

antioxidants after compounding and multiple extrusions (calculated from FTIR by means of the corresponding IR extinction coefficient, see Section 2.3.2.1 (a) in Chapter 2). Again, it is clear that compared with virgin polymers, the compounding step has generally no significant effect on the degree of unsaturation in LLDPE except in few cases (e.g. trans-vinylene in IrganoxHP136 stabilised VP-8770 and Ultrinox626 stabilised PL-1840, vinyl group in Ultrinox626 stabilised FM-1570). Moreover, the differences in the total-double-bond concentration for all the extruded polymers (P_0 , $P_1 \sim P_5$) containing any of the single antioxidant was shown to be very limited with the exception of the cases mentioned above (see Tables A5.3 to A5.6 in Appendix).

Figures 5.12, 5.13(a) and 5.13(b) compare the changes with extrusion passes in trans-vinylene concentration in these stabilised LLDPE samples. It is shown that the concentration of trans-vinylene in stabilised z-LLDPE is much lower than its concentration in the metallocene polymers (see Figure 5.12) due to the original low content of trans-vinylene in virgin Ziegler polymer. Figure 5.13(a) shows that compared with the unstabilised extruded analogues, the range of changing in trans-vinylene concentration generally becomes smaller for all the m-LLDPE polymers stabilised with the hindered phenol (Irg1076 and IrgE201) and lactone (IrgHP136) antioxidants upon multiple extrusions. However, stabilising the z-LLDPE with any examined single antioxidant leads to a larger range of changing in trans-vinylene concentration upon multiple extrusions compared to the unstabilised polymer. For the phosphite AO, Ultrinox626, always causes more significant change in the concentration of trans-vinylene after extrusions in the case of the m-LLDPE polymer containing lower SCB content, especially for FM-1570. Figure 5.13(a) shows that, in the unstabilised FM-1570 polymer, the trans-vinylene concentration, relative to the virgin polymer, decreases after the first extrusion but then with further extrusions it increases, though the percentage change is still at negative value, and after five extrusions it almost assesses the concentration of the unprocessed virgin polymer; in the case of the same polymer stabilised with Ultrinox626, there is a very large increase in the concentration of trans-vinylene (with respect to the virgin polymer) with extrusion passes. Moreover, Figure 5.13(b) indicates that similar to the unstabilised polymers (see Figure 5.11), the trans-vinylene concentration in all

the LLDPE polymers stabilised with single antioxidants tends to increase in most cases with more extrusion passes.

In contrast to trans-vinylene, the vinyl concentration in virgin z-LLDPE is much higher than that in the virgin metallocene polymers, see Figure 5.14. It is shown in Figure 5.15(a) that the hinder phenol and lactone antioxidants generally show no much difference in their effects on the changes of vinyl concentration in the extruded LLDPE polymers. Meanwhile, similar to the situation of unstabilised polymers (see Figure 5.11), both stabilised metallocene and Ziegler-type polymers generally show reduction in their vinyl concentration after multiple extrusions, and the largest extent of vinyl decrease can be observed in the extruded m-LLDPE having the highest SCB content (VP-8770, see Figure 5.15(b)). Furthermore, both stabilised and unstabilised z-LLDPE show an overall lower extent of decrease in vinyl concentration compared to the corresponding metallocene polymers, see Figure 5.15(b).

Figure 5.16 shows that the vinylidene concentration in all stabilised m-LLDPE polymers increases with increasing extrusion passes. It is clear from Figure 5.17(a) that the vinylidene concentration in the stabilised m-LLDPE is generally lower than that in the corresponding unstabilised polymers after TSE extrusions, but the situation is totally different in the case of z-LLDPE polymer. For the stabilised z-LLDPE, there are only relatively small changes in the amount of vinylidene after extrusion for different passes; however, a steady increase in vinylidene concentration with more extrusion passes can be observed in z-LLDPE stabilised with the phosphite antioxidant, Ultrinox626. Meanwhile, just like the case of unstabilised polymers (see Figure 5.11), the stabilised m-LLDPE with the lowest SCB content (FM-1570) shows the greatest increase in vinylidene concentration upon multi-pass extrusions (see Figure 5.17(b)).

5.2.2.3. Effects on the Level of Carbonyl Containing Compounds

The carbonyl concentration in virgin LLDPE as well as in extruded polymers containing single antioxidants is highlighted in Tables A5.3 to A5.6 (see Appendix). Generally, the addition of single antioxidants in the compounding

step (P_0) can lead to an enhancement of carbonyl concentration in all the polymers examined, especially for the LLDPE stabilised with Irganox1076 (see Figure 5.18). It is indicated from Figure 5.19(a) that, compared to the unstabilised polymers, compounding the LLDPE polymers with the hindered phenol antioxidant, Irganox1076, can result in a significant increase in the concentration of carbonyl compounds; however, the addition of phosphite lowers the carbonyl concentration in m-LLDPE upon multiple extrusions. In contrast to the situation of m-LLDPE, z-LLDPE stabilised with phosphite shows a considerable increase in carbonyl concentration upon multi-pass extrusions.

Figure 5.18 shows the changes of carbonyl concentration in different extruded LLDPE polymers containing single antioxidants. It is interesting to note that the extruded m-LLDPE stabilised by Ultrinox626 gave the lowest amount of carbonyl compounds, even though the z-LLDPE polymer containing the same phosphite antioxidant gave a considerable increase in the level of carbonyl concentration with increasing extrusion passes. It is also clear in Figure 5.19(b) that the amount of carbonyl compounds in all the stabilised LLDPE polymers increases with more extrusion passes. Meanwhile, similar to the case of unstabilised polymers (see Figure 5.11), the z-LLDPE always presents the largest extent of increase in carbonyl concentration among the stabilised polymers no matter what antioxidant was used. Figures 5.20 to 5.23 show the FTIR spectra in carbonyl region for the extruded LLDPE polymers stabilised with different single antioxidants.

5.2.2.4. Effects on the Extent of Branching

Table 5.7 gives the changes of short chain branches (SCB) after multiple extrusions of two representative polymers containing different single antioxidants. Overall, there is no significant change in the SCB content upon TSE extrusions, although the stabilised m-LLDPE show a very slight decrease compared to the virgin analogue.

5.2.2.5. Effects on the Discoloration of Extruded Polymers

Table 5.8 and Figure 5.24 show the effect of extrusion on the discolouration of polymers (YI-YI₀) containing single antioxidants. It is clear that the compounding step as well as multiple extrusions generally result in increased discolouration of all stabilised polymers. IrganoxE201 has the most adverse effect on the yellowing of all the extruded polymers, whereas the Ultrinox626 (phosphite) and Irganox1076 (hindered phenol) antioxidants give rise to much lower extent of polymer discolouration.

5.2.3. Synergistic and Antagonistic Effects of Antioxidant Mixtures on Stabilisation of Extruded LLDPE

Due to the limitation of the effectiveness of single antioxidant in polymer stabilisation during melt processing, combinations of different types of antioxidants have been extensively investigated and widely used in industry. The objects of this part of work were to examine the effective and to further verify the stabilisation mechanisms of single antioxidants established in the former section by analysing the interactions between antioxidants and polymers as well as different antioxidants. Furthermore, it is important to optimise the effective of AO packages required for m-LLDPE stabilisation during melt processing on the synergistic and antagonistic effects reflected by different antioxidant mixtures. To understand the effects of the combined antioxidants on the rheological and molecular characteristics of LLDPE during extrusion, some typical commercial antioxidant mixtures were physically mixed and added into PL-1840 (this polymer was chosen as a representative of m-LLDPE polymers).

5.2.3.1. Effects on the Melt Stability

The melt flow performances of extruded LLDPE stabilised by different AO mixtures are shown in Tables A5.7 and A5.8 (see Appendix). Compared to the virgin polymers, it can be seen that the melt flow behaviour of LLDPE (MI, MFR) after compounding (P₀) with any AO mixtures have almost no changes. It is also clear from Figure 5.25 that when hindered phenol (Irganox1076 or

IrganoxE201) and phosphite (Irgafos168, Ultrinox626, IrgafosP-EPQ or Weston399) antioxidants were combined, they were more effective in reducing the range of MI change of PL-1840 upon multiple extrusions compared to the polymer singly stabilised with each of the hindered phenols. Moreover, the addition of γ -lactone (IrganoxHP136) in the hindered phenol/phosphite AO mixtures results in further reduction in the extent of MI variation for the extruded PL-1840 polymer.

Figures 5.26 and 5.27 show that the addition of lactone (IrganoxHP136) in the hindered phenol /phosphite AO mixtures can evidently increase their effectiveness in LLDPE melt stabilisation. Among the AO mixtures examined, the combination of Irganox1076, Irgafos168 and IrganoxHP136 is most effective in improving the melt stability of PL-1840 upon multiple extrusions. The MFR changes of extruded PL-1840 containing different combined antioxidants show very similar results to those outlined discussed above (see Figure 5.28). The mixture of Irganox1076, Irgafos168 and IrganoxHP136 antioxidants performs most effectively in terms of restricting the increase of MFR value, which corresponds to the broadening of molecular weight distribution of the extruded polymers.

Figures 5.29 and 5.30 show the effects of two commercial AO mixtures on the melt stability of different LLDPE upon multi-pass extrusions. It is found that both antioxidants combined are more effective for the stabilisation of m-LLDPE with higher SCB content (VP-8770). In general, the addition of IrganoxXP490 antioxidant results in a better overall stabilisation effect in both Metallocene and Ziegler polymers, especially for m-LLDPE polymers (see Figure 5.31). The major difference between these two antioxidants is that IrganoxXP490 which contains the phosphite IrgP-EPQ has higher relative concentration of hindered phenol and less phosphite than in the case for IrganoxHP2921, which contains Irgafos168 as the phosphite.

5.2.3.2. Effects on the Degree of Unsaturation

Figures 5.32 to 5.37 show the variations of unsaturated groups in PL-1840 polymer containing different AO mixtures after compounding and multiple extrusions (see the detailed results in Tables A5.9 to A5.11 in Appendix). It is shown that compounding AO mixtures generally results in an enhancement of trans-vinylene and vinylidene concentrations, but reduction in vinyl concentration (except for the polymer stabilised with Irgafos168 contained AO mixtures) compared to that in virgin polymer (see Figure 5.35). In general, the concentrations of trans-vinylene and vinylidene groups in all stabilised PL-1840 increase after multiple extrusions, whereas considerable decrease in vinyl concentration can be observed in the extruded polymer containing AO mixtures (see Figures 5.33, 5.35 and 5.37). Additionally, the use of different hindered phenols in AO mixtures shows no significant impact on the changes in vinyl and vinylidene concentrations, but it affects the changing trend of trans-vinylene concentration in PL-1840 subjected to multiple extrusions.

Figures 5.38(a) and 5.38(b) indicate further that although the phosphorus content in all stabilised PL-1840 was fixed at 0.006 w% (see Table 5.2), the different phosphite antioxidants in the AO mixtures has considerable effect on the production of trans-vinylene in stabilised PL-1840, leading to different extents of variation in trans-vinylene concentration in PL-1840 after multi-pass extrusions, with the trans-vinylene concentration generally increasing with more extrusion passes. It is also clear that the amount of vinyl groups in PL-1840 stabilised with Irgafos168 combined AO mixtures evidently tends to decrease with increasing extrusion passes, while the vinyl concentration in PL-1840 containing other AO mixtures overall shows no significant change upon multiple extrusions. The vinylidene concentrations in PL-1840 containing different AO mixtures all tend to increase with the number of extrusion passes (see Figures 5.38(a) and 5.38(b)). Figure 5.38(b) shows that, in general, the presence of lactone antioxidant (IrganoxHP136) in AO mixtures does not greatly affect the changes in the concentrations of unsaturated groups in extruded PL-1840 polymers;

meanwhile, the use of different hindered phenols (Irg1076 or IrgE201) has no significant effect either on the variation of unsaturated groups.

The variations of double bond concentrations in different LLDPE stabilised by two commercial AO mixtures after multiple extrusions are shown in Figure 5.39. Compared with the amount of unsaturated groups in extruded PL-1840 containing AO mixtures of Irganox1076, IrgafosP-EPQ, IrganoxHP136 (500: 1000: 250 ppm) and Irganox1076, Irgafos168, IrganoxHP136 (500: 1250: 250 ppm), it can be seen that the PL-1840 polymer stabilised by the commercial antioxidants with the same AO combination presents the similar tendency in the change of each kind of double bond upon multi-pass extrusions (see Figures 5.32, 5.34 and 5.36). It is also interesting to note from Figure 5.40 that the changes of individual unsaturated group in different LLDPE polymers containing 1750ppm IrganoxHP2921 (Irg1076: Irgafos168: IrgHP136 = 2: 4: 1) resemble each other in the tendency with more extrusion passes. However, an evident difference can be observed from the changes in trans-vinylene concentration in different polymers stabilised with 1500ppm IrganoxXP490 (Irg1076: IrgafosP-EPQ: IrgHP136 = 3: 2: 1) with increasing extrusion passes. It can be found further from Figure 5.41 that the extent of concentration changes of all kinds of double bonds in LLDPE containing IrganoxXP490 is overall smaller than that in the corresponding polymers stabilised with IrganoxHP2921 upon multiple extrusions.

5.2.3.3. Effects on the Level of Carbonyl Containing Compounds

Figure 5.42 indicates that compounding AO mixtures in PL-1840 generally leads to increase in carbonyl concentration compared to that in the virgin polymer (see Table A5.12 for the detailed results). It is also clear from Figure 5.43 that the amount of carbonyl compounds in all stabilised PL-1840 tends to increase with increasing passes of extrusions, and the addition of IrganoxHP136 in the AO combinations has no significant effects on the changes of carbonyl concentration. Among the AO mixtures, the IrganoxE201 (biological hindered phenol) contained antioxidants show the best effectiveness on restricting the increase of carbonyl compounds in extruded PL-1840 polymers. Figures 5.44 and 5.45

reveal further that the combination of hindered phenol and phosphite can effectively reduce the formation of carbonyl compound in the extruded PL-1840 polymer, and the presence of lactone in these AO mixtures basically results in similarity in the production of carbonyl groups in PL-1840 stabilised with different phosphite containing AO mixtures upon multi-pass extrusions.

The effects of the two commercial AO mixtures on the carbonyl concentrations in different LLDPE during melt extrusion have also been examined and the results are shown in Figures 5.46 and 5.47. It is worth noting that the compounding of both IrganoxXP490 and IrganoxHP2921 antioxidants can lead to a great enhancement of carbonyl concentration in Dowlex2045E polymer (z-LLDPE). Meanwhile, it can be clearly seen from Figure 5.48 that the LLDPE stabilised with IrganoxHP2921 overall contain lower amounts of carbonyl compounds than that stabilised with IrganoxXP490.

5.2.3.4. Effects on the Discoloration

It is shown in Figures 5.49 that the yellow index difference ($YI - YI_0$) value of all LLDPE containing the AO mixtures increases with more extrusion passes (see Table 5.9 for details), and the addition of IrganoxHP136 antioxidant causes more severe discolouration in extruded PL-1840 polymers. It can also be found from Figure 5.49 that compared to the corresponding AO mixtures containing synthetic hindered phenol (Irganox1076), the use of biological antioxidant (IrganoxE201) overall result in much greater increase of YI value in the stabilised PL-1840 after multiple extrusions; and meanwhile, the presence of TMP in the mixed antioxidants can reduce the level of discolouration in PL-1840 polymer subjected to multi-pass extrusions. Figures 5.50 and 5.51 show that the AO mixtures containing different phosphites generally present similar influence on the variation of discolouration in stabilised PL-1840 polymer after multiple extrusions. In addition, it is shown from Figures 5.52 and 5.53 that the use of both commercial AO mixtures, IrganoxHP2921 and IrganoxXP490 leads to considerable increase in the level of discolouration for z-LLDPE after TSE extrusions. Meanwhile, IrganoxHP2921 shows much less effects on the

discolouration of m-LLDPE with higher SCB content (VP-8770) than IrganoxXP490 when subjected to multi-pass extrusions.

5.3. DISCUSSION

5.3.1. Stabilisation Mechanisms of LLDPE Polymers in the Presence of Different Antioxidants Used Singly

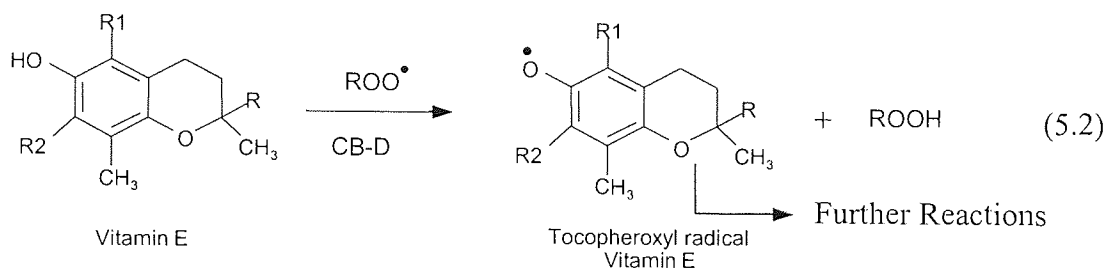
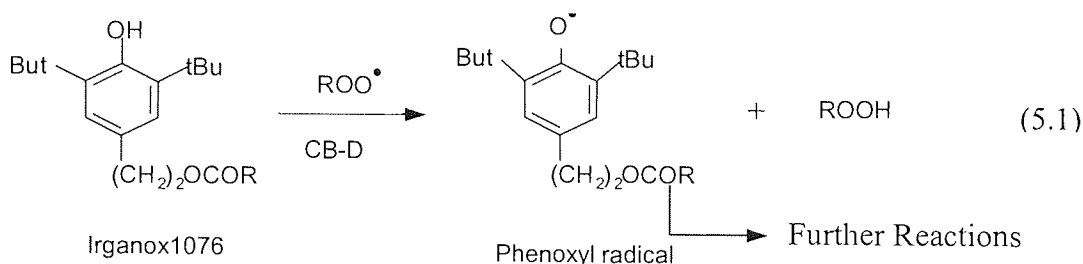
5.3.1.1. Effects of Antioxidants on the Melt Stability of LLDPE Polymers

Thermal oxidation of LLDPE takes place under extrusion conditions of high temperature, high shear rate and the presence of small concentration of oxygen and leads to structural variations (e.g. crosslinking and chain scission) that are responsible for formation of oxidative defects during processing, particularly in the case of m-LLDPE which has a higher melt viscosity (due to its narrower MWD), compared to z-LLDPE, and this causes more processing difficulties. The primary object of compounding antioxidants in LLDPE melt is to inhibit the thermal oxidative degradation and control the rheological characteristic changes. Therefore, the stabilisation role and mechanisms of the different types of antioxidants examined here need to be understood in order to develop the most effective antioxidant packages for melt processing of these polymers.

The melt flow behaviour of stabilised LLDPE shown in Figure 5.7 indicates that all the antioxidants examined offer generally a higher stabilisation activity in the m-LLDPE polymer having the lowest SCB content, i.e. FM-1570. In contrast, these AO's resulted in the lowest effectiveness in the melt stabilisation of the z-LLDPE polymer, Dowlex2045E. The MFR changes shown in Figure 5.9 support these findings whereby the stabilised FM-1570 polymer shows the lowest MFR increase with extrusion passes (corresponding to least broadening of MWD), while Dowlex2045E shows the highest increase in MFR.

Figures 5.8 and 5.10 compare the extent of melt stabilisation imparted by the antioxidants in the different LLDPE compared to their corresponding

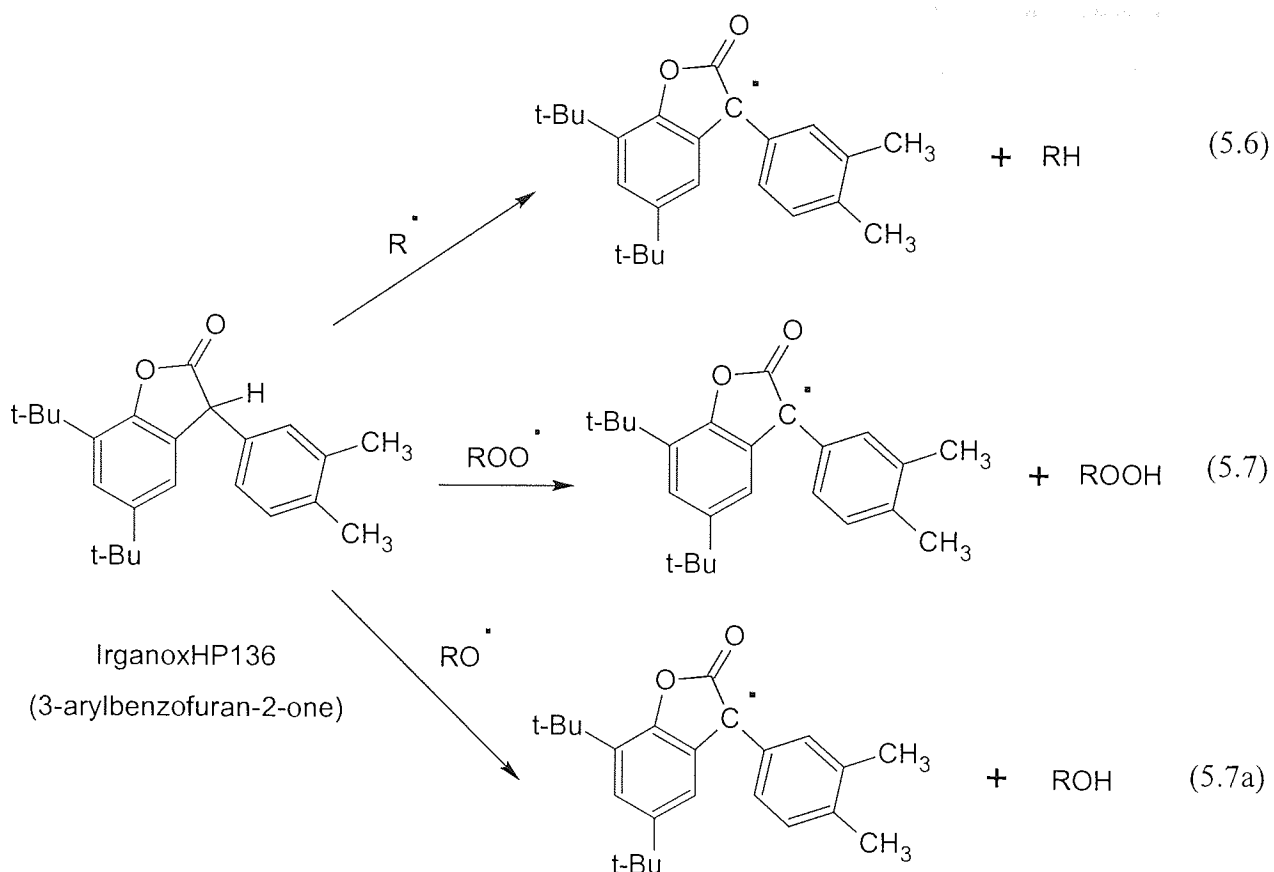
unstabilised polymers. It is evident that both hindered phenols examined (Irganox1076 and IrganoxE201) can effectively stabilise the polymer melts during multiple extrusions (with the exception of PL-1840, and the reason for this is not very clear) and their antioxidant action is predominated by their CB-D activity; donating hydrogen to macro-alkylperoxy radicals ROO^\bullet , see Reactions 5.1 and 5.2 [109, 111, 112].



The antioxidant reactions 5.1 and 5.2 occur in direct competition with hydrogen abstraction by the alkylperoxy radicals (ROO^\bullet) from the polymer substrate (see Reaction 5.3), thus the more effective is the CB-D antioxidant, the less important the hydrogen abstraction reaction becomes and thus the concentration of R^\bullet generated can be expected to be lower. Since the addition of alkyl radicals to vinyl groups plays an important role in the crosslinking reaction of oxidising LLDPE during multiple extrusion (see Reactions 5.4 and 5.5), phenolic antioxidants would be expected to contribute to reducing the extent of crosslinking as well as broadening of MWD of the polymers (especially for z-LLDPE) associated with predominance of crosslinking reaction (see Figures 5.7 and 5.8). The efficiency of melt stabilisation exhibited by the hindered phenols has also been supported by a generally more stable melt pressure experienced during multi-pass extrusions of stabilised polymers (see Table 5.5) compared to that of the unstabilised counterparts (see Table 4.1 in Chapter 4).

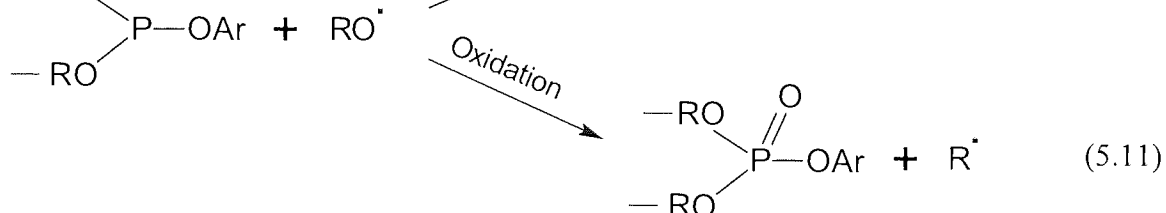
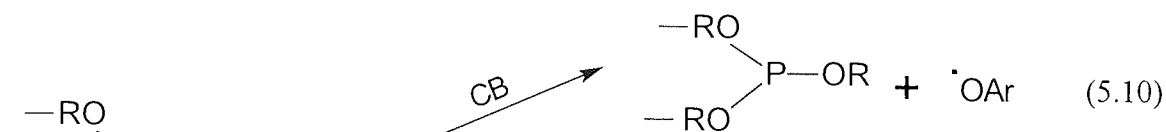
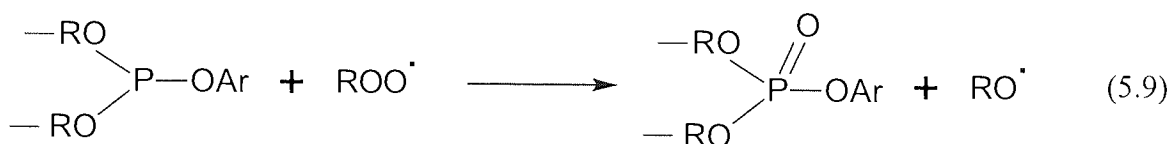
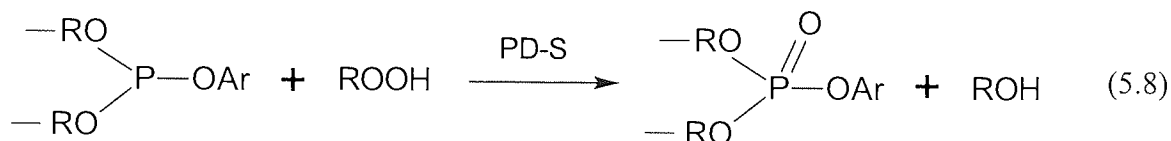


The melt flow behaviour of stabilised LLDPE (see Figures 5.7 to 5.10) indicates that the lactone antioxidant (IrganoxHP136) has good performance in stabilising the polymer melts during multiple extrusions (compared to the MI and MFR changes of the unstabilised counterparts shown in Figures 5.8 and 5.10). It is clear that the presence of IrganoxHP136 can greatly reduce the extent of MI decrease (corresponding to reduction in extent of increase in crosslinking) as well as MFR enhancement (corresponding to reduction in extent of MWD broadening) for the stabilised polymers, especially in the case of the m-LLDPE polymer with lower comonomer content (e.g. FM-1570) and the z-LLDPE. The effectiveness of IrganoxHP136 is also reflected in the overall more stable melt pressures and power consumptions during LLDPE multiple extrusions compared to the unstabilised polymers (see Table 5.5 and Table 4.1 in Chapter 4). The good melt stabilising effect of the lactone antioxidant can, most likely, be attributed to its high ability of donating a hydrogen to the oxidation intermediates. Previous studies have demonstrated that the lactone antioxidant IrganoxHP136 operates efficiently under conditions where both alkyl (R^\bullet) and alkyl peroxy (ROO^\bullet) radicals are present in the system, i.e. under normal extrusion conditions. It can effectively trap these radicals and decrease the production of macro-alkyl radicals, thus inhibit both crosslinking and chain scission reactions (see Reactions 5.6, 5.7 and 5.7a) [143].



Figures 5.8 and 5.10 show that m-LLDPE stabilised with the phosphite ester antioxidant (Ultranox626) presents generally a lower effectiveness during multiple extrusions compared to the other antioxidants examined. The drastic drop in MI and greater increase in MFR with more extrusion passes suggest a significant crosslinking and MWD broadening of the extruded polymers. However, this organic phosphite antioxidant is shown to be fairly effective on the melt stabilisation of z-LLDPE, especially for the polymer subjected to only one pass extrusion. The reason for this AO performance is not very clear and is considered probably due to the Ziegler catalyst residue in this polymer that favours the stabilisation activities. The phosphite ester primarily functions as a stoichiometric peroxide decomposer (PD-S) reducing hydroperoxides to alcohols (preventive mechanism, see Reaction 5.8) [120]. Although phosphite antioxidants can also contribute to some chain breaking activity through deactivating both ROO^\bullet (see Reaction 5.9) and RO^\bullet (see Reaction 5.10) radicals [119], it is not a highly effective chain breaking antioxidant due to its much weaker electron donating ability. Meanwhile, if an oxidation reaction occurs instead of

substitution (as shown in Reaction 5.11) then alkyl (R^\bullet) radicals are formed which can propagate the autoxidative chain. So normally, phosphite antioxidants are rarely used on their own to stabilise polymers, but instead are often used in combination with alkylperoxyl and/or alkyl radical scavengers, in order to improve the stabilising effectiveness.

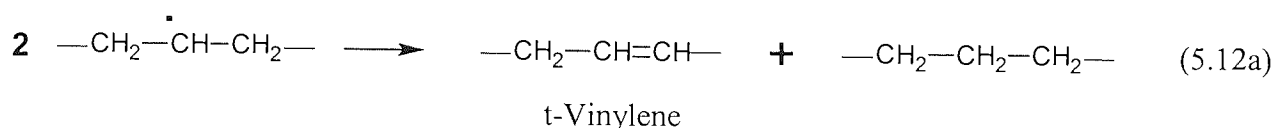
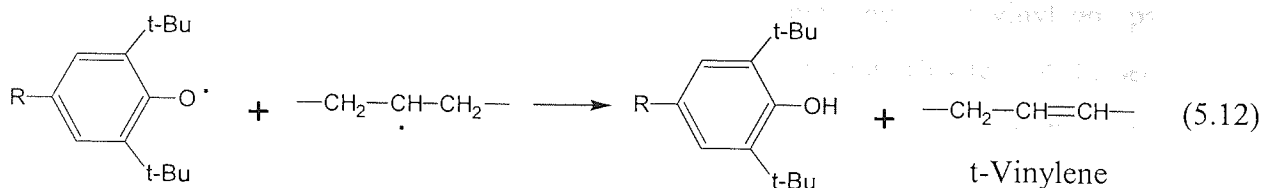


Based on the results of melt flow measurement of the stabilised polymers, it can be concluded that the antioxidant with higher ability of donating hydrogen (CB-D mechanism) generally presents a higher activity in melt stabilisation during multiple extrusions of LLDPE. On the other hand, the polymers with lower vinyl concentration (e.g. FM-1570) and lower density (easier for the diffusion of antioxidant in the polymer melt, e.g. VP-8770) show a higher extent of melt stability upon multi-pass extrusions when compounded with the antioxidants examined (see Figures 5.7 and 5.9).

5.3.1.2. Effects of Antioxidants on Structural Changes in LLDPE Polymers

Figures 5.12, 5.14 and 5.16 show that the trend in changes of different double bonds is not too different in the case of the different polymers stabilised with hindered phenols (Irg1076 and IrgE201) and lactone (IrgHP136) antioxidants. However, stabilisation of the FM-1570 polymer (the m-LLDPE with the lowest comonomer content) with phosphite, Ultrinox626, shows a very different behaviour upon multiple extrusions in terms of changes in trans-vinylene (see Figures 5.12 and 5.13).

Compared to the unstabilised polymers, the uses of hindered phenols (Irganox1076 and IrganoxE201) and lactone (IrganoxHP136) antioxidants do not show significant effect on the composition of the unsaturated groups that are present in both extruded m-LLDPE and z-LLDPE polymers (see Figures A5.1 to A5.4 in Appendix). Figures 5.12 shows that the lower comonomer containing m-LLDPE (FM-1570 and PL-1840) stabilised with phenolic antioxidants (as well as lactone) generally contain in absolute value less trans-vinylene upon multiple extrusions than the stabilised VP-8770 which has higher comonomer content, but the extent of change with respect to the virgin FM-1570 and PL-1840 is lower, i.e. relatively lower decrease in trans-vinylene can be observed for these polymers after extrusions, see Figures 5.13(a) and 5.13(b). The lower reduction of trans-vinylene in the lower comonomer content m-LLDPE can be accounted for, at least in part, by the reaction of secondary macro-alkyl radicals (expected to be the primary alkyl radicals formed in the oxidation of LLDPE with lower SCB content) with phenoxyl radicals during thermal oxidation, see Reaction 5.12. However, it is unreasonable to ignore the significant contribution to the variation of trans-vinylene from the other reactions that occur in the absence of phenolic antioxidants (see Reaction 5.12a); as the differences in trans-vinylene concentration change between unstabilised (see Figure 5.11) and stabilised (with hindered phenol and lactone) samples (see Figure 5.13) are not very large for most polymers after multi-pass extrusions [128, 129].



It is also worth noting from Figures 5.13(a) and 5.13(b) that much more trans-vinylene groups were produced in the presence of the phosphite Ultrinox626 in FM-1570 (m-LLDPE with the lowest SCB content) compared to the other stabilised metallocene polymers upon multiple extrusions. This is expected to be due to the disproportionation reaction of secondary macro-alkyl radicals (see Reaction 5.12a) that are the predominant alkyl radicals in this grade of m-LLDPE polymer, as they can be generated *via* the reduction of alkyl peroxy (ROO[•]) and alkoxy (RO[•]) radicals in the presence of phosphite antioxidant (see Reactions 5.9 and 5.11). However, it is not clear as to why the extruded PL-1840 polymer having similar comonomer content does not show such an increase (quite small change with respect to the virgin polymer) in trans-vinylene concentration when stabilised with Ultrax626 (see Figure 5.13(b)).

Figures 5.15(a) and 5.15(b) show that similar to the case of unstabilised polymers (see Figure 5.11), the vinyl concentration in the LLDPE stabilised with all the antioxidants examined generally decreases (with respect to the virgin polymers) upon multiple extrusions. A consequence of the function of phenolic and lactone antioxidants is a decrease in the macro-alkyl radicals in the polymer melt, thus the use of these antioxidants can be expected to lower the production of vinyl group through the reactions of alkyl and derived radicals (see Reaction 4.10 to 4.12 in Chapter 4); on the other hand, they can also reduce the chance of occurrence of crosslinking as a result from the addition reaction of vinyl group with alkyl radicals (see Reaction 5.4). Thus overall, a smaller extent of change in vinyl concentration upon more extrusion passes can be observed for the

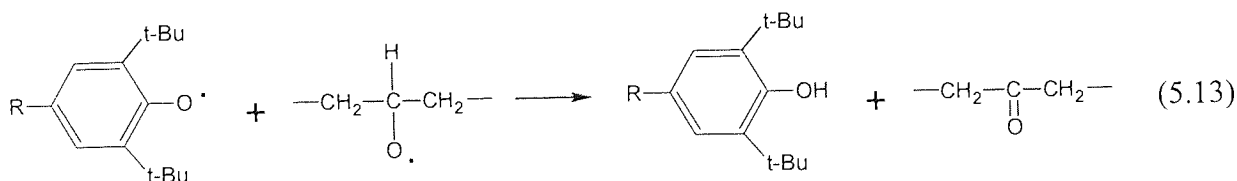
stabilised (phenol or lactone) LLDPE originally containing more vinyl groups compared to the corresponding unstabilised polymer (e.g. Dowlex2045E, see Figure 5.15(a)). Figure 5.15(b) shows further that vinyl concentration in m-LLDPE stabilised with any of the single antioxidants used generally results in much larger extent of decrease after multiple extrusions when compared to corresponding stabilised z-LLDPE polymer. This is similar to the case shown in the extrusion of unstabilised polymers (see Figure 5.11) and is mainly due to the much lower original vinyl content in the virgin metallocene polymers.

The overall lower increase of vinylidene concentration in the Ultrinox626 and IrgHP136 stabilised VP-8770 (the m-LLDPE having the highest SCB content) compared to the unstabilised polymer (see Figure 5.17(a)) indicates the effectiveness of these antioxidants in inhibiting the formation of active (alkyl, alkoxyl and peroxy) radicals involving short chain branch (SCB), as these radicals are the most important intermediates leading to the yield of vinylidene group during multiple extrusions (see Reaction 4.13 to 4.15 in Chapter 4). However, comparing Figure 5.17(b) with Figure 5.11, it can be seen that generally, the use of all the antioxidants examined has no significant effect on the variation of vinylidene concentration in the extruded polymers compared to the corresponding unstabilised extruded counterparts.

It is clear from Figures 5.18 and 5.19(a) that the carbonyl concentration in the m-LLDPE polymers containing Irganox1076 is higher than for other antioxidants. This is mainly due to the presence of a large ester absorption at 1739 cm^{-1} in the spectrum of Irganox1076 (see Figure A2.1 in Appendix). The changes in the FTIR spectra in the carbonyl region for the different stabilised polymers are shown in Figures 5.20 to 5.23. It is important to note that an ester absorption peak at 1739 cm^{-1} is always present in the virgin unprocessed metallocene polymers (much lower absorption of this peak in the virgin z-LLDPE). This is mainly due to the fact that these polymers were stabilised by the manufacturers (generally low level of stabilisation for the purpose of storage and shipping) and almost certainly the stabilisation package used would include a hindered phenol such as Irganox1076 and hence the 1739 cm^{-1} absorption (virgin unstabilised and unoxidised polyethylene should not have any significant absorptions in the

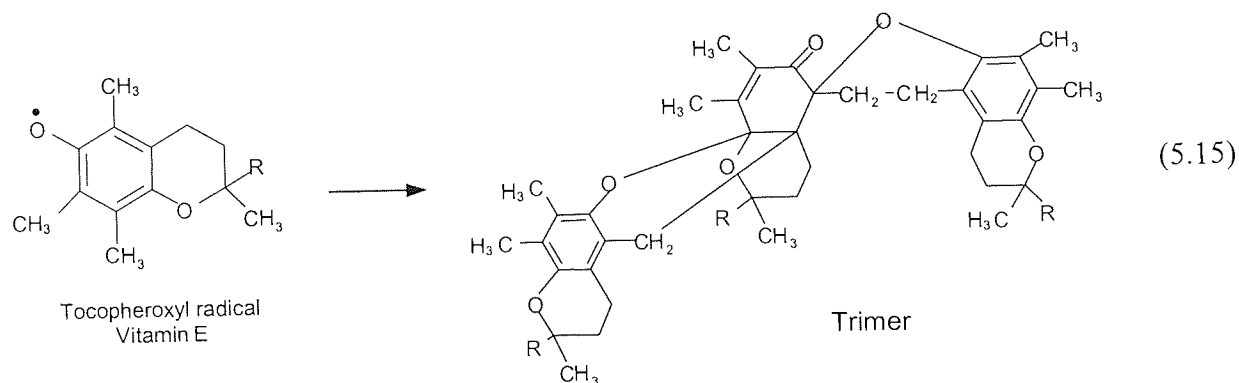
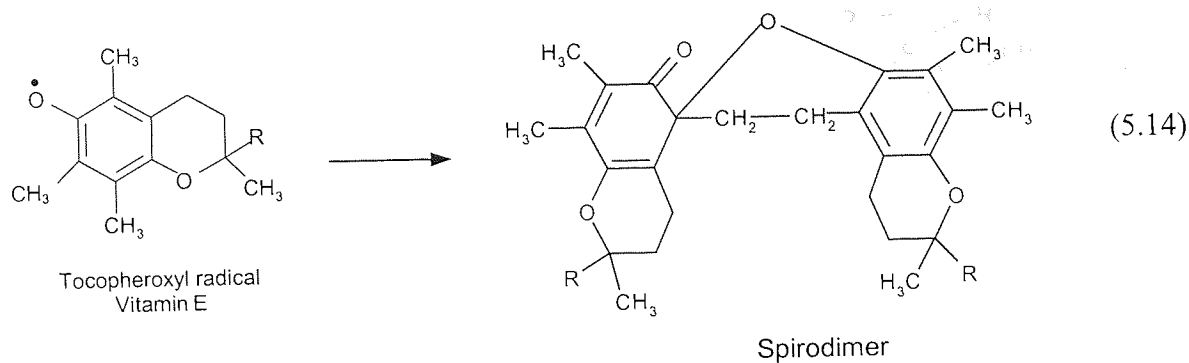
carbonyl region). Therefore, only the extent of changes in carbonyl content in extruded polymers relative to that present in the virgin unprocessed counterparts, will be considered here.

The phenolic antioxidants such as Irganox1076 can act as Lewis acid to some extent in LLDPE melt, thus its presence is favourable to some acid-catalysed reactions leading to the formation of carboxylic acids and unsaturated ketones (see Reactions 4.31 to 4.34 and 4.38 in Chapter 4) [93, 101]. Meanwhile, the disappearance of aldehyde peak in the FTIR spectra of Irganox1076 stabilised LLDPE (evident absorbance of aldehydes can be observed in the FTIR spectra of unstabilised polymers from Figures 4.35 to 4.40 in Chapter 4) further confirms the occurrence of some oxidation reactions that transform aldehydes into carboxylic acids under the catalysis of acid (see Reactions 4.31 and 4.32 in Chapter 4) [101]. Following the above discussion, then the consumption of the AO Irganox1076 upon multi-pass extrusions should result in a drop in the production of acids and unsaturated ketones, thus more ketones can form and accumulate in the polymer. Meanwhile, the evident increase of absorption at 1739 cm^{-1} attributed to ester for extruded LLDPE stabilised with Irganox1076 (compared to the virgin unprocessed polymers, see Figure 5.20) assumes that the esterification reaction between carboxylic acid and alcohol cannot be ignored. In addition to the formation paths of ketone discussed in Chapter 4, the increased yield of ketone in Irganox1076 stabilised LLDPE has also been suggested to result from the interaction of phenoxyl radicals (the residue of phenolic antioxidant after donating a hydrogen) with alkoxyl radicals formed in the decomposition of hydroperoxides during TSE extrusion (see Reaction 5.13) [129]. The alkoxyl radicals are transformed into ketone whereas the phenoxyl radical is transformed back into the original phenol molecule.

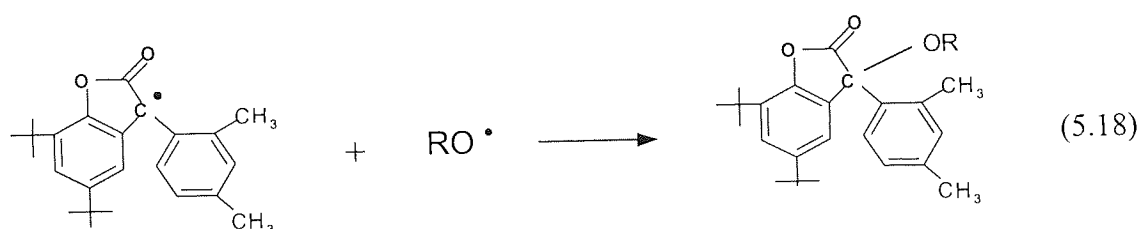
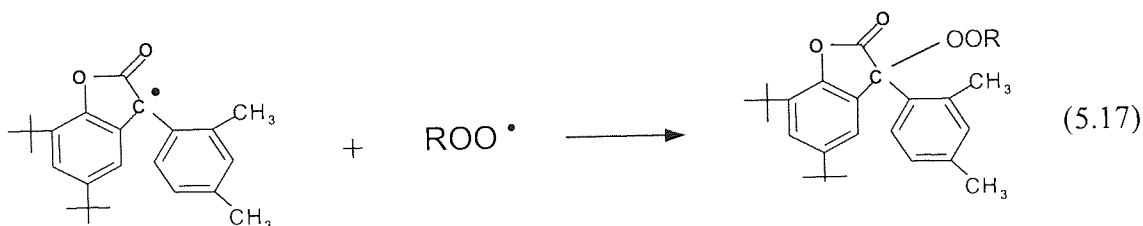
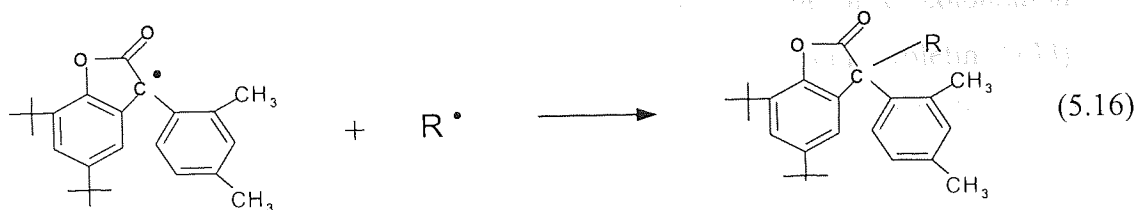


It is also clear from Figure 5.19(b) that in the case of the z-LLDPE, there is much larger increase in carbonyl concentration when the polymer is stabilised with all the antioxidants examined, particularly with Irganox1076 and Ultrinox626 (with respect to the corresponding virgin unprocessed polymer) in comparison with the other m-LLDPE (see Figure 5.19(b)). This indicates that the z-LLDPE undergoes much more oxidative degradation relative to the extent of degradation of metallocene polymers stabilised with the same antioxidants and extruded under the same conditions. It is shown from the FTIR spectra in carbonyl region (see Figure 5.20 to 5.23) that the most significant difference in the composition of carbonyl compounds between z-LLDPE containing phosphite with that of z-LLDPE containing other antioxidants is the disappearance of aldehyde absorbance (1730 cm^{-1}) and the considerable increase in 1714 and 1697 cm^{-1} peaks attributed to ketones and carboxylic acids in the phosphite stabilised polymer. The stabilising function of phosphite AO (see Reactions 5.8 to 5.11) is favourable for the decomposition of hydroperoxides and oxygen containing radicals, which prevents the yield of aldehyde *via* the transformation of these groups. Meanwhile, more alcohols would be expected to be produced through the PD-S reaction of phosphite (see Reaction 5.8) and their further oxidation in presence of Ziegler catalyst residue may lead to the formation of carboxylic acids. As a result, ketone and carboxylic acid become the two major compounds that account for the existence of great amount of carbonyls contained in Ultrinox626 stabilised z-LLDPE (see Figure 5.18). Reaction 5.13 is proposed to be a primary route for the formation of ketone when the phenoxyl radicals were yielded through Reaction 5.10.

Figure 5.19(b) shows that the differences in carbonyl change in all metallocene polymers stabilised with Irganox1076 and Ultrinox626 are very small. In the case of polymers stabilised with IrganoxE201, the increase in the carbonyl concentration may be due at least in part to the build-up of AO oxidation products which contain carbonyl absorptions such as spirodimer and trimer (see Reactions 5.14 and 5.15). These products were shown previously [140, 142] to form during extrusion of polyethylenes stabilised with vitamin E antioxidant.



In both the IrganoxE201 and lactone stabilised m-LLDPE polymers, it seems that there is a noticeable increase with extrusion passes in the extent of change of carbonyl concentration (relative to virgin unprocessed polymers, see Figure 5.19(b)), particularly in VP-8770 containing highest comonomer, as well as significant increase in the 1718 cm^{-1} band attributed to ketone; whereas in the case of z-LLDPE stabilised with these antioxidants, there is a very notable increase in both the 1730 and 1718 cm^{-1} bands attributed to aldehydes and ketones (see Figures 5.21 and 5.22). However, in the case of the lactone AO, all the LLDPE stabilised with this AO show lower carbonyl concentration compared to the corresponding unstabilised polymers after multi-pass extrusions (see Figure 5.19(a)). The primary 3-arylbenzofuran-2-one radicals formed in the first antioxidant step is expected to react further with alkyl, alkoxyl and peroxy radicals (see Reactions 5.16 to 5.18) resulting in their deactivation.

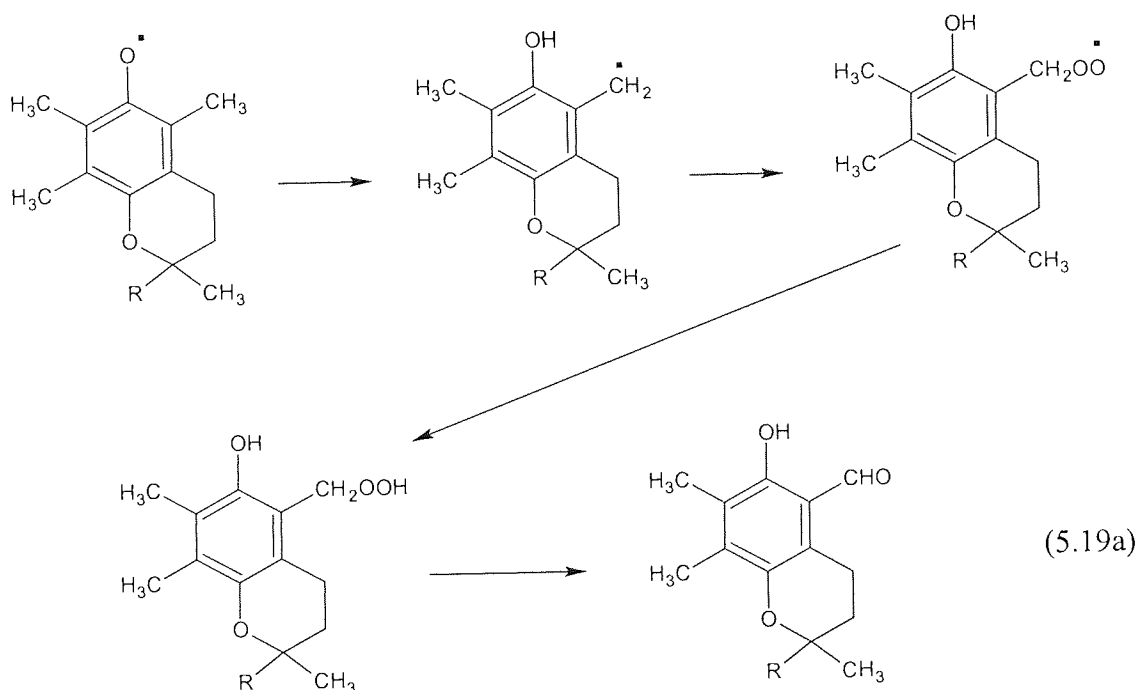
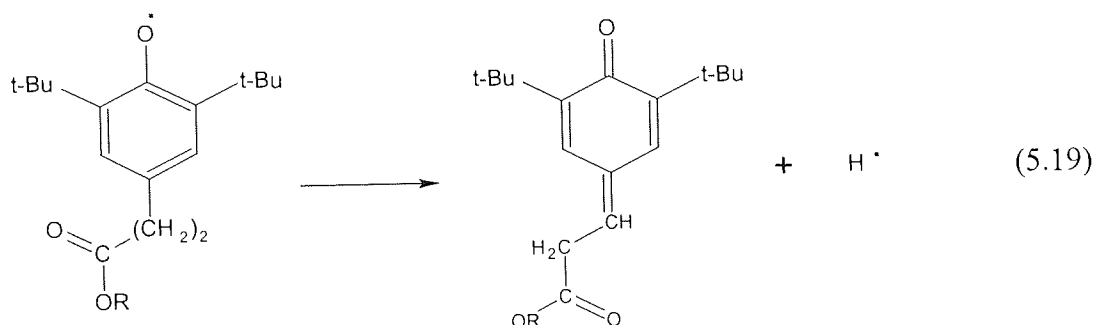


For the extrusion of LLDPE, the loss of short chain branches (SCB) is generally accompanied by the occurrence of chain scission and the generation of SCB is caused by crosslinking. The slight decrease of SCB content in the stabilised VP-8770 (m-LLDPE) compared to the virgin polymer (see Table 5.7) indicates that the primary reactions that affect the branching of the extruded polymers may be, at least in part, based on chain scission reactions. These reactions are very helpful in keeping a more constant melt viscosity and melt flow behaviour in the cases of both metallocene and Ziegler LLDPE, in which crosslinking is generally the predominant reaction during TSE extrusion. Compared with the unstabilised polymers (see Table 4.3 in Chapter 4), there are very small changes in SCB content in the presence of all the antioxidants in the polymers subjected to different passes of extrusions (P_1 and P_3).

5.3.1.3. Effects of Antioxidants on the Discolouration of LLDPE Polymers

All the antioxidants used here are shown to cause more discolouration to all the LLDPE polymers with increasing extrusion passes, see Table 5.8 and Figure 5.24. Generally, IrganoxE201 results in the largest extent of discolouration and

the phosphite, Ultrinox626, gives rise to lowest extent of discolouration. Phosphites are known to result in decreasing discolouration in polyolefins [133]. In the case of both hindered phenols, Irganox1076 and IrganoxE201, the reason for discolouration is by and large due to the formation of antioxidant oxidation products based on quinonoid type and aldehydic type products, see Reactions 5.19 and 5.19a [111, 142]. The reason for discolouration produced from IrganoxHP136 is not very clear and requires further investigation.



5.3.2. Melt Stabilisation Mechanisms of Antioxidant Mixtures in LLDPE

The higher effectiveness of hindered phenol and phosphite ester combined AO systems in melt stabilisation of PL-1840 (m-LLDPE) can be observed directly from the overall lower melt pressures of PL-1840 containing AO mixtures (indicating lower extents of crosslinking) compared to that of the single AO stabilised counterparts during multiple extrusions (see Tables 5.5 and 5.6). The synergistic effects of phenol-phosphite AO system on the stabilisation of LLDPE are highlighted in Scheme 5.2, which is similar to mechanisms suggested to be responsible for the co-operative effect of IrganoxE201 with phosphite, Ultrinox626 [130, 140, 142]. Phosphite ester is known to act as peroxide decomposer (PD-S mechanism) leading to reduction of hydroperoxides (ROOH), which formed in the polymer as a consequence of the antioxidant activity of hindered phenol (e.g. Irganox 1076, see Scheme 5.2, Reaction a); meanwhile alcohol is formed and the phosphite is oxidised to the corresponding phosphate (see Scheme 5.2, Reaction b). Additionally, IrganoxE201 has been shown to be a more effective melt stabiliser in the PL-1840 polymer than the Irganox1076-based AO system (Irganox 1076: Ultrinox626) even though the former was used at a lower concentration (see Figures 5.25 and 5.28). The higher antioxidant activity of the IrganoxE201-based system is mainly attributed to its highly efficient alkylperoxyl radical trapping capability resulting from the higher stability of the formed tocopheroxyl radical, compared to the phenoxyl radical formed from Irganox1076 [140, 142].

The presence of different phosphite antioxidants (used at the same phosphorus content, 0.006 wt% P) in the phenol-phosphite AO mixtures can significantly affect their performance as melt stabilisers in m-LLDPE (see Figures 5.26 and 5.27). The melt flow behaviour of extruded PL-1840 polymer stabilised by AO systems containing Irganox1076 and some typical phosphite antioxidants show that, Irganfos168 exhibits the most effective performance on the polymer stabilisation when combined with hindered phenols, whereas, Ultrinox626 and IrgafosP-EPQ present similar and the lowest effectiveness on the stabilisation of PL-1840 melt. As shown in Scheme 5.2, Irganfos168 is a hindered phosphite ester and has relatively strong tendency to undergo chain-breaking reactions (as well

The diagram illustrates the proposed mechanism for the degradation of Irganox 1076 and Irgafos 168. The scheme includes the following components:

- Chemical Structures:**
 - Irganox 1076:** A bisphenol structure with two phenolic rings, each substituted with a tert-butyl group and a (CH₃)₃C group. It is shown in its radical cation form (ROO[•]).
 - Irgafos 168:** A phosphite structure consisting of a central phosphorus atom bonded to three phenyl groups, each substituted with a tert-butyl group and a (CH₃)₃C group.
 - Radical Species:** ROO[•], RO[•], and a radical species derived from Irganox 1076 (HO-C(CH₃)₂-C(CH₃)₂-C(CH₃)₃).
 - Reaction Intermediates:** ROOH, ROH, and a radical species derived from Irgafos 168 (HO-C(CH₃)₂-C(CH₃)₂-C(CH₃)₃).
- Reaction Pathways:**
 - a:** Reaction of ROO[•] with Irganox 1076 to form ROOH and a radical species.
 - b:** Reaction of ROOH with Irgafos 168 to form ROH and a radical species.
 - c:** Reaction of RO[•] with Irganox 1076 to form a radical species.
 - d:** Reaction of RO[•] with Irgafos 168 to form a radical species.
 - e:** Reaction of a radical species with Irganox 1076 to form a radical species.
 - f:** Reaction of a radical species with Irgafos 168 to form a radical species.

Although Weston399 has relatively weaker chain breaking activity due to the unhindered aryl structure, it shows higher effectiveness on m-LLDPE melt

stabilisation than the other two phosphite antioxidants, Ultrinox626 and IrgafosP-EPQ. One reason could be due to the presence of three phenoxyl groups connected to the phosphorus atom in Weston399 structure (compared to only one in Ultrinox626 and two in IrgafosP-EPQ), see Table 2.3 in Chapter 2 for the molecular structures, Weston399 has more chances to undergo chain-breaking reactions (see Scheme 5.2 Reaction d) leading to the improvement of its stabilising effect. On the other hand, its liquid state enable Weston399 to be better spread in the polymer melt during processing and thus to perform more effectively as antioxidant. In addition, it is shown that the presence of the polyhydric alcohol, TMP, in the IrganoxE201 and Ultrinox626 AO combination can also impart a better performance to this stabilisation system (see Figures 5.25 and 5.28). This is mainly due to the plasticising function of TMP in polymer melt, which can be observed from the evidently lower power consumption during extrusions of PL-1840 containing TMP (see Table 5.6 for AO-E3), leading to a better dispersion of antioxidants in the stabilised polymer.

The use of lactone antioxidant (e.g. IrganoxHP136) in the phenol-phosphite AO combinations can further improve their stabilising functions for PL-1840 polymer upon multiple extrusions (see Figures 5.25 and 5.28). It has been reported that 3-arylbenzofuran-2-one can act effectively as a complementary chain breaking antioxidant, operating efficiently under processing conditions where alkyl (R^\bullet) and alkyl peroxy (ROO^\bullet) radicals are present in the polymers [143, 144, 145]. Thus lactone antioxidant has the ability to retard or inhibit the crosslinking and other chain reactions related to these radicals. Scheme 5.3 shows the synergistic actions and proposed mechanisms for the possible transformations and interactions between IrganoxHP136 and Irgafos168 (representative of phosphite AO's) [143]. The co-operative antioxidant actions of the lactone and phosphite are considered to be mainly responsible for the high extents of melt stability of the stabilised PL-1840 during TSE extrusions. The synergistic complementary effect between Irganox1076 (hindered phenol) and IrganoxHP136 (lactone) can also make contribution to the excellent stabilisation performance of these three AO combinations. Moreover, the AO mixtures

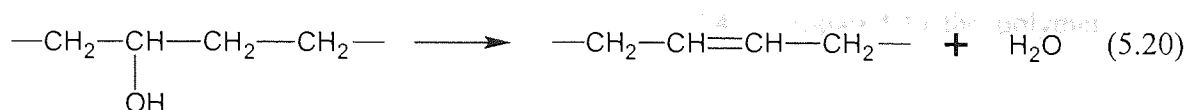
The diagram illustrates the degradation pathways of Irganox HP136 and Irgafos 168. Key components include:

- Irganox HP136**: A hindered phenol derivative with two tert-butyl groups and a 2,4,6-trimethylphenyl group.
- Irgafos 168**: A phosphine oxide derivative with three 2,4,6-trimethylphenyl groups.
- Radical Reactions**:
 - $R^\bullet + O_2 \rightarrow ROO^\bullet$
 - ROO^\bullet can undergo various reactions (a, b, c, d, e, f, g) leading to different products.
 - ROO^\bullet can react with R^\bullet or ROO^\bullet to form a cyclic peroxide (c).
 - ROO^\bullet can react with $PD-S$ to form ROH and a phosphine oxide (d).
 - ROO^\bullet can react with $Irgafos\ 168$ to form a phosphine oxide and a radical (e).
 - ROO^\bullet can react with CB to form a phosphine oxide and a radical (f).
 - ROO^\bullet can react with $CB-D$ to form $ROOH$ (a) or a radical adduct (b).
 - ROO^\bullet can react with $Irganox\ HP136$ to form a radical adduct (i).
 - ROO^\bullet can react with $Irganox\ HP136$ to form a radical adduct (g).
- Other Reactions**:
 - ROH can be formed from ROO^\bullet (d).
 - $ROOH$ can be formed from ROO^\bullet (a).
 - RO^\bullet can be formed from ROO^\bullet (e, f).
 - RO^\bullet can react with CB to form a radical adduct (f).
 - RO^\bullet can react with $CB-D$ to form a radical adduct (b).
 - RO^\bullet can react with $Irganox\ HP136$ to form a radical adduct (i).
 - RO^\bullet can react with $Irganox\ HP136$ to form a radical adduct (g).

273

Results presented in Figures 5.29 and 5.30 reveal that two commercial antioxidant blends based on three-AO combinations of Irganox1076 and IrganoxHP136 as well as either of the phosphites, Irgafos168 or IrgafosP-EPQ, show similar stabilising effects in the z-LLDPE polymer and are more effective in m-LLDPE containing more comonomers (VP-8770), indicating that the synergistic stabilisation action of these combined antioxidants may perform more efficiently for the polymer melt in which more alkyl peroxy radicals present (e.g. VP-8770, due to the higher SCB content). Meanwhile, the advantage of using higher concentrations of the hindered phenol (Irganox1076) in such AO combinations has also been confirmed (750 ppm in IrganoxXP490 compared to 500 ppm in IrganoxHP2921) from the better stabilisation performance of IrganoxXP490 in m-LLDPE melts (see Figure 5.31).

Examination of the concentrations of unsaturated groups has shown that compared to the unstabilised and singly stabilised (Irganox1076) PL-1840, the combination of Irganox1076 with Irgafos168 or Weston399 generally lead to the largest extent of increase in trans-vinylene in multi-pass extruded polymer (see Figures 5.32, 5.33 and 5.11). As alcohol is produced under the function of phosphite AO based on PD-S mechanism (see Scheme 5.2 Reaction b) and it can further transform into trans-vinylene through an acid-catalysed reaction (see Reaction 5.20), it is reasonable to suppose that Irgafos168 and Weston399 present more effective synergistic actions with hindered phenol (Irganox1076) compared to the other phosphite antioxidants examined while hydroperoxide is the most important oxidation intermediates. The presence of IrganoxHP136 (lactone) in phenol-phosphite AO system results in different changes of trans-vinylene concentration in extruded PL-1840 depending on the extrusion conditions and the nature of phosphite AO (see Figures 5.33 and 5.38(b)), which may lead to the dominance of different reactions in PL-1840 melt stabilisation. In addition, the use of biological hindered phenol, IrganoxE201, instead of Irganox1076 in the phenol-phosphite AO system can cause some, but not significant changes in trans-vinylene concentration (see Figures 5.32 and 5.33) in extruded polymers, and this is considered mainly due to the more effective chain breaking ability of this phenolic antioxidant.



The vinyl concentration in extruded PL-1840 stabilised with Irganox1076-phosphite AO mixtures generally decrease compared to the virgin polymer, with the exception of Irganox1076/ Irgafos168 stabilised PL-1840 (see Figure 5.35). Much more vinyl groups were found produced in the one-pass extruded PL-1840 polymer containing Irganox1076/ Irgafos168 and it is probably because that Irgafos168 is very effective in the transformation of hydroperoxides into alcohols (PD-S mechanism) during the first extrusion of the polymer, therefore, more alcohols on the end of polymer chains (primary alcohols) were also formed and they can transform further into vinyl groups *via* a similar reaction to that shown in Reaction 5.20. The vinyl concentration tends to decrease with increasing extrusion passes due to the consumption of Irgafos168 and the occurrence of higher extent of crosslinking involving vinyl group (see Figure 5.25). Figure 5.35 also shows that the vinyl concentration in most Irganox1076-phosphite stabilised PL-1840 is lower than that in Irganox1076 single stabilised polymer and the reason for this result is not very clear. Adding IrganoxHP136 (lactone) in this phenol-phosphite AO system seems to have no significant effect on the vinyl concentration in the extruded polymer no matter what phosphite antioxidant was used (see Figure 4.38(b)). Moreover, the use of another hinder phenol (IrganoxE201 rather than Irganox1076) in the phenol-phosphite combined antioxidants seems not significantly to affect the vinyl concentration in the stabilised PL-1840 upon multiple extrusions (see Figures 5.34 and 5.35).

Figures 5.36 and 5.37 show that there are only small differences in vinylidene concentration in the PL-1840 stabilised by different phenol-phosphite AO mixtures upon multiple extrusions, and adding the lactone antioxidant, IrganoxHP136, has very little effect on vinylidene concentration in the extruded polymers (also see Figure 5.38(b)). Therefore, it can be assumed that vinylidene concentration in extruded PL-1840 is not significantly affected by the difference of the phenol-phosphite based stabilisation system. Meanwhile, the combination of Irganox1076/phosphite (as well as the lactone) generally leads to production

of more vinylidene groups in the extruded PL-1840 compared to the polymer only containing hindered phenol (see Figure 5.37).

The effects of two commercial phenol-phosphite-lactone combined antioxidants on the concentrations of unsaturated groups in different LLDPE polymers (see Figures 5.39 and 5.40) show that the Irgafos168 contained AO mixture (IrganoxHP2921, Irganox1076: Irgafos168: IrganoxHP136 = 2:4:1) can significantly increase the trans-vinylene concentration in the polymers when multi-pass extrusions were carried out. This confirms further the major formation route of trans-vinylene in the presence of Irganox1076 and Irgafos168 discussed before. Additionally, the much more vinyl groups in P_0 extruded z-LLDPE containing IrganoxHP2921 (see Figure 5.39) are most likely on account of the more terminal alkyl radicals that present in this polymer, which can transform further into primary alcohols under the function of Irgafos168, and then vinyl groups (see Reaction 5.20). Very similar extent of increase in vinyl concentration in m-LLDPE containing IrganoxHP2921 after compounding step (P_0) can also be observed from Figure 5.40. There is no evident difference in vinylidene concentration in all the examined polymers stabilised by these two commercial AO mixtures after extrusions. In general, the changes of unsaturated groups in extruded LLDPE containing commercial phenol-phosphite-lactone AO systems correspond well with the results obtained from the polymer stabilised by the similar AO combinations that were achieved in compounding step. Moreover, Figure 5.41 indicates that the difference in the composition of this three-AO commercial stabilising package can significantly affect the content of various unsaturated groups in LLDPE polymers upon multi-pass extrusions.

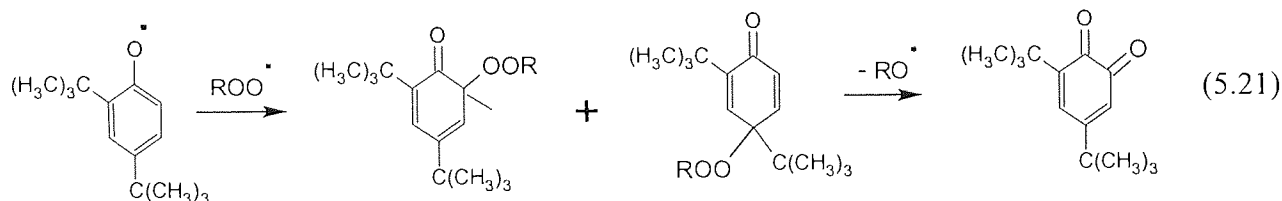
The carbonyl concentrations in PL-1840 are generally similar for the polymers stabilised by Irganox1076 and different phosphite antioxidants under the same extrusion conditions (see Figure 5.42), and the three-AO containing polymer always has much lower carbonyl content compared to the hindered phenol single stabilised PL-1840, indicating the higher effectiveness of this AO combination in stabilising m-LLDPE during extrusion (see Figure 5.43). In the mean time, there is no evident effect on the amount of carbonyl compounds in extruded polymers when lactone (IrganoxHP136) was added into the phenol-phosphite AO systems

(see Figure 5.43). However, it is worth noting that the PL-1840 stabilised by AO mixtures containing Irgafos168 overall have lower carbonyl concentrations after multiple extrusions (see Figures 5.44 and 5.45). This should be attributed to the very effective peroxide deactivation activity of Irgafos168, avoiding the yield of more carbonyl compounds *via* peroxide decomposition. Furthermore, the extruded PL-1840 stabilised by IrganoxE201/Ultranox626 AO system contains relatively less carbonyl compounds compared to the counterpart containing Irganox1076/Ultranox626 mixtures under the same extrusion conditions (see Figures 5.42 and 5.43). The higher effectiveness of IrganoxE201 on polymer stabilisation through CB-D mechanism, lowering the production of macro-alkyl radicals, is suggested to account for the formation of less carbonyl compounds in the extruded polymers. Figures 5.46 to 5.48 indicate that all LLDPE polymers (especially *z*-LLDPE) stabilised with Irgafos168 involved phenol-phosphite-lactone commercial AO system (IrganoxHP2921) generally contain less carbonyl compounds than those stabilised with the other similar commercial AO combination (IrganoxXP490) after TSE extrusions, and this confirms further the advantage of Irgafos168 in reducing the carbonyl production in processed LLDPE when combined with hindered phenols.

The FTIR spectra in carbonyl region for extruded PL-1840 containing Irganox1076 and different phosphites (see Figure 5.54) show that, the different phosphite antioxidants almost have no effect on the composition of carbonyl compounds in the extruded polymers, and the addition of lactone (IrganoxHP136) in phenol-phosphite AO system does not significantly affect the carbonyl composition either. Similarly, the use of IrganoxE201 instead of Irganox1076 in phenol-phosphite combination has not been found to lead to evident changes in carbonyl composition in the stabilised PL-1840 upon multi-pass extrusions (see Figures 5.54 and 5.55). The dominant absorbance peak of ester is mainly attributed to the ester group contained in Irganox1076 and the esters produced from esterification reaction of carboxylic acids and alcohols, which formed *via* the PD-S stabilisation mechanism of phosphite, seems to be less important. The stronger absorbance of ketones indicates the importance of ketone formation via the interaction of phenoxyl and alkoxyl radicals (see Reaction 5.13). The carbonyl composition of different extruded LLDPE

stabilised by commercial AO mixture, IrganoxXP490 (Irg1076: IrgP-EPQ: HP136 = 3:2:1), has been shown in FTIR spectra in Figure 5.56. It can be seen that the carbonyl composition is very similar for stabilised metallocene polymers. However, z-LLDPE contains much more ketone when multi-pass extrusions were carried out, indicating the formation of more secondary alkoxy radicals with increasing extrusion passes. Meanwhile, the considerable concentration of carboxylic acid in extruded z-LLDPE is supposed to be attributed to further oxidation of alcohols produced by the stabilising function of phosphites under the catalysis of Ziegler catalyst residue.

The comparison of yellow index (YI) of extruded PL-1840 stabilised by Irganox1076 and different phosphite antioxidants (see Figures 5.49 to 5.51) reveals that the polymer containing Irgafos168 shows the highest level of discolouration and the Ultrinox626 contained polymer shows the least. This indicates to some extents the capability of phosphite antioxidant undergoing chain breaking reactions (see Scheme 5.2, Reaction d), as the products of these reactions, phenoxyl radicals, can further interact with peroxy and alkoxy radicals and transform into some coloured products (see Reaction 5.21) [117].



The presence of lactone antioxidant (IrganoxHP136) in phenol-phosphite AO system can remarkably increase the extent of discolouration in the extruded PL-1840. This is most likely due to the yellowing caused by the coloured materials transformed from the benzofuranone radicals (see Scheme 5.3 Reaction c and h). IrganoxE201 can also lead to more serious discolouration in the extruded PL-1840, and the coloured products derived from IrganoxE201 has been described in Reaction 5.19a. The presence of the polyhydric alcohol, TMP, in the AO system can give a lower extent of discolouration, as shown in Figure 5.46. Finally, the effect of two commercial phenol-phosphite-lactone AO systems on the discolouration of different LLDPE has been examined (see Figures 5.52 and

5.53). It is indicated that the IrgafosP-EPQ containing AO mixtures (IrganoxXP490) are more liable to cause higher extent of discolouration in the extruded m-LLDPE with higher SCB content (VP-8770). This is considered to be due to the higher phenolic AO content (Irg1076) in IrganoxXP490, leading to the production of more coloured quinonoid structure (see Reaction 5.19) in the extruded VP-8770, in which macro-alkyl and peroxy radicals are more likely to be formed during extrusions.

Table 5.4. TSE Extrusion Characteristics of P₀ for LLDPE Compounded with Single and Combined Antioxidants

| Single Antioxidant or AO Mixture Code | Polymer Code | Screw Speed (rpm) | T _{die} (°C) | Output Rate (kg/hr) | Pressure (psi)±5% | I (A) ±0.5 | Power Consumption (kW.h/kg) |
|--|-----------------|-------------------------|--------------------------|------------------------|----------------------|---------------|-----------------------------------|
| Single Antioxidants | | | | | | | |
| Irganox1076 | FM-1570 | 100 | 210 | 4.0 | 645 | 10.0 | 0.30 |
| | PL-1840 | 100 | 210 | 4.0 | 720 | 10.5 | 0.32 |
| | VP-8770 | 100 | 210 | 4.0 | 855 | 10.0 | 0.30 |
| | Dowlex2045E* | 100 | 210 | 4.0 | 765 | 8.5 | 0.26 |
| IrganoxHP136 | FM-1570 | 100 | 210 | 4.0 | 650 | 10.0 | 0.30 |
| | PL-1840 | 100 | 210 | 4.0 | 730 | 10.0 | 0.30 |
| | VP-8770 | 100 | 210 | 4.0 | 880 | 10.5 | 0.32 |
| | Dowlex2045E | 100 | 210 | 4.0 | 860 | 9.5 | 0.29 |
| Ultranox626 | FM-1570 | 100 | 210 | 4.0 | 655 | 10.0 | 0.30 |
| | PL-1840 | 100 | 210 | 4.0 | 720 | 10.0 | 0.30 |
| | VP-8770 | 100 | 210 | 4.0 | 860 | 10.0 | 0.30 |
| | Dowlex2045E | 100 | 210 | 4.0 | 870 | 10.0 | 0.30 |
| IrganoxE201 | FM-1570 | 100 | 210 | 4.0 | 670 | 10.0 | 0.30 |
| | PL-1840 | 100 | 210 | 4.0 | 740 | 10.0 | 0.30 |
| | VP-8770 | 100 | 210 | 4.0 | 860 | 10.0 | 0.30 |
| | Dowlex2045E | 100 | 210 | 4.0 | 860 | 9.5 | 0.29 |
| Antioxidant (AO) Mixtures[#] | | | | | | | |
| AO-A1 | PL-1840 | 100 | 210 | 4.0 | 680 | 10.0 | 0.30 |
| AO-A2 | PL-1840 | 100 | 210 | 4.0 | 685 | 10.5 | 0.32 |
| AO-B1 | PL-1840 | 100 | 210 | 4.0 | 645 | 10.5 | 0.32 |
| AO-B2 | PL-1840 | 100 | 210 | 4.0 | 670 | 10.5 | 0.32 |
| AO-C1 | PL-1840 | 100 | 210 | 4.0 | 640 | 10.5 | 0.32 |
| AO-C2 | PL-1840 | 100 | 210 | 4.0 | 675 | 10.5 | 0.32 |
| AO-D1 | PL-1840 | 100 | 210 | 4.0 | 675 | 10.5 | 0.32 |
| AO-D2 | PL-1840 | 100 | 210 | 4.0 | 675 | 10.5 | 0.32 |
| AO-E1 | PL-1840 | 100 | 210 | 4.0 | 670 | 10.1 | 0.31 |
| AO-E2 | PL-1840 | 100 | 210 | 4.0 | 670 | 10.0 | 0.30 |
| AO-E3 | PL-1840 | 100 | 210 | 4.0 | 650 | 8.5 | 0.26 |
| AO-F | PL-1840 | 100 | 210 | 4.0 | 670 | 10.0 | 0.30 |
| | VP-8770 | 100 | 210 | 4.0 | 730 | 10.2 | 0.31 |
| | Dowlex2045E | 100 | 210 | 4.0 | 815 | 10.0 | 0.30 |
| AO-G | PL-1840 | 100 | 210 | 4.0 | 655 | 10.5 | 0.32 |
| | VP-8770 | 100 | 210 | 4.0 | 760 | 10.0 | 0.30 |
| | Dowlex2045E | 100 | 210 | 4.0 | 830 | 10.0 | 0.30 |

* Old batch polymer was used

For the codes of AO mixtures see Table 5.2

Table 5.5. TSE Extrusion Characteristics of P₁-P₅ for Stabilised LLDPE
Containing Single Antioxidants

| Single Antioxidant | Polymer Code | Extrusion Passes | Screw Speed (rpm) | T _{die} (°C) | Output Rate (kg/hr) | Pressure (psi)+5% | I (A) ±0.5 | Power Consumption (kW.h/kg) |
|--------------------|--------------|------------------|-------------------|-----------------------|---------------------|-------------------|------------|-----------------------------|
| Irganox1076 | FM-1570 | 1 | 100 | 265 | 4.8 | 470 | 11.0 | 0.28 |
| | | 3 | | | 4.8 | 470 | 11.0 | 0.28 |
| | | 5 | | | 4.8 | 470 | 11.0 | 0.28 |
| | PL-1840 | 1 | 100 | 265 | 4.7 | 530 | 11.0 | 0.28 |
| | | 3 | | | 4.7 | 550 | 11.5 | 0.30 |
| | | 5 | | | 4.7 | 530 | 11.0 | 0.28 |
| | VP-8770 | 1 | 100 | 265 | 4.8 | 600 | 11.5 | 0.29 |
| | | 3 | | | 4.7 | 590 | 11.5 | 0.30 |
| | | 5 | | | 4.8 | 600 | 12.0 | 0.30 |
| | Dowlex2045E | 1 | 100 | 265 | 4.8 | 610 | 11.0 | 0.28 |
| | | 3 | | | 4.8 | 630 | 11.5 | 0.29 |
| | | 5 | | | 4.8 | 630 | 12.0 | 0.30 |
| IrganoxHP136 | FM-1570 | 1 | 100 | 265 | 4.8 | 465 | 11.0 | 0.28 |
| | | 3 | | | 4.8 | 465 | 11.0 | 0.28 |
| | | 5 | | | 4.8 | 465 | 11.0 | 0.28 |
| | PL-1840 | 1 | 100 | 265 | 4.8 | 535 | 11.0 | 0.28 |
| | | 3 | | | 4.8 | 530 | 11.0 | 0.28 |
| | | 5 | | | 4.8 | 545 | 11.5 | 0.29 |
| | VP-8770 | 1 | 100 | 265 | 4.7 | 620 | 11.0 | 0.28 |
| | | 3 | | | 4.8 | 620 | 11.0 | 0.28 |
| | | 5 | | | 4.7 | 590 | 11.5 | 0.30 |
| | Dowlex2045E | 1 | 100 | 265 | 4.8 | 700 | 12.0 | 0.30 |
| | | 3 | | | 4.8 | 670 | 12.0 | 0.30 |
| | | 5 | | | 4.8 | 660 | 12.0 | 0.30 |
| Ultranox626 | FM-1570 | 1 | 100 | 265 | 4.8 | 460 | 11.0 | 0.28 |
| | | 3 | | | 4.8 | 485 | 11.0 | 0.28 |
| | | 5 | | | 4.8 | 500 | 11.0 | 0.28 |
| | PL-1840 | 1 | 100 | 265 | 4.8 | 520 | 11.0 | 0.28 |
| | | 3 | | | 4.8 | 550 | 11.0 | 0.28 |
| | | 5 | | | 4.8 | 570 | 11.5 | 0.29 |
| | VP-8770 | 1 | 100 | 265 | 4.8 | 620 | 11.0 | 0.28 |
| | | 3 | | | 4.6 | 610 | 11.5 | 0.30 |
| | | 5 | | | 4.7 | 620 | 11.5 | 0.30 |
| | Dowlex2045E | 1 | 100 | 265 | 4.8 | 670 | 12.0 | 0.30 |
| | | 3 | | | 4.8 | 700 | 12.0 | 0.30 |
| | | 5 | | | 4.8 | 710 | 12.0 | 0.30 |
| IrganoxE201 | FM-1570 | 1 | 100 | 265 | 4.8 | 470 | 11.0 | 0.28 |
| | | 3 | | | 4.7 | 460 | 11.0 | 0.28 |
| | | 5 | | | 4.8 | 470 | 11.0 | 0.28 |
| | PL-1840 | 1 | 100 | 265 | 4.8 | 550 | 11.5 | 0.29 |
| | | 3 | | | 4.8 | 550 | 11.0 | 0.28 |
| | | 5 | | | 4.8 | 550 | 11.5 | 0.29 |
| | VP-8770 | 1 | 100 | 265 | 4.8 | 620 | 12.0 | 0.30 |
| | | 3 | | | 4.7 | 600 | 11.5 | 0.30 |
| | | 5 | | | 4.7 | 600 | 11.5 | 0.30 |
| | Dowlex2045E | 1 | 100 | 265 | 4.8 | 700 | 11.5 | 0.29 |
| | | 3 | | | 4.8 | 690 | 12.0 | 0.30 |
| | | 5 | | | 4.8 | 690 | 12.5 | 0.32 |

Table 5.6. TSE Extrusion Characteristics of P₁~P₅ for Stabilised LLDPE Containing AO Mixtures

| AO Mixture Code * | Polymer Code | Extrusion Passes | Screw Speed (rpm) | T _{die} (°C) | Output Rate (kg/hr) | Pressure (psi) | I (A) | Power Consumption (kW.h/kg) |
|-------------------|--------------|------------------|-------------------|-----------------------|---------------------|----------------|-------|-----------------------------|
| AO-A1 | PL-1840 | 1 | 100 | 265 | 4.8 | 495 | 11.5 | 0.29 |
| | | 3 | | | 4.8 | 490 | 11.5 | 0.29 |
| | | 5 | | | 4.8 | 485 | 11.5 | 0.29 |
| AO-A2 | PL-1840 | 1 | 100 | 265 | 4.8 | 485 | 11.5 | 0.29 |
| | | 3 | | | 4.8 | 490 | 11.5 | 0.29 |
| | | 5 | | | 4.8 | 480 | 11.5 | 0.29 |
| AO-B1 | PL-1840 | 1 | 100 | 265 | 4.8 | 480 | 11.5 | 0.29 |
| | | 3 | | | 4.8 | 490 | 11.5 | 0.29 |
| | | 5 | | | 4.8 | 505 | 11.5 | 0.29 |
| AO-B2 | PL-1840 | 1 | 100 | 265 | 4.8 | 480 | 11.5 | 0.29 |
| | | 3 | | | 4.8 | 485 | 11.5 | 0.29 |
| | | 5 | | | 4.8 | 490 | 12.0 | 0.30 |
| AO-C1 | PL-1840 | 1 | 100 | 265 | 4.7 | 430 | 11.5 | 0.30 |
| | | 3 | | | 4.8 | 480 | 11.5 | 0.29 |
| | | 5 | | | 4.8 | 505 | 11.5 | 0.29 |
| AO-C2 | PL-1840 | 1 | 100 | 265 | 4.8 | 470 | 11.5 | 0.29 |
| | | 3 | | | 4.8 | 490 | 11.5 | 0.29 |
| | | 5 | | | 4.8 | 490 | 11.5 | 0.29 |
| AO-D1 | PL-1840 | 1 | 100 | 265 | 4.8 | 490 | 11.5 | 0.29 |
| | | 3 | | | 4.8 | 480 | 11.5 | 0.29 |
| | | 5 | | | 4.7 | 500 | 11.5 | 0.30 |
| AO-D2 | PL-1840 | 1 | 100 | 265 | 4.8 | 490 | 11.5 | 0.29 |
| | | 3 | | | 4.8 | 490 | 11.5 | 0.29 |
| | | 5 | | | 4.8 | 475 | 11.5 | 0.29 |
| AO-E1 | PL-1840 | 1 | 100 | 265 | 4.8 | 500 | 11.0 | 0.28 |
| | | 3 | | | 4.8 | 490 | 11.0 | 0.28 |
| | | 5 | | | 4.8 | 480 | 11.0 | 0.28 |
| AO-E2 | PL-1840 | 1 | 100 | 265 | 4.8 | 480 | 11.0 | 0.28 |
| | | 3 | | | 4.8 | 485 | 11.0 | 0.28 |
| | | 5 | | | 4.8 | 480 | 11.0 | 0.28 |
| AO-E3 | PL-1840 | 1 | 100 | 265 | 4.8 | 465 | 9.8 | 0.25 |
| | | 3 | | | 4.8 | 500 | 9.9 | 0.25 |
| | | 5 | | | 4.8 | 480 | 10.0 | 0.25 |
| AO-F | PL-1840 | 1 | 100 | 265 | 4.8 | 430 | 11.5 | 0.29 |
| | | 3 | | | 4.7 | 475 | 11.5 | 0.30 |
| | | 5 | | | 4.7 | 490 | 11.5 | 0.30 |
| | VP-8770 | 1 | 100 | 265 | 4.8 | 535 | 11.5 | 0.29 |
| | | 3 | | | 4.7 | 550 | 12.0 | 0.31 |
| | | 5 | | | 4.7 | 570 | 11.5 | 0.30 |
| | Dowlex2045E | 1 | 100 | 265 | 4.8 | 610 | 11.5 | 0.29 |
| | | 3 | | | 4.8 | 680 | 11.8 | 0.30 |
| | | 5 | | | 4.8 | 655 | 12.0 | 0.30 |
| AO-G | PL-1840 | 1 | 100 | 265 | 4.8 | 475 | 11.8 | 0.30 |
| | | 3 | | | 4.8 | 490 | 11.8 | 0.30 |
| | | 5 | | | 4.8 | 500 | 11.5 | 0.29 |
| | VP-8770 | 1 | 100 | 265 | 4.6 | 550 | 11.0 | 0.29 |
| | | 3 | | | 4.6 | 545 | 11.0 | 0.29 |
| | | 5 | | | 4.6 | 530 | 11.0 | 0.29 |
| | Dowlex2045E | 1 | 100 | 265 | 4.8 | 630 | 11.8 | 0.30 |
| | | 3 | | | 4.8 | 660 | 12.0 | 0.30 |
| | | 5 | | | 4.8 | 670 | 12.0 | 0.30 |

* See Table 5.2 for the Code of AO mixtures (Page 243)

Table 5.7. SCB Content (weight %) in TSE Processed LLDPE (265°C, 100rpm)
Containing Different Single Antioxidants (Measured by ^{13}C -NMR)

| Polymer | Virgin | Pass | Extent of SCB (wt % 1-Octene) From ^{13}C -NMR | | | |
|------------------|------------|------|---|-------|-------------|-------------|
| | | | Antioxidant | | | |
| | | | Irganox1076 | HP136 | IrganoxE201 | Ultranox626 |
| VP-8770 | 28.2 | 1 | 26.4 | 26.4 | 26.6 | 26.3 |
| | | 3 | 26.6 | 26.3 | 26.7 | 26.0 |
| Dowlex 2045E* | 10.5 (Old) | 1 | 10.5 | 9.8 | 9.7 | 9.8 |
| | 9.6 (New) | 3 | 10.8 | 10.0 | 9.6 | 10.0 |

* Dowlex2045E containing Irganox1076 is old batch polymer (SCB content = 10.5);
Dowlex2045E containing other antioxidants are new batch polymers (SCB content = 9.6).

Table 5.8. Yellow Index (YI) and Its Changes (YI-YI₀) of TSE Extruded LLDPE
Containing Single Antioxidant Measured by Spectrophotometry

| Extrusion Pass | | P ₀ | | P ₁ | | P ₃ | | P ₅ | |
|----------------|-------------|----------------|----------------------|----------------|----------------------|----------------|----------------------|----------------|----------------------|
| Polymer | Antioxidant | YI | YI-YI ₀ * | YI | YI-YI ₀ * | YI | YI-YI ₀ * | YI | YI-YI ₀ * |
| FM-1570 | Irganox1076 | -2.37 | 0.35 | 0.67 | 3.39 | 4.06 | 6.78 | 7.43 | 10.2 |
| | HP136 | -1.83 | 0.89 | 1.42 | 4.14 | 5.49 | 8.21 | 8.85 | 11.6 |
| | Ultranox626 | -4.89 | -2.17 | -2.86 | -0.14 | 0.27 | 2.99 | 3.82 | 6.54 |
| | IrganoxE201 | 0.88 | 3.6 | 3.51 | 6.23 | 9.74 | 12.5 | 15.0 | 17.7 |
| PL-1840 | Irganox1076 | -2.93 | -2.65 | -1.51 | -1.23 | 1.74 | 2.02 | 5.36 | 5.64 |
| | HP136 | -3.07 | -2.79 | -0.67 | -0.39 | 4.22 | 4.50 | 9.22 | 9.50 |
| | Ultranox626 | -3.34 | -3.06 | -0.91 | -0.63 | 4.12 | 4.40 | 10.5 | 10.8 |
| | IrganoxE201 | -1.94 | -1.66 | 2.66 | 2.94 | 11.5 | 11.8 | 20.0 | 20.2 |
| VP-8770 | Irganox1076 | 3.56 | 0.76 | 7.79 | 4.99 | 11.0 | 8.15 | 13.6 | 10.8 |
| | HP136 | 4.57 | 1.77 | 8.06 | 5.26 | 12.7 | 9.90 | 15.9 | 13.1 |
| | Ultranox626 | 3.78 | 0.98 | 5.85 | 3.05 | 9.81 | 7.01 | 16.8 | 14.0 |
| | IrganoxE201 | 7.93 | 5.13 | 10.8 | 8.02 | 15.8 | 13.0 | 20.3 | 17.5 |
| Dowlex2045E ** | Irganox1076 | 10.3 | 6.86 | 13.4 | 10.0 | 17.8 | 14.4 | 20.2 | 16.8 |
| | HP136 | -1.97 | 0.80 | 6.78 | 9.55 | 13.7 | 16.4 | 19.9 | 22.7 |
| | Ultranox626 | -4.46 | -1.69 | -0.67 | -2.10 | 3.14 | 5.91 | 5.38 | 8.15 |
| | IrganoxE201 | -0.76 | 2.01 | 8.04 | 10.8 | 17.3 | 20.0 | 22.8 | 25.6 |

* YI₀ is the yellow index of corresponding virgin polymers

** Dowlex2045E containing Irganox1076 is old batch polymer and the YI₀ = 3.44;
Dowlex2045E containing other antioxidants are new batch polymers and the YI₀ = -2.77.

Table 5.9. Yellow Index (YI) and Its Changes (YI-YI₀) of TSE Extruded LLDPE Containing Antioxidant Mixtures (Measured by Spectrophotometry)

| Extrusion Pass | | P ₀ (210°C) | | P ₁ (265°C) | | P ₃ (265°C) | | P ₅ (265°C) | |
|----------------|-------------|------------------------|----------------------|------------------------|----------------------|------------------------|----------------------|------------------------|----------------------|
| Antioxidant * | Polymer ** | YI | YI-YI ₀ # | YI | YI-YI ₀ # | YI | YI-YI ₀ # | YI | YI-YI ₀ # |
| AO-A1 | PL-1840 | -3.56 | -1.82 | -1.44 | 0.30 | 1.48 | 3.22 | 3.73 | 5.47 |
| AO-A2 | PL-1840 | -3.14 | -1.40 | -1.53 | 0.21 | 2.05 | 3.79 | 5.22 | 6.96 |
| AO-B1 | PL-1840 | -3.99 | -2.25 | -2.36 | -0.62 | -0.67 | 1.07 | 1.60 | 3.34 |
| AO-B2 | PL-1840 | -3.92 | -2.18 | -1.57 | 0.17 | 1.10 | 2.84 | 4.63 | 6.37 |
| AO-C1 | PL-1840 | -4.33 | -2.59 | -2.25 | -0.51 | 0.48 | 2.22 | 2.70 | 4.44 |
| AO-C2 | PL-1840 | -4.82 | -3.08 | -1.85 | -0.11 | 1.96 | 3.70 | 4.93 | 6.67 |
| AO-D1 | PL-1840 | -3.72 | -1.98 | -1.61 | 0.13 | 0.27 | 2.01 | 2.51 | 4.25 |
| AO-D2 | PL-1840 | -4.00 | -2.26 | -1.64 | 0.10 | 0.97 | 2.71 | 4.11 | 5.85 |
| AO-E1 | PL-1840 | -3.05 | -1.31 | 3.12 | 4.86 | 7.36 | 9.10 | 13.4 | 15.1 |
| AO-E2 | PL-1840 | -3.13 | -1.39 | 2.82 | 4.56 | 8.86 | 10.6 | 14.7 | 16.4 |
| AO-E3 | PL-1840 | -1.85 | -0.11 | 2.87 | 4.61 | 5.51 | 7.25 | 9.58 | 11.3 |
| AO-F | PL-1840 | -4.56 | -2.82 | -1.48 | 0.26 | 1.85 | 3.59 | 4.81 | 6.55 |
| | VP-8770 | 5.77 | 4.27 | 9.27 | 7.77 | 13.6 | 12.1 | 17.0 | 15.5 |
| | Dowlex2045E | -1.13 | 1.64 | 2.35 | 5.12 | 9.57 | 12.3 | 12.8 | 15.6 |
| AO-G | PL-1840 | -2.06 | -0.32 | -0.41 | 1.33 | 2.40 | 4.14 | 4.15 | 5.89 |
| | VP-8770 | 3.07 | 1.57 | 6.28 | 4.78 | 8.76 | 7.26 | 10.3 | 8.77 |
| | Dowlex2045E | 0.92 | 3.69 | 5.31 | 8.08 | 12.4 | 15.2 | 14.9 | 17.7 |

* See Table 5.2 for the Code of AO mixtures (Page 243)

** The LLDPE used are all new batch polymers, and their YI₀ are respectively:

PL-1840, -1.74; VP-8770, 1.50; Dowlex2045E, -2.77

YI₀ is the yellow index of corresponding virgin polymers

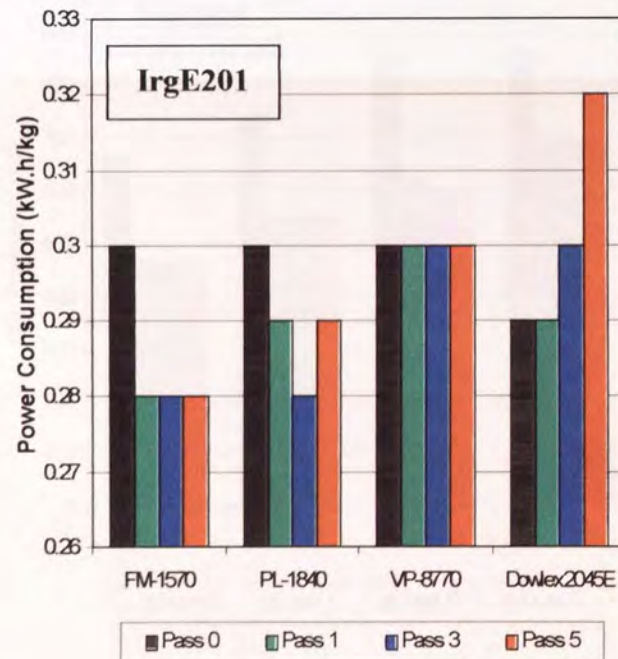
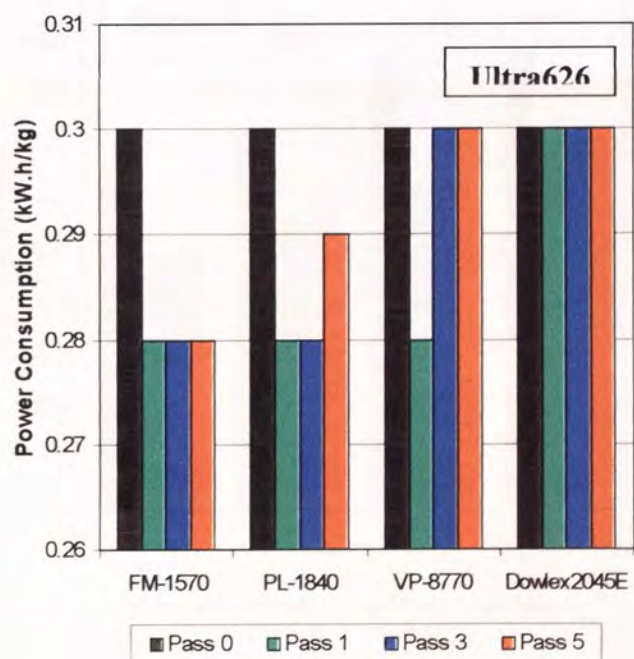
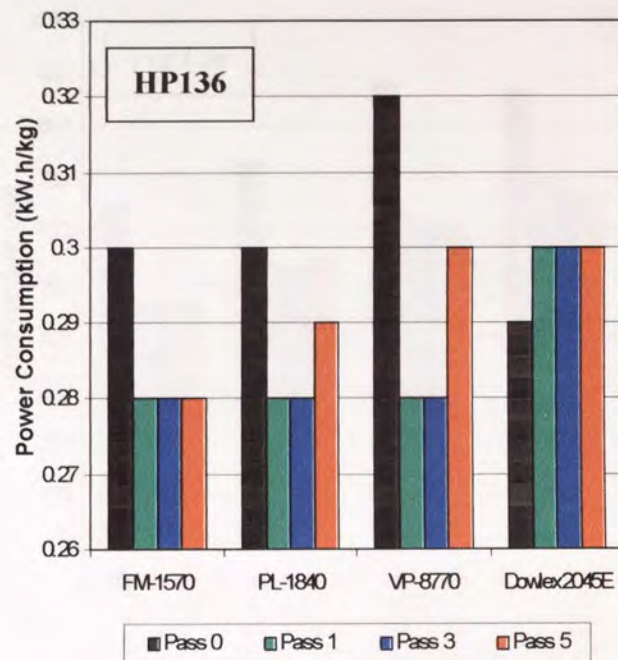
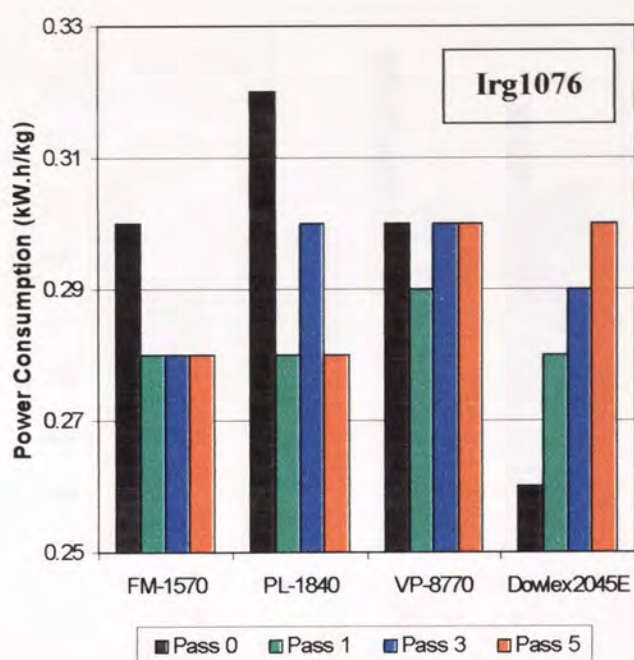


Figure 5.1. Power Consumption of TSE Extrusion for LLDPE Stabilised with Single Antioxidants (210°C, 100rpm, 4.0kg/hr for P₀, 265°C, 100rpm, 4.8kg/hr for P₁~P₅)

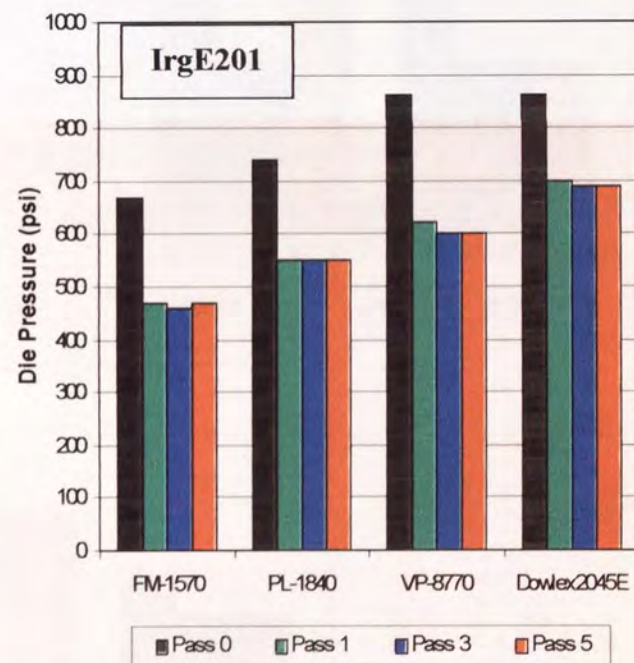
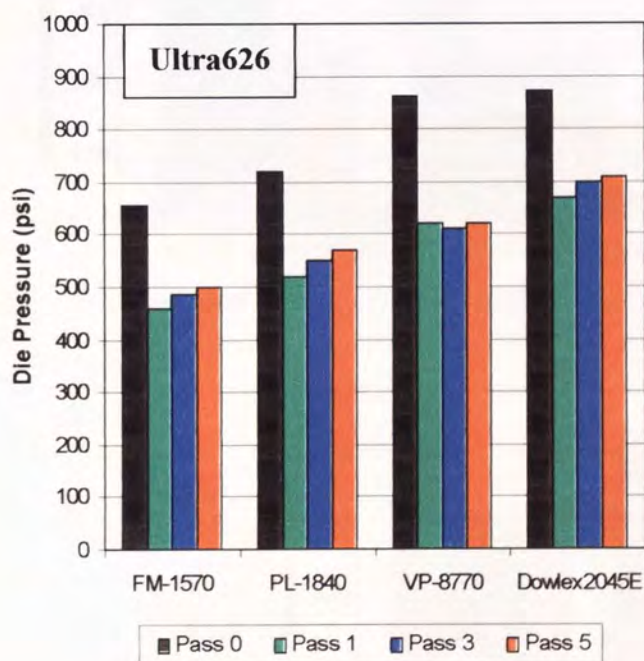
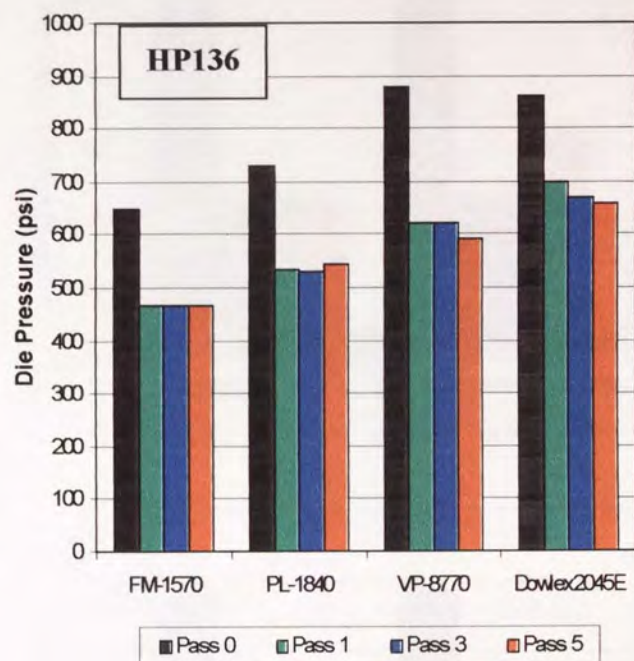
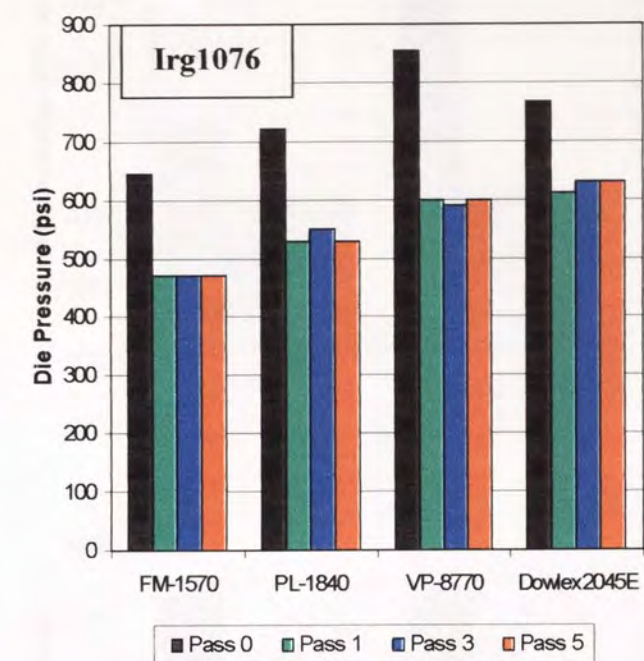


Figure 5.2. Die Pressure of TSE Extrusion for LLDPE Stabilised with Single Antioxidants (210°C, 100rpm, 4.0kg/hr for P₀, 265°C, 100rpm, 4.8kg/hr for P₁~P₅)

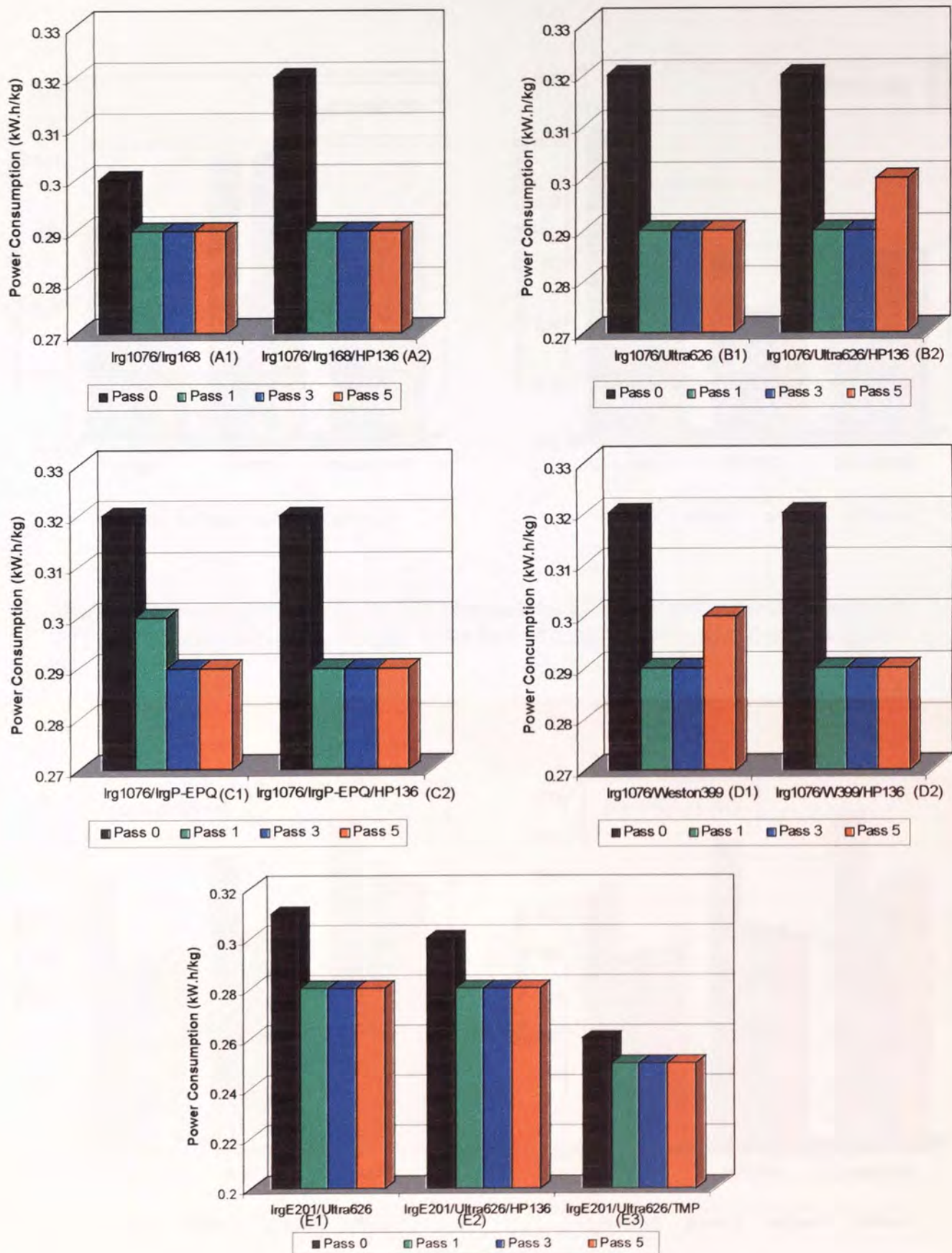


Figure 5.3. Power Consumption of TSE Extrusion for **PL-1840** Stabilised with Antioxidant Mixtures (210°C, 100rpm, 4.0kg/hr for P₀, 265°C, 100rpm, 4.8kg/hr for P₁~P₅)

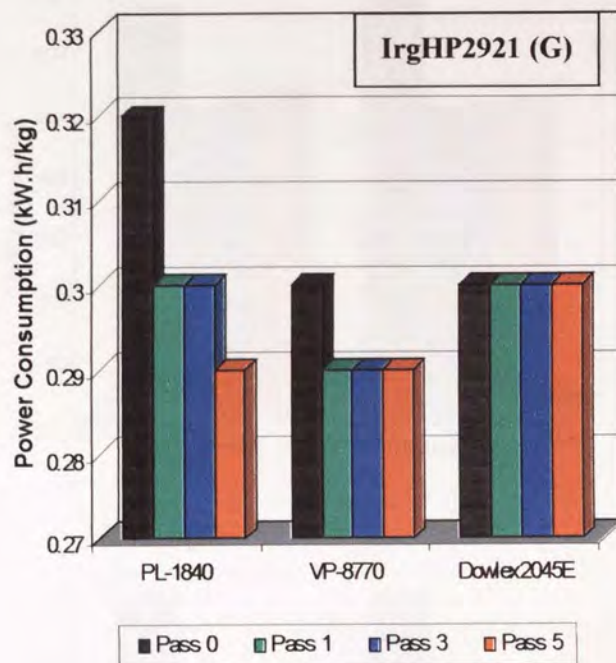
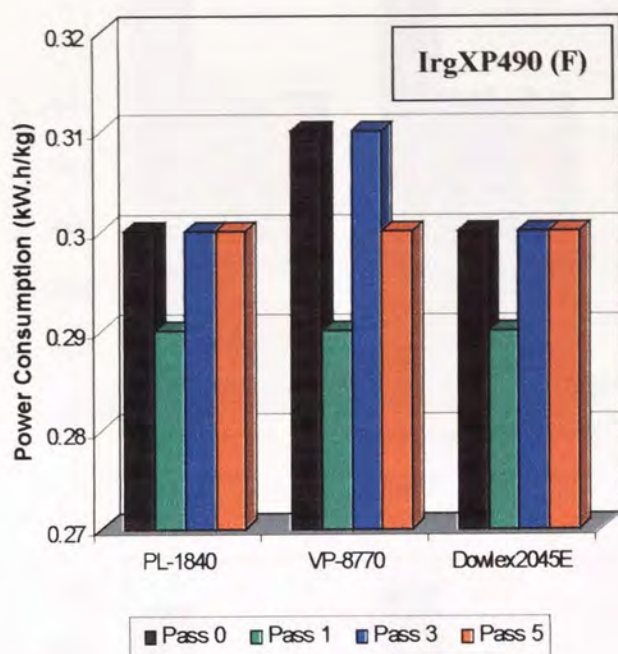


Figure 5.4. Power Consumption of TSE Extrusion for LLDPE Stabilised with Commercial Antioxidants (210°C, 100rpm, 4.0kg/hr for P₀, 265°C, 100rpm, 4.8kg/hr for P₁~P₅)

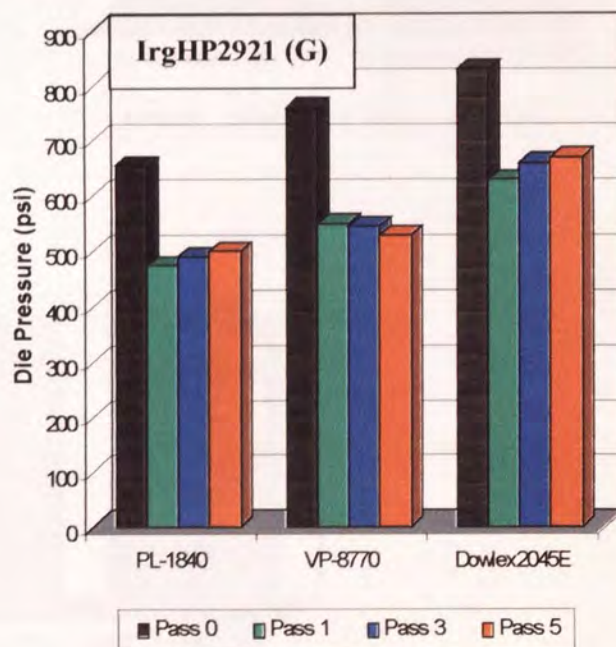
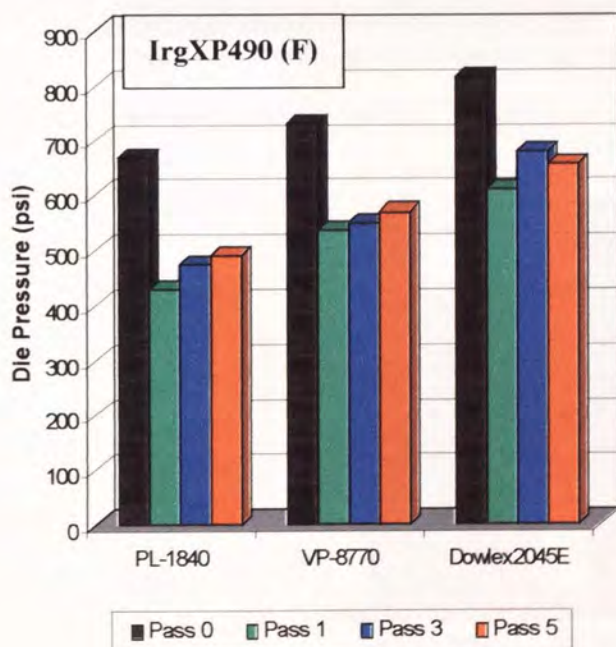


Figure 5.5. Die Pressure of TSE Extrusion for LLDPE Stabilised with Commercial Antioxidants (210°C, 100rpm, 4.0kg/hr for P₀, 265°C, 100rpm, 4.8kg/hr for P₁~P₅)

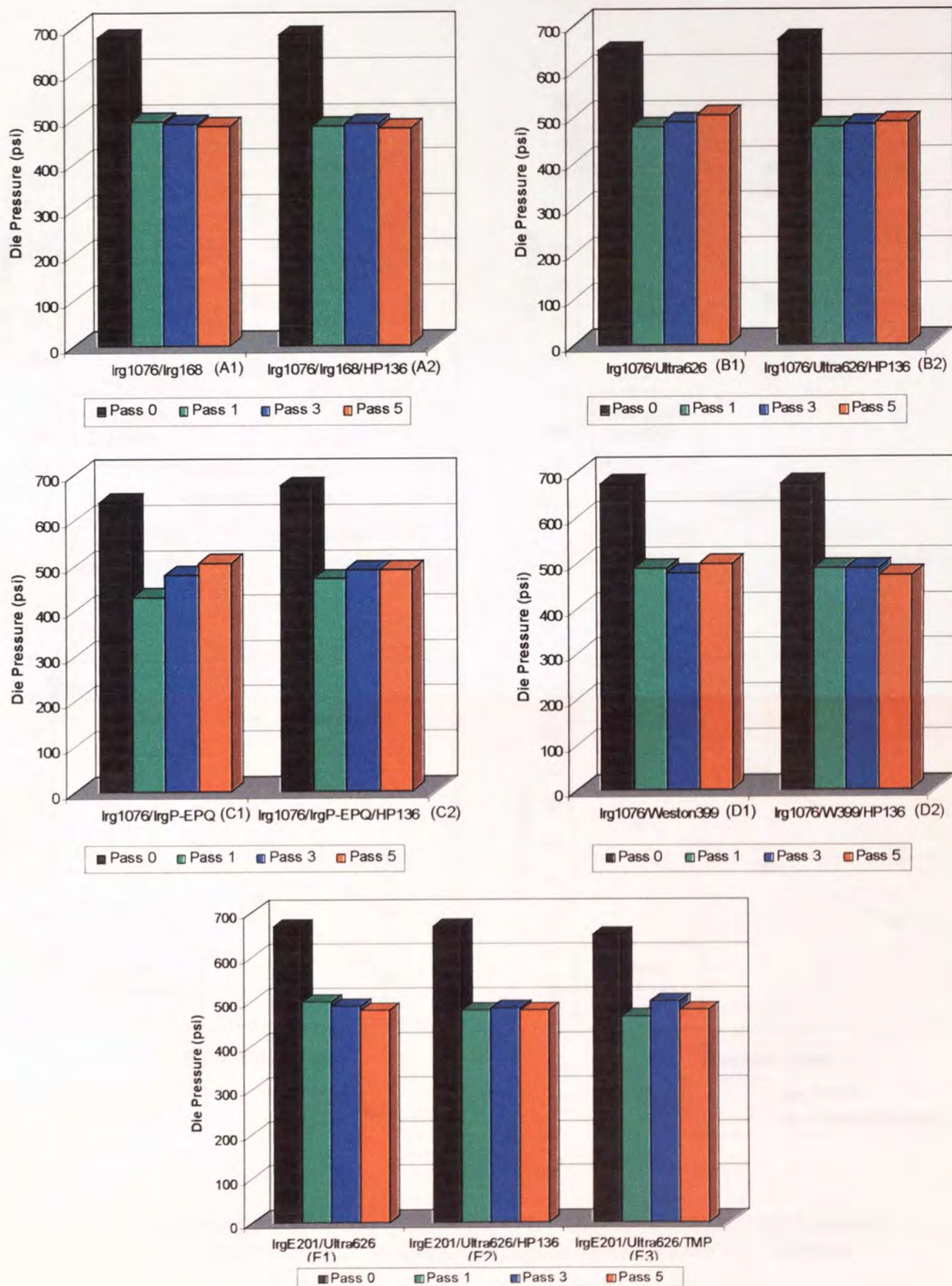
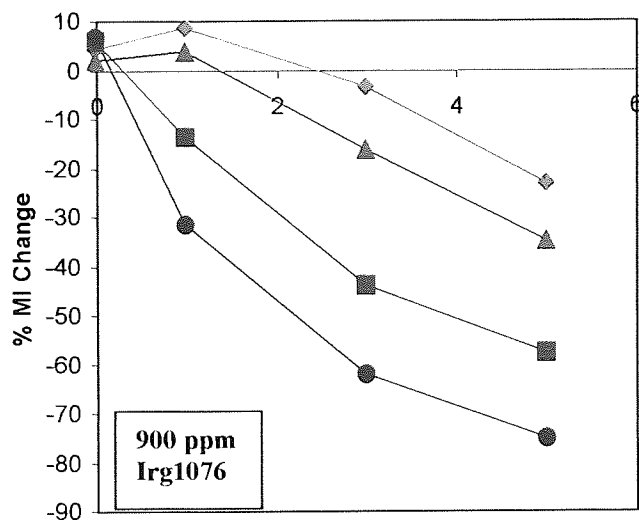
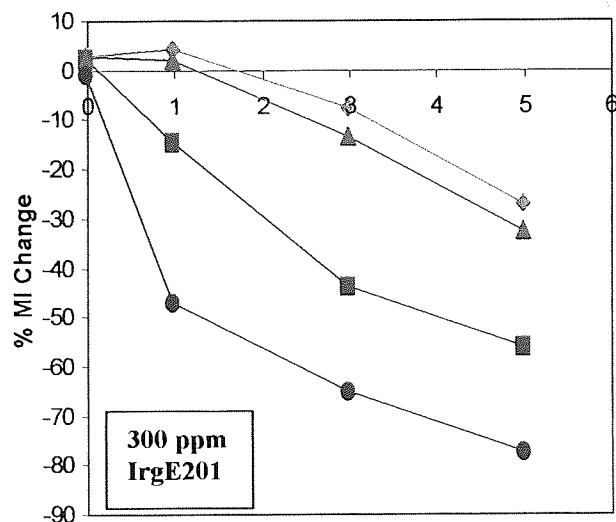
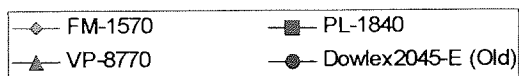


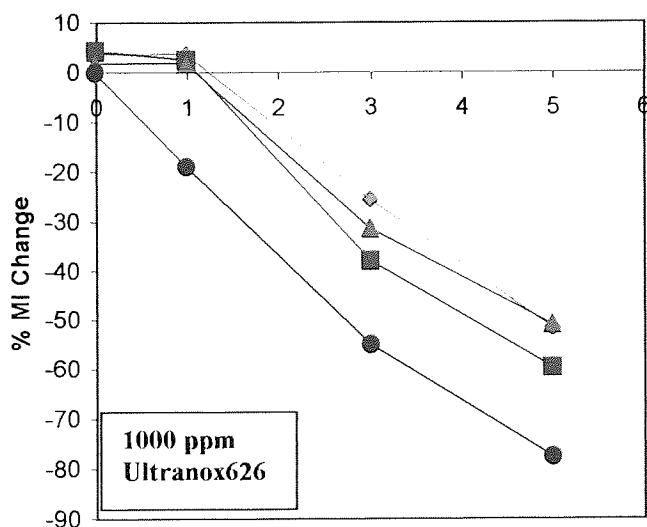
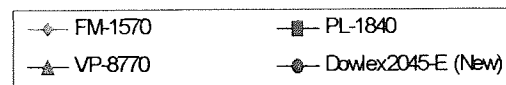
Figure 5.6. Die Pressure of TSE Extrusion for **PL-1840** Stabilised by Antioxidant Mixtures (210°C, 100rpm, 4.0kg/hr for P₀, 265°C, 100rpm, 4.8kg/hr for P₁~P₅)



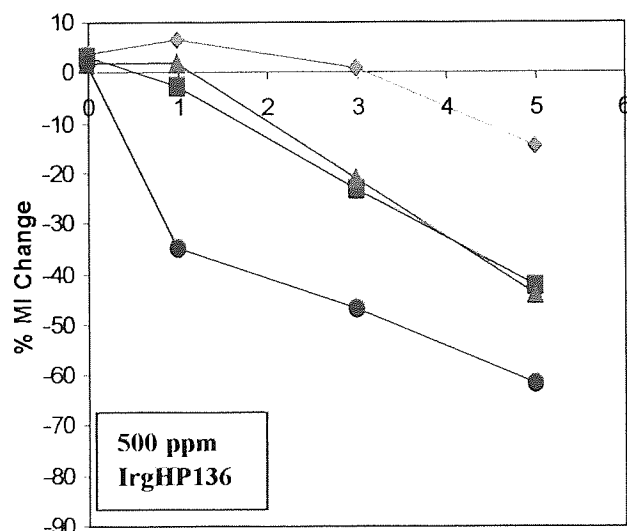
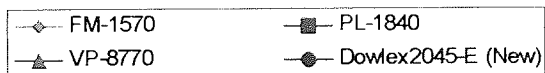
Extrusion Passes



Extrusion Passes



Extrusion Passes



Extrusion Passes



Figure 5.7. Percentage MI Change with Passes for Different TSE Processed LLDPE Polymers Containing Single Antioxidants (265°C, 100rpm)

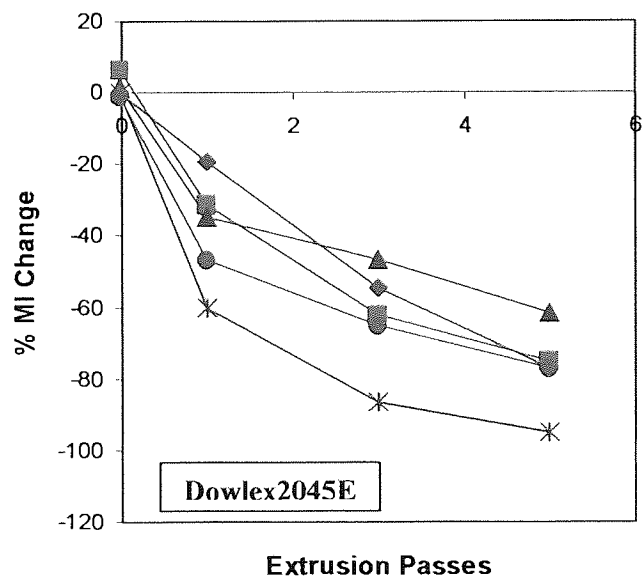
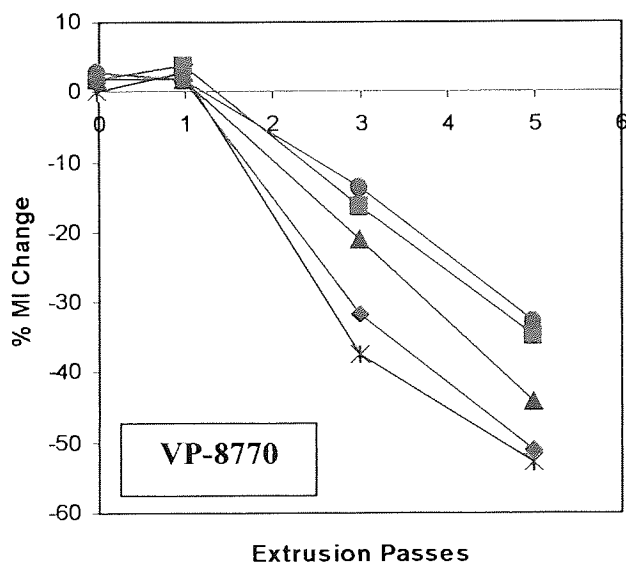
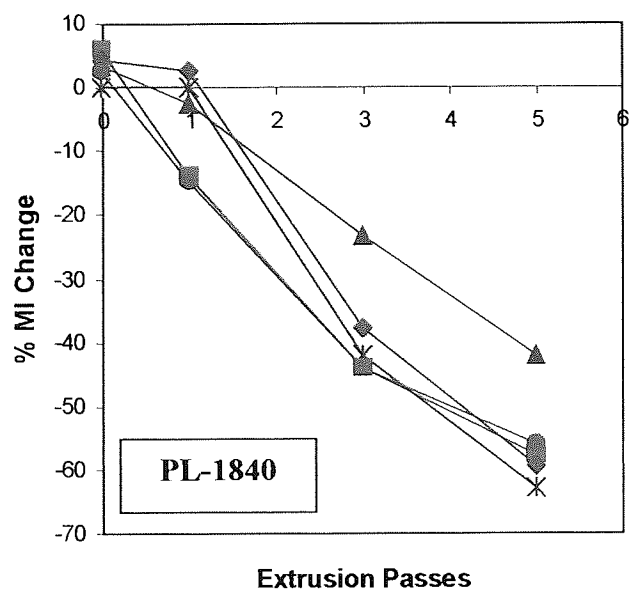
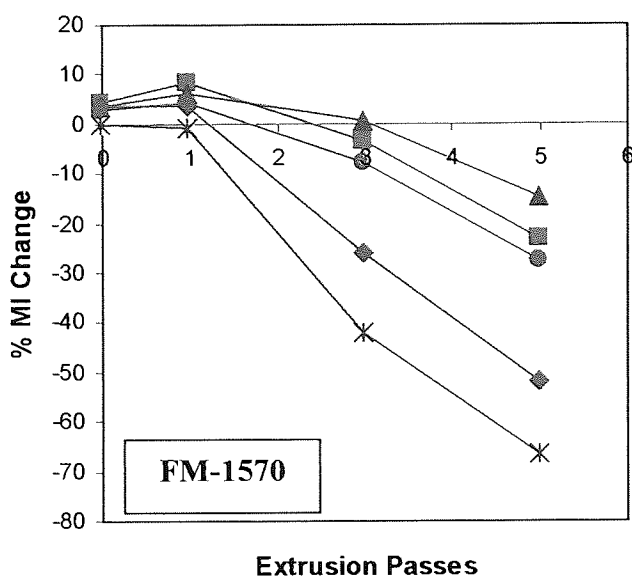


Figure 5.8. Percentage MI Change with Passes for Each of the Extruded LLDPE Polymers Containing Different Single Antioxidants (265°C, 100rpm)

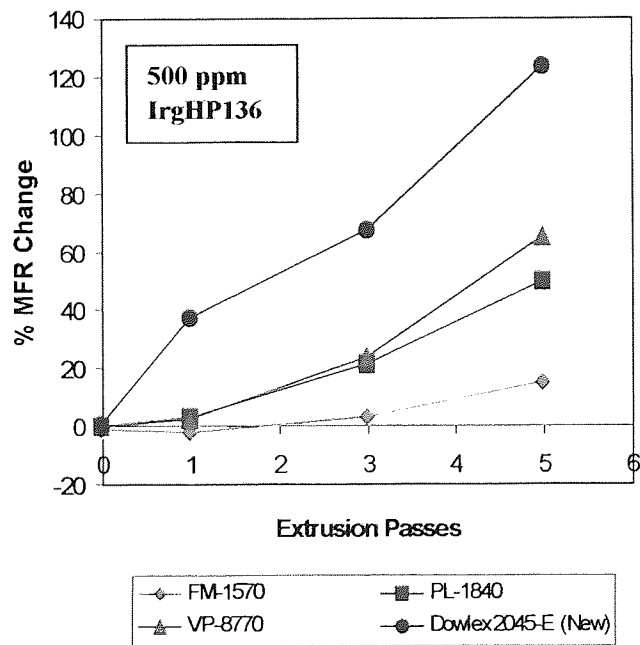
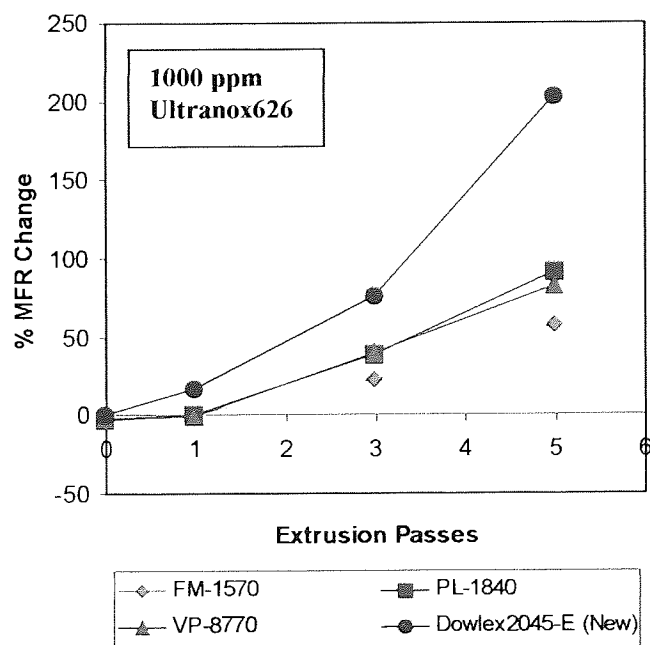
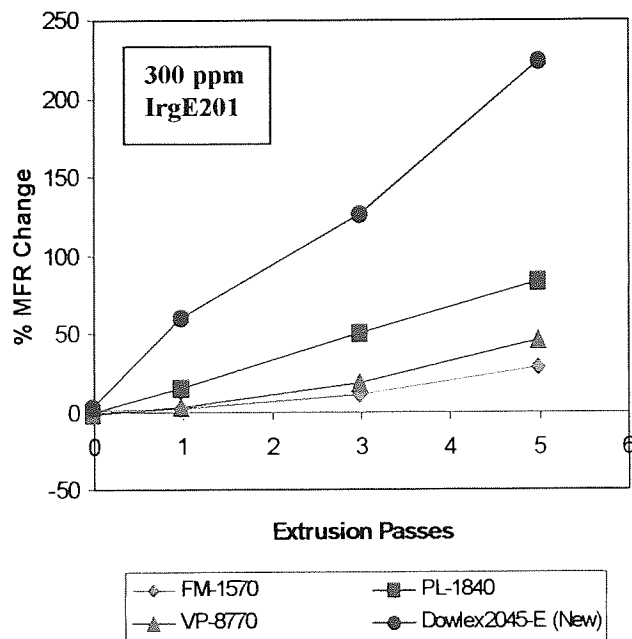
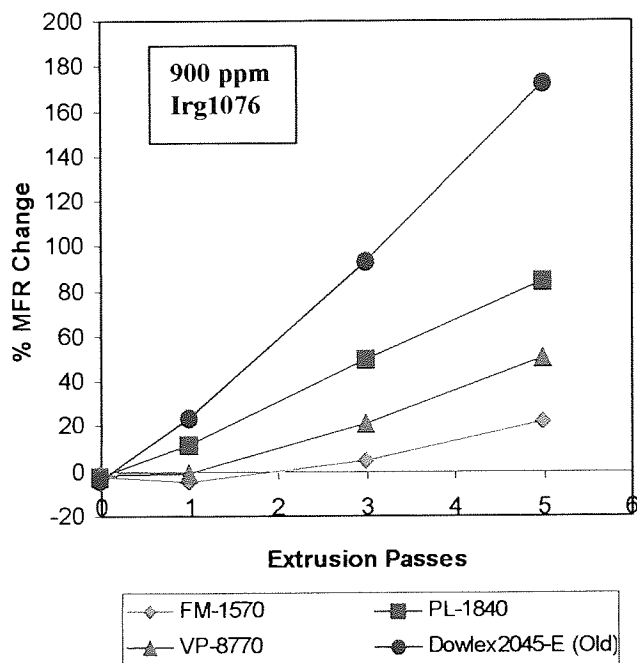


Figure 5.9. Percentage MFR Change with Passes for Different TSE Processed LLDPE Polymers Containing Single Antioxidants (265°C, 100rpm)

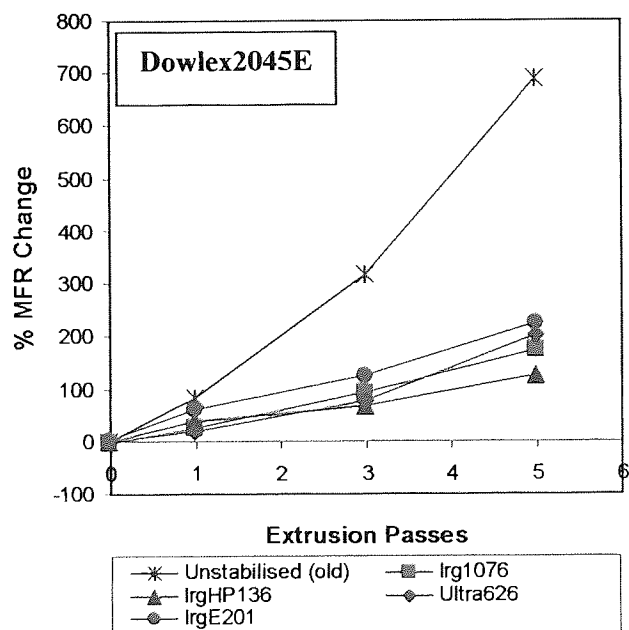
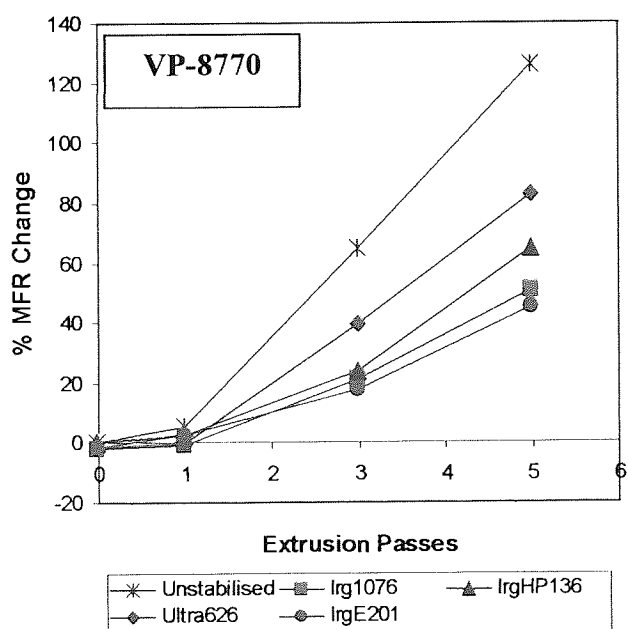
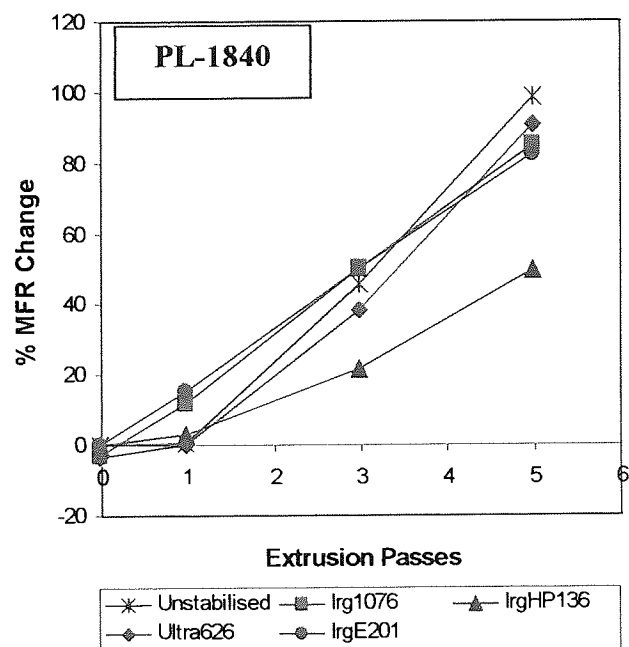
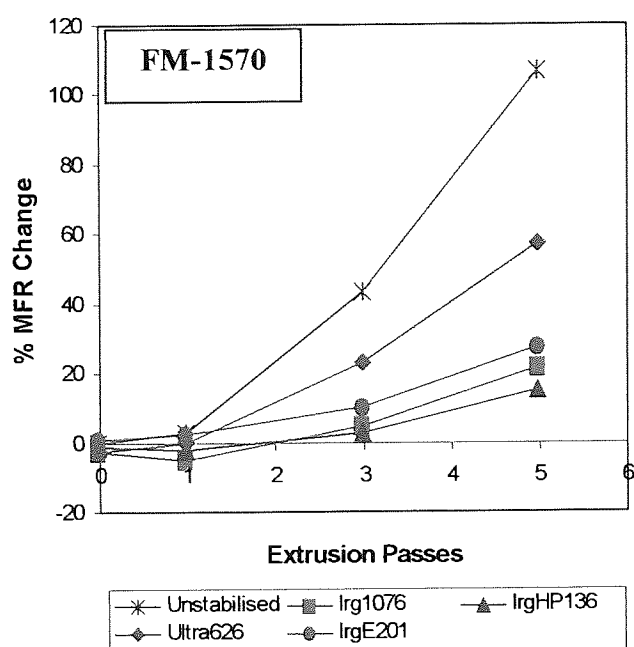


Figure 5.10. Percentage MFR Change with Passes for Each of the Extruded LLDPE Polymers Containing Different Single Antioxidants (265°C, 100rpm)

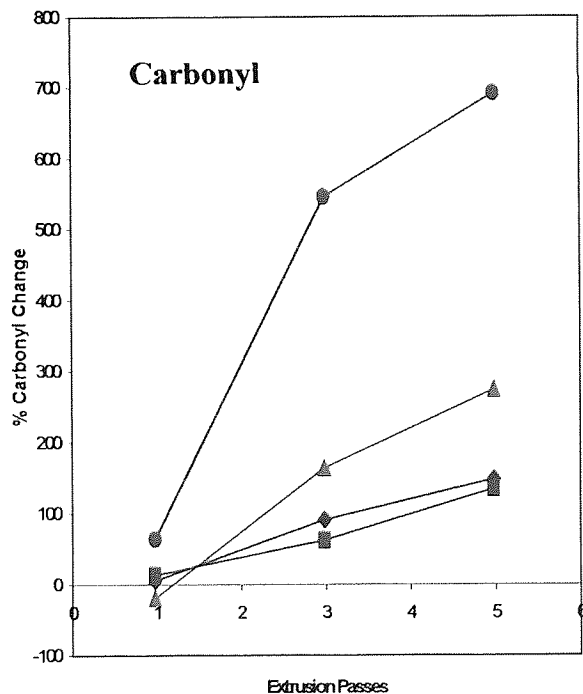
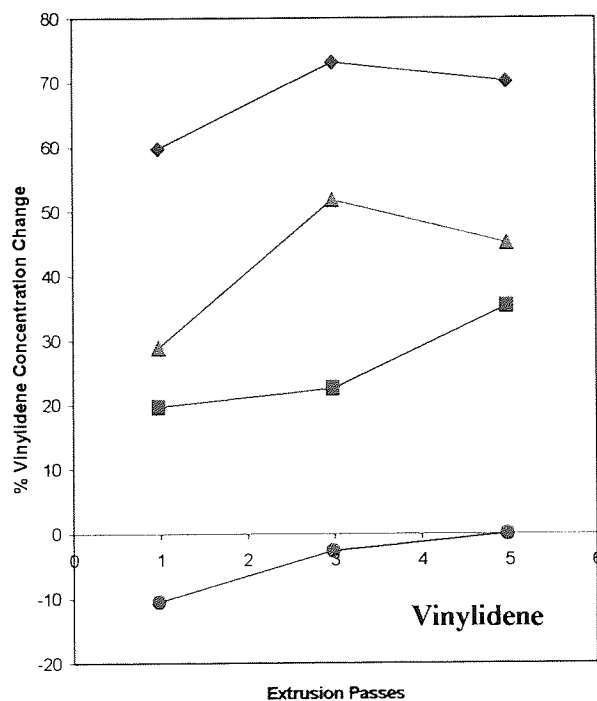
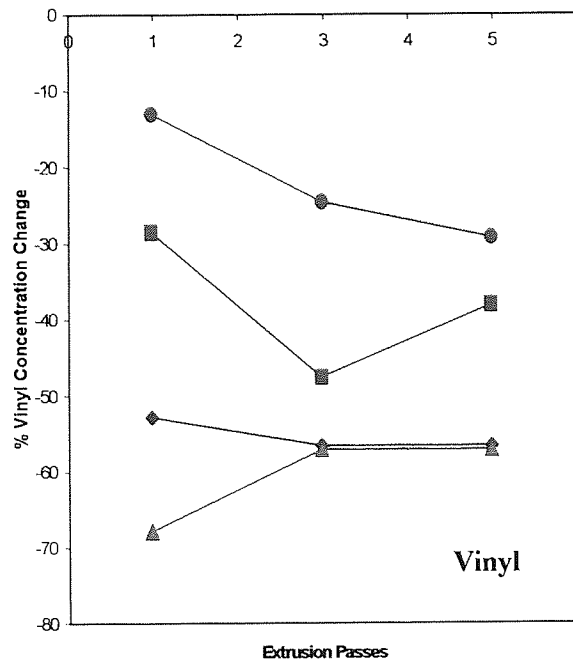
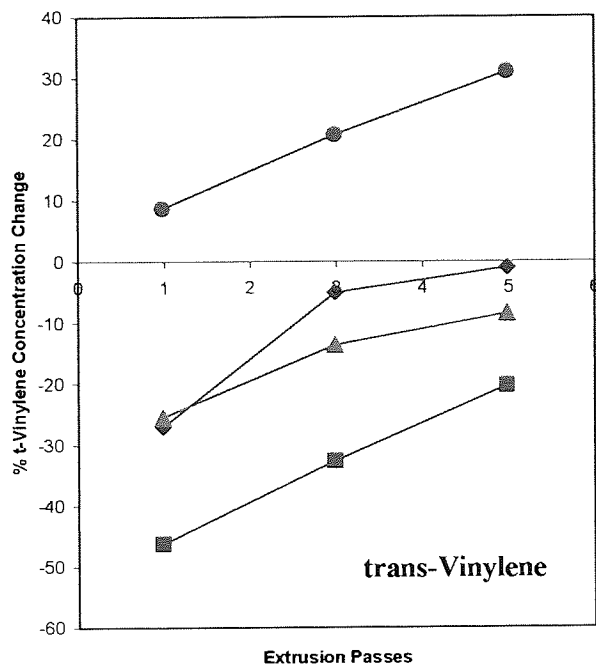


Figure 5.11. Percentage Concentration Change of Unsaturated Groups and Carbonyl Compounds in **Unstabilised LLDPE** Polymers Extruded at 265°C

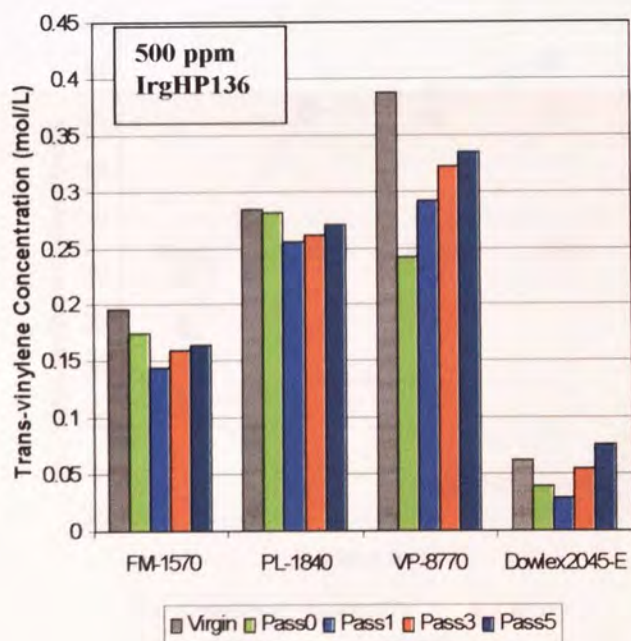
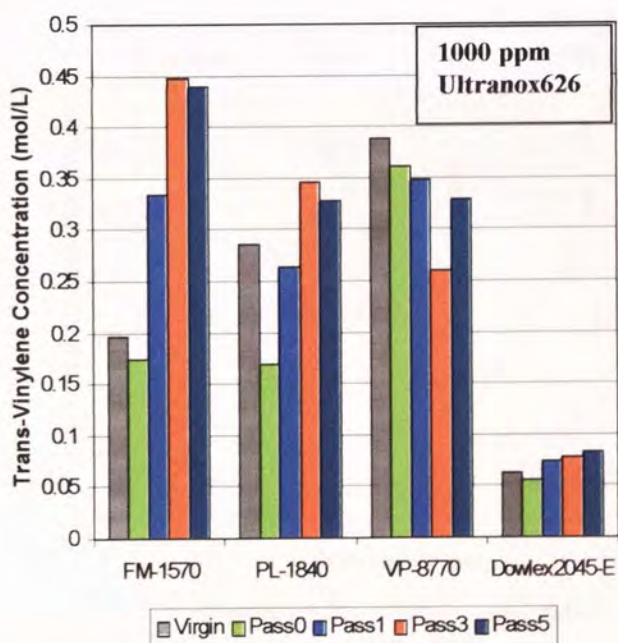
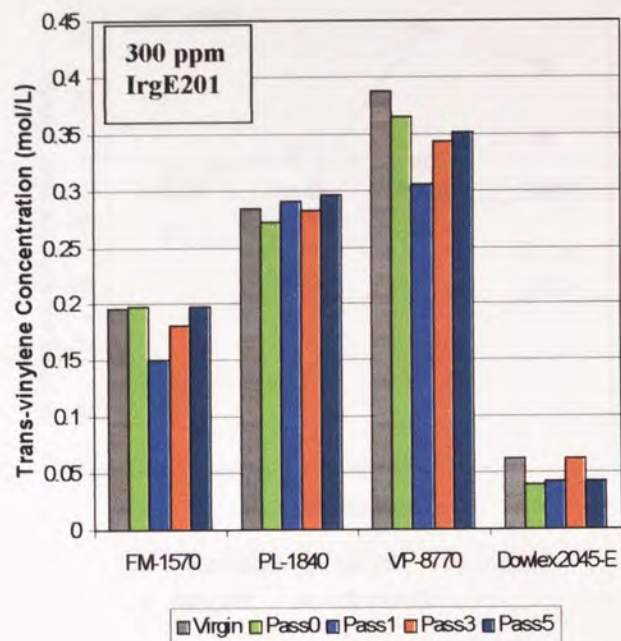
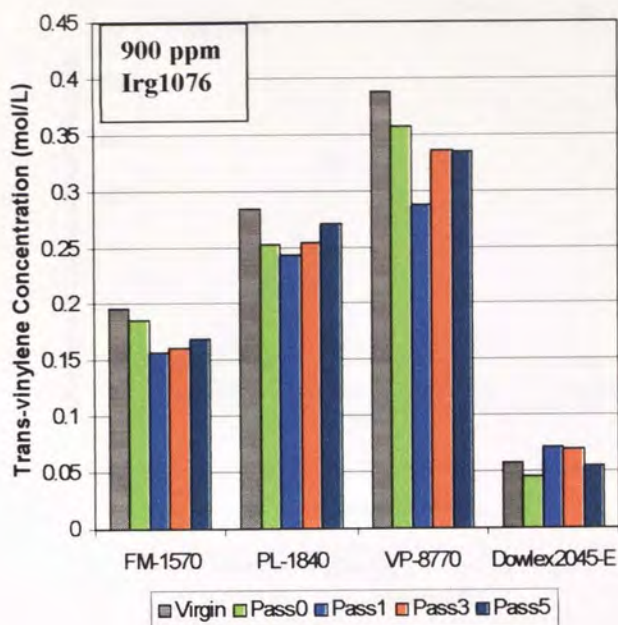


Figure 5.12. Concentration of Trans-vinylene as a Function of Extrusion Passes for TSE Processed LLDPE Polymers Containing Single Antioxidants (265°C, 100rpm)

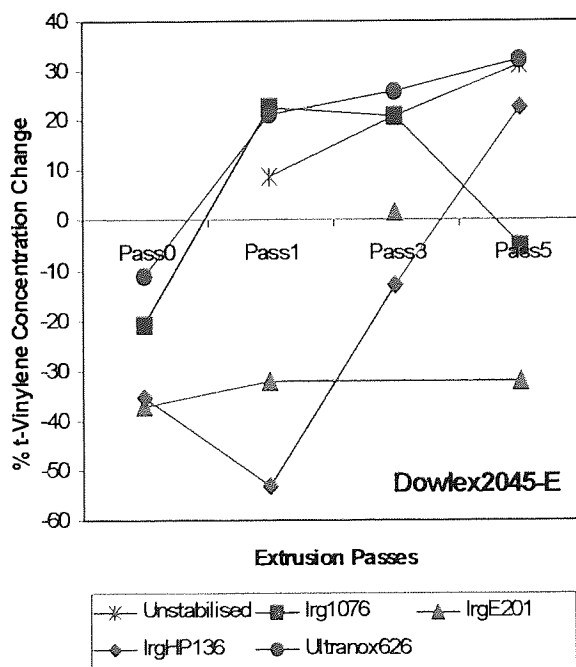
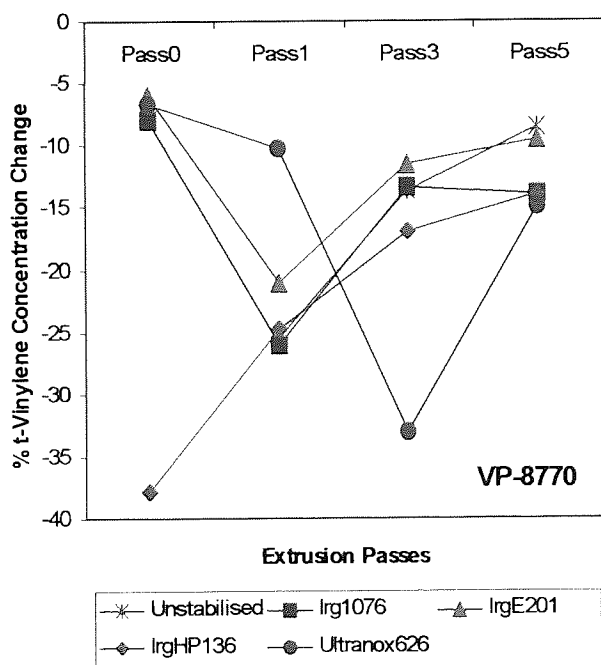
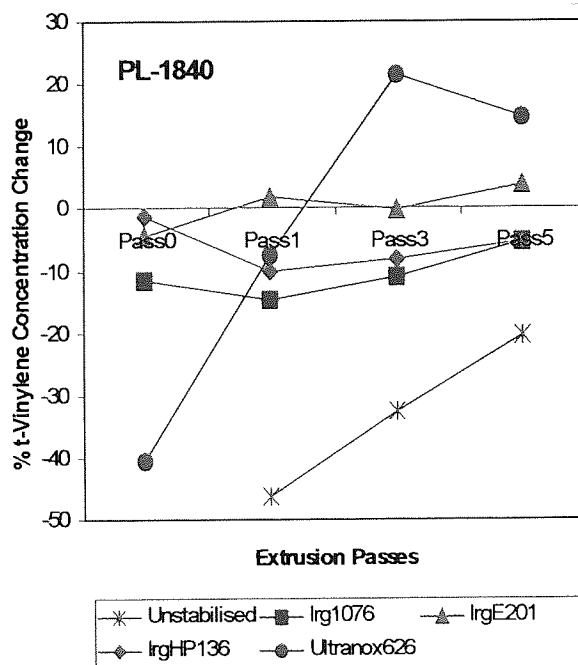
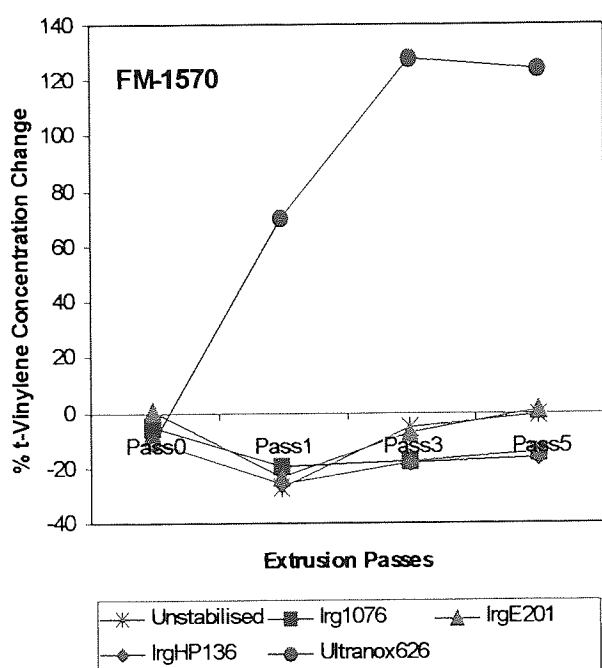


Figure 5.13(a). Percentage Concentration Change of Trans-vinylene with Extrusion Passes for Individual LLDPE Polymers Containing Different Single Antioxidants Extruded under the Condition of 265°C, 100rpm

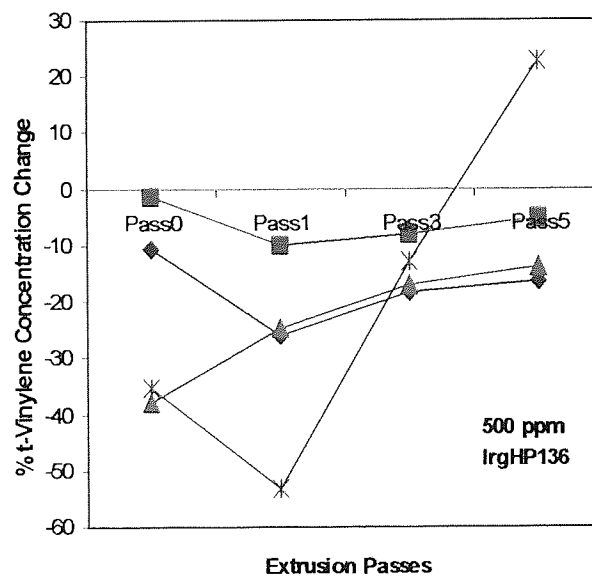
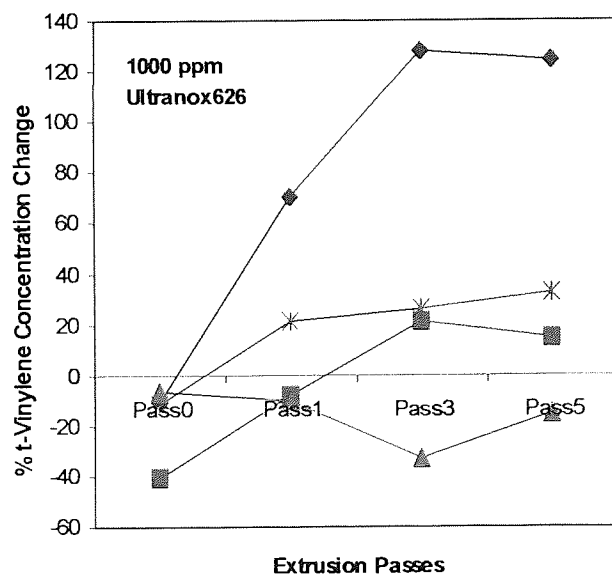
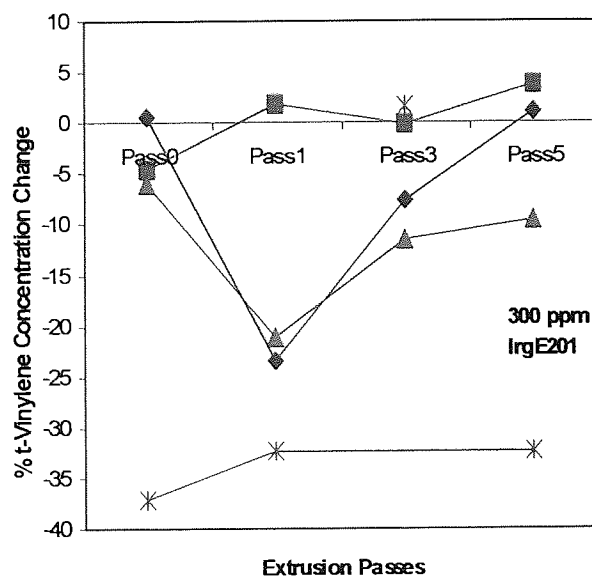
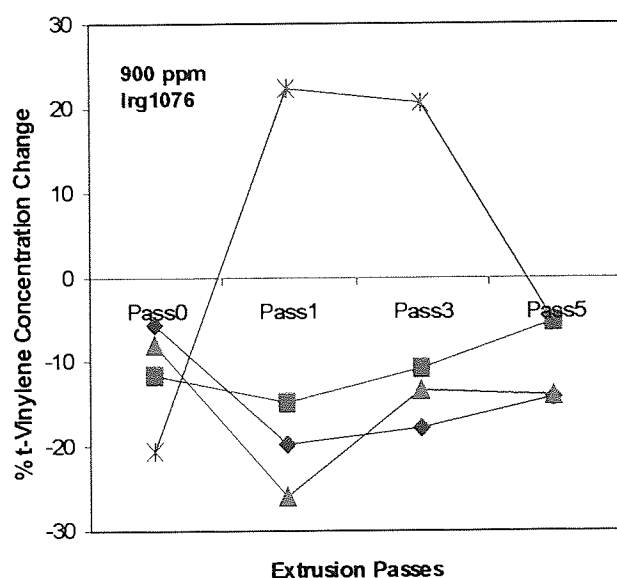


Figure 5.13(b). Percentage Concentration Change of Trans-vinylene with Extrusion Passes for Different LLDPE Polymers Containing Single Antioxidants Extruded under the Condition of 265°C, 100rpm

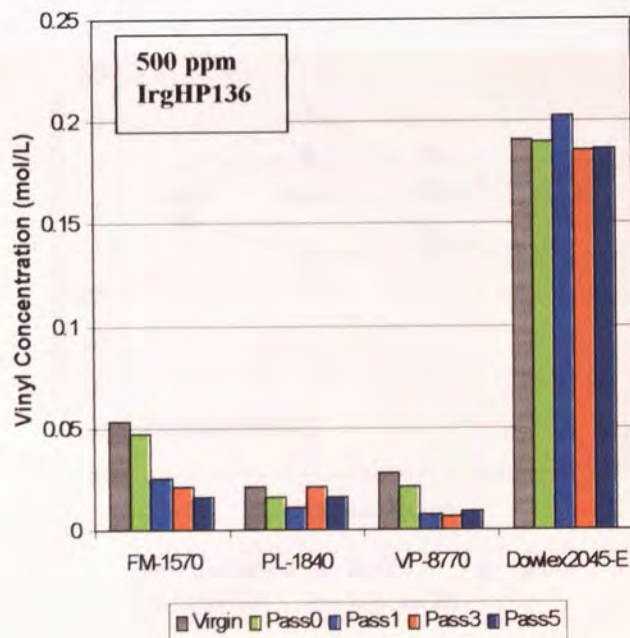
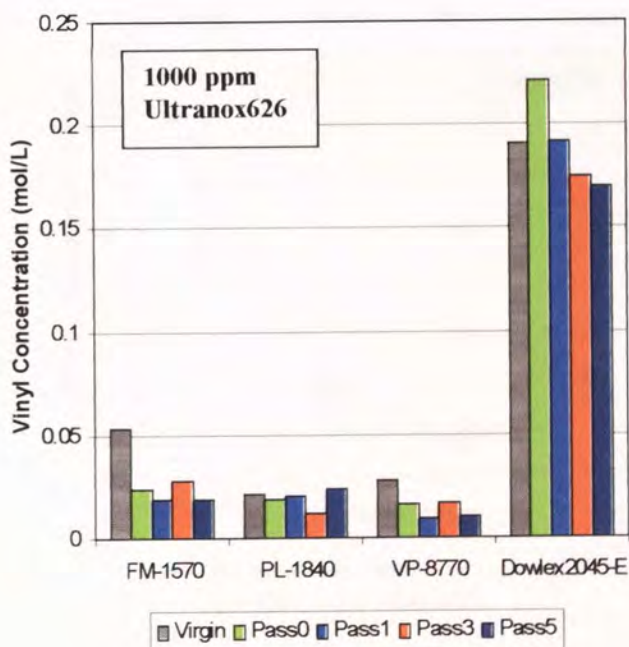
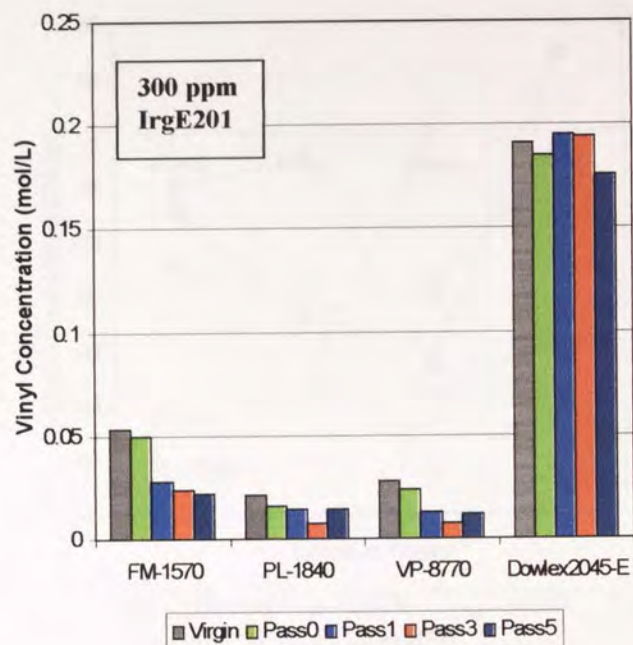
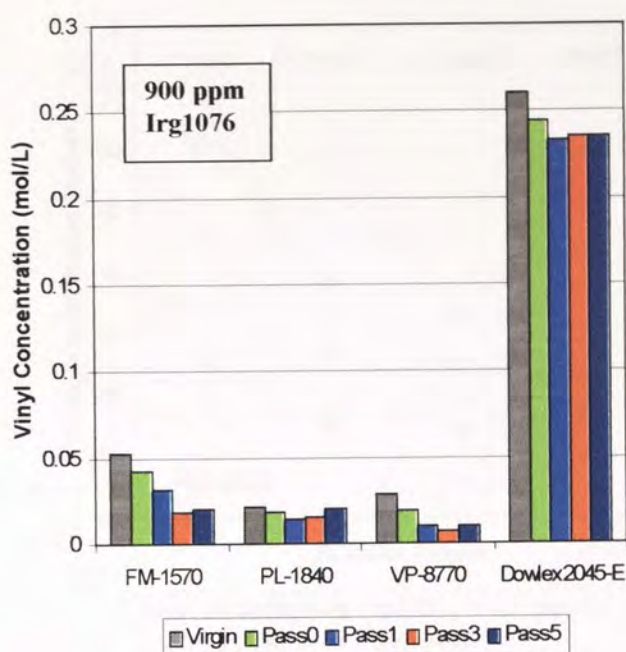


Figure 5.14. Concentration of Vinyl as a function of Extrusion Passes for TSE Processed LLDPE Polymers Containing Single Antioxidants (265°C, 100rpm)

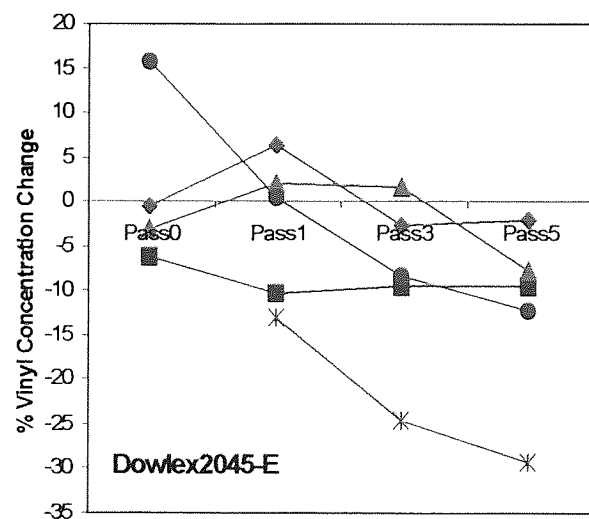
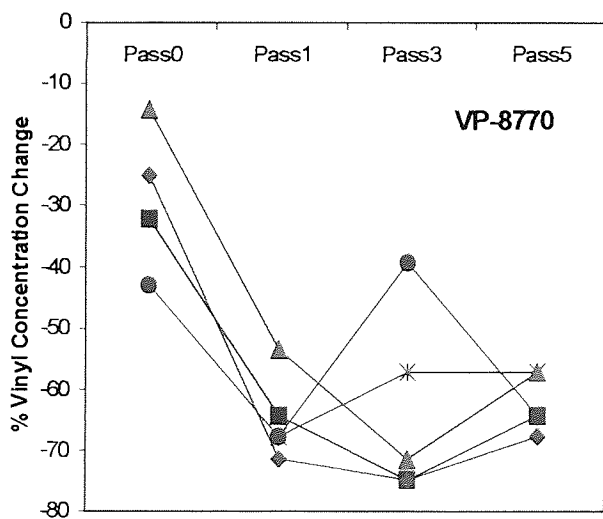
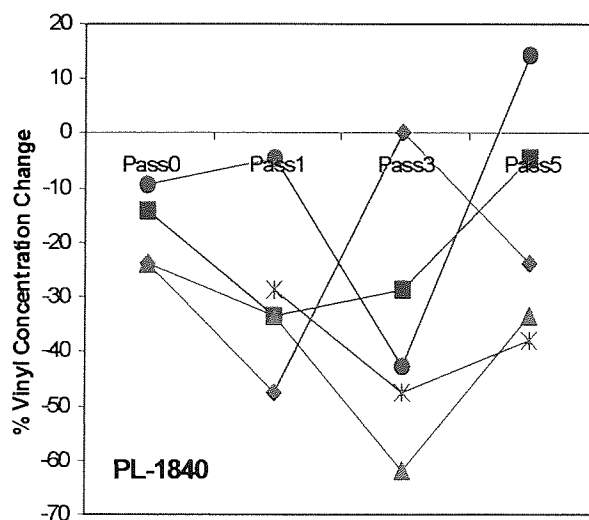
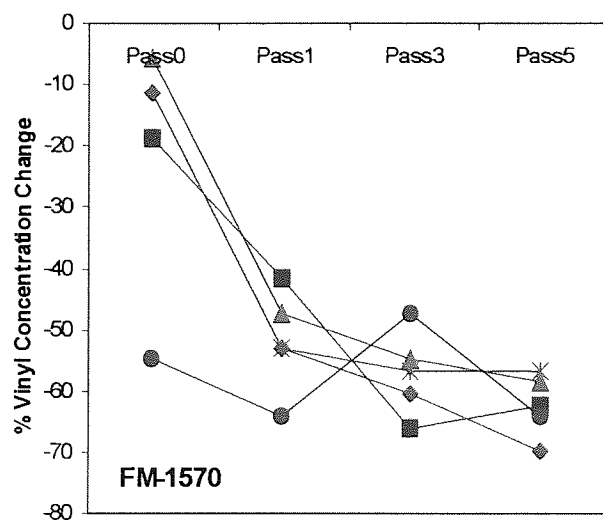


Figure 5.15(a). Percentage Concentration Change of Vinyl with Extrusion Passes for Individual LLDPE Polymers Containing Different Single Antioxidants Extruded under the Condition of 265°C, 100rpm

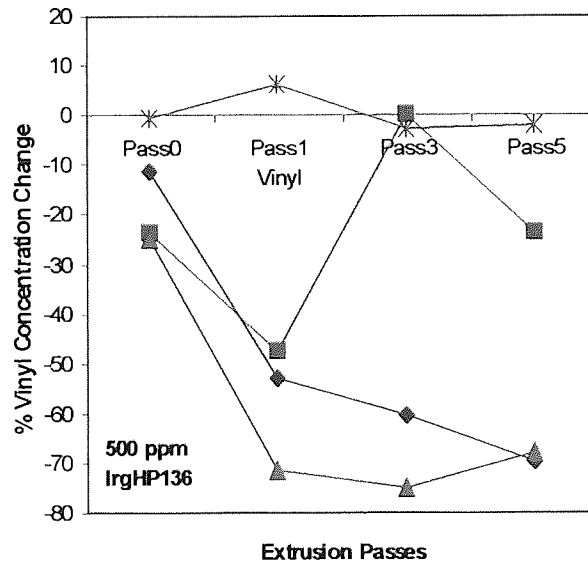
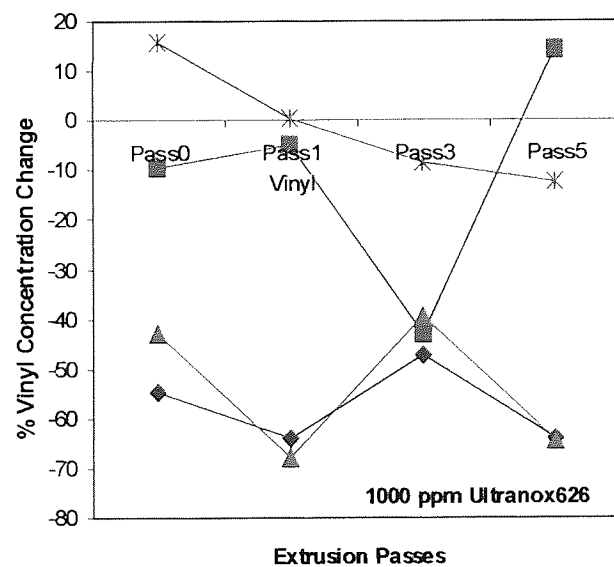
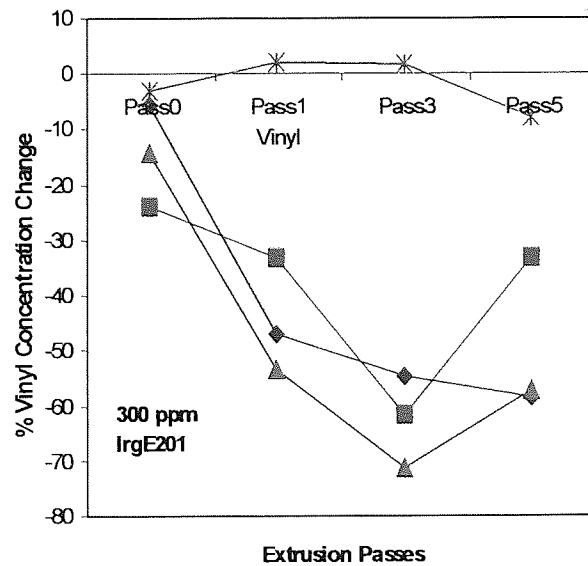
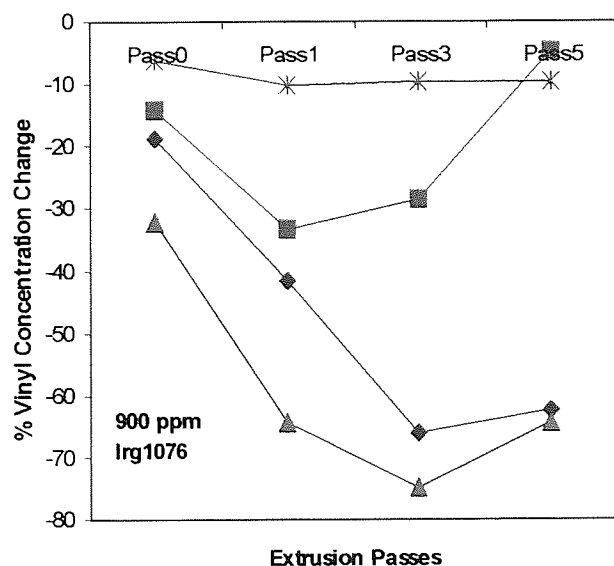


Figure 5.15(b). Percentage Concentration Change of Vinyl with Extrusion Passes for Different LLDPE Polymers Containing Single Antioxidants Extruded under the Condition of 265°C, 100rpm

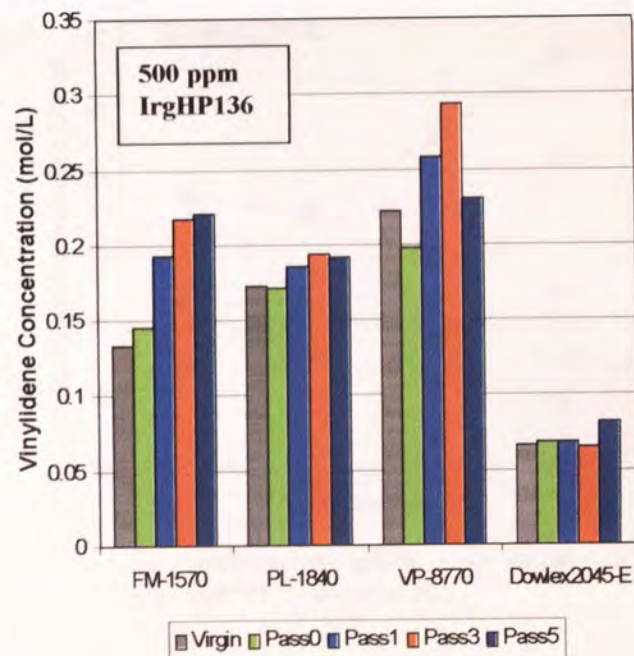
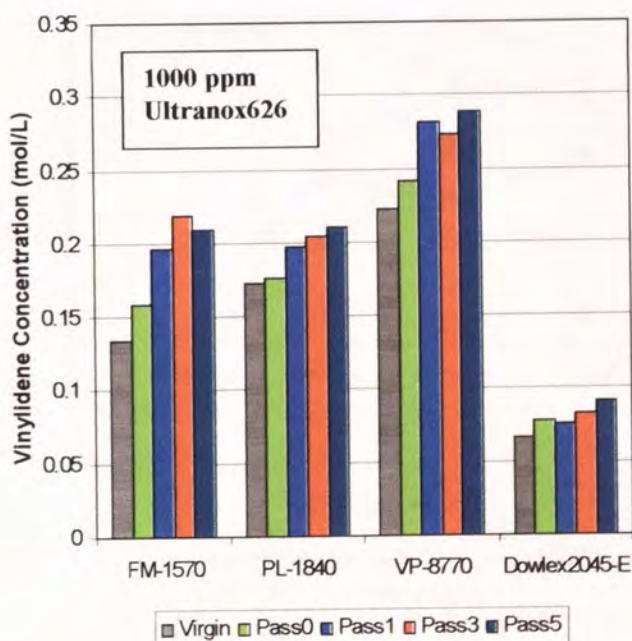
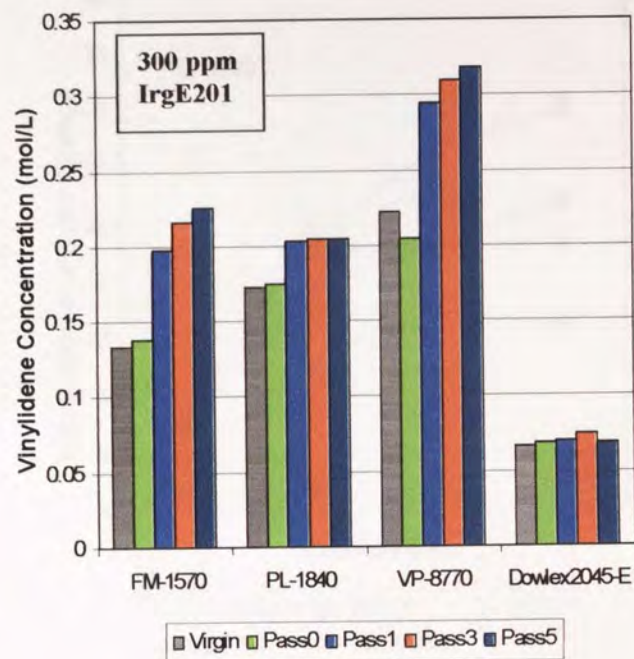
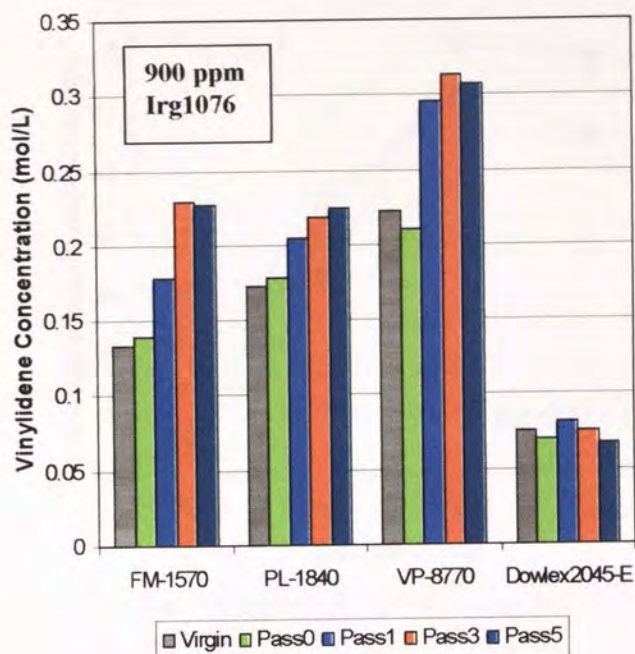


Figure 5.16. Concentration of Vinylidene as a Function of Extrusion Passes for TSE Processed LLDPE Polymers Containing Single Antioxidants (265°C, 100rpm)

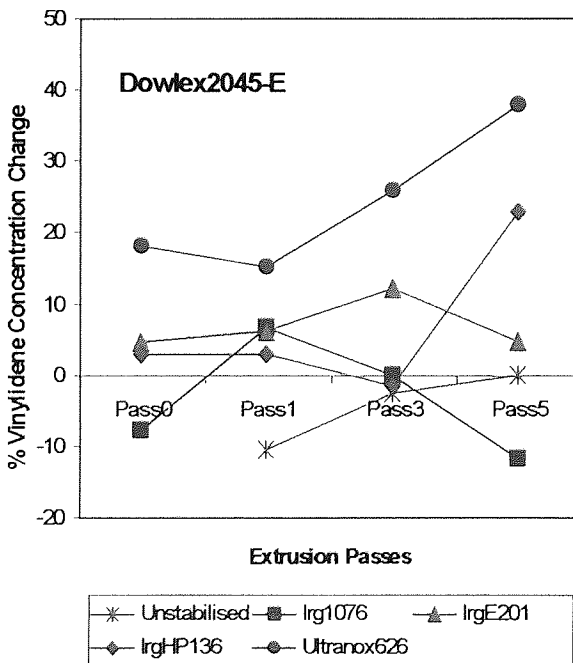
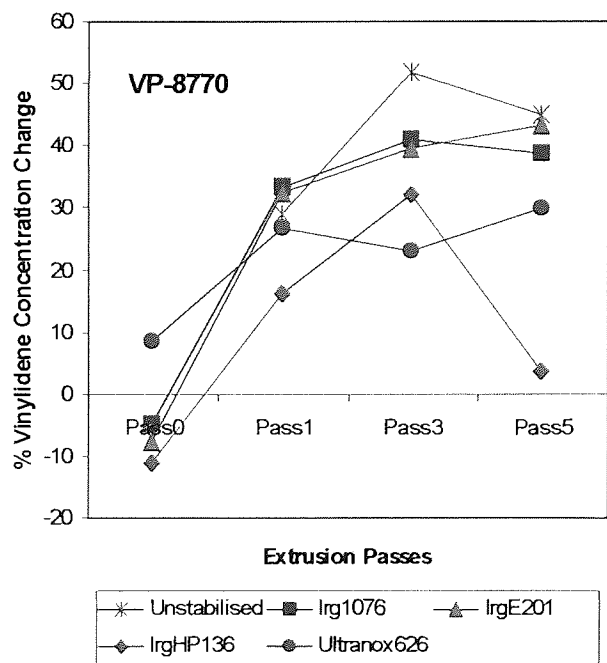
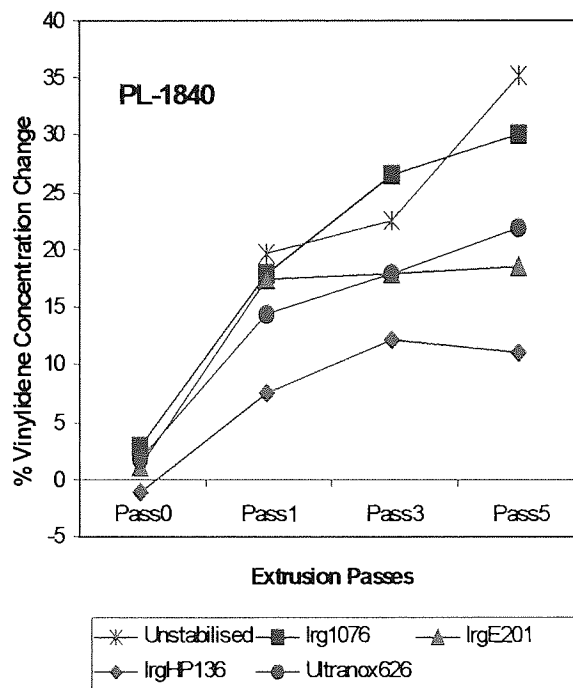
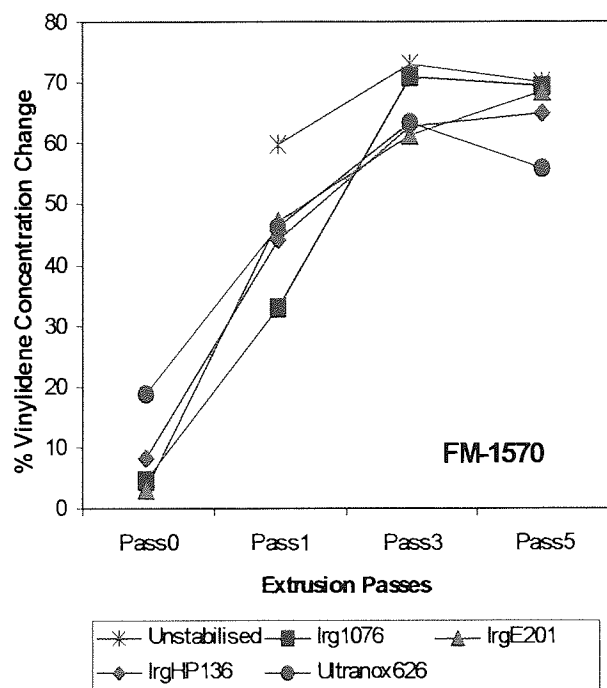


Figure 5.17(a). Percentage Concentration Change of Vinylidene with Extrusion Passes for Individual LLDPE Polymers Containing Different Single Antioxidants Extruded under the Condition of 265°C, 100rpm

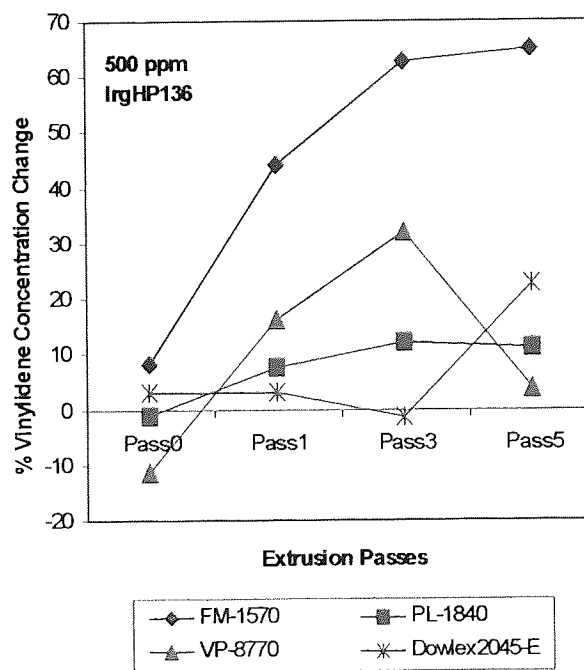
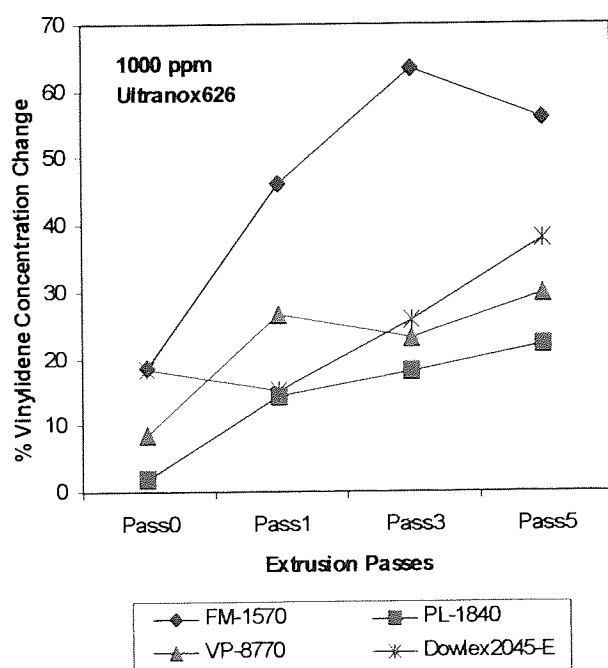
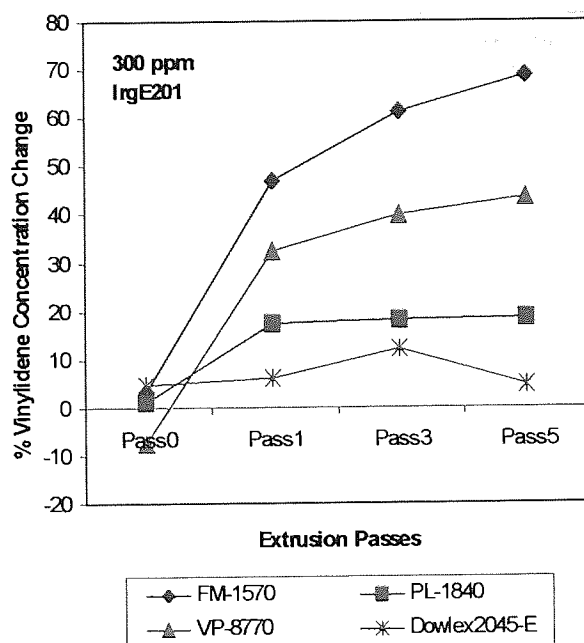
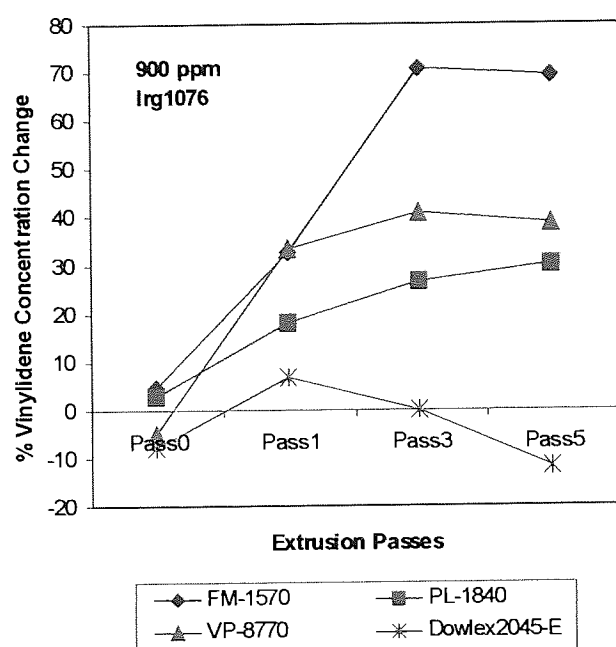


Figure 5.17(b). Percentage Concentration Change of Vinylidene with Extrusion Passes for Different LLDPE Polymers Containing Single Antioxidants Extruded under the Condition of 265°C, 100rpm

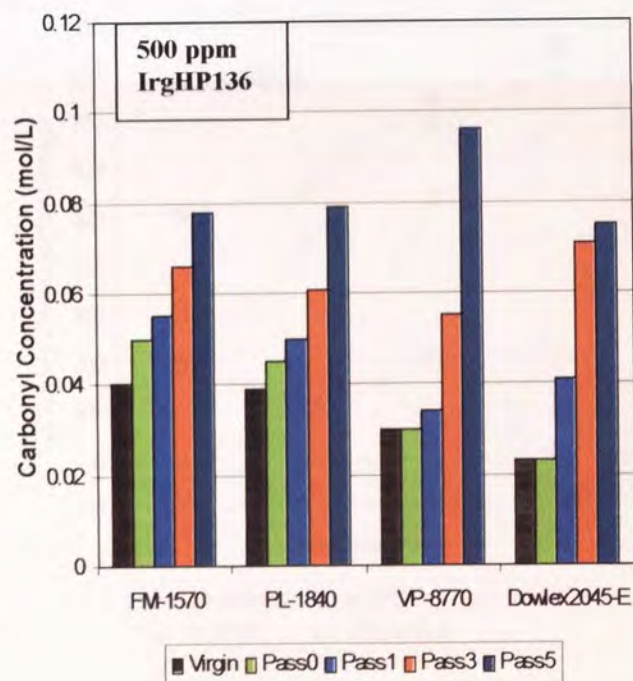
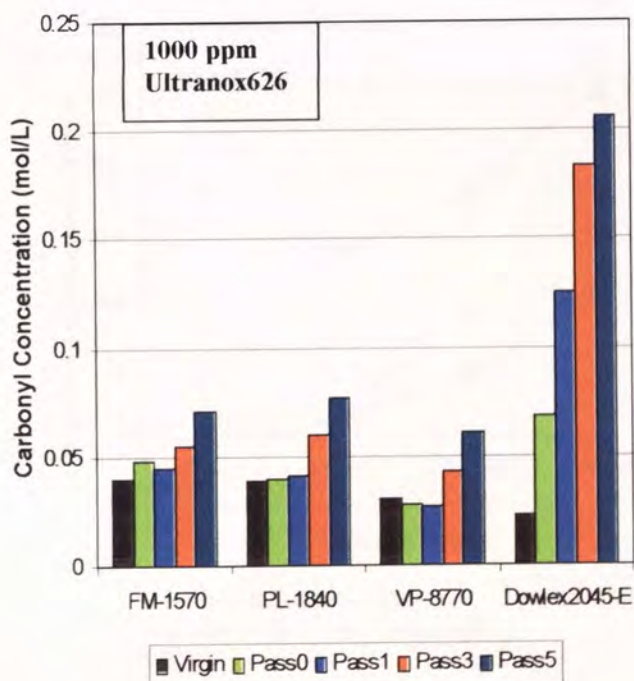
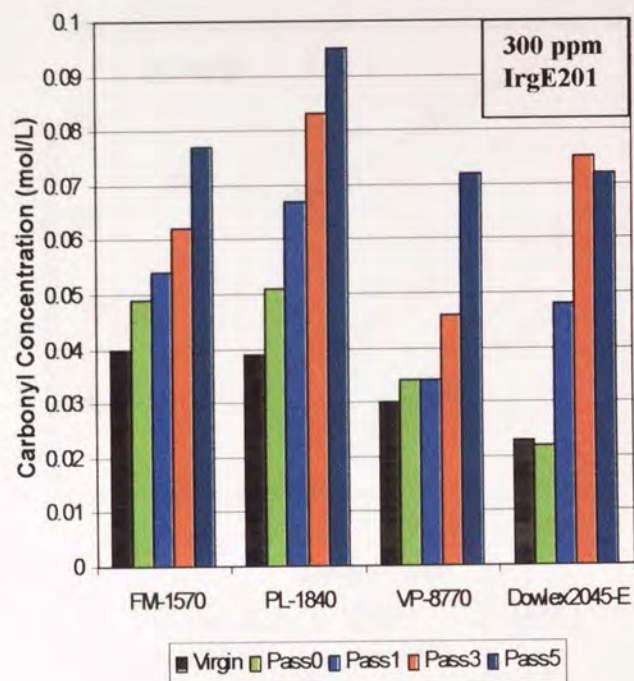
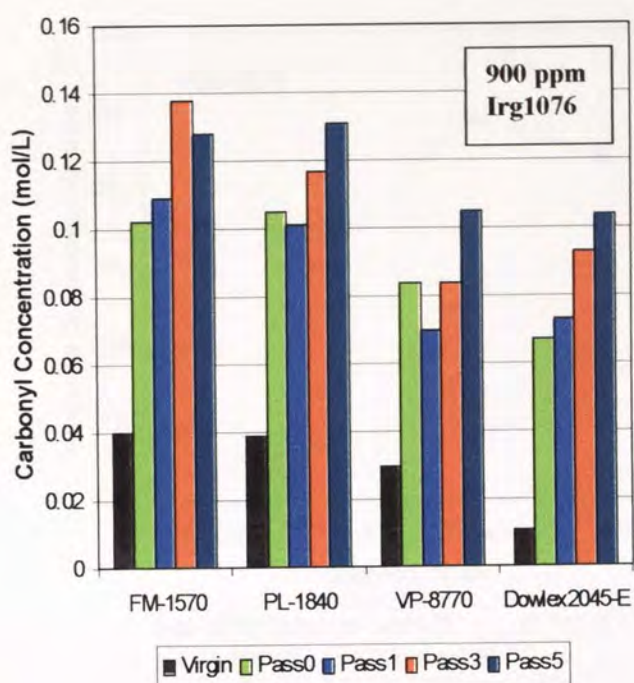


Figure 5.18. Concentration of Carbonyl Compounds (determined by FTIR in carbonyl region of $1680\sim1780\text{ cm}^{-1}$) as a Function of Extrusion Passes for Different TSE Processed LLDPE Polymers Containing Single Antioxidants (265°C , 100rpm)

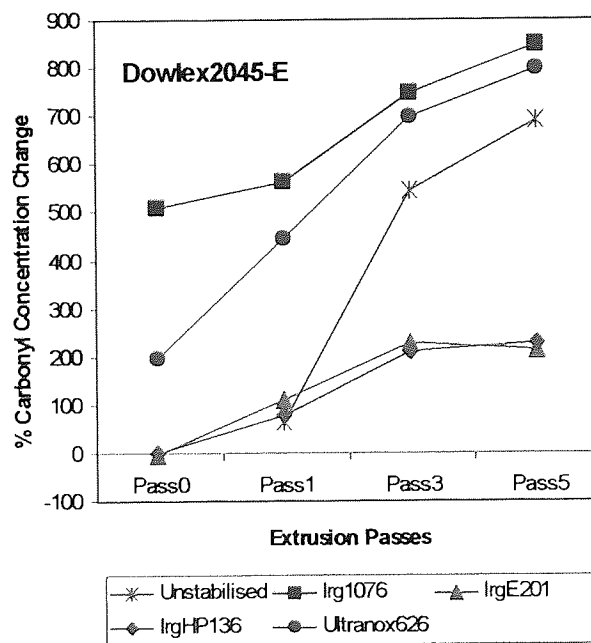
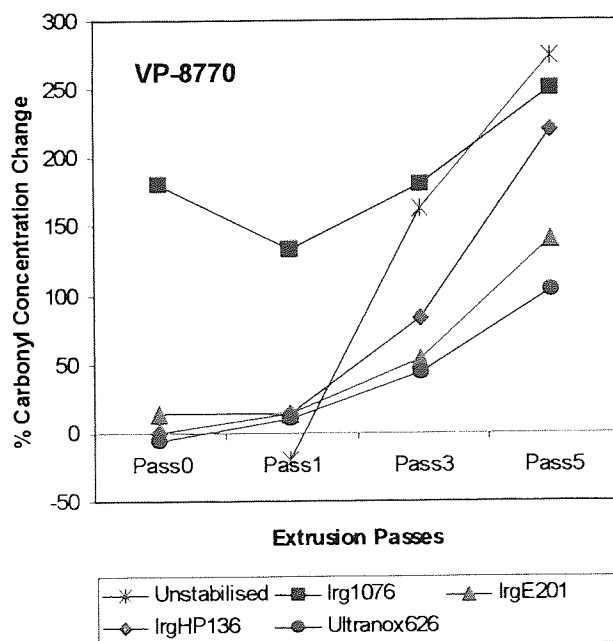
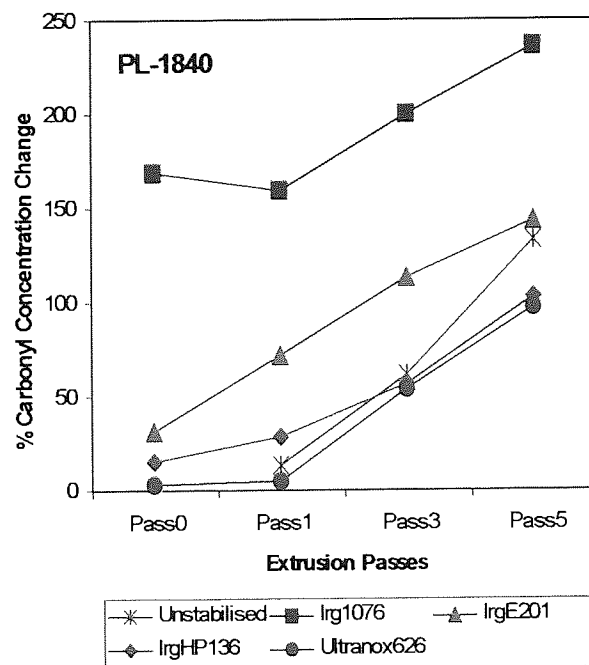
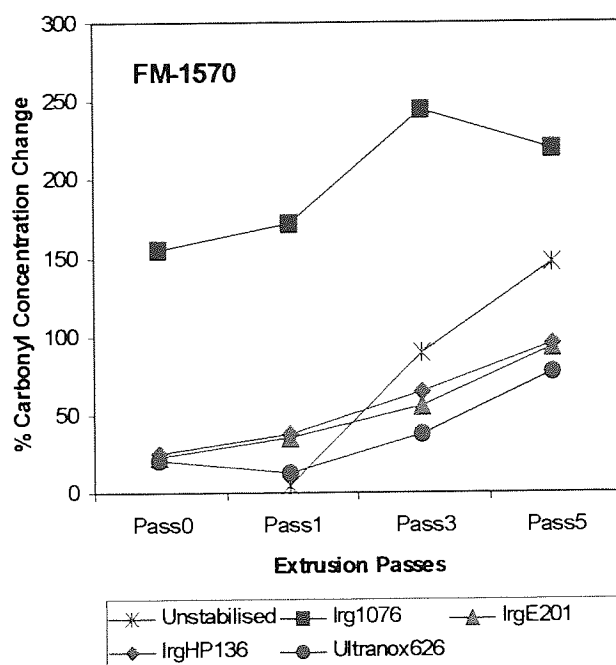


Figure 5.19(a). Percentage Concentration Change of Carbonyl Groups with Extrusion Passes for Individual LLDPE Polymers Containing Different Single Antioxidants Extruded under the Condition of 265°C, 100rpm

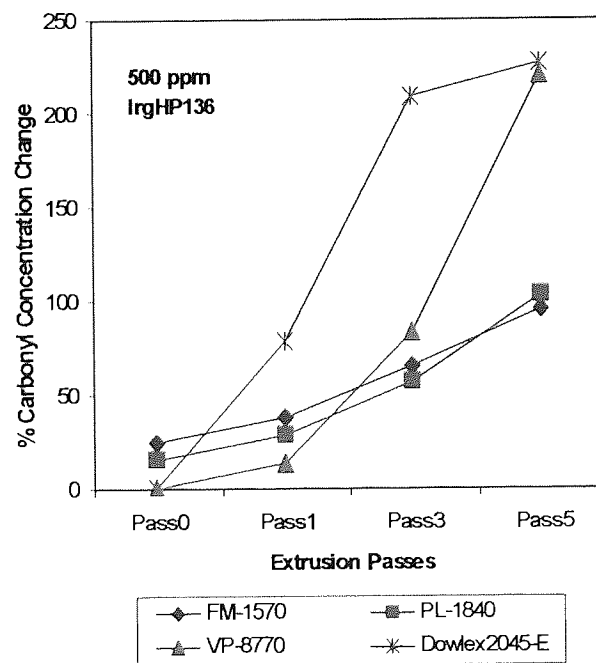
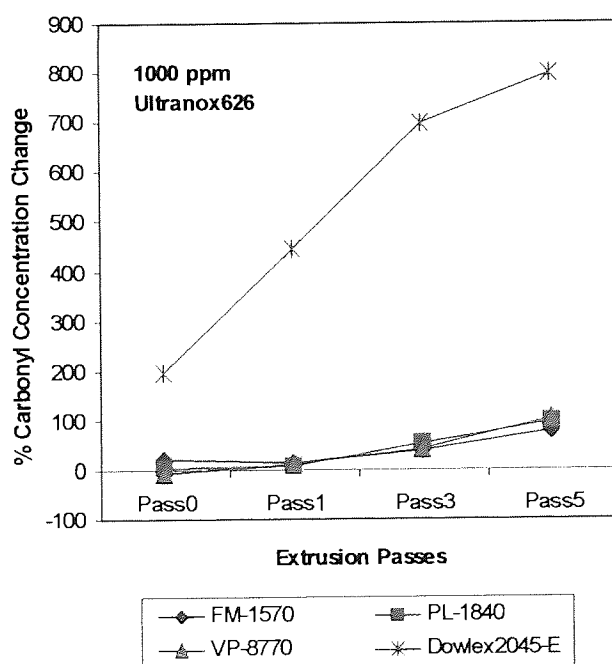
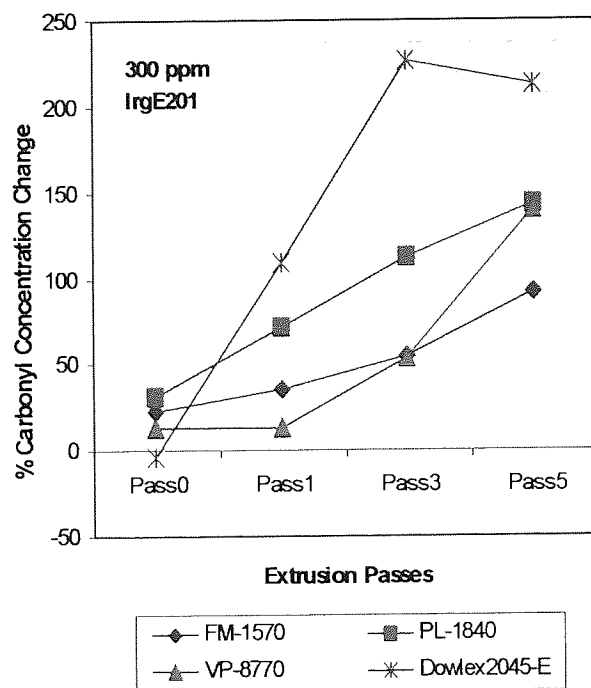
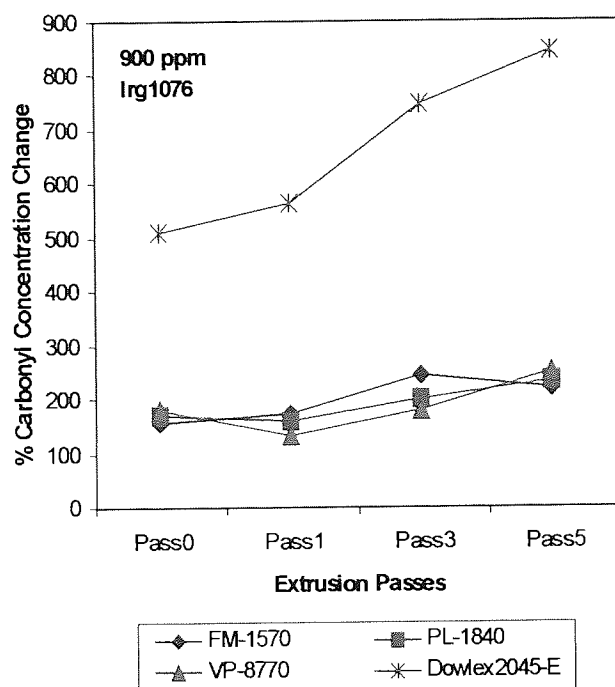


Figure 5.19(b). Percentage Concentration Change of Carbonyl Groups with Extrusion Passes for Different LLDPE Polymers Containing Single Antioxidants Extruded under the Condition of 265°C, 100rpm

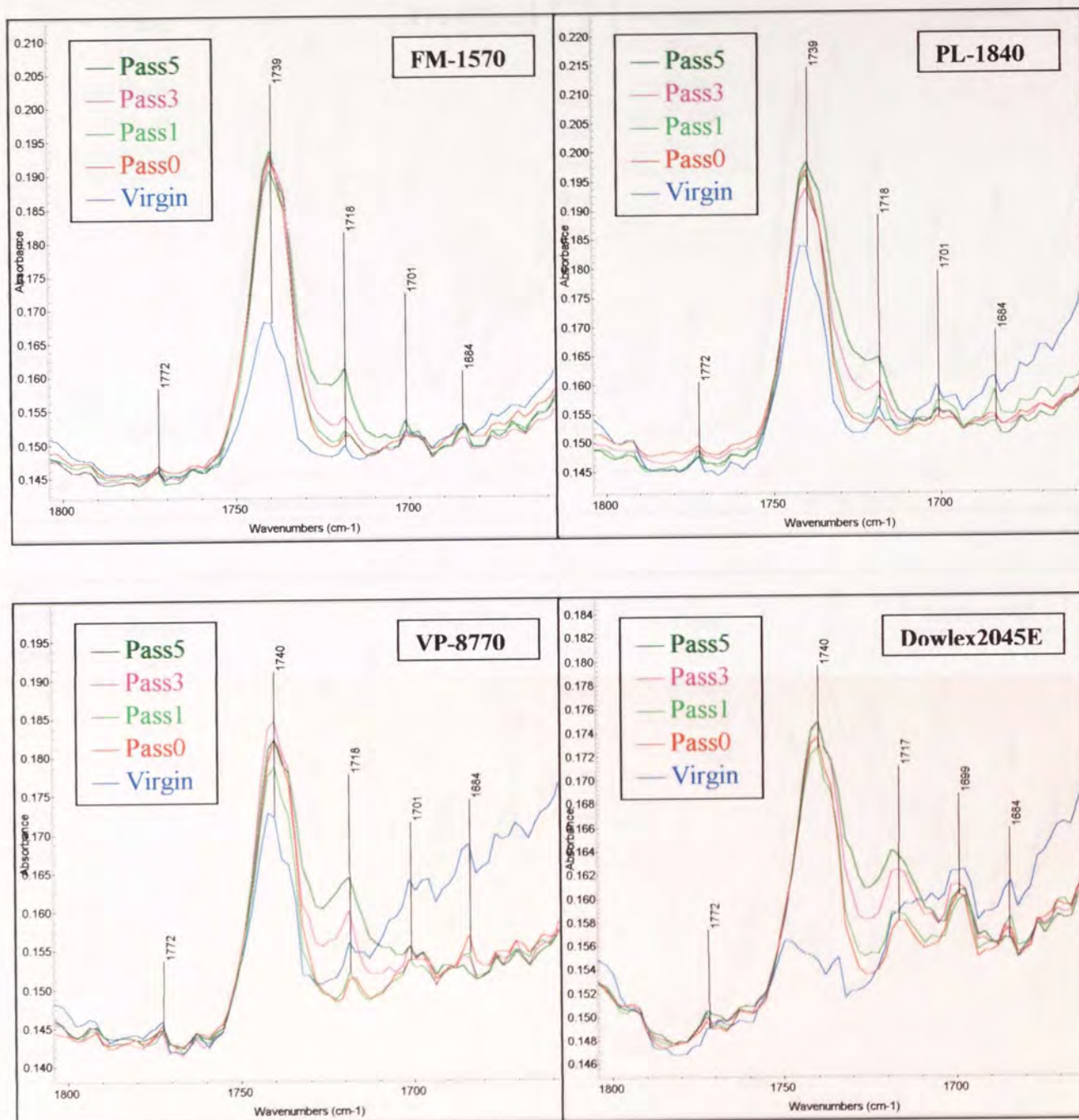


Figure 5.20. FTIR Spectra in Carbonyl Region for TSE Processed (265°C, 100rpm) LLDPE Polymers Containing **Irganox1076** (1772 cm⁻¹ γ -Lactone, 1739 cm⁻¹ Ester, 1718 cm⁻¹ Ketone, 1699~1701 cm⁻¹ Carboxylic acid, 1684~1685 cm⁻¹ Unsaturated ketone)

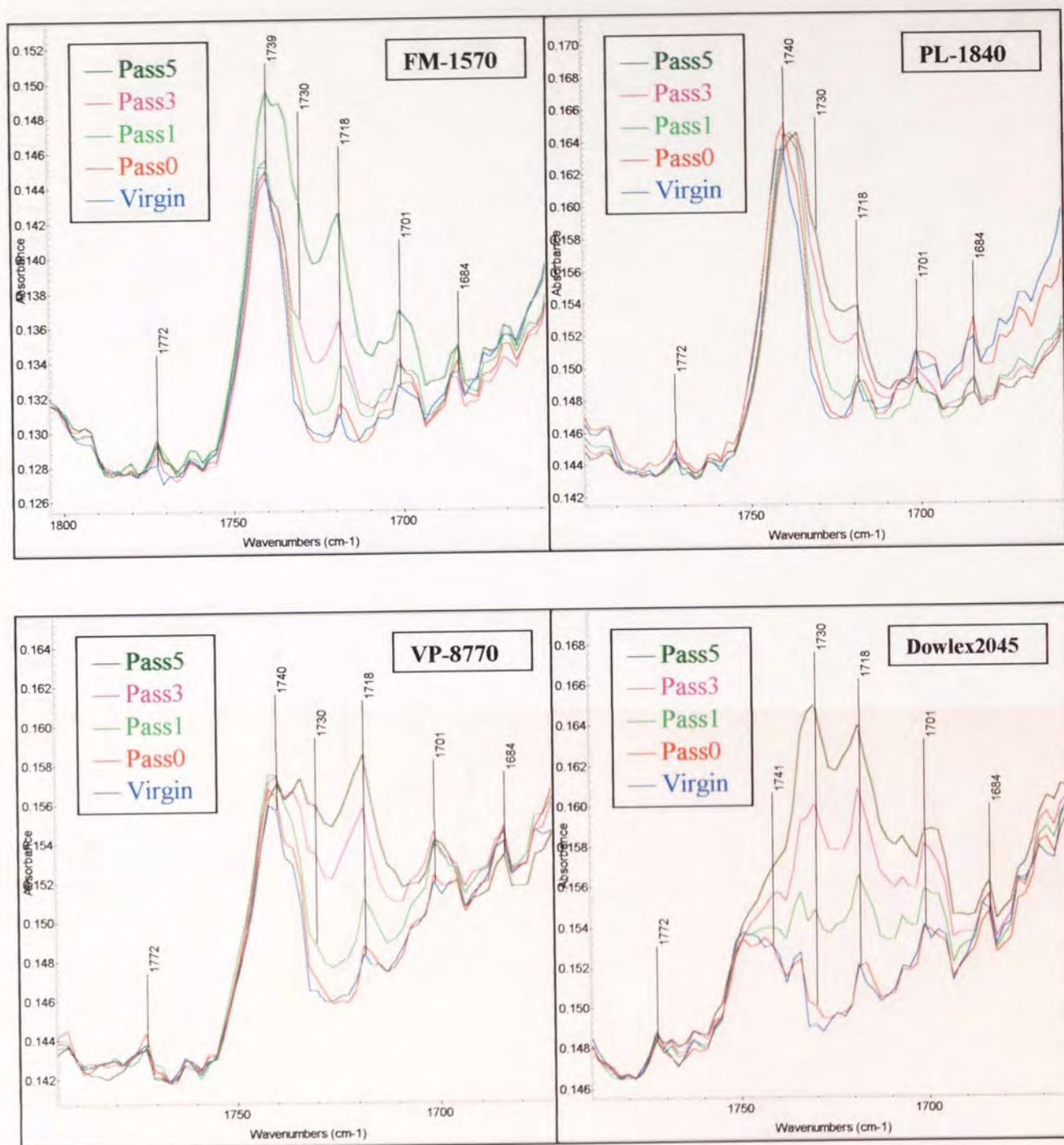


Figure 5.21. FTIR Spectra in Carbonyl Region for TSE Processed (265°C, 100rpm) LLDPE Polymers Containing **IrganoxE201** (1772 cm⁻¹ γ -Lactone, 1739~1741 cm⁻¹ Ester, 1730 cm⁻¹ Aldehyde, 1718 cm⁻¹ Ketone, 1701 cm⁻¹ Carboxylic acid, 1684 cm⁻¹ Unsaturated ketone)

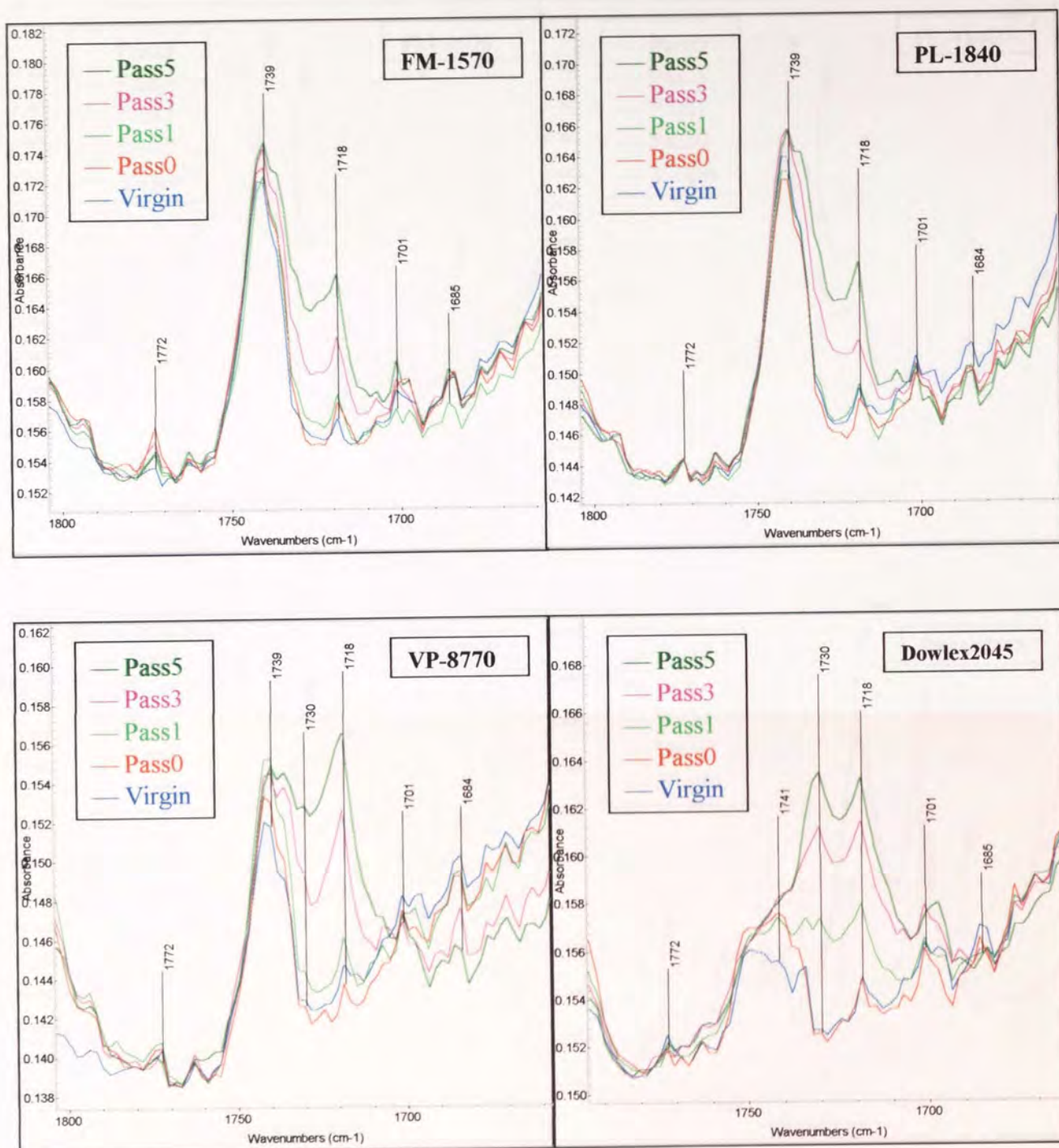


Figure 5.22. FTIR Spectra in Carbonyl Region for TSE Processed (265°C, 100rpm) LLDPE Polymers Containing **IrganoxHP136** (1772 cm⁻¹ γ -Lactone, 1739~1741 cm⁻¹ Ester, 1730 cm⁻¹ Aldehyde, 1718 cm⁻¹ Ketone, 1701 cm⁻¹ Carboxylic acid, 1684~1685 cm⁻¹ Unsaturated ketone)

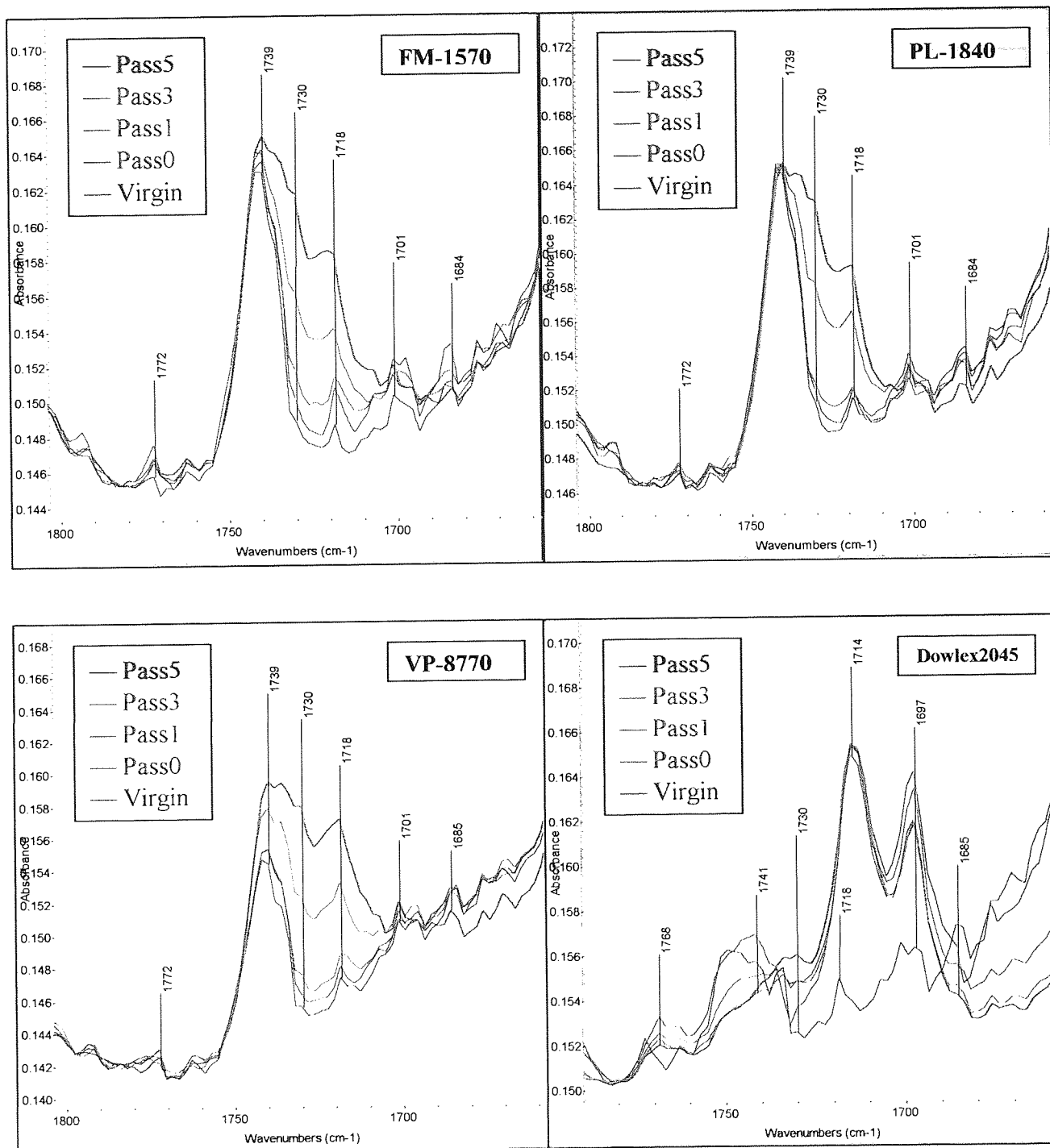


Figure 5.23. FTIR Spectra in Carbonyl Region for TSE Processed (265°C, 100rpm) LLDPE Polymers Containing **Ultranox626** (1768~1772 cm⁻¹ γ -Lactone, 1739~1741 cm⁻¹ Ester, 1730 cm⁻¹ Aldehyde, 1714~1718 cm⁻¹ Ketone, 1697~1701 cm⁻¹ Carboxylic acid, 1684~1685 cm⁻¹ Unsaturated ketone)

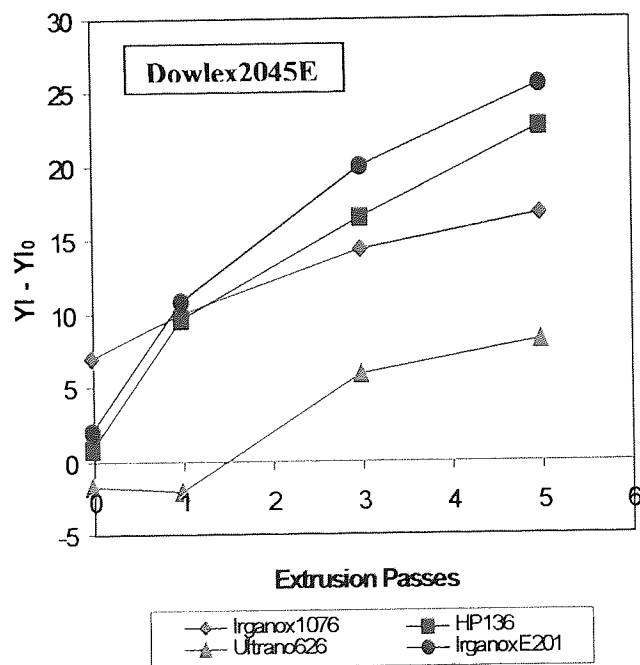
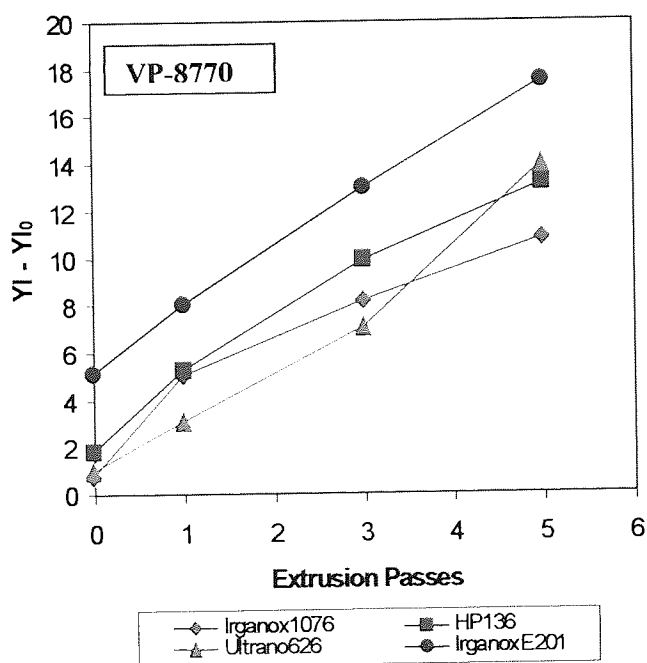
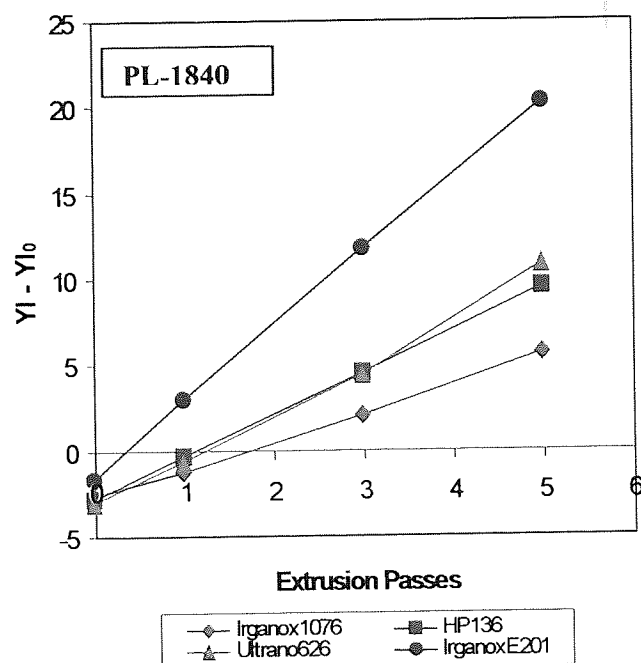
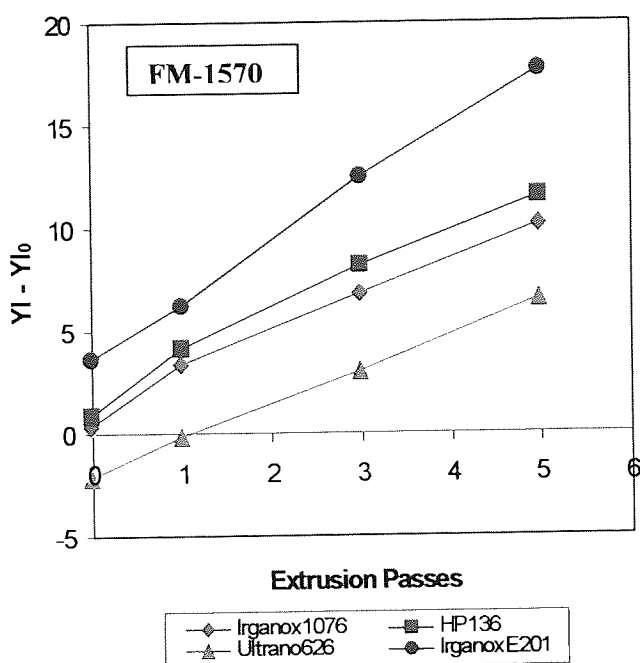


Figure 5.24. Yellow Index Change ($YI - YI_0$) for TSE Processed LLDPE Polymers Containing Single Antioxidants (265°C , 100rpm)

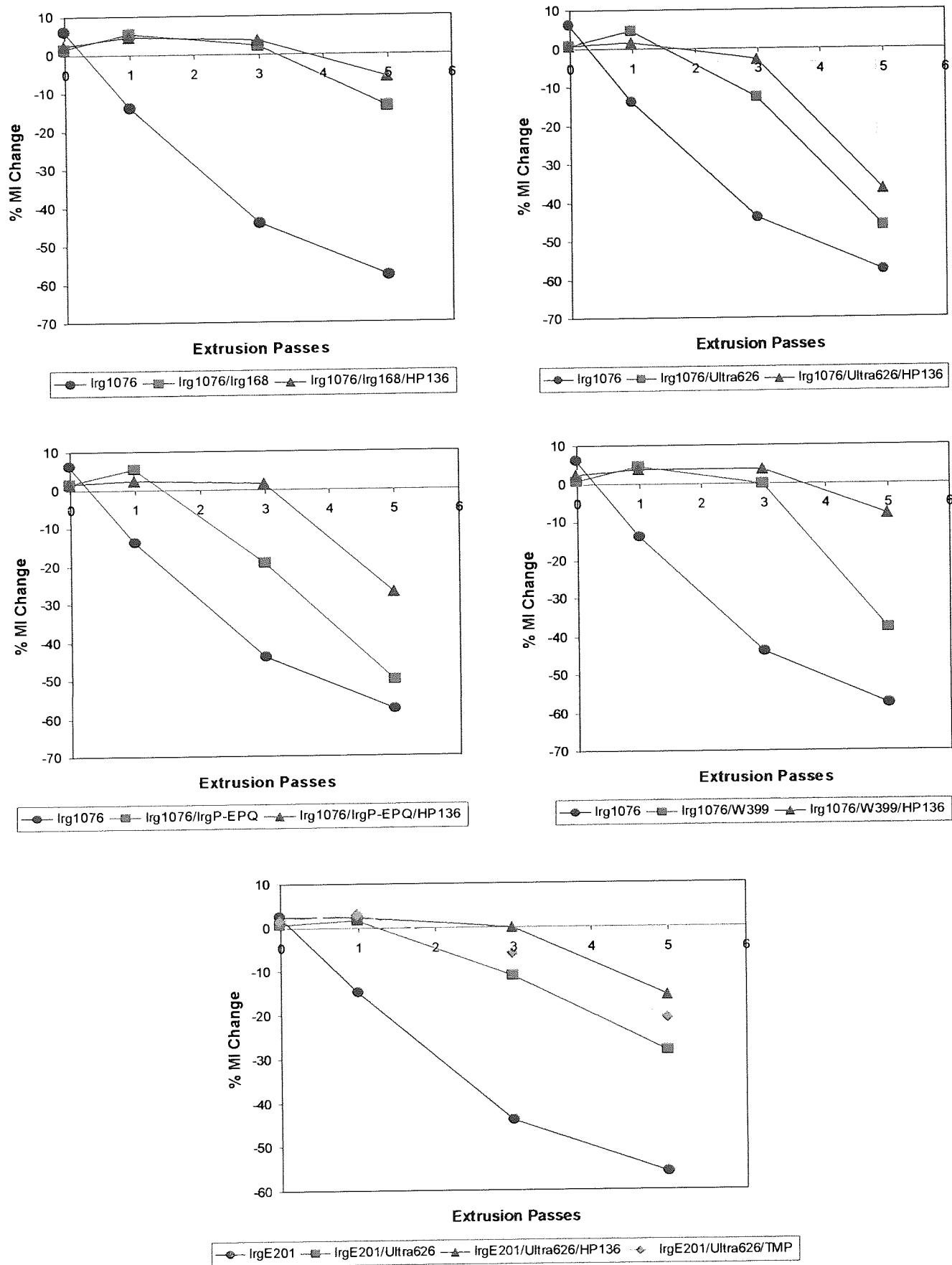


Figure 5.25. Percentage MI Change with Extrusion Passes for TSE Processed **PL-1840** Containing Different Antioxidant Mixtures (265°C, 100rpm, see Table 5.2 for AO composition)

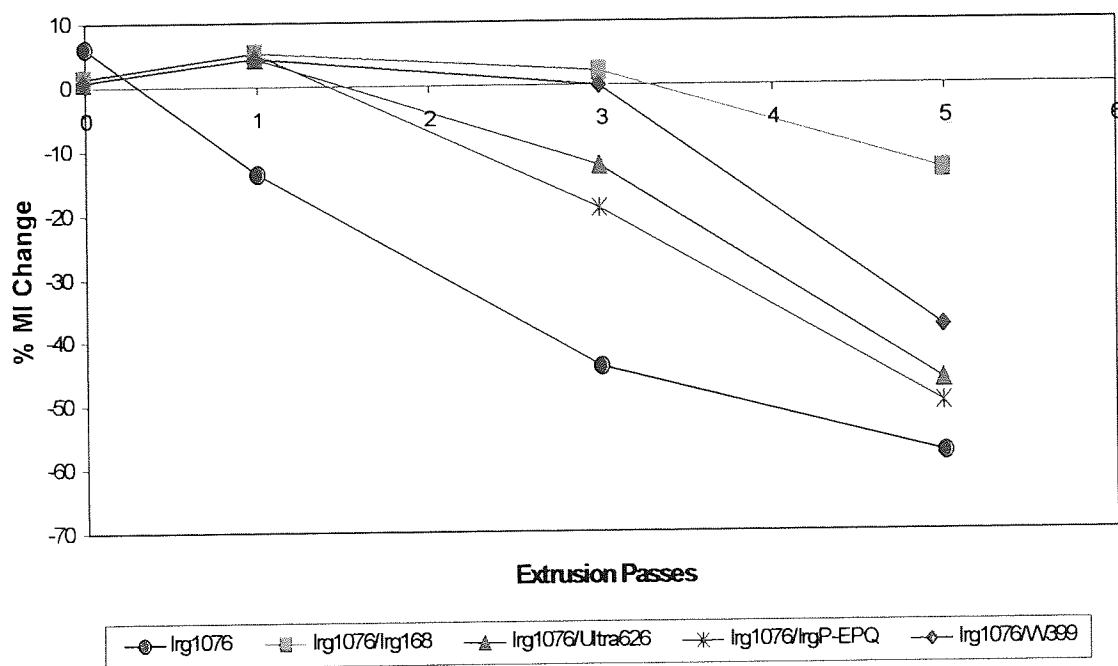


Figure 5.26. Percentage MI Change with Extrusion Passes for TSE Processed **PL-1840** Containing Irg1076 and Different Phosphite Antioxidants (265°C, 100rpm, see Table 5.2 for AO composition)

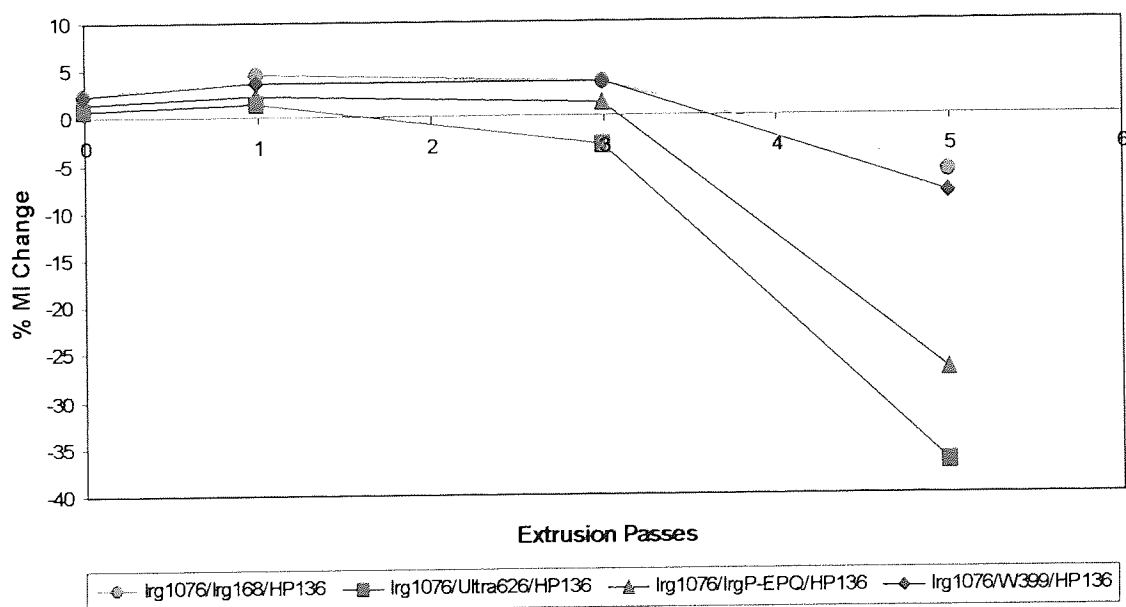


Figure 5.27. Percentage MI Change with Extrusion Passes for TSE Processed **PL-1840** Containing Irg1076, HP136 and Different Phosphite Antioxidants (265°C, 100rpm, see Table 5.2 for AO composition)

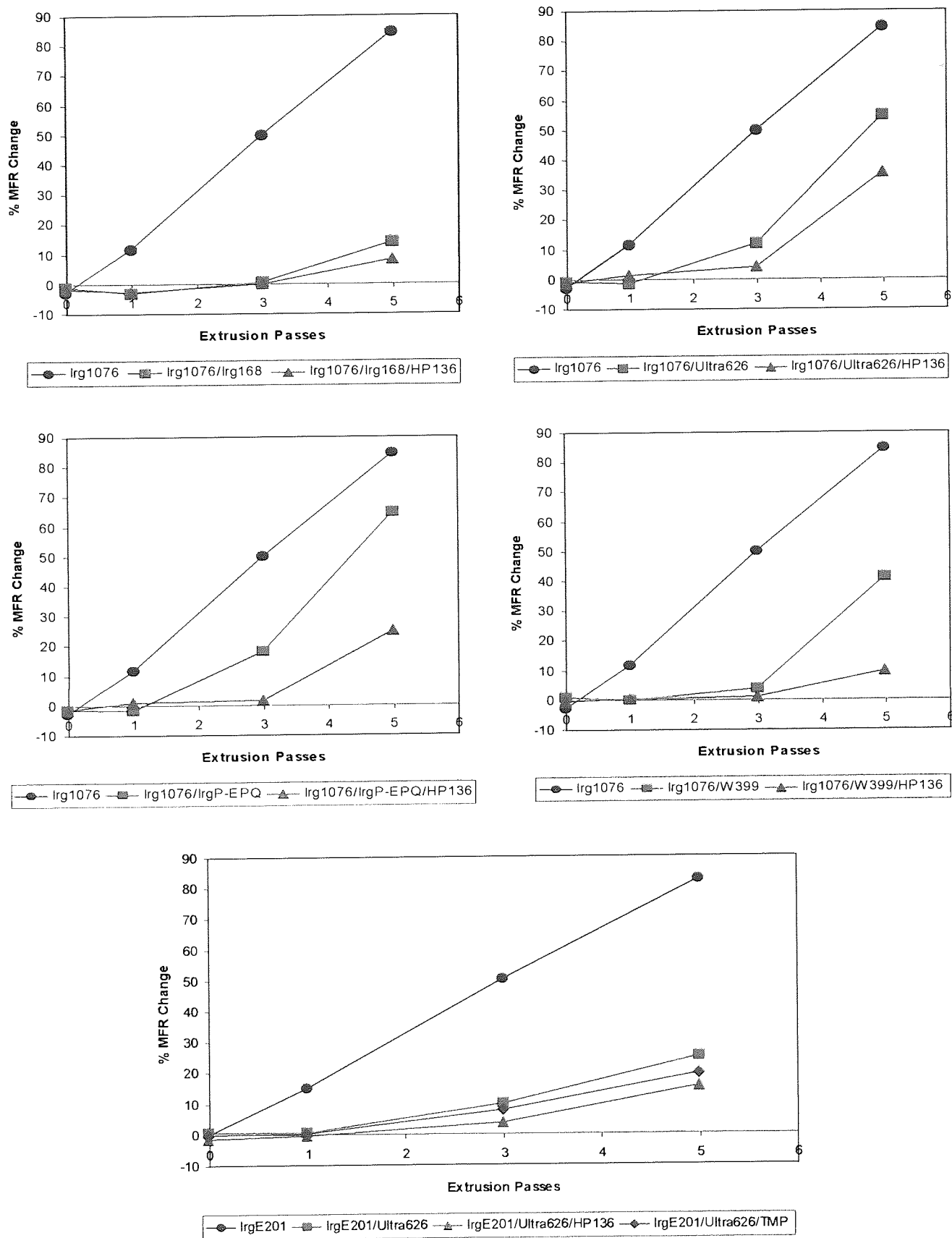


Figure 5.28. Percentage MFR Change with Extrusion Passes for TSE Processed **PL-1840** Containing Different Antioxidant Mixtures (265°C, 100rpm)

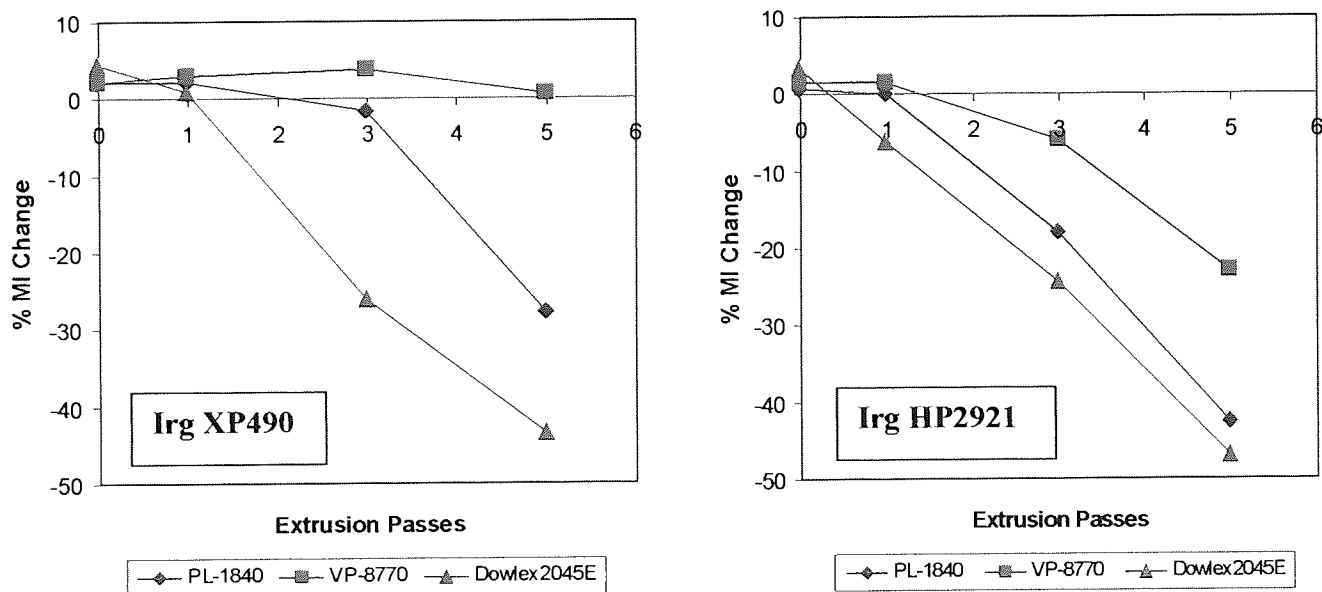


Figure 5.29. Percentage MI Change with Extrusion Passes for TSE Processed LLDPE Containing Commercial Antioxidant Mixtures (265°C, 100rpm, **IrgXP490** – Irg1076: IrgP-EPQ: HP136 = 3:2:1, **IrgHP2921** – Irg1076: Irg168: HP136= 2:4:1)

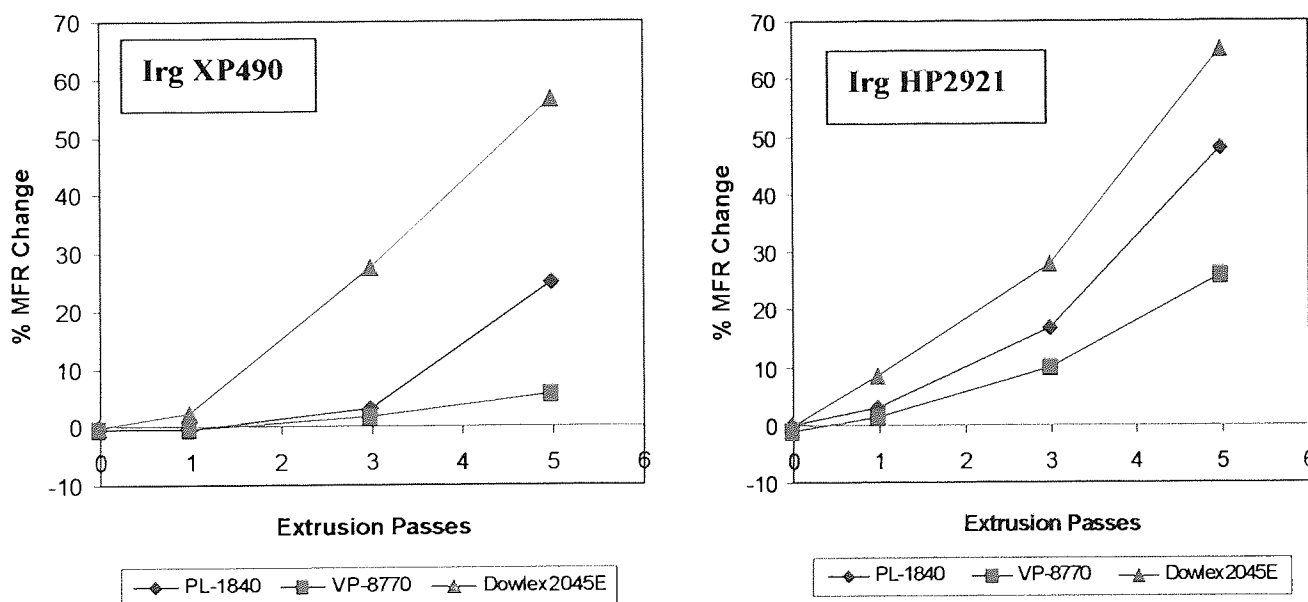


Figure 5.30. Percentage MFR Change with Extrusion Passes for TSE Processed LLDPE Containing Commercial Antioxidant Mixtures (265°C, 100rpm, **IrgXP490** – Irg1076: IrgP-EPQ: HP136 = 3:2:1, **IrgHP2921** – Irg1076: Irg168: HP136= 2:4:1)

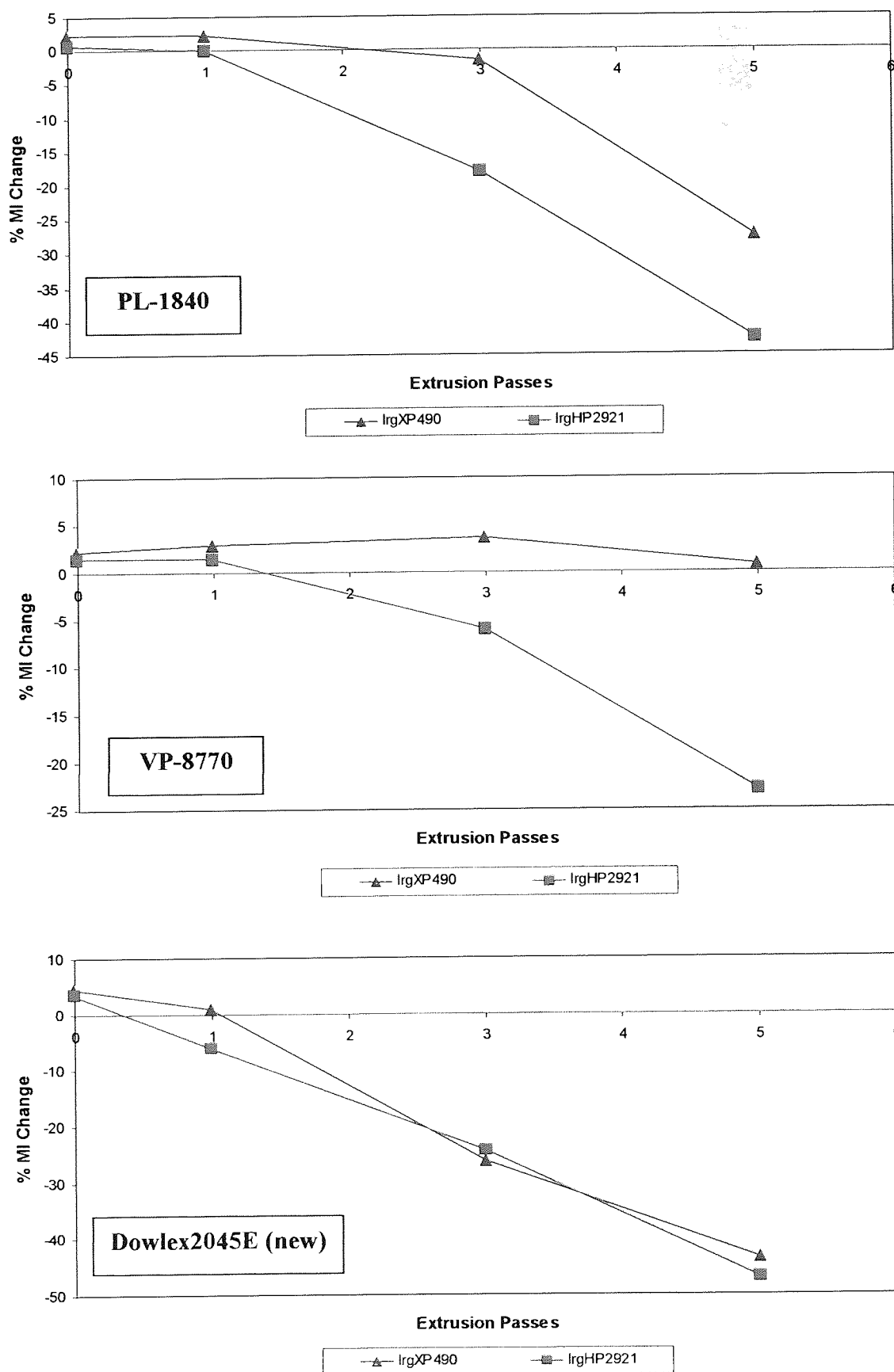


Figure 5.31. Percentage MI Change with Extrusion Passes for Extruded LLDPE Containing Different Commercial Antioxidant Mixtures (265°C, 100rpm)

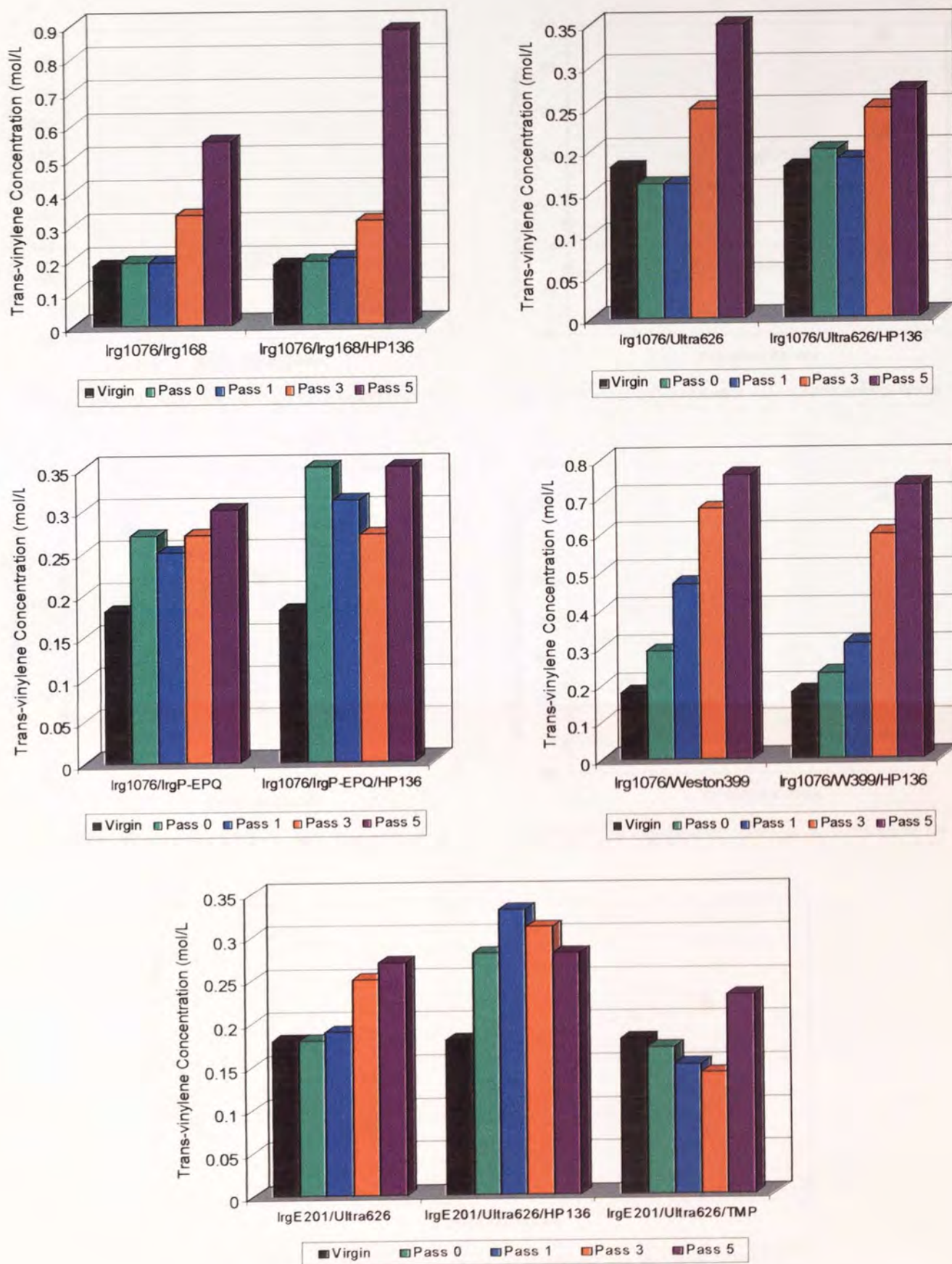


Figure 5.32. Changes in Trans-vinylene Concentration with Extrusion Passes for TSE Processed PL-1840 Containing Different Antioxidant Mixtures (265°C, 100rpm)

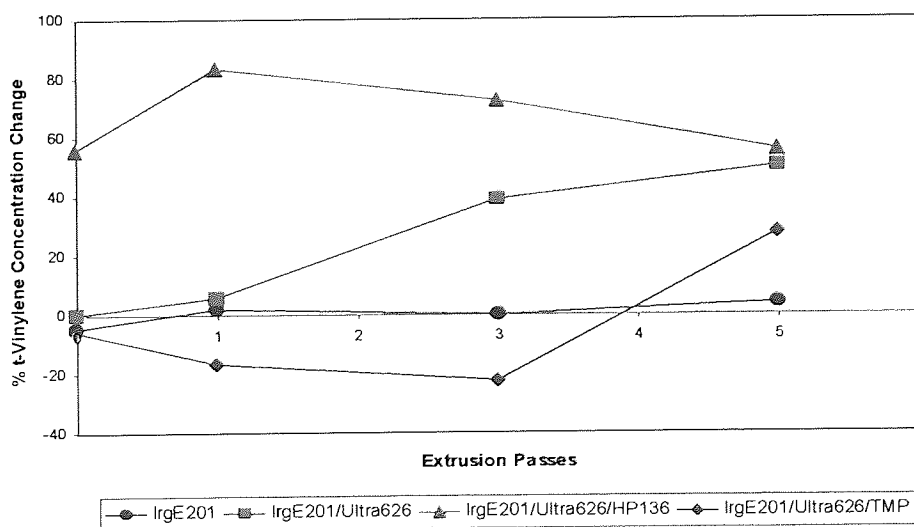
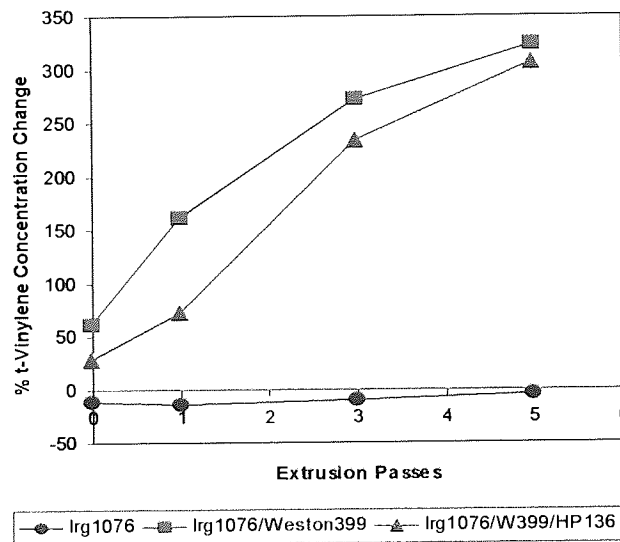
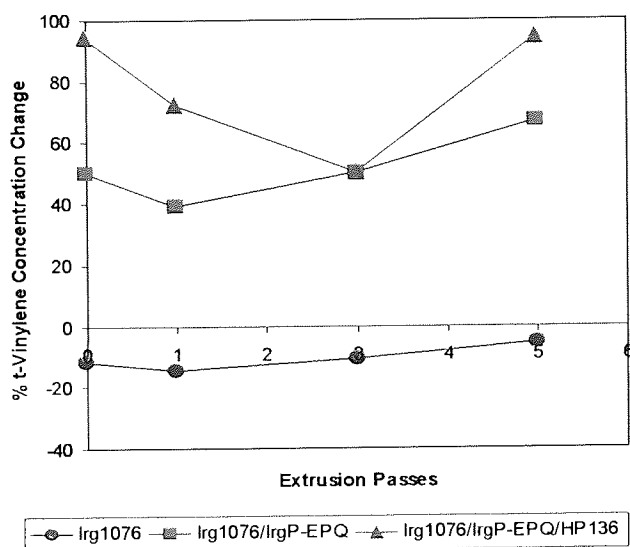
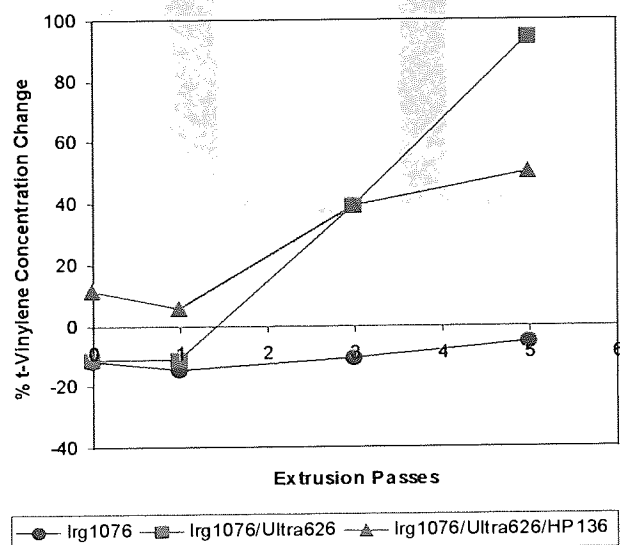
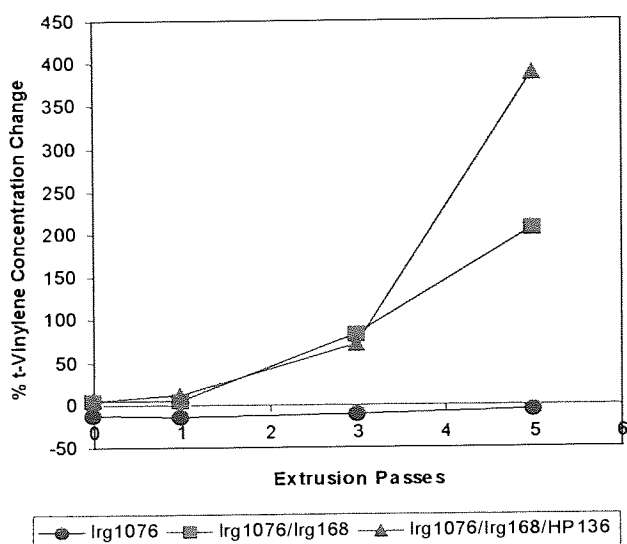


Figure 5.33. Percentage Concentration Change of Trans-vinylene with Extrusion Passes for TSE Processed PL-1840 Containing Different Antioxidant Mixtures (265°C, 100rpm)

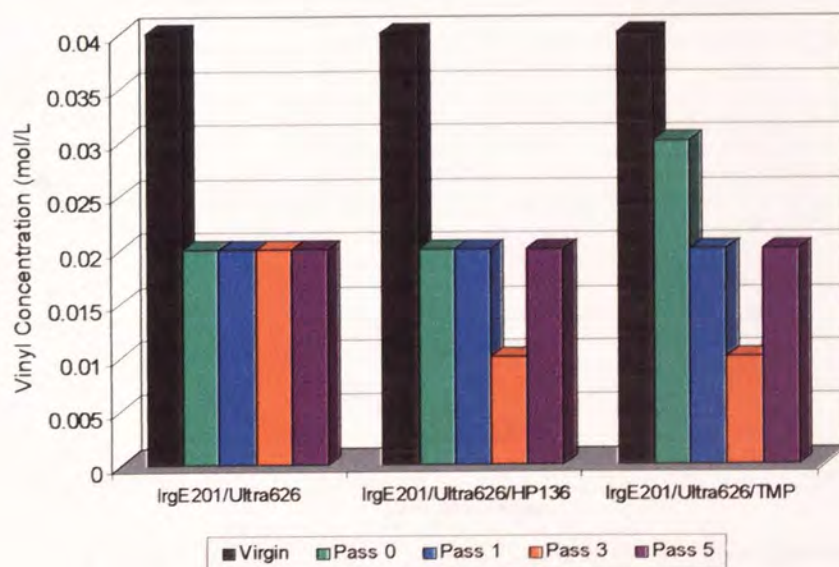
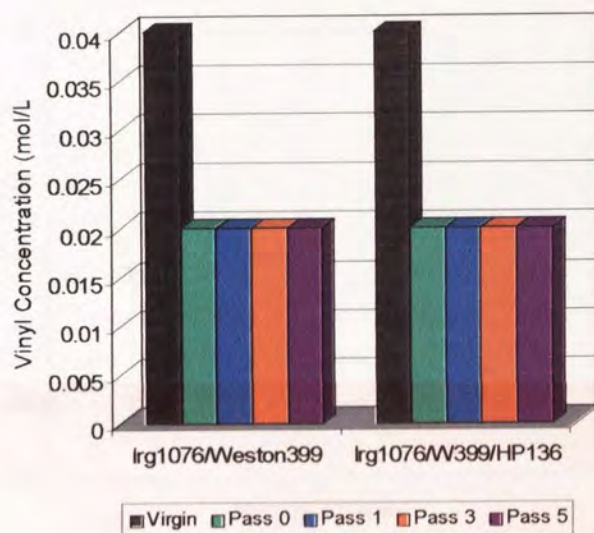
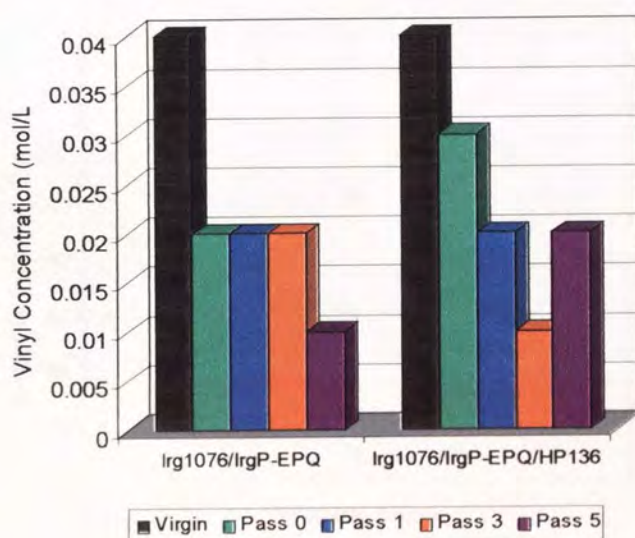
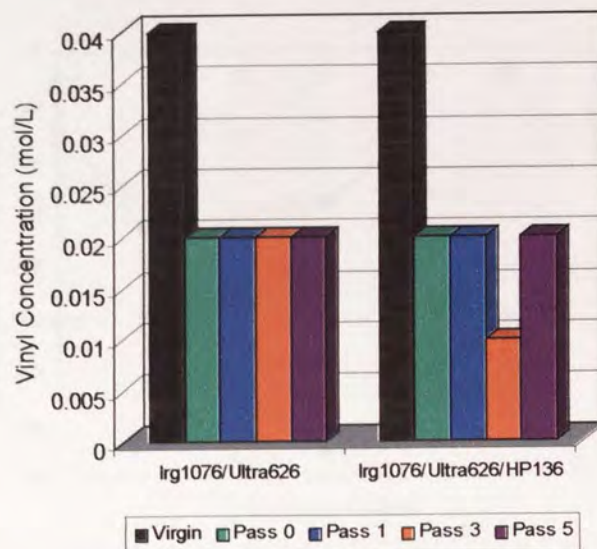
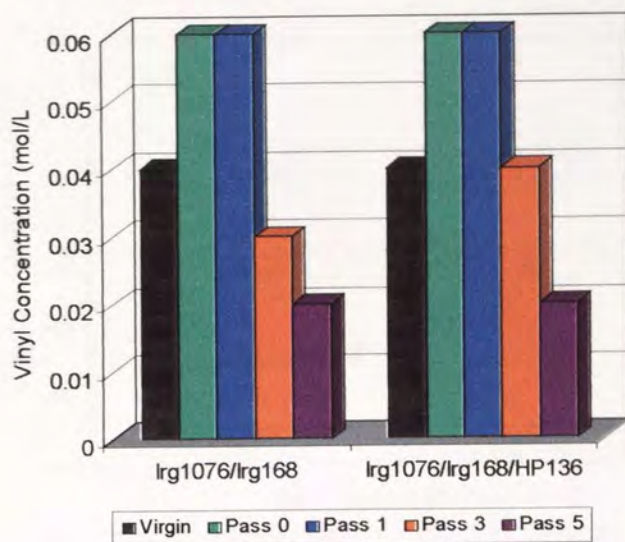


Figure 5.34. Changes in Vinyl Concentration with Extrusion Passes for TSE Processed **PL-1840** Containing Different Antioxidant Mixtures (265°C, 100rpm)

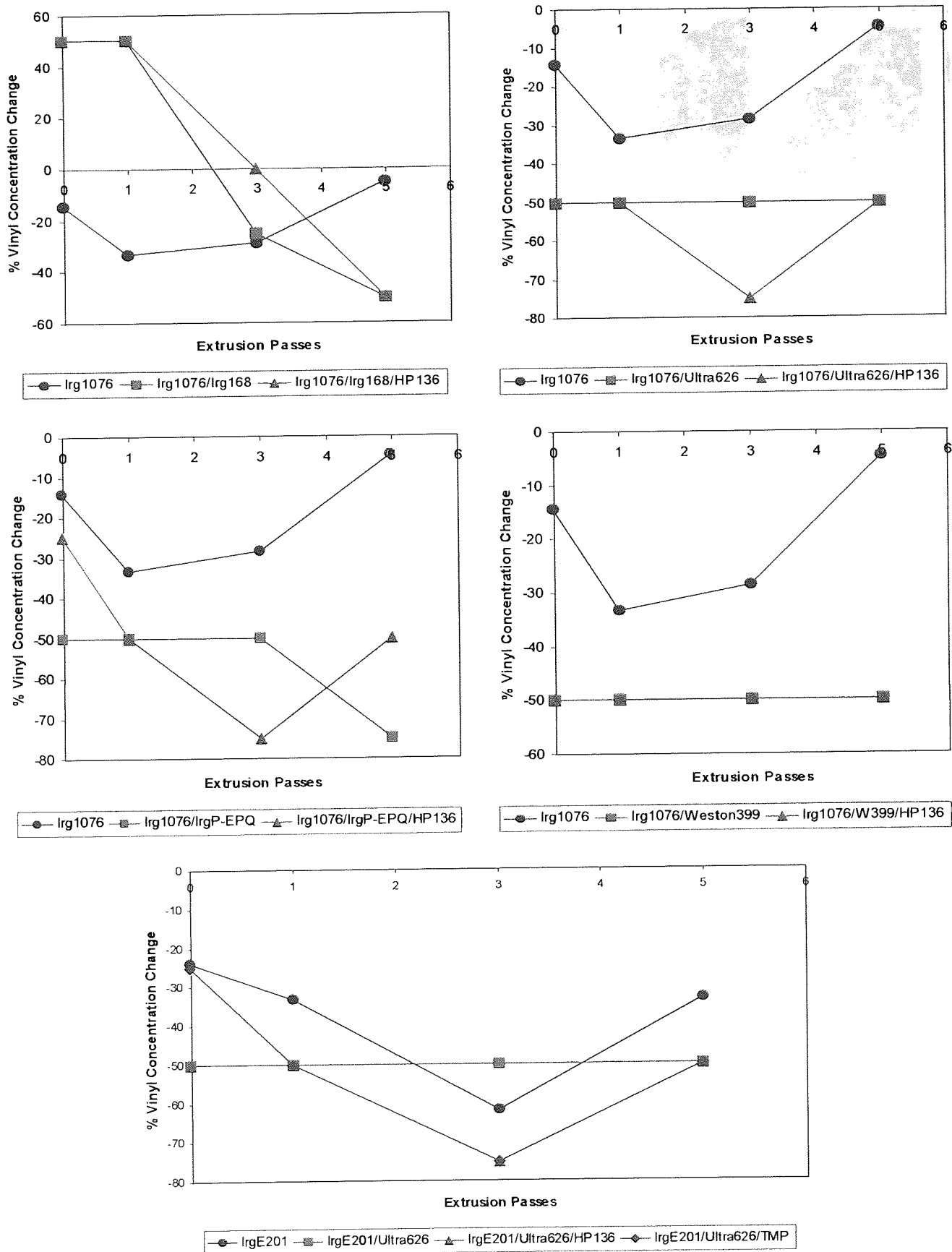


Figure 5.35. Percentage Concentration Change of Vinyl Group with Extrusion Passes for TSE Processed **PL-1840** Containing Different Antioxidant Mixtures (265°C, 100rpm)

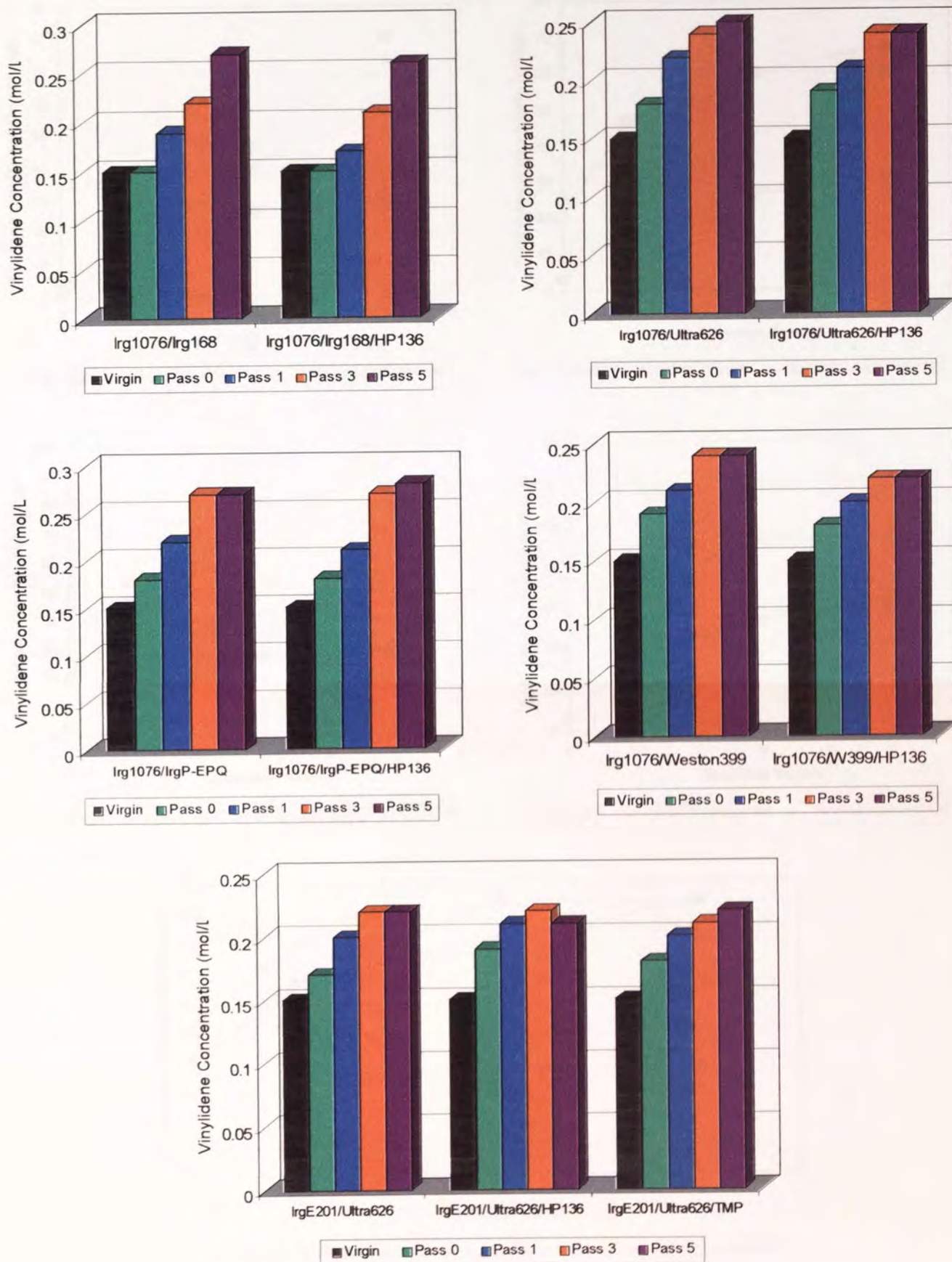


Figure 5.36. Changes in Vinylidene Concentration with Extrusion Passes for TSE Processed PL-1840 Containing Different Antioxidant Mixtures (265°C, 100rpm)

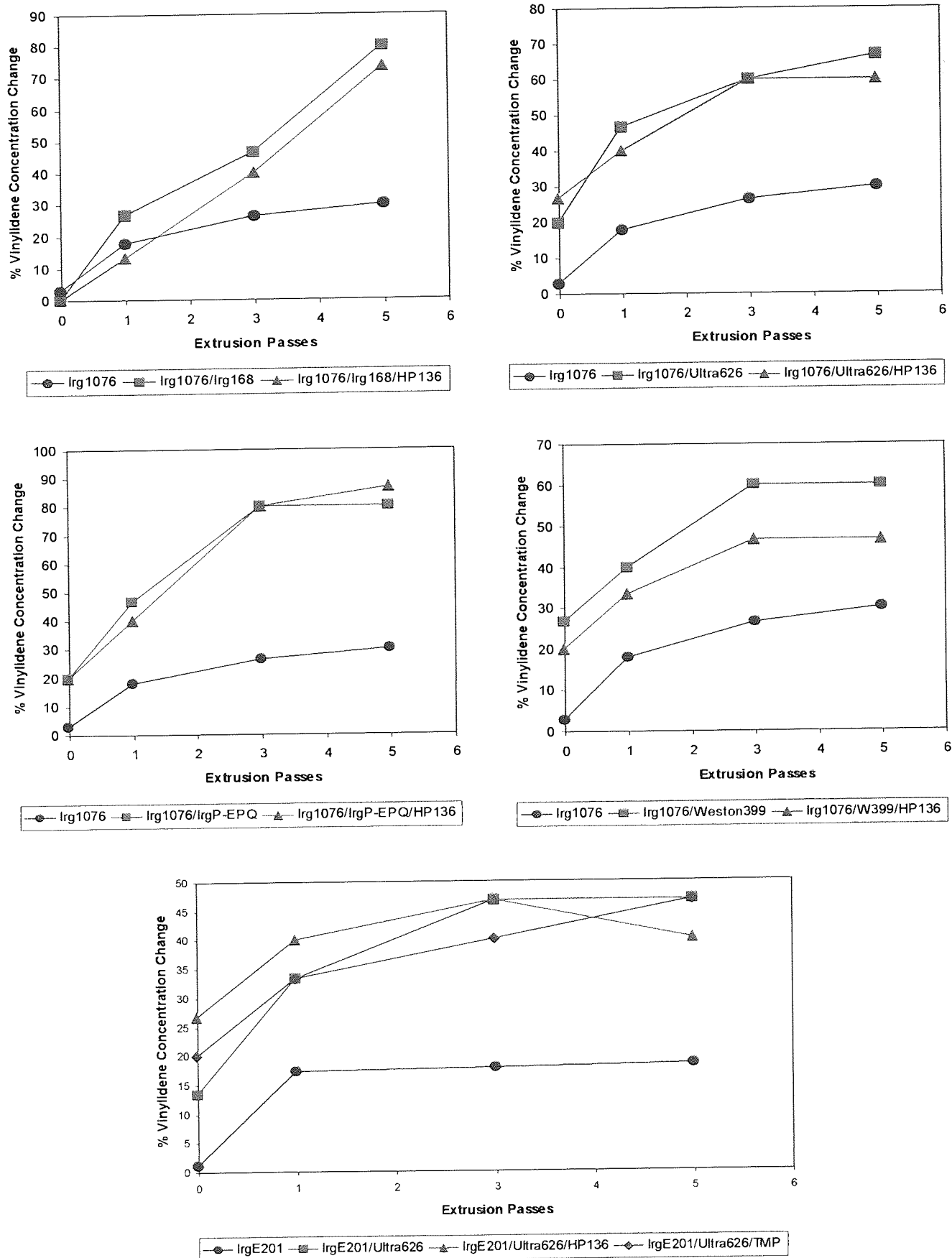


Figure 5.37. Percentage Concentration Change of Vinylidene Group with Extrusion Passes for TSE Processed **PL-1840** Containing Different Antioxidant Mixtures (265°C, 100rpm)

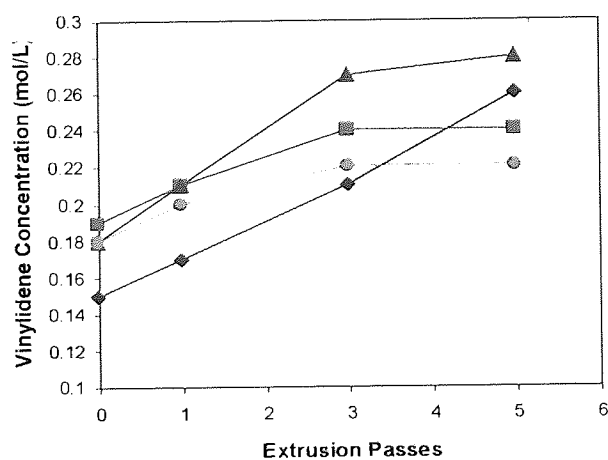
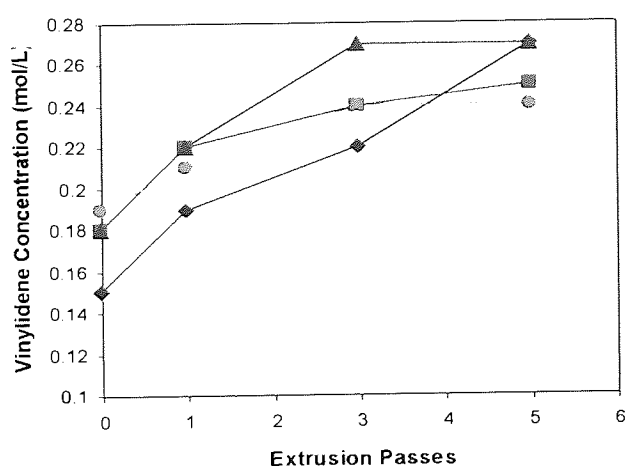
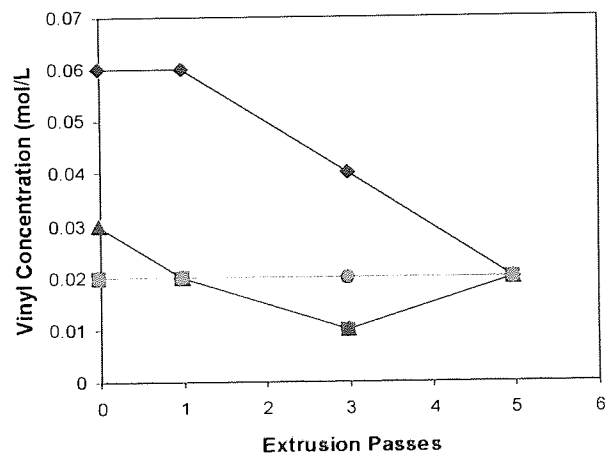
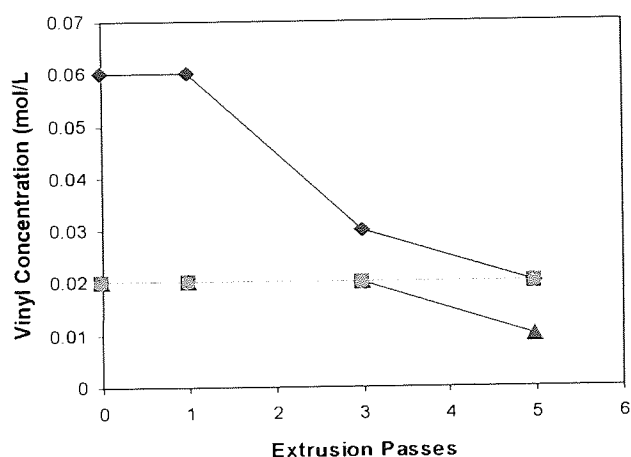
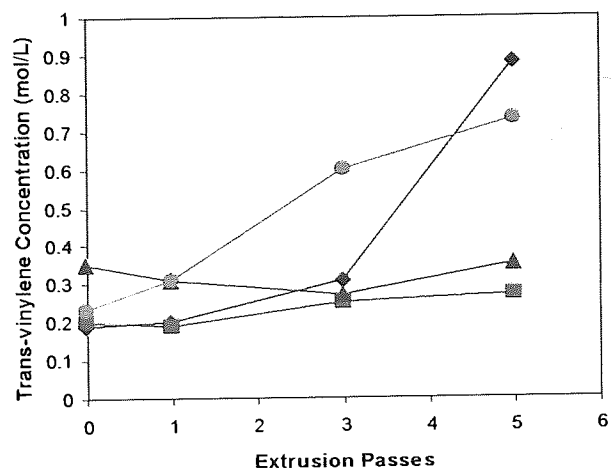
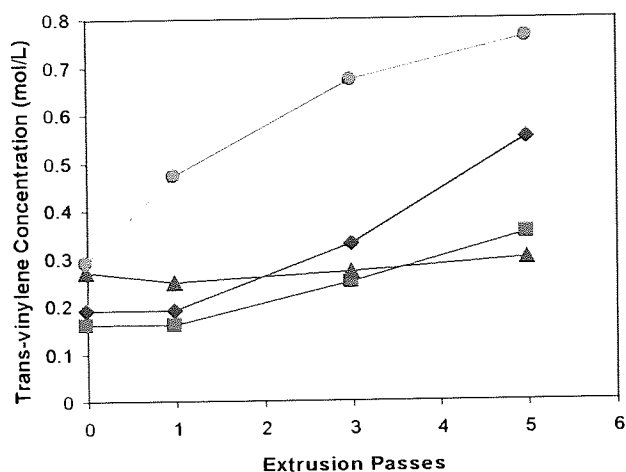


Figure 5.38(a). Changes of Unsaturated Group Concentrations with Extrusion Passes for TSE Processed PL-1840 Containing Different Antioxidant Mixtures (265°C, 100rpm)

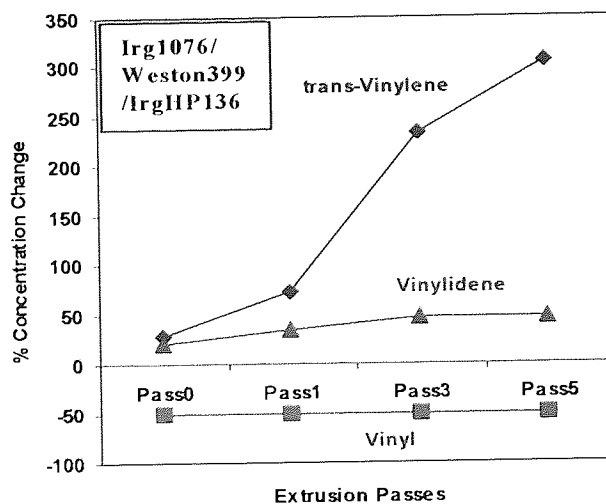
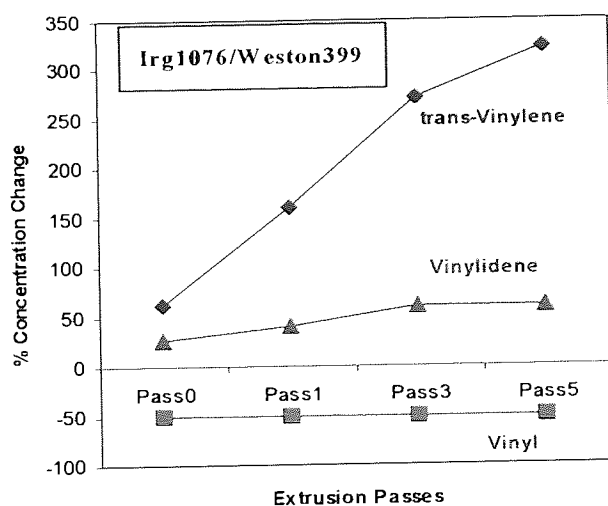
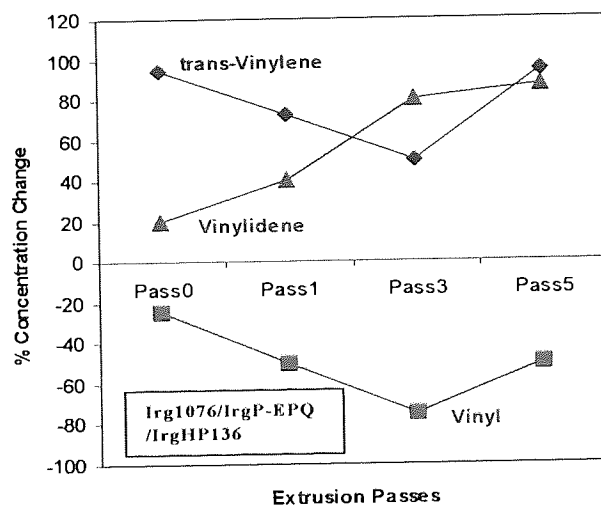
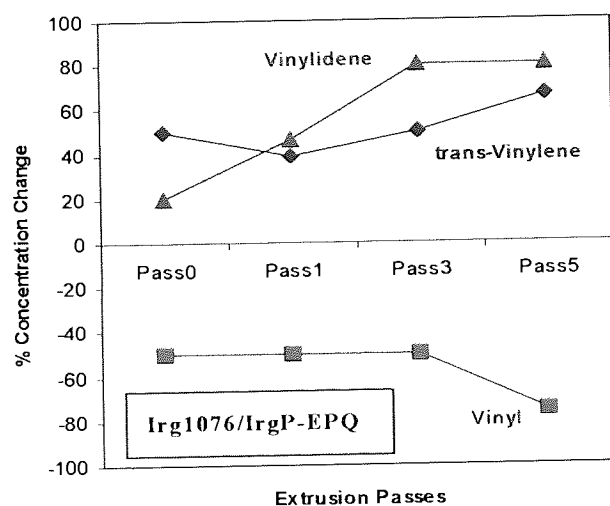
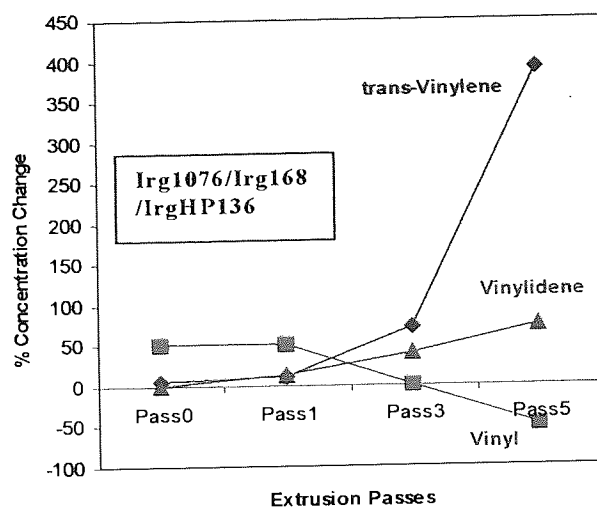
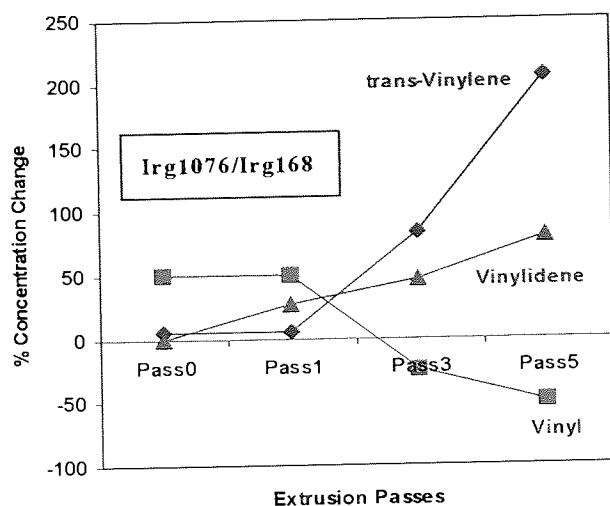


Figure 5.38(b) continue to next Page...

Figure 5.38(b) continued....

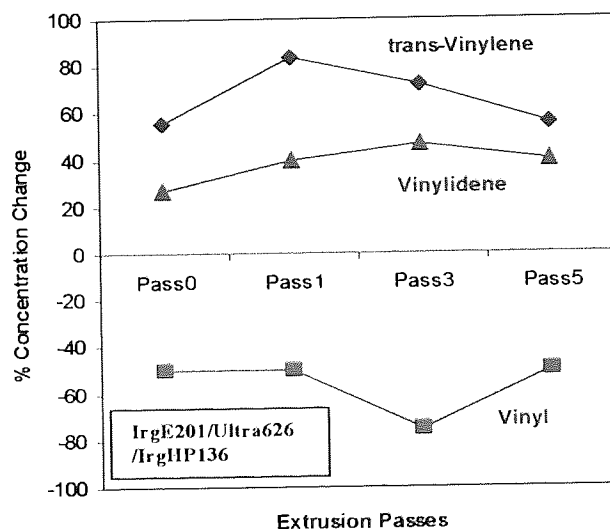
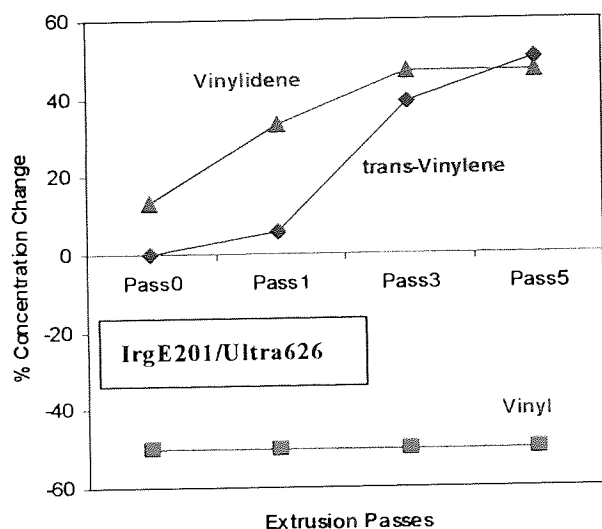
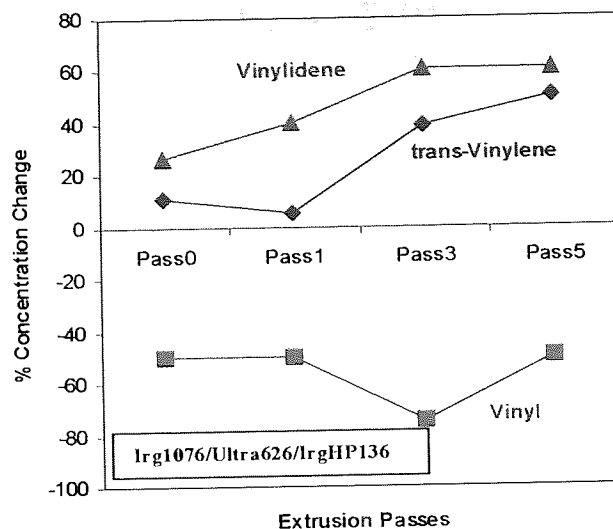
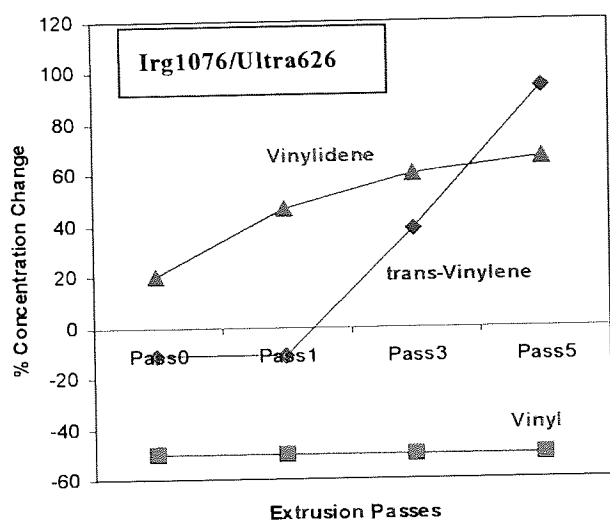


Figure 5.38(b). Percentage Concentration Change of Unsaturated Groups with Extrusion Passes for TSE Processed **PL-1840** Containing Different Antioxidant Mixtures (265°C, 100rpm)

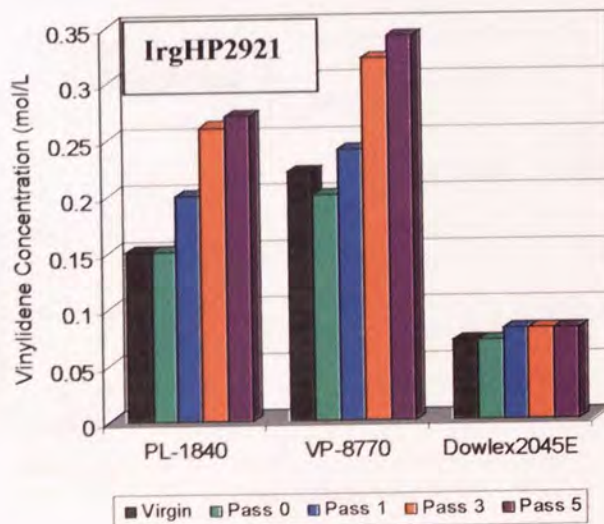
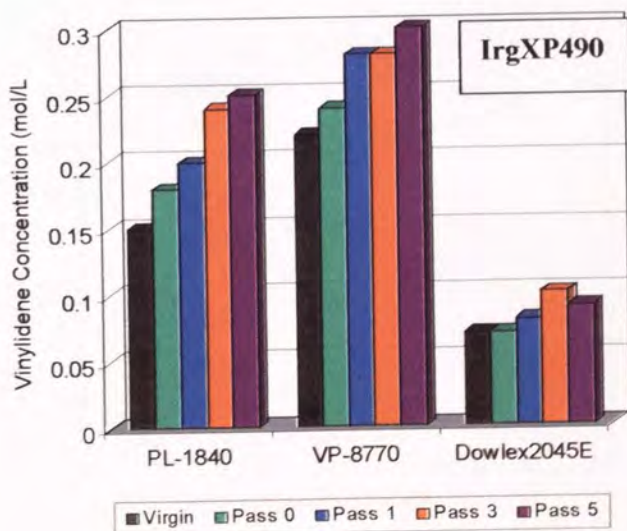
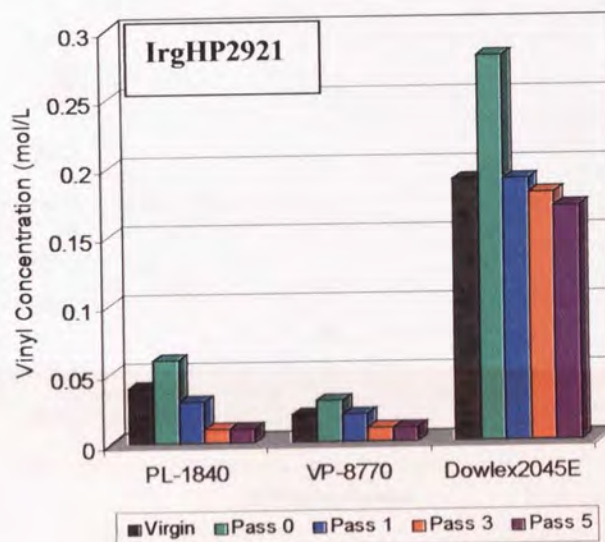
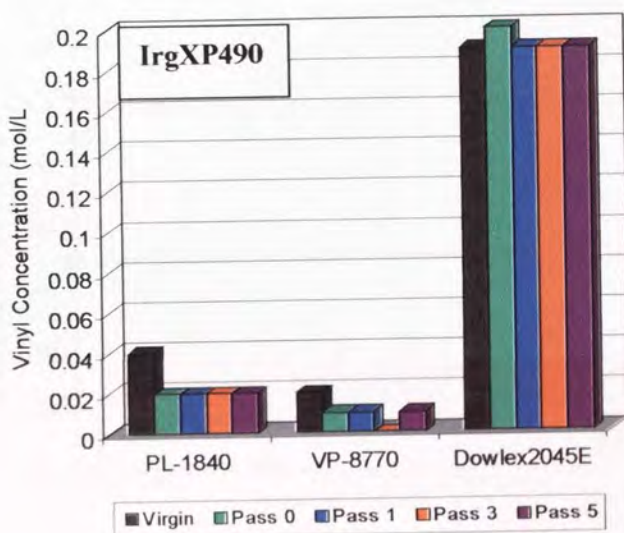
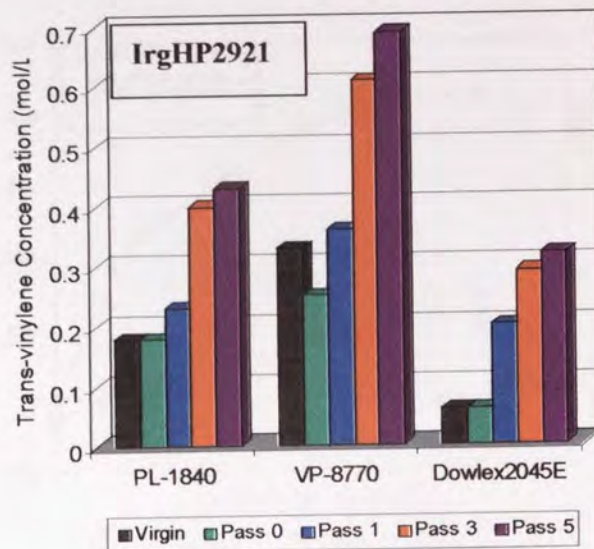
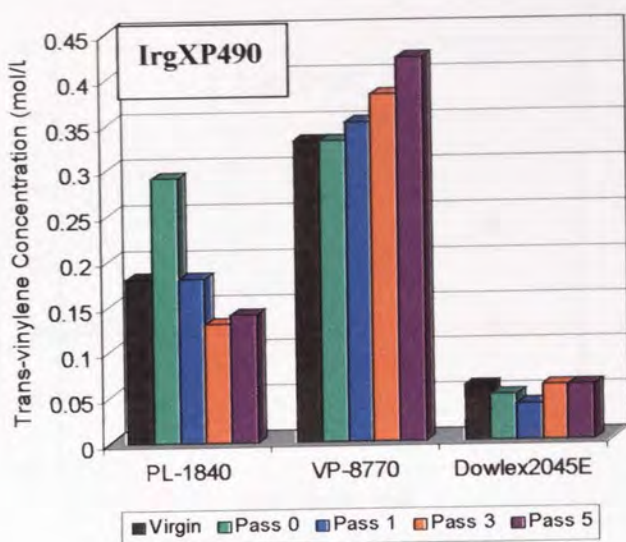


Figure 5.39. Double Bond Concentration Change with Extrusion Passes for TSE Processed LLDPE Polymers Containing Commercial Antioxidant Mixtures (265°C, 100rpm)

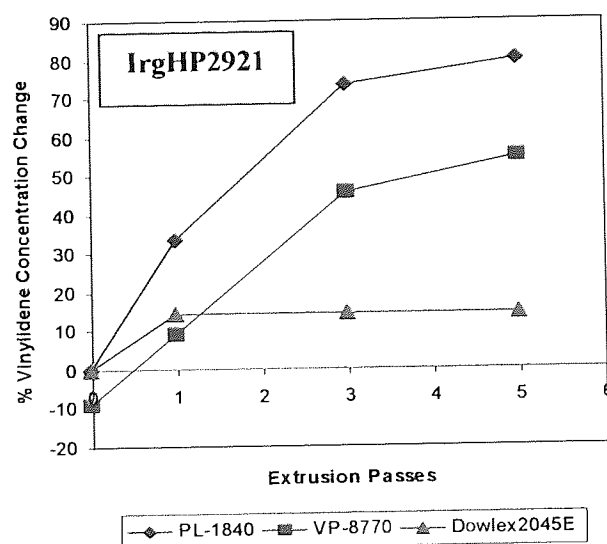
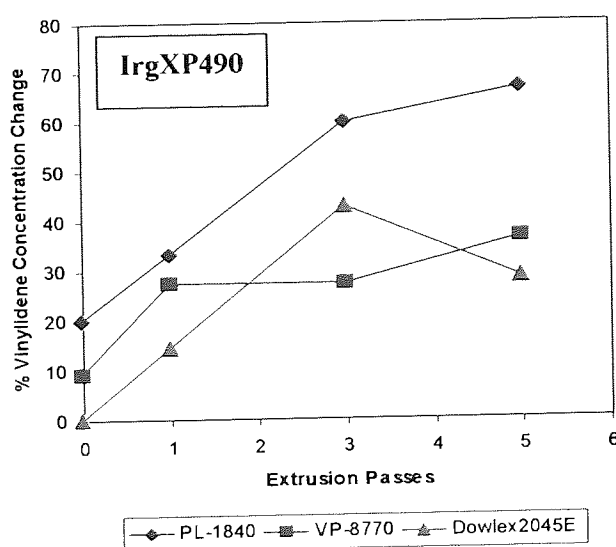
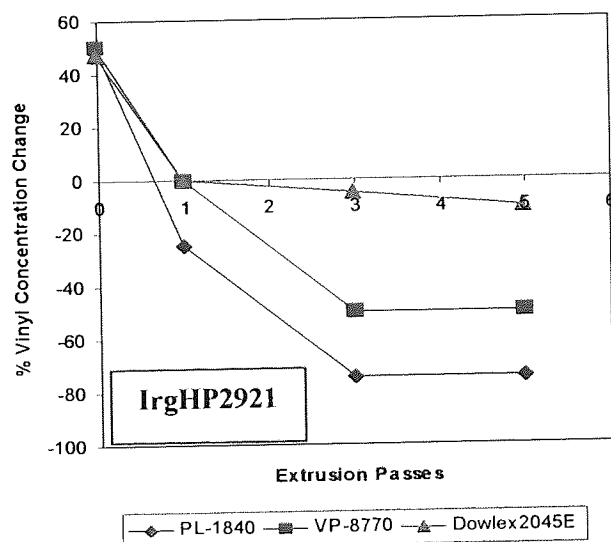
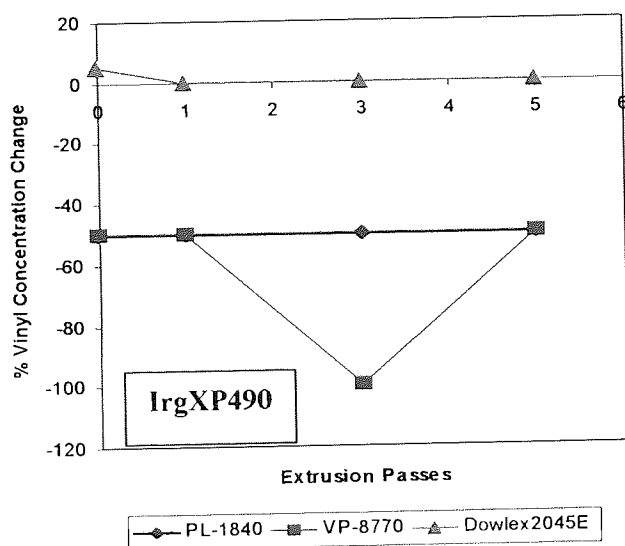
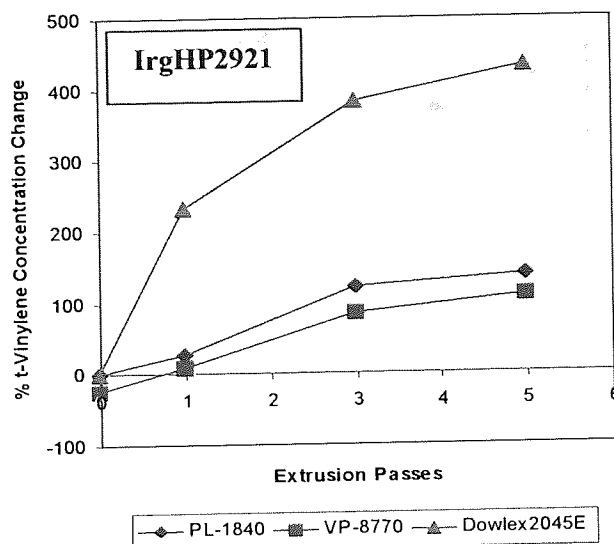
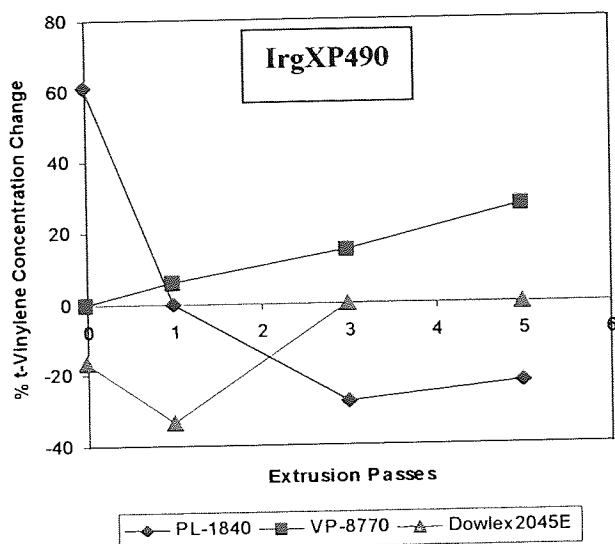


Figure 5.40. Percentage Change of Double Bond Concentrations with Extrusion Passes for TSE Processed LLDPE Polymers Containing Commercial Antioxidant Mixtures (265°C, 100rpm)

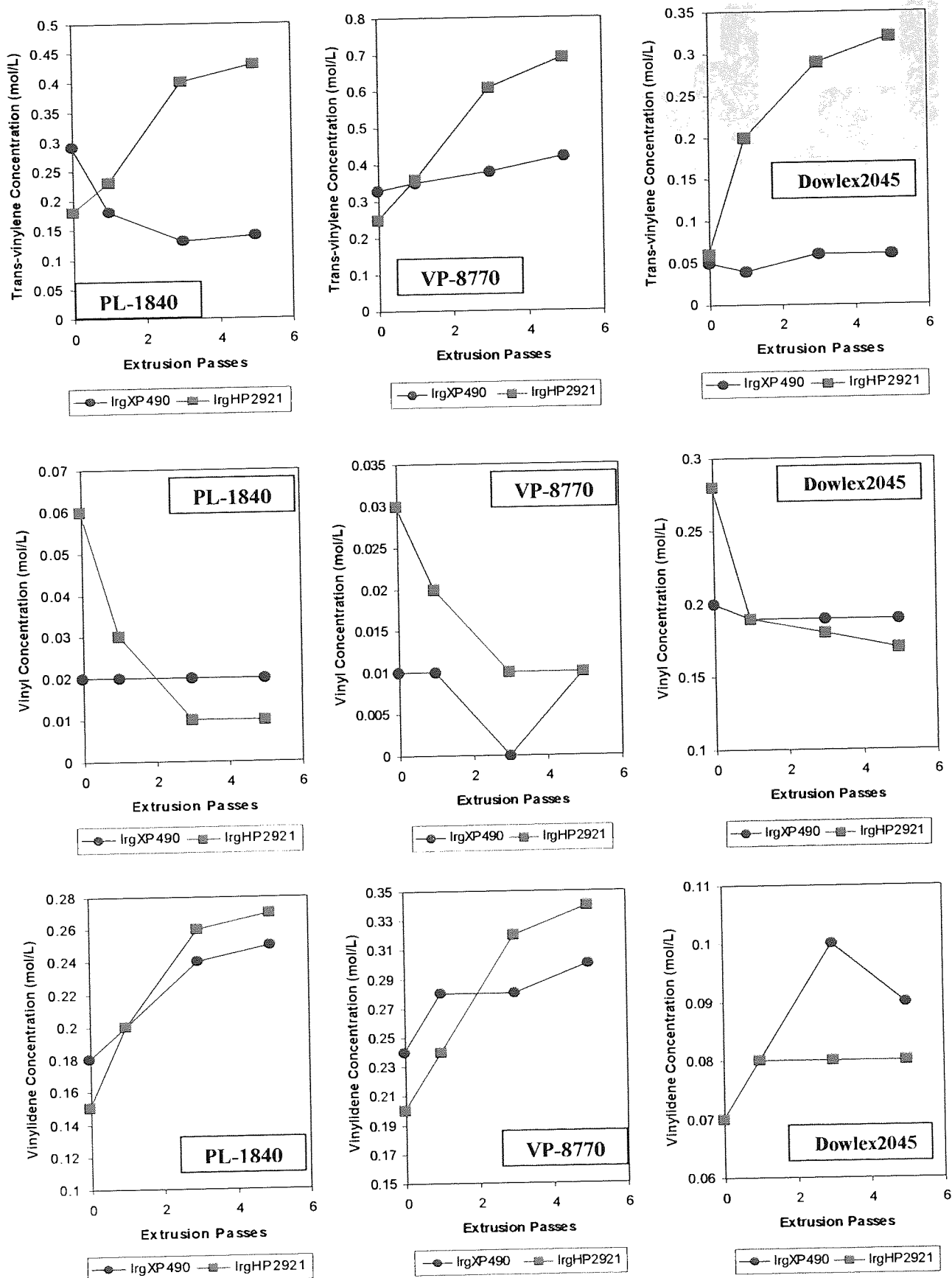


Figure 5.41. The Changes of Unsaturated Concentrations with Extrusion Passes for TSE Processed LLDPE Polymers Containing Different Commercial Antioxidant Mixtures (265°C, 100rpm)

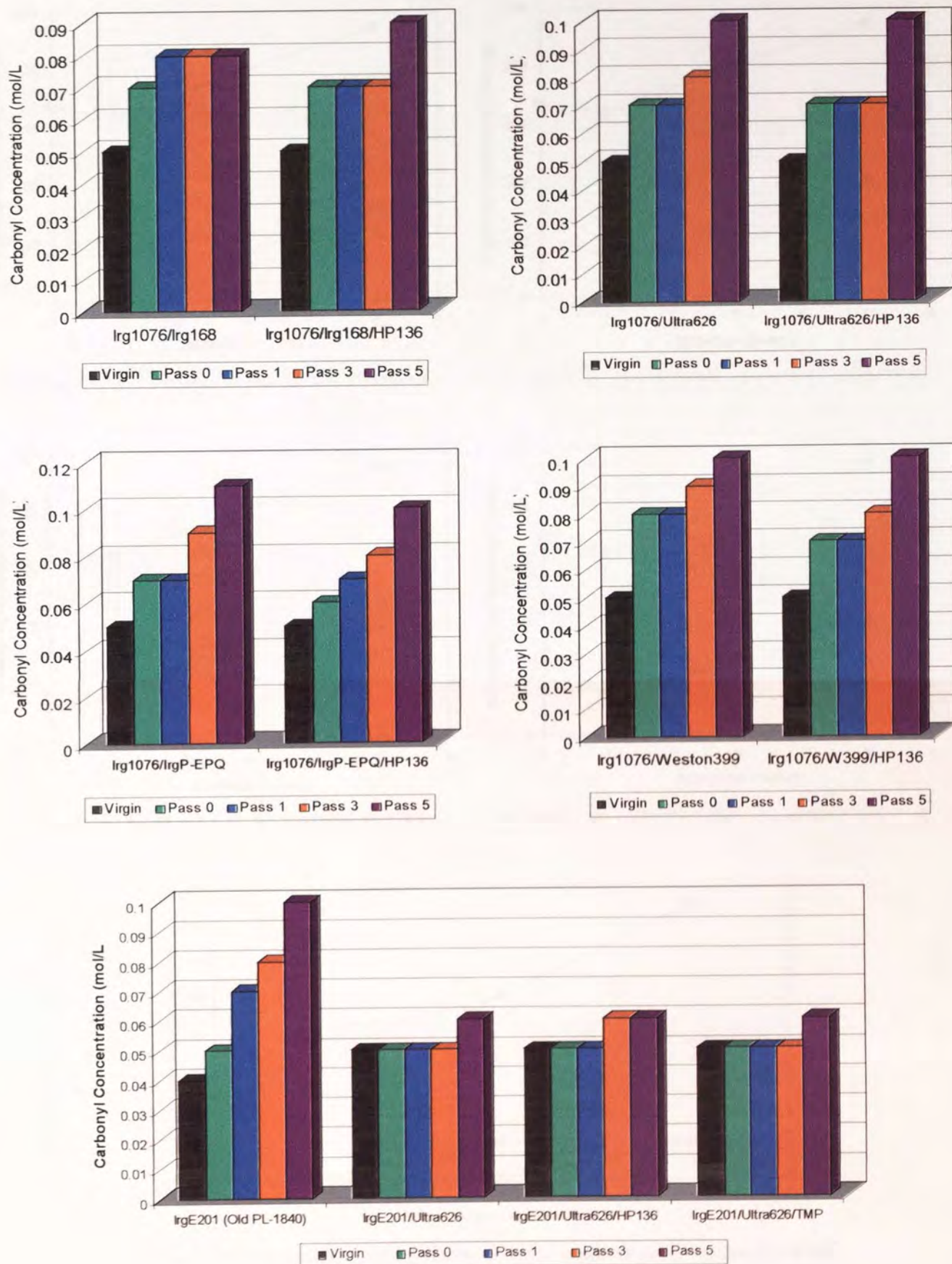


Figure 5.42. Changes in Carbonyl Concentration with Extrusion Passes for TSE Processed PL-1840 Containing Different Antioxidant Mixtures (265°C, 100rpm)

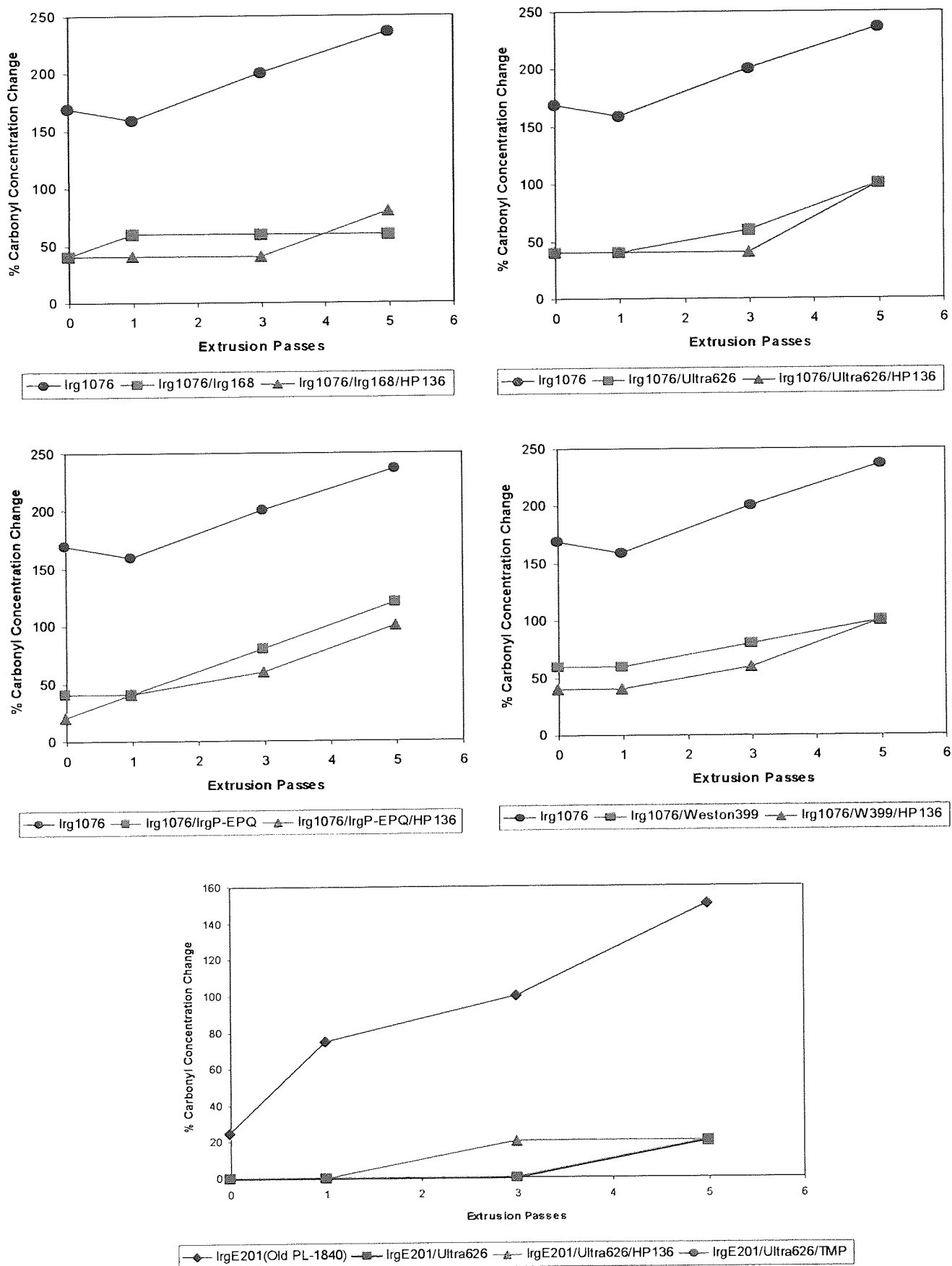


Figure 5.43. Percentage Concentration Change of Carbonyl Group with Extrusion Passes for TSE Processed **PL-1840** Containing Different Antioxidant Mixtures (265°C, 100rpm)

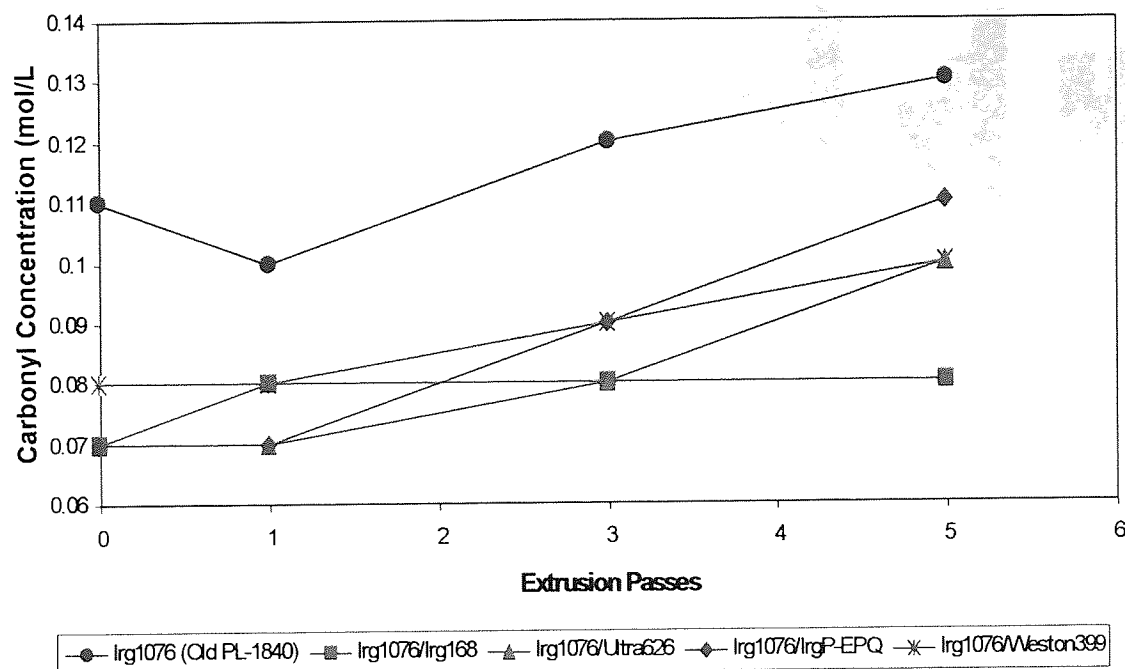


Figure 5.44. Changes of Carbonyl Concentrations with Extrusion Passes for TSE Processed **PL-1840** Containing Irg1076 and Different Phosphite Antioxidants (265°C, 100rpm, see Table 5.2 for AO composition)

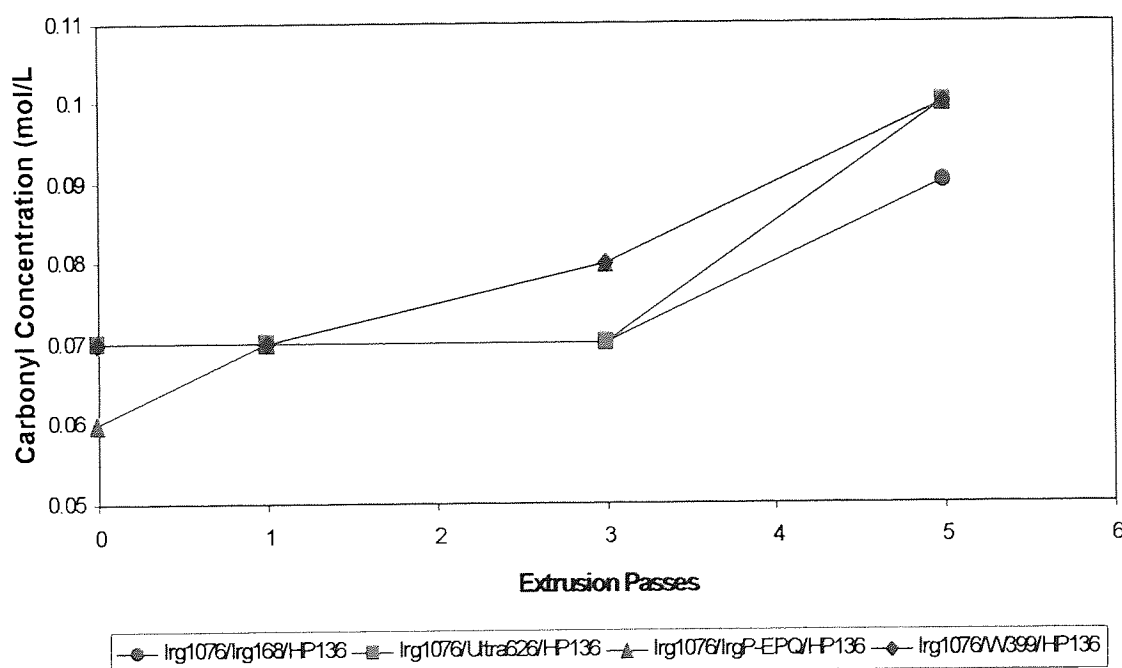


Figure 5.45. Changes of Carbonyl Concentrations with Extrusion Passes for TSE Processed **PL-1840** Containing Irg1076, HP136 and Different Phosphite Antioxidants (265°C, 100rpm, see Table 5.2 for AO composition)

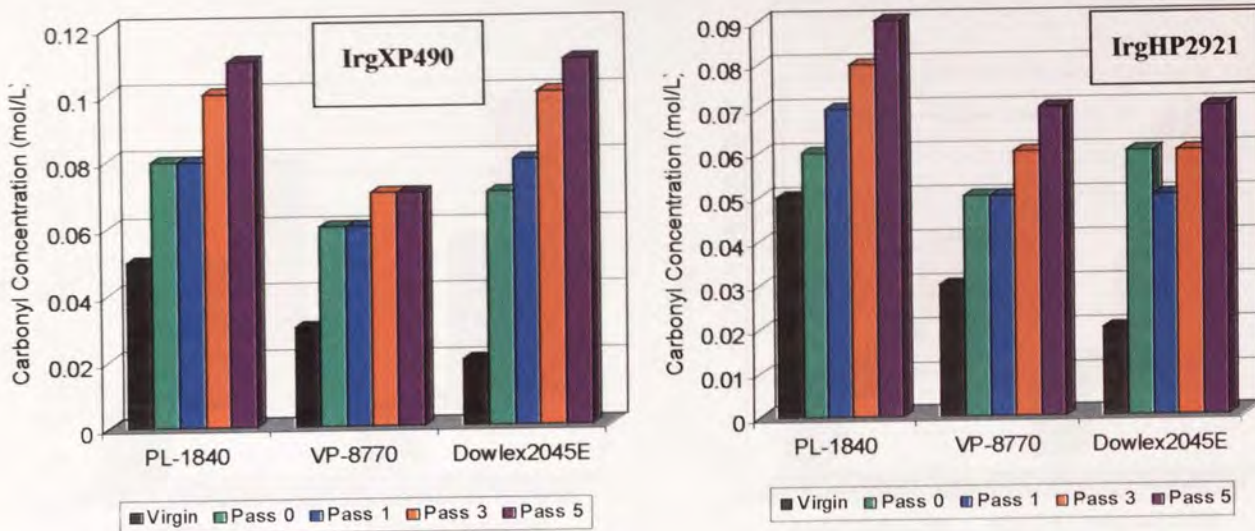


Figure 5.46. Carbonyl Concentration Change with Extrusion Passes for TSE Processed LLDPE Polymers Containing Commercial Antioxidant Mixtures (265°C, 100rpm, **IrgXP490** – Irg1076: IrgP-EPQ: HP136 = 3:2:1, **IrgHP2921** – Irg1076: Irg168: HP136= 2:4:1)

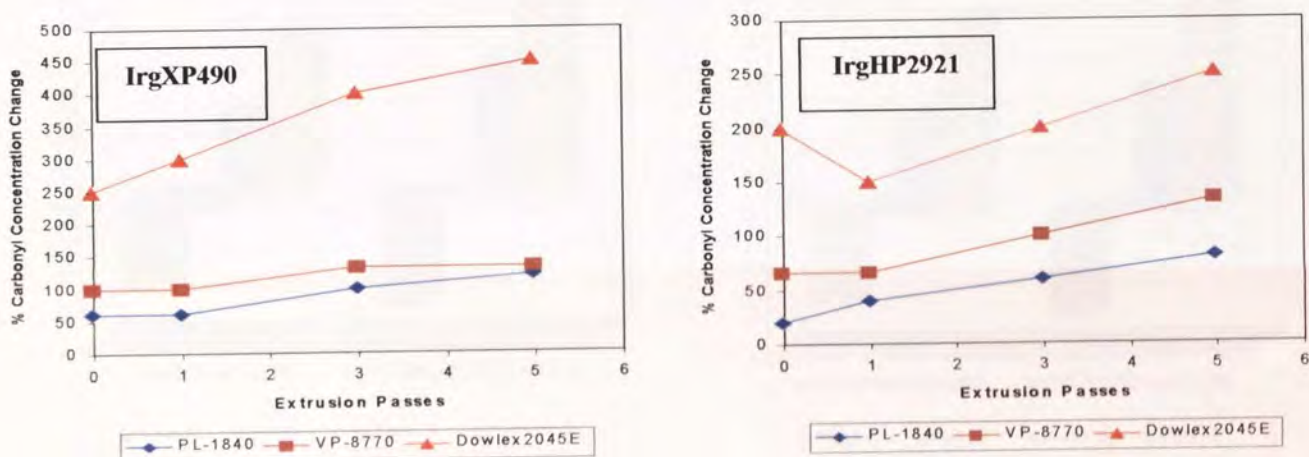


Figure 5.47. Percentage Concentration Change of Carbonyl Group with Extrusion Passes for TSE Processed LLDPE Polymers Containing Commercial Antioxidant Mixtures (265°C, 100rpm,)

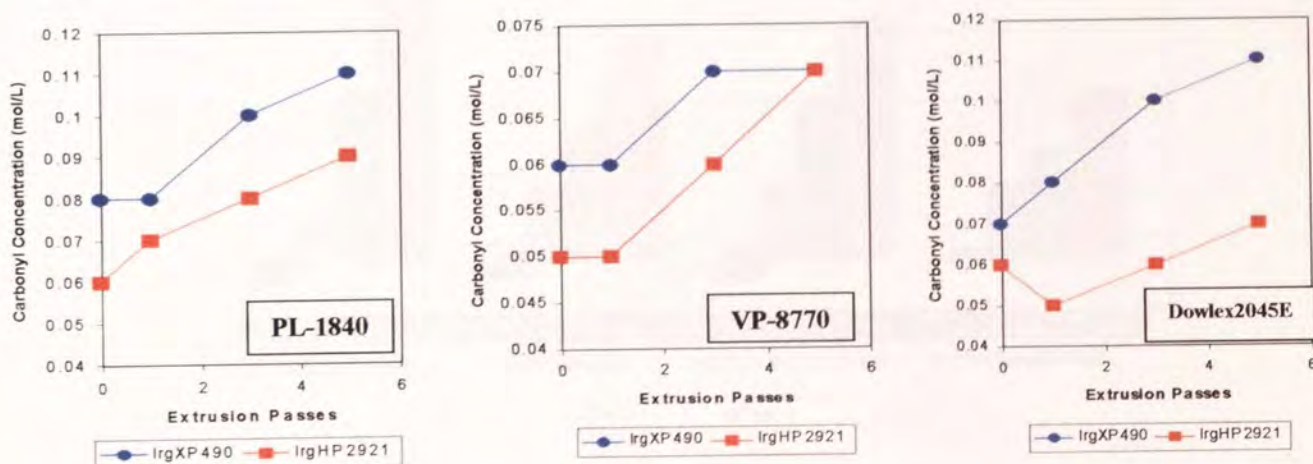


Figure 5.48. The Changes of Carbonyl Concentrations with Extrusion Passes for TSE Processed LLDPE Polymers Containing Different Commercial Antioxidant Mixtures (265°C, 100rpm)

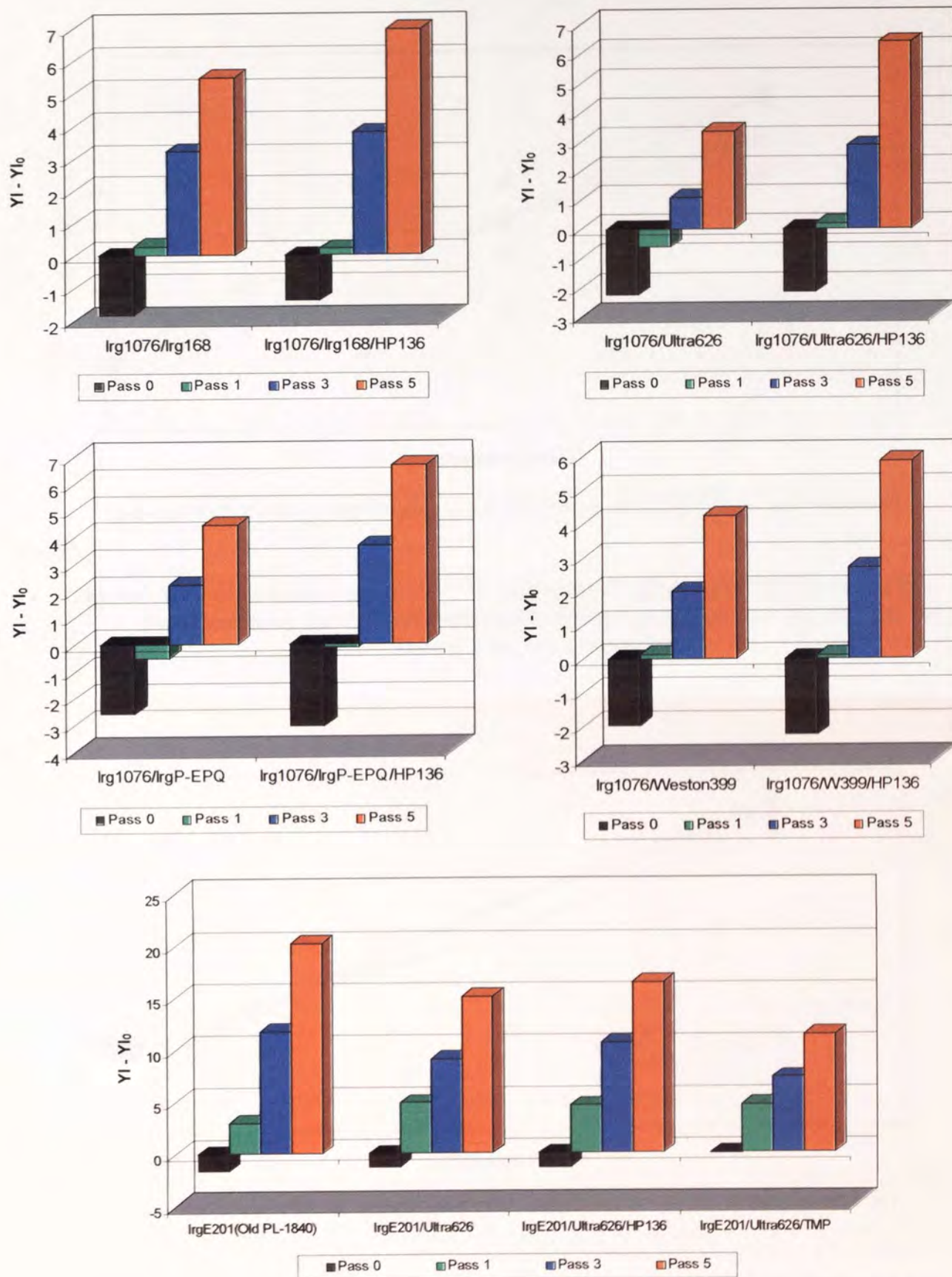


Figure 5.49. Yellow Index Change (YI-YI₀) with Extrusion Passes for TSE Processed PL-1840 Containing Different Antioxidant Mixtures (265°C, 100rpm)

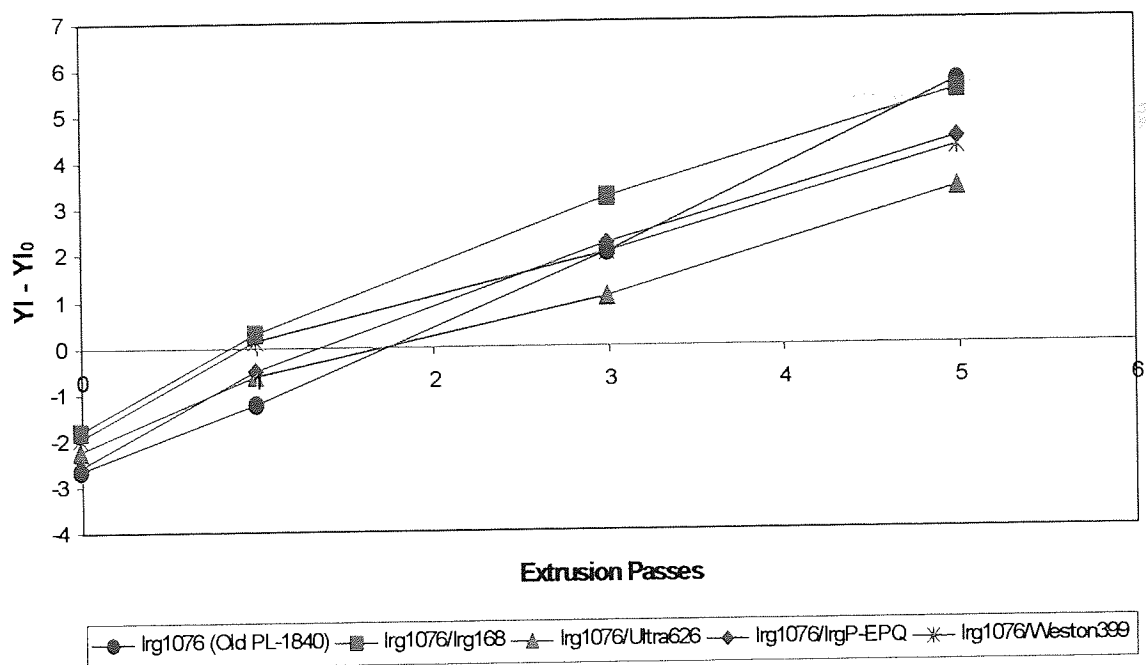


Figure 5.50. Yellow Index Change ($YI - YI_0$) with Extrusion Passes for TSE Processed **PL-1840** Containing Irg1076 and Different Phosphite Antioxidants (265°C, 100rpm, see Table 5.2 for AO composition)

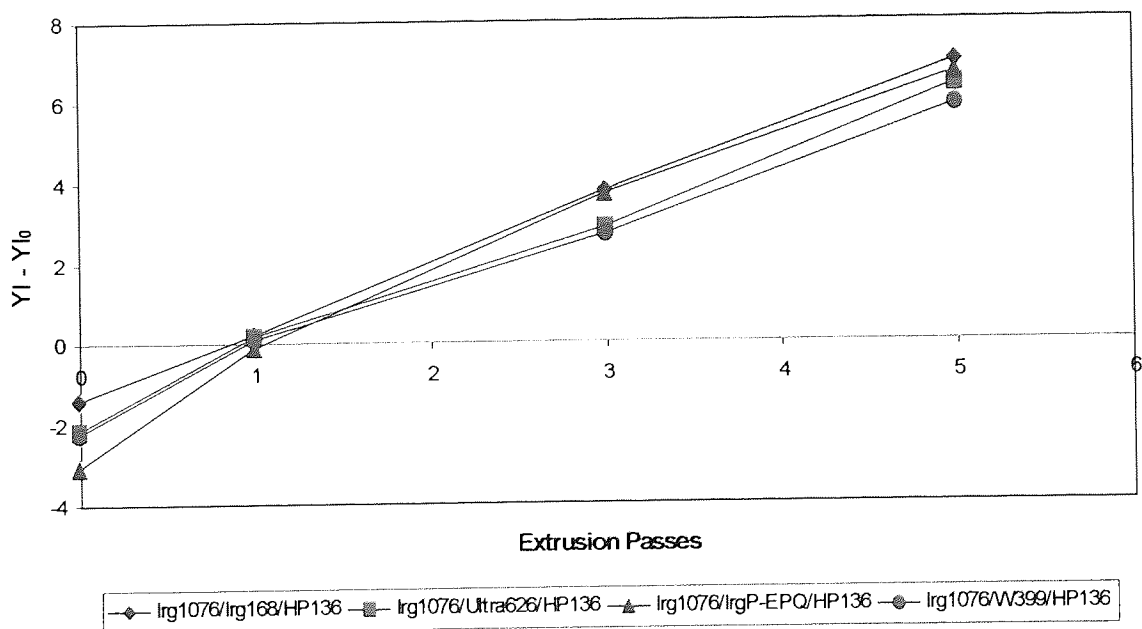


Figure 5.51. Yellow Index Change ($YI - YI_0$) with Extrusion Passes for TSE Processed **PL-1840** Containing Irg1076, HP136 and Different Phosphite Antioxidants (265°C, 100rpm, see Table 5.2 for AO composition)

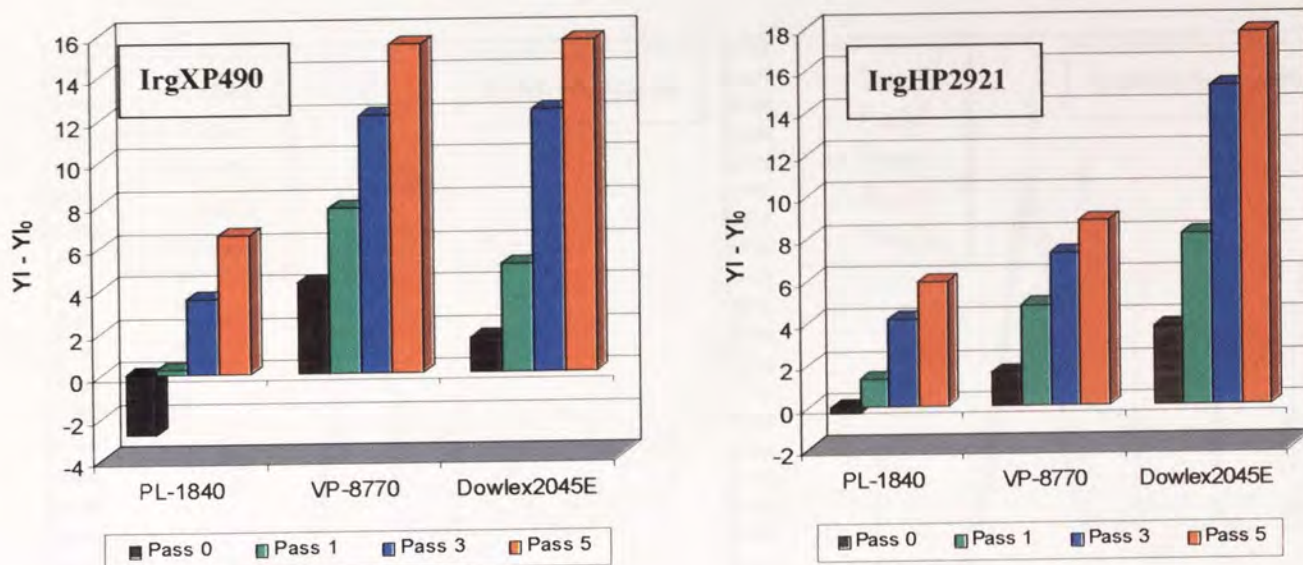


Figure 5.52. Yellow Index Change (YI-YI₀) with Extrusion Passes for Different Extruded LLDPE Polymers Containing Commercial Antioxidant Mixtures (265°C, 100rpm, **IrgXP490** – Irg1076: IrgP-EPQ: HP136 = 3:2:1, **IrgHP2921** – Irg1076: Irg168: HP136= 2:4:1)

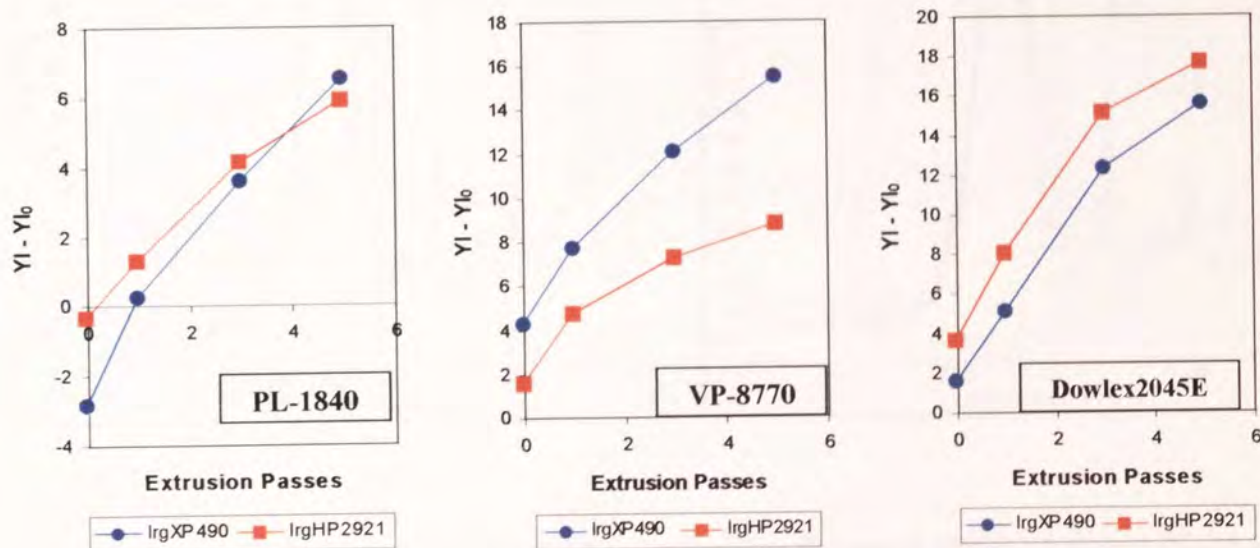


Figure 5.53. Yellow Index Change (YI-YI₀) with Extrusion Passes for TSE Processed LLDPE Polymers Containing Different Commercial Antioxidant Mixtures (265°C, 100rpm, **IrgXP490** – Irg1076: IrgP-EPQ: HP136 = 3:2:1, **IrgHP2921** – Irg1076: Irg168: HP136= 2:4:1)

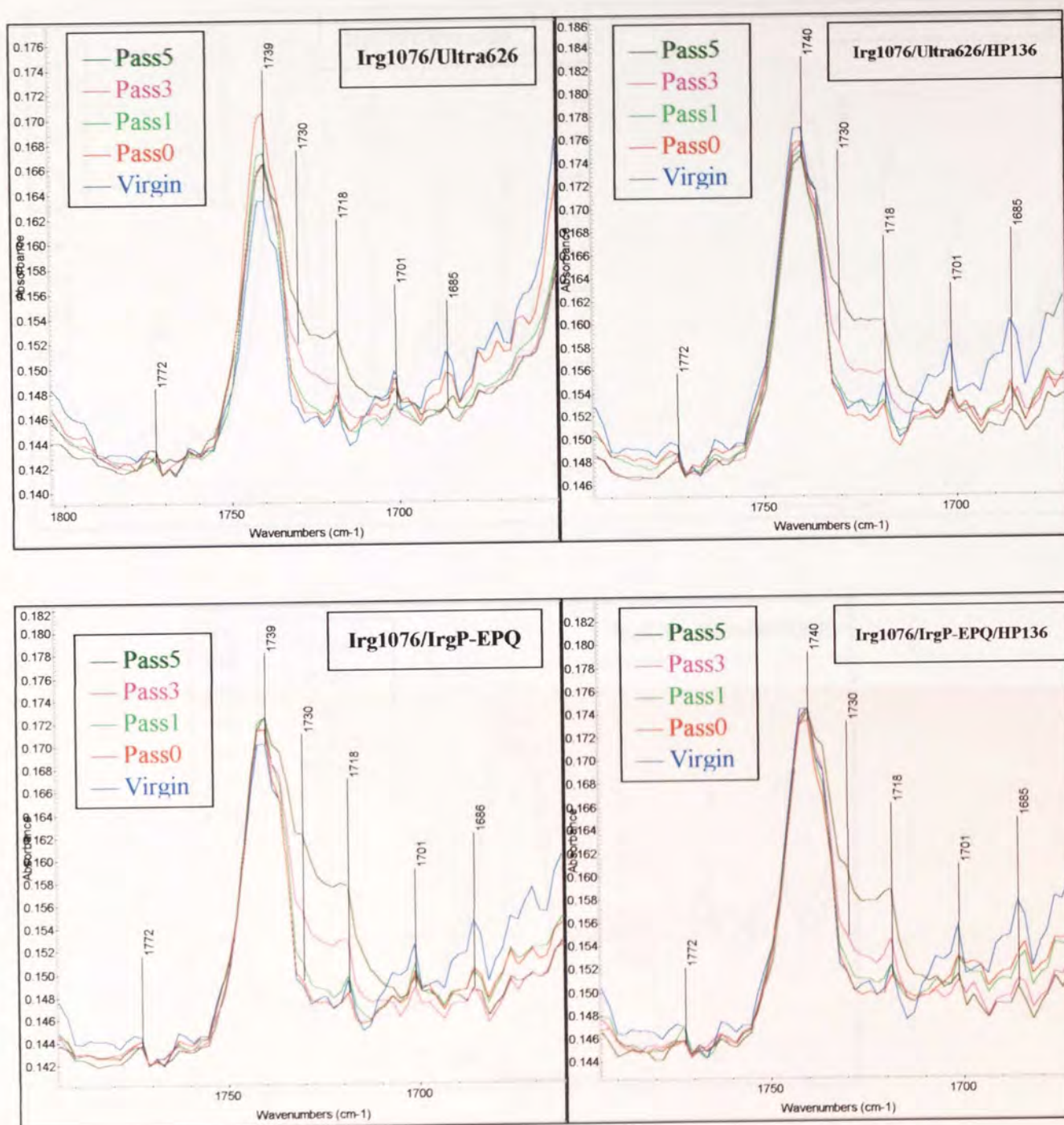


Figure 5.54. FTIR Spectra in Carbonyl Region for TSE Processed (265°C, 100rpm) **PL-1840** Containing **Irganox1076** and Other Antioxidants (1772cm⁻¹ γ -Lactone, 1739~1740 cm⁻¹ Ester, 1730 cm⁻¹ Aldehyde, 1718 cm⁻¹ Ketone, 1701 cm⁻¹ Carboxylic acid, 1685 cm⁻¹ Unsaturated ketone)

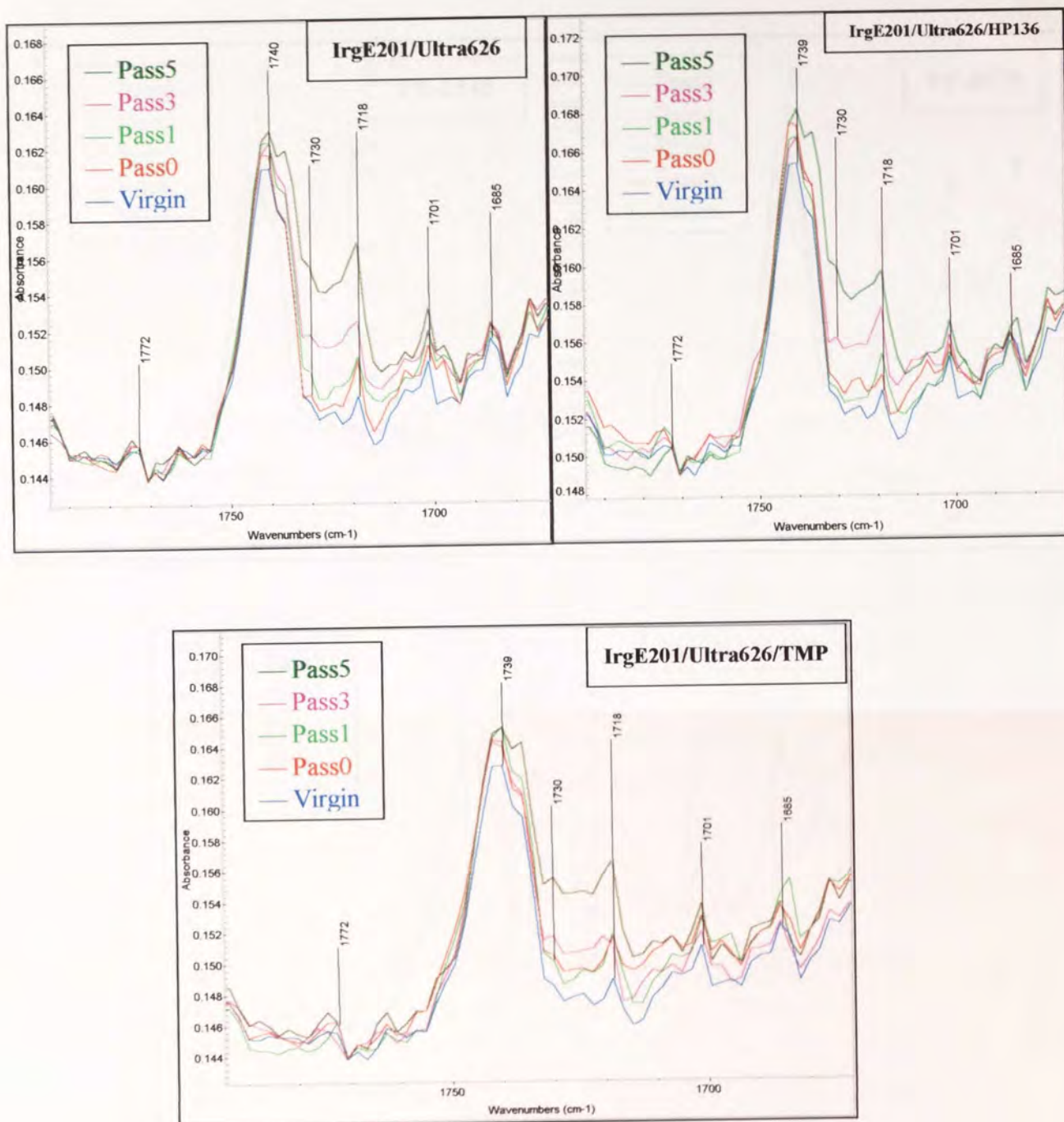


Figure 5.55. FTIR Spectra in Carbonyl Region for TSE Processed (265°C, 100rpm) **PL-1840** Containing **IrganoxE201** and Other Antioxidants (1772 cm⁻¹ γ -Lactone, 1739~1740 cm⁻¹ Ester, 1730 cm⁻¹ Aldehyde, 1718 cm⁻¹ Ketone, 1701 cm⁻¹ Carboxylic acid, 1685 cm⁻¹ Unsaturated ketone)

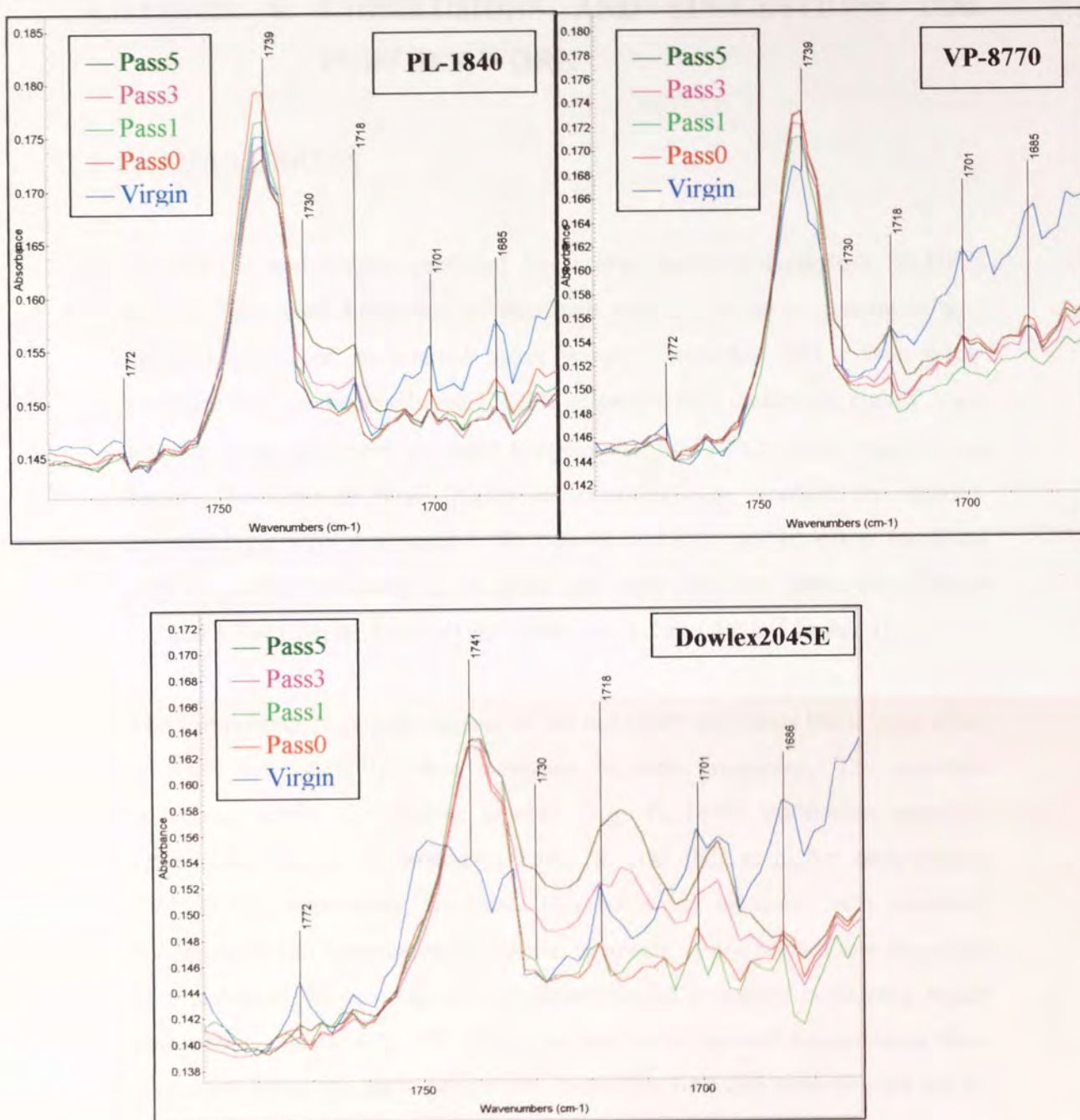


Figure 5.56. FTIR Spectra in Carbonyl Region for TSE Processed (265°C, 100rpm) LLDPE Polymers Containing **IrganoxXP490** (1772 cm⁻¹ γ -Lactone, 1739~1741 cm⁻¹ Ester, 1730 cm⁻¹ Aldehyde, 1718 cm⁻¹ Ketone, 1701 cm⁻¹ Carboxylic acid, 1685 cm⁻¹ Unsaturated ketone)

CHAPTER 6. CONCLUSIONS AND SUGGESTIONS FOR FURTHER WORK

6.1. CONCLUSIONS

1. Metallocene and Ziegler catalyzed linear low density polyethylene (LLDPE) showed significant differences in their melt stability during processing in both closed chamber of an internal mixer (torque rheometer) and a twin screw extruder. For metallocene-based LLDPE polymers, they underwent mainly chain scission when processed at lower temperatures ($< 220^{\circ}\text{C}$); while crosslinking became predominant when higher temperatures were applied. In contrast, crosslinking always dominated in the case of z-LLDPE and its extent increased with increasing processing temperatures and more extrusion passes (see Figures 3.2 and 3.3 in Chapter 3 as well as Figures 4.4, 4.5 and 4.8 in Chapter 4).
2. The comonomer (1-octene) content in the m-LLDPE polymers has a large effect on their melt stability when subjected to melt processing. The polymers containing lower comonomer content (e.g. PL-1840) underwent generally crosslinking during processing in both TR and TSE at higher temperatures ($235\sim 285^{\circ}\text{C}$); meanwhile, the extent of crosslinking increased with increasing temperatures and more extrusion passes. However, it was shown that the extent of crosslinking in the case of metallocene-based polymers containing higher comonomer content (e.g. VP-8770) decreased with elevated temperatures when processed under the same conditions. Basically, the more comonomers the m-LLDPE contains, the more would the polymer be susceptible to chain scission when processed at higher temperatures (see Figures 3.2 and 3.3 in Chapter 3 as well as Figures 4.4, 4.5 and 4.8 in Chapter 4).
3. Crosslinking and chain scission are competing reactions in the case of both metallocene and Ziegler-based LLDPE polymers when subjected to melt

processing. As a result, the molecular weight distribution, MWD (inferred indirectly from MFR measurement), of all processed polymers, particularly for z-LLDPE, became broader owing to oxidative degradation. The MWD tended generally to become broader with increasing processing temperature and more extrusion passes for all the polymers examined. Based on the results of rheological measurements, a comonomer concentration limit (≈ 20 wt%) is suggested to exist for m-LLDPE, so that polymers containing comonomer less than this limit showed generally similar melt stability during processing; whereas, those with higher comonomer content showed different melt flow behaviour when processing at higher temperatures (see Figures 3.2 to 3.4 in Chapter 3 as well as Figures 4.4 to 4.23 in Chapter 4).

4. The chain scission of m-LLDPE processed at lower temperatures ($< 235^{\circ}\text{C}$) is mainly due to the high shear force caused by their higher melt viscosity. Moreover, the β -scission of alkyl, alkoxy and peroxy radicals produced in the polymer oxidation is another major reason for the scission of polymer chains, especially at higher processing temperatures. The crosslinking of LLDPE was found to be closely related to the vinyl group concentration originally contained in the polymers. The addition reaction of vinyl group to macro-alkyl radicals makes a great contribution to the predominance of polymer crosslinking. Additionally, processing at higher temperatures favours the occurrence of crosslinking reactions not involving vinyl group, such as the recombination of alkyl, alkoxy radicals, as the lower melt viscosity of LLDPE polymers at higher temperature makes it easier for these radicals to move and combine with each other. Similarly, the polymer with lower density (higher comonomer content) is more likely to undergo this kind of crosslinking even at lower processing temperatures. The crosslinking reactions that occur in m-LLDPE with higher comonomer content generally led to long-chain branching and formation of polymer network. In contrast, z-LLDPE tended to undergo crosslinking reactions that resulted in short-chain branching and linear molecule enlargement (see

Figures 3.1 to 3.3, 3.6 and Tables 3.1, 3.2 in Chapter 3 as well as Figures 4.3, 4.4, 4.11, 4.14, 4.15, 4.17, 4.19, 4.21, 4.22, 4.24, 4.28 and 4.46 in Chapter 4).

5. The melt processing led to variation in unsaturation in LLDPE polymers. But in most cases, the polymer originally containing more amount of a specific unsaturated group will still have higher concentration of this group after processing under all conditions examined. Trans-vinylene group can be both produced and decomposed during melt processing of LLDPE polymers and the disproportionation of secondary alkyl radicals is the major route of tran-vinylene formation for LLDPE polymers containing lower comonomer content. Vinyl group was also produced in LLDPE polymers when subjected to melt processing. However, most of the reactions forming vinyl group can lead to polymer chain scission. The formation of vinylidene group always involves the transformation of short chain branches. As vinylidene is a relatively stable unsaturated group, its concentration increased in most polymers examined after melt processing. Moreover, all these unsaturated groups can be involved in the reactions forming conjugated structures, which play a very important role in polymer discolouration, during melt processing of LLDPE polymers (see Table 3.2 and Figures 3.5 to 3.7 in Chapter 3 as well as Figures 4.24 to 4.30, 4.43, 4.44 and 4.47 to 4.50 in Chapter 4).
6. More carbonyl compounds were generally produced in both metallocene and Ziegler LLDPE polymers with increasing processing temperatures. The z-LLDPE polymer was shown to be more susceptible to oxidative degradation than m-LLDPE during melt processing due to its much higher extent of increase in carbonyl concentration. Meanwhile, the m-LLDPE having higher comonomer content underwent greater extent of degradation when processing at higher temperatures or subjected to more extrusion passes. The differences in the amount and composition of carbonyl compounds in LLDPE polymers after TR and TSE processing are mainly attributed to the different processing duration and oxygen pressure. Furthermore, an approximate linear relationship was found

between the concentrations of carbonyl compounds and individual unsaturated groups in extruded LLDPE polymers based on the grade (comonomer content) and type (metallocene or Ziegler). The z-LLDPE basically showed the smallest changes in unsaturated groups with the increase in carbonyl content, indicating larger extent of oxidative degradation (see Figure 3.8 to 3.13 in Chapter 3 as well as Figures 4.34 to 4.40 and 4.45 in Chapter 4).

7. For the processing of m-LLDPE in a closed mixer (TR), esters were found to be the major carbonyl products formed when the polymers were processed at lower temperatures (220~250°C). The esterification of carboxylic acids and alcohols is the main reason for the formation of esters. The increased cleavage of oxygen containing (peroxyl and alkoxyl) radicals made ketones and carboxylic acids become the most important carbonyl compounds when m-LLDPE polymers were processed at higher temperatures (>250°C). In contrast, ketones and carboxylic acids were always seen to be the dominant carbonyl products in z-LLDPE after TR processing under all conditions examined, indicating the higher susceptibility of this polymer's oxygen containing radicals to cleavage. Ketones were generally produced from the breakdown of tertiary peroxyl or alkoxyl radicals as well as the transformation of hydroperoxides. Carboxylic acids were mainly produced through the oxidation of aldehydes, which were the major carbonyl compounds formed from the β -scission of secondary peroxyl or alkoxyl radicals, under the activation of hydroperoxides (see Figures 3.9 to 3.13 in Chapter 3).
8. In the case of processing m-LLDPE polymers in an extruder (TSE), ketones and aldehydes were generally observed as the major carbonyl products and their productions increased with more extrusion passes and increasing temperature. In addition, carboxylic acids and γ -lactones were also found formed in m-LLDPE containing higher comonomer content under certain extrusion conditions (e.g. Pass1 at 285°C). The higher concentration of hydroperoxides formed in m-LLDPE due to the higher oxygen pressure during TSE extrusion is suggested to account for the fact that more aldehydes and less carboxylic acids were produced

in these polymers compared to the case of processing in TR, as a large amount of hydroperoxides were more likely to undergo bimolecular decomposition to form ketones than to react with aldehydes to form carboxylic acids. In contrast to the m-LLDPE polymers, although ketones and aldehydes were basically still the dominant carbonyl products in extruded z-LLDPE, more carboxylic acids were produced in this polymer during TSE extrusions (particularly when only one-pass extrusion was carried out) and it reveals the lower tendency for hydroperoxides to undergo bimolecular decomposition in Ziegler-based LLDPE. Moreover, TSE extrusion was shown generally to have no significant effect on the overall amount of short chain branching in all the processed polymers (see Figures 4.35 to 4.42 in Chapter 4).

9. For the antioxidants examined in this work, the chain-breaking donor (CB-D) antioxidants, i.e. hindered phenol, γ -lactone, presented generally higher activity in melt stabilisation of LLDPE polymers when singly used during TSE extrusion. However, the peroxide decomposers, phosphite ester (PD-S), were shown to be fairly effective in stabilisation of z-LLDPE melt, suggesting the presence of more hydroperoxides in this polymer during TSE extrusion. Compared to the unstabilised polymers, the use of single antioxidants examined in this work can lead to differences in the variation of unsaturated group concentrations in both extruded metallocene and Ziegler LLDPE polymers to some extent. For a specific unsaturated group, the polymers containing a phosphite antioxidant and the singly stabilized z-LLDPE generally showed more differences in the concentration change compared with the corresponding unstabilised polymers extruded under the same conditions. Meanwhile, compounding LLDPE polymers with any examined single antioxidant (except for Irg1076) generally resulted in decrease of carbonyl concentration in both m-LLDPE and z-LLDPE polymers extruded for multiple passes with respect to the unstabilised polymers, with the exception of z-LLDPPE stabilized with phosphite AO, Ultrinox626 (see Figures 5.8, 5.10, 5.13(a), 5.15(a), 5.17(a) and 5.19(a) in Chapter 5).

10. Ketone was the most important carbonyl product in the extruded polymers singly stabilized with all the antioxidants examined. The presence of phenoxyl radicals in the hindered phenol containing polymers was more favorable to the formation of ketone. The use of phenolic antioxidants generally favored the formation of carboxylic acids and unsaturated ketones, meanwhile, led to the decrease of aldehyde production in the extruded polymers. The LLDPE stabilized with lactone generally showed small difference in carbonyl content compared to the unstabilised polymers after extrusions, and their carbonyl compositions were similar to those in the polymers containing biological hindered phenol (IrgE201). Phosphite AO was shown to be more effective in stabilization of z-LLDPE by means of preventing aldehyde from formation and correspondingly, more carboxylic acids were produced during extrusions. In addition, the generation of oxidation transformation products of hindered phenol and lactone antioxidants during TSE extrusion can lead to larger extent of discoloration for all the extruded LLDPE compared to the corresponding unstabilised polymers (see Figures 5.20 to 5.24 and Table 5.8 in Chapter 5 as well as Table 4.4 in Chapter 4).
11. The combination of hindered phenol and phosphite antioxidants showed synergistic effects on the stabilisation of m-LLDPE melt during TSE extrusion. Furthermore, the biological hindered phenol had better stabilization activity than the synthetic one. The phosphite AO with higher chain-breaking ability generally performed more effectively in the phenol-phosphite stabilization system. The addition of lactone in the phenol-phosphite combination can improve further the effectiveness of this antioxidant package in stabilisation of m-LLDPE melt due to the synergistic actions between lactone and phosphite antioxidants. Moreover, the presence of polyhydric alcohol (TMP) in the phenol-phosphite system can also impart it a better performance in m-LLDPE stabilisation. The phenol-phosphite-lactone AO combination showed higher stabilisation effectiveness for m-LLDPE containing higher comonomer content during extrusions. As the major antioxidant, hindered phenol needs to be used

at a relatively higher concentration in this three-AO package in order to obtain the best performance in melt stabilisation of LLDPE polymers (see Figures 5.25 to 5.31 in Chapter 5).

12. Compared to the unstabilised polymer, more trans-vinylene and vinylidene groups were produced in the extruded m-LLDPE stabilised with phenol-phosphite combined AO package. Meanwhile, the combination of hindered phenol and phosphite antioxidants can greatly lower the carbonyl concentration in the extruded m-LLDPE with respect to the polymer singly stabilised with hindered phenol. Generally, the effectiveness of antioxidants and antioxidant combinations is not only depends on their chemical structures, but also depends on their physical properties, e.g. solid or liquid, as well as the characteristics of the stabilized LLDPE polymers. In most cases, the liquid antioxidants show better stabilisation performance, and the stabilised LLDPE polymers with lower density and lower content of unsaturated groups show higher extent of melt stability upon multi-pass extrusions (see Figures 5.11, 5.25 to 5.30, 5.38(b), and 5.42 to 5.45 in Chapter 5).

6.2. SUGGESTIONS FOR FURTHER WORK

1. The LLDPE polymers used in this work have already been stabilised by the manufacturer to impart a basic stability to the polymers in storage and transportation. It would be valuable to find a proper solvent capable of extracting all the antioxidants out of the polymers without any adverse effect on the polymers, and then to compare the oxidation behaviour of the extracted polymers during melts processing with the work conducted in this study.
2. In this work, the TSE extrusions of all unstabilised LLDPE polymers were carried out under atmospheric conditions. Further work may be taken under the oxygen deficient conditions, e.g. under the flow of nitrogen. This will help

understand the effect of oxygen pressure (concentration) on the oxidation behavior of these polymers during multi-pass extrusions.

3. In order to have a more comprehensive understanding of the stabilisation effectiveness of the antioxidants and their combination used in this work, it would be useful to examine their performance in other metallocene-based LLDPE polymers having different types of comonomers (e.g. hexene, butene).
4. Further work still need to be carried out to develop more effective multi-component stabilising packages for specific m-LLDPE polymers, based on the mechanistic investigation in thermal oxidation and stabilisation of metallocene polymers conducted in this work.

REFERENCES

of Olefin Polymerization

1. T. O. J. Kresser, in **Polyolefin Plastics**, Van Nostrand Reinhold Company, New York, Chapter 1: "Historical Development", Chapter 2: "Physical Properties", Chapter 3: "Chemistry of Polyolefins", Chapter 4: "The Manufacture of Polyolefin Plastics", (1969)
2. T. Keii, in **Kinetics of Ziegler-Natta Polymerization**, Kodansha, Tokyo, Chapter 1: "Introduction – Ziegler-Natta Heterogeneous System", Chapter 5: "Ethylene Polymerization", (1972)
3. I. Pasquon, A. Valvassori and G. Sartori, in **The Stereochemistry of Macromolecules, Volume 1**, A. D. Ketley (Ed.), Marcel Dekker, New York, Chapter 4: "The Copolymerisation of Olefins by Ziegler-Natta Catalysts" (1967)
4. W. Kaminsky, **New Polymers by Metallocene Catalysis**, Macromol. Chem. Phys., 197, 3907-3945 (1996)
5. F. Ciardelli, A. Altomare, M. Michelotti, **From Homogeneous to Supported Metallocene Catalysts**, Catal. Today, 41 (1-3), 149-157 (1998)
6. K. B. Sinclair and R.B. Wilson, **Metallocene Catalysts: A Revolution of Olefin Polymerisation**, Chem. Ind., (21), 857-862, (1994)
7. J. C. Stevens, **Constrained Geometry and Other Single Site Metallocene Polyolefin Catalysts: A Revolution in Olefin Polymerization**, Stud. Surf. Sci. Catal., 101 (11th International Congress on Catalysis – 40th Anniversary, 1996, Part A), 11-20 (1996)
8. C. Lehtinen, P. Starck and B. Lofgren, **Co- and Terpolymerization of Ethene and α -Olefins with Metallocenes**, J. Polym. Sci., Part A: Polym. Chem., 35, 307-318 (1997)
9. M. Arndt, W. Kaminsky and U. Weingarten, **Ethene/Propene Copolymerisation by [Me₂C(3-RCp)(Flu)]ZrCl₂/MAO (R=H, Me, isoPr, tert Bu)**, Macromol. Chem. Phys., 199 (6), 1135 (1998)
10. K. Soga, J. R. Park, T. Shiono, **Copolymerisation of Ethylene and Propylene with a CpTiCl₃/SiO₂-MAO Catalyst System**, Polym. Commun., 32(10), 310-313 (1991)
11. D. O. Jordan, Chapter 1: "**Ziegler-Natta Polymerization**" in Reference 3
12. J. C. W. Chien, D. He, **Olefin Copolymerisation with Metallocene Catalysts, I. Comparison of Catalysts**, J. Polym. Sci., Part A: Polym. Chem., 29, 1585 (1991)

13. H. Hocker, **Directed Polymer Synthesis for Industrial Applications**, Macromol. Symp., 101, 1-9 (1996)
14. A. Todo and N. Kashiwala, **Structure and Properties of New Olefin Polymers**, Macromol. Symp., 101, 301-308 (1996)
15. J. B. P. Soares and A. E. Hamielec, **Metallocene / Aluminoxane Catalysts for Olefin Polymerisation – A Review**, Polymer Reaction Engineering, 3 (2), 131-200 (1995)
16. W. Kaminsky, **New Polyolefins by Metallocene Catalysts**, Pure and Appl. Chem., 70 (6), 1229 (1998)
17. J. Koivumaki and J.V. Seppala, **Copolymerisation of Ethylene and 1-hexadecene with Cp_2ZrCl_2 -methylaluminoxane Catalyst**, Polym. Commun., 9 (34), 1958-1959 (1993)
18. T. Uozumi, T. Toneri, K. Soga, **Copolymerization of Ethylene and 1-octene with Cp^*TiCl_3 as Catalyst Supported on 3-Aminopropyltrimethoxysilane treated SiO_2** , Macromol. Rapid Commun., 18, 9-15 (1997)
19. F. Garbassi, L. Gila, A. Proto, **Metallocenes: New Catalysts for New Polyolefins**, Polym. News, 19 (12), 367-371 (1994)
20. W. Kaminsky, **New Polymers by Metallocene Catalysis**, Macromol. Chem. Phys., 197 (12), 3907-3945 (1996)
21. P. S. Subramanian and K. J. Chou, **Molecular Modelling Studies of the Metallocene-catalysed Polymer Reactions**, Trends Polym. Sci. (Cambridge, U.K.), 3 (10), 324-329 (1995)
22. G. Balbontin, I. Camurati, T. Dallocco and R. C. Zeigler, **Linear Low-Density Polyethylene – Catalyst System Effect on Polymer Microstructure**, J. Mole. Cata. A – Chemical, 98 (3), 123-133 (1995)
23. S. P. Chum, C. I. Kao and G. Knight, in **Metallocene-Based Polyolefins, Volume 1**, J. Scheirs and W. Kaminsky (Ed.), Wiley Series in Polymer Science Publishers, New York, Chapter 12: "Structure, properties and preparation of polyolefins produced by single site technology", (2000)
24. A. Marigo, G. Cingano, C. Marega, R. Zannetti, G. Ferrara, G. Paganetto, **Small-angle and Wide-angle X-ray-scattering Characterization of 1-Hexene Linear Low-density Polyethylene**, Macromol. Chem. Phys., 196 (8), 2537-2544 (1995)
25. T. Shimoura, M. Kohno, N. Inoue, T. Asanuma, R. Sugimoto, T. Iwatani, O. Uchida, S. Kimura, S. Harima, H. Zenkoh and E. Tanaka, **Recent Advances in Olefin Polymerisation**, Macromol. Symp., 101, 289-299 (1996)

26. G. A. Campbell and A. K. Babel, **Physical Properties and Processing Conditions Correlations of the LDPE/LLDPE Tubular Blown Films**, *Macromol. Symp.*, 101, 199-206 (1996)
27. Y. M. Kim and J. K. Park, **Effect of Short-chain Branching on the Blown Film Properties of Linear Low-density Polyethylene**, *J. Appl. Polym. Sci.*, 61 (13), 2315-2324 (1996)
28. S.W. Shang and R.D. Kamla, **Influence of Processing Conditions on the Physical Properties of LLDPE Blown Films**, *J. Plastic. Film and Sheeting*, 11, 21-37 (1995)
29. D. M. Simpson and D. G. Onell, **Blown Film Resins – Solid-state Structure Comparison Between Standard LLDPE and Enhanced Performance LLDPE**, *TAPPI Journal*, 78 (8), 170-174 (1995)
30. Y. Liu and R. W. Truss, **Tensile Yielding and Microstructures of Blends of Isotactic Polypropylene and Linear Low-density Polyethylene**, *J. Polym. Sci., Part B: Polym. Phys.*, 33 (5), 813-822 (1995)
31. P. L. Joskowicz, A. Munoz, J. Barrera, A. J. Muller, **Calorimetric Study of Blends of Low-density Polyethylene (LDPE) and Linear Low-density Polyethylene (LLDPE) Temperature Rising Elution Fractionation (TREF) Fractions**, *Macromol. Chem. Phys.*, 196 (1), 385-398 (1995)
32. G. Ritzau, **Effect of Shear Modification on the Rheological Behaviour of Two Low-Density Polyethylene (LDPE) Grades**, *Polym. Eng. Sci.*, 29 (4), 214-226 (1989)
33. A. Munoz-Escalona and P. Lafuente, **Rheological Behaviour of Metallocene Catalysed High Density Polyethylene Blends**, *Polymer*, 38 (3), 589-594 (1997)
34. J. F. Vega, A. Munoz-Escalona, A. Santamaria, M. E. Munoz and P. Lafuente, **Comparison of the Rheological Properties of Metallocene-Catalyzed and Conventional High-Density Polyethylenes**, *Macromolecules*, 29, 960-965 (1996)
35. J. M. Carella, **Comments on the Paper "Comparison of the Rheological Properties of Metallocene-Catalyzed and Conventional High-Density Polyethylenes"**, *Macromolecules*, 29, 8280-8281 (1996)
36. C. Y. Cheng, in **Metallocene-Based Polyolefins, Volume 2**, J. Scheirs and W. Kaminsky (Ed.), Wiley Series in Polymer Science Publishers, Chapter 20: "Extrusion Characteristics of Metallocene Based Polyolefins", (2000)
37. H. N. Cheng, **Determination of polyethylene Branching through Computerized ¹³C NMR Analysis**, *Polymer Bulletin*, 16, 445-452 (1986)

38. G. C. Pandey, **Quantification of α -Olefin Co-polymer in Linear Low-Density Polyethylene by Fourier Transform Infrared Spectroscopy**, *Process Control and Quality*, 7, 173-177 (1995)
39. S. A. Karoglanian and I. R. Harrison, **A Temperature Rising Elution Fractionation Study of Short Chain Branching Behaviour in Ultra Low Density Polyethylene**, *Polym. Eng. Sci.*, 36 (5), 731-736 (1996)
40. T. M. Liu and I. R. Harrison, **A DSC Method of Measuring Short-Chain Branching Distribution in Linear Low Density Polyethylene**, *Thermochimica Acta*, 233, 167-171 (1994)
41. D. C. Bugada and A. Rudin, **Branching in Low Density Polyethylene by ^{13}C -NMR**, *Eur. Polym. J.*, 23 (10), 809-818 (1987)
42. M. D. Pooter, P. B. Smith, K. K. Dohrer, K. F. Bennett, M. D. Meadows, C. G. Smith, H. P. Schouwenaars and R. A. Geerards, **Determination of the Composition of Common Linear Low Density Polyethylene Copolymers By ^{13}C -NMR Spectroscopy**, *J. Appl. Polym. Sci.*, 42, 399-408 (1991)
43. **Standard Test Method for Determination of Linear Low Density Polyethylene (LLDPE) Composition by Carbon-13 Nuclear Magnetic Resonance**, ASTM Standard D 5017-91, (1991)
44. T. Usami and S. Takayama, **Identification of Branches in Low-Density Polyethylenes by Fourier Transform Infrared Spectroscopy**, *Polymer J.*, 16 (10), 731-738 (1984)
45. W. F. Maddams, **Infrared Spectroscopic Studies on Polyethylene, 7: The Use of the Methyl Deformation Band for Branch Characterisation**, *Makromol. Chem.*, 189, 333-339 (1988)
46. R. Arnaud, J-Y Moisan and J. Lemaire, **Primary Hydroperoxidation in Low-Density Polyethylene**, *Macromolecules*, 17, 332-336 (1984)
47. G. Williams, M. R. Kamal and D. G. Cooper, **Thermo-oxidative Degradation of Linear Low Density Polyethylene Melts**, *Polym. Degrad. Stab.*, 42 (1), 61-68 (1993)
48. I. Mingozi and S. Nascetti, **Chemical Composition Distribution and Molecular Weight Distribution Determination of Ethylene, 1-Butene Linear Low-Density Polyethylene (LLDPE)**, *Int. J. Polym. Anal. Charac.*, 3, 59-73 (1996)
49. J. J. Mara and K. P. Menard, **Characterization of Linear Low Density Polyethylene by Temperature Rising Elution Fractionation and By Differential Scanning Calorimetry**, *Acta Polymer*, 45, 378-380 (1994)

50. L. N. Mizerovskii and V. V. Afanas'eva, **Low-Density Polyethylene: Melting Curves From Differential Scanning Calorimetry**, Russian J. Phys. Chem., 70 (1), 159-160 (1996)
51. P. Starck, **Studies of the Comonomer Distributions in Low Density Polyethylenes Using Temperature Rising Elution Fractionation and Stepwise Crystallization by DSC**, Polymer International, 40, 111-122 (1996)
52. R. T. Johnston and E. J. Morrison, in **Polymer Durability**, R. Clough, N. Billingham and K.T. Gillen (Ed.), Amer. Chem. Soci., Chapter 39: "Thermal Scission and Cross-linking during Polyethylene Melt Processing", (1996)
53. T. Wang, **The Determination of the composition of Unsaturation in Polybutadiene Chain**, Ph.D. Thesis, Aston University, 1992
54. **Standard Test Method for Vinyl and Trans Unsaturation in Polyethylene by Infrared Spectrophotometry**, ASTM Standard D 6248-98, (1999)
55. J. K. Rogers, **Exxon Expands Line of Metallocene Products**, Mod. Plast., (11), (1993)
56. J. K. Rogers, **Exxon; Full Speed Ahead on Gas Phase Metallocene Polyethylene**, Mod. Plast., (15), (1993)
57. D. Rotman, A. Wood, **Dow and Exxon Jostle in Race to Bring Metallocene Products to the Market**, Chem. Week., Sept. 15th, (1993)
58. A. Montagna, J. C. Floyd, **Exxon Cites Breakthrough in Olefins Polymerisation**, Mod. Plast., (61), (July 1991)
59. W. Chen and Z. Jing, **Research and Development on Metallocene Catalysis for Olefin Polymerization**, Polym. Bull. (Chinese), (1), 54-58 (1997)
60. K. W. Swogger, G. M. Lancaster, S. Y. Lai, T. I. Butler, **Improving Polymer Processability Utilizing Constrained Geometry Single-Site Catalyst Technology**, J. Plas. Film & Sheeting, 11 (2), 102-112 (1995)
61. K. Mehta, M.C. Chen and C.Y. Yin, Chapter 21: "**Film Applications for Metallocene-based Propylene Polymers**" in Reference 36
62. R. C. Portnoy and J. D. Domine, Chapter 22: "**Medical Applications of Metallocene Catalysed Polyolefins**", in Reference 36
63. S. Betso, L.T. Kale and J.J. Hemphill, Chapter 23: "**Constrained Geometry-catalysed Polyolefins in Durable Wire and Cable Applications**", in Reference 36
64. G. Graff, **Strong Sales Defy Slow Economy**, Purchasing, May 2nd, 2002

65. N. Grassie and G. Scott, in **Polymer Degradation and Stabilisation**, Cambridge University Press, Cambridge, Chapter 4: "Oxidation of Polymers", (1985)
66. S. Al-Malaika, in **Atmospheric Oxidation and Antioxidants, Volume I**, G. Scott (Ed.), Elsevier Science Publishers B.V., The Netherlands, Chapter 2: "Autoxidation", (1993)
67. O. Chiantore and M. Guaita, **Experimental and Methodological Aspects in the Characterization of Polymers Undergoing Degradation**, J. Appl. Polym. Sci.: Appl. Polym. Symp., 52, 1-10 (1993)
68. T. J. Henman, in **Developments in Polymer Stabilisation-1**, G. Scott (Ed.), Applied Science Publishers, London, Chapter 2: "Melt Stabilisation of Polypropylene", (1979)
69. A. Gopferich, **Mechanisms of Polymer Degradation and Erosion**, Biomaterials, 17(2), 103-114 (1996)
70. M. U. Amin, G. Scott and L. M. K. Tillekeratne, **Mechanism of the Photo-Initiation Process in Polyethylene**, Eur. Polym. J., 11, 85-89 (1975)
71. T. J. Henman, in **Degradation and Stabilisation of Polyolefins**, N. Allen (Ed.), Elsevier Applied Science Publications, London, Chapter 2: "Controlled Crosslinking and Degradation", (1983)
72. S. S. Stivala, J. Kimura, S. M. Gabbay, Chapter 3: "**Thermal Degradation and Oxidative Processes**" in Reference 71
73. C. H. Lee, C. E. Lee, J. H. Han and K. S. Suh, **Thermal Degradation Study of Polyethylene Using ¹H-NMR**, Jpn. J. Appl. Phys., 35 (4A), 2145-2148 (1996)
74. M. Iring and F. Tudos, **Thermal Oxidation of Polyethylene and Polypropylene: Effects of Chemical Structure and Reaction Conditions on the Oxidation Process**, Prog. Polym. Sci., 15, 217-262 (1990)
75. Y. A. Shlyapnikov and I. A. Serenkova, **High-temperature Oxidation and Stabilization of Polymers**, Polym. Degrad. Stab., 35, 67-76 (1992)
76. A. H. Willbourn, **Polymethylene and Structure of polyethylene: Study of Short-chain Branching, Its Nature and Effects**, J. Polym. Sci., 34, 569-597 (1959)
77. W. L. Hawkins, in **Polymer Stabilisation**, W. L. Hawkins (Ed.), Wiley - Interscience, Chapter 1: "Environmental Deterioration of Polymers", (1972)
78. S. Moss and H. Zweifel, **Degradation and Stabilization of High Density Polyethylene During Multiple Extrusions**, Polym. Degrad. Stab., 25, 217-245 (1989)

79. W. L. Hawkins in **Degradation and Stabilisation of Polymers**, G. Geuskens (Ed.), Applied Science Publishers Ltd., Chapter 4: "The Thermal Oxidation of Polyolefins – Mechanisms of Degradation and Stabilisation", (1975)
80. S. H. Hamid, **Ultraviolet-induced Degradation of Ziegler-Natta and Metallocene Catalyzed Polyethylenes**, J. Appl. Polym. Sci., 78, 1591-1596 (2000)
81. K. B. Chakraborty and G. Scott, **The Effects of Thermal Processing on the Thermal Oxidative and Photo-oxidative Stability of LDPE**, Eur. Poly. J., 13, 731-737 (1977)
82. J-M Ginhac, J-L Gardette, R. Arnaud, J. Lemaire, **Influence of Hydroperoxides on the Photothermal Oxidation of Polyethylene**, Makromol. Chem., 182, 1017-1025 (1981)
83. P. Dole, J. Chauchard, **Thermooxidation of Poly(ethylene-co-methylacrylate) and Poly(methylacrylate) Compared to Oxidative Thermal Ageing of Polyethylene**, Polym. Degrad. Stab., 53 (1), 63-72 (1996)
84. S. H. Hamid, W. H. Prichard, **Application of Infrared Spectroscopy in Polymer Degradation**, Polym. – Plast. Technol. Eng., 27 (3), 303-334 (1988)
85. L. Yang, F. Heatley, T. G. Blease and R. I. G. Thompson, **A Study of the Mechanism of the Oxidative Thermal Degradation of Poly(ethylene oxide) and Poly(propylene oxide) Using ^1H and ^{13}C -NMR**, Eur. Polym. J., 32 (5), 535-547 (1996)
86. A. Torikai, **Photo- and Radiation-induced Degradation of Synthetic Polymers: Polymer Structure and Stability**, Angew. Makromol. Chem., 216, 225-241 (1994)
87. A. C. Albertsson, S. Karlsson, **Degradation of Polyethylene (PE) and Degradation Products**, Polym. Mater. Sci. Eng., 62, 976-978 (1990)
88. J. P. Redfern, **Polymer and Other Degradation Studies Using Thermal Analysis Techniques**, J. Appl. Polym. Sci.: Appl. Polym. Symp., 55, 65-86 (1994)
89. R. G. Davidson, **Polymer Degradation Studies by FTIR**, Prog. Pac. Polym. Sci. 2, Proc. Pac. Polym. Conf., 2nd, Vol. (ISS/PTTL), 101-111 (1992)
90. J. Pielichowski, K. Pielichowski, **Application of Thermal Analysis for the Investigation of Polymer Degradation Processes**, J. Therm. Anal., 43 (2), 505-508 (1995)
91. I. S. Bhardwaj, V. Kumar, K. Palanivelu, **Thermal Characterisation of Low-density Polyethylene and Linear Low-density Polyethylene Blends**, Thermochim. Acta, 131, 241-246 (1988)

92. E. Foldes, **Degradation of HDPR and LLDPE in Closed Mixing Chamber: A Comparison. I. Changes in the Chemical Structure**, Polym. Bull. (Berlin), 18 (6), 525-532 (1987)
93. F. Gugumus, **Physico-chemical Aspects of Polyethylene Processing in Open Mixers 1: Review of Published Work**, Polym. Degrad. Stab., 66, 161-172 (1999)
94. F. Gugumus, **Formation of Ester Functional Groups in Oxidizing Polymers**, Polym. Degrad. Stab., 65, 5-13 (1999)
95. F. Gugumus, **Physico-chemical Aspects of Polyethylene Processing in Open Mixers 8: Various Reactions of Polyethylene Hydroperoxide in the Melt**, Polym. Degrad. Stab., 75, 131-142 (2002)
96. F. Gugumus, **Thermolysis of Polyethylene Hydroperoxides in the Melt 5. Mechanisms and Formal Kinetics of Product Formation**, Polym. Degrad. Stab., 76, 381-391 (2002)
97. A. Holmstrom and E. M. Sorvik, **Thermooxidative Degradation of Polyethylene. I. and II. Structural Changes Occuring in Low-Density Polyethylene, High-Density Polyethylene, and Tetratetracontane Heated in Air**, J. Polym. Sci., Polym. Chem. Ed., 16, 2555-2586 (1978)
98. H. N. Cheng, F. C. Schilling and F. A. Bovey, **¹³C Nuclear Magnetic Resonance Observation of the Oxidation of Polyethylene**, Macromolecules, 9 (2), 363-365 (1976)
99. H. Hinsken, S. Moss, J-R Pauquet and H. Zweifel, **Degradation of Polyolefins During Melt Processing**, Polym. Degrad. Stab., 34, 279-293 (1991)
100. F. Gugumus, **Re-examination of the Thermal Oxidation Reactions of Polymers 2. Thermal Oxidation of Polyethylene**, Polym. Degrad. Stab., 76, 329-340 (2002)
101. F. Gugumus, **Re-examination of the Thermal Oxidation Reactions of Polymers 3. Various Reactions in Polyethylene and Polypropylene**, Polym. Degrad. Stab., 77, 147-155 (2002)
102. J. Petruj and J. Marchal, **Mechanism of Ketone Formation in the Thermooxidation and Radiolytic Oxidation of Low Density Polyethylene**, Radiat. Phys. Chem., 16, 27-36 (1980)
103. J. Lacoste, **Polyethylene Hydroperoxide Decomposition Products**, Polym. Degrad. Stab., 34 (1-3), 309-323 (1991)
104. E. Fanton, A. Tidjani and R. Arnaud, **Hydroperoxidation in the Low-Temperature Thermooxidation of Linear Low Density Polyethylene**, Polymer, 35 (2), 433-434 (1994)

105. A. Harlin, **Thermal-mechanical Degradation of Linear Polyethylene Copolymer Polymerised with two Supported Catalyst Systems**, Polym. Degrad. Stab., 42, 89-94 (1993)
106. **Standard Test Method for Flow Rates of Thermoplastics by Extrusion Plastometer**, ASTM Standard D 1238-95, (1995)
107. G. Scott, in **Developments in Polymer Stabilisation - 4**, G. Scott (Ed.), Applied Science Publishers, London, Chapter 1: "Mechanism of Antioxidant Action", (1981)
108. S. Al-Malaika, in **Comprehensive Polymer Science**, G.C. Eastwood (Ed.), Pergamon Press Publishers, New York, Chapter 19: "Effects of Antioxidants and Stabilisers", (1989)
109. G. Scott, Chapter 4: "Antioxidants Chain Breaking" in Reference 66
110. S. Al-Malaika, **Mechanisms of Antioxidant Action and Stabilisation Technology – The Aston Experience**, Polym. Degrad. Stab., 34, 1-36 (1991)
111. J. Pospisil and S. Nespurek, **Chain Breaking Stabilisers in Polymers: the Current Status**, Polym. Degrad. Stab., 49, 99-110 (1995)
112. N. Grassie and G. Scott, in **Polymer Degradation and Stabilisation**, Cambridge University and Press, Cambridge, Chapter 5: "Antioxidants and Stabilisers", (1985)
113. S. Girois, P. Delprat, L. Audouin, J. Verdu, **Kinetic Study of the Photostabilisation of Polypropylene Films by an Hydroxyphenylbenzotriazole**, Polym. Degrad. Stab., 64, 107-114 (1999)
114. I. Bauer, S. Korner, B. Pawelke, S. Al-Malaika and W. D. Habicher, **Hydroperoxide Decomposing Ability and Hydrolytic Stability of Organic Phosphites Containing Hindered Amine Moieties (HALS-Phosphites)**, Polym. Degrad. Stab., 62, 175-186 (1998)
115. J. R. Shelton, Chapter 2: "Stabilization Against Thermal Oxidation", in Reference 77
116. I. Bauer, W. D. Habicher, C. Rautenberg and S. Al-Malaika, **Antioxidant Interaction Between Organic Phosphites and Hindered Amine Light Stabilisers During Processing and Thermoxidation of Polypropylene**, Polym. Degrad. Stab., 48, 427-440 (1995)
117. I. Bauer, W. D. Habicher, S. Korner and S. Al-Malaika, **Antioxidant Interaction Between Organic Phosphites and Hindered Amine Light Stabilisers: Effects During Photooxidation of Polypropylene – II**, Polym. Degrad. Stab., 55, 217-224 (1997)

118. J. Pospisil, **Chemical and Photochemical Behaviour of Phenolic Antioxidants in Polymer Stabilisation: State of the Art Report, Part 1**, Polym. Degrad. Stab., 40, 217-232, (1993)
119. K. Schwetlick, T. Konig, C. Ruger, J. Pionteck and W.D. Habicher, **Chain - Breaking Antioxidant Activity of Phosphite Esters**, Polym. Degrad. Stab., 15, 97-108 (1986)
120. C. Neri, S. Constanzi, R. Riva, R. Farris and R. Colombo, **Mechanism of Action of Phosphites in Polyolefin Stabilisation**, Polym. Degrad. Stab., 49, 65-69, (1995)
121. S. Al-Malaika, **Some Aspects of Polymer Stabilisation**, Int. J. Polym. Mater., 24 (1-4), 47-58 (1994)
122. S. Al-Malaika, **A Critique on Stabilization Technology in Polyolefins**, Polym. - Plast. Technol. Eng., 27 (2), 261-301 (1988)
123. I. Bachert, **Stabilizing Plastics in Processing and Use**, Plastics, Additives and Compounding, 2 (9), 18-21 (2000)
124. H. Clariant, **Polymer Stabilizers: Some Recent Developments**, Plastics, Additives and Compounding, 2 (4), 34-36 (2000)
125. N. C. Billingham, in **Atmospheric Oxidation and Antioxidants-2**, G. Scott (Ed.), Elsevier Applied Science Publications, London, Chapter 4: "The Physical Chemistry of Polymer Oxidation and Stabilisation", (1985)
126. G. Scott (Ed.) Chapter 9: "Synergism and Antagonism", in Reference 66
127. Y. A. Shlyapnikov and N. K. Tyuleneva, **Inhibited Oxidation of Polyethylene: Anatomy of Induction Period**, Polym. Degrad. Stab., 56, 311-315 (1997)
128. F. Gugumus, **Thermolysis of Polyethylene Hydroperoxides in the Melt 4. Effect of Phenolic Antioxidants and Temperature on the Oxidation Product Formation**, Polym. Degrad. Stab., 76, 341-352 (2002)
129. F. Gugumus, **Thermolysis of Polyethylene Hydroperoxides in the Melt 6. Mechanisms and Formal Kinetics of Product Formation in the Presence of Phenolic Antioxidants**, Polym. Degrad. Stab., 77, 157-168 (2002)
130. S. Issenhuth, **The Antioxidant Role of Vitamin E in Polyolefins**, Ph.D Thesis, Aston University, Birmingham, (1996)
131. S. Issenhuth, **Unpublished Internal Reports**, Polymer Processing and Performance Research Unit, Aston University, Birmingham, (1997-1999)
132. J. F. Robinson and K. A. Robinson, in **Contemporary Chemical Analysis**, Prentice Hall, NJ, Page42, (1998)

133. U. Daraz, **Unpublished Internal Reports**, Polymer Processing and Performance Research Unit, Aston University, Birmingham, (1998-2000)
134. S. Issenhuth, **Unpublished Internal Report 4: Metallocene LLDPE: Investigation of Processing Stability and Melt Stabilisation**, Polymer Processing and Performance Research Unit, Aston University, Birmingham, March, (1998)
135. J. L. Gardette, **Extinction Coefficients**, Private Communication with Dr. S. Al-Malaika, November, (2000)
136. **Standard Test Method for Yellowness Index of Plastics**, ASTM Standard D 1925-70, (1977)
137. S. Mui, **"Rheometer Standard Operating Procedure"**, Unpublished Internal Report, Polymer Processing and Performance Research Unit, Aston University, Birmingham, (2000)
138. H. Weston, **"Insight into Polyethylene's Behaviour During Extrusion Via Capillary Rheometry"**, BSc Thesis in Applied Chemistry, Aston University, Birmingham, (2002)
139. O. Chiantore, S. Tripodi, C. Sarmoria and E. Valles, **Mechanism and Molecular Weight Model for Thermal Oxidation of Linear ethylene-butene Copolymer**, *Polymer*, **42**, 3981-3987 (2001)
140. S. Al-Malaika, H. Ashley and S. Issenhuth, **The Antioxidant Role of α -tocopherol in Polymers. 1. The Nature of Transformation Products of α -tocopherol Formed During Melt Processing of LDPE**, *J. Polymer. Science: Part A: Polymer Chemistry*, **32**, 3099-3113 (1994)
141. G.W. Burton, T. Doba, E.J. Gabe, L. Hughes, F.L. Lee, L. Prasad and K.U. Ingold, **Autoxidation of Biological Molecules. 4. Maximising the Antioxidant Activity of Phenols**, *J.Am.Chem.Soc.*, **107**, 7053-7065 (1985)
142. S.Al-Malaika and S. Issenhuth, **The Antioxidant Role of α -tocopherol in Polymers. 3. The Nature of Transformation Products During Polyolefin Extrusion**, *Polym.Deg.stab.*, **65**, 143 (1999)
143. J. R. Pauquet, **Breakthrough Chemistry for Processing Stabilisation of Polypropylene**, *J. Pure Applied Chem.*, **36** (11), 1717-1730 (1999)
144. P. Nesvadba and C. Krohnke, **A New Class of Highly Active Phosphorus Free Processing Stabilisers for Polymers**, in Additives '97, Executive Conference Management, New Orleans, (1997)

APPENDIX

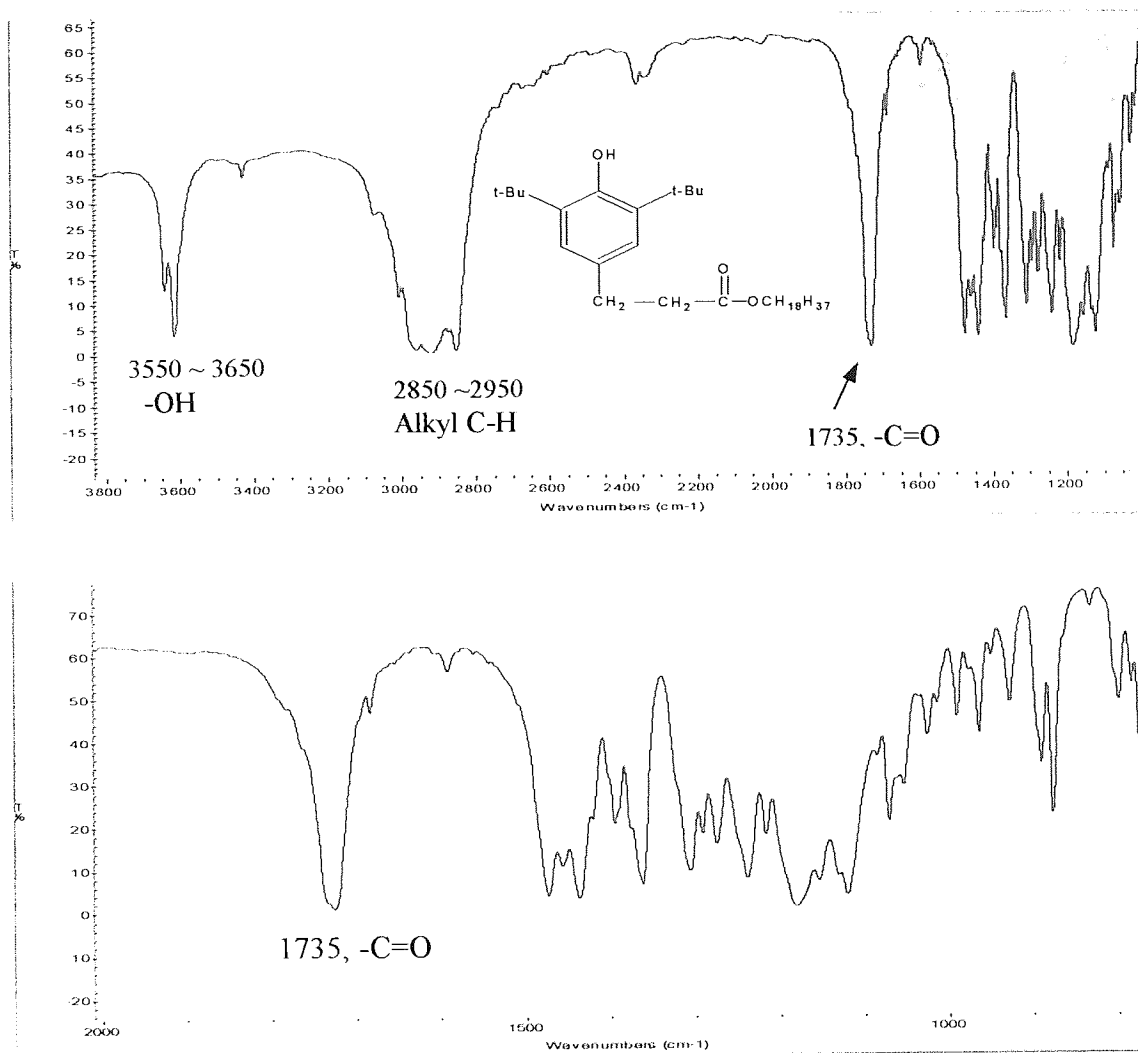


Figure A2.1. FTIR Spectrum of Irganox 1076 and the Expansion at 2000~900 cm⁻¹ (KBR windows)

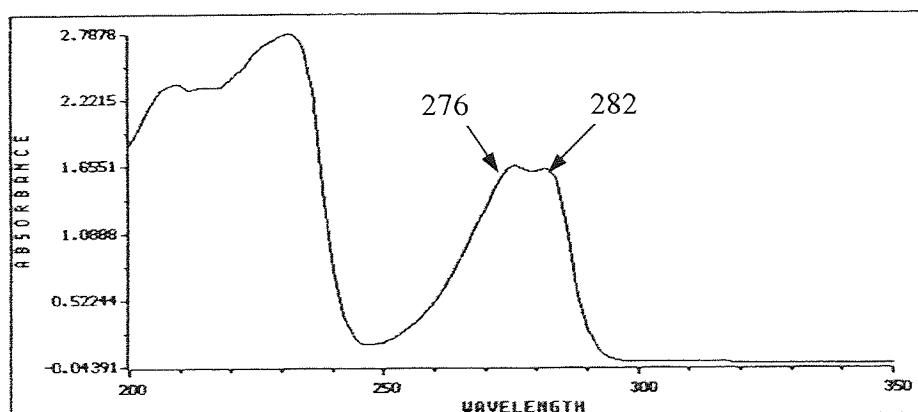


Figure A2.2. UV Spectrum of Irganox 1076 in Hexane

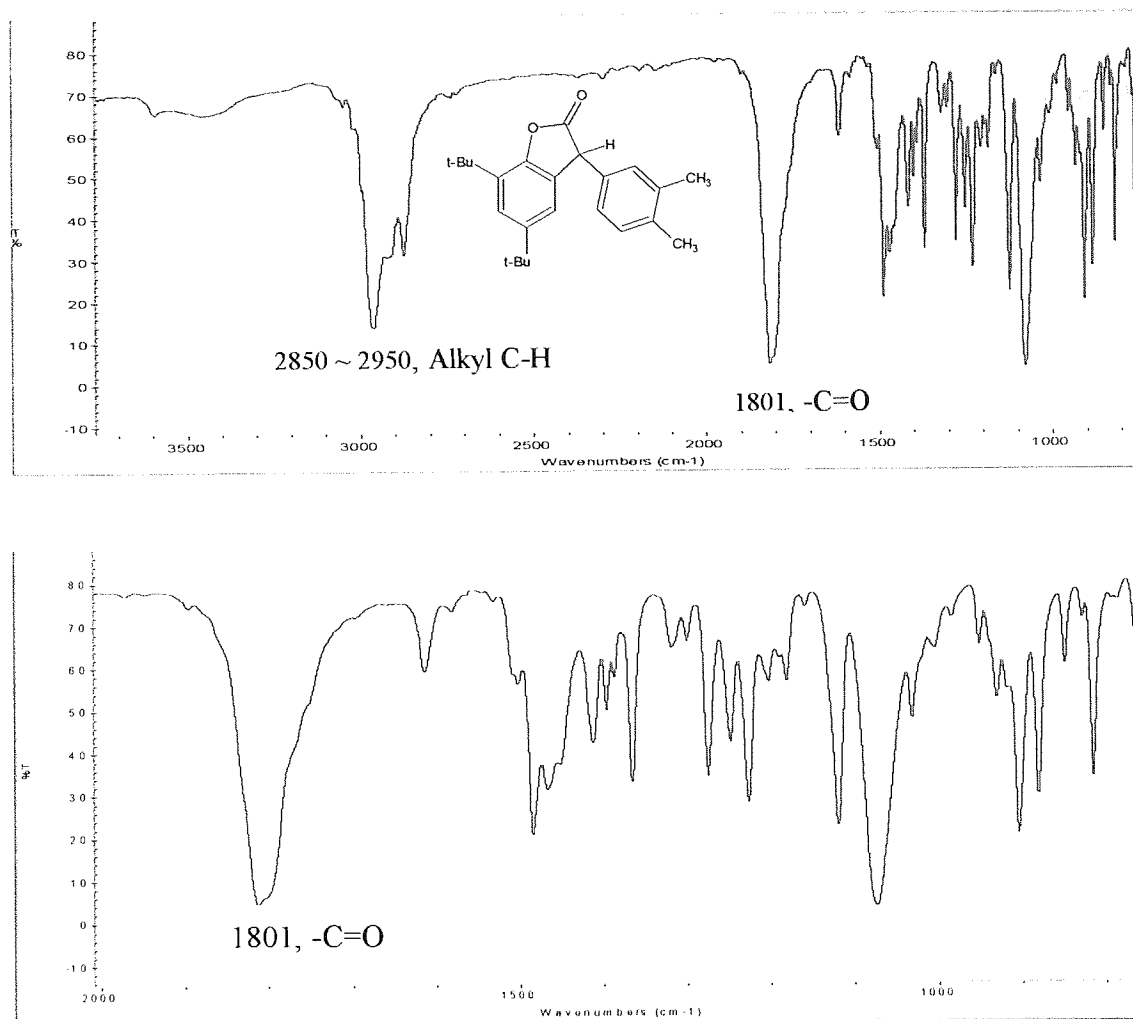


Figure A2.3. FTIR Spectrum of Irganox HP136 and the Expansion at 2000~900 cm^{-1} (KBR windows)

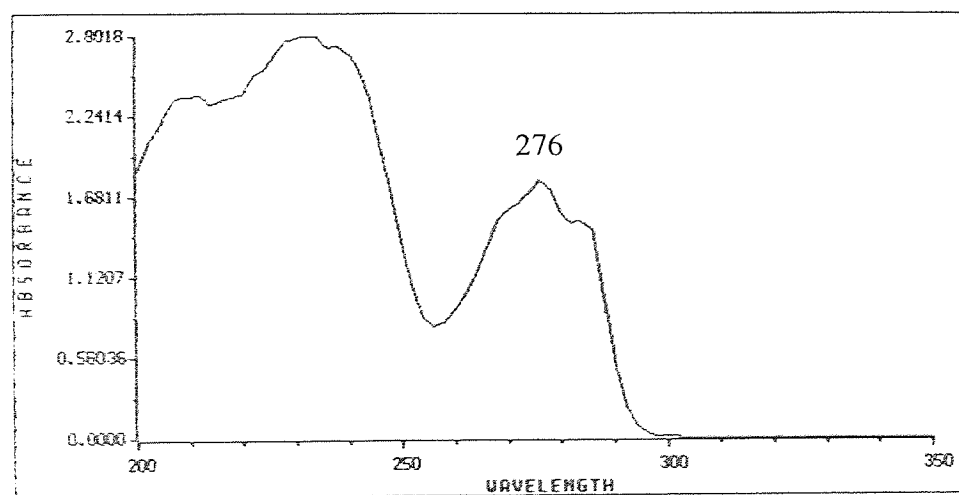


Figure A2.4. UV Spectrum of Irganox HP136 in Hexane

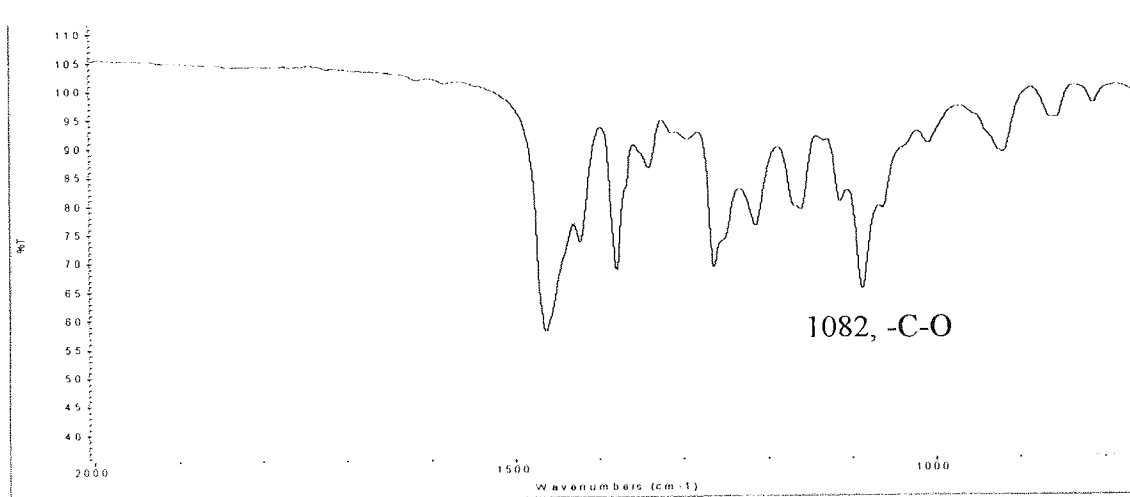
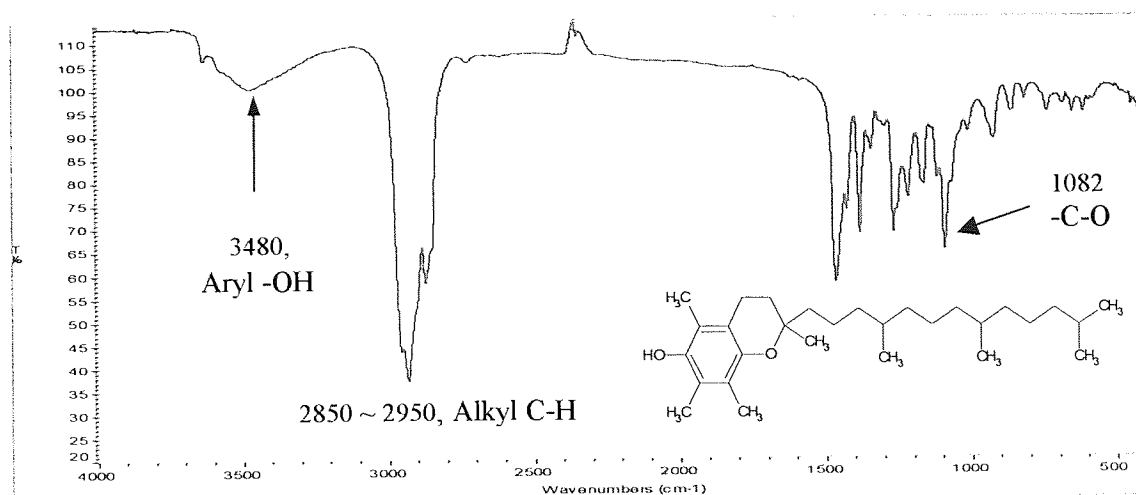


Figure A2.5. FTIR Spectrum of Irganox E201 and the Expansion at 2000~900 cm⁻¹ (KBR windows)

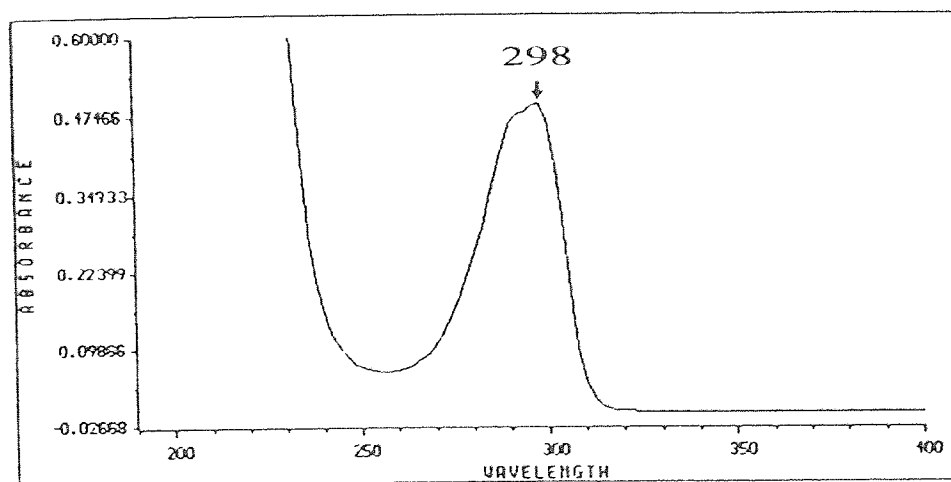


Figure A2.6. UV Spectrum of Irganox E201 in Hexane

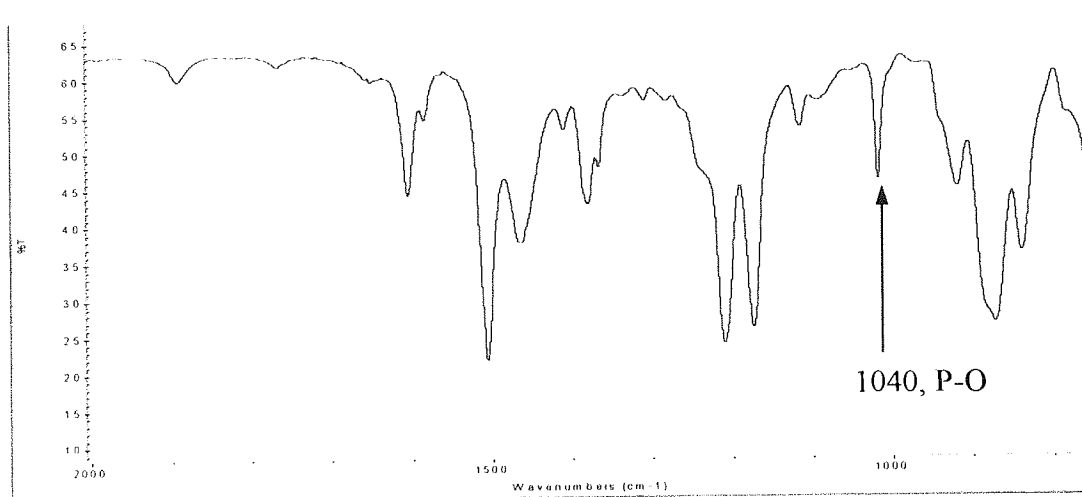
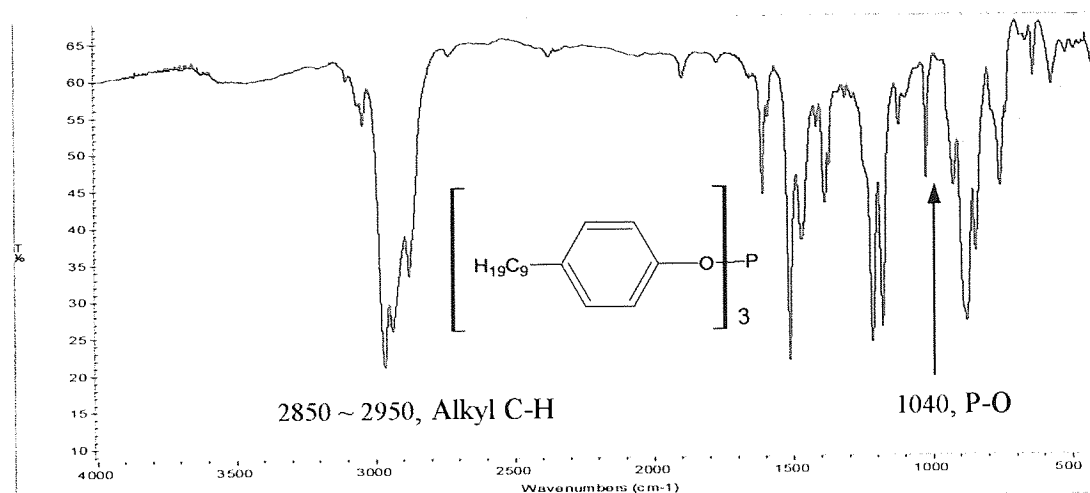


Figure A2.7. FTIR Spectrum of Weston 399 and the Expansion at 2000~900 cm⁻¹ (KBr windows)

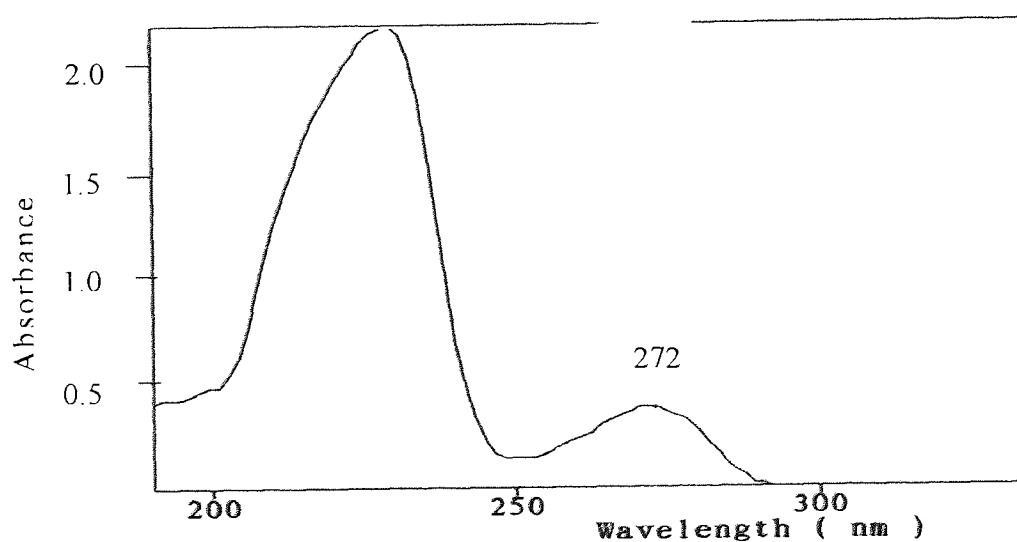


Figure A2.8. UV Spectrum of Weston 399 in Hexane

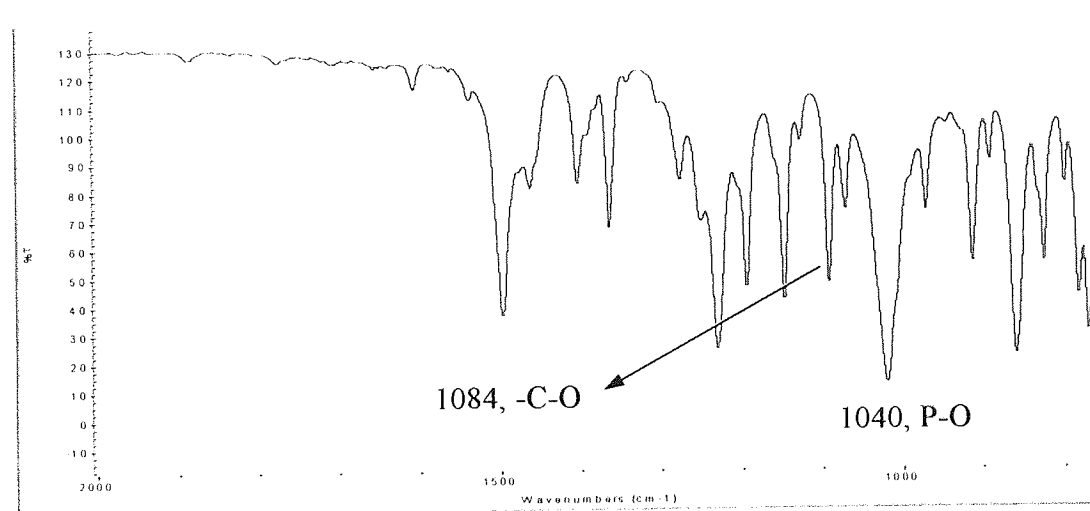
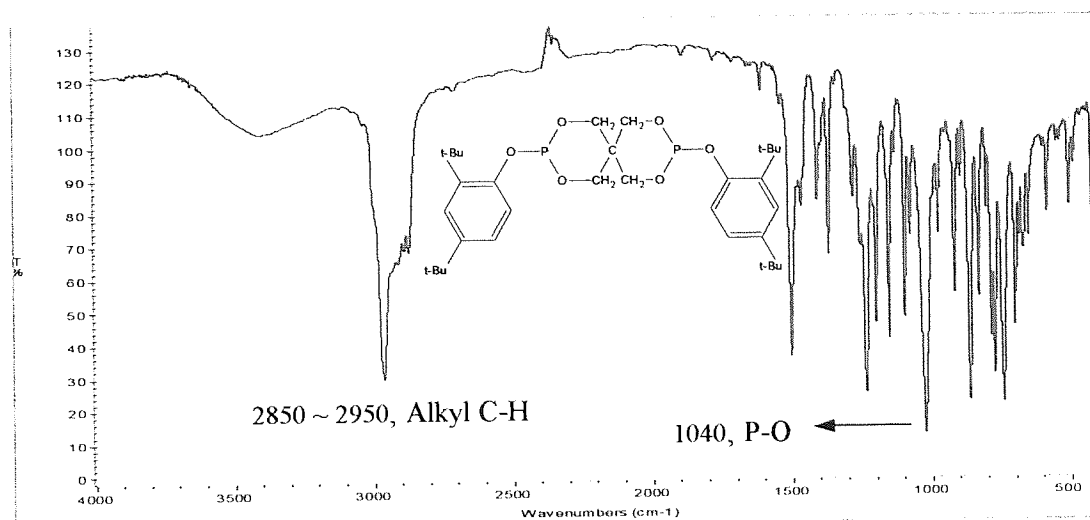


Figure A2.9. FTIR Spectrum of Ultrinox 626 and the Expansion at 2000~900 cm⁻¹ (KBR windows)

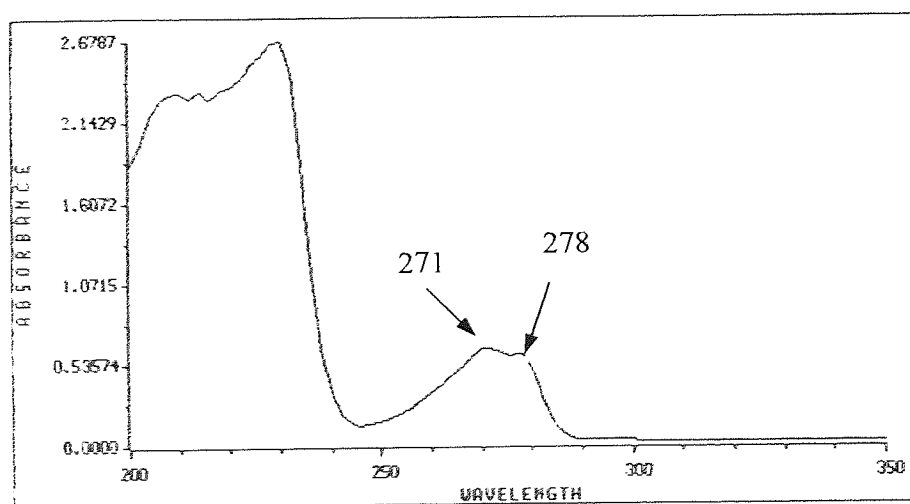


Figure A2.10. UV Spectrum of Ultrinox 626 in Hexane

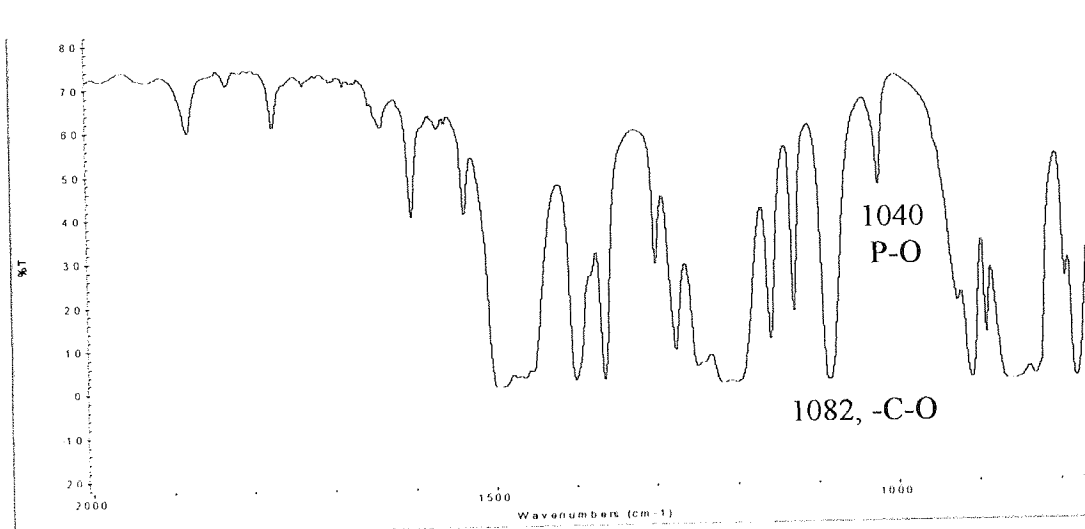
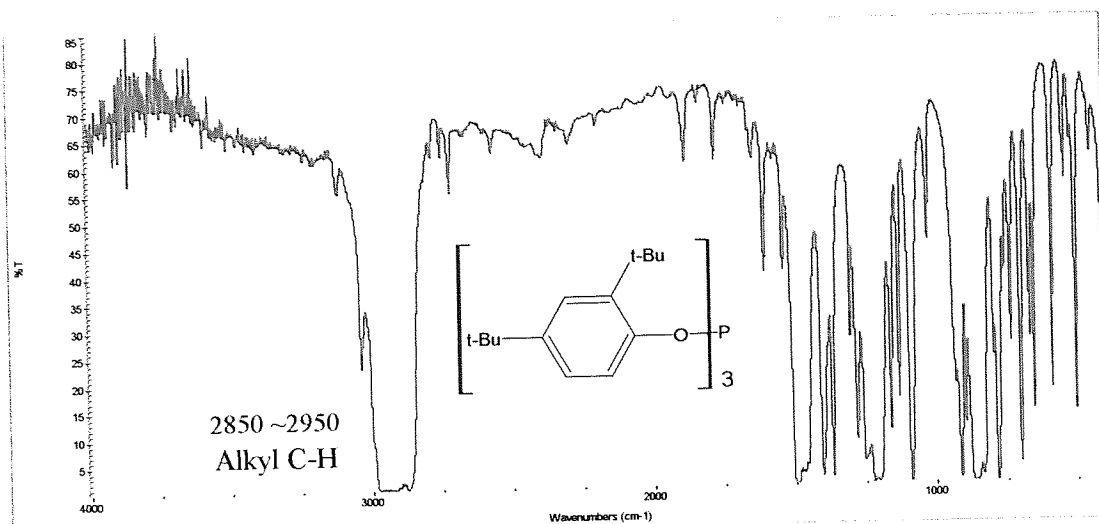


Figure A2.11. FTIR Spectrum of Irgafos 168 and the Expansion at 2000~900 cm⁻¹ (mixture with Nujol)

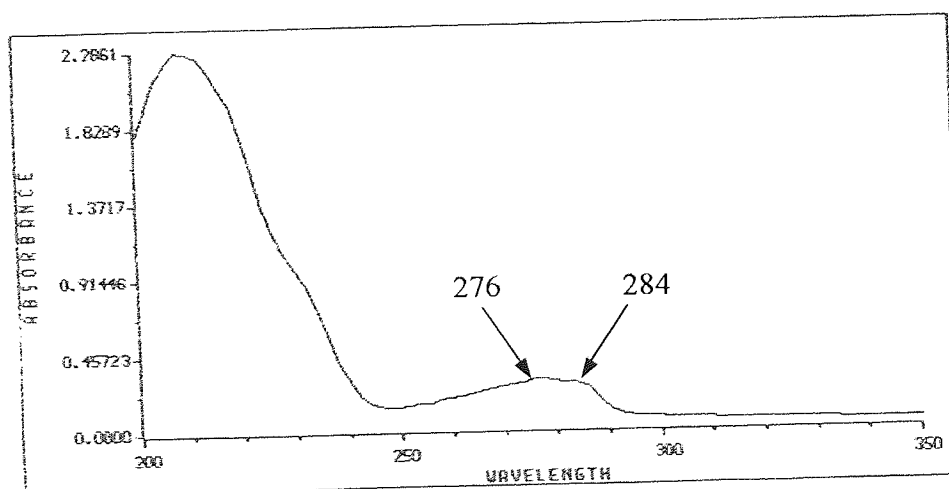


Figure A2.12. UV Spectrum of Irgafos 168 in Hexane

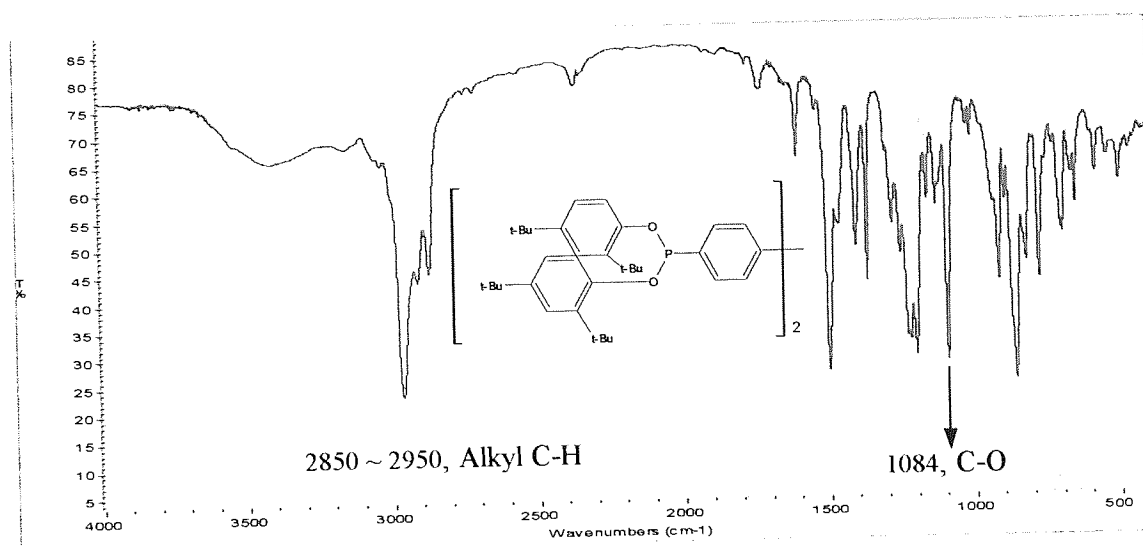


Figure A2.13. FTIR Spectrum of Irgafos P-EPQ and the Expansion at 2000~900 cm^{-1} (KBR windows)

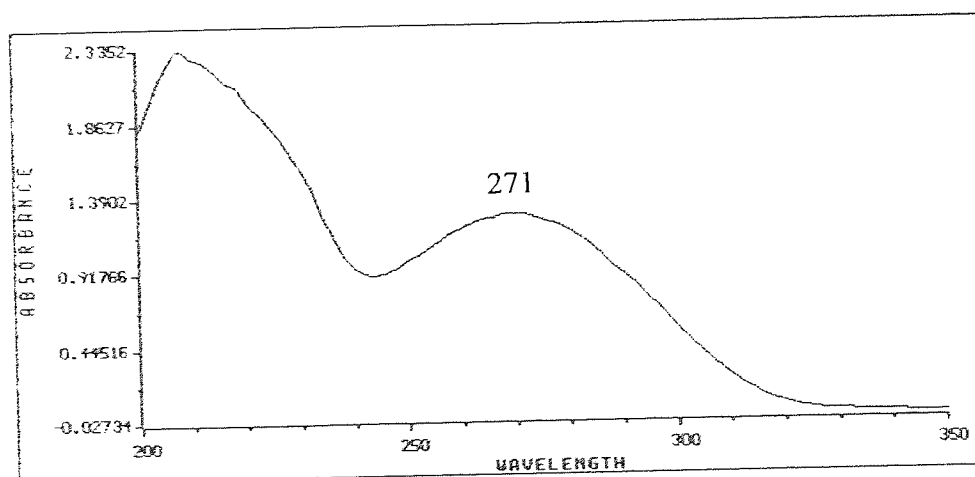


Figure A2.14. UV Spectrum of Irgafos P-EPQ in Hexane

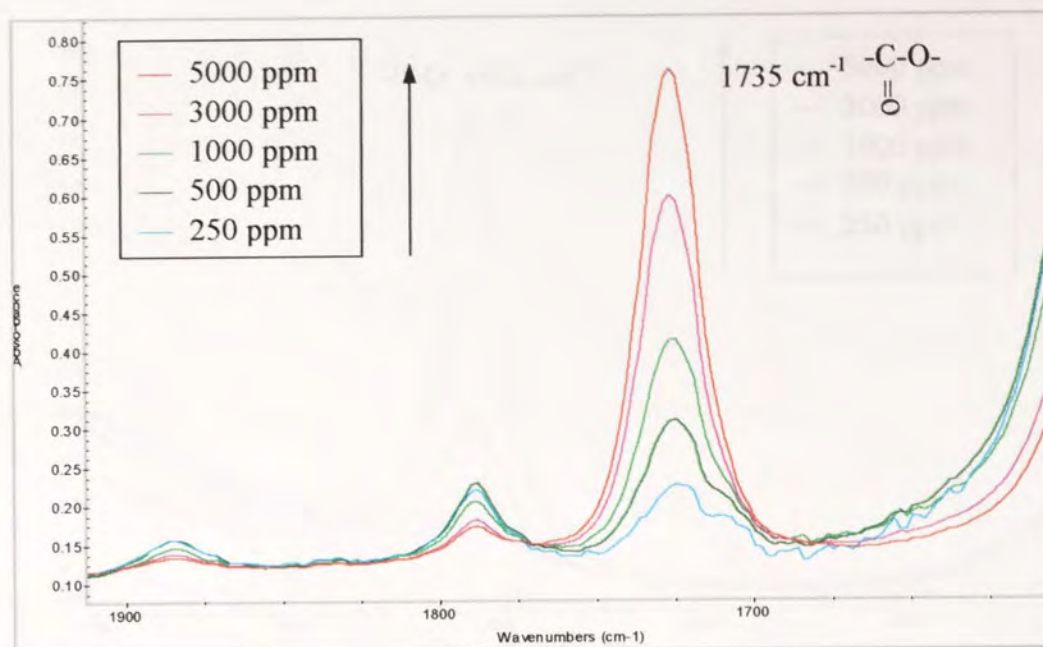


Figure A2.15. FTIR Spectra of Irganox1076 Standard Solutions (DCM) (the Numbers are ppm concentration of each solution)

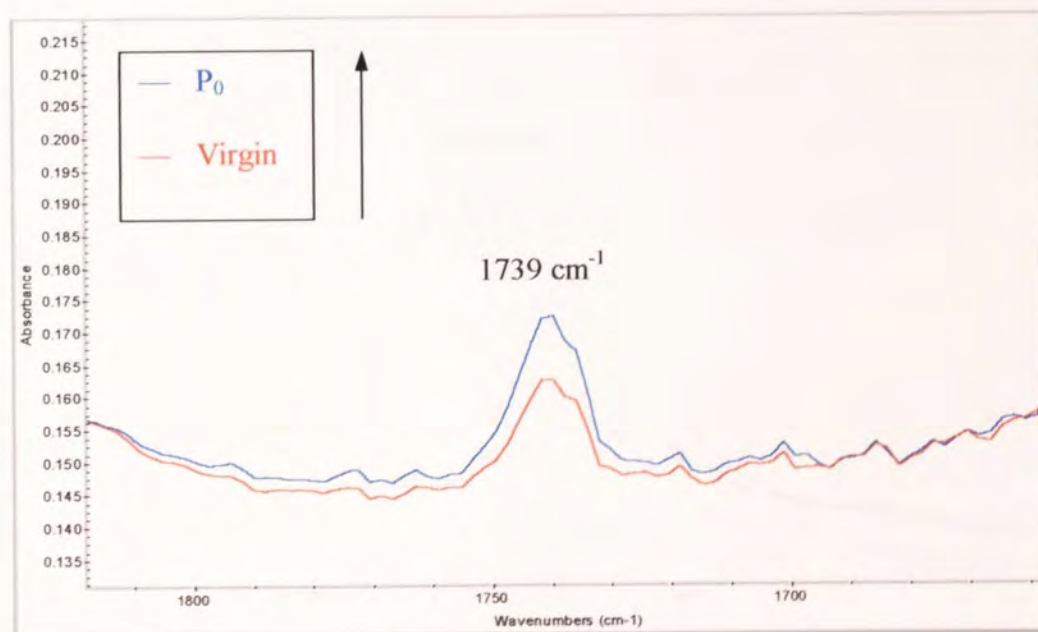


Figure A2.16. FTIR Spectrum of TSE Processed PL-1840, P_0 (Irg1076:Irg168=500:1250 ppm)

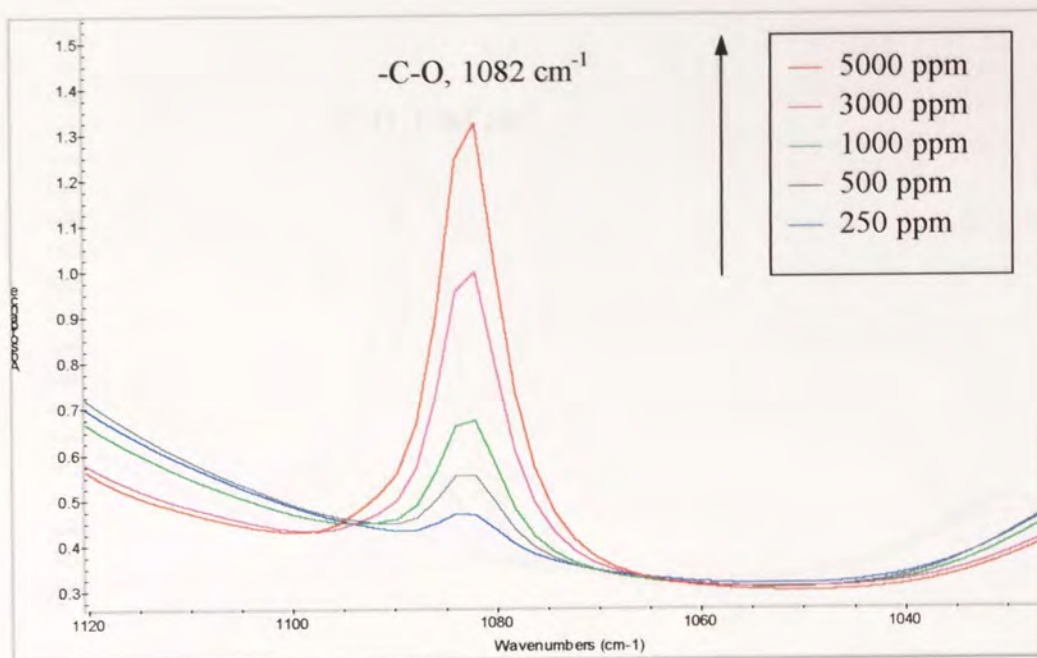


Figure A2.17. FTIR Spectra of Irgafos168 Standard Solutions (DCM) (the Numbers are ppm concentration of each solution)

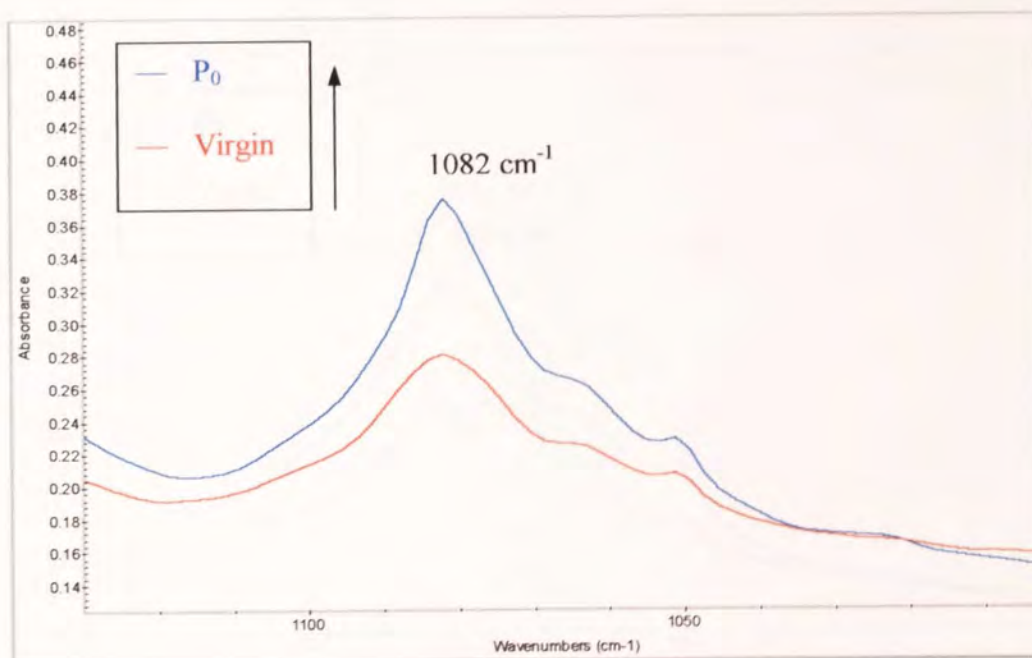


Figure A2.18. FTIR Spectrum of TSE Processed PL-1840, P₀ (Irg1076:Irg168:HP168=500:1250:250 ppm)

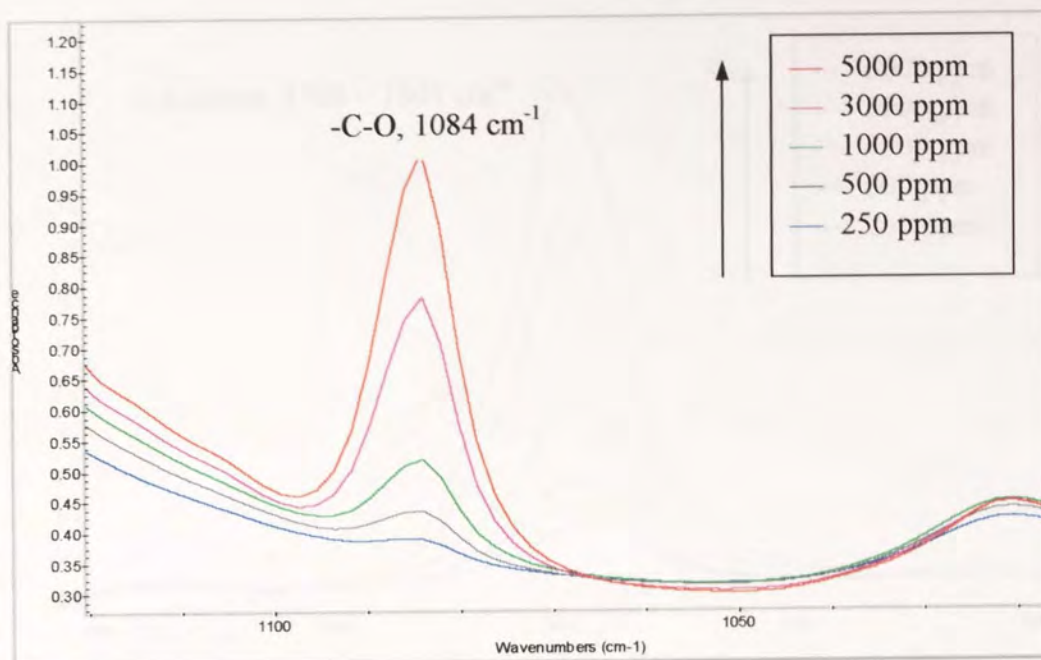


Figure A2.19. FTIR Spectra of Irgafos P-EPQ Standard Solutions (DCM) (the Numbers are ppm concentration of each solution)

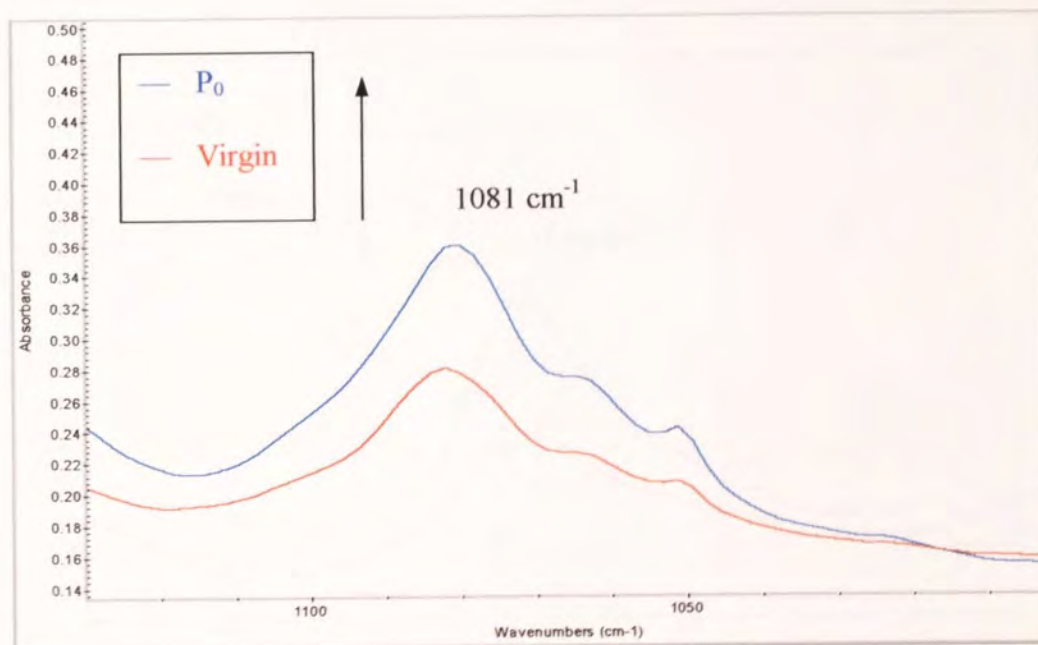


Figure A2.20. FTIR Spectrum of TSE Processed PL-1840, P_0 (Irg1076:IrgP-EPQ=500: 1000 ppm)

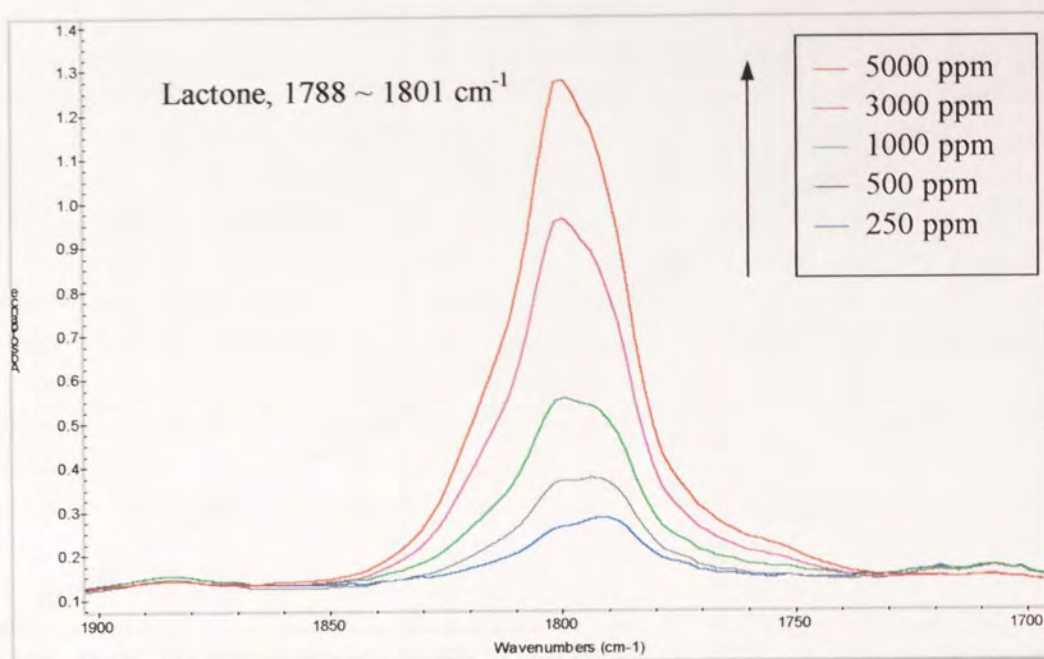


Figure A2.21. FTIR Spectra of Irganox HP136 Standard Solutions (DCM) (the Numbers are ppm concentration of each solution)

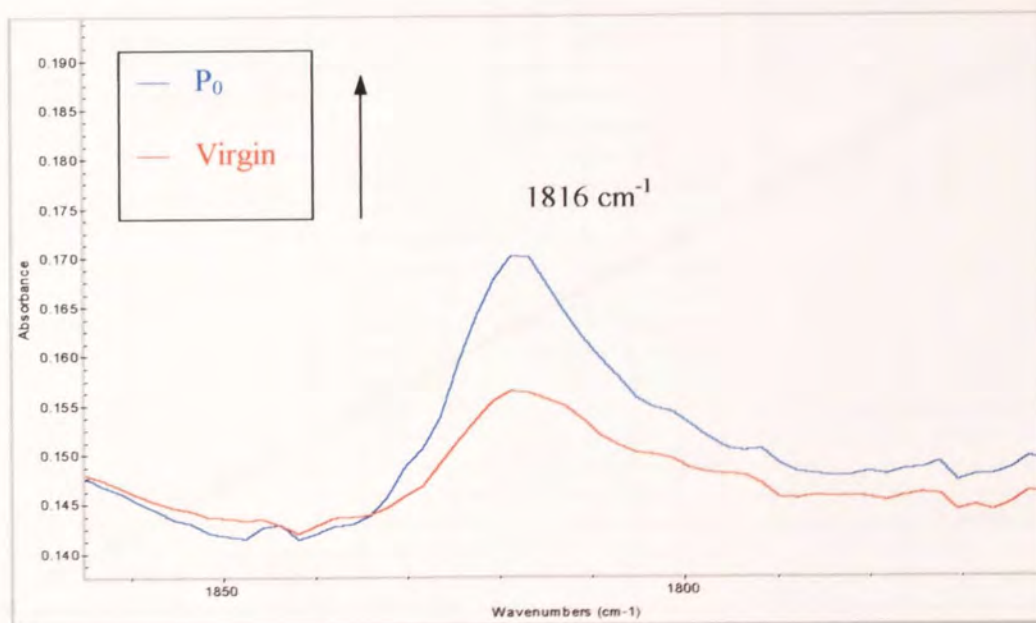


Figure A2.22. FTIR Spectrum of TSE Processed PL-1840, P₀ (Irg1076:IrgP-EPQ:HP136=500:1000:250 ppm)

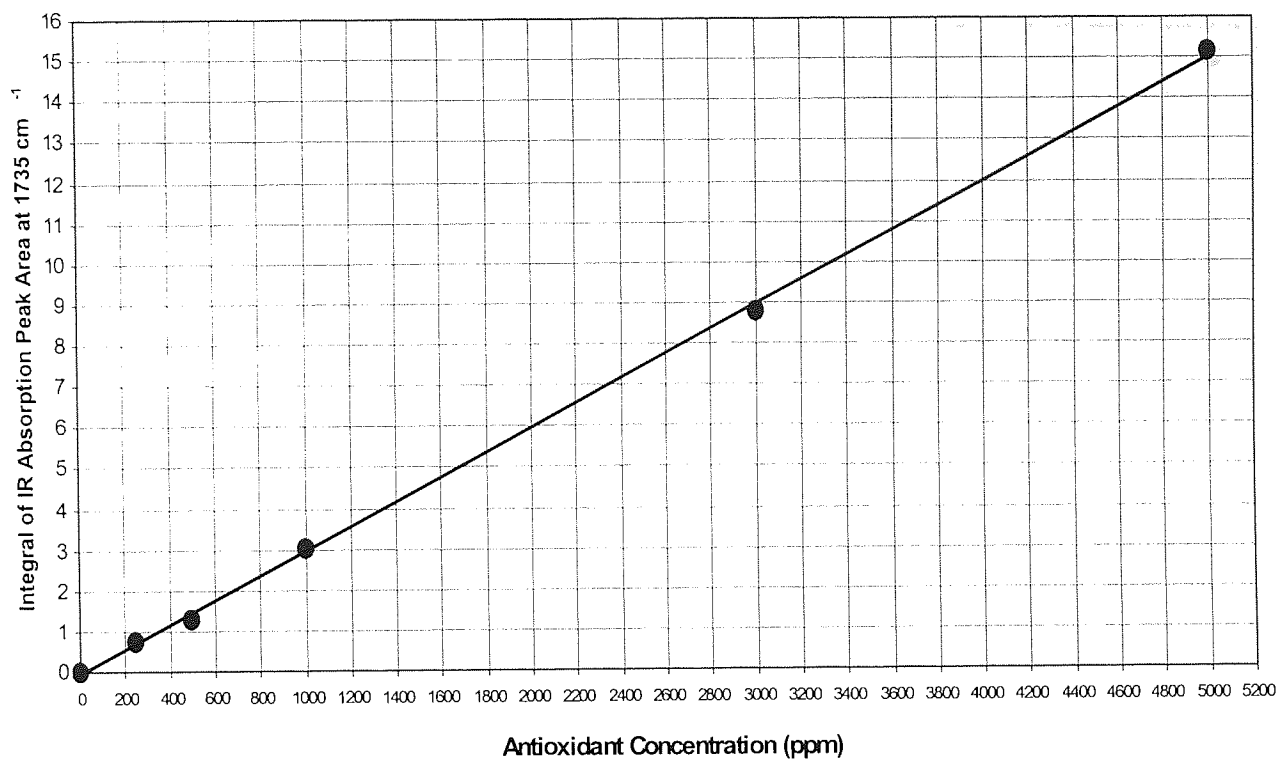


Figure A2.23. Calibration Curve of Irganox 1076

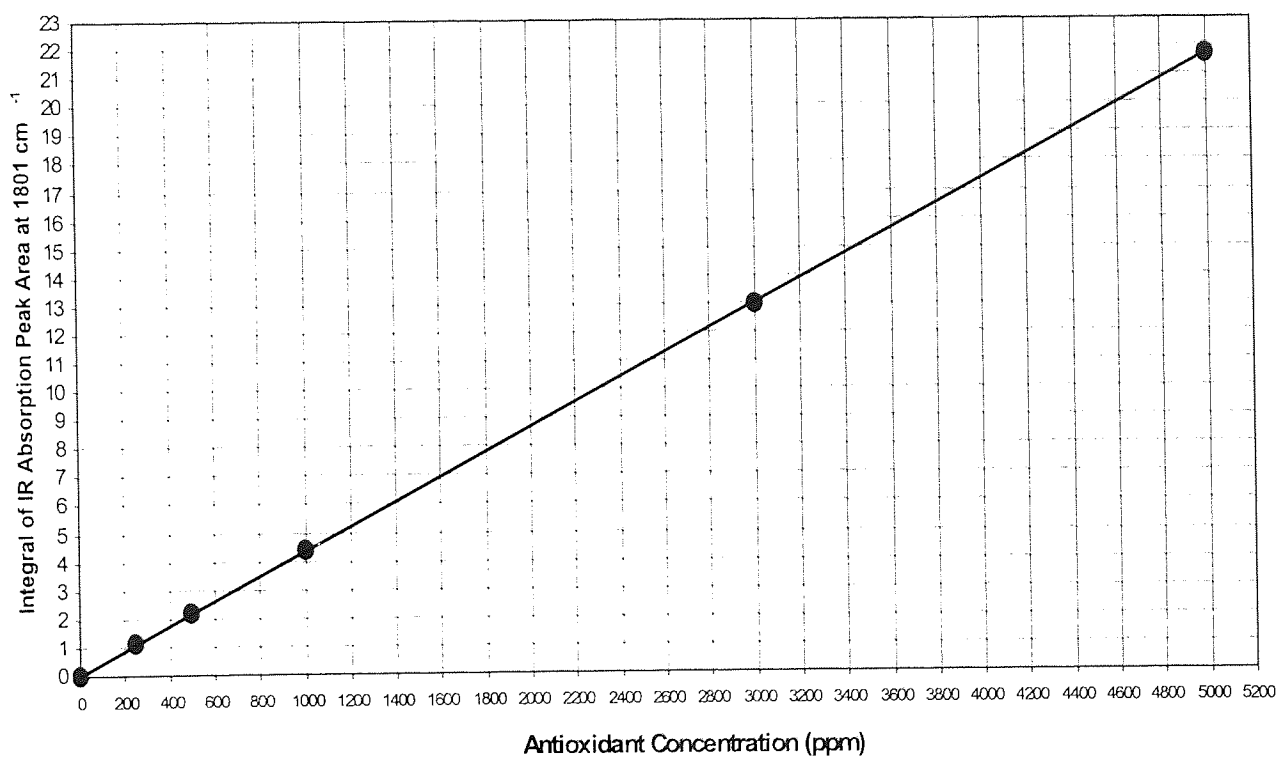


Figure A2.24. Calibration Curve of Irganox HP136

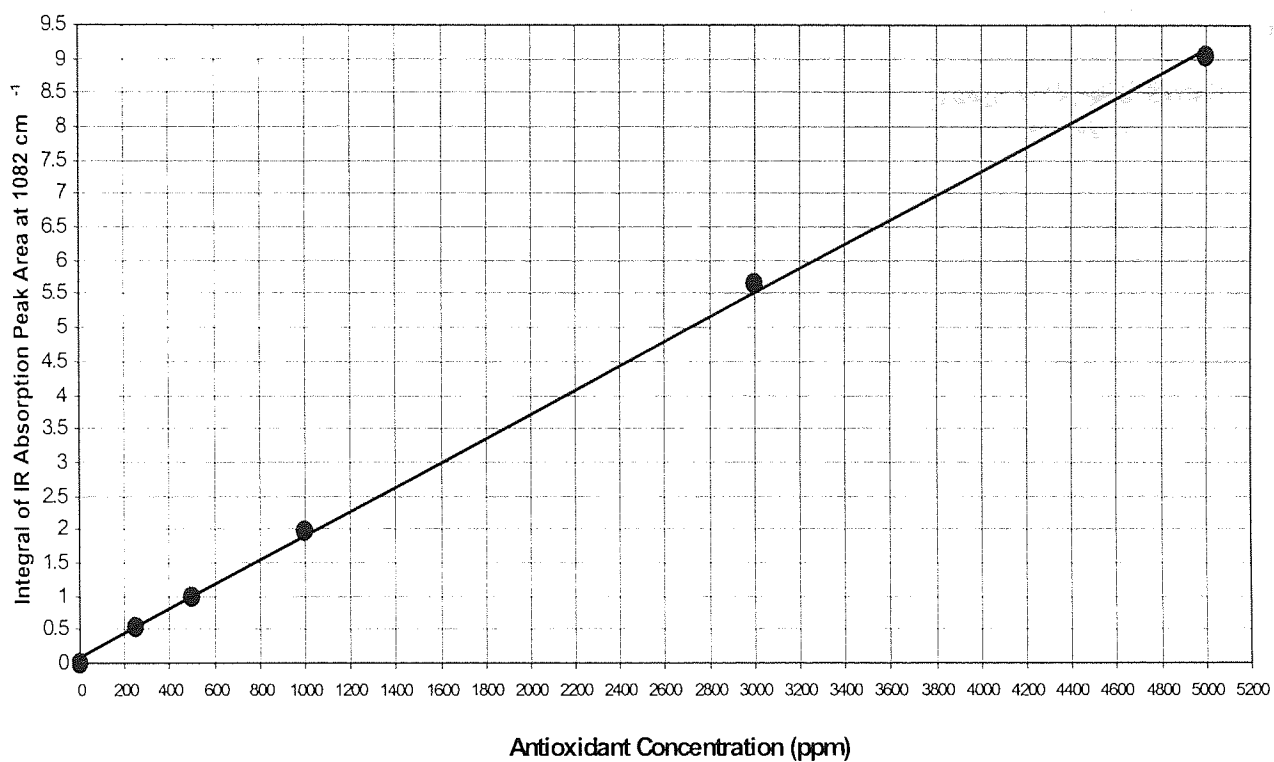


Figure A2.25. Calibration Curve of Irgafos 168

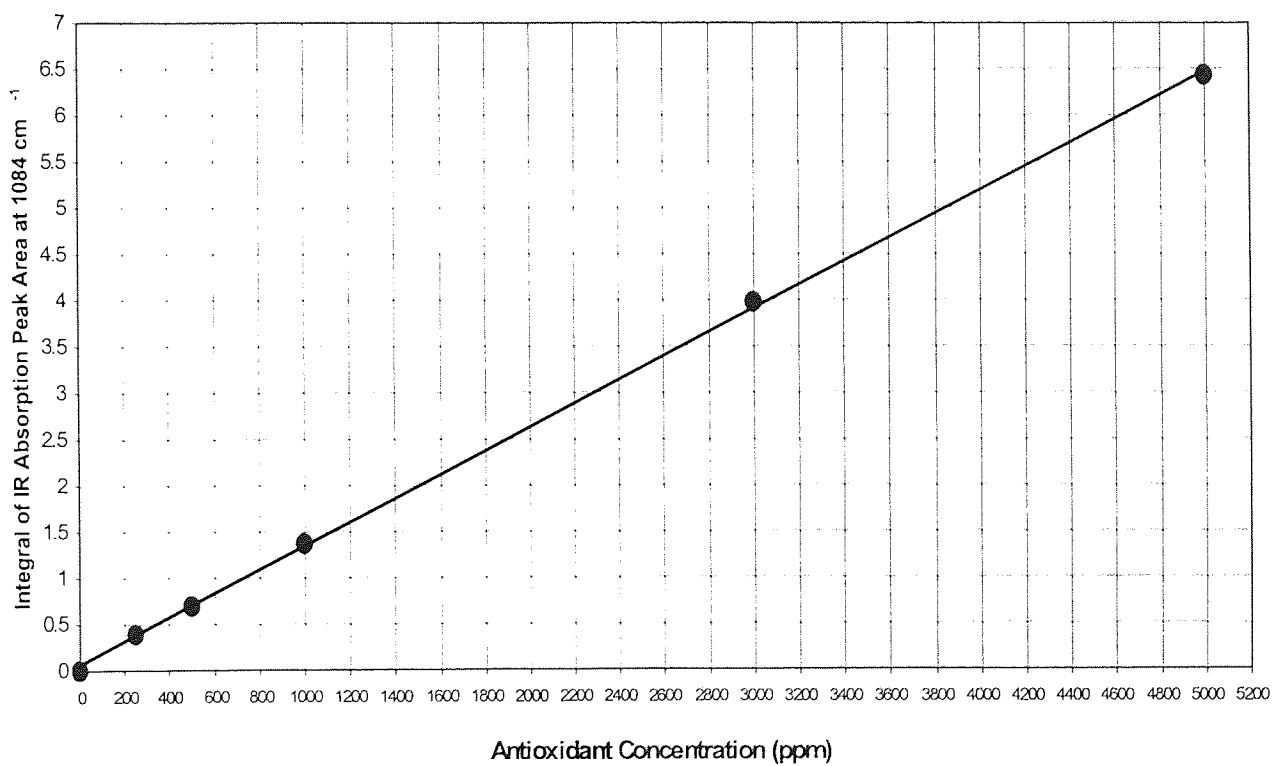


Figure A2.26. Calibration Curve of Irgafos P-EPQ

Table A3.1 Branching Amount (from ^{13}C -NMR) and Relative Concentrations of Double Bonds (from IR absorption area index) Contained in Virgin LLDPE (measured in Aston)

| Polymer Code | Dowlex2045-E | FM-1570 | PL-1840 | VP-8770 | EG 8150 |
|---|------------------------|---------|---------|---------|---------|
| Branching Amount I-Octene (w%) | 10.5 | 11.6 | 13.4 | 28.2 | 36.2 |
| Density (g/cm^3) | 0.92 | 0.92 | 0.91 | 0.89 | 0.87 |
| Group | Relative Concentration | | | | |
| Trans-Vinylene, $-\text{CH}=\text{CH}-$ | 0.028 | 0.069 | 0.095 | 0.211 | 0.255 |
| Vinyl, $-\text{CH}=\text{CH}_2$ | 0.143 | 0.062 | 0.034 | 0.043 | 0.029 |
| Vinylidene, $>\text{C}=\text{CH}_2$ | 0.061 | 0.128 | 0.157 | 0.282 | 0.488 |
| Total Double Bond | 0.232 | 0.259 | 0.286 | 0.536 | 0.772 |

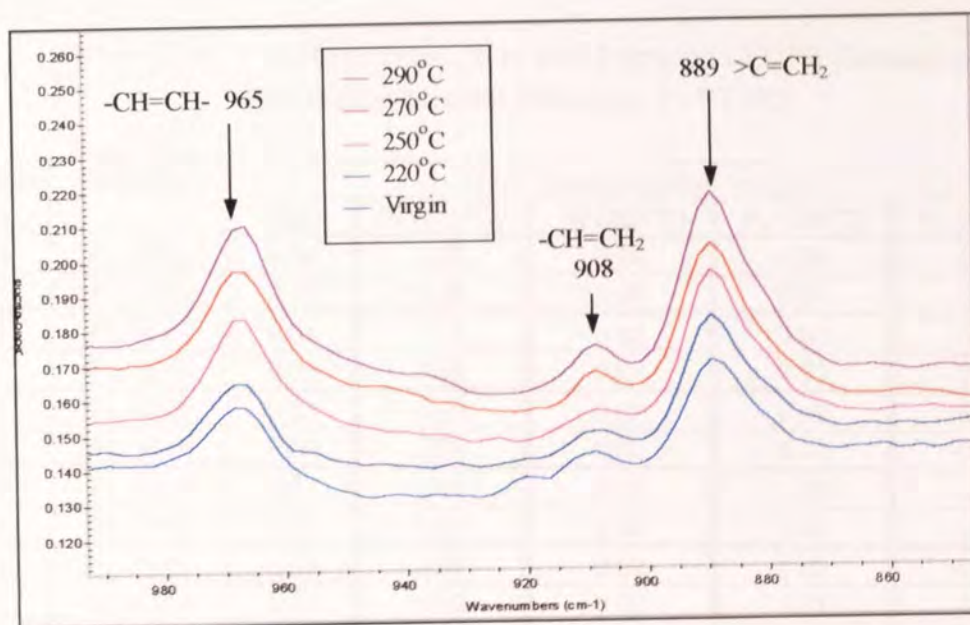


Figure A3.1. FTIR Spectrums of TR Processed PL-1840 (60rpm, 10min) at the Region of Unsaturated Groups

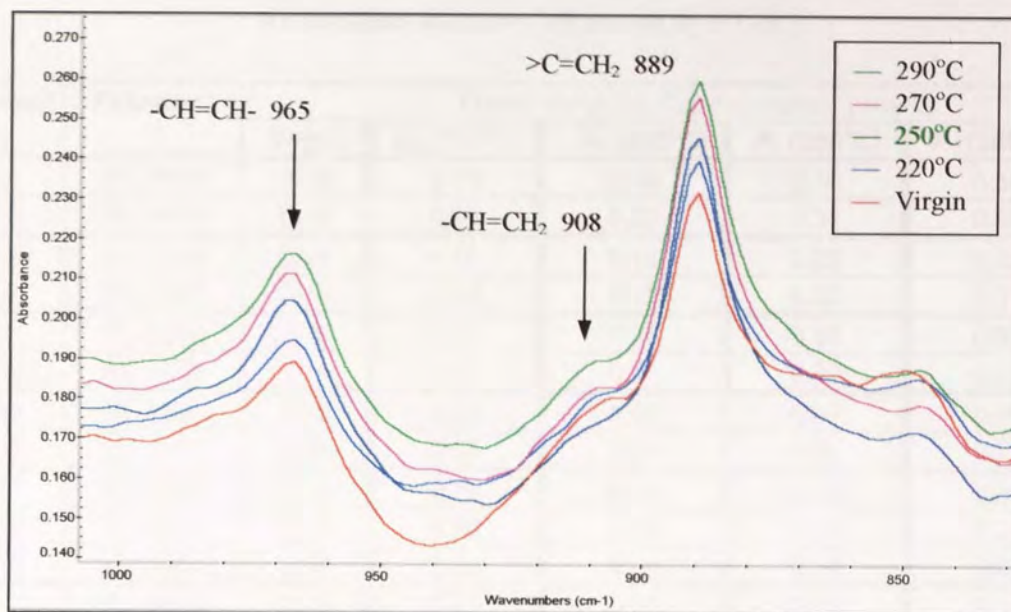


Figure A3.2. FTIR Spectrums of TR Processed EG8150 (60rpm, 10min) at the Region of Unsaturated Groups

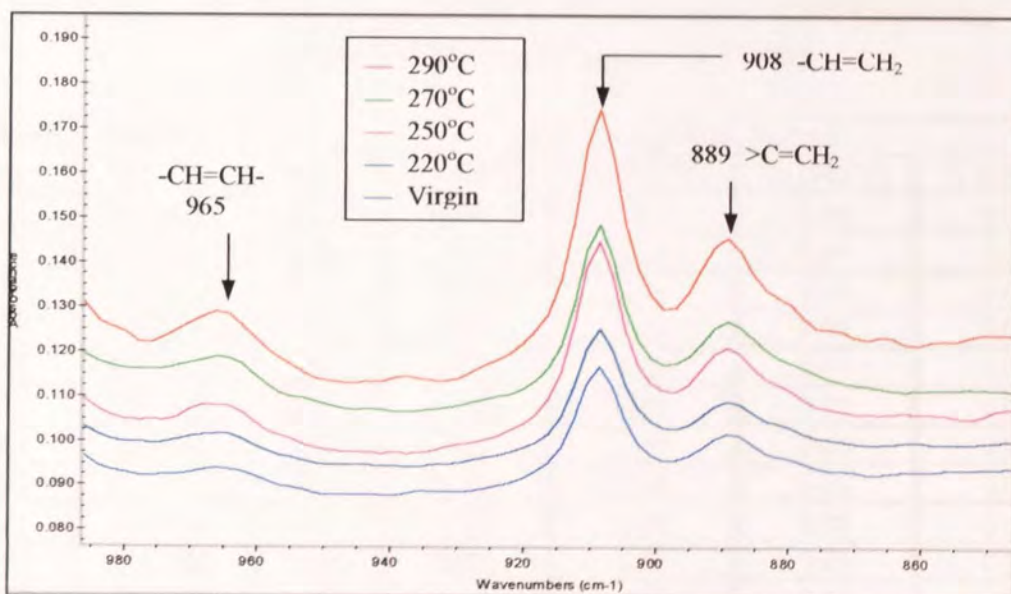


Figure A3.3. FTIR Spectrums of TR Processed Dowlex2045-E (60rpm, 10min) at the Region of Unsaturated Groups

Table A4.1. MI, HMI and MFR of TSE Processed LLDPE Polymers

| MI (g/10min) | | | | | | | | | | | | |
|-------------------|------|------|------|------|------|------|------|------|------|------|------|------|
| Temperatutre (°C) | 210 | | | 235 | | | 265 | | | 285 | | |
| Pass | P1 | P3 | P5 | P1 | P3 | P5 | P1 | P3 | P5 | P1 | P3 | P5 |
| FM-1570 | 1.39 | 1.40 | 1.42 | 1.48 | 1.24 | 0.73 | 1.42 | 0.83 | 0.48 | 1.35 | 0.81 | 0.51 |
| PL-1840 | 1.21 | 1.22 | 1.23 | 1.22 | 1.04 | 0.66 | 1.16 | 0.67 | 0.43 | 1.12 | 0.69 | 0.44 |
| PL-1880 | 1.13 | 1.15 | 1.15 | 1.14 | 0.79 | 0.39 | 1.10 | 0.60 | 0.41 | 1.03 | 0.60 | 0.39 |
| VP-8770 | 1.08 | 1.06 | 0.89 | 1.09 | 0.64 | 0.37 | 1.07 | 0.65 | 0.49 | 1.12 | 0.78 | 0.70 |
| Dowlex2045-E | 1.15 | 0.42 | 0.11 | 0.88 | 0.22 | 0.07 | 0.48 | 0.16 | 0.06 | 0.48 | 0.08 | 0.03 |
| HMI (g/10min) | | | | | | | | | | | | |
| Temperatutre (°C) | 210 | | | 235 | | | 265 | | | 285 | | |
| Pass | P1 | P3 | P5 | P1 | P3 | P5 | P1 | P3 | P5 | P1 | P3 | P5 |
| FM-1570 | 55.0 | 54.1 | 55.1 | 57.1 | 53.0 | 44.1 | 56.4 | 46.0 | 38.3 | 55.7 | 46.9 | 40.4 |
| PL-1840 | 44.8 | 45.7 | 45.4 | 44.9 | 43.1 | 36.4 | 44.0 | 36.7 | 32.2 | 44.0 | 38.6 | 33.4 |
| PL-1880 | 37.7 | 37.7 | 38.2 | 37.5 | 34.2 | 27.6 | 37.0 | 31.9 | 29.4 | 36.5 | 33.7 | 32.6 |
| VP-8770 | 33.2 | 32.6 | 31.0 | 33.0 | 28.1 | 24.5 | 33.4 | 31.8 | 32.9 | 36.4 | 40.0 | 45.3 |
| Dowlex2045-E | 44.4 | 31.9 | 23.6 | 37.3 | 25.7 | 17.4 | 31.5 | 24.0 | 17.0 | 32.5 | 18.8 | 11.2 |
| MFR (HMI / MI) | | | | | | | | | | | | |
| Temperatutre (°C) | 210 | | | 235 | | | 265 | | | 285 | | |
| Pass | P1 | P3 | P5 | P1 | P3 | P5 | P1 | P3 | P5 | P1 | P3 | P5 |
| FM-1570 | 40 | 39 | 39 | 39 | 43 | 60 | 40 | 55 | 80 | 41 | 58 | 79 |
| PL-1840 | 37 | 38 | 37 | 37 | 41 | 55 | 38 | 55 | 75 | 39 | 56 | 76 |
| PL-1880 | 33 | 33 | 33 | 33 | 43 | 71 | 34 | 53 | 72 | 35 | 56 | 84 |
| VP-8770 | 31 | 31 | 35 | 30 | 44 | 66 | 31 | 49 | 67 | 33 | 51 | 65 |
| Dowlex2045-E | 39 | 76 | 215 | 42 | 117 | 249 | 66 | 150 | 283 | 68 | 235 | 373 |

Table A4.2. Double Bond Concentration (from IR extinction coefficient) of TSE Processed FM-1570

| Temperature (°C) | Pass | t-Vinylene | Vinyl | Vinylidene | Total Double Bond |
|---------------------|------|-----------------|-----------------|-----------------|-------------------|
| | | Content (mol/L) | Content (mol/L) | Content (mol/L) | Content (mol/L) |
| Vingin FM-1570 | | 0.20 | 0.05 | 0.13 | 0.38 |
| 210 | 1 | 0.18 | 0.05 | 0.16 | 0.39 |
| | 3 | 0.17 | 0.03 | 0.20 | 0.40 |
| | 5 | 0.14 | 0.03 | 0.21 | 0.38 |
| 235 | 1 | 0.16 | 0.03 | 0.20 | 0.39 |
| | 3 | 0.18 | 0.02 | 0.24 | 0.44 |
| | 5 | 0.18 | 0.01 | 0.23 | 0.42 |
| 265 | 1 | 0.14 | 0.03 | 0.21 | 0.38 |
| | 3 | 0.19 | 0.02 | 0.23 | 0.44 |
| | 5 | 0.19 | 0.02 | 0.23 | 0.44 |
| 285 | 1 | 0.19 | 0.03 | 0.22 | 0.44 |
| | 3 | 0.23 | 0.04 | 0.26 | 0.53 |
| | 5 | 0.22 | 0.04 | 0.24 | 0.50 |

Table A4.3. Double Bond Concentration (from IR extinction coefficient) of TSE Processed PL-1840

| Temperature (°C) | Pass | t-Vinylene | Vinyl | Vinylidene | Total Double Bond |
|---------------------|------|-----------------|-----------------|-----------------|-------------------|
| | | Content (mol/L) | Content (mol/L) | Content (mol/L) | Content (mol/L) |
| Vingin PL-1840 | | 0.29 | 0.02 | 0.17 | 0.48 |
| 210 | 1 | 0.29 | 0.02 | 0.19 | 0.50 |
| | 3 | 0.24 | 0.02 | 0.19 | 0.45 |
| | 5 | 0.19 | 0.02 | 0.19 | 0.40 |
| 235 | 1 | 0.20 | 0.03 | 0.21 | 0.44 |
| | 3 | 0.25 | 0.01 | 0.23 | 0.49 |
| | 5 | 0.23 | 0.02 | 0.22 | 0.47 |
| 265 | 1 | 0.15 | 0.02 | 0.21 | 0.38 |
| | 3 | 0.19 | 0.01 | 0.21 | 0.41 |
| | 5 | 0.23 | 0.01 | 0.23 | 0.47 |
| 285 | 1 | 0.23 | 0.02 | 0.24 | 0.49 |
| | 3 | 0.23 | 0.02 | 0.24 | 0.49 |
| | 5 | 0.26 | 0.01 | 0.24 | 0.51 |

Table A4.4. Double Bond Concentration (from IR extinction coefficient) of TSE Processed PL-1880

| Temperature (°C) | Pass | t-Vinylene | Vinyl | Vinylidene | Total Double Bond |
|---------------------|------|-----------------|-----------------|-----------------|-------------------|
| | | Content (mol/L) | Content (mol/L) | Content (mol/L) | Content (mol/L) |
| Vingin PL-1880 | | 0.24 | 0.04 | 0.14 | 0.42 |
| 210 | 1 | 0.18 | 0.03 | 0.16 | 0.37 |
| | 3 | 0.15 | 0.02 | 0.19 | 0.36 |
| | 5 | 0.16 | 0.01 | 0.23 | 0.40 |
| 235 | 1 | 0.17 | 0.01 | 0.21 | 0.39 |
| | 3 | 0.18 | 0.01 | 0.24 | 0.43 |
| | 5 | 0.19 | 0.01 | 0.24 | 0.44 |
| 265 | 1 | 0.14 | 0.02 | 0.20 | 0.36 |
| | 3 | 0.19 | 0.01 | 0.26 | 0.46 |
| | 5 | 0.18 | 0.01 | 0.23 | 0.42 |
| 285 | 1 | 0.18 | 0.03 | 0.25 | 0.46 |
| | 3 | 0.20 | 0.03 | 0.25 | 0.48 |
| | 5 | 0.21 | 0.02 | 0.27 | 0.50 |

Table A4.5. Double Bond Concentration (from IR extinction coefficient) of TSE Processed VP-8770

| Temperature (°C) | Pass | t-Vinylene | Vinyl | Vinylidene | Total Double Bond |
|---------------------|------|-----------------|-----------------|-----------------|-------------------|
| | | Content (mol/L) | Content (mol/L) | Content (mol/L) | Content (mol/L) |
| Vingin VP-8770 | | 0.39 | 0.03 | 0.22 | 0.64 |
| 210 | 1 | 0.36 | 0.01 | 0.24 | 0.61 |
| | 3 | 0.32 | 0.01 | 0.31 | 0.64 |
| | 5 | 0.33 | 0.01 | 0.31 | 0.65 |
| 235 | 1 | 0.23 | 0.01 | 0.28 | 0.52 |
| | 3 | 0.33 | 0.01 | 0.30 | 0.64 |
| | 5 | 0.35 | 0.01 | 0.34 | 0.70 |
| 265 | 1 | 0.29 | 0.01 | 0.29 | 0.59 |
| | 3 | 0.34 | 0.01 | 0.34 | 0.69 |
| | 5 | 0.36 | 0.01 | 0.32 | 0.69 |
| 285 | 1 | 0.33 | 0.01 | 0.33 | 0.67 |
| | 3 | 0.32 | 0.01 | 0.33 | 0.66 |
| | 5 | 0.38 | 0.02 | 0.34 | 0.74 |

Table A4.6. Double Bond Concentration (from IR extinction coefficient) of TSE Processed Dow

| Temperature (°C) | Pass | t-Vinylene | Vinyl | Vinylidene | Total Double |
|---------------------|------|-----------------|-----------------|-----------------|--------------|
| | | Content (mol/L) | Content (mol/L) | Content (mol/L) | Content |
| Virgin Dowlex2045-E | | 0.06 | 0.26 | 0.08 | 0.4 |
| 210 | 1 | 0.06 | 0.26 | 0.07 | 0.3 |
| | 3 | 0.06 | 0.24 | 0.07 | 0.3 |
| | 5 | 0.06 | 0.22 | 0.07 | 0.3 |
| 235 | 1 | 0.07 | 0.24 | 0.09 | 0.4 |
| | 3 | 0.06 | 0.23 | 0.08 | 0.3 |
| | 5 | 0.07 | 0.21 | 0.07 | 0.3 |
| 265 | 1 | 0.06 | 0.23 | 0.07 | 0.3 |
| | 3 | 0.07 | 0.20 | 0.07 | 0.3 |
| | 5 | 0.08 | 0.18 | 0.08 | 0.3 |
| 285 | 1 | 0.06 | 0.24 | 0.08 | 0.3 |
| | 3 | 0.07 | 0.23 | 0.08 | 0.3 |
| | 5 | 0.11 | 0.19 | 0.10 | 0.4 |

Table A4.7. Content of Carbonyl Groups (from IR extinction coefficient)
Contained in TSE Processed LLDPE

| Extrusion Temperature (°C) | | | 210 | 235 | 265 | 285 |
|----------------------------|----------------|------|-----------------|-----------------|-----------------|-----------------|
| Polymer | Virgin Content | Pass | Content (mol/L) | Content (mol/L) | Content (mol/L) | Content (mol/L) |
| FM-1570 | 0.04 (mol/L) | 1 | 0.04 | 0.04 | 0.04 | 0.04 |
| | | 3 | 0.05 | 0.06 | 0.08 | 0.08 |
| | | 5 | 0.05 | 0.09 | 0.10 | 0.10 |
| PL-1840 | 0.04 (mol/L) | 1 | 0.04 | 0.05 | 0.04 | 0.04 |
| | | 3 | 0.05 | 0.05 | 0.06 | 0.06 |
| | | 5 | 0.05 | 0.07 | 0.09 | 0.09 |
| PL-1880 | 0.04 (mol/L) | 1 | 0.04 | 0.06 | 0.04 | 0.04 |
| | | 3 | 0.04 | 0.05 | 0.07 | 0.07 |
| | | 5 | 0.05 | 0.08 | 0.08 | 0.08 |
| VP-8770 | 0.03 (mol/L) | 1 | 0.03 | 0.03 | 0.02 | 0.02 |
| | | 3 | 0.03 | 0.05 | 0.08 | 0.08 |
| | | 5 | 0.04 | 0.10 | 0.11 | 0.11 |
| Dowlex2045-E | 0.01 (mol/L) | 1 | 0.02 | 0.02 | 0.02 | 0.02 |
| | | 3 | 0.03 | 0.09 | 0.07 | 0.07 |
| | | 5 | 0.16 | 0.13 | 0.09 | 0.09 |

Table A5.1. MI and Its Change of TSE Processed LLDPE Containing Single Sta
(265°C, 100rpm, 4.8kg/h)

| AO | Polymer Code | Virgin | P ₀ * (210°C) | | P ₁ (265°C) | | P ₃ (265°C) | | M |
|-----------------|-----------------------------|-----------------|--------------------------|---------------|------------------------|---------------|------------------------|---------------|-----|
| | | MI (g/10min) | MI (g/10min) | Change (%) | MI (g/10min) | Change (%) | MI (g/10min) | Change (%) | |
| Irg1076 | FM-1570 | 1.43 | 1.49 | 4.20 | 1.55 | 8.39 | 1.38 | -3.50 | 1.1 |
| | PL-1840 | 1.16 | 1.23 | 6.03 | 1.00 | -13.8 | 0.65 | -44.0 | 0.4 |
| | VP-8770 | 1.04 | 1.06 | 1.92 | 1.08 | 3.85 | 0.87 | -16.4 | 0.6 |
| | Dowlex2045-E (Old Batch) | 1.21 | 1.29 | 6.61 | 0.83 | -31.4 | 0.46 | -62.0 | 0.3 |
| HP136 | FM-1570 | 1.43 | 1.48 | 3.50 | 1.52 | 6.29 | 1.44 | 0.70 | 1.2 |
| | PL-1840 | 1.16 | 1.20 | 3.45 | 1.13 | -2.59 | 0.89 | -23.3 | 0.6 |
| | VP-8770 | 1.04 | 1.06 | 1.92 | 1.06 | 1.92 | 0.82 | -21.2 | 0.4 |
| | Dowlex2045E (New Batch) | 1.15 | 1.17 | 1.74 | 0.75 | -34.8 | 0.61 | -47.0 | 0.4 |
| Ultranox 626 | FM-1570 | 1.43 | 1.48 | 3.5 | 1.48 | 3.50 | 1.06 | -25.9 | 0.6 |
| | PL-1840 | 1.16 | 1.21 | 4.31 | 1.19 | 2.59 | 0.72 | -37.9 | 0.4 |
| | VP-8770 | 1.04 | 1.06 | 1.92 | 1.06 | 1.92 | 0.71 | -31.7 | 0.3 |
| | Dowlex2045E (New Batch) | 1.15 | 1.15 | 0.00 | 0.93 | -19.1 | 0.52 | -54.8 | 0.3 |
| Irganox E201 | FM-1570 | 1.43 | 1.47 | 2.80 | 1.49 | 4.20 | 1.32 | -7.69 | 1.1 |
| | PL-1840 | 1.16 | 1.19 | 2.59 | 0.99 | -14.7 | 0.65 | -44.0 | 0.4 |
| | VP-8770 | 1.04 | 1.07 | 2.88 | 1.06 | 1.92 | 0.90 | -13.5 | 0.6 |
| | Dowlex2045E (New Batch) | 1.15 | 1.14 | -0.87 | 0.61 | -47.0 | 0.40 | -65.2 | 0.3 |

* P₀ was carried out at 210°C, 100rpm and 4.0kg/h

Table A5.2. MFR and Its Change of TSE Processed LLDPE Containing Single
(265°C, 100rpm, 4.8kg/h)

| Stabiliser | Polymer Code | Virgin MFR | P ₀ * (210°C) | | P ₁ (265°C) | | P ₃ (265°C) | | F |
|-----------------|-----------------------------|------------|--------------------------|------------|------------------------|------------|------------------------|------------|---|
| | | | MFR | Change (%) | MFR | Change (%) | MFR | Change (%) | |
| Irg1076 | FM-1570 | 39 | 38 | -2.56 | 37 | -5.12 | 40 | 2.56 | 4 |
| | PL-1840 | 38 | 37 | -2.63 | 42 | 10.5 | 57 | 50.0 | 7 |
| | VP-8770 | 30 | 29 | -3.33 | 30 | 0.00 | 36 | 20.0 | 4 |
| | Dowlex2045-E (Old Batch) | 36 | 34 | -5.56 | 44 | 22.2 | 69 | 91.7 | 9 |
| HP136 | FM-1570 | 39 | 38 | -2.56 | 38 | -2.56 | 40 | 2.56 | 4 |
| | PL-1840 | 38 | 38 | 0.00 | 39 | 2.63 | 46 | 21.1 | 4 |
| | VP-8770 | 30 | 30 | 0.00 | 31 | 3.33 | 37 | 23.3 | 4 |
| | Dowlex2045E (New Batch) | 30 | 30 | 0.00 | 41 | 36.7 | 49 | 63.3 | 6 |
| Ultranox 626 | FM-1570 | 39 | 38 | -2.56 | 39 | 0.00 | 47 | 20.5 | 6 |
| | PL-1840 | 38 | 36 | -5.26 | 38 | 0.00 | 52 | 36.8 | 7 |
| | VP-8770 | 30 | 29 | -3.33 | 30 | 0.00 | 41 | 36.7 | 4 |
| | Dowlex2045E (New Batch) | 30 | 30 | 0.00 | 35 | 16.7 | 52 | 73.3 | 6 |
| Irganox E201 | FM-1570 | 39 | 39 | 0.00 | 39 | 0.00 | 43 | 10.3 | 4 |
| | PL-1840 | 38 | 38 | 0.00 | 43 | 13.2 | 57 | 50.0 | 4 |
| | VP-8770 | 30 | 29 | -3.33 | 30 | 0.00 | 35 | 16.7 | 4 |
| | Dowlex2045E (New Batch) | 30 | 30 | 0.00 | 47 | 56.7 | 67 | 123 | 4 |

* P₀ was carried out at 210°C, 100rpm and 4.0kg/h

Table A5.3. Concentrations of Double Bonds and Carbonyl Compounds in Extruded L Containing Irg1076 (Calculation Based on IR Extinction Coefficients, see Table 2.10 in C

| Polymer Code | Pass | T-Vinylene (mol/L) | Vinyl (mol/L) | Vinylidene (mol/L) | Total Double Bonds (mol/L) | Carbonyl (mol/L) |
|--------------------------|--------|--------------------|---------------|--------------------|----------------------------|------------------|
| FM-1570 | Virgin | 0.20 | 0.05 | 0.13 | 0.38 | 0.0 |
| | 0 | 0.19 | 0.04 | 0.14 | 0.37 | 0.1 |
| | 1 | 0.16 | 0.03 | 0.18 | 0.37 | 0.1 |
| | 3 | 0.16 | 0.02 | 0.23 | 0.41 | 0.1 |
| | 5 | 0.17 | 0.02 | 0.23 | 0.42 | 0.1 |
| PL-1840 | Virgin | 0.29 | 0.02 | 0.17 | 0.48 | 0.0 |
| | 0 | 0.25 | 0.02 | 0.18 | 0.45 | 0.1 |
| | 1 | 0.24 | 0.01 | 0.20 | 0.45 | 0.1 |
| | 3 | 0.25 | 0.02 | 0.22 | 0.49 | 0.1 |
| | 5 | 0.27 | 0.02 | 0.23 | 0.52 | 0.1 |
| VP-8770 | Virgin | 0.39 | 0.03 | 0.22 | 0.64 | 0.0 |
| | 0 | 0.36 | 0.02 | 0.21 | 0.59 | 0.0 |
| | 1 | 0.29 | 0.01 | 0.30 | 0.60 | 0.0 |
| | 3 | 0.34 | 0.01 | 0.31 | 0.66 | 0.0 |
| | 5 | 0.33 | 0.01 | 0.31 | 0.65 | 0.1 |
| Dowlex2045-E (Old Batch) | Virgin | 0.06 | 0.26 | 0.08 | 0.40 | 0.0 |
| | 0 | 0.05 | 0.24 | 0.07 | 0.36 | 0.0 |
| | 1 | 0.07 | 0.23 | 0.08 | 0.38 | 0.0 |
| | 3 | 0.07 | 0.24 | 0.08 | 0.39 | 0.0 |
| | 5 | 0.06 | 0.24 | 0.07 | 0.37 | 0.1 |

Table A5.4. Concentrations of Double Bonds and Carbonyl Compounds in Extruded I Containing HP136 (Calculation Based on IR Extinction Coefficients, see Table 2.10 in C

| Polymer Code | Pass | T-Vinylene (mol/L) | Vinyl (mol/L) | Vinylidene (mol/L) | Total Double Bonds (mol/L) | Carbonyl (mol/L) |
|-------------------------|--------|--------------------|---------------|--------------------|----------------------------|------------------|
| FM-1570 | Virgin | 0.20 | 0.05 | 0.13 | 0.38 | 0 |
| | 0 | 0.18 | 0.05 | 0.15 | 0.38 | 0 |
| | 1 | 0.15 | 0.03 | 0.19 | 0.37 | 0 |
| | 3 | 0.16 | 0.02 | 0.22 | 0.40 | 0 |
| | 5 | 0.16 | 0.02 | 0.22 | 0.40 | 0 |
| PL-1840 | Virgin | 0.29 | 0.02 | 0.17 | 0.48 | 0 |
| | 0 | 0.28 | 0.02 | 0.17 | 0.47 | 0 |
| | 1 | 0.26 | 0.01 | 0.19 | 0.46 | 0 |
| | 3 | 0.26 | 0.02 | 0.19 | 0.47 | 0 |
| | 5 | 0.27 | 0.02 | 0.19 | 0.48 | 0 |
| VP-8770 | Virgin | 0.39 | 0.03 | 0.22 | 0.64 | 0 |
| | 0 | 0.24 | 0.02 | 0.20 | 0.46 | 0 |
| | 1 | 0.29 | 0.01 | 0.26 | 0.56 | 0 |
| | 3 | 0.32 | 0.01 | 0.29 | 0.62 | 0 |
| | 5 | 0.33 | 0.01 | 0.23 | 0.57 | 0 |
| Dowlex2045E (New Batch) | Virgin | 0.06 | 0.19 | 0.07 | 0.32 | 0 |
| | 0 | 0.04 | 0.19 | 0.07 | 0.30 | 0 |
| | 1 | 0.03 | 0.20 | 0.07 | 0.30 | 0 |
| | 3 | 0.05 | 0.19 | 0.07 | 0.31 | 0 |
| | 5 | 0.08 | 0.19 | 0.08 | 0.35 | 0 |

Table A5.5. Concentrations of Double Bonds and Carbonyl Compounds in Extruded LLDPE Containing Ultrinox626 (Calculation Based on IR Extinction Coefficients, see Table 2.10 in Chapter 2)

| Polymer Code | Pass | T-Vinylene (mol/L) | Vinyl (mol/L) | Vinylidene (mol/L) | Total Double Bonds (mol/L) | Carbonyl (mol/L) |
|-------------------------|--------|--------------------|---------------|--------------------|----------------------------|------------------|
| FM-1570 | Virgin | 0.20 | 0.05 | 0.13 | 0.38 | 0.04 |
| | 0 | 0.17 | 0.02 | 0.16 | 0.35 | 0.05 |
| | 1 | 0.33 | 0.02 | 0.20 | 0.55 | 0.05 |
| | 3 | 0.45 | 0.03 | 0.22 | 0.70 | 0.06 |
| | 5 | 0.44 | 0.02 | 0.21 | 0.67 | 0.07 |
| PL-1840 | Virgin | 0.29 | 0.02 | 0.17 | 0.48 | 0.04 |
| | 0 | 0.17 | 0.02 | 0.18 | 0.37 | 0.04 |
| | 1 | 0.26 | 0.02 | 0.20 | 0.48 | 0.04 |
| | 3 | 0.35 | 0.01 | 0.20 | 0.56 | 0.06 |
| | 5 | 0.33 | 0.02 | 0.21 | 0.56 | 0.08 |
| VP-8770 | Virgin | 0.39 | 0.03 | 0.22 | 0.64 | 0.03 |
| | 0 | 0.36 | 0.02 | 0.24 | 0.62 | 0.03 |
| | 1 | 0.35 | 0.01 | 0.28 | 0.64 | 0.03 |
| | 3 | 0.26 | 0.02 | 0.27 | 0.55 | 0.04 |
| | 5 | 0.33 | 0.01 | 0.29 | 0.63 | 0.06 |
| Dowlex2045E (New Batch) | Virgin | 0.06 | 0.19 | 0.07 | 0.32 | 0.02 |
| | 0 | 0.06 | 0.22 | 0.08 | 0.36 | 0.07 |
| | 1 | 0.08 | 0.19 | 0.08 | 0.35 | 0.12 |
| | 3 | 0.08 | 0.18 | 0.08 | 0.34 | 0.18 |
| | 5 | 0.08 | 0.17 | 0.09 | 0.34 | 0.21 |

Table A5.6. Concentrations of Double Bonds and Carbonyl Compounds in Extruded LLDPE Containing IrganoxE201 (Calculation Based on IR Extinction Coefficients, see Table 2.10 in Chapter 2)

| Polymer Code | Pass | T-Vinylene (mol/L) | Vinyl (mol/L) | Vinylidene (mol/L) | Total Double Bonds (mol/L) | Carbonyl (mol/L) |
|-------------------------|--------|--------------------|---------------|--------------------|----------------------------|------------------|
| FM-1570 | Virgin | 0.20 | 0.05 | 0.13 | 0.38 | 0.04 |
| | 0 | 0.20 | 0.05 | 0.14 | 0.39 | 0.05 |
| | 1 | 0.15 | 0.03 | 0.20 | 0.38 | 0.05 |
| | 3 | 0.18 | 0.02 | 0.22 | 0.42 | 0.06 |
| | 5 | 0.20 | 0.02 | 0.23 | 0.45 | 0.08 |
| PL-1840 | Virgin | 0.29 | 0.02 | 0.17 | 0.48 | 0.04 |
| | 0 | 0.27 | 0.02 | 0.18 | 0.47 | 0.05 |
| | 1 | 0.29 | 0.01 | 0.20 | 0.50 | 0.07 |
| | 3 | 0.28 | 0.01 | 0.20 | 0.49 | 0.08 |
| | 5 | 0.30 | 0.01 | 0.21 | 0.52 | 0.10 |
| VP-8770 | Virgin | 0.39 | 0.03 | 0.22 | 0.64 | 0.03 |
| | 0 | 0.37 | 0.02 | 0.21 | 0.60 | 0.03 |
| | 1 | 0.31 | 0.01 | 0.29 | 0.61 | 0.03 |
| | 3 | 0.34 | 0.01 | 0.31 | 0.66 | 0.05 |
| | 5 | 0.35 | 0.01 | 0.32 | 0.68 | 0.07 |
| Dowlex2045E (New Batch) | Virgin | 0.06 | 0.19 | 0.07 | 0.32 | 0.02 |
| | 0 | 0.04 | 0.19 | 0.07 | 0.30 | 0.02 |
| | 1 | 0.04 | 0.20 | 0.07 | 0.31 | 0.05 |
| | 3 | 0.06 | 0.19 | 0.07 | 0.32 | 0.08 |
| | 5 | 0.04 | 0.18 | 0.07 | 0.29 | 0.07 |

Table A5.7. MI and Its Change of TSE Processed LLDPE Containing Antioxidant Mixtures (265°C, 100rpm, 4.8kg/h)

| Antioxidant Mixtures (Code) * | Polymer ** | Virgin MI (g/10min) | P ₀ *** (210°C) | | P ₁ (265°C) | | P ₃ (265°C) | | P ₅ (265°C) | |
|-------------------------------|-------------|---------------------|----------------------------|------------|------------------------|------------|------------------------|------------|------------------------|------------|
| | | | MI (g/10min) | Change (%) | MI (g/10min) | Change (%) | MI (g/10min) | Change (%) | MI (g/10min) | Change (%) |
| AO-A1 | PL-1840 | 1.34 | 1.36 | 1.49 | 1.41 | 5.22 | 1.37 | 2.24 | 1.16 | -13.4 |
| AO-A2 | PL-1840 | 1.34 | 1.37 | 2.24 | 1.40 | 4.48 | 1.39 | 3.73 | 1.26 | -5.97 |
| AO-B1 | PL-1840 | 1.34 | 1.35 | 0.75 | 1.40 | 4.48 | 1.17 | -12.7 | 0.72 | -46.3 |
| AO-B2 | PL-1840 | 1.34 | 1.35 | 0.75 | 1.36 | 1.49 | 1.30 | -2.99 | 0.85 | -36.6 |
| AO-C1 | PL-1840 | 1.34 | 1.36 | 1.49 | 1.41 | 5.22 | 1.08 | -19.4 | 0.67 | -50.0 |
| AO-C2 | PL-1840 | 1.34 | 1.36 | 1.49 | 1.37 | 2.24 | 1.36 | 1.49 | 0.98 | -26.9 |
| AO-D1 | PL-1840 | 1.34 | 1.35 | 0.75 | 1.40 | 4.48 | 1.34 | 0.00 | 0.83 | -38.1 |
| AO-D2 | PL-1840 | 1.34 | 1.37 | 2.24 | 1.39 | 3.73 | 1.39 | 3.73 | 1.23 | -8.21 |
| AO-E1 | PL-1840 | 1.34 | 1.35 | 0.75 | 1.36 | 1.49 | 1.19 | -11.2 | 0.96 | -28.4 |
| AO-E2 | PL-1840 | 1.34 | 1.37 | 2.24 | 1.37 | 2.24 | 1.34 | 0.00 | 1.13 | -15.7 |
| AO-E3 | PL-1840 | 1.34 | 1.36 | 1.49 | 1.38 | 2.99 | 1.26 | -5.97 | 1.06 | -20.9 |
| AO-F | PL-1840 | 1.34 | 1.37 | 2.24 | 1.37 | 2.24 | 1.32 | -1.49 | 0.97 | -27.6 |
| | VP-8770 | 1.35 | 1.38 | 2.22 | 1.39 | 2.96 | 1.40 | 3.70 | 1.36 | 0.74 |
| | Dowlex2045E | 1.15 | 1.20 | 4.35 | 1.16 | 0.87 | 0.85 | -26.1 | 0.65 | -43.5 |
| AO-G | PL-1840 | 1.34 | 1.35 | 0.75 | 1.34 | 0.00 | 1.10 | -17.9 | 0.77 | -42.5 |
| | VP-8770 | 1.35 | 1.37 | 1.48 | 1.37 | 1.48 | 1.27 | -5.93 | 1.04 | -23.0 |
| | Dowlex2045E | 1.15 | 1.19 | 3.48 | 1.08 | -6.09 | 0.87 | -24.4 | 0.61 | -47.0 |

* See Table 5.2 for the Code of AO mixtures (Page 243)

** The LLDPE used are all new batch polymers

*** P₀ was carried out at 210°C, 100rpm and 4.0kg/h

Table A5.8. MFR and Its Change of TSE Processed LLDPE Containing Antioxidant Mixture (265°C, 100rpm, 4.8kg/h)

| Antioxidant Mixtures (Code) * | Polymer ** | Virgin MFR | P ₀ *** (210°C) | | P ₁ (265°C) | | P ₃ (265°C) | | P ₅ (265°C) | |
|-------------------------------|-------------|------------|----------------------------|------------|------------------------|------------|------------------------|------------|------------------------|------------|
| | | | MFR | Change (%) | MFR | Change (%) | MFR | Change (%) | MFR | Change (%) |
| AO-A1 | PL-1840 | 37.9 | 37.5 | -1.06 | 36.7 | -3.17 | 38.1 | 0.53 | 43.2 | 14.0 |
| AO-A2 | PL-1840 | 37.9 | 37.2 | -1.85 | 36.8 | -2.9 | 37.9 | 0.00 | 41.0 | 8.18 |
| AO-B1 | PL-1840 | 37.9 | 37.6 | -0.79 | 37.4 | -1.32 | 42.4 | 11.9 | 58.6 | 54.6 |
| AO-B2 | PL-1840 | 37.9 | 37.5 | -1.06 | 38.4 | 1.32 | 39.4 | 3.96 | 51.4 | 35.6 |
| AO-C1 | PL-1840 | 37.9 | 37.3 | -1.58 | 37.2 | -1.85 | 44.8 | 18.2 | 62.4 | 64.6 |
| AO-C2 | PL-1840 | 37.9 | 37.3 | -1.58 | 38.3 | 1.06 | 38.5 | 1.58 | 47.3 | 24.8 |
| AO-D1 | PL-1840 | 37.9 | 38.2 | 0.79 | 37.9 | 0.00 | 39.3 | 3.69 | 53.5 | 41.2 |
| AO-D2 | PL-1840 | 37.9 | 37.7 | -0.53 | 38 | 0.26 | 38.3 | 1.06 | 41.5 | 9.50 |
| AO-E1 | PL-1840 | 37.9 | 38.1 | 0.53 | 38.1 | 0.53 | 41.7 | 10.0 | 47.4 | 25.1 |
| AO-E2 | PL-1840 | 37.9 | 37.4 | -1.32 | 37.8 | -0.26 | 39.3 | 3.69 | 43.7 | 15.3 |
| AO-E3 | PL-1840 | 37.9 | 37.9 | 0.00 | 38.0 | 0.26 | 40.8 | 7.65 | 45.3 | 19.5 |
| AO-F | PL-1840 | 37.9 | 37.7 | -0.53 | 37.7 | -0.53 | 39.1 | 3.17 | 47.4 | 25.1 |
| | VP-8770 | 28.5 | 28.4 | -0.35 | 28.4 | -0.35 | 29.0 | 1.75 | 30.1 | 5.61 |
| | Dowlex2045E | 29.5 | 29.4 | -0.34 | 30.2 | 2.37 | 37.6 | 27.5 | 46.2 | 56.6 |
| AO-G | PL-1840 | 37.9 | 37.9 | 0.00 | 39.0 | 2.90 | 44.3 | 16.9 | 56.1 | 48.0 |
| | VP-8770 | 28.5 | 28.2 | -1.05 | 28.9 | 1.40 | 31.3 | 9.82 | 35.9 | 26.0 |
| | Dowlex2045E | 29.5 | 29.4 | -0.34 | 32.0 | 8.47 | 37.7 | 27.8 | 48.7 | 65.1 |

* See Table 5.2 for the Code of AO mixtures (Page 243)

* The LLDPE used are all new batch polymers

** P₀ was carried out at 210°C, 100rpm and 4.0kg/h

Table A5.9. Trans-vinylene Concentration in TSE Extruded LLDPE Containing Antioxidant Mixture (Measured by FT-IR)

| Antioxidant Code | Polymer * | Trans- vinylene Concentration (mol/L) | | | | |
|------------------|-------------|---------------------------------------|------------------------|------------------------|------------------------|------------------------|
| | | Virgin | P ₀ (210°C) | P ₁ (265°C) | P ₃ (265°C) | P ₅ (265°C) |
| AO-A1 | PL-1840 | 0.18 | 0.19 | 0.19 | 0.33 | 0.55 |
| AO-A2 | PL-1840 | 0.18 | 0.19 | 0.20 | 0.31 | 0.88 |
| AO-B1 | PL-1840 | 0.18 | 0.16 | 0.16 | 0.25 | 0.35 |
| AO-B2 | PL-1840 | 0.18 | 0.20 | 0.19 | 0.25 | 0.27 |
| AO-C1 | PL-1840 | 0.18 | 0.27 | 0.25 | 0.27 | 0.30 |
| AO-C2 | PL-1840 | 0.18 | 0.35 | 0.31 | 0.27 | 0.35 |
| AO-D1 | PL-1840 | 0.18 | 0.29 | 0.47 | 0.67 | 0.76 |
| AO-D2 | PL-1840 | 0.18 | 0.23 | 0.31 | 0.60 | 0.73 |
| AO-E1 | PL-1840 | 0.18 | 0.18 | 0.19 | 0.25 | 0.27 |
| AO-E2 | PL-1840 | 0.18 | 0.28 | 0.33 | 0.31 | 0.28 |
| AO-E3 | PL-1840 | 0.18 | 0.17 | 0.15 | 0.14 | 0.23 |
| AO-F | PL-1840 | 0.18 | 0.29 | 0.18 | 0.13 | 0.14 |
| | VP-8770 | 0.33 | 0.33 | 0.35 | 0.38 | 0.42 |
| | Dowlex2045E | 0.06 | 0.05 | 0.04 | 0.06 | 0.06 |
| AO-G | PL-1840 | 0.18 | 0.18 | 0.23 | 0.40 | 0.43 |
| | VP-8770 | 0.33 | 0.25 | 0.36 | 0.61 | 0.69 |
| | Dowlex2045E | 0.06 | 0.06 | 0.20 | 0.29 | 0.32 |

* The LLDPE used are all new batch polymers

Table A5.10. Vinyl Concentration in TSE Extruded LLDPE Containing Antioxidant Mixture (Measured by FT-IR)

| Antioxidant Code | Polymer * | Vinyl Concentration (mol/L) | | | | |
|------------------|-------------|-----------------------------|------------------------|------------------------|------------------------|------------------------|
| | | Virgin | P ₀ (210°C) | P ₁ (265°C) | P ₃ (265°C) | P ₅ (265°C) |
| AO-A1 | PL-1840 | 0.04 | 0.06 | 0.06 | 0.03 | 0.02 |
| AO-A2 | PL-1840 | 0.04 | 0.06 | 0.06 | 0.04 | 0.02 |
| AO-B1 | PL-1840 | 0.04 | 0.02 | 0.02 | 0.02 | 0.02 |
| AO-B2 | PL-1840 | 0.04 | 0.02 | 0.02 | 0.01 | 0.02 |
| AO-C1 | PL-1840 | 0.04 | 0.02 | 0.02 | 0.02 | 0.01 |
| AO-C2 | PL-1840 | 0.04 | 0.03 | 0.02 | 0.01 | 0.02 |
| AO-D1 | PL-1840 | 0.04 | 0.02 | 0.02 | 0.02 | 0.02 |
| AO-D2 | PL-1840 | 0.04 | 0.02 | 0.02 | 0.02 | 0.02 |
| AO-E1 | PL-1840 | 0.04 | 0.02 | 0.02 | 0.02 | 0.02 |
| AO-E2 | PL-1840 | 0.04 | 0.02 | 0.02 | 0.01 | 0.02 |
| AO-E3 | PL-1840 | 0.04 | 0.03 | 0.02 | 0.01 | 0.02 |
| AO-F | PL-1840 | 0.04 | 0.02 | 0.02 | 0.02 | 0.02 |
| | VP-8770 | 0.02 | 0.01 | 0.01 | 0.00 | 0.01 |
| | Dowlex2045E | 0.19 | 0.20 | 0.19 | 0.19 | 0.19 |
| AO-G | PL-1840 | 0.04 | 0.06 | 0.03 | 0.01 | 0.01 |
| | VP-8770 | 0.02 | 0.03 | 0.02 | 0.01 | 0.01 |
| | Dowlex2045E | 0.19 | 0.28 | 0.19 | 0.18 | 0.17 |

* The LLDPE used are all new batch polymers

Table A5.11. Vinylidene Concentration in TSE Extruded LLDPE Containing Antioxidant Mixture (Measured by FT-IR)

| Antioxidant Code | Polymer * | Vinylidene Concentration (mol/L) | | | | |
|------------------|-------------|----------------------------------|------------------------|------------------------|------------------------|------------------------|
| | | Virgin | P ₀ (210°C) | P ₁ (265°C) | P ₃ (265°C) | P ₅ (265°C) |
| AO-A1 | PL-1840 | 0.15 | 0.15 | 0.19 | 0.22 | 0.27 |
| AO-A2 | PL-1840 | 0.15 | 0.15 | 0.17 | 0.21 | 0.26 |
| AO-B1 | PL-1840 | 0.15 | 0.18 | 0.22 | 0.24 | 0.25 |
| AO-B2 | PL-1840 | 0.15 | 0.19 | 0.21 | 0.24 | 0.24 |
| AO-C1 | PL-1840 | 0.15 | 0.18 | 0.22 | 0.27 | 0.27 |
| AO-C2 | PL-1840 | 0.15 | 0.18 | 0.21 | 0.27 | 0.28 |
| AO-D1 | PL-1840 | 0.15 | 0.19 | 0.21 | 0.24 | 0.24 |
| AO-D2 | PL-1840 | 0.15 | 0.18 | 0.20 | 0.22 | 0.22 |
| AO-E1 | PL-1840 | 0.15 | 0.17 | 0.20 | 0.22 | 0.22 |
| AO-E2 | PL-1840 | 0.15 | 0.19 | 0.21 | 0.22 | 0.21 |
| AO-E3 | PL-1840 | 0.15 | 0.18 | 0.20 | 0.21 | 0.22 |
| AO-F | PL-1840 | 0.15 | 0.18 | 0.20 | 0.24 | 0.25 |
| | VP-8770 | 0.22 | 0.24 | 0.28 | 0.28 | 0.30 |
| | Dowlex2045E | 0.07 | 0.07 | 0.08 | 0.10 | 0.09 |
| AO-G | PL-1840 | 0.15 | 0.15 | 0.20 | 0.26 | 0.27 |
| | VP-8770 | 0.22 | 0.20 | 0.24 | 0.32 | 0.34 |
| | Dowlex2045E | 0.07 | 0.07 | 0.08 | 0.08 | 0.08 |

* The LLDPE used are all new batch polymers

Table A5.12. Carbonyl Concentration in TSE Extruded LLDPE Containing Antioxidant Mixture (Measured by FT-IR)

| Antioxidant Code | Polymer * | Carbonyl Concentration (mol/L) | | | | |
|------------------|-------------|--------------------------------|------------------------|------------------------|------------------------|------------------------|
| | | Virgin | P ₀ (210°C) | P ₁ (265°C) | P ₃ (265°C) | P ₅ (265°C) |
| AO-A1 | PL-1840 | 0.05 | 0.07 | 0.08 | 0.08 | 0.08 |
| AO-A2 | PL-1840 | 0.05 | 0.07 | 0.07 | 0.07 | 0.09 |
| AO-B1 | PL-1840 | 0.05 | 0.07 | 0.07 | 0.08 | 0.10 |
| AO-B2 | PL-1840 | 0.05 | 0.07 | 0.07 | 0.07 | 0.10 |
| AO-C1 | PL-1840 | 0.05 | 0.07 | 0.07 | 0.09 | 0.11 |
| AO-C2 | PL-1840 | 0.05 | 0.06 | 0.07 | 0.08 | 0.10 |
| AO-D1 | PL-1840 | 0.05 | 0.08 | 0.08 | 0.09 | 0.10 |
| AO-D2 | PL-1840 | 0.05 | 0.07 | 0.07 | 0.08 | 0.10 |
| AO-E1 | PL-1840 | 0.05 | 0.05 | 0.05 | 0.05 | 0.06 |
| AO-E2 | PL-1840 | 0.05 | 0.05 | 0.05 | 0.06 | 0.06 |
| AO-E3 | PL-1840 | 0.05 | 0.05 | 0.05 | 0.05 | 0.06 |
| AO-F | PL-1840 | 0.05 | 0.08 | 0.08 | 0.10 | 0.11 |
| | VP-8770 | 0.03 | 0.06 | 0.06 | 0.07 | 0.07 |
| | Dowlex2045E | 0.02 | 0.07 | 0.08 | 0.10 | 0.11 |
| AO-G | PL-1840 | 0.05 | 0.06 | 0.07 | 0.08 | 0.09 |
| | VP-8770 | 0.03 | 0.05 | 0.05 | 0.06 | 0.07 |
| | Dowlex2045E | 0.02 | 0.06 | 0.05 | 0.06 | 0.07 |

* The LLDPE used are all new batch polymers

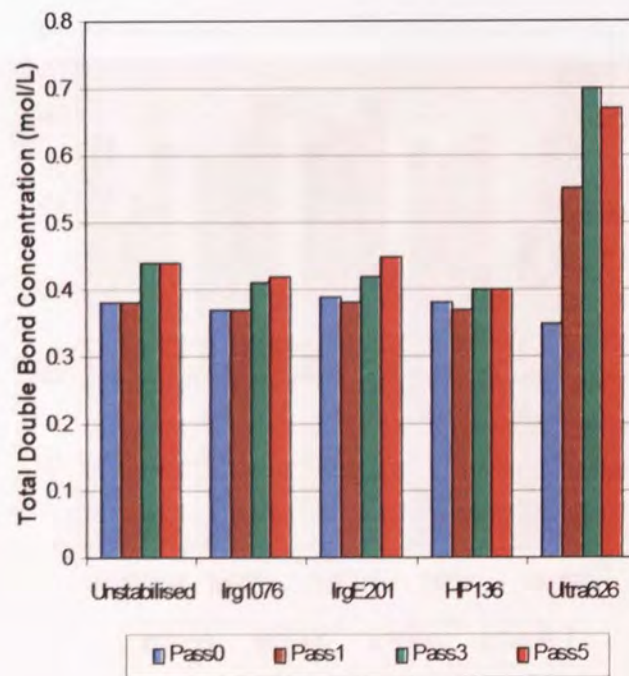
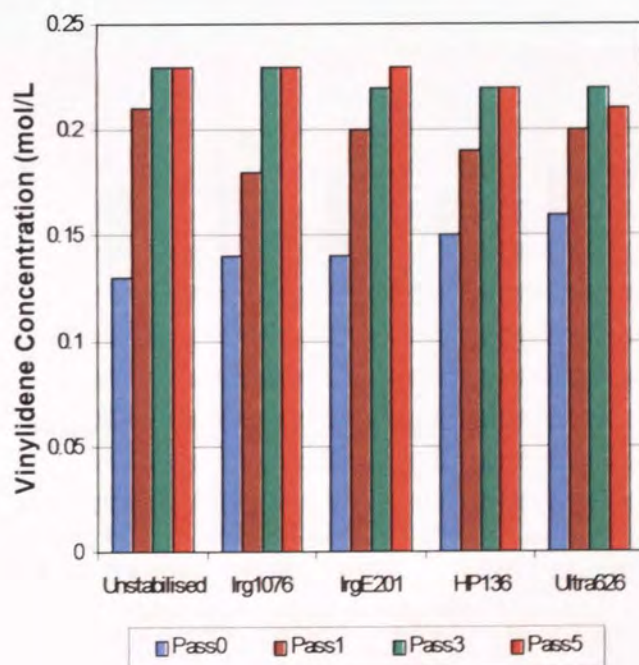
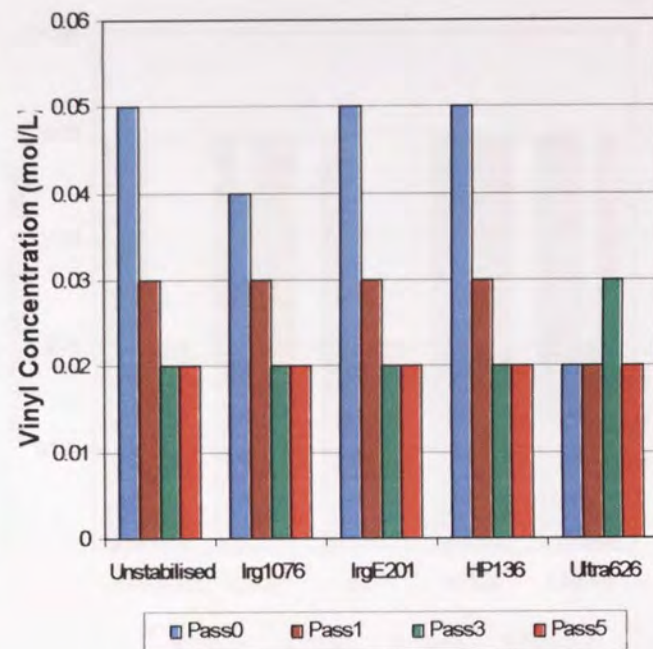
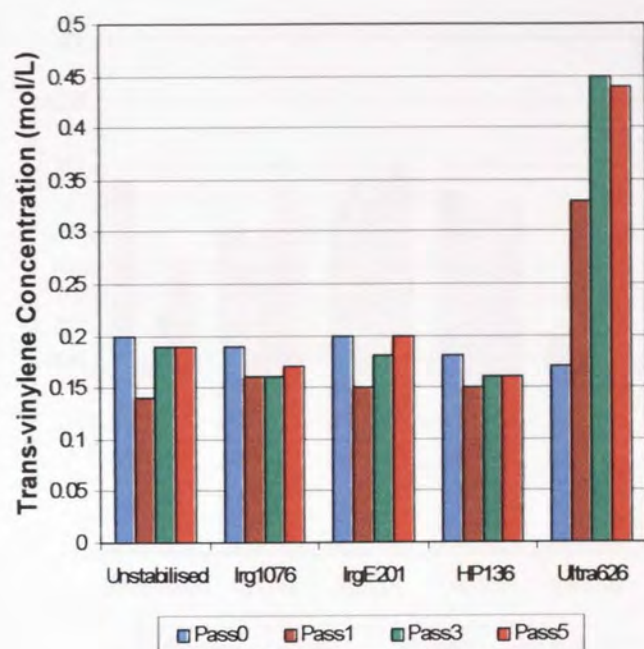


Figure A5.1. Concentration Changes of Double Bonds with Passes for Extruded FM-1570 Containing Different Single Antioxidants (265°C, 100rpm, Pass0 of unstabilised polymer represents the virgin sample)

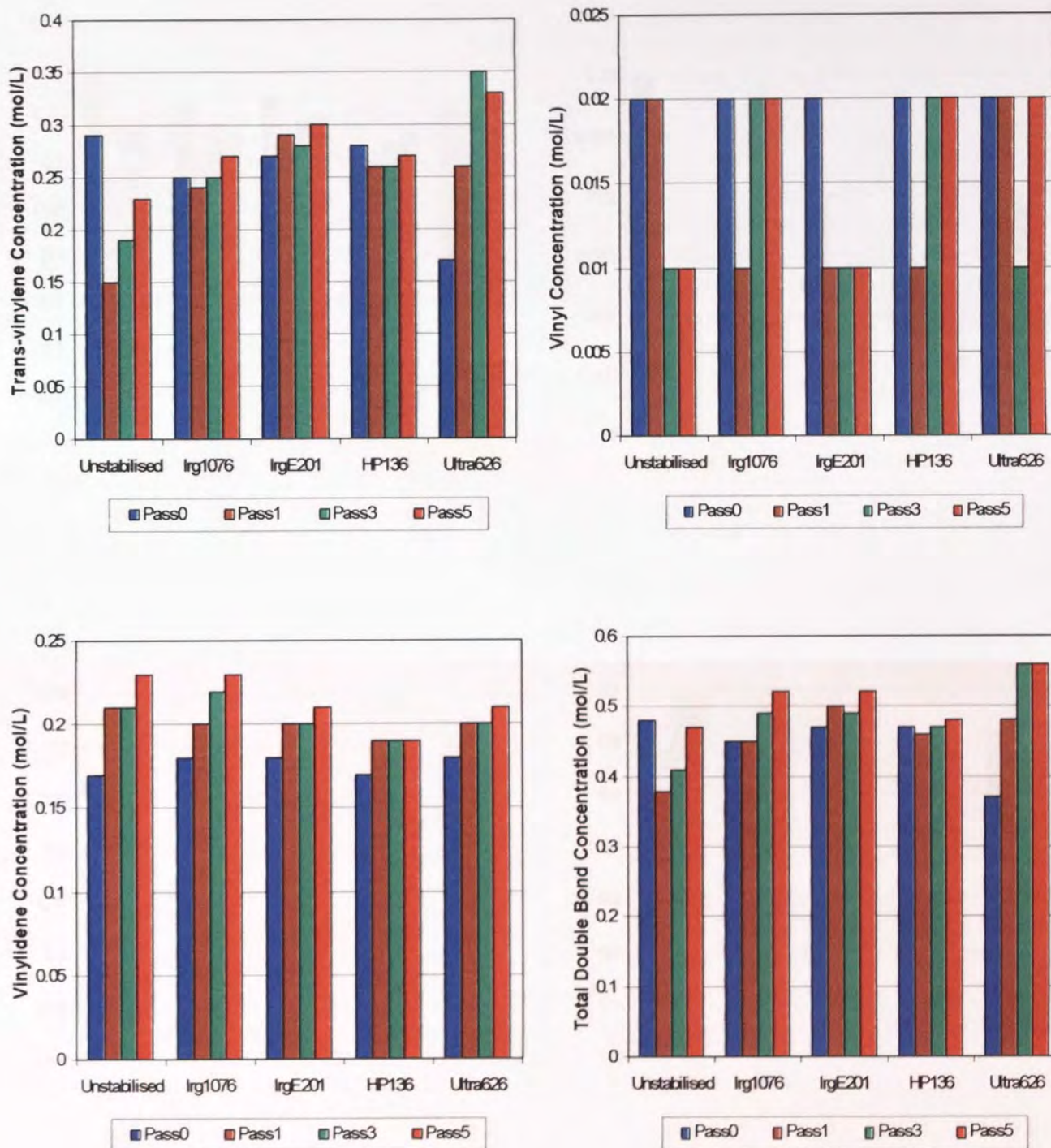


Figure A5.2. Concentration Changes of Double Bonds with Passes for Extruded PL-1840 Containing Different Single Antioxidants (265°C, 100rpm, Pass0 of unstabilised polymer represents the virgin sample)

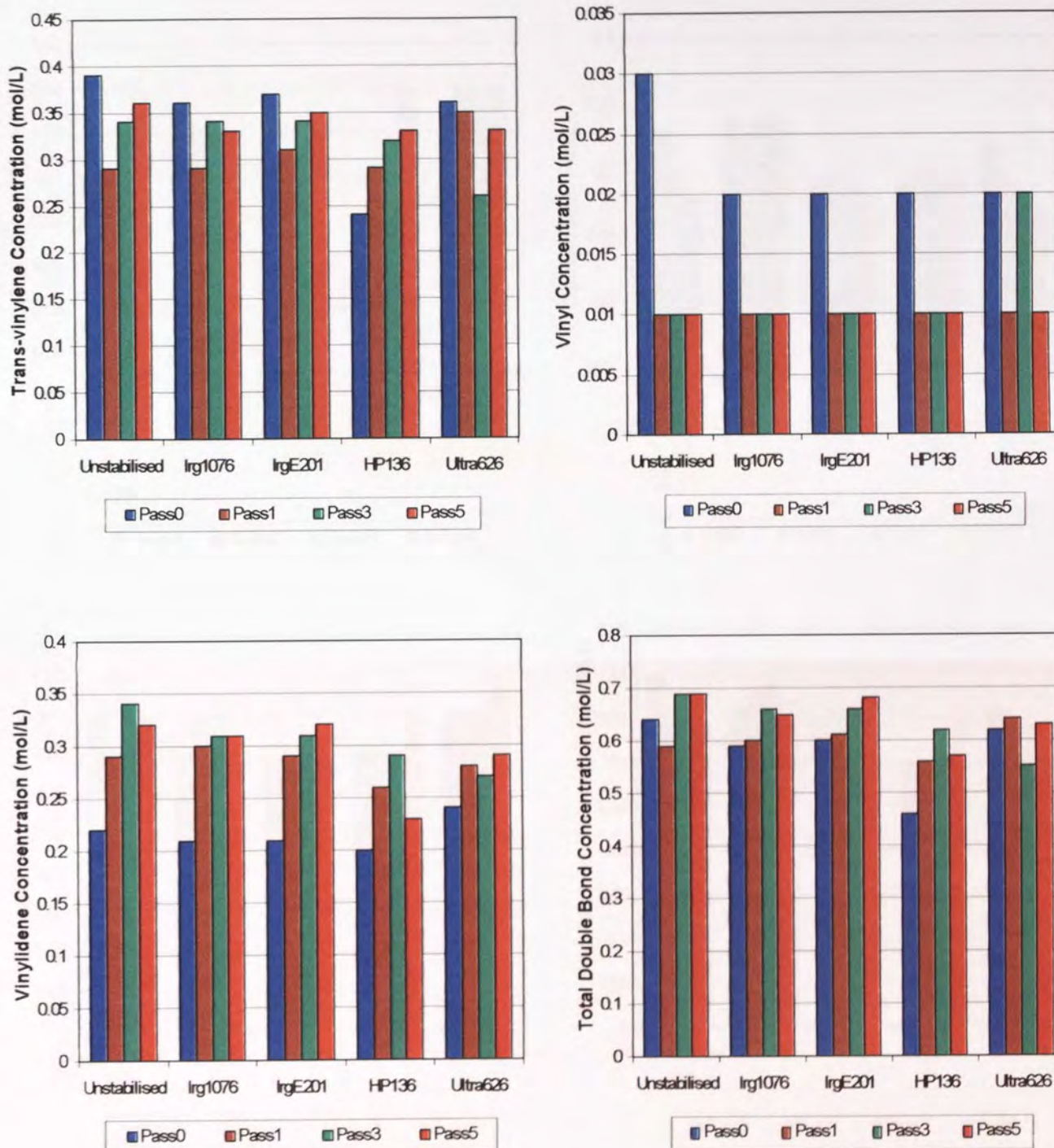


Figure A5.3. Concentration Changes of Double Bonds with Passes for Extruded VP-8770 Containing Different Single Antioxidants (265°C, 100rpm, Pass0 of unstabilised polymer represents the virgin sample)

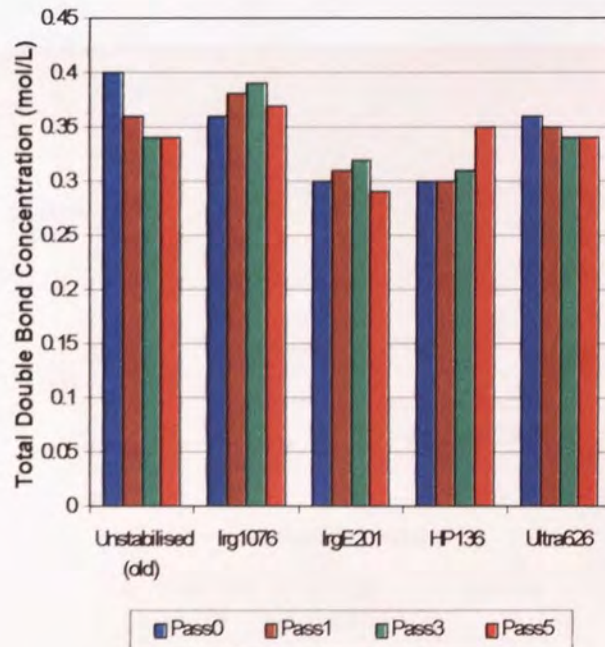
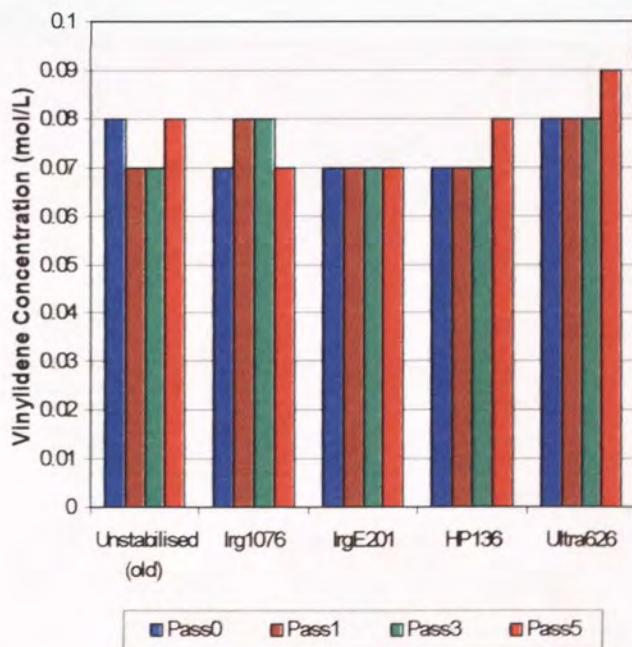
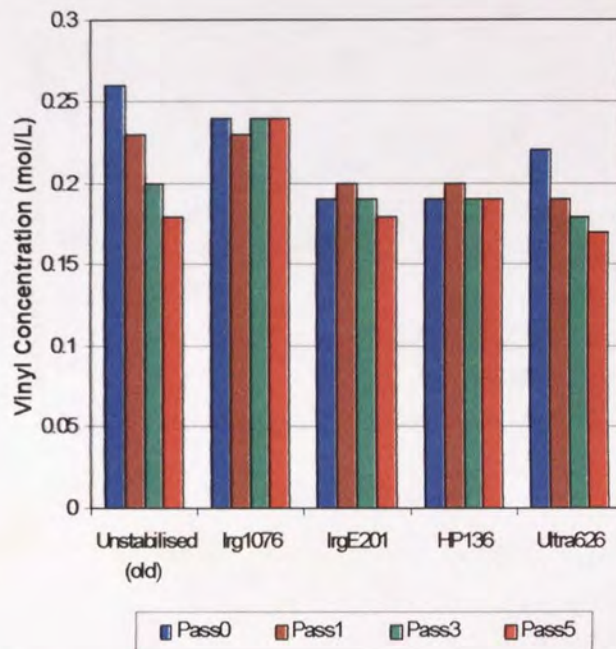
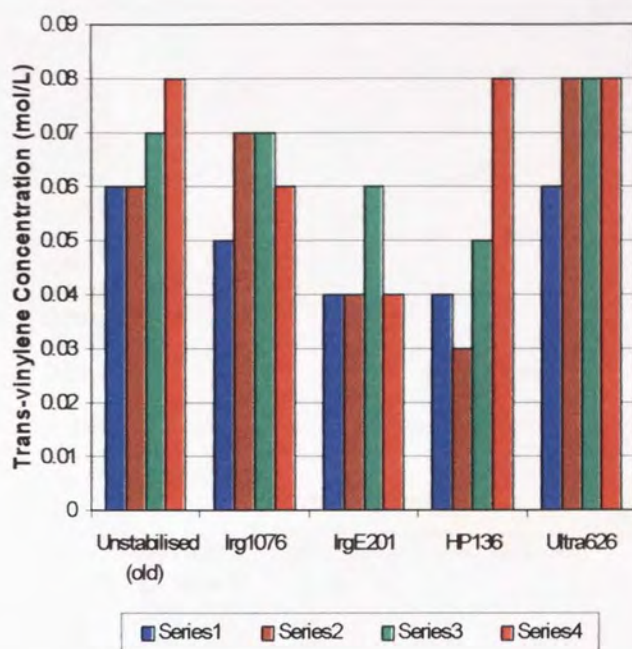


Figure A5.4. Concentration Changes of Double Bonds with Passes for Extruded Dowlex2045E Containing Different Single Antioxidants (265°C, 100rpm, Pass0 of unstabilised polymer represents the virgin sample, Dowlex2045E containing Irg1076 was old batch and the others were new batch polymers)

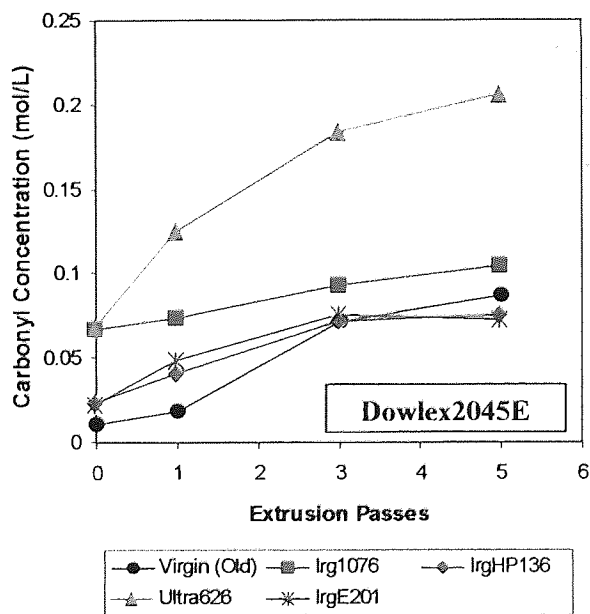
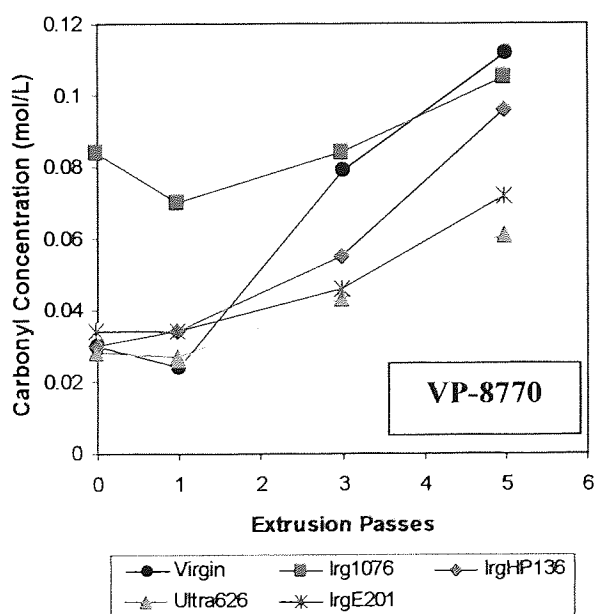
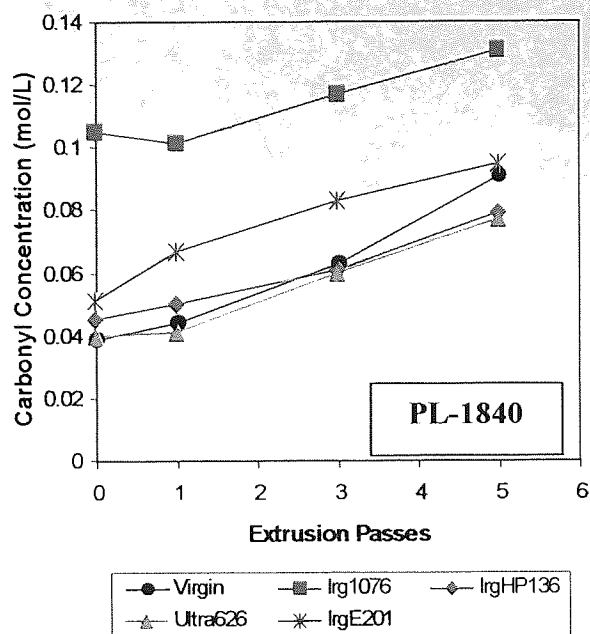
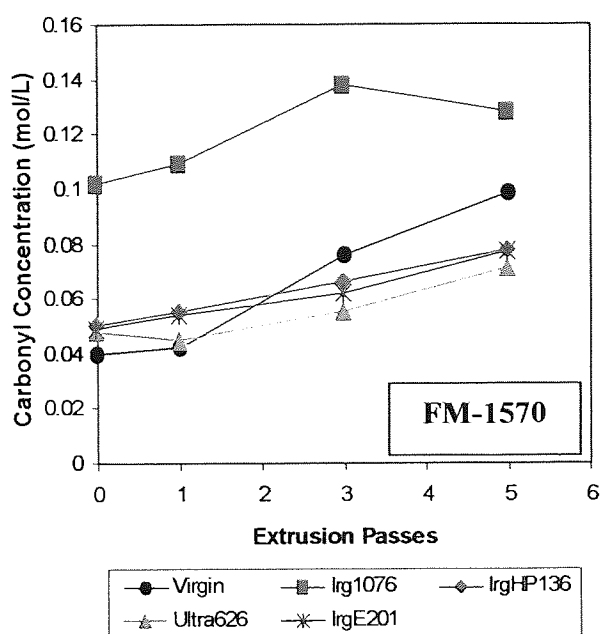


Figure A5.5. Carbonyl Concentration (determined by FTIR in carbonyl region of $1680\sim1780\text{ cm}^{-1}$) Change with Extrusion Passes for Extruded LLDPE Polymers Containing Different Single Antioxidants (265°C , 100rpm, virgin LLDPE with 0 pass represent unprocessed polymers)